3A Seismic Soil Structure Interaction Analysis

3A.1 Introduction

This appendix presents soil-structure interaction (SSI) analysis performed for the generic site conditions adopted for establishing seismic design loads and seismic adequacy of the Reactor Building (R/B) and Control Building (C/B) complex of the ABWR standard plant for a 0.3g safe shutdown earthquake (SSE) excitation. The free-field design spectra of SSE are described in Subsection 3.7.1 and are defined per Regulatory Guide 1.60. The SSI analysis results in the form of site-enveloped seismic responses at key locations in the R/B and C/B complex are presented herein.

In order to ensure the seismic adequacy of the R/B and C/B structures and the associated reactor and other equipment, an extensive seismic analysis is required. For a standard plant design, the analysis must be performed over a range of site parameters. The site parameters considered and their ranges together form the generic site conditions. The generic site conditions are selected to provide an adequate seismic design margin for the standard plant located at any site with site parameters within the range of parameters considered in this study. For sites to be located with these facilities, site-specific geotechnical data will be developed and submitted to the NRC demonstrating compatibility with the design analyses assumptions (see Subsection 2.3.1.2).

This appendix details the basis for selecting the site conditions and analysis cases, and the method of the seismic soil-structure interaction analysis. A description of the input motion and damping values, the structural model, and the soil model are included. The parametric study SSI results as well as enveloping seismic responses are also presented.

Seismic adequacy of the R/B and C/B are demonstrated in Section 3.8 using the seismic design loads presented in this appendix, which are obtained as a result of application of the SSI on the methodology described in this appendix.

To demonstrate the seismic adequacy of the standard ABWR R/B design, a total of 22 SSI cases are analyzed for generic site conditions using the finite element method for the SSE condition. The enveloped results reported in this appendix form the design SSE loads.

3A.2 ABWR Standard Plant Site Plan

The typical site plan of the ABWR standard plant is shown in Figure 3A-1. The plan orientations are identified by 0°–180° and 90°–270° directions. The cross section along the 0°–180° is shown in Figure 3A-2. The R/B is nearly square in plan with dimensions of 56.6m x 59.6m. This building is deeply embedded with embedment depth of 25.7m. Adjacent to the R/B along the 0° direction is the C/B. This building is rectangular in plan having plan dimensions of 24m x 56m and the embedment depth of 23.2m. Adjacent to the C/B in the 0° direction farther away from the R/B is the turbine building (T/B) which is 106m long, 58.5m wide. All buildings are supported on separated basemats. The separation distance between the R/B and C/B is 2m. The separation distance between the C/B and T/B is 6m.

The primary objective of the analysis presented in this appendix is to obtain seismic responses for the R/B and C/B complex. Other buildings are considered in the seismic analysis when they are expected to affect the seismic responses of the R/B and C/B.

In the modeling of the buildings, the 0°–180° and 90°–270° directions are designated as X- and Y-axes, respectively. The Z-axis follows the elevations shown in Figure 3A-2. As evident from the site plan, the consideration of structure-to-structure interaction effect in the SSI analysis for the R/B and C/B is required only for X-direction. For the analysis in the Y-direction, the R/B and C/B are considered individually since the structure-to-structure interaction effect in this direction is expected to be less insignificant.

3A.3 Generic Site Conditions

This section describes the generic site conditions and their design parameters based on a range of soil properties used in the soil-structure interaction analysis described in this appendix.

The site conditions are varied to cover a range of expected site conditions in relatively high seismic areas where a nuclear power plant may be constructed.

From the SSI analysis point of view, site conditions can be characterized in terms of: (1) soil deposit depth above bedrock, (2) soil profile and properties, and (3) ground water level. Parametric variations in each of these three areas for establishing generic site design envelopes are presented as follows.

3A.3.1 Soil Deposit Depth

To encompass most of the potential site conditions, a broad range of soil deposit depth is considered. The minimum depth is the embedment depth for which the R/B is supported directly on rock. For this case, the soil depth is 25.7m which is the R/B embedment depth.

The other soil depths are determined using Reference 3A-1 as the guide. By maintaining the ratio of soil depth below the basemat to the basemat width to be approximately the same as for the Standard Plant design, the shallow depth is chosen to be 45.7m.

The deepest soil deposit considered in the Standard Plant is 91.5m. This depth is selected on the basis of a survey of sixty-two U.S. nuclear power plant sites, which indicates that the rock level in the majority of sites is located at a depth less than 61m from the ground surface. A 91.5m depth is, thus, a reasonable upper bound and, therefore, is selected to be the deep soil deposit case for this appendix. Between the shallow and deep soil cases, an intermediate depth is chosen to be at 61m.

In summary, the variations of soil deposit thickness are accounted for by considering the following four representative soil deposit depths.

Minimum (embedment depth)	25.7m
Shallow soil deposit	45.7m
Intermediate soil deposit	61.0m
Deep soil deposit	91.5m

3A.3.2 Soil Profile and Properties

The range of soil profiles considered in this appendix is based on the velocity profiles used in Reference 3A-1. A total of six velocity profiles are selected and shown in Figure 3A-3. These velocity profiles are designated with the abbreviations: UB, VP3, VP4, VP5, VP7 and an upper bound case with rigid soil properties (R cases).

The profile UB represents a soil profile of which the shear wave velocity at a depth z below the ground surface is obtained using the modulus parameter K_{2max} and the following equations.

$$G_{max}(z) = 218.8 K_{2max} \sqrt{\sigma_m(z)} \quad (3A\text{-}1)$$

$$V_s = \sqrt{G_{max} / \rho} \quad (3A\text{-}2)$$

where

G_{max} = maximum shear modulus, kPa

σ_m = effective mean pressure (kPa) at depth (z); it is assumed equal to 0.7 times the effective overburden pressure, which corresponds to the use of an at rest coefficient of lateral pressure equal to 0.55.

K_{2max} = modulus parameter

ρ = mass density

V_s = shear wave velocity

This soil profile is assumed to consist of seven horizontal layers. The K_{2max} value, total unit weight, and Poisson's ratio for each layer are as shown in Table 3A-1.

Note that for submerged layers the Poisson's ratio is to be adjusted such that the minimum P-wave velocity of water is retained. The values of average shear wave velocity, shown in Figure

3A-3 for UB, are computed using Equations 3A-1 and 3A-2 at the mid-depth of each layer for the ground water level at a depth of 0.61m below grade.

The profiles UB, VP3 through VP5 are selected based on three generalized soil zones shown in Figure 3A-4: a soil zone (sands, silts, clays, and gravely soils), a transition zone, and a soft rock and well-cemented soil zone. Velocity profile UB represents an average profile of the soil zone; VP3 and VP4 bound the transition zone, and VP5 represents an average profile for well-cemented soil zone. Those velocity profiles are smooth curves representative of the average variation of shear modulus with depth that can be expected within each of the soil zones.

The profile VP7 represents a hard rock site with a uniform shear wave velocity of 1524 m/s. The profile for R cases represents an upper bound profile with rigid soil properties (uniform shear wave velocity of 6096 m/s).

The lower bound shear wave velocity for the top 9m of soil among all profiles considered is 303 m/s. The upper bound velocity is 6096 m/s. This constitutes a wide range of potential site conditions that are suitable for nuclear power plants.

The general soil layer properties (layer thickness, total unit weight, and Poisson's ratio) defined for the UB profile are also adopted for all other profiles except for VP7 and R. The profiles VP7 and R are considered to be uniform elastic half-space with a constant Poisson's ration of 0.3. The unit weight density for VP7 profile is the same as UB profile. The unit weight density for R profiles is 2.2 t/m^3. The base rock in all soil profiles is modeled using density 2.2 t/m^3, shear wave velocity of 1594 m/s. Poisson's ratio of 0.3, and material damping of 1%. The average shear wave velocities in layers for all soil profiles are tabulated in Table 3A-2.

The shear modulus and material damping of soil are strain dependent. Figure 3A-5 shows the variation of shear modulus and damping ratio with shear strain for various soil profiles considered. The soil curves shown correspond to average curves of Reference 3A-6. On the basis of the recommendations made in Reference 3A-3 the soil material damping of a hysteretic nature is limited to a maximum of 15% of critical. In addition to use of average soil curves, a parametric study was performed in which the upper bound shear modulus soil degradation curve of Reference 3A-6 is used. This curve is the same as the shear modulus degradation curve reported in Reference 3A-7 for sands. The results of this case are presented in Section 3A.9.5. Variation of shear modulus and damping for rock profiles (VP5 and VP7) are shown in Figure 3A-6. The shear modulus reduction factors and damping ratios at various strain levels are shown in Tables 3A-3 and 3A-4. For VP7 profile, the free-field site response analysis results has shown that the strain-compatible shear modulus and material damping are essentially unchanged from their initial values. The SSI analysis for R profile is performed using uniform velocity of 6098 m/s.

3A.3.3 Ground Water Table

The effect of ground water on the soil properties is considered using the following procedure:

(1) Perform one dimensional convolution or deconvolution analysis for the horizontal excitation component to obtain strain compatible shear modulus, G, corresponding to the induced strain level. The corresponding shear wave velocity, Vs, is then computed as

$$V_s = \sqrt{G/\rho} \tag{3A-3}$$

(2) Compute the corresponding compression wave velocity, Vp, using the following equation.

$$V_p = V_s \sqrt{\frac{2(1-\mu)}{1-2\mu}} \tag{3A-4}$$

where μ is a Poisson's ratio. The lower bound of V_p for the submerged soil below water table is the compression wave velocity of water taken to be 1463 m/s. When the computed V_p of soil is smaller than 1463 m/s, adjustment of soil Poisson's ratio is required to increase the P-wave velocity.

In order to evaluate the effects of water table location variation (assuming no soil failure) on structural response, three water table locations are considered, namely, the high, intermediate, and low water tables. The high water table is the base case which is located at 0.61m below grade. The low water table is taken to be 25.7m which is at the base of the R/B foundation basemat. The intermediate water table is assumed at 12.2m below grade which is at about the midheight of the R/B embedment. Since the ground water may have more pronounced effects on soft sites, the UB profile with 45.7m depth of soil deposit is investigated for all three water tables defined above. The water table level for other site conditions is based on the basic high water table case which is at 0.61m below grade.

3A.3.4 Summary of Site Conditions

The above discussions cover the range of site parameters in terms of soil deposit depth, soil profile and properties, and water table location. Based on the Standard Plant experience (Reference 3A-1) that the shallower soil depth in general resulted in higher structural response, all velocity profiles, except the VP7 and R profiles which are uniform rock profiles with zero soil depth, are considered for the 45.7m shallow soil case, and only limited soil velocity profiles need to be considered for other depths. For the deeper deposits of 61m and 91.5m in depth, it is sufficient to consider only the lower bound UB and VP3 profiles. Consequently, the effects of variation in soil properties with depth is accounted for more representatively. The minimum soil depth of 25.7m is considered for the UB and VP3 profiles which adequately cover the range of soil profiles considered. As mentioned before, the water table variation is

taken into account by the UB profile for the shallow soil deposit case. The site conditions in terms of the combination of shear wave velocity profile, soil depth and ground water table locations are schematically summarized in Figure 3A-3.

3A.4 Input Motion and Damping Values

3A.4.1 Input Motion

The time-history method is used in performing the seismic soil-structure interaction analysis. Earthquake (input or control) motion in the form of synthetic acceleration time histories are generated as described in Subsection 3.7.1.2 for all three components designated as H_1, H_2, and V. The H_1 and H_2 are the two horizontal components mutually perpendicular to each other. In the SSI analyses, H_1 and H_2 components are used in the horizontal X-(0°) and Y-(90°) directions, respectively. The V component is used in the vertical Z-direction.

The input motion (or control motion) is defined at the finished grade in the free-field. The motion is assumed to be generated by vertically propagating plane seismic shear waves for the horizontal components and compression waves for the vertical component.

3A.4.2 Damping Values

The structural components damping values used in the seismic analysis are in accordance with those specified in Regulatory Guide 1.61. These values for the SSE are summarized in Table 3.7-1.

The soil material damping values used for the SSI analysis are based on the strain-compatible soil damping values resulting from the free-field site response analysis as described in Subsection 3A.6. The strain-dependent soil damping versus strain is described in Subsection 3A.3.2.

3A.5 Soil-Structure Interaction Analysis Method

3A.5.1 Introduction

Nuclear Island structures are massive structures typically embedded to a considerable depth in a soil deposit. An important aspect in the seismic design of these structures is the evaluation of the dynamic interaction between the structures and the soil. Such interaction effects may significantly affect the response of the structures as well as the equipment systems.

The approach used to obtain seismic design envelopes in this appendix is based on the finite-element method using substructuring technique. The newly developed, two and three-dimensional (2-D and 3-D), linear finite element computer program SASSI (Reference 3A-4) is used. The program uses finite elements with complex moduli for modeling the structure and foundation properties and is based on the flexible volume method of substructuring and the frequency domain complex response method of analysis. Detailed descriptions of the complex response method and SSI methodology are presented in Subsections 3A.5.2 and 3A.5.3.

In performing the SSI analysis using the finite element method, the detailed structural models described in Subsection 3.7.2 are coupled with the soil model. Structural responses in terms of accelerations, forces, moments, and stresses are computed directly. Floor response spectra are obtained from the calculated response acceleration time histories (see Subsection 3.7.2.5). This effectively eliminates the need for a second step structural response analysis in which the fixed-based structural model is subjected to the base motions resulting from the first step SSI analysis. The direct solution also has an added advantage that the structural response to all components of base motion including rocking motion components for an embedded foundation is automatically accounted for in the solution.

The SSI analyses for the three directional earthquake components are performed separately. The maximum co-directional responses to each of the three earthquake components are combined using the SRSS method to obtain the combined maximum structural response in each selected degree of freedom of interest.

3A.5.2 Complex Response Method

For the dynamic analysis of a linear damped system, the equation of motion in the time domain at time t may be written in the following matrix form:

$$M\ddot{U} + D\dot{U} + KU = P \qquad (3A\text{-}5)$$

where $\ddot{U}$, $\dot{U}$ and U are respectively the acceleration, velocity and displacement vector at time t; K and M are the assembled total stiffness and mass matrices; D is the damping matrix and P is the dynamic load vector acting on the system at time t. For an SSI system for which the soil material damping is characterized by the constant hysteresis damping model and the foundation impedances are frequency dependent, the equation of motion is most conveniently formed and solved in the frequency domain using the complex response method. The application of the complex response method involves two solution steps: (1) steady-state response analysis to obtain the frequency response functions, and (2) Fourier analysis of the input and convolution to determine the transient response.

For the steady-state harmonic excitation at the circular frequency ω, the exciting force vector is written in the form:

$$P(t) = P^{*} \cdot e^{i\omega t} \qquad (3A\text{-}6)$$

where P^{*} is a complex constant vector representing the applied force amplitude and the phase angle.

The steady-state displacement response is also harmonic with the frequency ω and can accordingly be written as

$$U(t) = U^{*} \cdot e^{i\omega t} \qquad (3A\text{-}7)$$

Substitution of Equations 3A-6 and 3A-7 into Equation 3A-5 yields the matrix equation

$$C^*U^* = P^* \tag{3A-8}$$

where C* is the frequency dependent complex dynamic stiffness matrix in the form

$$C^* = K + i\omega D - \omega^2 M \tag{3A-9}$$

Equation 3A-8 is a system of linear equations with the complex coefficient matrix which can be solved for the complex response vector U^* for each frequency. The solution for U^* for a unit applied force, i.e., $P^* = 1$, is the transfer function.

For a system with material damping, the first two terms of Equation 3A-9 can be combined into a complex stiffness matrix K^*

$$K^* = K + i\omega D \tag{3A-10}$$

For a system with constant hysteresis material damping, K^* can be formed directly using complex shear moduli E_s^*, and complex constrained moduli E_p^*, defined by the following equations:

$$E_s^* = E_s\left(1-2\beta_s^2 + 2i\beta_s\sqrt{1-\beta_s^2}\right) \tag{3A-11}$$

$$E_p^* = E_p\left(1-2\beta_p^2 + 2i\beta_p\sqrt{1-\beta_p^2}\right) \tag{3A-12}$$

Where E_s and E_p are the real numbers corresponding to the shear and constrained moduli of the material, respectively, and β_s and β_p are the critical damping ratios associated with S-waves and P-waves, respectively. For practical applications, β_s and β_p are usually taken to be equal, i.e., $\beta_s = \beta_p = \beta$, in which case the Poisson's ratio is a real number.

Using the transfer function solution obtained from the complex response method, the transient excitations such as earthquake motions or applied dynamic loads, can be analyzed by decomposing the input excitation into Fourier components with period $N \bullet \Delta t$, where Δt is the time interval of digitization of excitation and N is the number of digitized points. Using the discrete representation, the discretized load function P (t) is defined by the series.

$$P_K = P(K \cdot \Delta t),\ K = 1, 2, ...,N \tag{3A-13}$$

which can be expanded into a discrete Fourier series in the form

$$P(t) = Re \sum_{s=1}^{N/2} P_s^* e^{i\omega_s t} \quad (3A\text{-}14)$$

where ω_s are the discrete circular frequencies defined by:

$$\omega_s = \frac{2\pi s}{N \cdot \Delta t} \quad (3A\text{-}15)$$

and P^* is complex amplitude defined by

$$P_s^* = \frac{1}{N} \sum_{K=1}^{N-1} P_k \exp(-i\omega_s k\Delta t);\ s = 0,\ s = \frac{N}{2} \quad (3A\text{-}16)$$

$$P_s^* = \frac{2}{N} \sum_{K=1}^{N-1} P_k \exp(-i\omega_s k\Delta t);\ 1 \le s \text{ and} \le \frac{N}{2} \quad (3A\text{-}17)$$

The numerical operations in Equations 3A-16 and 3A-17 are performed using the efficient Fast Fourier Transform (FFT) algorithm. This technique requires that N be a power of 2 which can always be achieved by adding trailing zeros to the discrete excitation time series. For damped systems these trailing zeros also serve as a quiet zone which allows the transient response motions to die out at the end of the duration to avoid cyclic overlapping error in the discrete Fourier transform procedure.

Once the P_s values are obtained, the Fourier transform of the transient response can be obtained by convolution of the transfer function and the Fourier coefficient, P_s, giving the complex frequency response function U_s for each discrete frequency ω_s.

Finally the transient response in the time domain U(t) can be obtained by the Fourier synthesis, i.e.,

$$U(t) = Re \sum_{s=0}^{N/2} U_s^* e^{i\omega_s t} \quad (3A\text{-}18)$$

Numerically, this operation is performed using the inverse Fast Fourier Transform algorithm. In principle, the system of complex linear equations defined by Equation 3A-8 has to be solved for each of the 1 + N/2 frequencies shown in Equation 3A-15. For the excitation defined by a real time function, the highest frequency corresponds to $1/(2\Delta t)$. This is called the Nyquist (or folding) frequency. The choice of Δt usually results in the Nyquist frequency which is much higher than the highest frequency of interest. The series in Equation 3A-15 can thus be truncated at some lower frequency number, s_{cut}. The corresponding cutoff frequency is

$$f_{cut} = \frac{s_{cut}}{N \cdot \Delta t} \quad s = 0,...,s_{cut} < \frac{N}{2} \tag{3A-19}$$

and only s_{cut} solution to Equation 3A-8 are required. For seismic analysis, s_{cut} is still a large number (typically of the order of 500). In practice Equation 3A-8 is solved for only a limited number of frequencies in the frequency range of interest. The solutions for the remaining frequencies are obtained by interpolation in the frequency domain.

3A.5.3 Methodology and Analysis Procedure

The flexible volume substructuring method used in SASSI considers the structure(s) and the foundation(s) to be partitioned as shown in Figure 3A-7. In this partitioning, the structure (Figure 3A-7) consists of the superstructure plus the basement minus the excavated soil. The foundation (Figure 3A-7), consists of the original site, i.e., the site without soil excavation for the structure basement. Interaction between the structure and the foundation occurs at all basement nodes. For seismic analysis, the equation of motion for substructure C in Figure 3A-7 can be written in the frequency domain as follows:

$$\begin{bmatrix} C_{ss}^* & C_{si}^* \\ C_{is}^* C_{ii}^* - C_f^* + X_f^* \end{bmatrix} \begin{Bmatrix} U_s^* \\ U_f^* \end{Bmatrix} = \begin{Bmatrix} O \\ X_f^* \bullet U_f'^* \end{Bmatrix} \tag{3A-20}$$

where the submatrices C^* are the complex dynamic stiffness matrices and defined by the following relation:

$$C^* = K^* - \omega^2 M \tag{3A-21}$$

where K^* is the complex stiffness matrix and M is the mass matrix, and ω is the excitation circular frequency. The subscripts used in Equation 3A-20 are defined in Figure 3A-7. The matrix X_f^* is the impedance computed for all the interacting nodes, $U_f'^*$ is the free–field motion and U_s^* and U_f^* are the complex total displacements of the superstructure and foundation nodes, respectively.

The complex modulus method of material representation described in the previous subsection is used to compute the complex stiffness of the elements allowing for variation of material damping in each element.

Based on the above equation of motion, the solution to the harmonic soil structure interaction problem can be achieved in the following five steps.

(1) Solve the site response problem. This step involves determining the free-field displacement amplitude $U_f'^*$ within the excavated volume. The site is modeled by horizontal soil layers resting on rigid base or elastic halfspace. The halfspace at the

bottom boundary is modeled using the variable depth method in which an extra layer of soil with a total depth of 1.5λ (where λ is the shear wave length in the halfspace) is added to the soil profile. Thus, the added soil layer depth varies with frequency. Furthermore, the added soil column is subdivided into n sublayers. A value of n = 10 is adequate and is used in the analyses.

In addition to variable depth soil layer, the halfspace simulation also uses viscous dashpots in the horizontal and vertical directions at the base of the added soil layer.

SASSI is a linear analysis program. The iteration on strain-dependent soil properties cannot be directly incorporated in the analysis. It is therefore, necessary first to perform the one-dimensional free-field soil column deconvolution analysis to obtain the equivalent linear soil properties compatible with seismic strains induced in the free-field. These properties are then used for the SASSI site response analysis. The free-field site response analysis is described in Subsection 3A.6.

(2) Solve the impedance problem. This step involves determining the matrix X_f^* which can be obtained efficiently from a series of 2-D plane strain or 3-D axisymmetric solution of sub-structure (b) in Figure 3A-7. The halfspace simulation, if requested in Step 1, will be automatically included in this step of analysis as well.

(3) Form the load vector. The seismic excitation load vector in Equation 3A-20 can be computed from the product of solutions in Steps 1 and 2.

(4) Form the complex dynamic stiffness matrix. This step involves forming the coefficient matrix C^* in the left-hand side of Equation 3A-20. The superstructure is modeled using finite elements from the finite element library of SASSI. The foundation is modeled using two sets of elements. The first set is used to represent excavated soil in the basement volume. Usually brick elements are used in 3-D analysis and four-node plane strain elements are used in 2-D analysis. The second set of elements are used to model the embedded portion of the superstructure such as the basement or side walls of the structural foundation below the grade. Similarly, brick and plane strain elements and/or plate elements are used for this purpose.

In the finite element discretization of the basement volume, the element side dimensions are selected to be smaller than or equal to 0.2 λ where λ is the shortest shear wave length of interest in the soil layer. Thus the maximum side dimension of the elements in the foundation model are governed by the shear wave velocity of the soil layer and highest frequency of interest in the analysis.

In selecting the highest frequency of analysis, the frequency content of input motion and fixed-base modal frequencies and modal mass participation factor of the superstructure are considered. Generally, it is adequate to solve the SSI problem for

frequencies up to the fixed-base modal frequency whose fixed-base cumulative modal mass amounts to 90% of the total mass.

Furthermore, if the nodal points for which responses are to be computed are located on the subcomponents of the superstructure model, then the local modal frequencies corresponding to these subcomponents should be considered in selecting the highest frequency of analysis.

(5) Solve the structural problem. This step involves solving the linear equation of Equation 3A-20 for each frequency.

For seismic excitation, the above steps are performed at several selected frequencies. These frequencies are usually selected to be close to major fixed-base modal frequencies of the structure and those of its subcomponents that are of interest. An effective interpolation scheme is used to compute the response at all frequencies required by the Fourier Transform Techniques to compute the response in time domain.

3A.6 Free-Field Site Responses Analysis

The behavior of soil is nonlinear under seismic excitation. The soil nonlinearity is caused by primary and secondary nonlinear effects. The primary nonlinearity is associated with the state of deformations induced by the free-field ground motion. The secondary nonlinearity is attributed to the SSI effects. This secondary effect on structural response is usually not significant and is neglected in the appendix.

The soil nonlinearity is approximately accounted for by an iterative process to obtain equivalent linear soil properties of shear modulus and material damping corresponding to effective strains developed in the free-field. The strain-compatible properties are then assigned to be the linear soil properties in the SSI analysis. These properties also determine the maximum element size of the foundation model using the finite-element approach.

The free-field site response analysis is performed using computer program SHAKE (Reference 3A-5) which employs the principle of one-dimensional propagation of waves in the vertical direction for a system of homogeneous, visco-elastic soil layers. An equivalent linear method is used to compute strain-compatible shear modulus and material damping for each soil layer. All sites except for the upper bound R profile defined in Table 3A-5 are analyzed using the H_1 and H_2 horizontal components of input motion at the ground surface. The free-field site response analysis is not performed for the R profile, since the next hardest profile VP7 already shows that the shear modulus and material damping corresponding to the induced strain level are essentially the same as their initial values at low strains. Therefore, the SSI analysis for the R profile is performed using the initial modulus and a conservative material damping of 1%.

In all analysis cases, the input motion was prescribed at the grade level.

Table 3A-6 summarizes the results of SSE free-field response analyses in terms of the strain-compatible shear wave velocity, averaged for all soil layers of the soil deposit, and the natural frequency of the soil column. These frequencies vary from 1.18 CPS to >33 CPS reflecting the wide range of dynamic soil properties and soil deposit configurations considered in this appendix.

For the vertical earthquake component, the P-wave velocity corresponding to the calculated strain-compatible shear modulus (or shear wave velocity) for each layer is determined following the steps described in Subsection 3A.3.3. The soil damping associated with the P-wave is considered to be the same as the final iterated damping associated with the shear wave.

3A.7 Soil-Structure Interaction Analysis Cases

To establish design envelopes of seismic responses of the R/B and C/B, SSI analyses of these buildings are performed for a total of 22 cases using the properties of the 14 generic sites defined in Subsection 3A.6. SSI cases are summarized in Table 3A-7. The analyses cases can be categorized into two groups. In group 1, 3-D SSI analysis of the R/B and C/B are performed individually without consideration to structure-to-structure interaction effects (cases 1 through 16 in Table 3A-7). In group 2, 2-D SSI analysis of the R/B and C/B are performed considering individual building as well as multiple buildings including the turbine building to evaluate the structure-to-structure interaction effects (cases 17 through 22 in Table 3A-7).

Group 1 includes cases which consider variation of shear wave velocity, depth to base rock, depth to water table, separation of the basement walls from side soil medium as well as concrete cracked condition. Variation of shear wave velocity includes cases from the upper bound R cases to softest UB profiles in the 0°–180° (X) and vertical (Z) direction. Only selected profiles to cover the range of shear wave velocities are used in the 90°–270° (Y) direction. Separation of side wall is allowed for one story for both the R/B and C/B. For R/B the separation considered is 7.5m and for C/B is 4.4m. For cracked condition, properties of the building walls are reduced by 50% and the RCCV by 30%. Variation of depth to base rock is considered for two soil profiles UB and VP3 where the effect is expected to be more significant due to contrast of velocity between the rock and the respective soil velocity. Variation of depth to water table was considered for the UB profile only where larger variation in P-wave velocity is expected due to submerged conditions.

In group 2 of SSI analysis cases, the effect of structure-to-structure interaction is evaluated. These cases are analyzed using 2-D option of SASSI in the 0°–180° (X) direction. In order to provide a one to one comparison, both the R/B and C/B are analyzed individually and together with T/B(R/B + C/B + T/B cases in Table 3A-7) using UB, VP3, and VP5 velocity profiles. The effects of structure-to-structure interaction are evaluated using the 2-D results. These results are compared with the respective 3-D results of each building.

The enveloping results are based on enveloping the responses of the governing SSI cases to cover a wide range of site conditions and variation in ground motion, soil foundation separation and change of structural properties due to concrete cracked condition.

3A.8 Analysis Models

3A.8.1 Reactor Building Structural Models

The structural model of the R/B complex including the reactor pressure vessel and internal components as described in Subsection 3.7.2.1.5.1.1 is used in SSI analysis. The model figures are shown as Figures 3A-8 and 3A-9.

In the SASSI analyses of the R/B, the properties of the outer walls represented by the outer stick below the grade in Figure 3A-8 are adjusted to subtract the properties of the four embedded outer walls. These walls, as described in the following subsection, are modeled as part of the finite element foundation model.

The SSI model of the R/B is a quarter model taking advantage of the two planes of symmetry. The model properties and boundary conditions are adjusted to correspond to the quarter model. In order to include the coupling effects, rigid arms are added to the stick models at each floor elevation to obtain the response of extreme floor locations. The rigid arms are shown in Figures 3A-10 and 3A-11 in the XZ and YZ planes, respectively.

In the 2-D SSI analyses the structural model properties (stiffness and mass) are converted into values corresponding to per unit foundation depth (dimension in the third direction) to maintain compatibility with the 2-D foundation model.

3A.8.2 Reactor Building Foundation Models

3A.8.2.1 2-D Foundation Model

The 2-D model consists of the R/B foundation model for X–direction of analysis. The model developed for X-direction is also applicable for the vertical analysis. The same R/B model in conjunction with the 2-D control and turbine buildings models is used for structure-to-structure interaction cases.

The foundation model of the R/B below grade is shown in Figure 3A-12. This model consists of 60 four-node plane strain elements with the properties of concrete to represent the base slab. The side walls are modeled by beam elements. The base slab and side wall elements are massless since the mass of all structural components is already included in the structural model. The stick models are connected to the base slab by rigid beams at their respective footprints (see Figure 3A-12)

The finite element mesh in the XZ plane representing the excavated soil elements for the R/B foundation is shown in Figure 3A-13. This model consists of 384 four-node plane strain

elements. The strain-compatible equivalent linear soil properties obtained from the free-field analysis are used for the soil finite elements.

To properly transfer the rotation of the stick model to the base slab (and vice versa), a set of rigid beams are placed at the top of the slab connecting each stick to its respective footprint (see Figure 3A-12). The stick representing the outer walls of the R/B is connected to the side walls by a set of rigid beams in horizontal directions to reflect the direct contact condition of the outside wall with the soil.

3A.8.2.2 3-D Foundation Model

By taking advantage of two planes of symmetry, the quarter model of R/B foundation is constructed as shown in Figure 3A-14. The excavated soil volume is shown in Figure 3A-15. The nodal points of the finite element mesh at different elevations are shown in Figures 3A-16 through 3A-24. A total of 504 brick elements are used for modeling the excavated soil in the embedded foundation volume. The base slab is modeled with 81 plate elements with rigid properties due to large thickness of the slab (see Figure 3A-16). The exterior walls of the building are also modeled with plate elements with concrete properties as shown in Figures 3A-25 and 3A-26.

The outer stick of the R/B model (Figure 3A-8) is connected to the base slab and the side walls with rigid beams as shown in Figure 3A-14. Since the sectional properties of the R/B stick model below grade are mainly due to the properties of the four side walls modeled explicitly by the plate elements, the stick model below grade, with adjusted properties, is connected to the side walls in both directions with rigid beams at each respective floor elevation (see Figure 3A-14). The foundation model shown is used in conjunction with the UB profile. For stiffer sites (VP and HR) foundation models with coarser element size is used to reduce the computer cost.

3A.8.3 Control Building Structural Model

The C/B model as described in Subsection 3.7.2.1.5.1.2 is used in SSI analysis. The model is shown in Figure 3A-27. The model has 8 lumped masses connected by massless beam elements. The shear rigidity in the direction of excitation is provided by the parallel walls. The bending rigidity includes the cross wall contribution. In the vertical direction a single mass point is used for each slab to represent the vertical slab frequency. The stick model with rigid arms is shown in Figure 3A-28. The rigid arms located at each floor elevation are used to obtain the response of extreme floor locations to include the coupling effect. Similarly, in the SASSI model of the C/B, the properties of the outer walls below the grade are subtracted from the stick model properties at respective locations. The walls are modeled as part of the finite element foundation model. The SSI model is also a quarter of model, taking advantage of two planes of symmetry in the building.

For the 2-D SSI model, the structural model properties are divided by the depth of the model to maintain compatibility with the 2-D foundation model.

3A.8.4 Control Building Foundation Models

3A.8.4.1 2-D Foundation Model

A 2-D model of the C/B foundation for X-direction of analysis was developed. The model for the X direction is also applicable for the vertical analysis.

The foundation model of the C/B in the XZ plane below grade is shown in Figure 3A-29. This model consists of 14 four-node plane strain elements with the properties of concrete to represent the base slab. The cross walls of the C/B are modeled by beam elements. The base slab and side wall elements are massless since the mass of all structural components is already included in the structural model. The structural model is connected to the base slab by a rigid beam connecting Node 2126 through Node 2130 at the top of the slab and another rigid beam connecting node 2106 through 2110 at the bottom of the slab (see Figure 3A-29). The rigid beams are not extended to the edge of the basemat in order to include the effect of basemat flexibility in the analysis.

The finite element mesh in the XZ plane representing the excavated soil elements for the C/B foundation is shown in Figure 3A-30. This model consists of 154 four-node plane strain elements. The strain-compatible equivalent linear properties obtained from the free-field analysis are used for the soil finite elements (see Appendix 3A.6 for additional information on free field analyses).

To properly transfer the rotation of the stick model to the base slab (and vice versa), a set of rigid beams are placed at the bottom of the slab connecting Nodes 2106 through Nodes 2110. The stick representing the walls of the C/B are connected to the cross walls by a set of rigid beams in the horizontal directions to reflect the direct contact condition of the outside wall with the soil.

3A.8.4.2 3-D Foundation Model

By taking advantage of two planes of symmetry, the quarter model of the C/B foundation is constructed as shown in Figure 3A-31. The excavated soil model is shown in Figure 3A-32. A total of 120 brick elements are used for modeling the excavated soil in the embedded foundation volume. The nodal points of the foundation model are shown in Figures 3A-33 through 3A-43. The base slab is modeled with 60 plate elements (see Figure 3A-33). The exterior walls of the building below grade are modeled with plate elements as shown in Figures 3A-44 and 3A-45.

The foundation model and the connection of the building stick model to the foundation are shown in Figure 3A-31. As shown in the figure, the base of the stick model is connected to the base slab by a set of rigid beams to maintain rotation compatibility. Rigid beams are placed in the walls at respective floor elevations (see Figure 3A-31) but the stick model is connected to the wall parallel to the direction of shaking. For this reason the rigid beams on the other side wall are not fully extended in the full depth of the wall so that mainly the stiffness of the wall parallel to the shaking direction is considered compatible with the assumption used in

development of stick model. For shaking in the other direction, stick model is similarly connected to the side wall which is parallel to the direction of shaking. The model shown is used in conjunction with the UB soil velocity profile. For stiffer profiles coarser models are used to reduce computer cost.

3A.8.5 Turbine Building Structural and Foundation Models

The turbine building model considered is shown in Figure 3A-46. It consists of two concentric lumped-mass beam sticks representing the building structures and the turbine generator pedestal. This simple representation is sufficient since the turbine building response is of no concern in this appendix and it is only used to evaluate its effect on the R/B and C/B. This effect can be adequately accounted for by maintaining the turbine building foundation configuration and the building total mass as well as the building fundamental frequency in the simplified model representation. Turbine building model is used in the 2-D SSI analysis in conjunction with the 2-D R/B and C/B models.

The foundation is assumed to be rigid for the purpose of evaluating the structure-to-structure interaction effect on the R/B and C/B. Figure 3A-46 also shows the 2-D foundation model.

3A.9 Analysis Results

In this section, typical SSI results are presented to show the effect of different parameters in terms of soil and structural properties on seismic responses of the plant structures and components. These results are grouped selectively in order to provide a reasonable basis for comparison of the results. In this section, only limited SSI responses in terms of acceleration response spectra and seismic forces at the key locations in the plant are presented. The complete seismic responses for all cases are presented in Section 3A.10.

For comparison study, the acceleration response spectra at 2% damping are shown for the following locations.

(1) Reactor Building

Location	Node No.	Respective Figure
RPV/MS Nozzle	33	3A-9
RCCV Top	89	3A-8
R/B Top	95	3A-8
Basemat	210 (UB model) 208 (all other models)	3A-14

(2) Control Building

C/B Top	108/181/183	3A-28
Basemat	102	3A-31

The seismic forces are presented at the following locations.

(1) Reactor Building

Location	Element No.	Respective Figure
Shroud Support	28	3A-9
RPV Skirt	69	3A-9
RSW Base	78	3A-8
Pedestal Base	86	3A-8
RCCV–Grade Level	89	3A-8
R/B–Grade Level	99	3A-8

(2) Control Building

C/B Grade Level	6	3A-27

For comparison study, the responses in each direction (X or Y or Z) due to shaking in the respective direction are presented. In Section 3A.10, however, the coupling effect due to shaking in all 3 directions are considered. In addition the results of the upper bound soil cases (rigid soil) are shown as a reference solution with the results of all selected groups.

3A.9.1 Effect of Soil Stiffness

In order to study the effect of soil stiffness on the SSI responses, both the R/B and C/B were analyzed in the horizontal X- and vertical Z-directions for the upper bound (R2) case, and soil with velocity profiles VP7, VP5, VP4, VP3, and UB1. The results due to horizontal X- shaking are shown in Figures 3A-47 through 3A-51 for the R/B. Figure 3A-47 shows the vertical response at the edge of the basemat due to horizontal shaking. The rocking frequency of the basemat increases as the soil stiffness increases. The results at other locations in the R/B show the successive shift in the peak frequency of the response due to the change in soil stiffness.

The results due to X-shaking for the C/B are shown in Figures 3A-52 through 3A-54. Similarly, a successive shift in the peak frequency of the response is observed.

The results in the vertical direction due to Z-shaking are shown in Figures 3A-55 through 3A-58 for the R/B and in Figures 3A-59 through 3A-60 for the C/B. As shown in these figures, the results are generally governed by the upper bound (R2) case results.

The results in terms of seismic forces are compared in Table 3A-8. As shown in this table, the results of the upper bound case generally governs the seismic responses. The results of all soil cases shown are used to obtain the enveloping results (Subsection 3A.10).

3A.9.2 Effect of Depth to Base Rock

In order to evaluate the effect of depth to base rock, both the R/B and C/B were analyzed in the X-direction using soil shear wave velocity profiles UB1 and VP3 for soil column depths of 25.7m, 45.7m, 61.0m, and 91.5m. The results for the R/B are compared with the upper bound case results in Figures 3A-61 through 3A-64 for the UB1 profile and in Figures 3A-65 through 3A-68 for the VP3 profile. As shown in these figures, the effect of the depth to base rock on the floor acceleration responses is insignificant except for the shallow soil site with 25.7m depth. In this case, the bottom of the basemat is resting on the base rock. Consequently, the responses for this case are larger than other soil cases considered. The results for the C/B are compared with the upper depth bound results in Figures 3A-69 through 3A-72. Similarly, except for the shallow soil case of 25.7m, the results of all other cases are relatively close. The results in terms of seismic forces are compared in Tables 3A-9 and 3A-10 for the UB and VP3 profiles, respectively. As shown in this table, except for the shallow soil case of 25.7m, the results are relatively close for other depth to base rock cases.

The results of all cases for depth to base rock study are used to obtain the enveloping responses (Subsection 3A.10)

3A.9.3 Effect of Depth to Ground Water Table

In order to evaluate the effect of depth to water table on the seismic responses, both the R/B and C/B were analyzed using the soil profile UB1D150 in the X- and Z-directions. The depth to water tables of 0.61m, 12.2m, and 25.7m were considered. The results in terms of acceleration response spectra due to horizontal X-shaking are shown in Figures 3A-73 through 3A-76 for the R/B and in Figures 3A-77 through 3A-78 for the C/B. As shown in these figures, the effect of depth to water table on horizontal responses is relatively small. The results due to vertical Z-shaking are shown in Figures 3A-80 through 3A-82 for the R/B and in Figures 3A-83 through 3A-84 for the C/B. As shown in these figures the effect of depth to water table is relatively more significant on the vertical responses. The results in terms of seismic forces are shown in Table 3A-11. The results in terms of axial loads for the shallow water table case are larger than other depths to water table cases considered. Seismic forces due to horizontal shaking are not affected significantly.

The results of all cases considered for the depth to water table are used to obtain the enveloping results (Subsection 3A.10)

3A.9.4 Effect of Concrete Cracking

In order to evaluate the effect of concrete cracking on the SSI responses, the upper bound case (R1) was analyzed using concrete cracked properties. These properties were obtained by reducing the stiffness of the R/B and C/B walls by 50%. Properties of the RCCV were reduced by 30%. The results of uncracked case due to horizontal X-shaking (R1UX) are compared with the results of the cracked case (R1CX) in Figures 3A-85 through 3A-88 for the R/B and in Figures 3A-89 and 3A-90 for the C/B. As expected, concrete cracking reduces the peak frequency of the response and amplifies the response at most locations. The effect on the basemat response is insignificant. The effect on the seismic forces is shown in Table 3A-12. Similarly, concrete cracking also affects the seismic forces in the plant structure.

Due to significance of concrete cracking on the seismic responses, the result of both cracked and uncracked cases are used with the results of other cases to obtain the enveloping results (Subsection 3A.10).

3A.9.5 Effects of Change in Soil Degradation Curve

For all SSI soil cases, strain-compatible soil properties were obtained using free-field SHAKE analysis results as discussed in Subsection 3A.6. For the free-field analysis, the strain-dependent soil properties were obtained from the generic Seed and Idriss soil curves (Reference 3A-6) using the mean curves. Recent data indicate that the amount of soil degradation due to shaking can be less than the mean values of the generic curves and is closer to the upper bound of the 1970 soil curves (Reference 3A-6). The soil shear modulus degradation curves (mean and upper bound) are shown in Figure 3A-91 The upper bound of the 1970 soil shear modulus curve is the same as the curve reported for sand in Reference 3A-7.

In order to evaluate the effect of change in soil degradation curves on SSI responses, the soil case with velocity profile VP3 and soil column depth of 45.7m was re-analyzed using the upper bound soil degradation curve. The results of the analysis in the horizontal X-direction for this case (SSI case VP3D1AX) are compared with the respective SSI case results using the mean curve (SSI case VP3D1X) and the very rigid soil case results (R1UX) for both the R/B and C/B in Figures 3A-92 through 3A-97. As shown in these results, the effect of change in soil degradation curve on the spectral values is insignificant. The effect on the seismic forces is shown in Table 3A-13. The effect on seismic forces is also insignificant.

Based on these results, variation of soil degradation for other soil cases was not considered warranted. The results based on mean soil degradation curve were used to obtain the enveloping responses.

3A.9.6 Effect of Side Soil-Wall Separation

In order to evaluate the effect of separation between the side walls and the side soil, the upper bound case was re-analyzed considering one story height separation for each building. For the R/B, R1 cases (R1UX and R1UZ) consider separation up to Elevation 4.8m (Figure 3A-8). For the C/B, R1 cases (R1UX and R1UZ) consider separation up to Elevation 3.5m (Figure 3A-27).

The spectral results for the R/B due to horizontal X-shaking are compared with the results of R2 cases (no separation) in Figures 3A-98 through 3A-101. The results due to vertical Z-shaking are shown in Figures 3A-102 through 3A-105. As expected, separation of side walls reduces the peak frequency of the response. The reduction is less significant for vertical responses. The effect on the basement response is insignificant.

The effect on the C/B responses are shown in Figures 3A-106 through 3A-109. Similarly, the separation effect is more pronounced in the horizontal responses.

The results in terms of seismic forces are shown in Table 3A-14. As shown in the table, the effect on the axial forces is relatively insignificant. However, seismic forces due to horizontal shaking are generally larger for the case with no separation. Due to considerable effect of side soil separation on the seismic responses, the results of both cases (R1 and R2) are used with the results of other SSI cases to obtain the enveloping results (Subsection 3A.10).

3A.9.7 Effect of Adjacent Buildings

In order to evaluate the effect of structure-to-structure interaction on the seismic responses, both the R/B and C/B were analyzed in the horizontal X-direction for soil profiles UB1D150, VP3D150, and VP5D150. Each building was analyzed individually using both the 2-D and 3-D models. The analysis was repeated using the multiple 2-D models of the reactor, control, and turbine buildings in one SSI model to consider structure-to-structure interaction effects. The results for the R/B are compared with the upper bound case results in Figures 3A-110 through 3A-121 for the soil profiles UB1D150, VP3D150, and VP5D150, respectively. As shown in these figures, the effect of structure-to-structure interaction on the R/B response is relatively insignificant and in general, tends to reduce the overall response of the building. The result of structure-to-structure interaction cases are either enveloped by the respective 3-D case results or the results of the upper bound case.

The results for the C/B are compared in Figures 3A-122 through 3A-127 for soil profiles UB1D150, VP3D150, and VP5D150, respectively. As shown in these results, the effect of structure-to-structure interaction is more pronounced in the response of the C/B. The SSI frequency of the R/B is present in the C/B response through a dip in the response spectrum. Similarly, the results of structure-to-structure cases generally are either enveloped by the respective 3-D case results or the results of the upper bound case. The results in terms of seismic forces are compared in Tables 3A-15 through 3A-17 for UB1, VP3, and VP5 soil velocity profiles. As shown in these tables, the results are generally governed by the upper bound cases.

The results in terms of seismic soil pressure were also computed. As expected, seismic soil pressure in between the R/B and C/B increased due to structure-to-structure interaction effect. The seismic soil pressure results obtained from analysis of individual buildings as well as multiple buildings were enveloped and used in the design of respective walls of each building. The enveloping seismic soil pressure results are shown in Table 3A-18.

Based on these results, except for seismic soil pressure, consideration to structure-to-structure interaction effect is not warranted for the purpose of obtaining enveloping seismic forces and floor acceleration response spectra. Consequently, the enveloping results presented in Section 3A.10 are based on the analysis of each individual building.

3A.9.8 Summary

On the basis of the analysis results for a wide range of site parameters and various analysis conditions presented in the preceding subsections, the following conclusions can be made.

(1) Stiffer sites result in higher structural responses, primarily due to less ground motion attenuation with depth in the free-field for stiffer sites. The R profile can be considered to be the upper bound profile.

(2) The effects of soil depth variation and ground water table variation on structural response for the same soil profile are relatively insignificant as compared to the effects of variation in shear wave velocities (i.e., soil stiffness) considered for a range of soil/rock profiles.

(3) The effect of structure-to-structure interaction on the R/B and C/B response is bounded by the response of the individual building considering all soil cases except for the seismic soil pressure between the R/B and C/B.

(4) The effects of concrete cracking and side soil separation on the floor acceleration response spectra are relatively significant.

3A.10 Site Enveloping Seismic Response

3A.10.1 Enveloping Maximum Structural Loads

The site-envelope seismic loads are established from the envelopes of all SASSI analysis results from 3-D SSI cases summarized in Table 3A-7 (Cases 1 through 16). The site-envelope seismic loads obtained are applicable for the design of the R/B and C/B structures and associated reactor and other equipment housed in the ABWR standard plant.

The enveloping maximum shear and moment distributions along the R/B walls, RCCV, RSW, pedestal and key RPV internal components are shown in Table 3A-19a through 3A-19d. The shear and moment are the envelope of all SSI cases additionally enveloped over the enveloped responses due to X-(0°–180°) and Y-(90°–270°) shaking. The torsional moments for building

structures are obtained using the enveloping shear force at each elevation multiplied by 5% eccentricity of the respective maximum floor dimension.

Similarly, the results for the C/B were obtained. These results are shown in Table 3A-20.

It should be noted that for design purposes, no credit has been taken for the reduction of horizontal forces at the R/B and C/B elements below the ground surface as predicted from analysis. The largest shear force above the ground surface is maintained as minimum for these elements.

The vertical loads are expressed in terms of enveloping absolute acceleration. The enveloping maximum acceleration values for the R/B and C/B are shown in Tables 3A-21a through 3A-21c and 3A-22. These acceleration values do not include the coupling effect and are only applicable for structural analysis in combination with the seismic loads due to horizontal shaking. For equipment design, however, SRSS was used to include the coupling vertical response due to horizontal shaking. These results are presented in Section 3A.10.3.

3A.10.2 Enveloping Floor Response Spectra

The site-envelope floor response spectra due to the 0.3g SSE are obtained according to the following steps.

(1) The calculated 2, 3, 5, and 10% damping response spectra of all SASSI 3-D cases are enveloped at all required locations in each of the three directions. In the vertical direction, where applicable, SRSS was used to include the coupling vertical response due to horizontal shaking.

(2) The envelope spectra in the two horizontal directions at each location obtained in step 1 are subsequently enveloped to form the bounding horizontal spectra.

(3) The envelope spectra were subsequently peak broadened by ±15%.

The site-envelope peak broadened SSE floor response spectra at critical damping ratios 2, 3, 5, and 10% for the R/B are shown in Figures 3A-128 through 3A-165 for the horizontal direction and in Figures 3A-166 through 3A-209 for the vertical direction including floor oscillator responses. The vertical responses for the reactor building walls also include the responses of the finite element model (Section 3H.1) for the upper bound R1 case. The results for the C/B are shown in Figures 3A-210 through 3A-228. For seismic design of equipment and piping, the alternative seismic input can be individual floor response spectra of each site condition considered in generating the site-envelope spectra.

Furthermore, vertical response spectra for floor oscillators should be used for the components supported by the floor slabs. However, for the components in the vicinity of the walls or on the walls, the building vertical response spectra at respective elevation can be used.

3A.10.3 Enveloping Maximum Absolute Accelerations

The site-envelope absolute acceleration responses (enveloping maximum zero period accelerations) are shown in Tables 3A-23a through 3A-23d and 3A-24 for the R/B and C/B. The vertical responses include the coupling vertical response due to horizontal shaking where applicable.

3A.10.4 Enveloping Maximum Relative Displacements

The site-envelope maximum relative displacements with respect to input motion at grade level in the free-field are shown in Tables 3A-25a through 3A-25d and 3A-26 for the R/B and C/B. These results may be used for design of components supported on the surrounding soil medium and connected to the respective building.

The site-envelope maximum relative displacements of the nodal points with respect to the base of each respective stick model are shown in Tables 3A-27a through 3A-27d and 3A-28. These results may be used for design of components located within the respective building.

3A.10.5 Summary

The site-envelope maximum seismic responses presented in Subsection 3A.10 envelop the maximum seismic SSE responses of the ABWR plant structures and components for a wide range of subsurface properties and conditions as well as the effect of concrete cracking and side soil-wall separation. These responses are used to design the ABWR plant structures and components.

3A.11 References

3A-1 7A25-3803-0006, Geotechnical Site Parameters for Advanced Boiling Water Reactor (ABWR) Standard Plant Design, Revision 0, April 2009.

3A-2 Not Used

3A-3 NUREG/CR-1161, Recommended Revisions to Nuclear Regulatory Commission Seismic Design Criteria, May 1980.

3A-4 Lysmer, J., Tabatabaie-Raissi, M., Tajirian, F., Vahdani, S., and Ostadan, F., SASSI--A System for Analysis of Soil-Structure Interaction, Report No. UC/B/GT/81-02, Geotechnical Engineering, University of California, Berkeley, CA, April, 1981; also Ostadan, F., Computer Program SASSI, CE (944), Theoretical, User's and Validation Manuals (1991), Bechtel Corporation, San Francisco, California

3A-5 Schnabel, P.B., Lysmer, J., and Seed, H.B., SHAKE--A Computer Program for Earthquake Response Analysis of Horizontally Layered Sites, Report No. RC 72-12, Earthquake Engineering Research Center, University of California, Berkeley, CA, 1972.

3A-6 Seed, H.B. and Idriss, I.M–Soil Moduli and Damping Factors for Dynamic Response Analysis, Report No. RC 70-10, Earthquake Engineering Research Center, University of California, Berkeley, CA, 1970.

3A-7 Idriss, I.M–Response of Soft Soil Sites During Earthquakes, H. Bolton Seed Memorial Symposium Proceedings, Volume 2, Bi Tech Publishers, May 1990.

Table 3A-1 Soil Properties for UB Profile

Layer Depth m (Nominal)	K_{2max}	Total Unit Weight t/m^3	Poisson's* ratio
0–9	140	1.92	0.38
9–15	140	2.00	0.35
15–22.5	140	2.00	0.35
22.5–30	140	2.00	0.35
30–45	160	2.09	0.32
45–60	160	2.09	0.32
60–90	240	2.17	0.30

* Total unit weight and Poisson's ratio for each layer are also used for other soil profiles. For rock profiles the total unit weight is 2.2 t/m^3 and Poisson's ratio is 0.3.

Table 3A-2 Average Shear Wave Velocities in Layers

Shear Wave Velocity Profiles						
Layer Depth (m) (nominal)	UB (m/s)	VP3 (m/s)	VP4 (m/s)	VP5 (m/s)	VP7 (m/s)	R (m/s)
0–9	303	549	732	887	1524	6096
9–15	374	576	738	893	1524	6096
15–22.5	418	585	756	912	1524	6096
22.5–30	455	610	762	915	1524	6096
30–45	524	622	768	918	1524	6096
45–60	573	643	793	930	1524	6096
60–90	758	674	817	945	1524	6096

Table 3A-3 Strain-Dependent Shear Modulus

Effective Shear Strain		Modulus Reduction Factor*	
γ_{eff}(%)	$LOG_{10}\gamma_{eff}$	UB, VP3 & VP4	VP5 & VP7
1.00E–4	–4.0	1.00	1.00
3.16E–4	–3.5	0.98	1.00
1.00E–3	–3.0	0.96	0.99
3.16E–3	–2.5	0.88	0.95
1.00E–2	–2.0	0.74	0.90
3.16E–2	–1.5	0.52	0.81
1.00E–1	–1.0	0.29	0.72
0.316	–0.5	0.15	0.40
1.00	0.0	0.06	0.40
10.00	1.0	0.06	0.40

* This is factor has to be applied to the shear modulus at low shear strain amplitudes defined here as 1E–4% to obtain the modulus at higher strain levels.

Table 3A-4 Strain-Dependent Soil Damping

Effective Shear Strain		% Of Critical Damping	
γ_{eff}(%)	$LOG_{10}\gamma_{eff}$	UB, VP3, VP4	VP5, VP7
1.00E–4	–4.0	0.60	0.60
3.16E–4	–3.5	0.8	0.70
1.00E–3	–3.0	1.7	0.8
3.16E–3	–2.5	3.1	1.1
1.00E–2	–2.0	5.6	1.5
3.16E–2	–1.5	9.6	2.1
1.00E–1	–1.0	15.00	3.0
0.316	–0.5	15.00	–
1.00	0.0	15.00	–
3.16	0.5	15.00	–
10.00	1.0	15.00	–

Table 3A-5 Case IDs for Site Conditions Considered

Soil Profile Depth m	Depth to Water Table m	Depth to Base Rock m	Shear Wave Velocity Profiles					
			UB	VP3	VP4	VP5	VP7*	R† Upper Bound
25.7	.61	25.7	UB1D85a	VP3D85a			–	–
45.7	.61	45.7	UB1D150	VP3D150	VP4D150	VP5D150		–
	12.2	45.7	UB2D150					
	25.7	45.7	UB3D150					
61	.61	61	UB1D200	VP3D200	–	–	–	–
91.5	.61	91.5	UB1D300	VP3D300	–	–	–	–

* These are uniform sites.

† These are uniform sites. One-story height separation (R1 Cases) and no separation of structures (R2 Cases) with side soil are considered for this site.

Table 3A-6 SSE Free-Field Site Response Results for all Soil Profiles (Average Properties)

Soil Profile ID	Average Shear Wave Velocity m/s	Soil Column Frequency (hertz)
UB1D85a	283	2.73
VP3D85a	499	4.82
UB1D150	320	1.75
UB2D150	320	1.75
UB3D150	320	1.75
VP3D150	487	2.67
VP4D150	659	3.60
VP5D150	877	4.80
UB1D200	345	1.41
VP3D200	483	1.98
UB1D300	431	1.18
VP3D300	486	1.33
VP7D300	1486	4.06
R Cases	6097	> 33

Table 3A-7 Summary of SSI Cases Considered (Reactor and Control Buildings)

Case No.	Soil Case ID	Soil Profile	Depth to Base Rock m	Depth to Water Table m	Uncracked/ Cracked	Input Motion	Dimension of Analysis	SSI Case ID (X)	(Y)	(Z)	Description
1	R1U	Upper Bound	NA	NA	UNCRKD	RG	3-D	R1UX	R1UY	R1UZ	Hard Rock, with separation
2	R2U	Upper Bound	NA	NA	UNCRKD	RG	3-D	R2UX	R2UY	R2UZ	Hard Rock, no separation
3	R1C	Upper Bound	NA	NA	CRKD	RG	3-D	R1CX	R1CY	NA	Cracked Case
4	VP7D150	VP7	45.7	NA	UNCRKD	RG	3-D	VP7D1X	VP7D1Y	VP7D1Z	SSI Cases
5	VP5D150	VP5	45.7	0.61	UNCRKD	RG	3-D	VP5DX	VP5DY	VP5DZ	SSI Cases
6	VP4D150	VP4	45.7	0.61	UNCRKD	RG	3-D	VP4D1X	—	—	SSI Cases
7	VP3D150	VP3	45.7	0.61	UNCRKD	RG	3-D	VP3D1X	VP3D1Y	VP3D1Z	SSI Cases
8	UB1D150	UB	45.7	0.61	UNCRKD	RG	3-D	UB1D1X	UB1D1Y	UB1D1Z	SSI Cases
9	VP3D85	VP3	25.7	0.61	UNCRKD	RG	3-D	VP3D3X	—	—	Depth to base rock study
10	VP3D200	VP3	61.0	0.61	UNCRKD	RG	3-D	VP3D4X	—	—	Depth to base rock study
11	VP3D300	VP3	91.5	0.61	UNCRKD	RG	3-D	VP3D5X	—	—	Depth to base rock study
12	UB1D85	UB	25.7	0.61	UNCRKD	RG	3-D	UB1D3X	—	—	Depth to base rock study
13	UB1D200	UB	61.0	0.61	UNCRKD	RG	3D	UB1D4X	—	—	Depth to base rock study
14	UB1D300	UB	91.5	0.61	UNCRKD	RG	3-D	UB1D5X	—	—	Depth to base rock study
15	UB2D150	UB	45.7	12.2	UNCRKD	RG	3-D	UB2D1X	—	UB2D1Z	Water table location study

Table 3A-7 Summary of SSI Cases Considered (Reactor and Control Buildings) (Continued)

Case No.	Soil Case ID	Soil Profile	Depth to Base Rock m	Depth to Water Table m	Uncracked/ Cracked	Input Motion	Dimension of Analysis	SSI Case ID (X)	(Y)	(Z)	Description
16	UB3D150	UB	45.7	25.7	UNCRKD	RG	3-D	UB3D1X	—	UB3D1Z	Water table location study
17	UB1D150	UB	45.7	0.61	UNCRKD	RG	2-D	UB1D1X2	—		One Building: R/B, C/B
18	VP3D150	VP3	45.7	0.61	UNCRKD	RG	2-D	VP3D1X2	—		One Building: R/B, C/B
19	VP5D150	VP5	45.7	0.61	UNCRKD	RG	2-D	VP5D1X2	—		One Building: R/B, C/B
20	UB1D150	UB	45.7	0.61	UNCRKD	RG	2-D	RCTUB1X	—		R/B + C/B + T/B
21	VP3D150	VP3	45.7	0.61	UNCRKD	RG	2-D	RCTVP3X	—		R/B + C/B + T/B
22	VP5D150	VP5	45.7	0.61	UNCRKD	RG	2-D	RCTVP5X	—		R/B + C/B + T/B

Table 3A-8 Effect Of Soil Stiffness on Maximum Forces

Beam Element	Location	Response Type	Soil Stiffness: Stiff R2UX/R2UZ	Stiff VP7D5X/VP7D5Z	Stiff VP5DX/VP5DZ	Soil Stiffness VP4D1X	Soft VP3D1X/VP3D1Z	Soft UB1D1X/UB1D1Z
a. Reactor Building								
28	Shroud Support	Shear	237	258	244	211	178	98
		Moment	14.14	15.49	15.03	12.82	10.66	6.35
		Axial	151	96	111		96	82
69	RPV Skirt	Shear	746	663	719	603	540	438
		Moment	38.36	42.11	40.32	34.94	32.11	20.92
		Axial	976	634	725		645	543
78	RSW Base	Shear	630	646	619	545	460	359
		Moment	32.10	32.94	31.27	28.01	23.37	17.63
		Axial	413	334	319		314	286
86	Pedestal Base	Shear	725	1,197	1,828	1,867	1,990	1,704
		Moment	60.20	198.40	319.22	333.73	347.27	319.12
		Axial	3,492	3,196	2,869		2,497	2,513
89	RCCV at Grade	Shear	14,620	14,330	13,120	12,120	10,130	7,269
		Moment	1,692.69	1,614.23	1,159.19	1,002.28	923.13	575.08
		Axial	22,490	20,000	15,140		12,090	12,100
99	R/B at Grade	Shear	27,630	26,650	27,730	24,760	20,790	11,430
		Moment	6,135.26	6,796.25	5,496.82	5,043.74	4,677.94	2,444.89
		Axial	17,050	20,070	15,040		12,610	12,310
b. Control Building								
6	C/B at Grade	Shear	4,353	4,957	4,716	4,462	3,497	2,564
		Moment	321.57	385.81	369.33	356.78	282.73	217.81
		Axial	3,360	3,616	3,429		3,180	2,998

Units: Shear & Axial Forces in Metric Ton (t); Moment in Meganewton-meters(MN-m)

Table 3A-9 Effect Of Depth to Base Rock, UB Case

Beam Element	Location	Response Type	R1UX	Depth to Base Rock (25.7m) UB1D3X	(45.7m) UB1D1X	(61.0m) UB1D4X	(91.5m) UB1D5X
a. Reactor Building							
28	Shroud Support	Shear	287	191	98	114	111
		Moment	18.83	11.07	6.35	7.09	7.06
69	RPV Skirt	Shear	798	647	438	449	427
		Moment	36.10	32.56	16.40	16.97	16.16
78	RSW Base	Shear	747	602	359	367	374
		Moment	38.88	30.24	17.63	17.78	17.84
86	Pedestal Base	Shear	2,218	2,481	1,704	1,830	1,668
		Moment	350.01	508.49	319.12	315.59	299.31
89	RCCV at Grade	Shear	17,010	10,070	7,269	10,940	8,104
		Moment	1,823.12	915.78	575.08	660.31	605.09
99	R/B at Grade	Shear	34,600	16,000	11,430	12,620	13,200
		Moment	8,073.12	4,055.19	2,444.89	2,719.48	2,535.10
b. Control Building							
6	C/B at Grade	Shear	5,624	2,425	2,564	2,320	2,294
		Moment	438.86	208.50	217.81	200.26	193.20

Units: Shear & Axial Forces in Metric Ton (t); Moment in Meganewton-meters (MN-m)

Table 3A-10 Effect Of Depth to Base Rock, VP3 Case

Beam Element	Location	Response Type	R1UX	Depth to Base Rock (25.7m) VP3D3X	(45.7m) VP3D1X	(61.0m) VP3D4X	(91.5m) VP3D5X
a. Reactor Building							
28	Shroud Support	Shear	287	178	178	166	164
		Moment	18.83	11.04	10.66	9.93	9.70
69	RPV Skirt	Shear	798	585	540	517	531
		Moment	43.85	35.68	32.11	28.55	29.01
78	RSW Base	Shear	747	515	460	442	427
		Moment	38.88	25.90	23.37	21.13	21.36
86	Pedestal Base	Shear	2,218	2,256	1,990	1,883	1,852
		Moment	350.01	425.04	347.27	326.77	236.57
89	RCCV at Grade	Shear	17,010	10,490	10,130	9,442	9,222
		Moment	1,823.12	887.63	923.13	759.65	727.48
99	R/B at Grade	Shear	34,600	20,270	20,790	17,720	18,020
		Moment	8,073.12	3,958.11	4,677.94	3,808.06	3,777.66
b. Control Building							
6	C/B at Grade	Shear	5,624	4,279	3,497	3,542	3,893
		Moment	438.86	310.39	282.73	287.35	31157

Units: Shear & Axial Forces in Metric Ton (t); Moment in Meganewton-Meters (MN-m)

Table 3A-11 Effect Of Depth to Water Table Location

Beam Element	Location	Response Type	R1UX/ R1UZ	GWT Below Grade (0.61m) UB1D1X/ UB1D1Z	(12.2m) UB2D1X/ UB2D1Z	(25.7m) UB3D1X/ UB3D1Z
a. Reactor Building						
28	Shroud Support	Shear	287	98	109	106
		Moment	18.83	6.35	6.31	7.35
		Axial	150	82	74	59
69	RPV Skirt	Shear	798	438	419	462
		Moment	43.85	20.92	20.30	21.78
		Axial	974	543	493	396
78	RSW Base	Shear	747	359	309	351
		Moment	38.88	17.63	14.84	16.87
		Axial	401	286	260	209
86	Pedestal Base	Shear	2,218	1,704	2,103	2,269
		Moment	350.01	319.12	392.28	414.15
		Axial	3,449	2,513	2,299	1,931
89	RCCV at Grade	Shear	17,010	7,269	7,973	7,326
		Moment	1823.12	575.08	402.80	604.31
		Axial	22,740	12,100	10,600	10,080
99	R/B at Grade	Shear	34,600	11,430	13,640	12,980
		Moment	8,073.12	2,444.89	3,136.28	3,034.29
		Axial	18,190	12,310	10,960	9,634
b. Control Building						
6	C/B at Grade	Shear	5,624	2,564	3,008	2,849
		Moment	430.86	217.81	253.12	240.66
		Axial	3,612	2,998	2,741	2,354

Units: Shear & Axial Forces in Metric Ton (t); Moment in Meganewton-meters (MN-m)

Table 3A-12 Effect of Concrete Cracking

Beam Element	Location	Response Type	Cracking Assumptions: Uncracked R1UX	Cracking Assumptions: Cracked R1CX
a. Reactor Building				
28	Shroud Support	Shear	287	414
		Moment	18.83	29.16
69	RPV Skirt	Shear	798	1,146
		Moment	43.85	69.16
78	RSW Base	Shear	747	1,043
		Moment	38.88	53.06
86	Pedestal Base	Shear	2,218	2,519
		Moment	350.01	483.19
89	RCCV at Grade	Shear	17,010	24,820
		Moment	1,823.12	1,504.39
99	R/B at Grade	Shear	34,600	36,790
		Moment	8,073.12	9,158.76
b. Control Building				
6	C/B at Grade	Shear	5,624	7,400
		Moment	438.86	593.52

Units: Shear & Axial Forces in Metric Ton (t); Moment in Meganewton-Meters (MN-m)

Table 3A-13 Effect of Change in Soil Degradation Curves

Beam Element	Location	Response Type	Soil Degradation Curves R1UX	Average VP3D1X	Upper Bound VP3D1AX
a. Reactor Building					
28	Shroud Support	Shear	287	178	252
		Moment	18.83	10.66	11.46
69	RPV Skirt	Shear	798	540	576
		Moment	43.85	32.11	34.74
78	RSW Base	Shear	747	460	508
		Moment	38.88	23.37	25.74
86	Pedestal Base	Shear	2,218	1,990	1,917
		Moment	350.01	347.27	350.89
89	RCCV at Grade	Shear	17,010	10,130	10,770
		Moment	1,823.12	923.13	951.48
99	R/B at Grade	Shear	34,600	20,790	22,090
		Moment	8,073.12	4,677.94	4,842.70
b. Control Building					
6	C/B at Grade	Shear	5,624	3,497	3,764
		Moment	438.86	282.74	308.14

Units: Shear & Axial Forces in Metric Ton (t); Moment in Metanewton-Meters (MN-m)

Table 3A-14 Effect Of Separation Between the Side Soil and Foundation Walls

Beam Element	Location	Response Type	Separating Assumptions: With Separation R1UX/R1UZ	Separating Assumptions: No Separation R2UX/R2UZ
a. Reactor Building				
28	Shroud Support	Shear	287	237
		Moment	18.83	14.14
		Axial	150	151
69	RPV Skirt	Shear	798	746
		Moment	43.85	38.36
		Axial	974	976
78	RSW Base	Shear	747	630
		Moment	38.88	32.10
		Axial	401	413
86	Pedestal Base	Shear	2,218	725
		Moment	350.01	60.20
		Axial	3,449	3,492
89	RCCV at Grade	Shear	17,010	14,620
		Moment	1,823.12	1,692.69
		Axial	22,740	22,490
99	R/B at Grade	Shear	34,600	27,630
		Moment	8,073.12	6,135.26
		Axial	18,190	17,050
b. Control Building				
6	C/B at Grade	Shear	5,624	4,353
		Moment	438.86	321.57
		Axial	3,612	3,360

Units: Shear & Axial Forces in Metric Ton (t); Moment in Meganewton-Meter (MN-m)

Table 3A-15 Effect Of Adjacent Buildings, UB Case

			Model in SASSI Analysis			
			3-D R/B	3-D R/B	2-D R/B	2-D R/B+C/B+T/B
Beam Element	Location	Response Type	ENV. of R1UX/R2UX	UB1D1X	UB1D1X2	RCTU1X
a. Reactor Building						
28	Shroud Support	Shear	287	98	115	106
		Moment	18.83	6.35	6.96	6.78
69	RPV Skirt	Shear	798	438	516	419
		Moment	43.85	20.92	25.98	21.52
78	RSW Base	Shear	747	359	377	325
		Moment	38.88	17.63	18.37	15.64
86	Pedestal Base	Shear	2,218	1,704	2,154	2,126
		Moment	350.01	319.12	395.93	394.83
89	RCCV at Grade	Shear	17,010	7,269	7,370	5,970
		Moment	1,823.12	575.08	626.28	594.40
99	R/B at Grade	Shear	34,600	11,430	15,380	13,700
		Moment	8,073.12	2,444.89	3,125.49	3,272.60
b. Control Building						
6	C/B at Grade	Shear	5,624	2,564	3,160	2,787
		Moment	438.86	217.81	264.69	266.69

Units: Shear & Axial Forces in Metric Ton (t); Moment in Meganewton-Meters (MN-m)

Table 3A-16 Effect Of Adjacent Buildings, VP3 Case

Beam Element	Location	Response Type	Model in SASSI Analysis: 3-D R/B ENV. of R1UX/R2UX	3-D R/B VP3D1X	2-D R/B VP3D1X2	2-D R/B+C/B+T/B RCTV3X
a. Reactor Building						
28	Shroud Support	Shear	287	178	181	153
		Moment	18.83	10.66	11.19	11.06
69	RPV Skirt	Shear	798	540	525	455
		Moment	43.85	32.11	27.84	24.77
78	RSW Base	Shear	747	460	420	382
		Moment	38.88	23.37	20.67	18.42
86	Pedestal Base	Shear	2,218	1,990	2,099	2,556
		Moment	350.01	347.27	352.66	326.87
89	RCCV at Grade	Shear	17,010	10,130	7,264	8,244
		Moment	1,823.12	923.13	662.46	688.26
99	R/B at Grade	Shear	34,600	20,790	14,680	18,690
		Moment	8,073.12	4,677.94	3,707.05	3,555.04
b. Control Building						
6	C/B at Grade	Shear	5,624	3,497	4,208	3,030
		Moment	438.86	282.74	363.25	257.40

Units: Shear & Axial Forces in MetricTon (t); Moment in Meganewton-Meters (MN-m)

Table 3A-17 Effect Of Adjacent Buildings, VP5 Case

Beam Element	Location	Response Type	Model in SASSI Analysis: 3-D R/B ENV. of R1UX/R2UX	3-D R/B VP5DX	2-D R/B VP5D1X2	2-D R/B+C/B+T/B RCTV5X
a. Reactor Building						
28	Shroud Support	Shear	287	244	330	335
		Moment	18.83	15.03	26.88	29.03
69	RPV Skirt	Shear	798	719	740	684
		Moment	43.8	40.32	39.41	36.12
78	RSW Base	Shear	747	619	579	567
		Moment	38.88	31.27	29.61	27.99
86	Pedestal Base	Shear	2,218	1,828	2,280	1,802
		Moment	350.01	319.22	383.06	343.54
89	RCCV at Grade	Shear	17,010	13,120	13,220	10,550
		Moment	1,823.12	1,159.19	1,014.04	1,001.29
99	R/B at Grade	Shear	34,600	27,730	28,690	22,070
		Moment	8,073.12	5,496.82	5,671.39	4,717.17
b. Control Building						
6	C/B at Grade	Shear	5,624	4,716	4,940	3,895
		Moment	438.86	369.33	393.75	289.53

Units: Shear & Axial Forces in MetricTon (t); Moment in Meganewton-meters (MN-m)

Table 3A-18 Effect of Adjacent Buildings Enveloping Seismic Soil Pressures

Elevation (m)	**R/B** (kPa)	**C/B** (kPa)
12.0 to 9.9	921.86	921.86
9.9 to 7.9	431.51	431.51
7.9 to 6.3	215.75	254.98
6.3 to 4.8	156.91	137.30
4.8 to 3.5	147.11	215.75
3.5 to 0.90	117.68	137.30
0.90 to –1.7	166.72	166.72
–1.7 to –3.8	235.37	235.37
–3.8 to –5.9	156.91	333.44
–5.9 to –8.2	392.28	392.28

Table 3A-19a ABWR Reactor Building Walls and Floors Summary of Enveloping Seismic Loads

Element No.	Node	Elev TMSL(m)	Max. Shear (t)	Max. Moment (MN-m)	Max. Torsion (MN-m)
93	95	49.70	8,700	519.77	254.98
	96	38.20	8,700	1,471.05	
94	96	38.20	19,000	2,059.47	539.39
	98	31.70	19,000	2,942.10	
96	98	31.70	25,000	3,628.59	715.91
	100	23.50	25,000	5,295.78	
98	100	23.50	35,000	5,688.06	1,078.77
	102	18.10	35,000	7,159.11	
99	102	18.10	40,000	7,257.18	1,176.84
	103	12.30	40,000	9316.65	
100	103	12.30	53,000	9,414.72	1,569.12
	104	4.80	53,000	13,729.80	1,569.12
101	104	4.80	53,000	13,729.80	1,569.12
	105	–1.70	53,000	16,671.90	
102	105	–1.70	53,000	16,671.90	1,569.12
	88	–8.20	53,000	20,594.70	

NOTE: (1) Seismic loads are the envelopes of horizontal X and Y direction responses

Table 3A-19b ABWR Reactor Building RCCV Summary of Enveloping Seismic Loads

Element No.	Node	Elev TMSL(m)	Max. Shear (t)	Max. Moment (Mn-m)	Max. Torsion (Mn-m)
87	89	31.70	9,500	951.28	74.53
	90	23.50	9,500	1,471.05	
88	90	23.50	23,000	1,765.26	362.86
	91	18.10	23,000	2,353.68	
89	91	18.10	25,000	3,138.24	402.09
	92	12.30	25,000	3,824.73	
90	92	12.30	25,000	4,609.29	402.09
	93	4.80	25,000	5,688.06	
91	93	4.80	25,000	5,982.27	402.09
	94	–1.70	25,000	7,257.18	
92	94	–1.70	26,000	7,257.18	421.70
	88	–8.20	26,000	8,826.30	

NOTE: (1) Seismic loads are the envelopes of horizontal X and Y direction responses

Table 3A-19c ABWR Reactor Building RSW/Pedestal Summary of Enveloping Seismic Loads

Element No.	Node	Elev TMSL(m)	Max. Shear (t)	Max. Moment (MN-m)	Max. Torsion (MN-m)
74	70	21.20	80	0	0.39
	78	18.44	80	2.06	
75	78	18.44	630	2.06	3.33
	79	17.02	630	10.79	
76	79	17.02	700	10.79	3.73
	80	15.60	700	20.59	
77	80	15.60	980	20.59	5.10
	81	13.95	980	36.29	
78	81	13.95	1,100	36.29	5.49
	82	12.30	1,100	53.94	
79	82	12.30	2,400	53,94	16.67
	71	8.20	2,400	107.88	
80	71	8.20	2,700	137.30	18.63
	83	7.00	2,700	156.91	
81	83	7.00	2,700	156.91	18.63
	72	4.50	2,700	215,75	
103	72	4.50	2,700	215.75	18.63
	84	3.50	2,700	245,18	
82	84	3.50	2,800	245.18	19.61
	73	1.70	2,800	294.21	

Table 3A-19c ABWR Reactor Building RSW/Pedestal Summary of Enveloping Seismic Loads (Continued)

Element No.	Node	Elev TMSL(m)	Max. Shear (t)	Max. Moment (MN-m)	Max. Torsion (MN-m)
83	73	1.70	29.42	294.21	20.59
	85	–0.18	29.42	343.25	
84	85	–0.18	29.42	343.25	20.59
	86	–2.10	29.42	402.09	
85	86	–2.10	30.40	402.09	21.58
	87	–4.70	30.40	470.74	
86	87	–4.70	31.38	470.74	21.58
	88	–8.20	31.38	588.42	

NOTE: (1) Seismic loads are the envelopes of horizontal X and Y direction responses

Table 3A-19d ABWR Reactor Building Key RPV/Internal Components Summary of Enveloping Seismic Loads

Element No.	Node	Elev TMSL(m)	Max. Shear (t)	Max. Moment (MN-m)	Max. Torsion (MN-m)
28	56	7.39	420	27.46	1.57
	27	6.75	420	29.42	1.57
69	46	9.29	1,200	58.842	9.61
	71	8.20	1,200	69.63	9.61

NOTE: (1) Seismic loads are the envelopes of horizontal X and Y direction responses

Table 3A-20 ABWR Control Building Summary of Enveloping Seismic Loads

Element No.	Node	Elev TMSL(m)	Max. Shear (t)	Max. Moment (MN-m)	Max. Torsion (MN-m)
7	108	22.2	4,000	50.01	117.68
	107	17.15	4,000	254.98	117.68
6	107	17.15	8,200	333.44	225.56
	106	12.3	8,200	686.49	225.56
5	106	12.3	11,000	735.53	294.21
	105	7.9	11,000	1,176.84	294.21
4	105	7.9	11,000	1,176.84	294.21
	104	3.5	11,000	1,667.19	294.21
3	104	3.5	11,000	1,667.19	294.21
	103	–2.15	11,000	2,255.61	294.21
2	103	–2.15	11,000	2,255.61	294.21
	102	–8.2	11,000	2,942.10	294.21

NOTE: (1) Seismic loads are the envelopes of horizontal x and y direction responses.

Table 3A-21a ABWR Reactor Building Walls and Floors Summary of Enveloping Maximum Vertical Accelerations

Node	Elev TMSL(m)	Location	Max. Vertical Acceleration (g)
95	49.70	R/B	0.62
96	38.20	R/B	0.51
98	31.70	R/B	0.47
100	23.50	R/B	0.43
102	18.10	R/B	0.38
103	12.30	R/B	0.34
104	4.80	R/B	0.31
105	–1.70	R/B	0.31
88	–8.20	R/B	0.30
107	31.70	R/B FLOOR	1.20
108	23.50	R/B FLOOR	1.55
109	18.10	R/B FLOOR	1.84
110	12.30	R/B FLOOR	1.02
111	4.80	R/B FLOOR	0.54
112	–1.70	R/B FLOOR	0.46

NOTE: Vertical values do not include the coupling effect due to horizontal shaking

Table 3A-21b ABWR Reactor Building RCCV Summary of Enveloping Maximum Vertical Accelerations

Node	Elev TMSL(m)	Location	Max. Vertical Acceleration (g)
89	31.70	RCCV	0.71
90	23.50	RCCV	0.67
91	18.10	RCCV	0.64
92	12.30	RCCV	0.57
93	4.80	RCCV	0.43
94	–1.70	RCCV	0.34
88	–8.20	RCCV	0.30

NOTE: Vertical values do not include the coupling effect due to horizontal shaking

Table 3A-21c ABWR Reactor Building RSW/PED Summary of Enveloping Maximum Vertical Accelerations

Node	Elev TMSL(m)	Location	Max. Vertical Acceleration (g)
70	21.20	RSW/PED	0.41
78	18.44	RSW/PED	0.41
79	17.02	RSW/PED	0.41
80	15.60	RSW/PED	0.40
81	13.95	RSW/PED	0.39
82	12.30	RSW/PED	0.38
71	8.20	RSW/PED	0.37
83	7.00	RSW/PED	0.36
72	4.50	RSW/PED	0.34
84	3.50	RSW/PED	0.34
73	1.70	RSW/PED	0.33
85	–0.18	RSW/PED	0.32
86	–2.10	RSW/PED	0.31
87	–4.70	RSW/PED	0.31
88	–8.20	RSW/PED	0.30

NOTE: Vertical values do not include the coupling effect due to horizontal shaking

Table 3A-22 ABWR Control Building
Summary of Enveloping Maximum Vertical Accelerations

Node	Elev TMSL(m)	Location	Max. Vertical Acceleration (g)
108	22.2	C/B STICK	0.37
107	17.15	C/B STICK	0.35
106	12.3	C/B STICK	0.32
105	7.9	C/B STICK	0.32
104	3.5	C/B STICK	0.31
103	–2.15	C/B STICK	0.31
102	–8.2	C/B STICK	0.30
113	17.15	C/B FLOOR	0.62
112	12.3	C/B FLOOR	0.58
111	7.9	C/B FLOOR	0.55
110	3.5	C/B FLOOR	0.51
109	–2.15	C/B FLOOR	0.49

NOTE: Vertical values do not include the coupling effect due to horizontal shaking.

Table 3A-23a ABWR Reactor Building Walls and Floors Summary of Enveloping Maximum Accelerations

Node No.	Elev TMSL(m)	Location	Max. Horizontal Acceleration (g)	Max. Vertical Acceleration (g)
95	49.70	R/B	1.44	1.03
96	38.20	R/B	1.10	0.83
98	31.70	R/B	0.93	0.80
100	23.50	R/B	0.75	0.63
102	18.10	R/B	0.59	0.50
103	12.30	R/B	0.47	0.39
104	4.80	R/B	0.32	0.33
105	–1.70	R/B	0.31	0.32
88	–8.20	R/B	0.31	0.33
107	31.70	R/B FLOOR	—	1.20
108	23.50	R/B FLOOR	—	1.55
109	18.10	R/B FLOOR	—	1.84
110	12.30	R/B FLOOR	—	1.02
111	4.80	R/B FLOOR	—	0.54
112	–1.70	R/B FLOOR	—	0.46

NOTE: (1) Horizontal accelerations are the envelopes of X and Y direction responses
(2) The results represent the maximum responses at the respective floor elevation

Table 3A-23b ABWR Reactor Building RCCV Summary of Enveloping Maximum Accelerations

Node No.	Elev TMSL(m)	Location	Max. Horizontal Acceleration (g)	Max. Vertical Acceleration (g)
89	31.70	RCCV	0.96	0.82
90	23.50	RCCV	0.82	0.95
91	18.10	RCCV	0.65	0.89
92	12.30	RCCV	0.55	0.77
93	4.80	RCCV	0.48	0.56
94	–1.70	RCCV	0.36	0.38
88	–8.20	RCCV	0.31	0.33

NOTE: (1) Horizontal accelerations are the envelopes of X and Y direction responses
(2) The results represent the maximum responses at the respective floor elevation

Table 3A-23c ABWR Reactor Building RSW/PED Summary of Enveloping Maximum Accelerations

Node No.	Elev TMSL(m)	Location	Max. Horizontal Acceleration (g)	Max. Vertical Acceleration (g)
70	21.20	RSW/PED	1.02	0.55
78	18.44	RSW/PED	0.92	0.55
79	17.02	RSW/PED	0.83	0.55
80	15.60	RSW/PED	0.73	0.52
81	13.95	RSW/PED	0.63	0.52
82	12.30	RSW/PED	0.58	0.51
71	8.20	RSW/PED	0.55	0.49
83	7.00	RSW/PED	0.53	0.49
72	4.50	RSW/PED	0.50	0.43
84	3.50	RSW/PED	0.50	0.41
73	1.70	RSW/PED	0.47	0.38
85	–0.18	RSW/PED	0.45	0.33
86	–2.10	RSW/PED	0.41	0.33
87	–4.70	RSW/PED	0.35	0.31
88	–8.20	RSW/PED	0.31	0.33

NOTE: (1) Horizontal accelerations are the envelopes of X and Y direction responses

(2) The results represent the maximum responses at the respective floor elevation

Table 3A-23d ABWR Reactor Building RPV/Internals Summary of Enveloping Maximum Accelerations

Node No.	Elev TMSL(m)	Location	Max. Horizontal Acceleration (g)	Max. Vertical Acceleration (g)
17	16.48	RPV	1.16	0.55
18	15.68	RPV	1.04	0.55
25	9.65	RPV	0.57	0.51
27	6.75	RPV	0.61	0.47
28	26.06	RPV	1.72	0.44
33	20.49	RPV	1.19	0.64
36	17.18	RPV	0.98	0.62
38	15.68	RPV	0.89	0.61
46	9.29	RPV	0.56	0.51
50	5.95	RPV	0.67	0.46
51	5.49	RPV	0.64	0.48
52	4.82	RPV	0.65	0.54
60	1.65	RPV	1.10	0.54
66	1.65	RPV	1.15	0.48

NOTE: (1) Horizontal accelerations are the envelopes of X and Y direction responses

Table 3A-24 ABWR Control Building Summary of Enveloping Maximum Accelerations

Node No.	Elev TMSL(m)	Location	Max. Acceleration (g) Horizontal	Vertical
108	22.2	C/B STICK	1.02	0.48
107	17.15	C/B STICK	0.72	0.44
106	12.3	C/B STICK	0.52	0.36
105	7.9	C/B STICK	0.34	0.33
104	3.5	C/B STICK	0.32	0.31
103	–2.15	C/B STICK	0.31	0.31
102	–8.2	C/B STICK	0.31	0.30
113	17.15	C/B FLOOR		0.62
112	12.3	C/B FLOOR		0.58
111	7.9	C/B FLOOR		0.55
110	3.5	C/B FLOOR		0.51
109	–2.15	C/B FLOOR		0.49

NOTE: (1) Horizontal accelerations are the envelopes of x and y direction responses.
(2) The results represent the maximum responses at the respective floor elevation.

Table 3A-25a ABWR Reactor Building Walls and Floors Summary of Enveloping Maximum Relative Displacements with Respect to Input Motion

Node No.	Elev TMSL(m)	Location	Max. Rel. Displacement (mm) Horizontal	Vertical
Reference Motion: Displacement at Free-Field Grade Level				
95	49.70	R/B	28.5	7.4
96	38.20	R/B	22.3	6.7
98	31.70	R/B	18.7	6.8
100	23.50	R/B	13.7	5.8
102	18.10	R/B	10.1	5.6
103	12.30	R/B	7.5	5.4
104	4.80	R/B	8.2	5.0
105	–1.70	R/B	8.8	4.7
88	–8.20	R/B	12.0	4.3

NOTE: (1) Horizontal displacements are the envelopes of X and Y direction responses
(2) The results represent the maximum responses at the respective floor elevation

Table 3A-25b ABWR Reactor Building RCCV Summary of Enveloping Maximum Relative Displacements with Respect to Input Motion

Node No.	Elev TMSL(m)	Location	Max. Rel. Displacement (mm) Horizontal	Vertical
Reference Motion: Displacement at Free-Field Grade Level				
89	31.70	RCCV	18.7	4.1
90	23.50	RCCV	13.7	6.6
91	18.10	RCCV	10.1	6.4
92	12.30	RCCV	7.5	5.6
93	4.80	RCCV	8.2	3.9
94	–1.70	RCCV	8.8	3.3
88	–8.20	RCCV	12.0	4.3

NOTE: (1) Horizontal displacements are the envelopes of X and Y direction responses
(2) The results represent the maximum responses at the respective floor elevation

Table 3A-25c ABWR Reactor Building RSW/PED Summary of Enveloping Maximum Relative Displacements with Respect to Input Motion

Node No.	Elev TMSL(m)	Location	Max. Rel. Displacement (mm) Horizontal	Vertical
Reference Motion: Displacement at Free-Field Grade Level				
70	21.20	RSW/PED	11.1	2.2
78	18.44	RSW/PED	9.5	2.2
79	17.02	RSW/PED	8.9	2.2
80	15.60	RSW/PED	8.1	2.2
81	13.95	RSW/PED	7.6	2.2
82	12.30	RSW/PED	7.6	2.7
71	8.20	RSW/PED	8.0	2.6
83	7.00	RSW/PED	8.1	2.6
72	4.50	RSW/PED	8.3	2.5
84	3.50	RSW/PED	8.4	2.4
73	1.70	RSW/PED	8.6	2.4
85	–0.18	RSW/PED	8.9	2.4
86	–2.10	RSW/PED	9.8	2.2
87	–4.70	RSW/PED	10.8	2.2
88	–8.20	RSW/PED	12.0	4.3

NOTE: (1) Horizontal displacements are the envelopes of X and Y direction responses
(2) The results represent the maximum responses at the respective floor elevation

Table 3A-25d ABWR Reactor Building RPV/Internals Summary of Enveloping Maximum Relative Displacements with Respect to Input Motion

Node No.	Elev TMSL(m)	Location	Max. Rel. Displacement (mm) Horizontal	Vertical
Reference Motion: Displacement at Free-Field Grade Level				
17	16.48	RPV	10.8	1.6
18	15.68	RPV	10.3	1.6
25	9.65	RPV	7.7	1.6
27	6.75	RPV	8.0	1.6
28	26.06	RPV	14.9	1.6
33	20.49	RPV	11.0	3.2
36	17.18	RPV	9.0	2.8
38	15.68	RPV	8.5	2.8
46	9.29	RPV	7.9	2.8
50	5.95	RPV	8.1	1.6
51	5.49	RPV	8.2	1.6
52	4.82	RPV	8.2	1.6
60	1.65	RPV	8.4	1.6
66	1.65	RPV	10.6	1.6

NOTE: (1) Horizontal accelerations are the envelopes of X and Y direction responses

Table 3A-26 ABWR Control Building Summary of Enveloping Maximum Relative Displacements with Respect to Input Motion

Node No.	Elev TMSL(m)	Location	Max. Rel. Displacement (mm) Horizontal	Vertical
Reference Motion: Displacement at Free-Field Grade Level				
108	22.2	C/B STICK	8.9	3.3
107	17.15	C/B STICK	9.0	3.3
106	12.3	C/B STICK	9.0	3.2
105	7.9	C/B STICK	9.7	3.1
104	3.5	C/B STICK	10.6	3.2
103	–2.15	C/B STICK	9.9	3.1
102	–8.2	C/B STICK	9.1	2.7
113	17.15	C/B FLOOR		1.5
112	12.3	C/B FLOOR		1.5
111	7.9	C/B FLOOR		1.5
110	3.5	C/B FLOOR		1.6
109	–2.15	C/B FLOOR		1.6

NOTE: (1) Horizontal accelerations are the envelopes of x and y direction responses.
(2) The results represent the maximum responses at the respective floor elevation.

Table 3A-27a ABWR Reactor Building Walls and Floors Summary of Enveloping Maximum Relative Displacements with Respect to Basemat

Node No.	Elev TMSL(m)	Location	Max. Rel. Displacement (mm) Horizontal	Vertical
Reference Motion: Displacement at Node 88				
95	49.70	R/B	24.1	7.4
96	38.20	R/B	19.0	6.7
98	31.70	R/B	15.6	6.8
100	23.50	R/B	11.4	5.8
102	18.10	R/B	8.2	5.6
103	12.30	R/B	5.7	5.3
104	4.80	R/B	3.8	4.9
105	–1.70	R/B	1.7	4.4
88	–8.20	R/B	0.0	4.0

NOTE: (1) Horizontal displacements are the envelopes of X and Y direction responses
(2) The results represent the maximum responses at the respective floor elevation

Table 3A-27b ABWR Reactor Building RCCV Summary of Enveloping Maximum Relative Displacements with Respect to Basemat

Node No.	Elev TMSL(m)	Location	Max. Rel. Displacement (mm) Horizontal	Vertical
Reference Motion: Displacement at Node 88				
89	31.70	RCCV	15.5	4.1
90	23.50	RCCV	11.9	6.6
91	18.10	RCCV	8.9	6.4
92	12.30	RCCV	5.8	5.6
93	4.80	RCCV	3.8	3.9
94	–1.70	RCCV	1.7	2.9
88	–8.20	RCCV	0.0	4.0

NOTE: (1) Horizontal displacements are the envelopes of X and Y direction responses
(2) The results represent the maximum responses at the respective floor elevation

Table 3A-27c ABWR Reactor Building RSW/PED Summary of Enveloping Maximum Relative Displacements with Respect to Basemat

Node No.	Elev TMSL(m)	Location	Max. Rel. Displacement (mm) Horizontal	Vertical
Reference Motion: Displacement at Node 88				
70	21.20	RSW/PED	8.8	2.2
78	18.44	RSW/PED	8.0	2.2
79	17.02	RSW/PED	7.4	2.2
80	15.60	RSW/PED	6.9	2.2
81	13.95	RSW/PED	6.3	2.7
82	12.30	RSW/PED	5.8	2.7
71	8.20	RSW/PED	4.6	2.6
83	7.00	RSW/PED	4.2	2.6
72	4.50	RSW/PED	3.4	2.4
84	3.50	RSW/PED	3.1	2.3
73	1.70	RSW/PED	2.5	2.0
85	–0.18	RSW/PED	2.7	2.0
86	–2.10	RSW/PED	1.6	1.4
87	–4.70	RSW/PED	1.3	1.4
88	–8.20	RSW/PED	0.0	4.0

NOTE: (1) Horizontal displacements are the envelopes of X and Y direction responses
(2) The results represent the maximum responses at the respective floor elevation

Table 3A-27d ABWR Reactor Building RPV/Internals Summary of Enveloping Maximum Relative Displacements with Respect to Basemat

Node No.	Elev TMSL(m)	Location	Max. Rel. Displacement (mm) Horizontal	Vertical
Reference Motion: Displacement at Node 88				
17	16.48	RPV	9.0	0.4
18	15.68	RPV	8.6	0.4
25	9.65	RPV	5.6	0.4
27	6.75	RPV	4.3	0.4
28	26.06	RPV	11.0	0.3
33	20.49	RPV	8.9	1.9
36	17.18	RPV	7.6	1.8
38	15.68	RPV	7.1	1.8
46	9.29	RPV	4.9	1.6
50	5.95	RPV	4.1	0.3
51	5.49	RPV	4.0	0.4
52	4.82	RPV	3.8	0.4
60	1.65	RPV	3.1	0.4
66	1.65	RPV	5.0	0.4

NOTE: (1) Horizontal displacements are the envelopes of X and Y direction responses

Table 3A-28 ABWR Control Building
Summary of Enveloping Maximum Relative Displacements with Respect to Basemat

Node No.	Elev TMSL(m)	Location	Max. Rel. Displacement (mm) Horizontal	Vertical
Reference Motion: Displacement at Node 102				
108	22.2	C/B STICK	6.6	3.0
107	17.15	C/B STICK	6.1	3.0
106	12.3	C/B STICK	6.4	2.9
105	7.9	C/B STICK	6.4	2.9
104	3.5	C/B STICK	7.6	2.8
103	-2.15	C/B STICK	2.6	2.6
102	-8.2	C/B STICK	0.0	0.0
113	17.15	C/B FLOOR		0.9
112	12.3	C/B FLOOR		0.9
111	7.9	C/B FLOOR		0.8
110	3.5	C/B FLOOR		0.7
109	-2.15	C/B FLOOR		0.5

NOTE: (1) Horizontal displacements are the envelopes of x and y direction responses.
(2) The results represent the maximum responses at the respective floor elevation.

Figure 3A-1 (Refer to Figure 1.2-1)

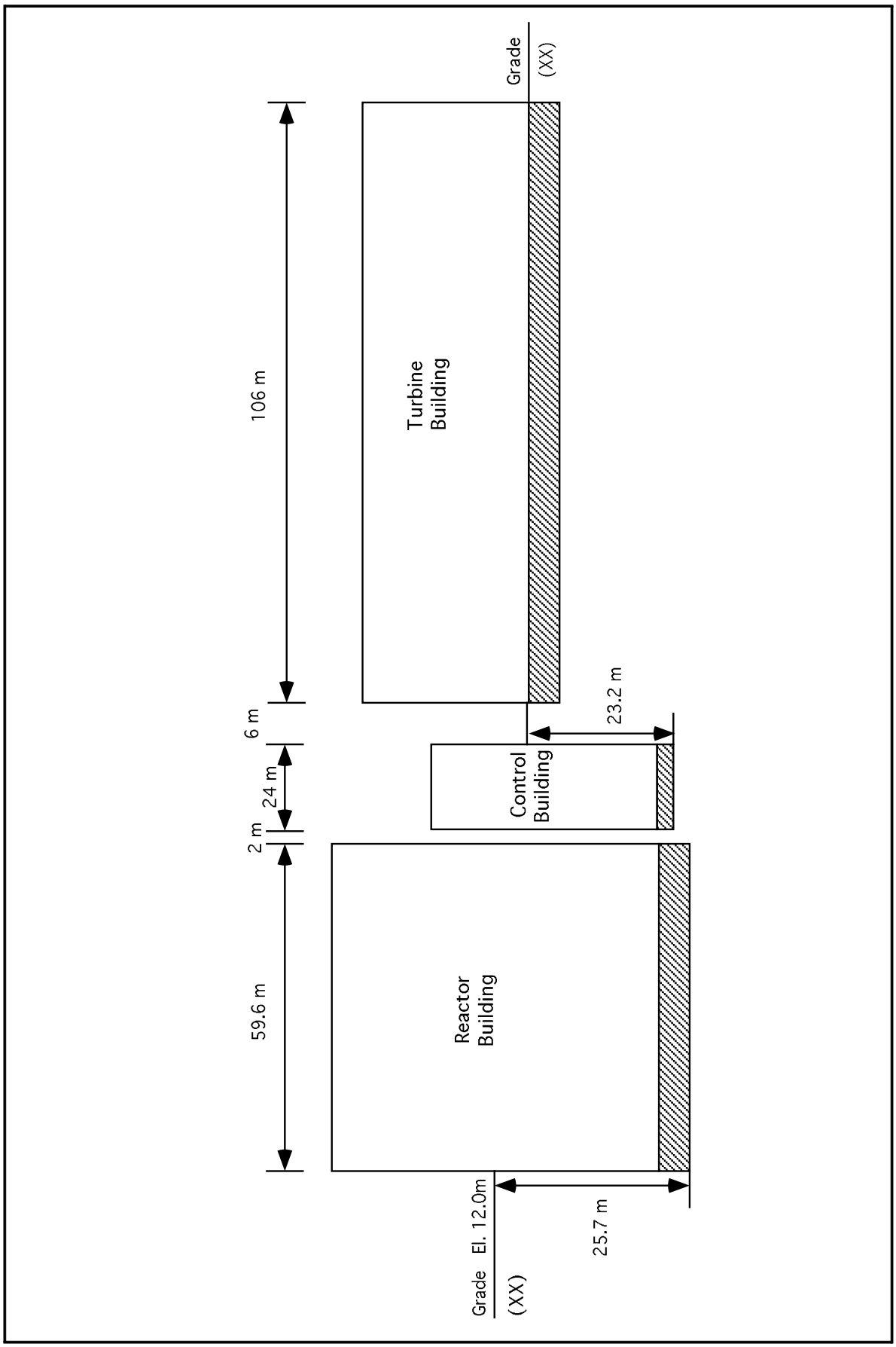

Figure 3A-2 0°–180° Section View

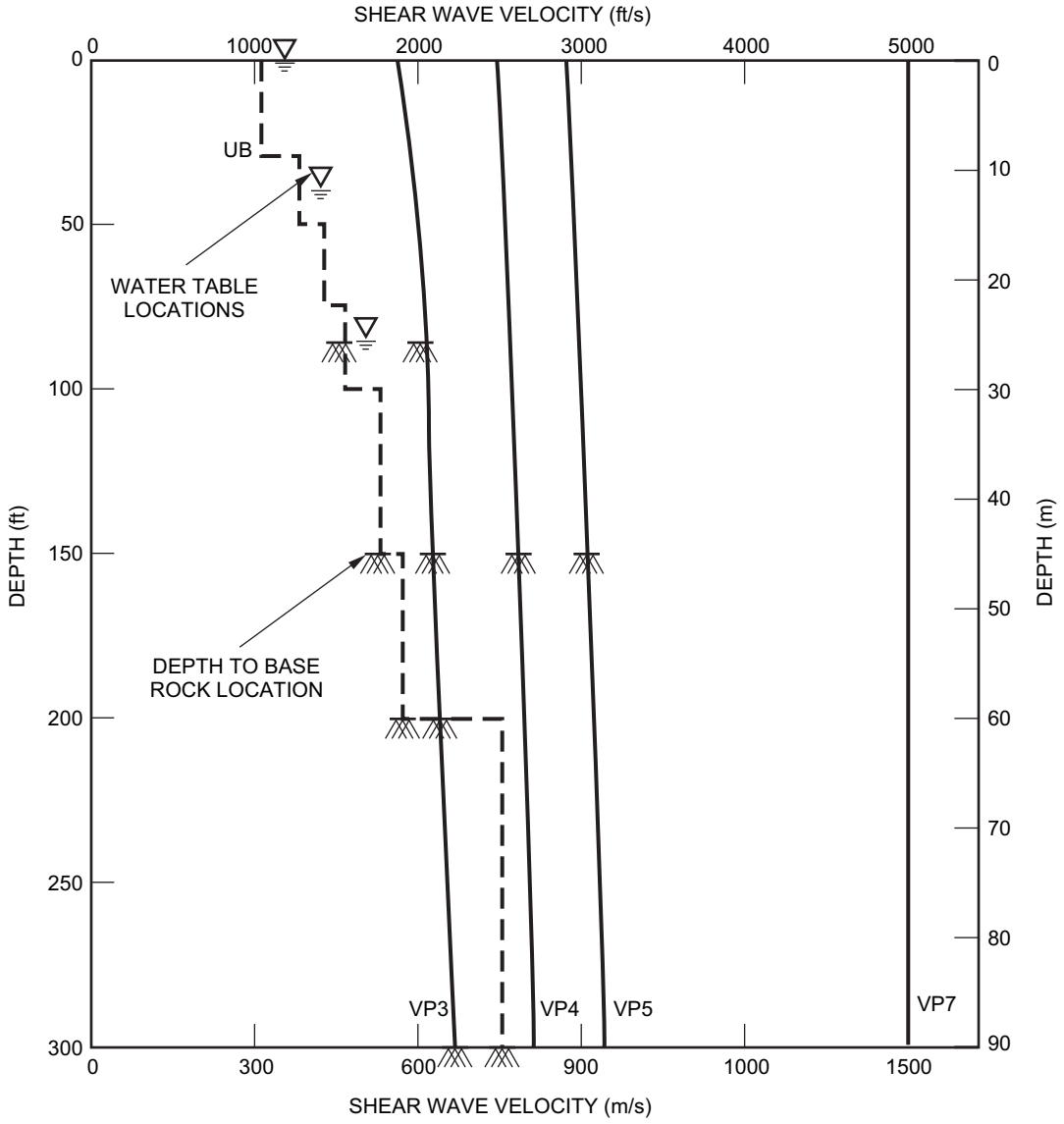

(1) FOR ALL VP CASES WATER TABLE IS AT .61 METERS.
(2) AN ADDITIONAL SITE WITH RIGID SOIL PROPERTIES (V_S = 6100 m/s) IS CONSIDERED

Figure 3A-3 Shear Wave Velocity Profiles Considered for SSI Analyses

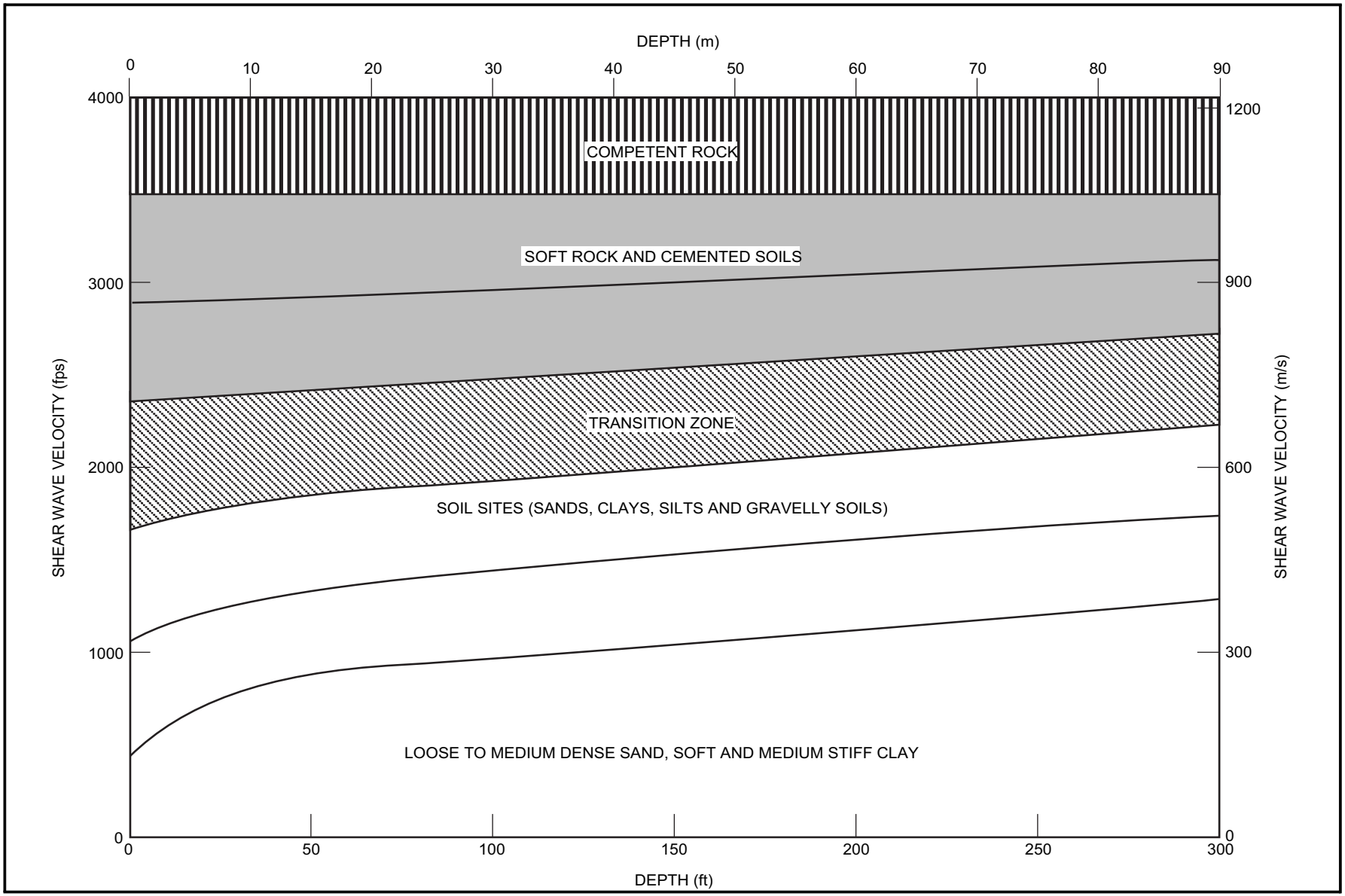

Figure 3A-4 Range of Shear Wave Velocities for Nuclear Power Plant Sites in High Seismic Areas

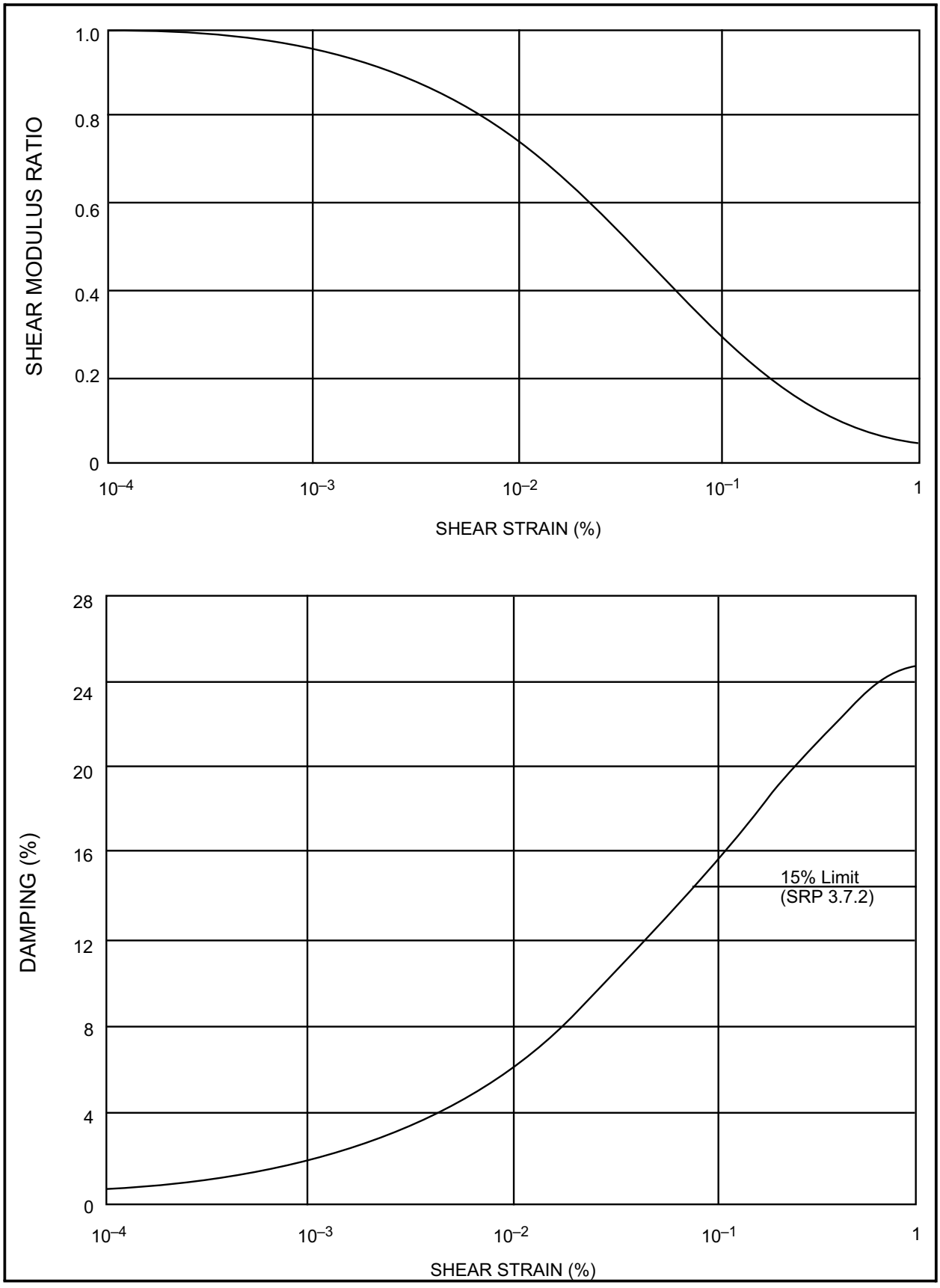

Figure 3A-5 Strain Dependent Soil Properties

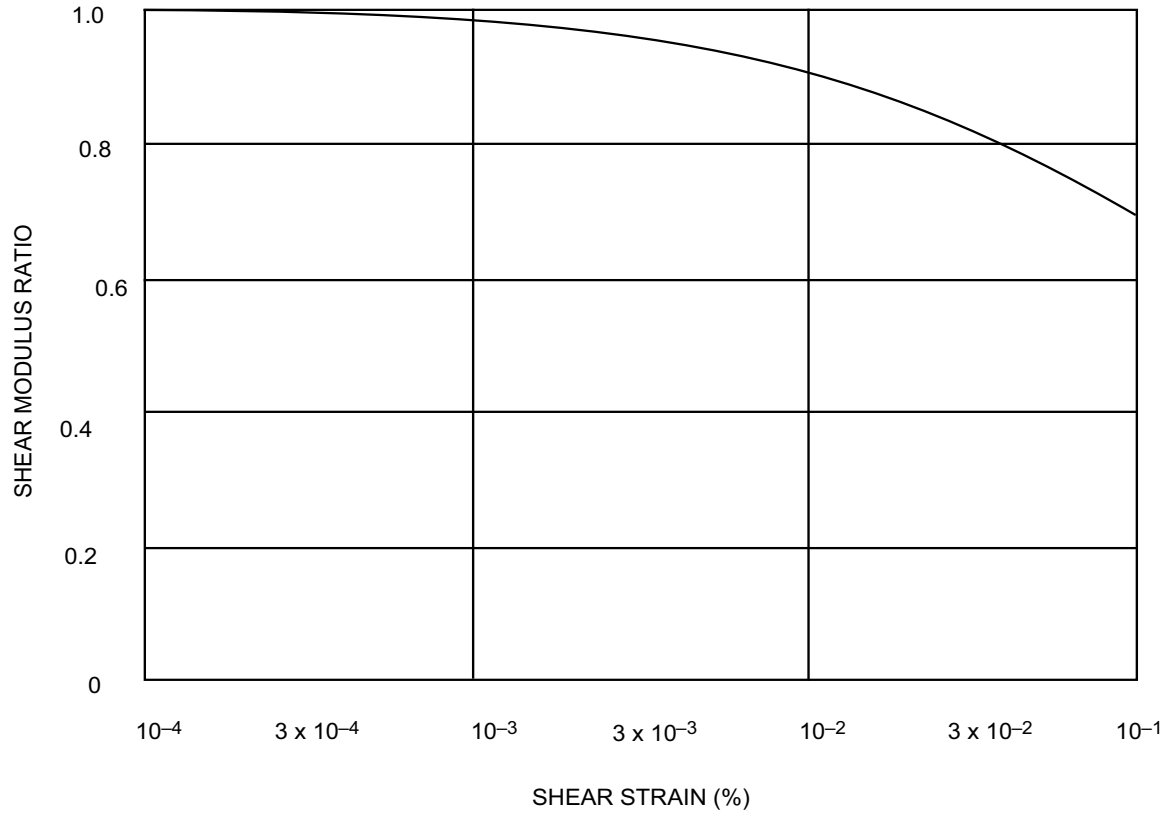

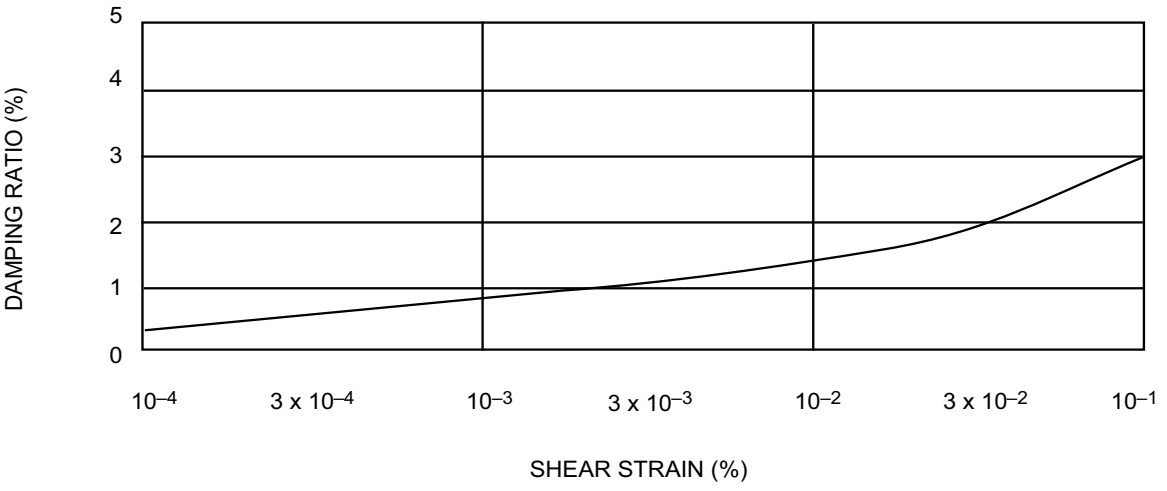

Figure 3A-6 Strain Dependent Rock Properties

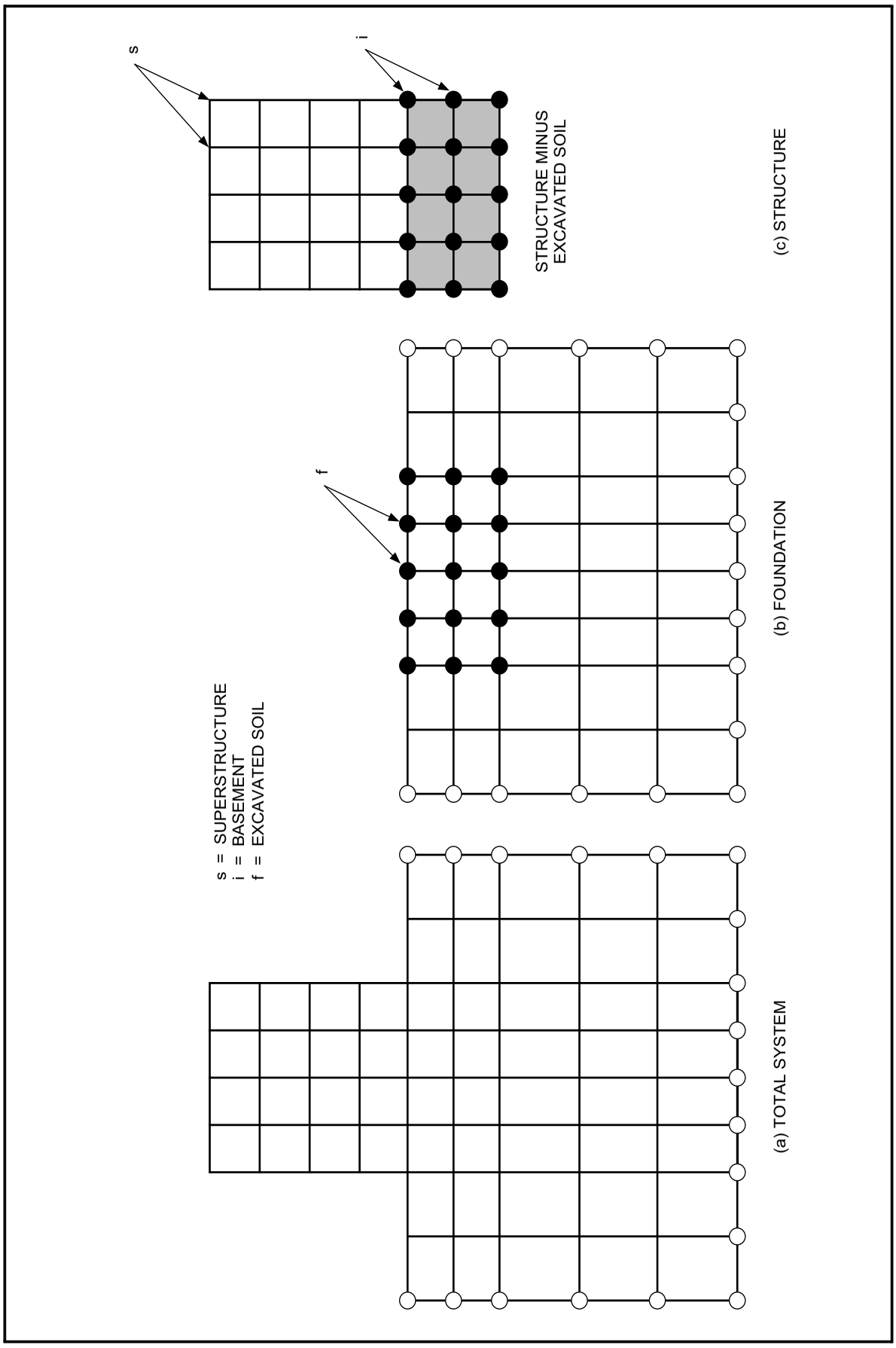

Figure 3A-7 Substructuring of Interaction Model

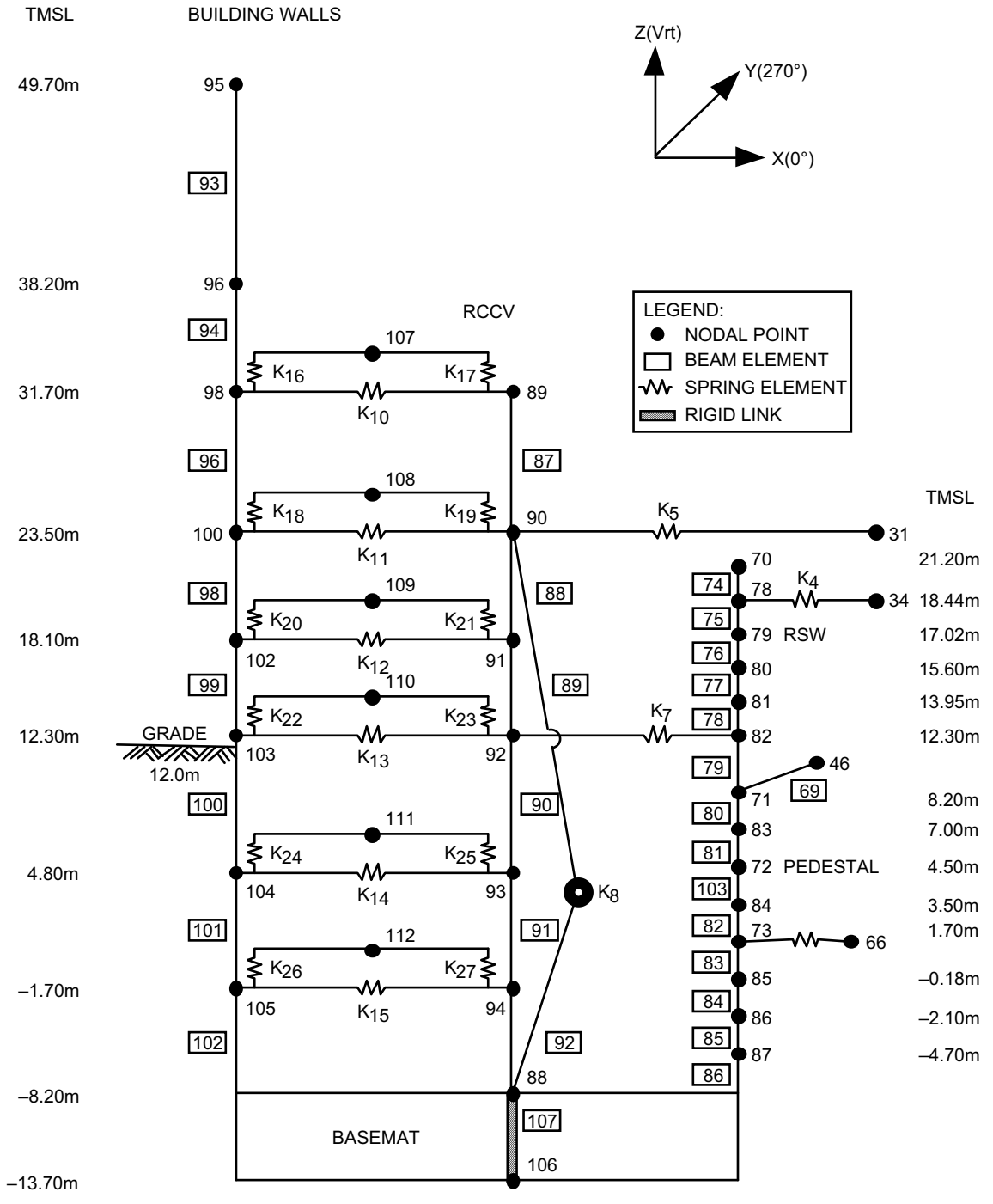

NOTE:
1. THE ROTATIONAL SPRING BETWEEN NODES 90 AND 88 IS PRESENT ONLY IN THE X-Z PLANE.

Figure 3A-8 Reactor Building Stick Model

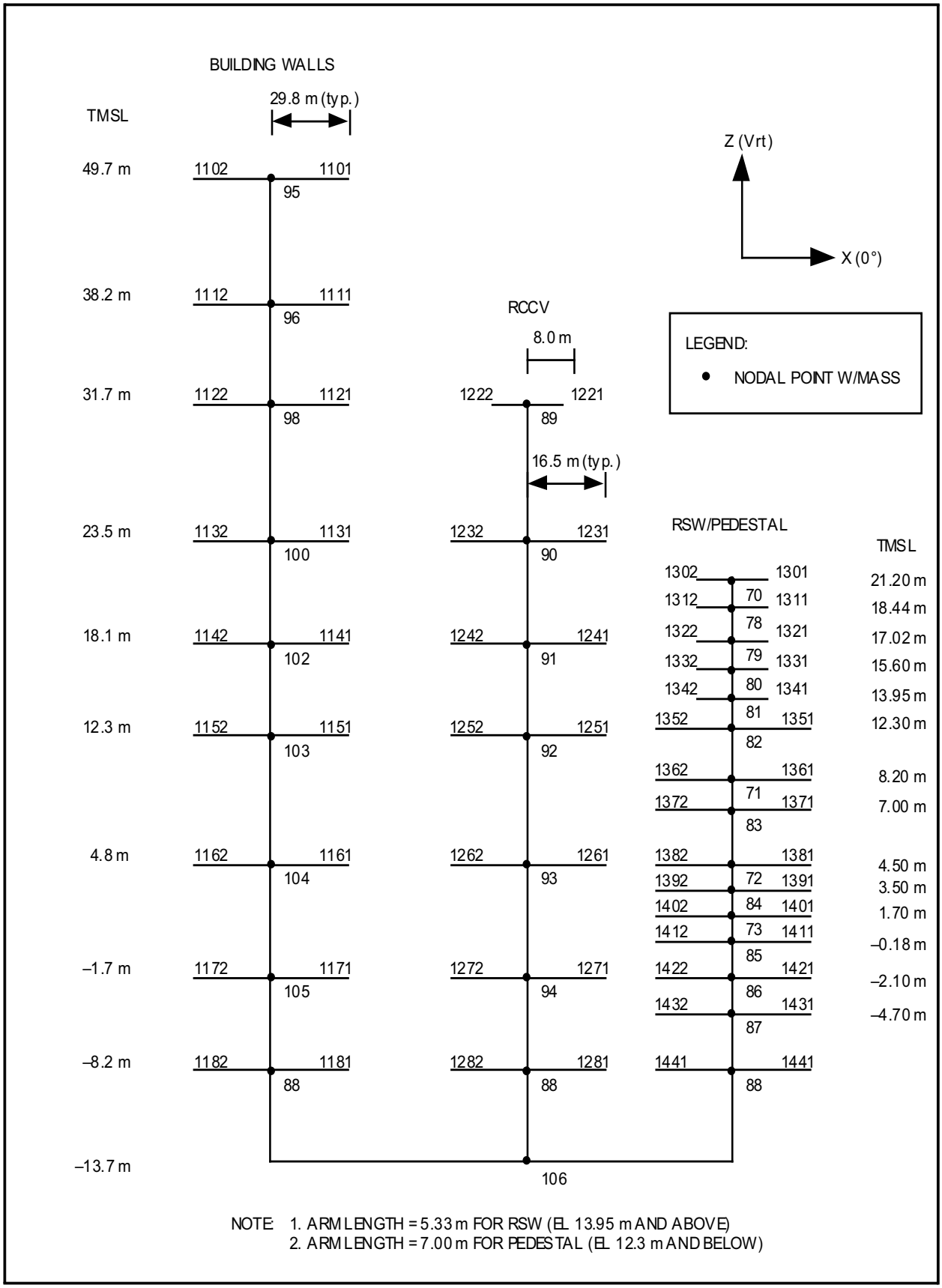

NOTE: 1. ARM LENGTH = 5.33 m FOR RSW (EL 13.95 m AND ABOVE)
2. ARM LENGTH = 7.00 m FOR PEDESTAL (EL 12.3 m AND BELOW)

Figure 3A-9 RPV Stick Model

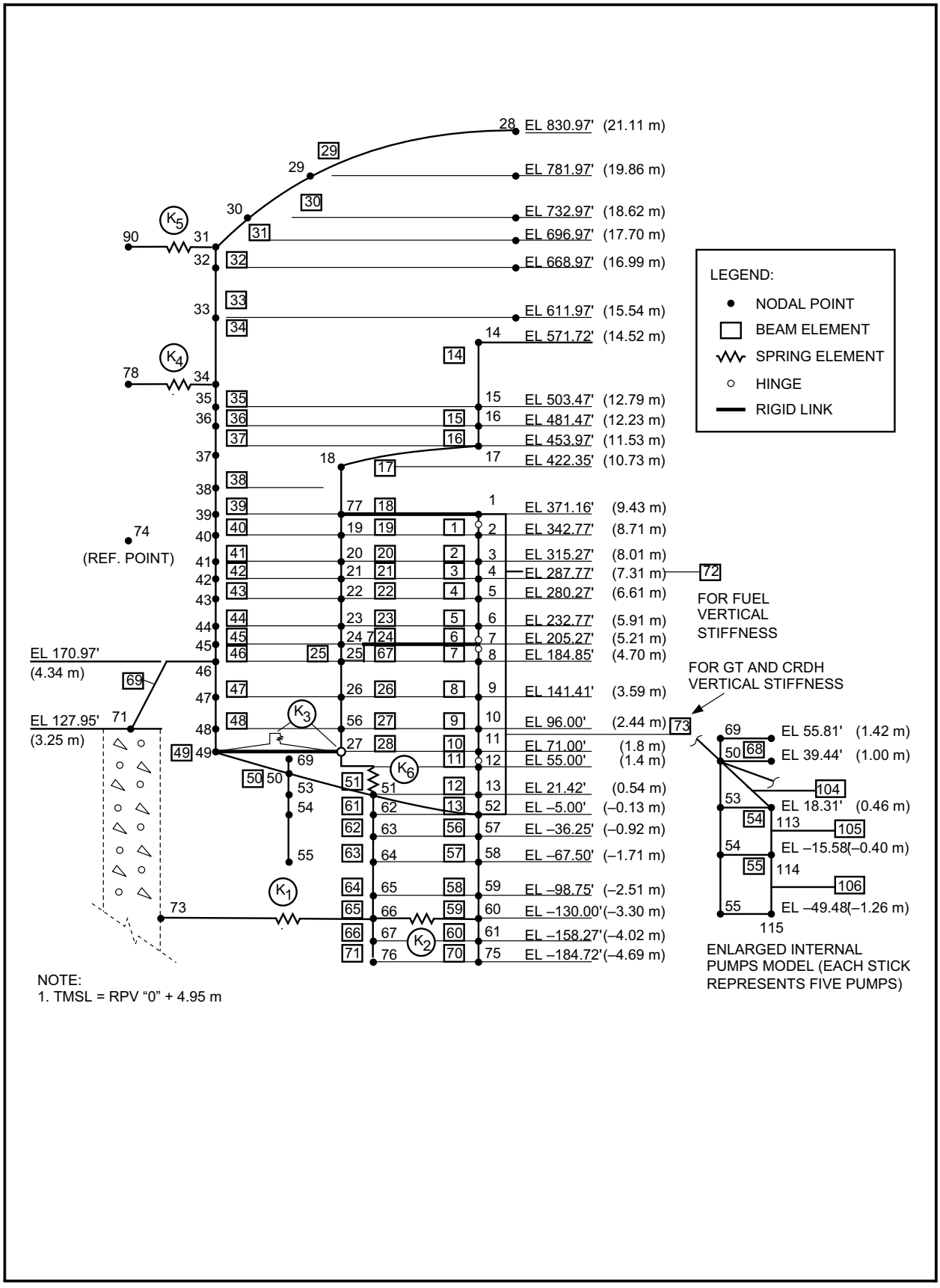

Figure 3A-10 Reactor Building Stick Model with Rigid Arms for X & Z Shaking

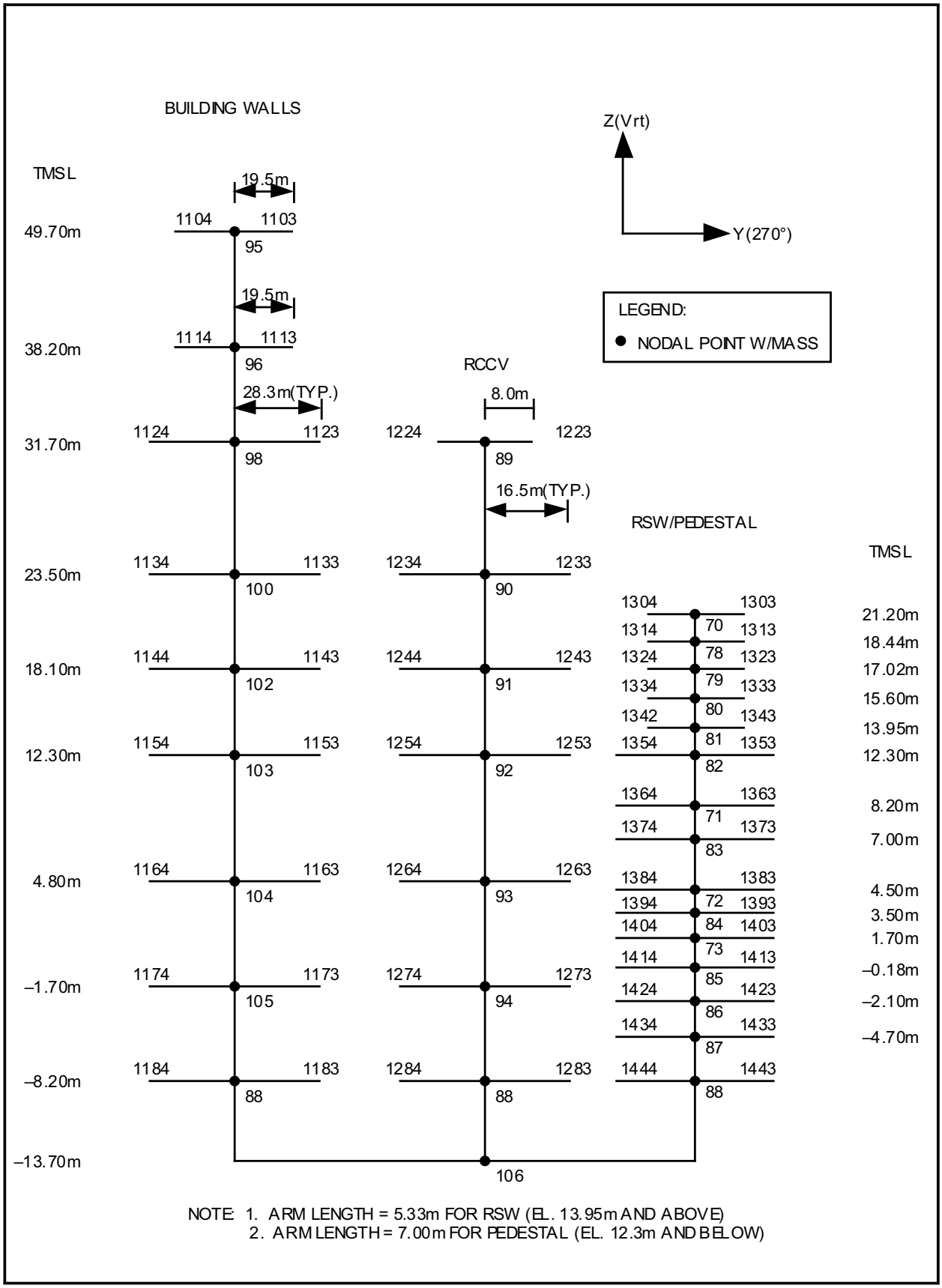

NOTE: 1. ARM LENGTH = 5.33m FOR RSW (EL. 13.95m AND ABOVE)
2. ARM LENGTH = 7.00m FOR PEDESTAL (EL. 12.3m AND BELOW)

Figure 3A-11 Reactor Building Stick Model with Rigid Arms for Y Shaking

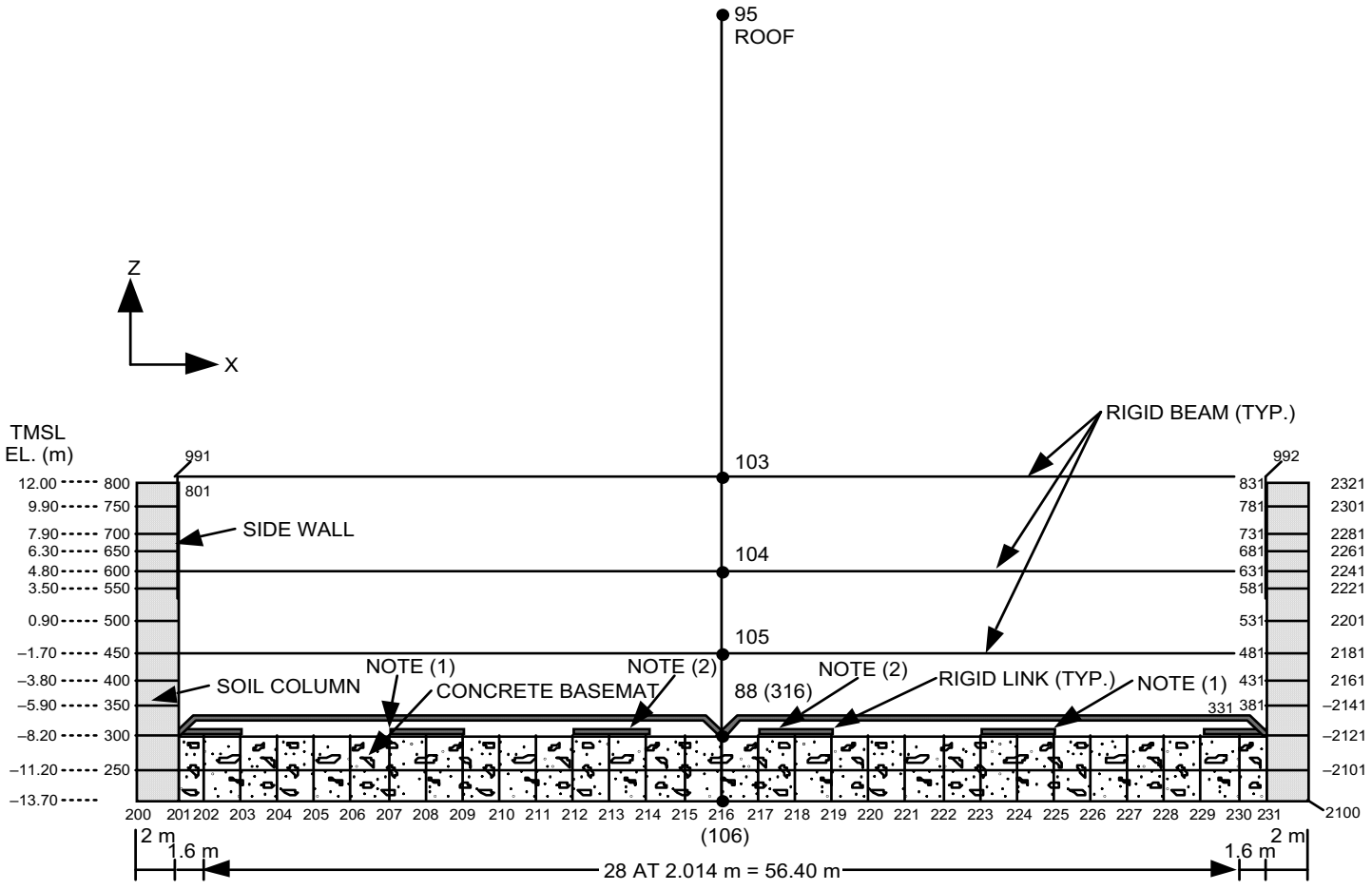

NOTES:
(1) FOOTPRINT CONNECTING TO RCCV STICK
(2) FOOTPRINT CONNECTING TO RSW/PEDESTAL STICK

Figure 3A-12 Reactor Building Foundation 2-D Model XZ Direction

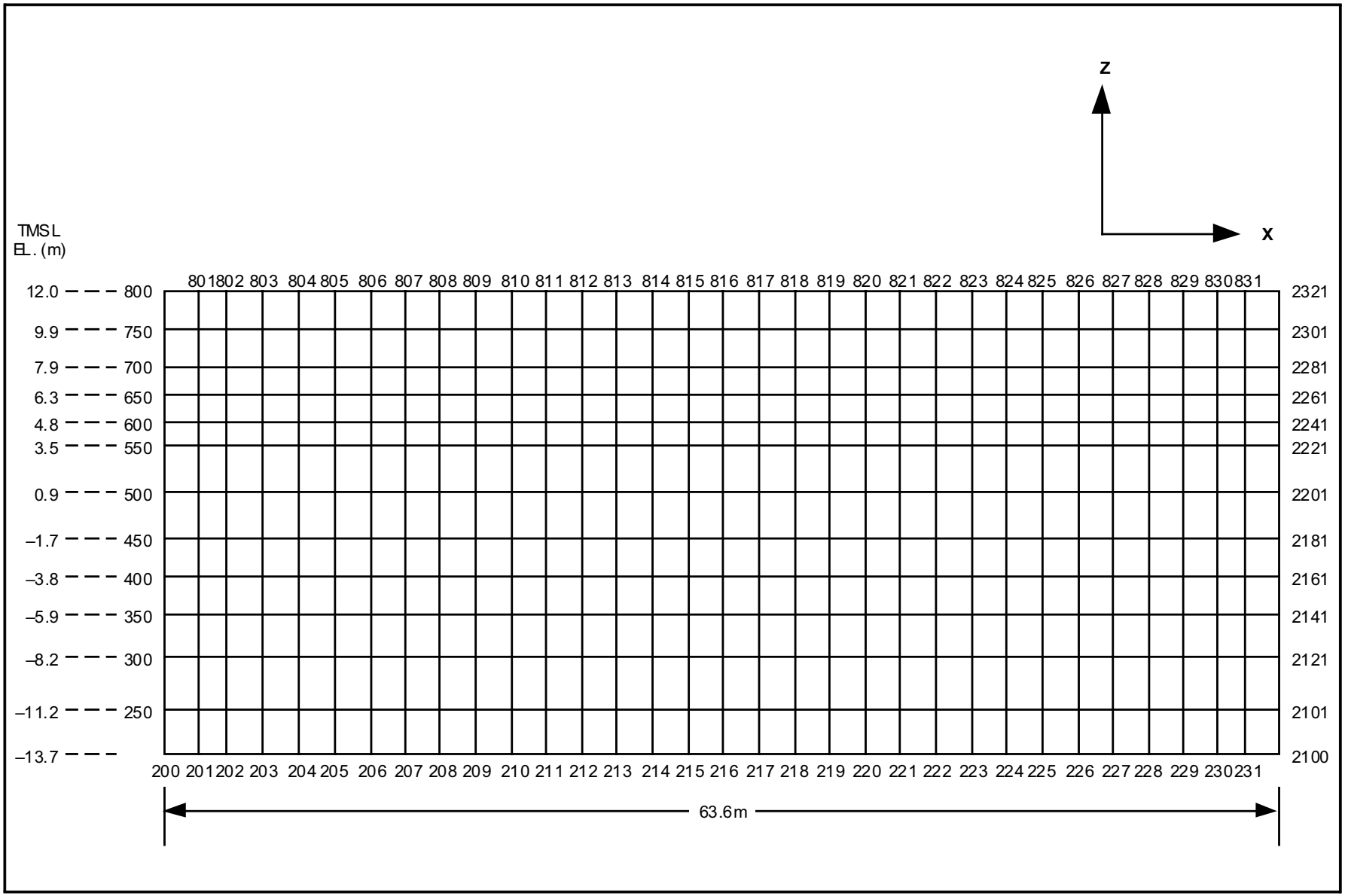

Figure 3A-13 The Excavated Soil Elements of Reactor Building 2-D Model

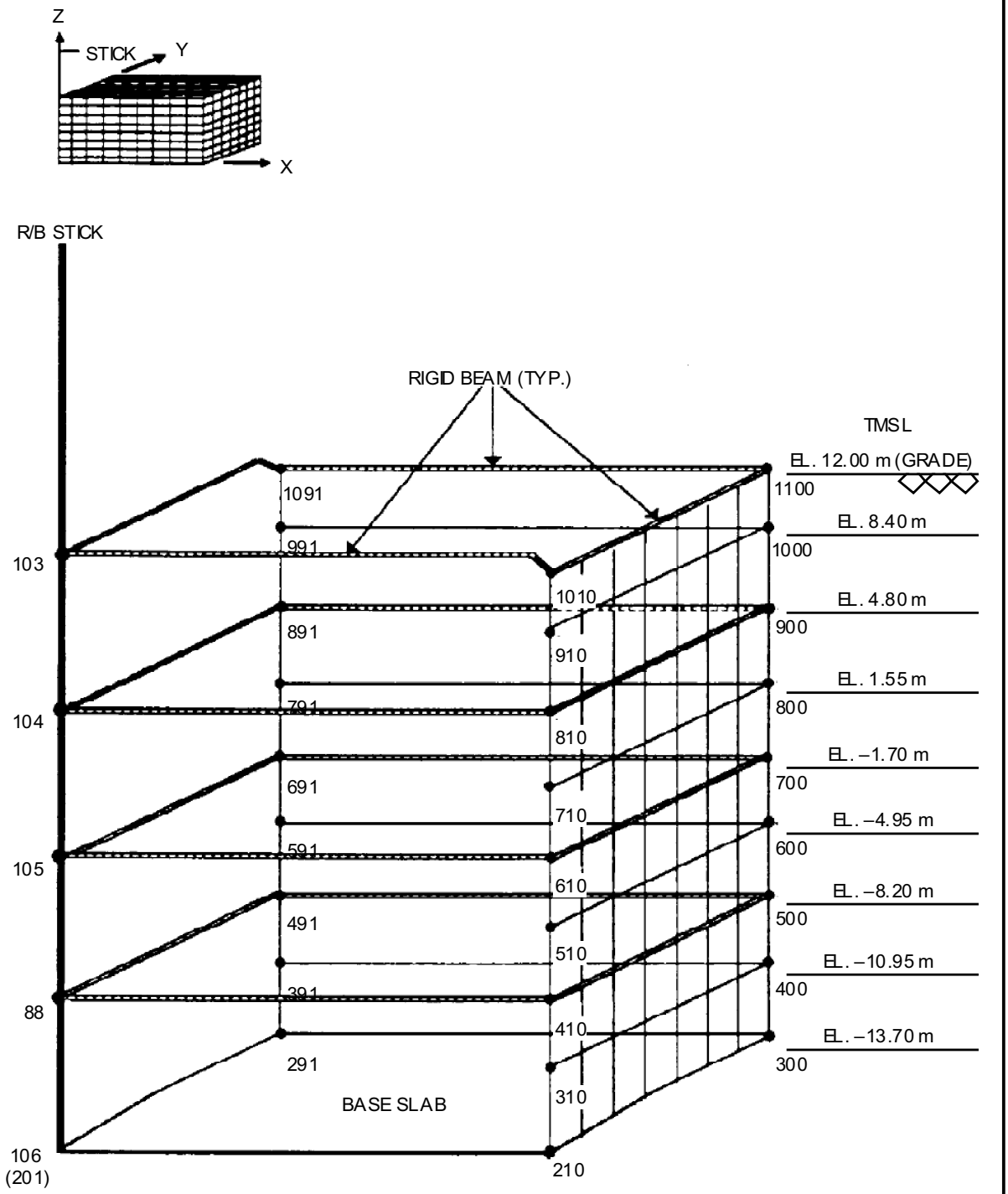

Figure 3A-14 Connection of the Main Stick to the Side Walls (For Reactor Building UB Cases)

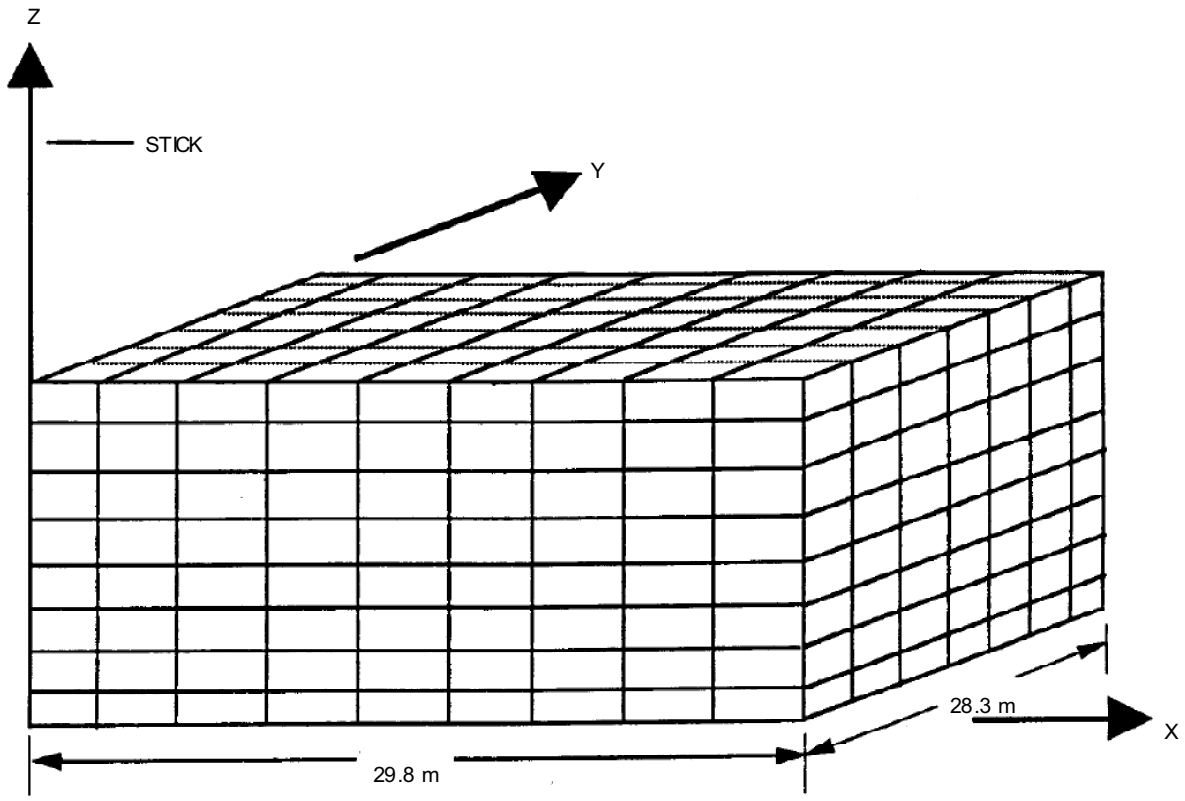

Figure 3A-15 R/B Excavated Soil Model (UB Soil Profiles)

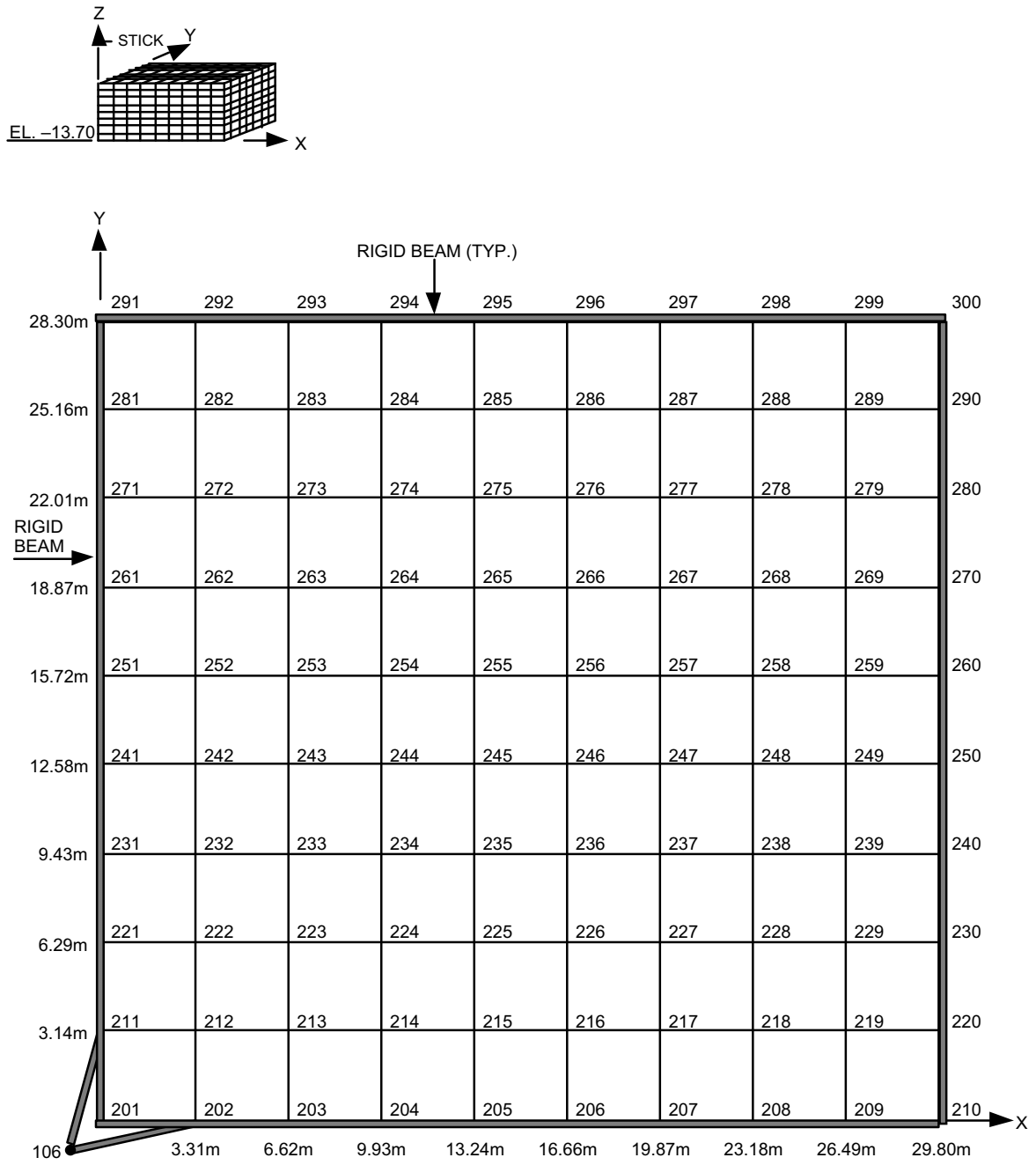

Figure 3A-16 UB Case: Nodal Points at Elevation –13.70m

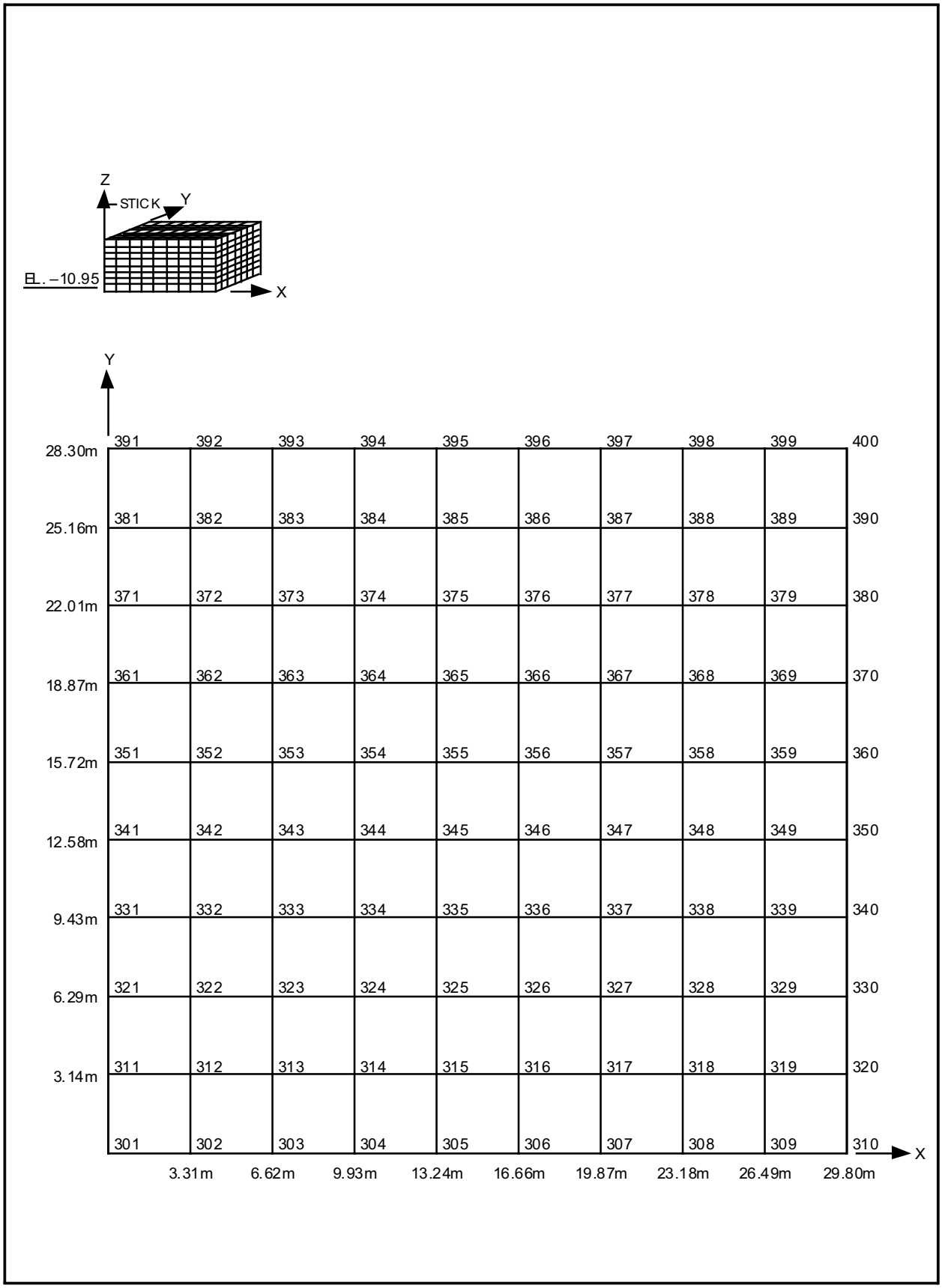

Figure 3A-17 UB Case: Nodal Points at Elevation –10.95m

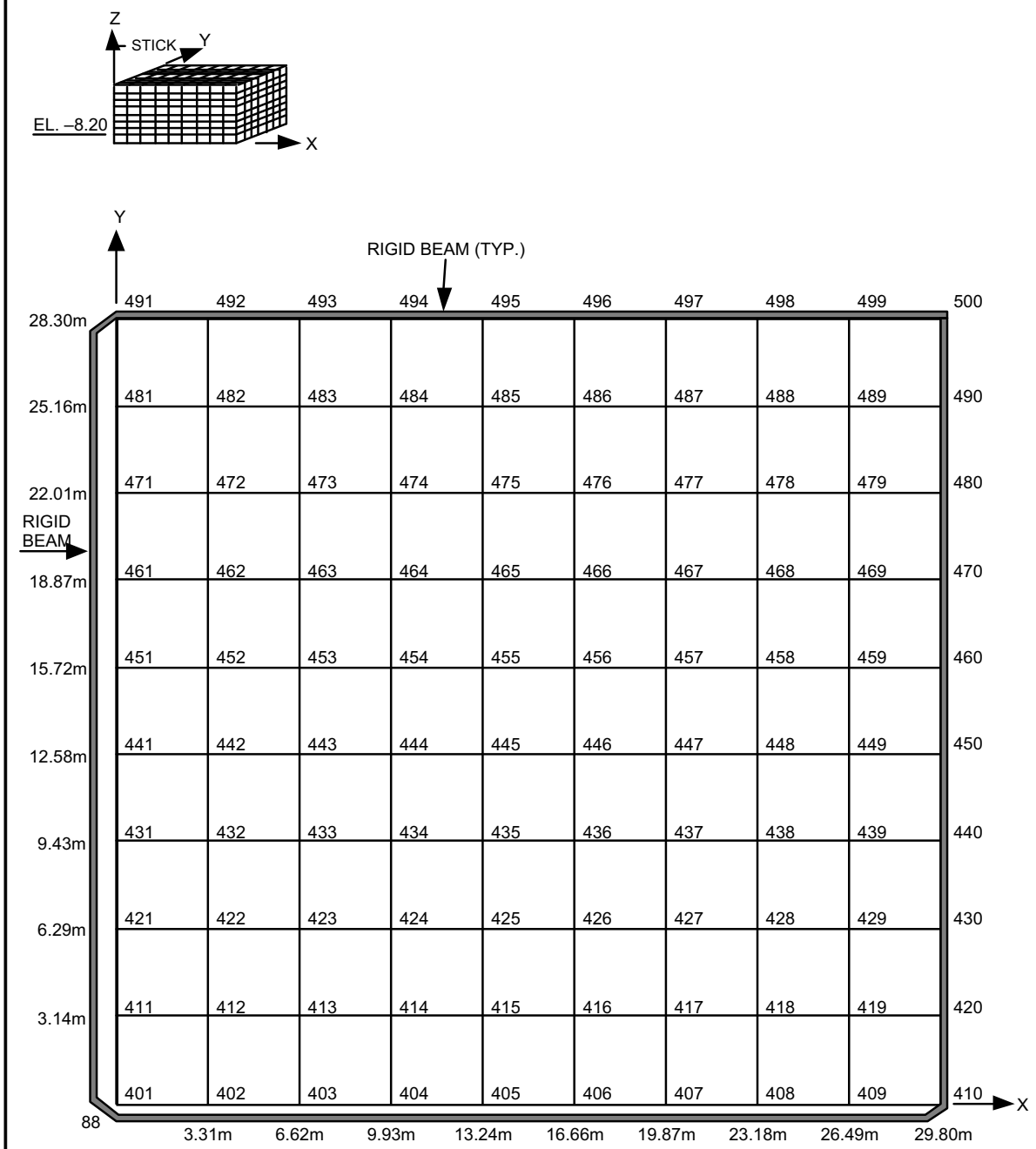

Figure 3A-18 UB Case: Nodal Points at Elevation –8.20m

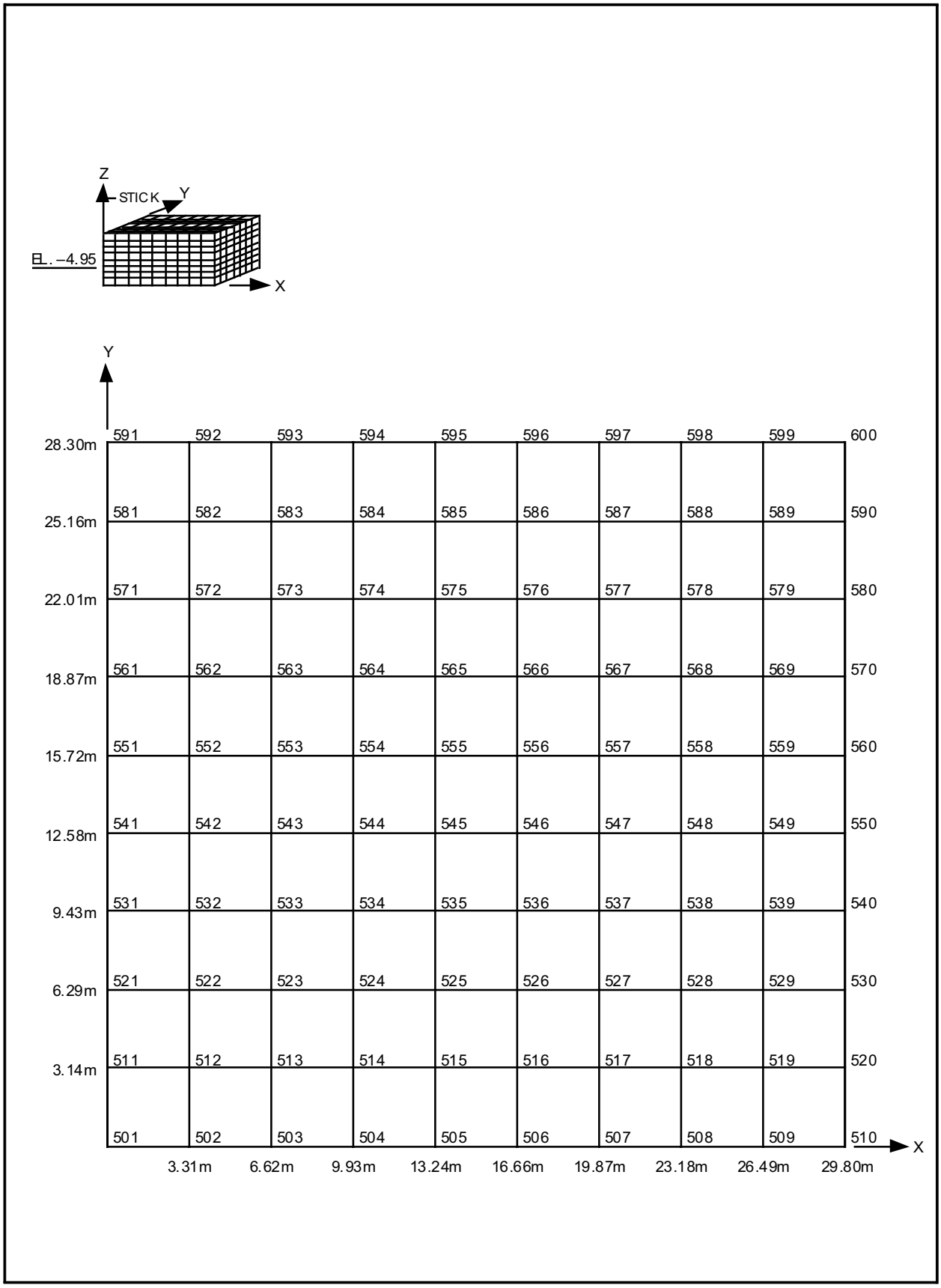

Figure 3A-19 UB Case: Nodal Points at Elevation –4.95m

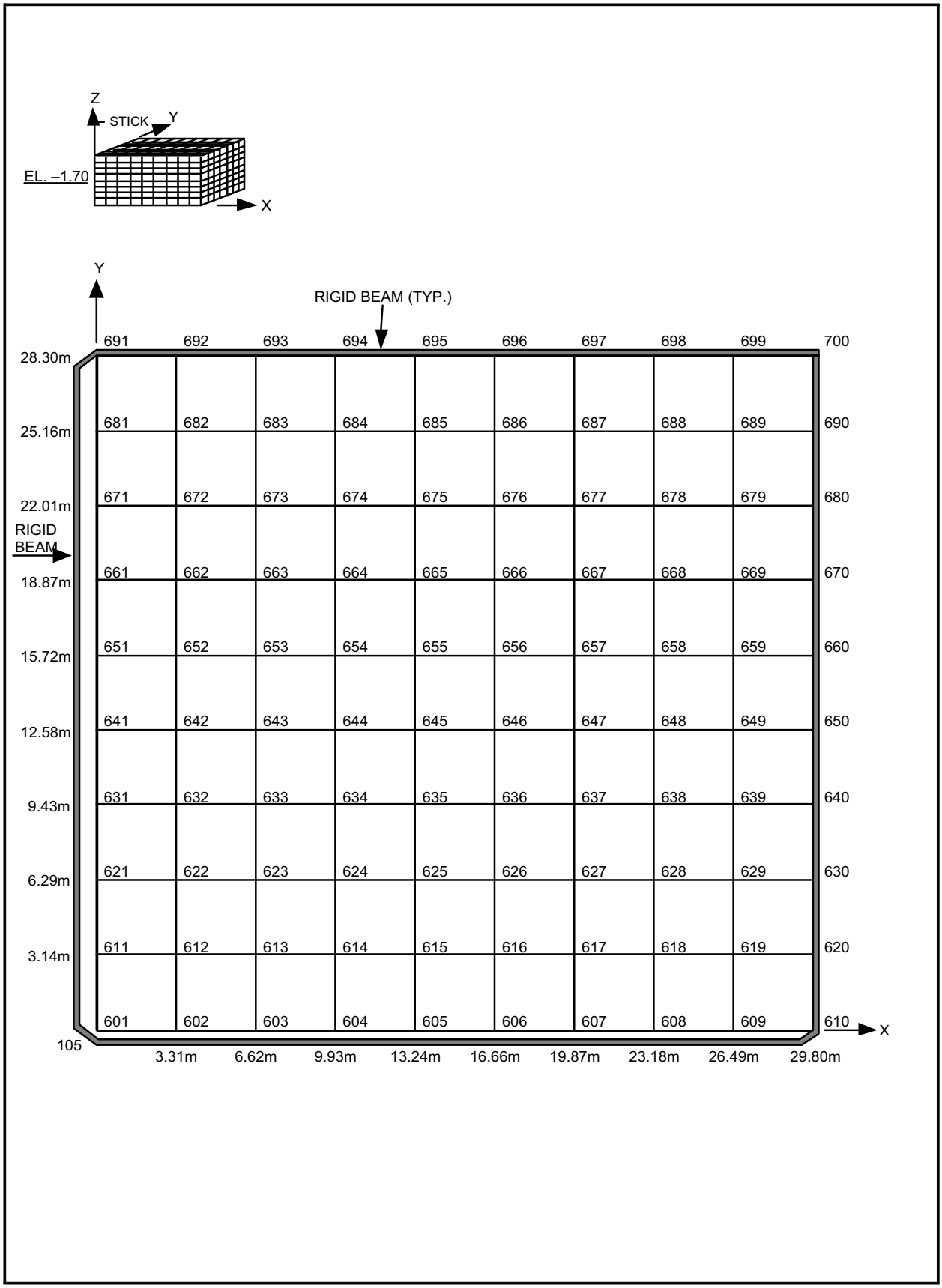

Figure 3A-20 UB Case: Nodal Points at Elevation –1.70m

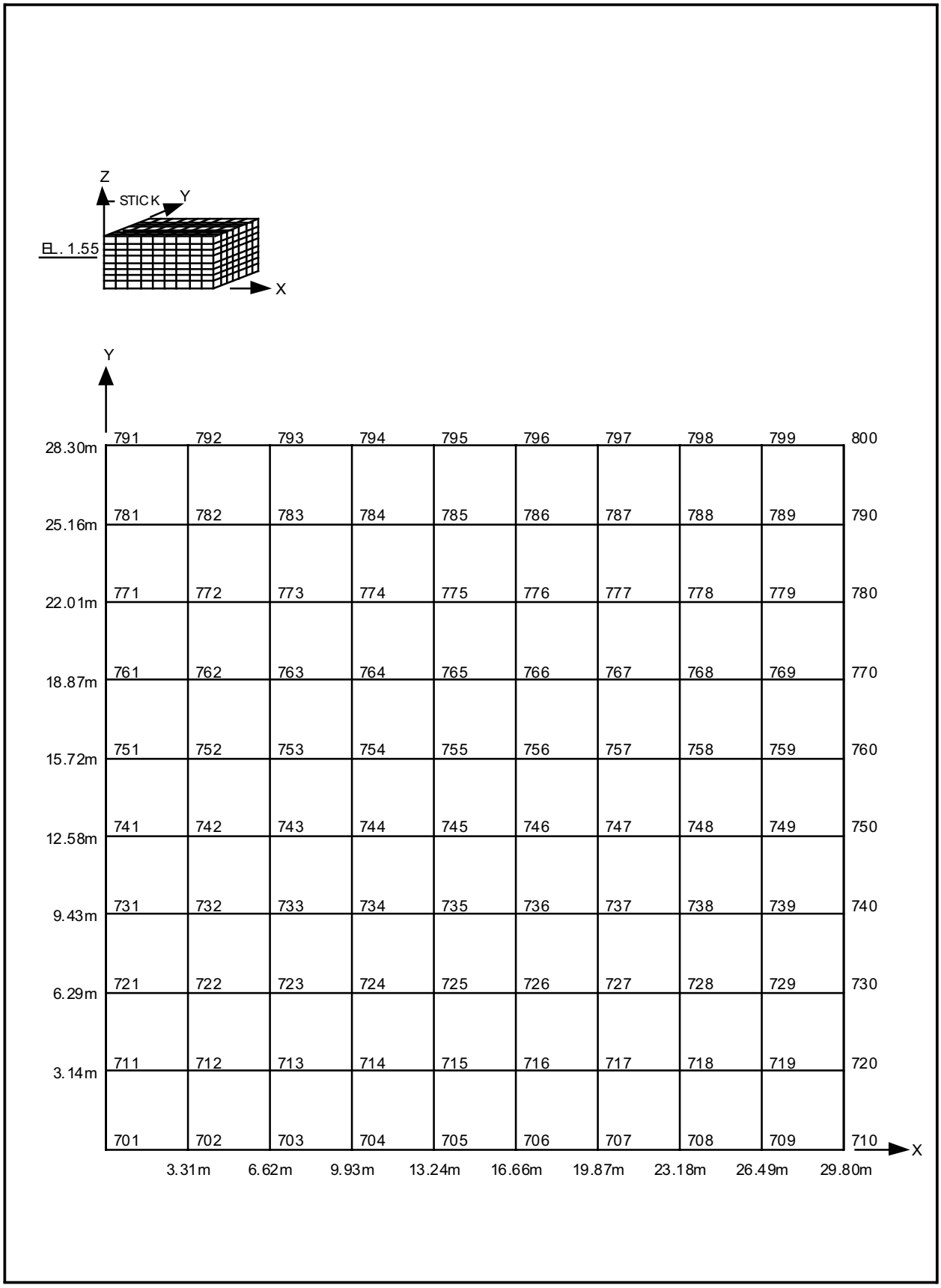

Figure 3A-21 UB Case: Nodal Points at Elevation 1.55m

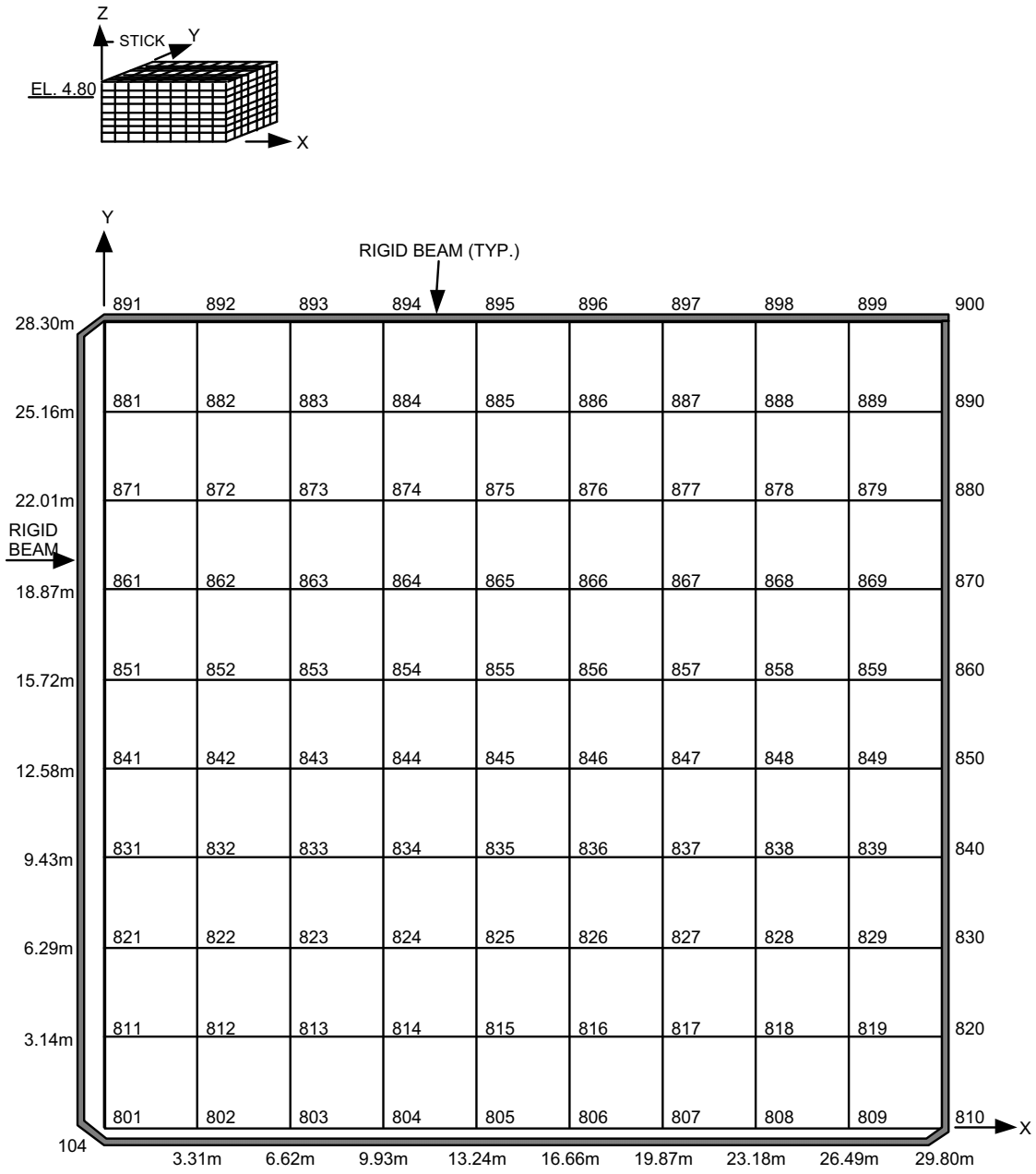

Figure 3A-22 UB Case: Nodal Points at Elevation 4.80m

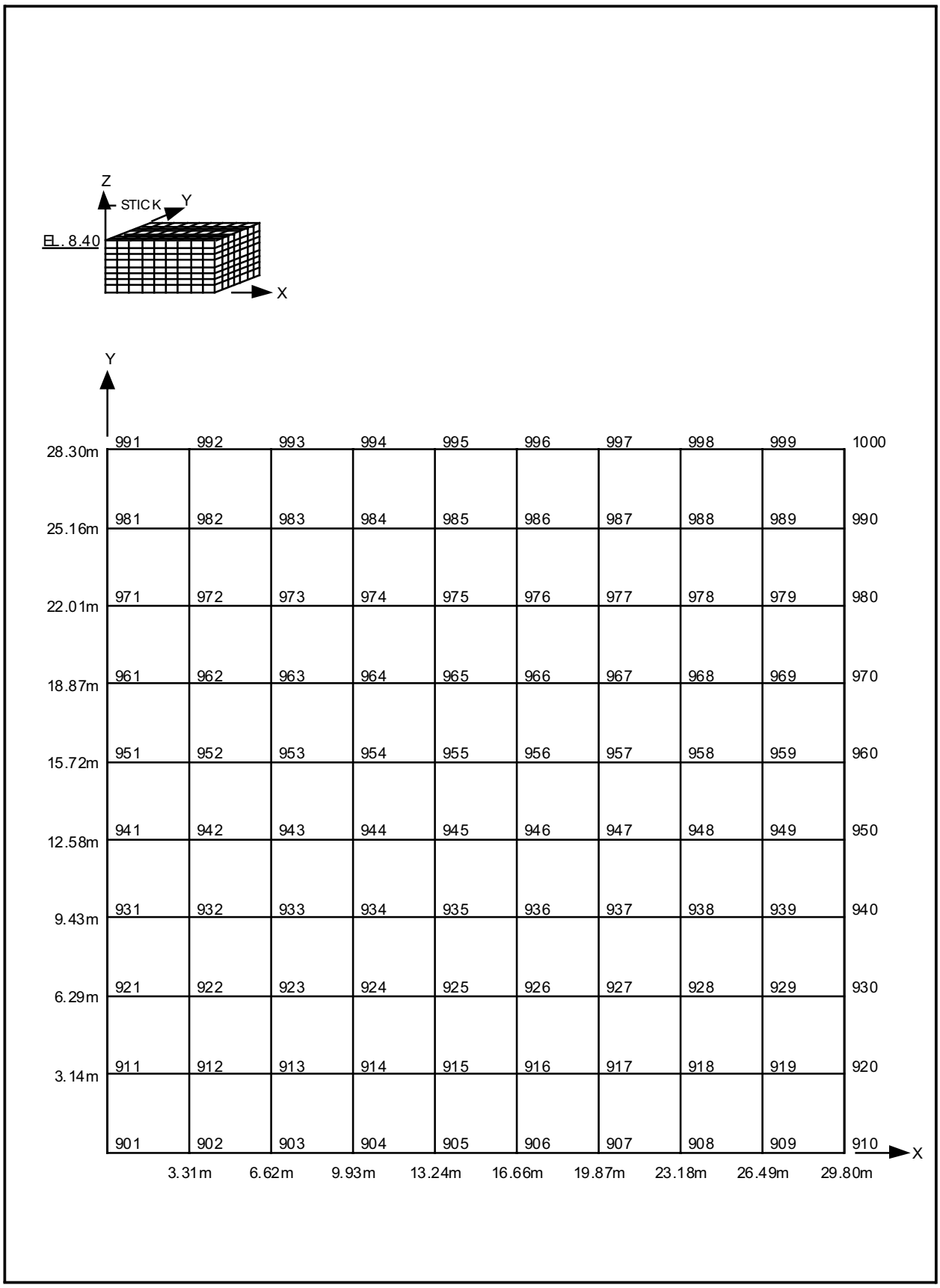

Figure 3A-23 UB Case: Nodal Points at Elevation 8.40m

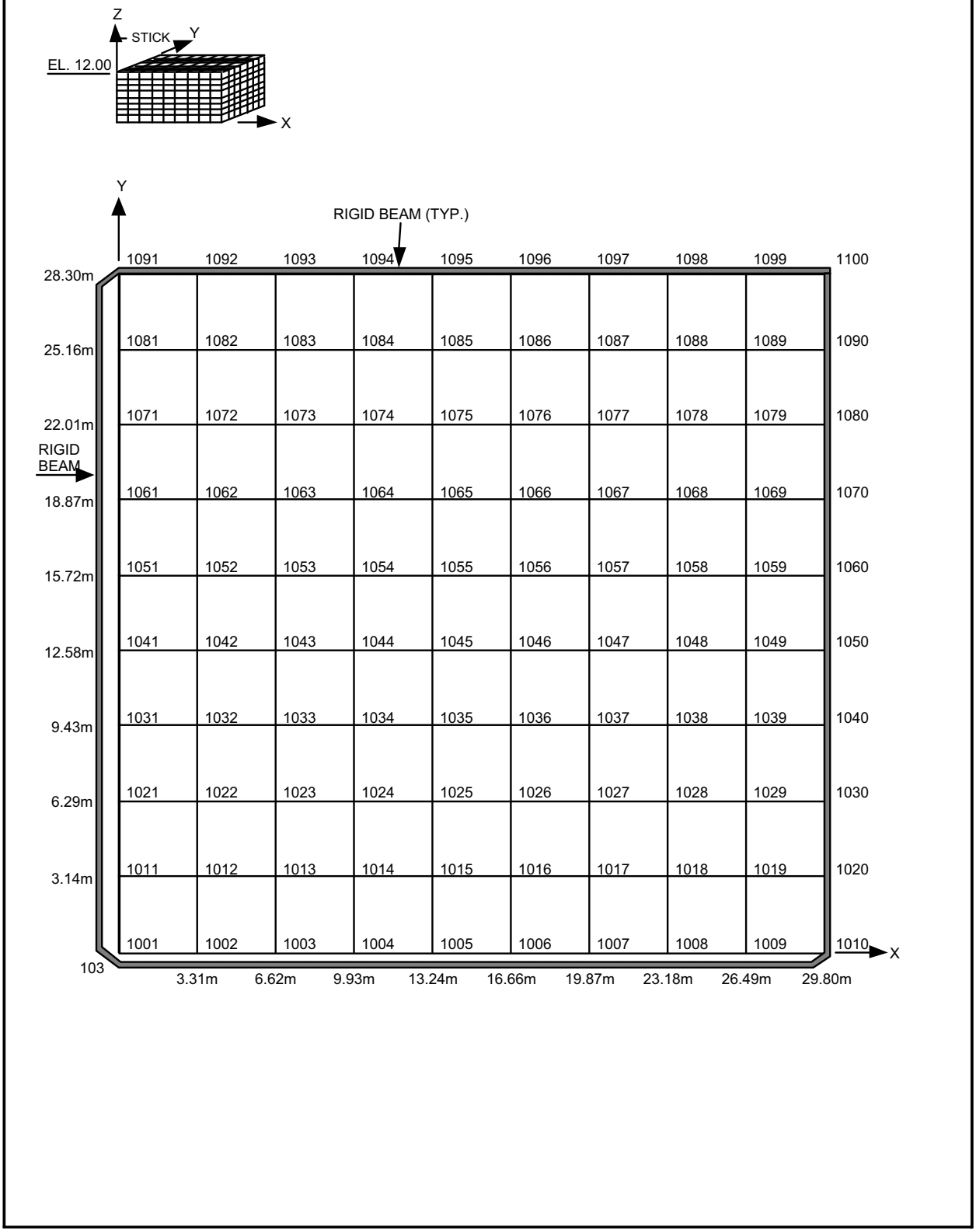

Figure 3A-24 UB Case: Nodal Points at Elevation 12.00m

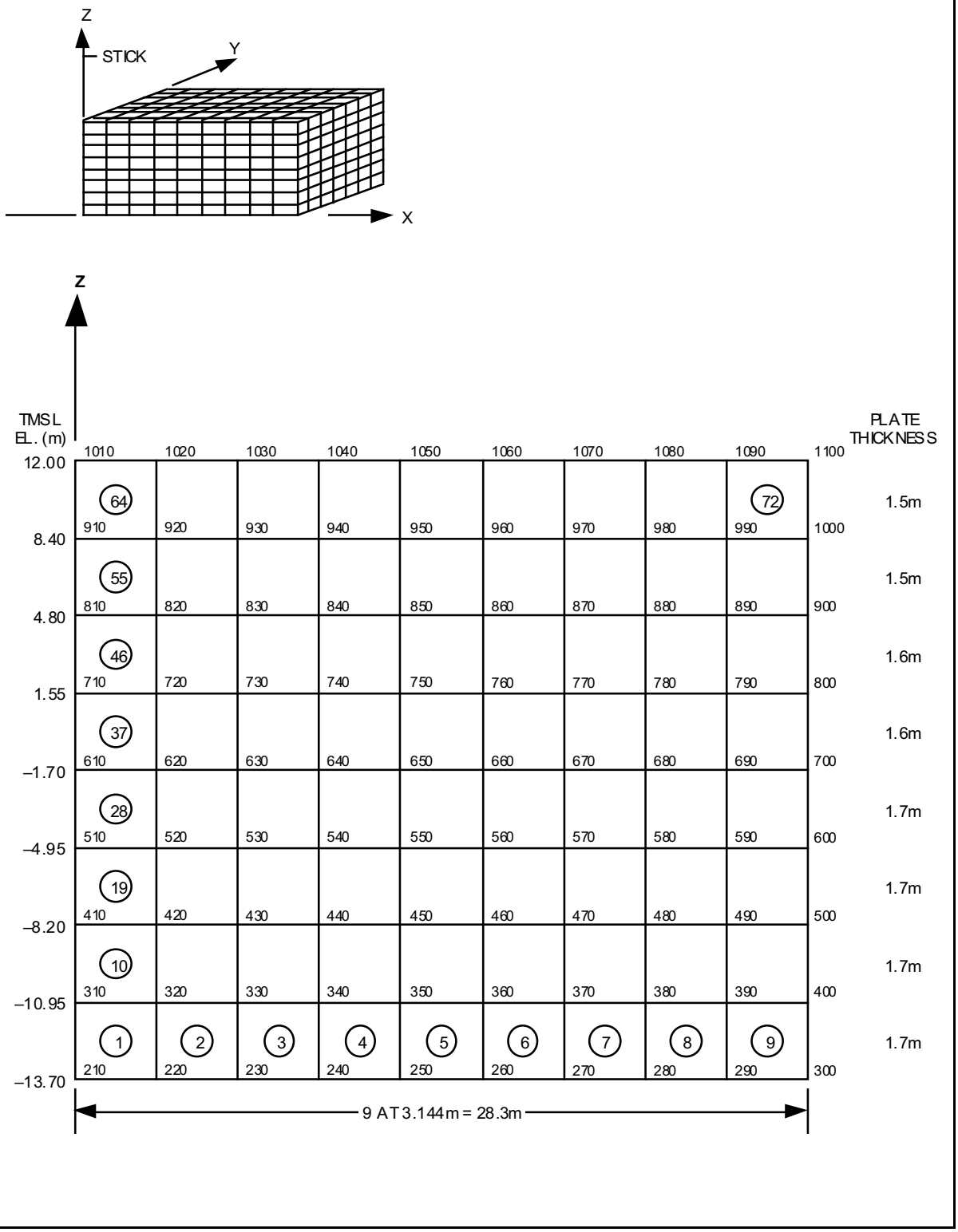

Figure 3A-25 Plate Elements of the Side Wall (X = 29.80m)

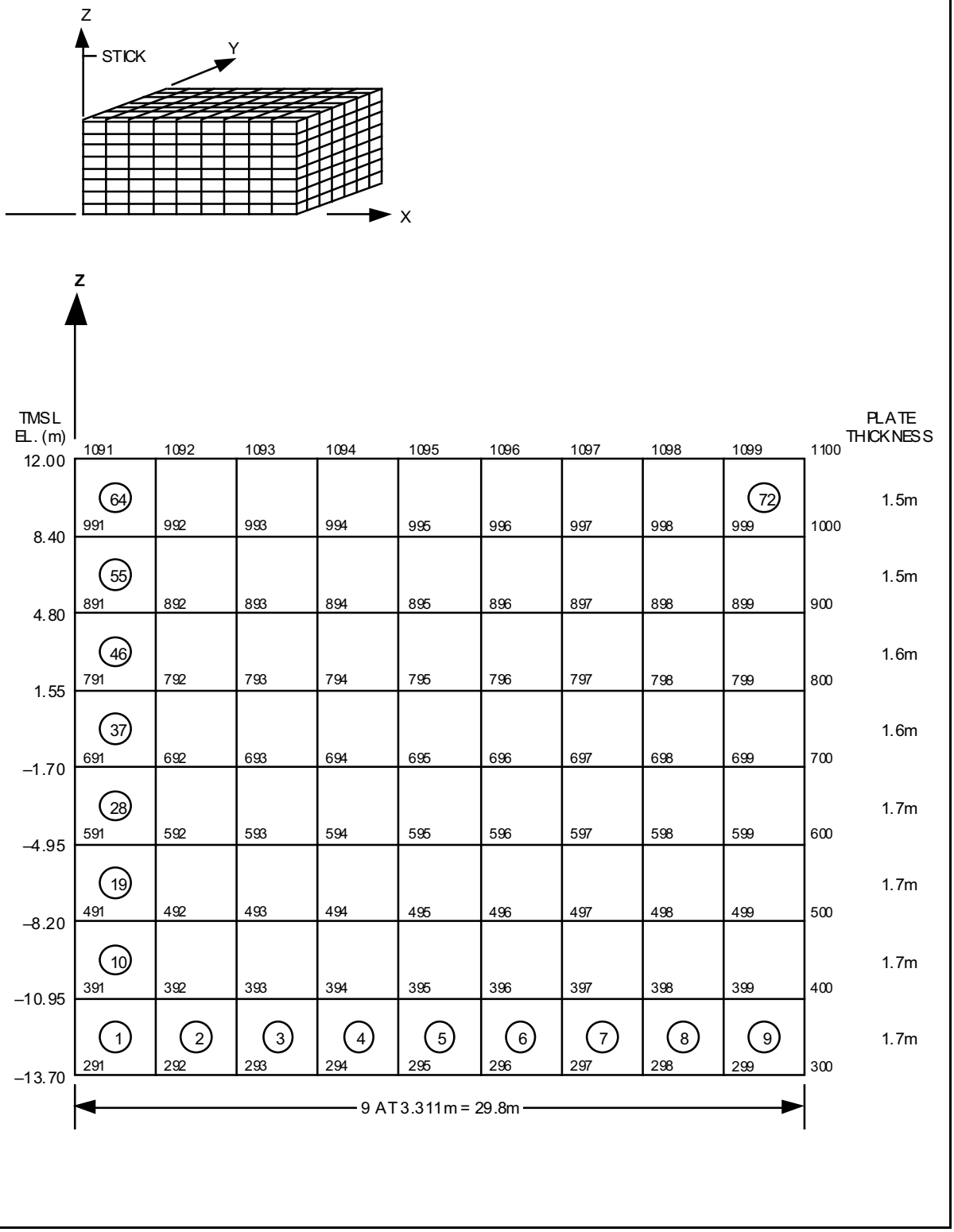

Figure 3A-26 Plate Elements of the Side Wall (Y = 28.30m)

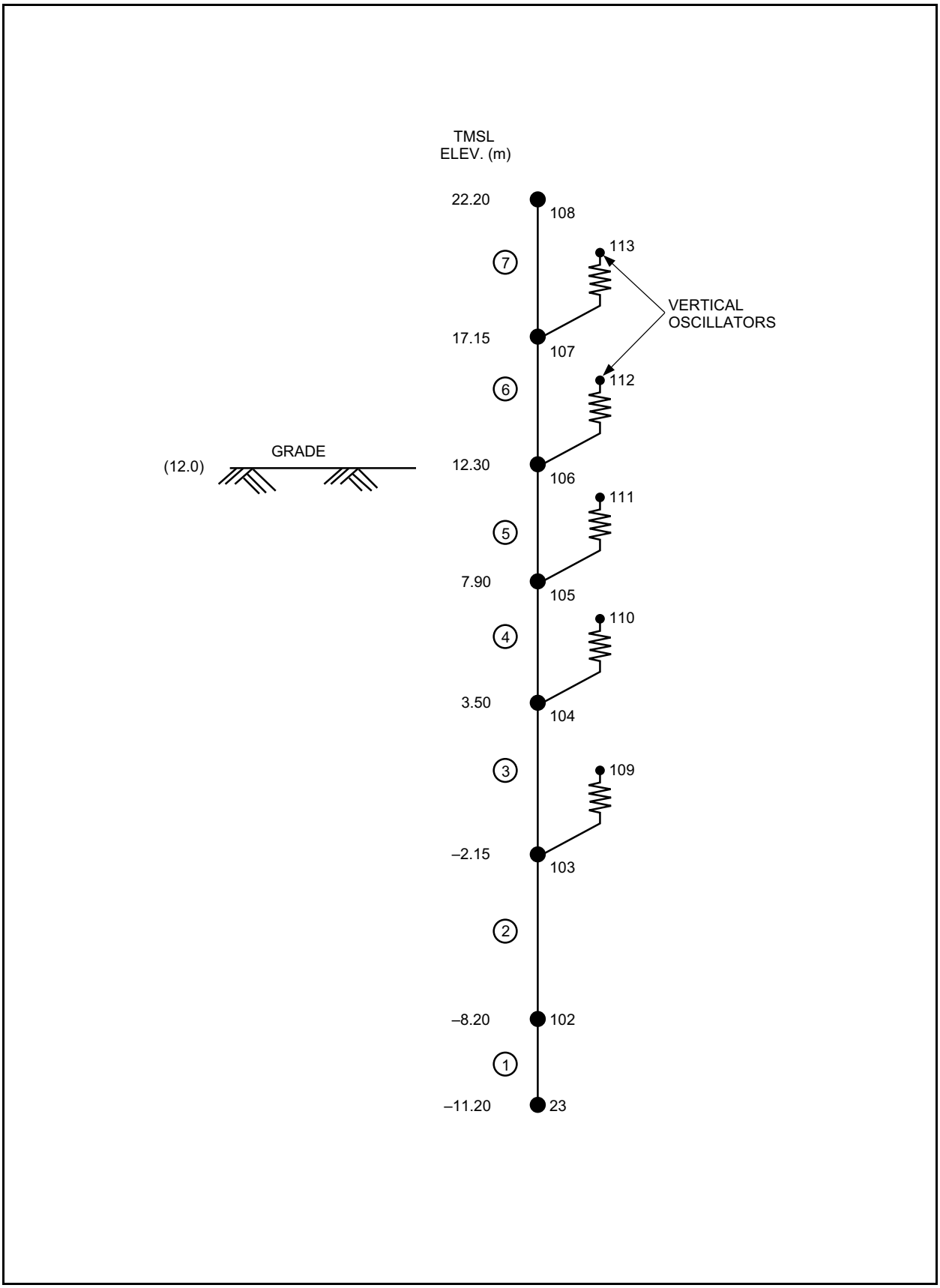

Figure 3A-27 Stick Model for the Control Building

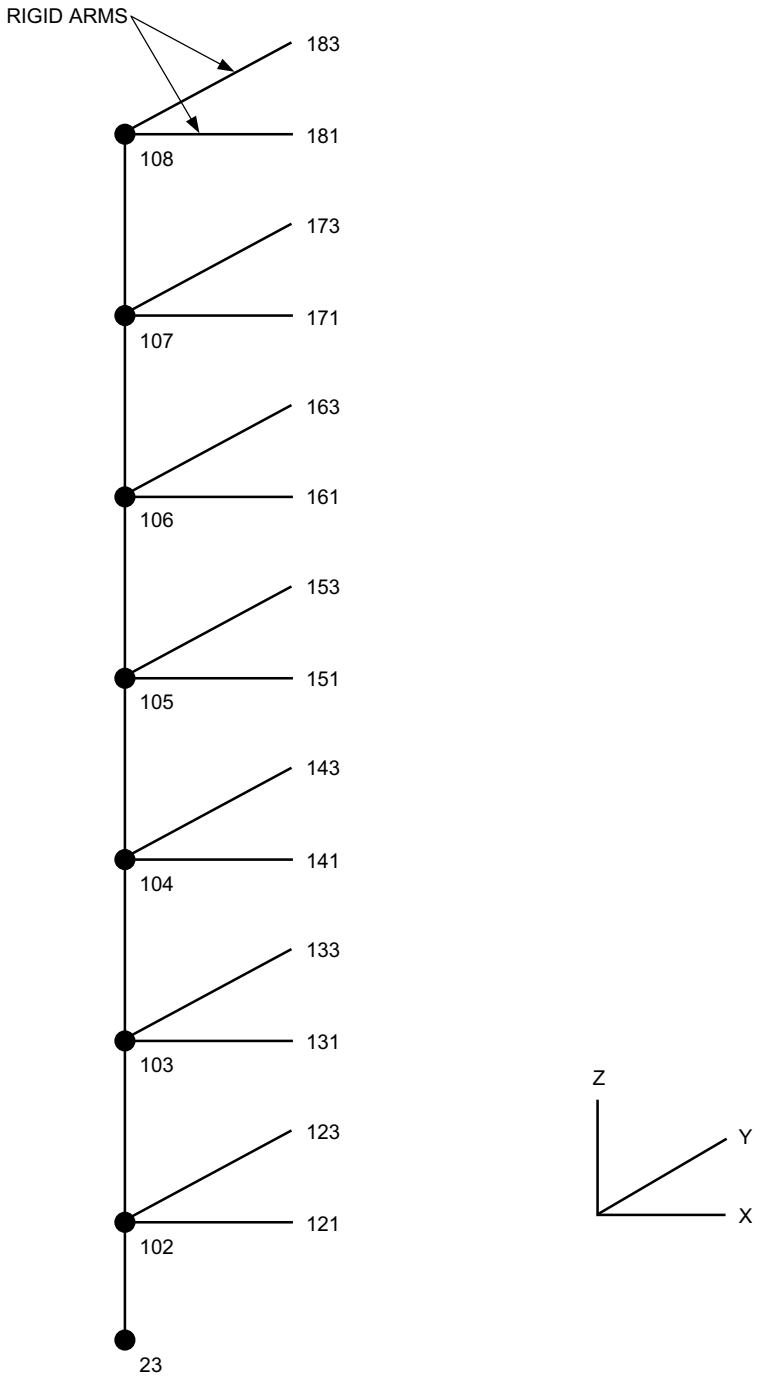

Figure 3A-28 1/4 Stick Model Showing Rigid Arms

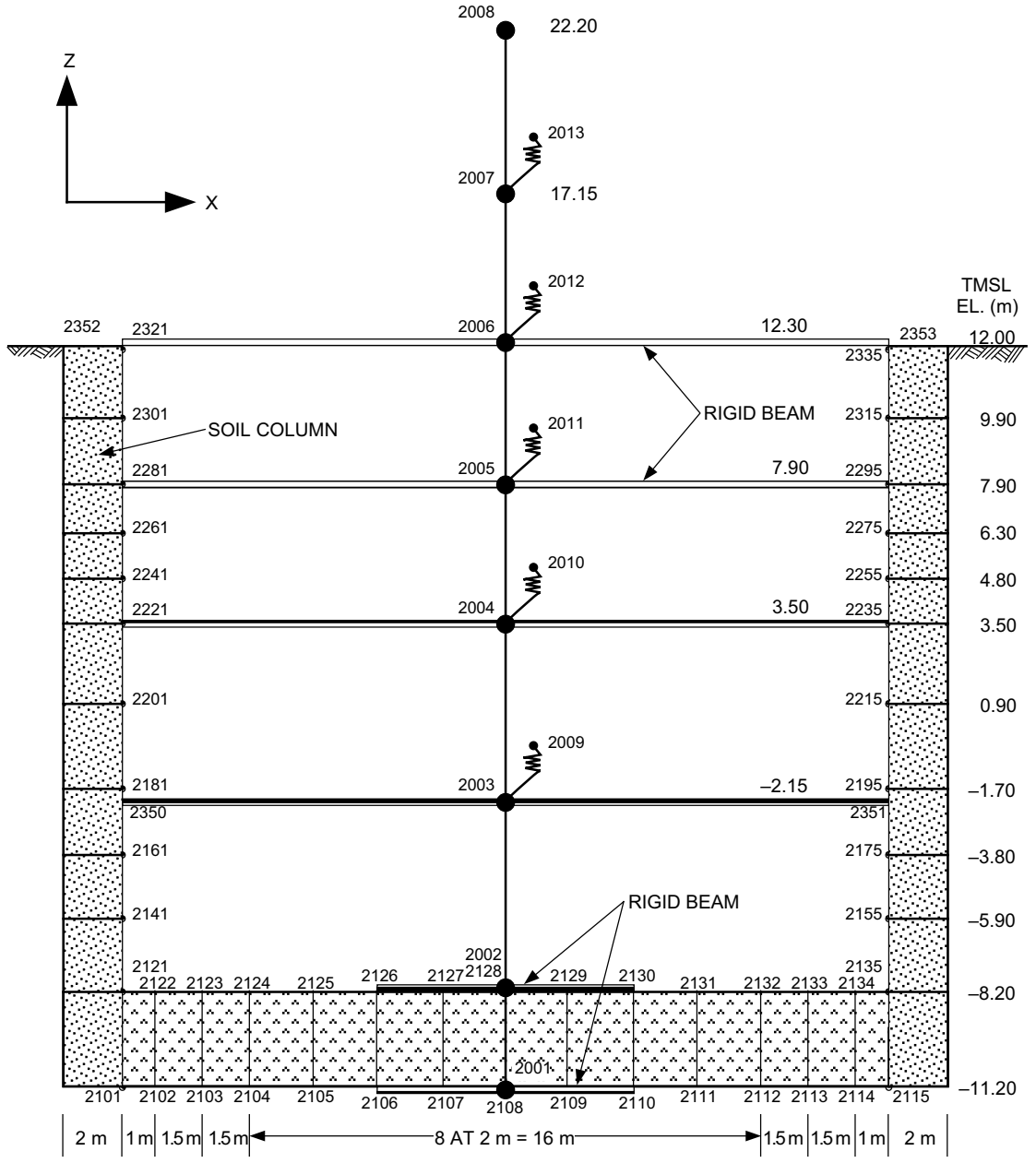

Figure 3A-29 Control Building Foundation 2-D Model XZ Direction

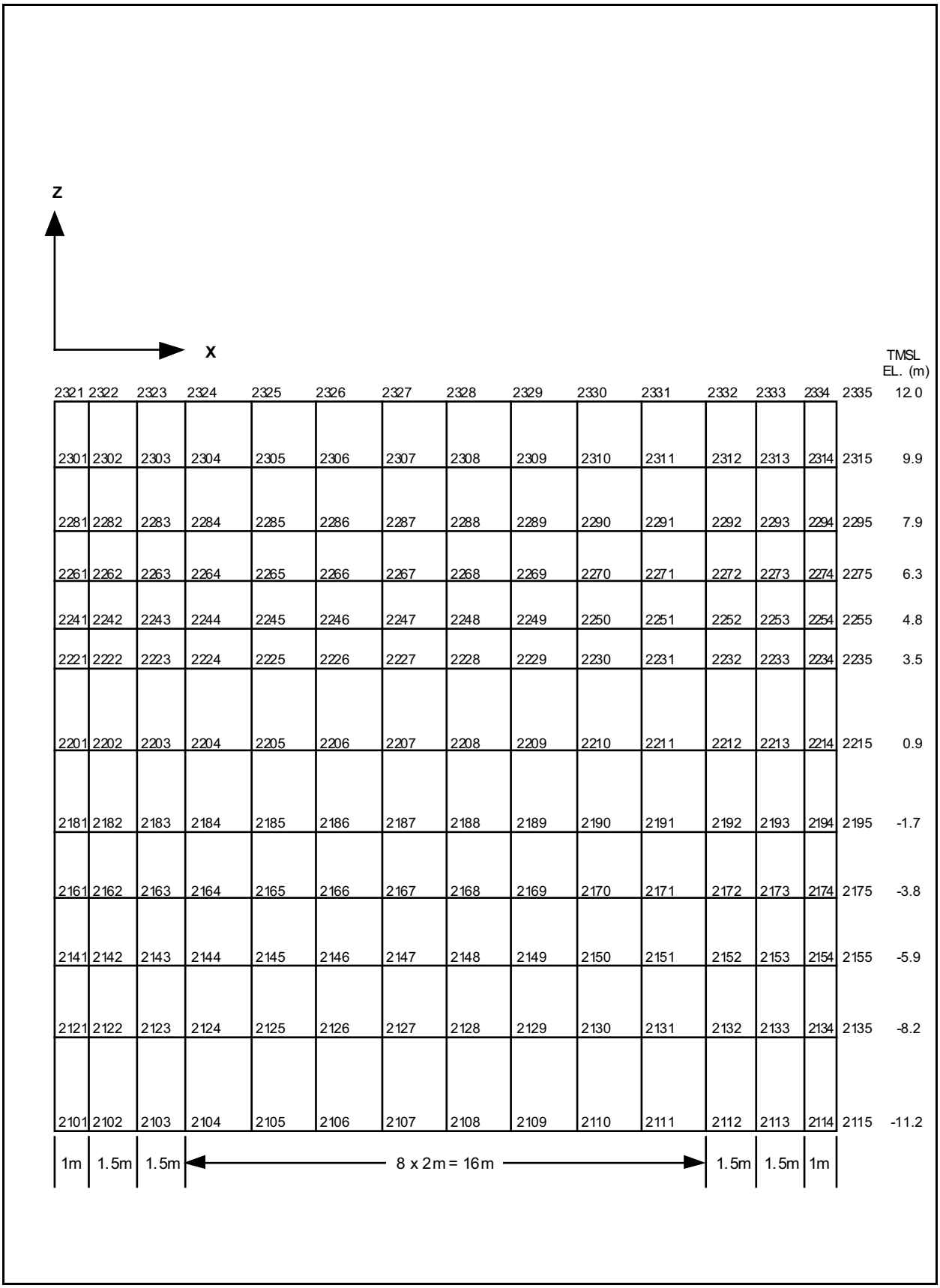

Figure 3A-30 Control Building Excavated Soil 2-D Model XZ Direction

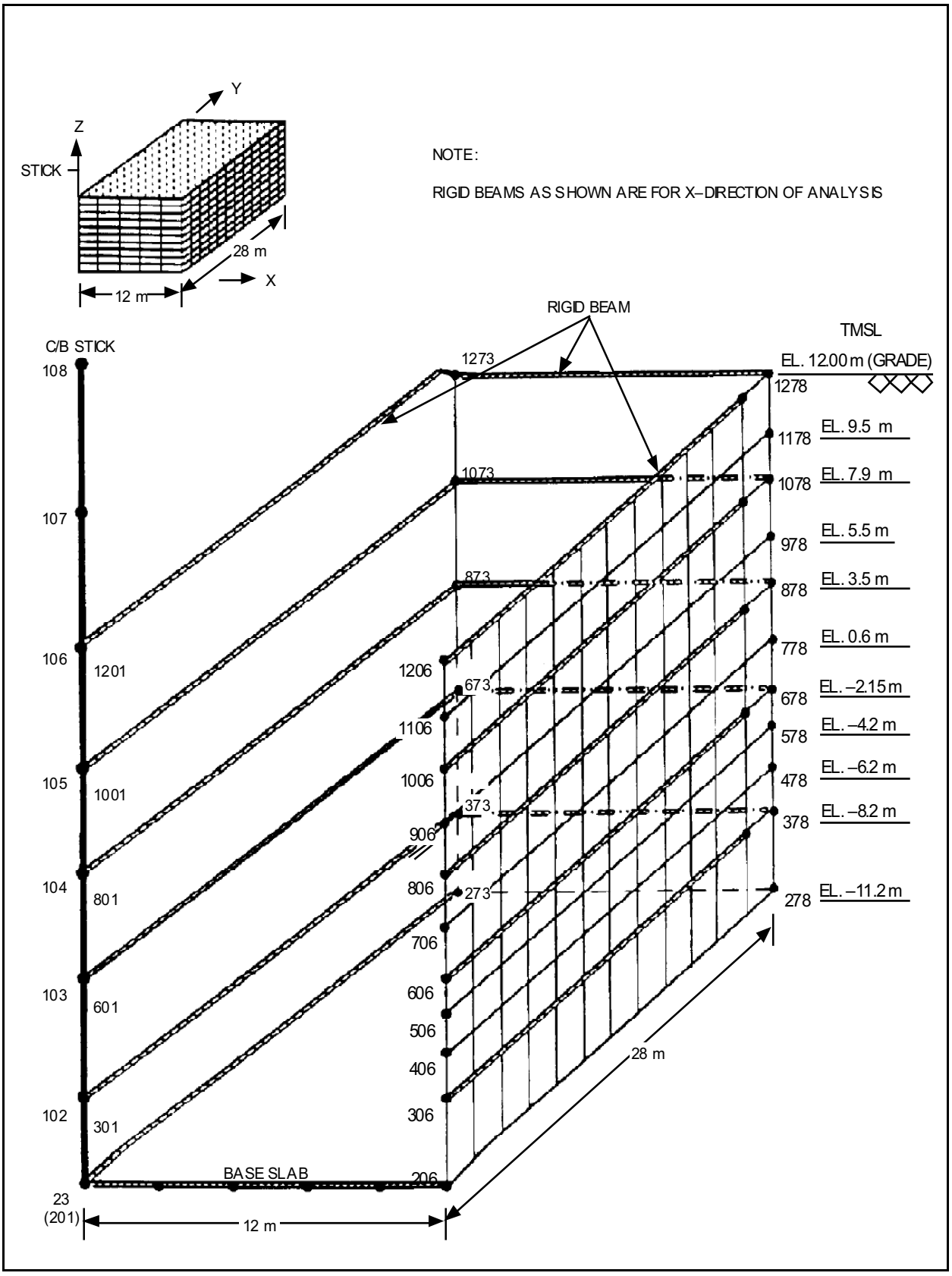

Figure 3A-31 Connection of the Main Stick to the Side Wall (Control Building for UB Soil Profiles)

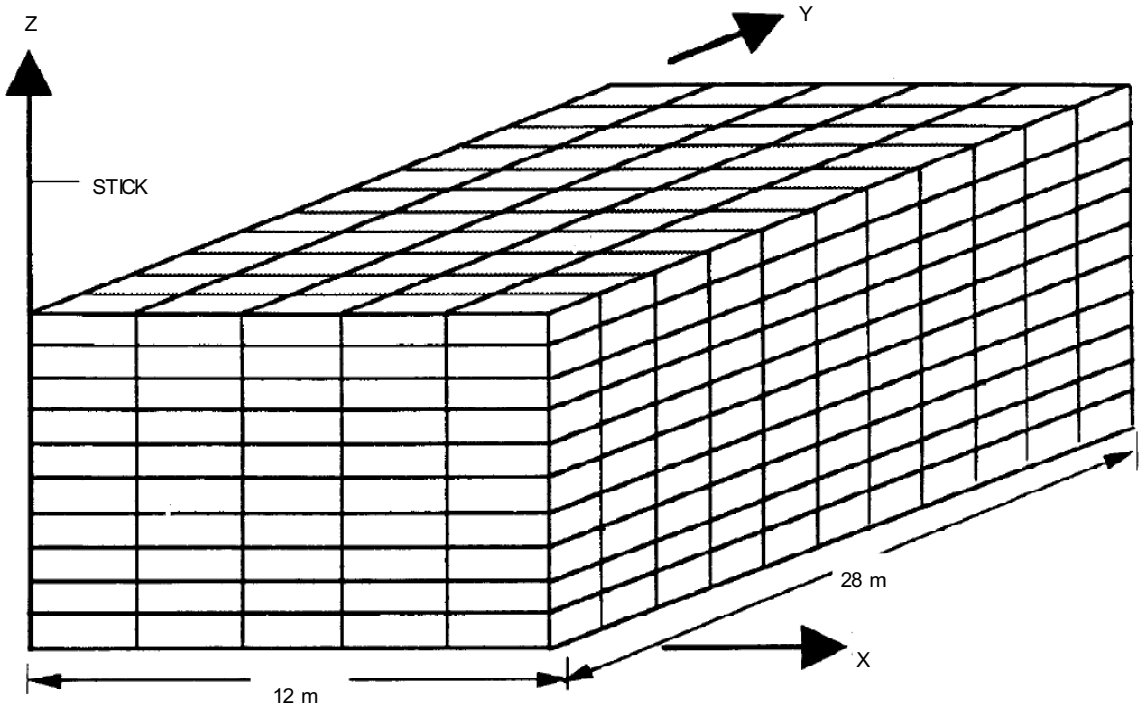

Figure 3A-32 C/B Excavated Soil Model (UB Soil Profiles)

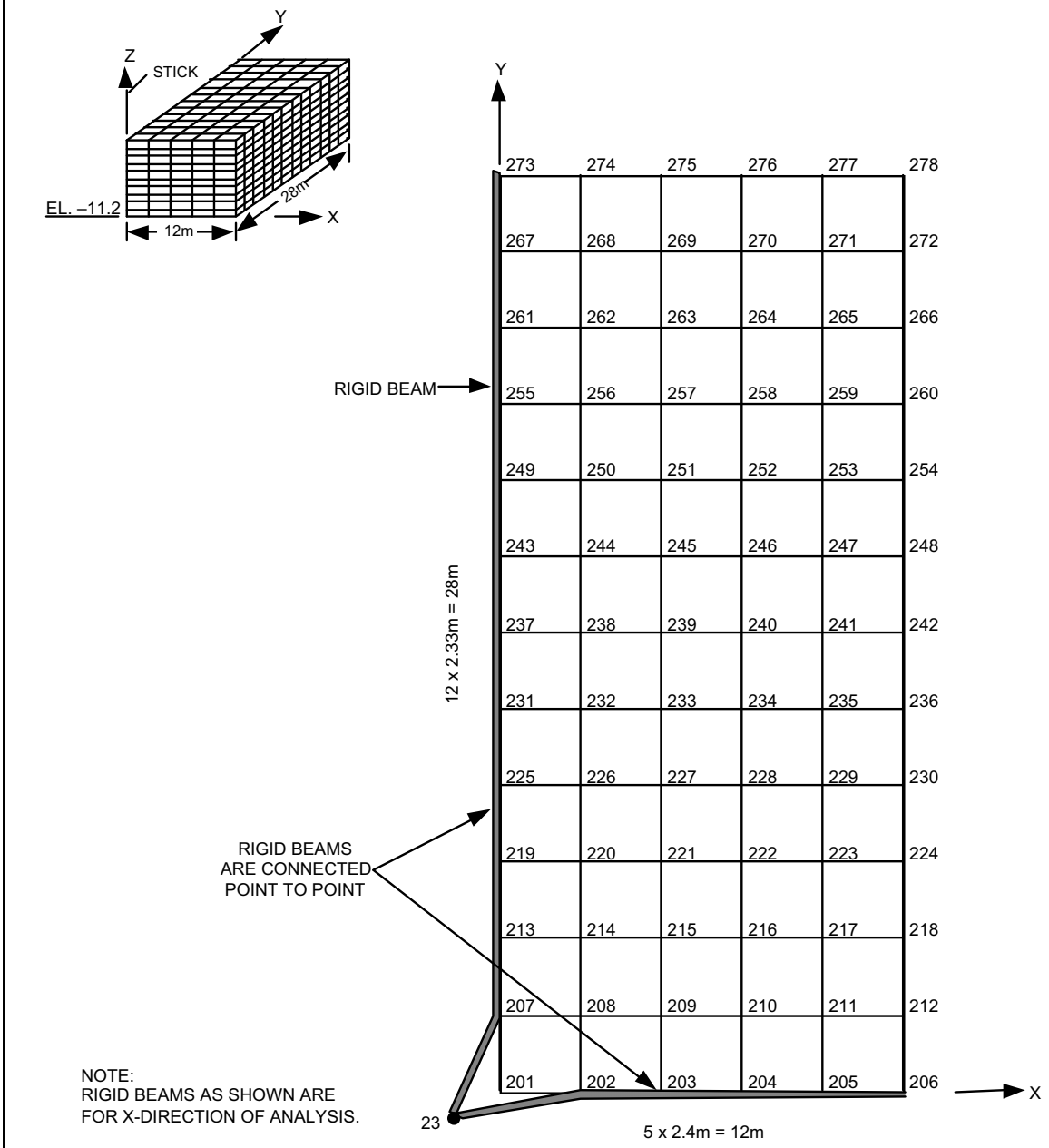

Figure 3A-33 UB Case: Nodal Points at Elevation –11.20m

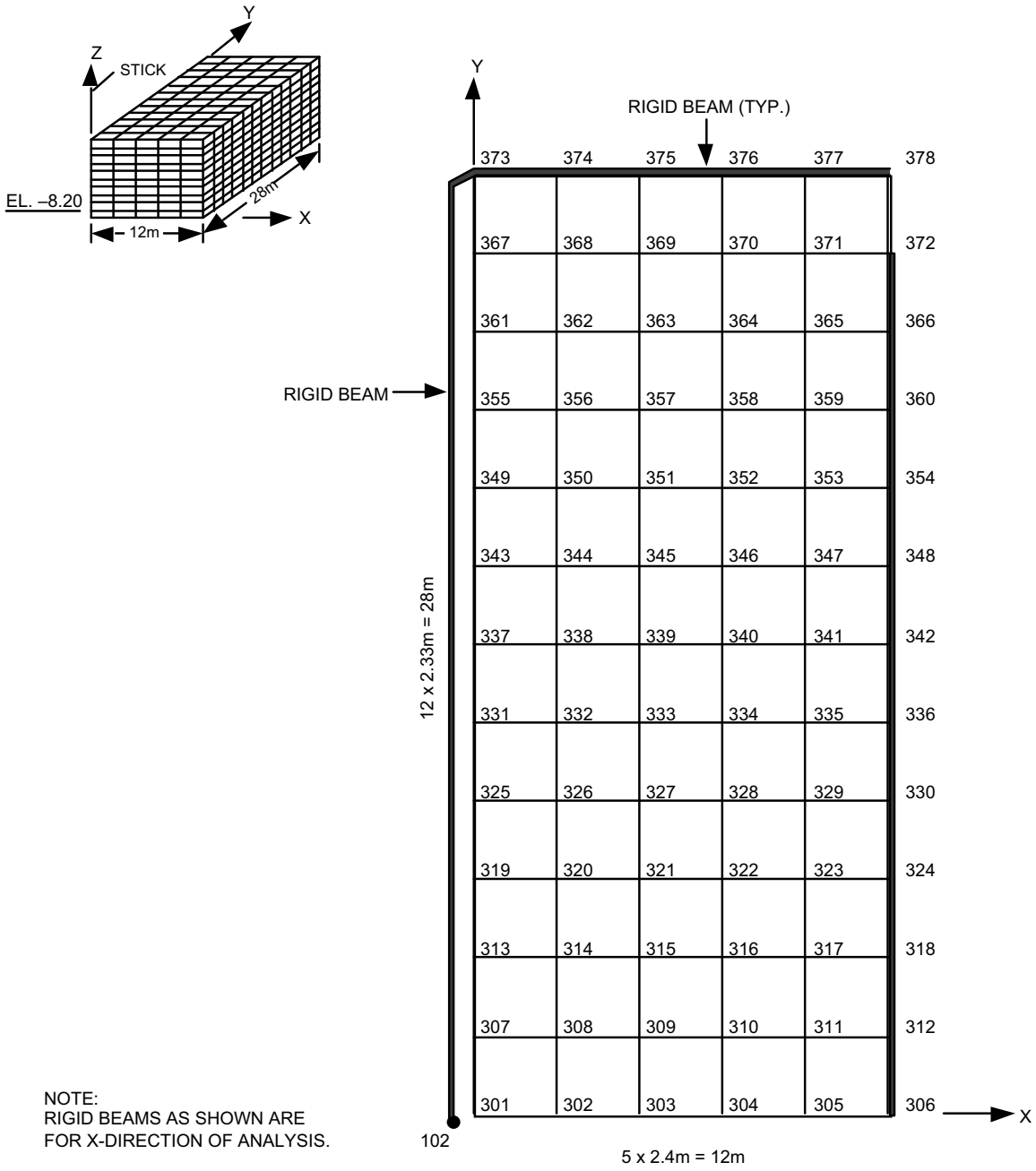

Figure 3A-34 UB Case: Nodal Points at Elevation –8.20m

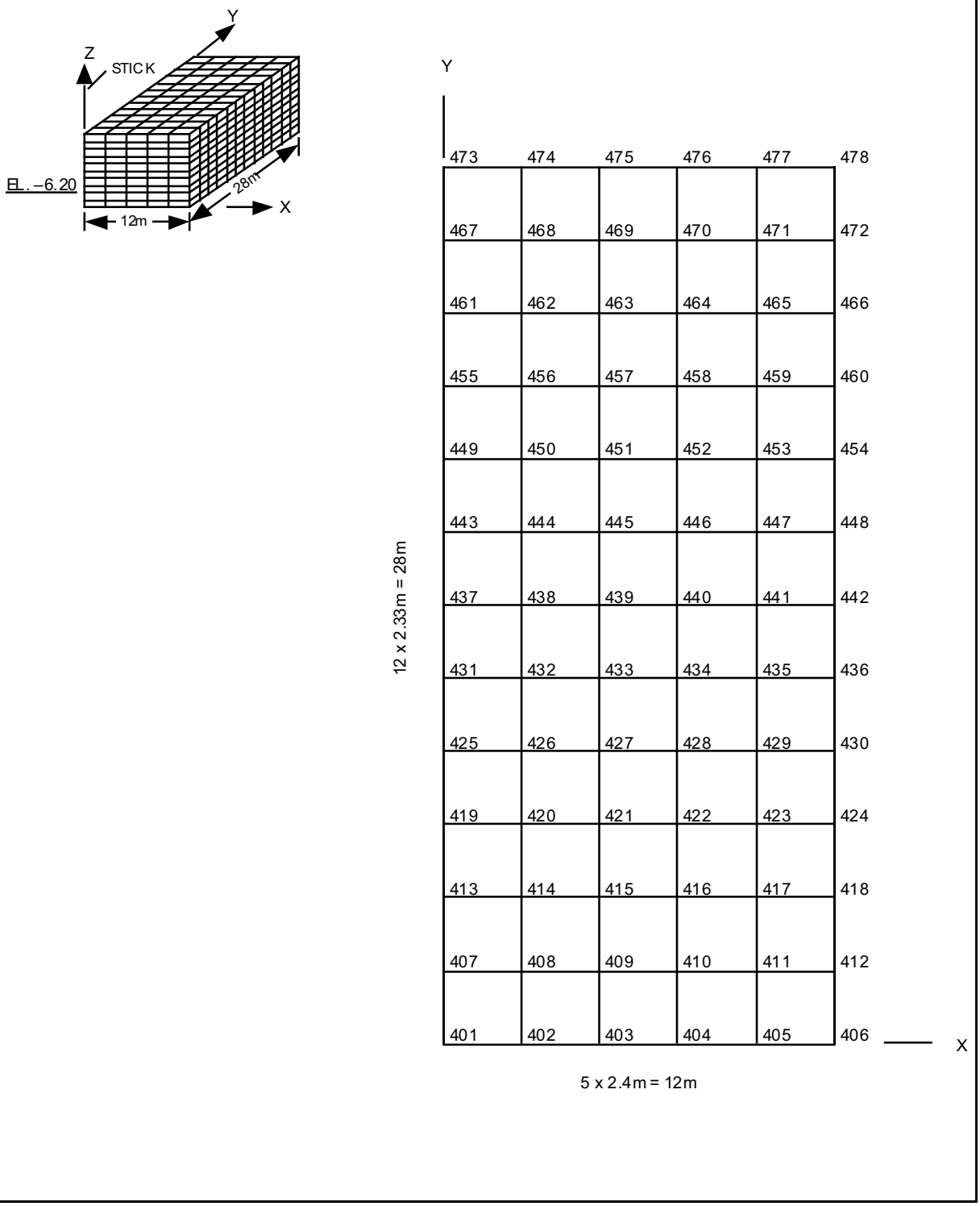

Figure 3A-35 UB Case: Nodal Points at Elevation –6.20m

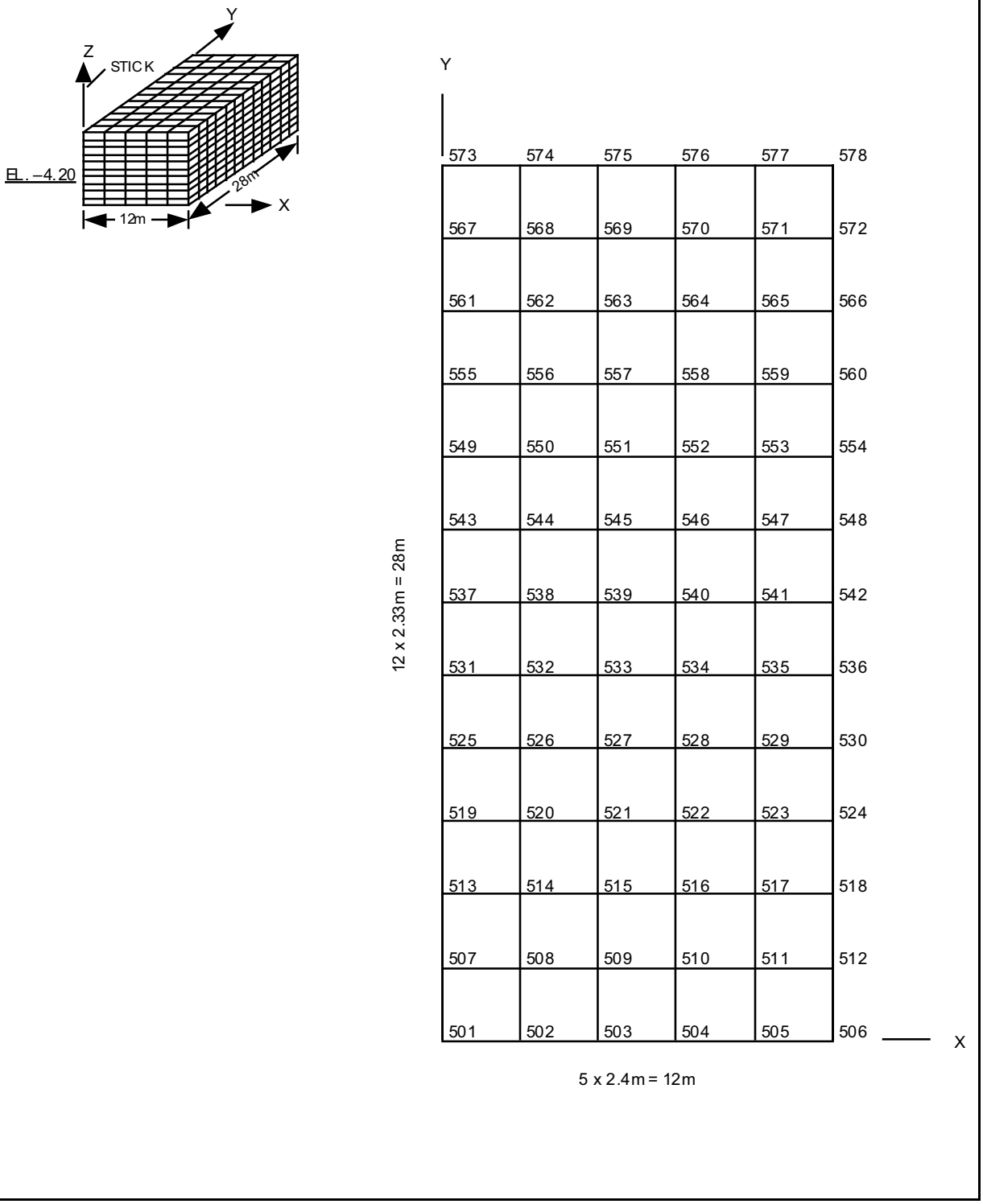

Figure 3A-36 UB Case: Nodal Points at Elevation –4.20m

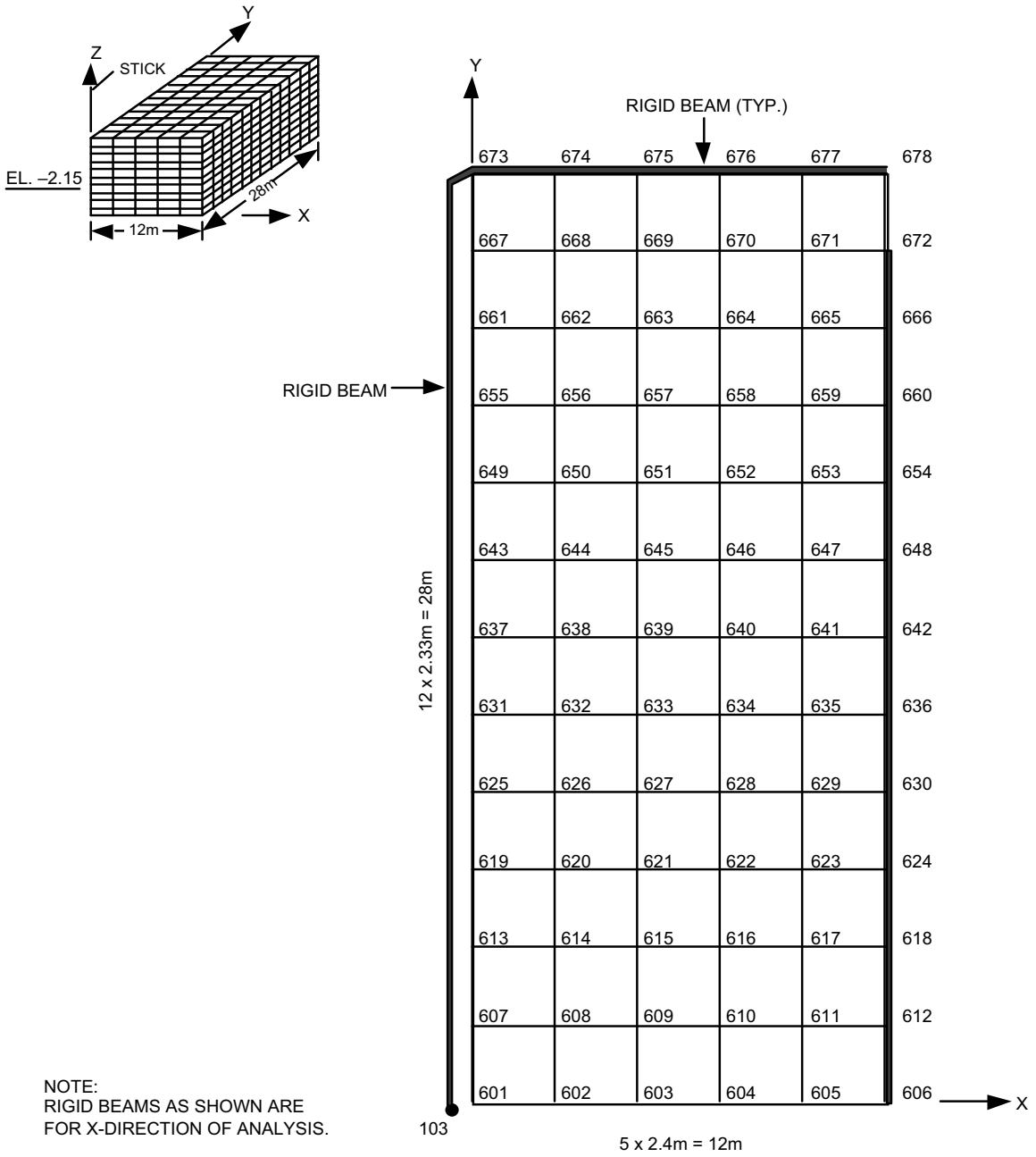

Figure 3A-37 UB Case: Nodal Points at Elevation –2.15m

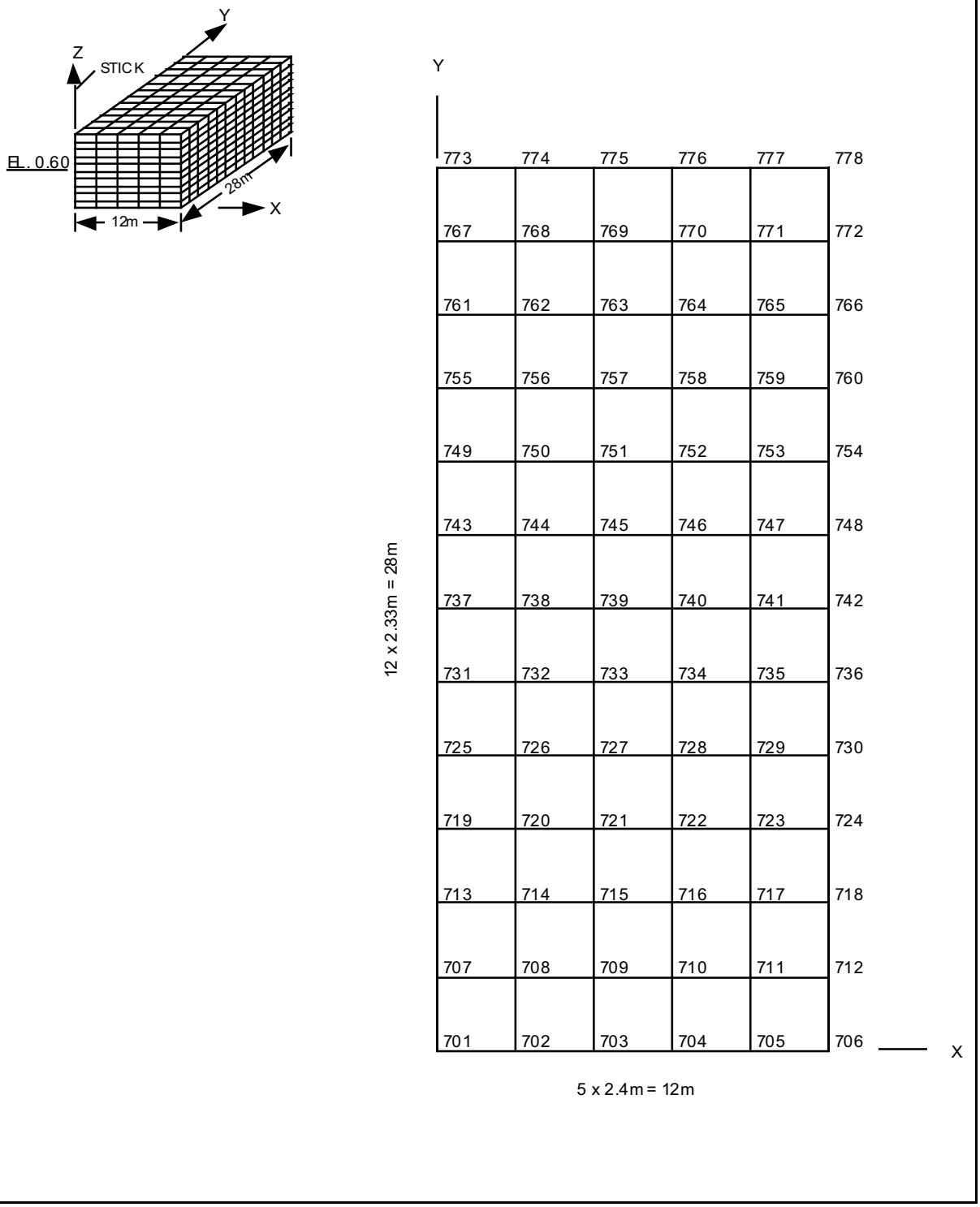

Figure 3A-38 UB Case: Nodal Points at Elevation 0.60m

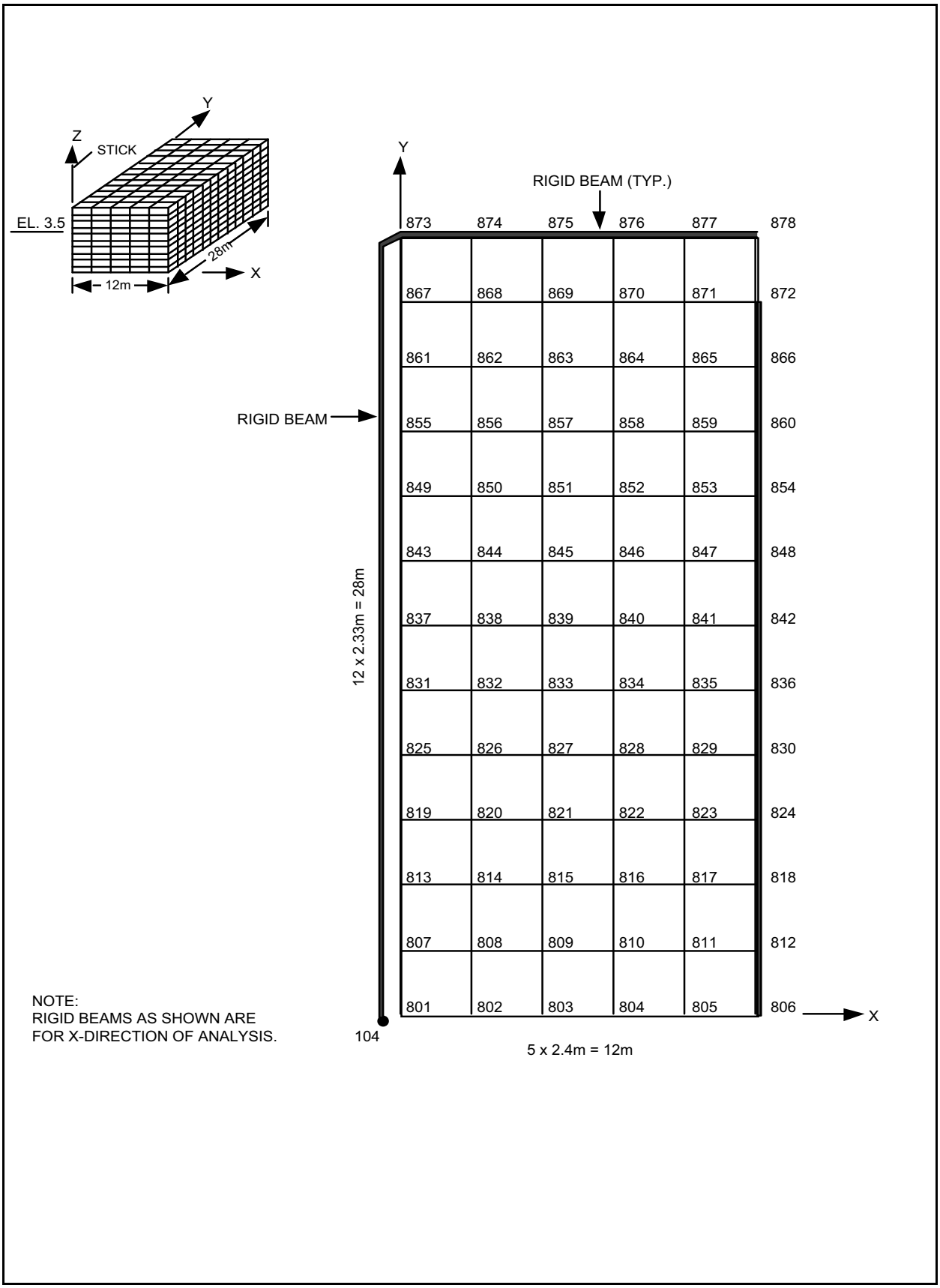

Figure 3A-39 UB Case: Nodal Points at Elevation 3.50m

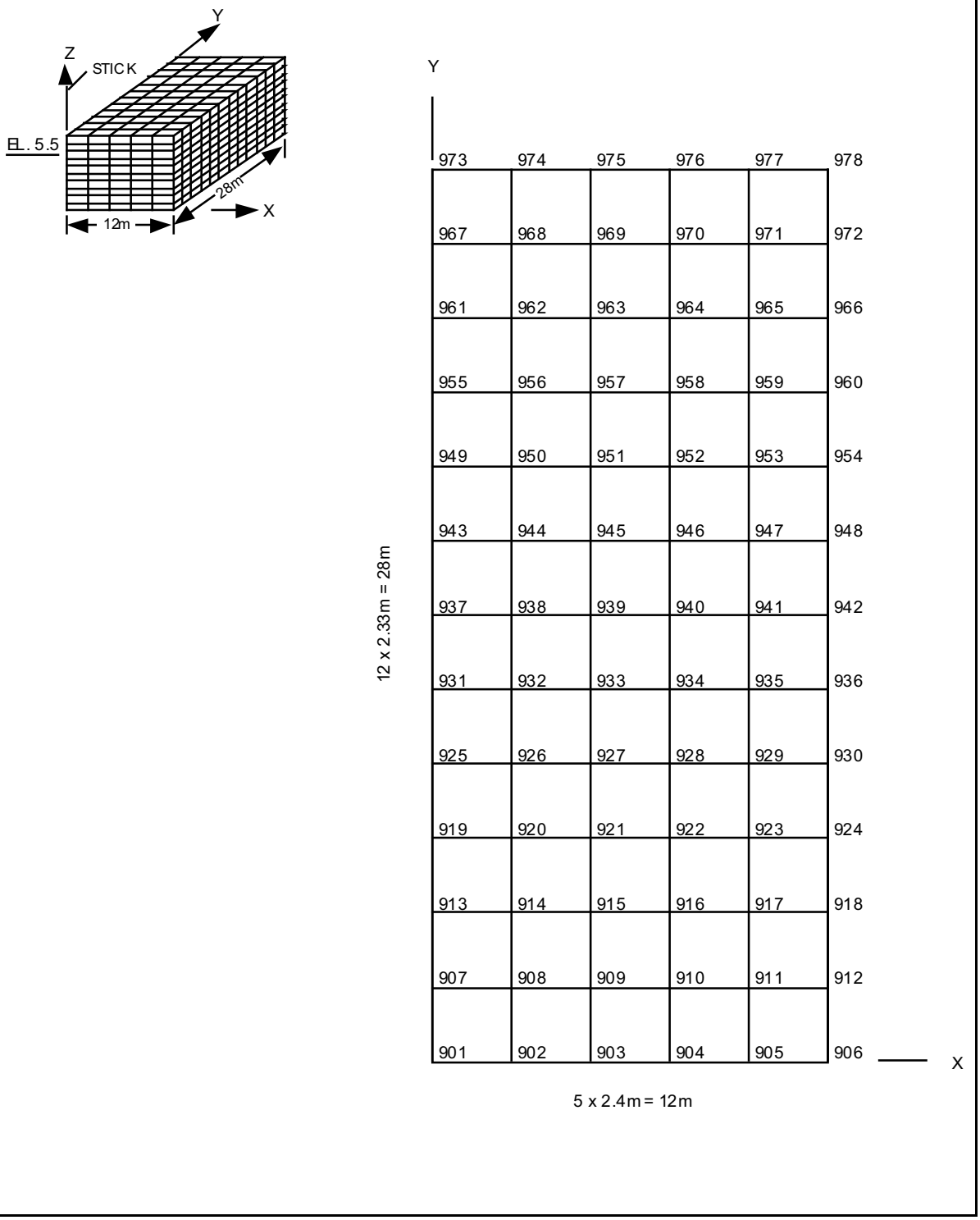

Figure 3A-40 UB Case: Nodal Points at Elevation 5.50m

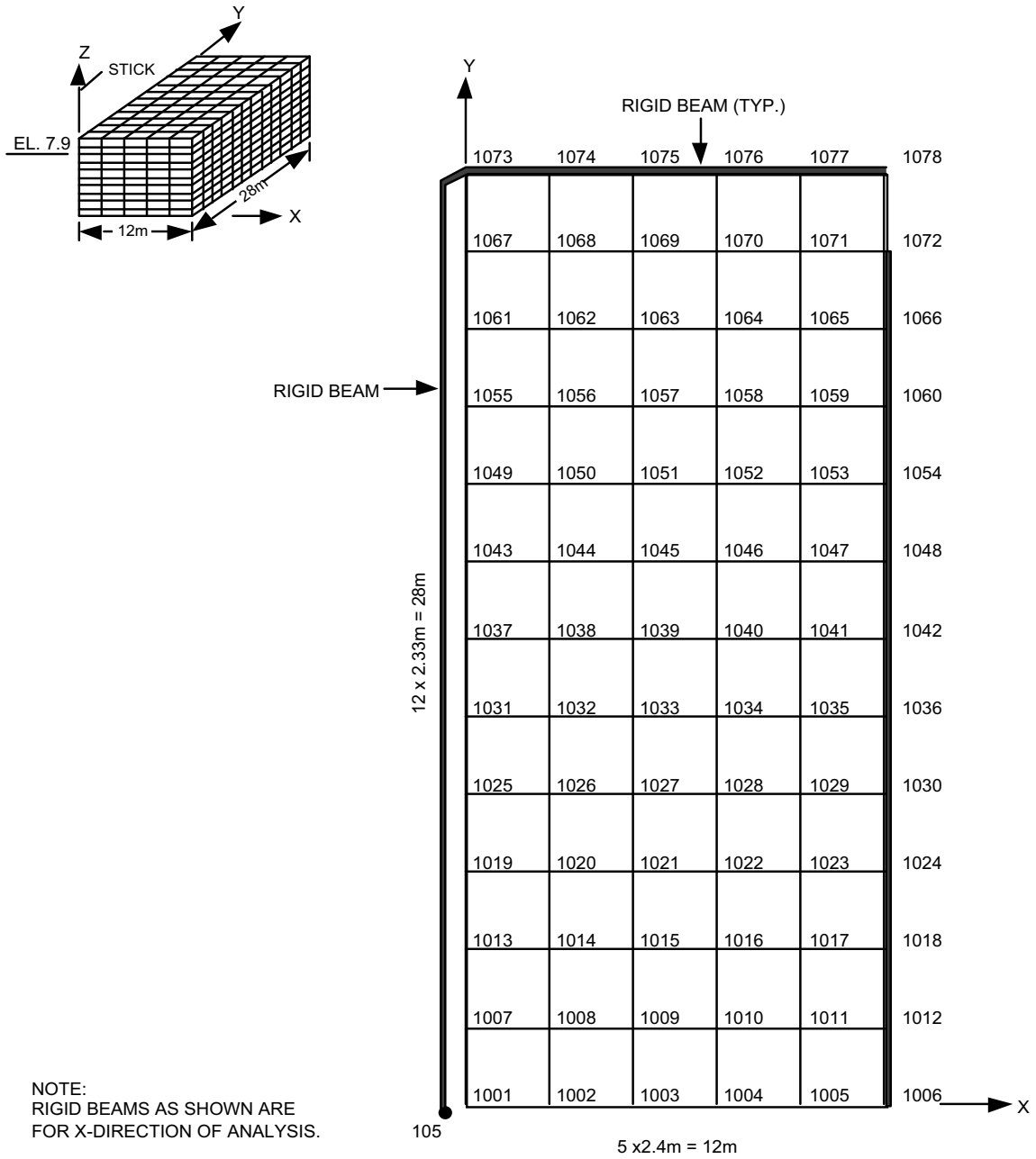

Figure 3A-41 UB Case: Nodal Points at Elevation 7.90m

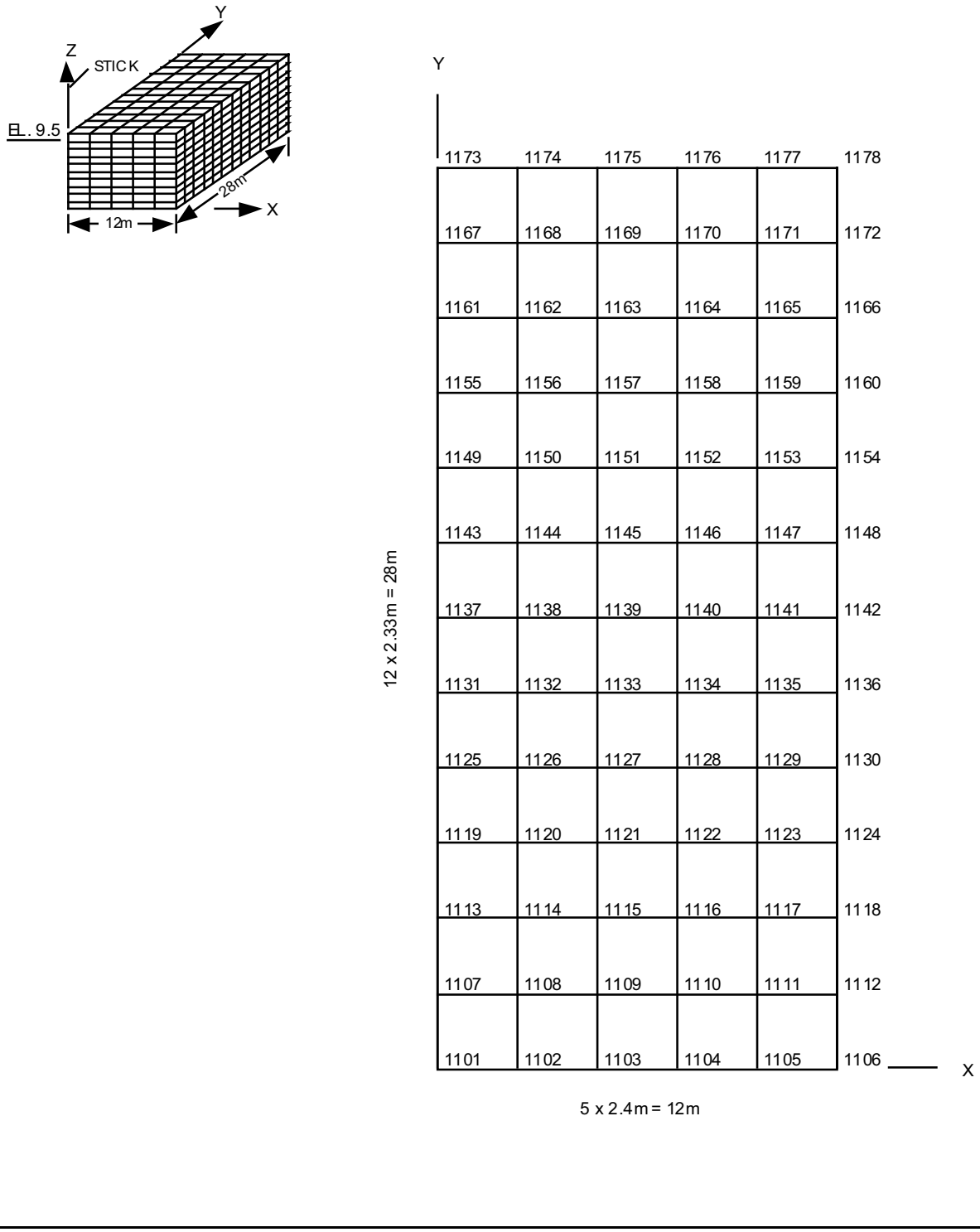

Figure 3A-42 UB Case: Nodal Points at Elevation 9.50m

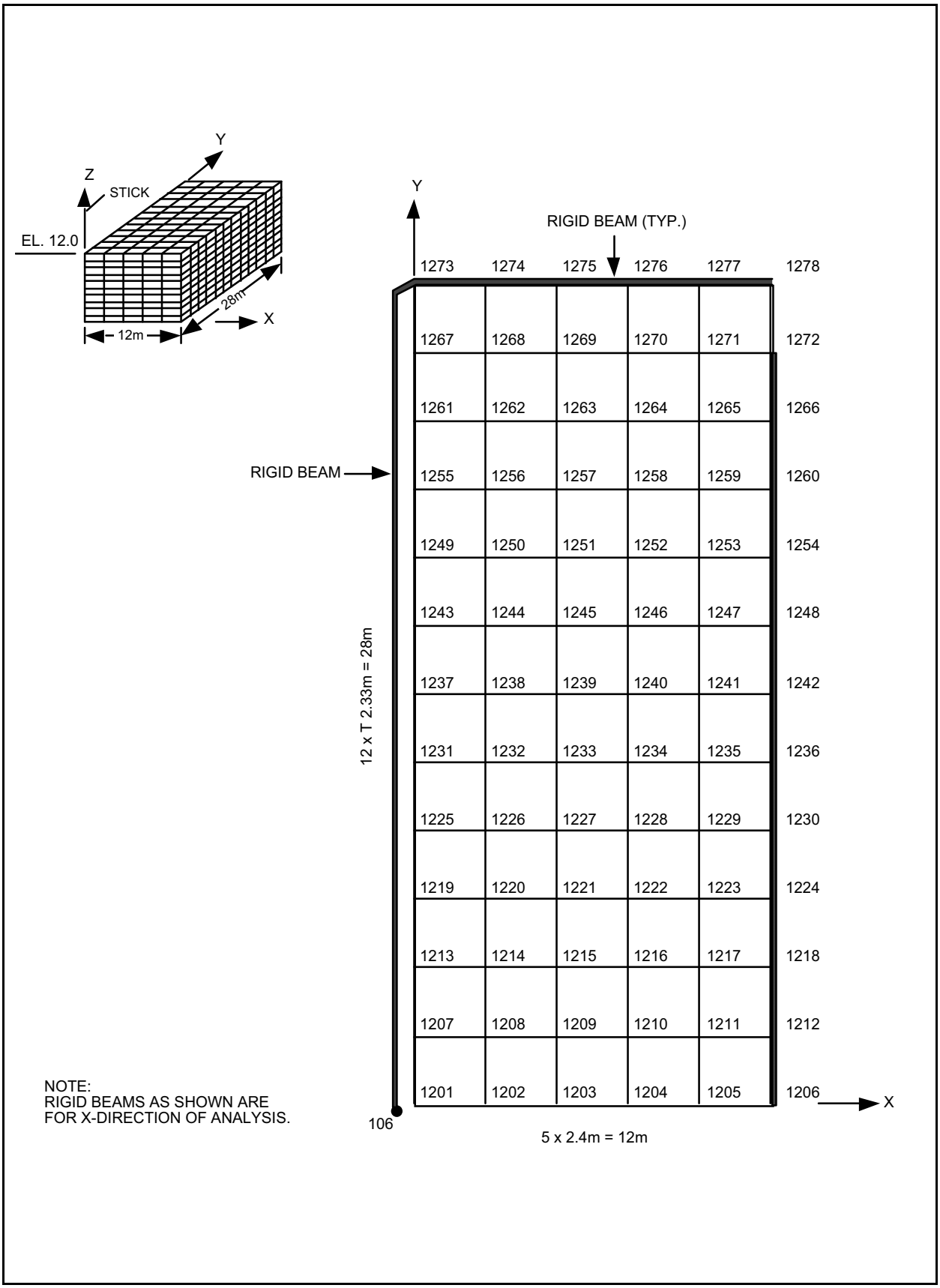

Figure 3A-43 UB Case: Nodal Points at Elevation 12.00m

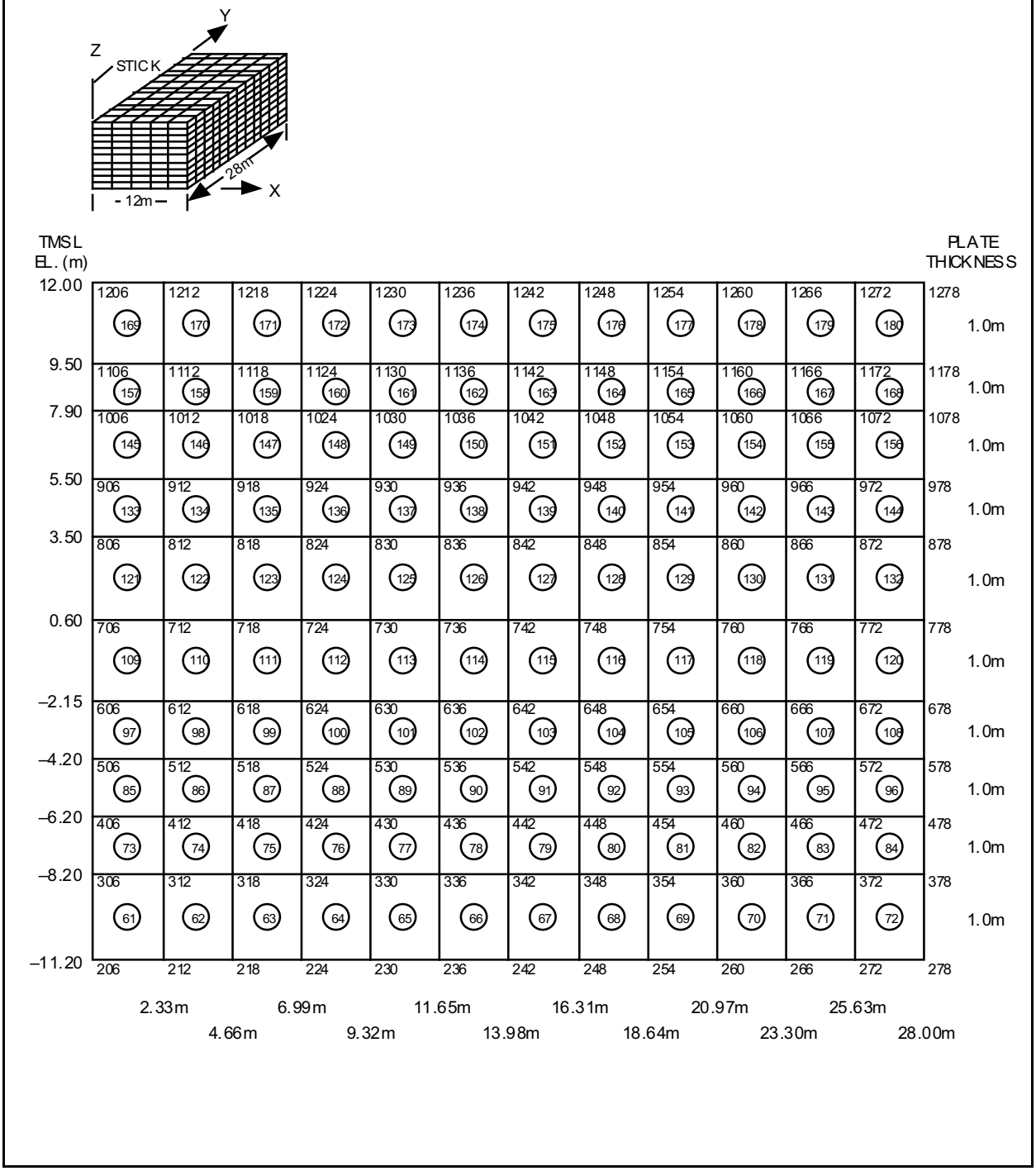

Figure 3A-44 Plate Elements of the Side Wall (X = 12.00m)

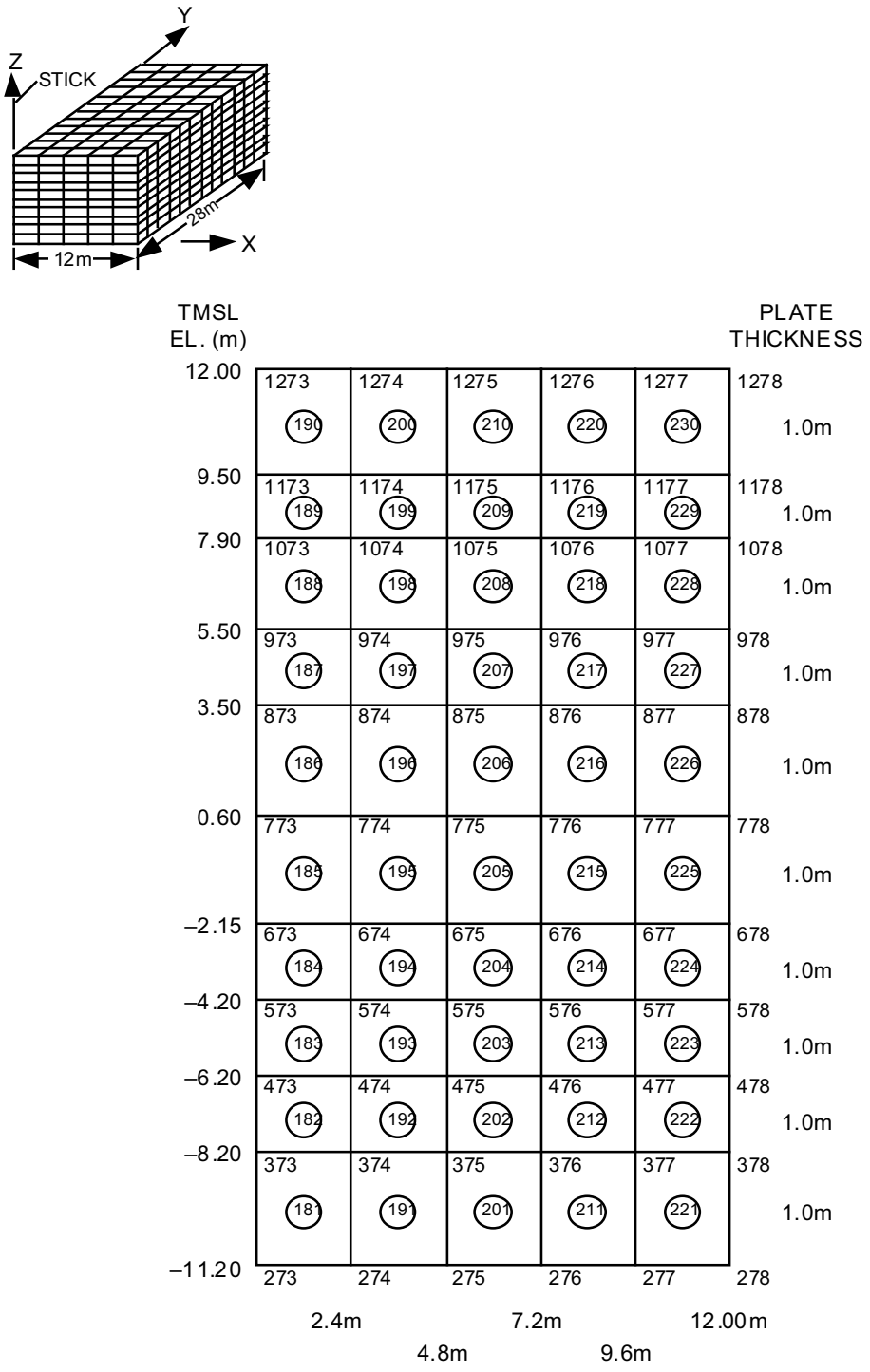

Figure 3A-45 Plate Elements of the Side Wall (Y = 28.00m)

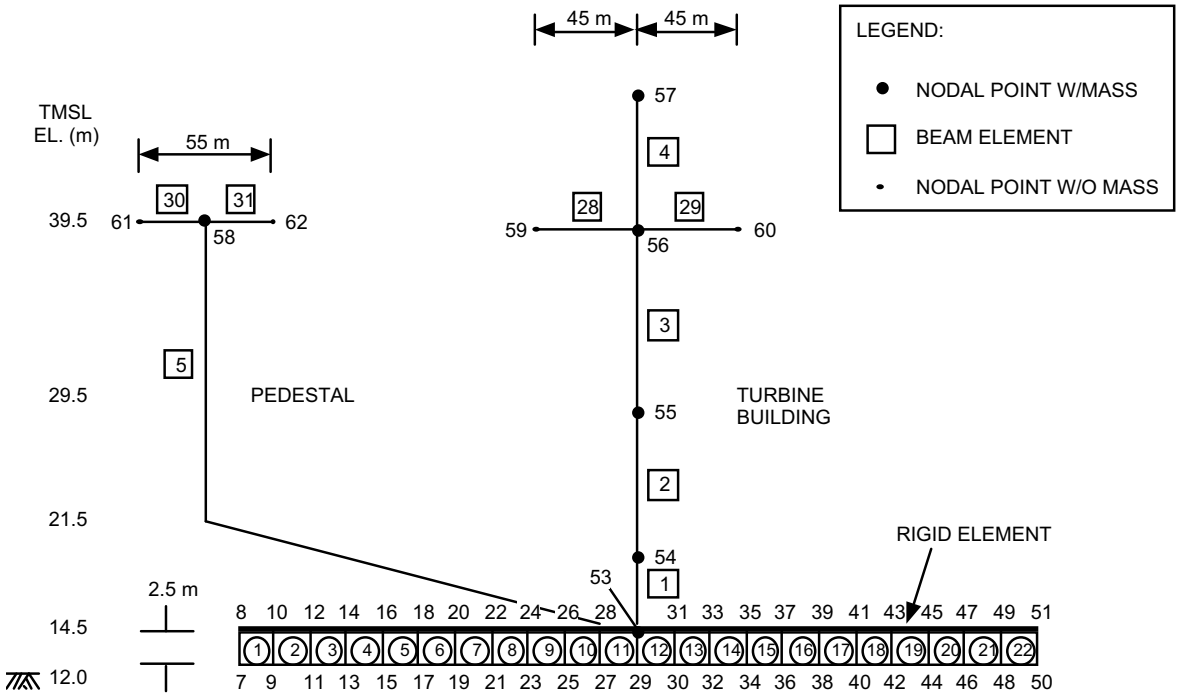

NOTE:

EXISTING STRUCTURE TO STRUCTURE SASSI 2D ANALYSIS USES THE NODE NUMBERS SHOWN ABOVE PLUS 2500 AS THE ACTUAL NODE NUMBERS.

Figure 3A-46 Turbine Building Model

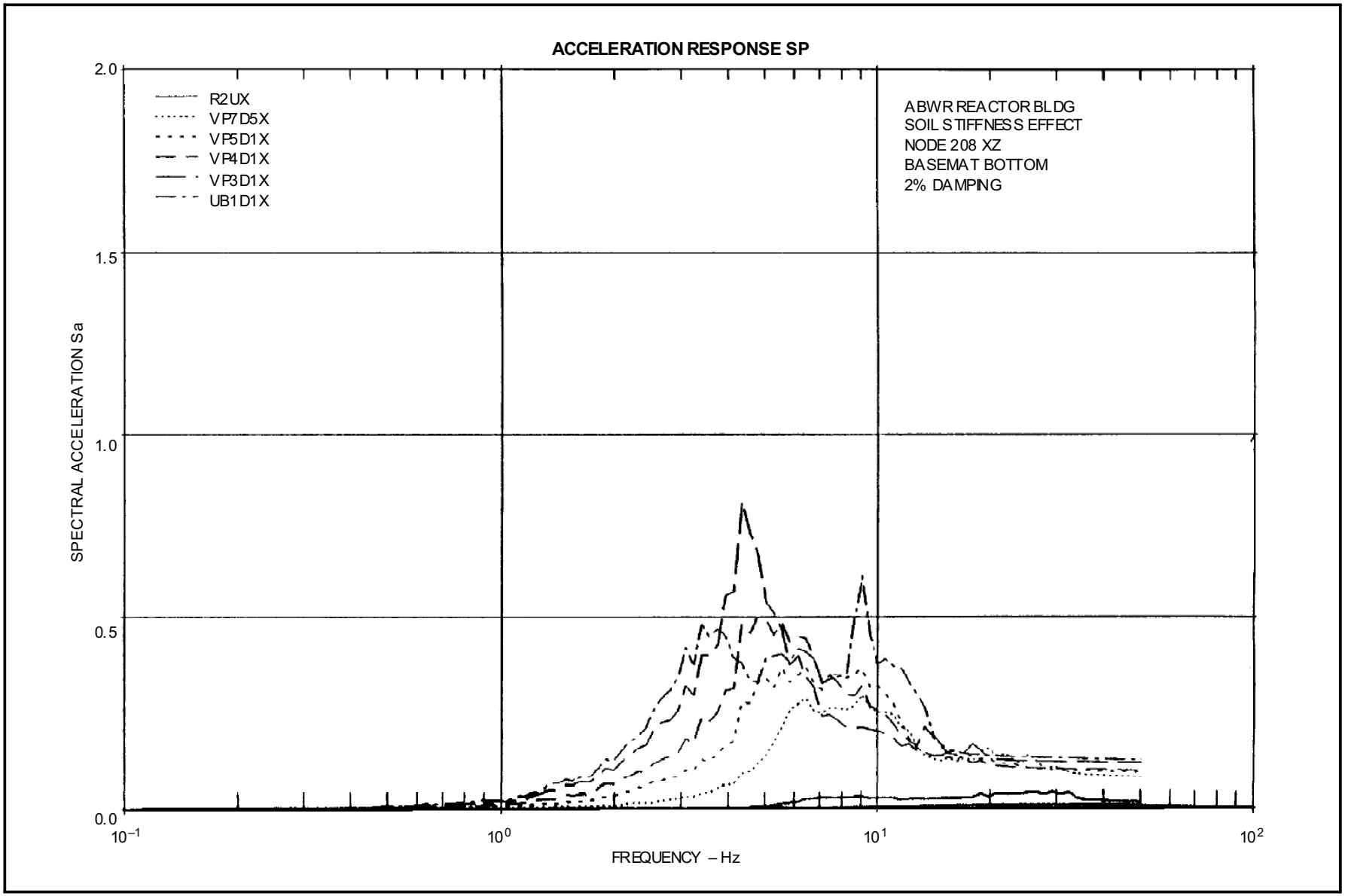

Figure 3A-47 ABWR Reactor Bldg. Soil Stiffness Effect, Node 208 XZ Basemat Bottom, 2% Damping

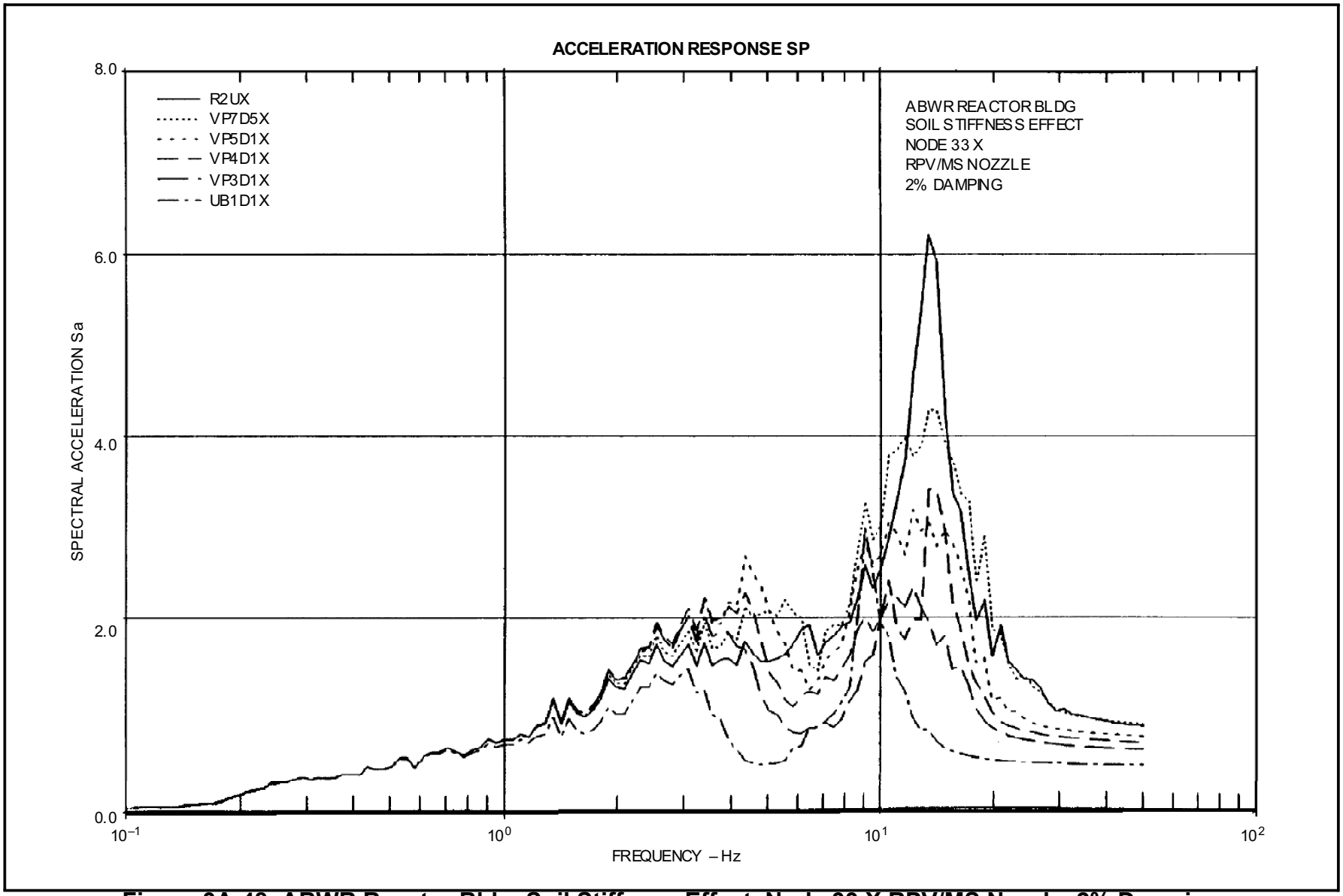

Figure 3A-48 ABWR Reactor Bldg. Soil Stiffness Effect, Node 33 X RPV/MS Nozzle, 2% Damping

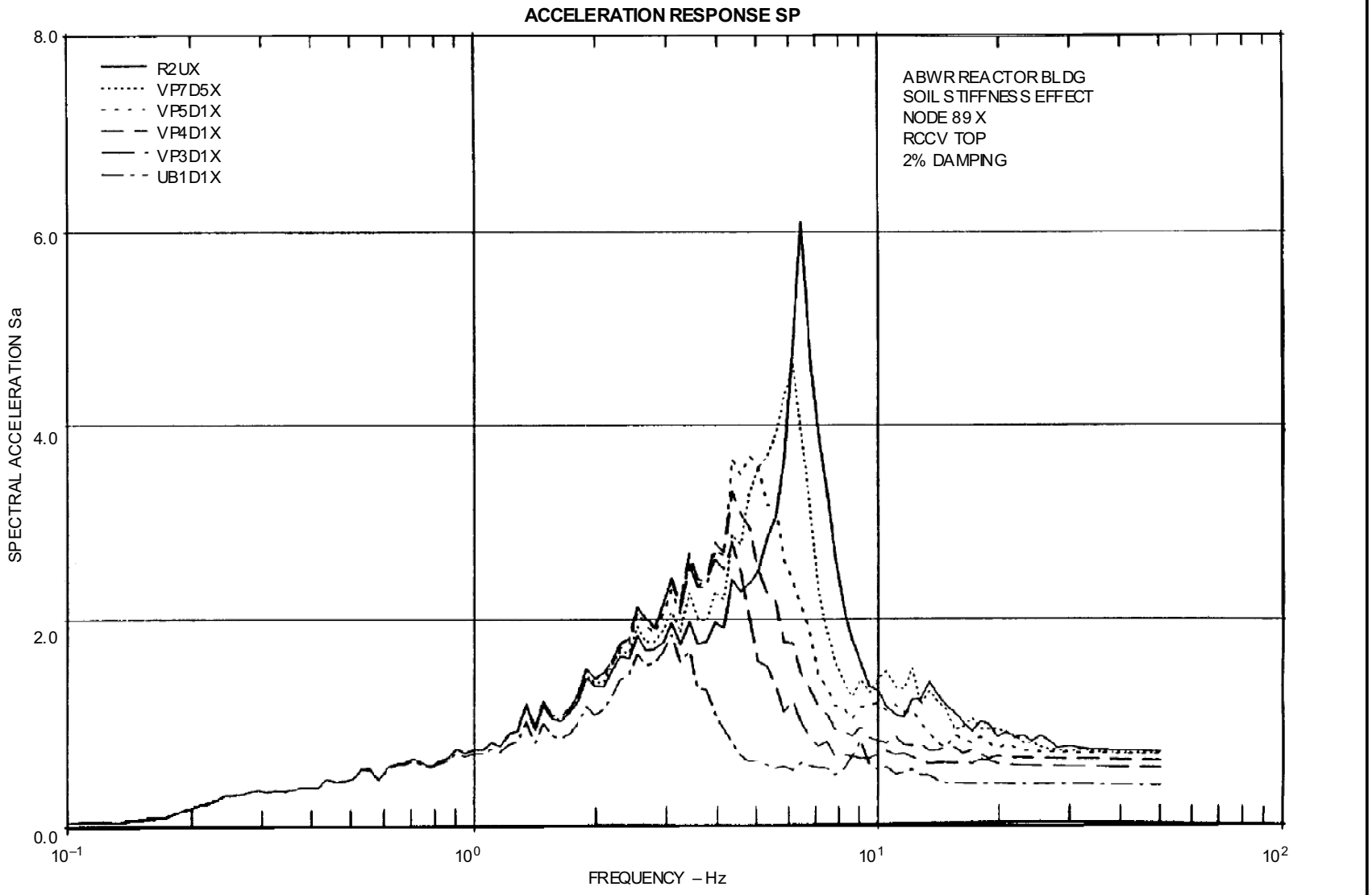

Figure 3A-49 ABWR Reactor Bldg. Soil Stiffness Effect, Node 89 X RCCV Top, 2% Damping

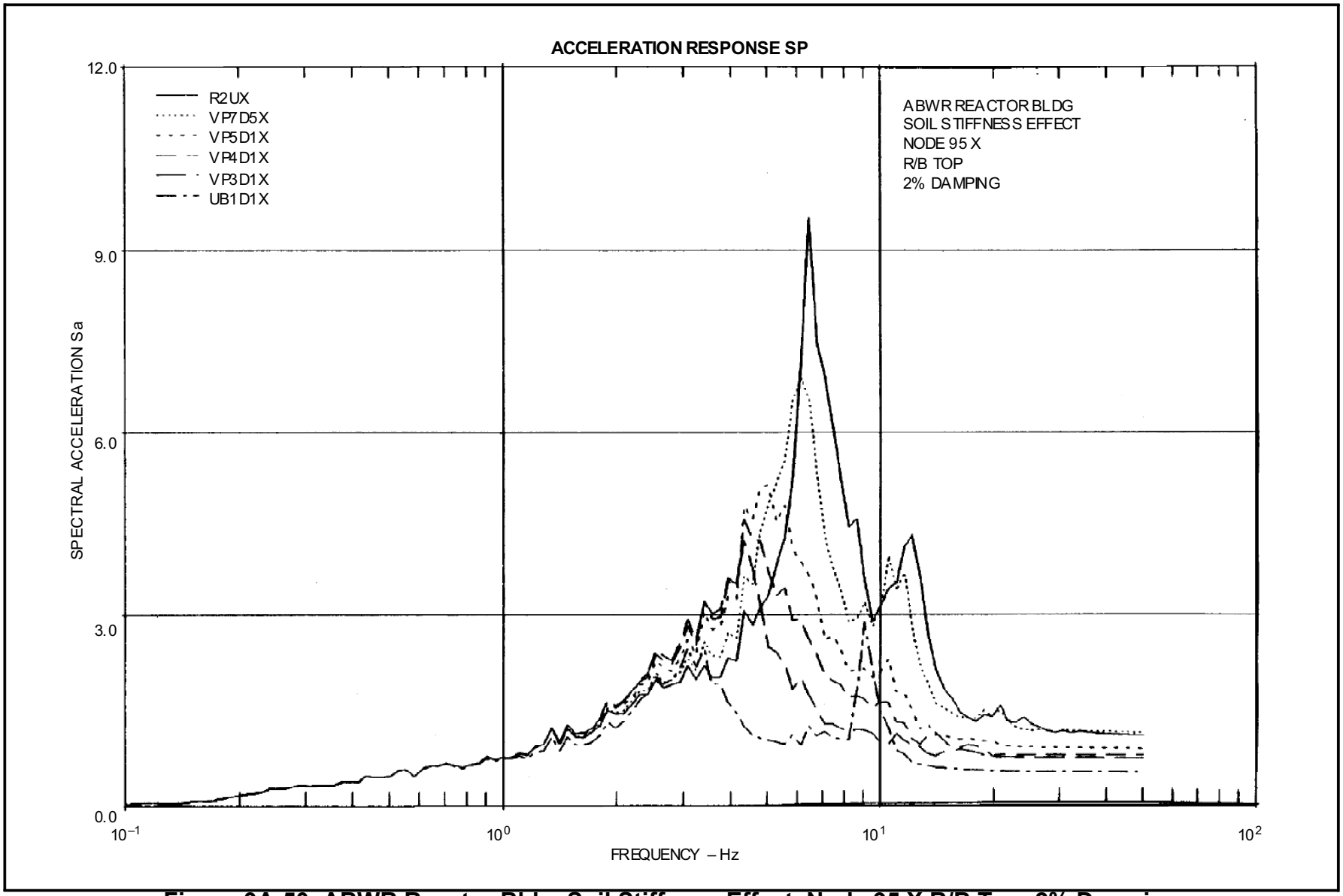

Figure 3A-50 ABWR Reactor Bldg. Soil Stiffness Effect, Node 95 X R/B Top, 2% Damping

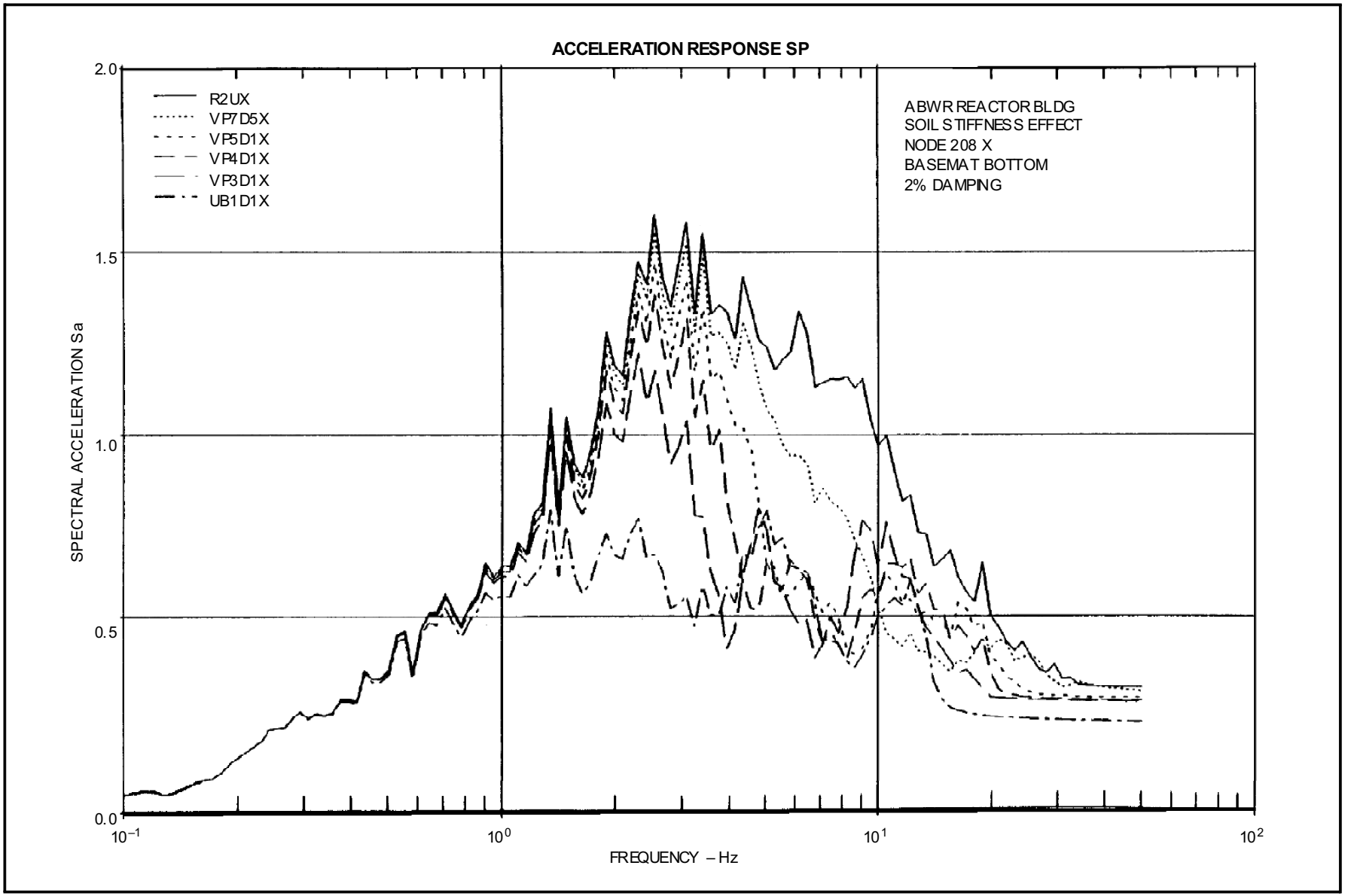

Figure 3A-51 ABWR Reactor Bldg. Soil Stiffness Effect, Node 208 X Basemat Bottom, 2% Damping

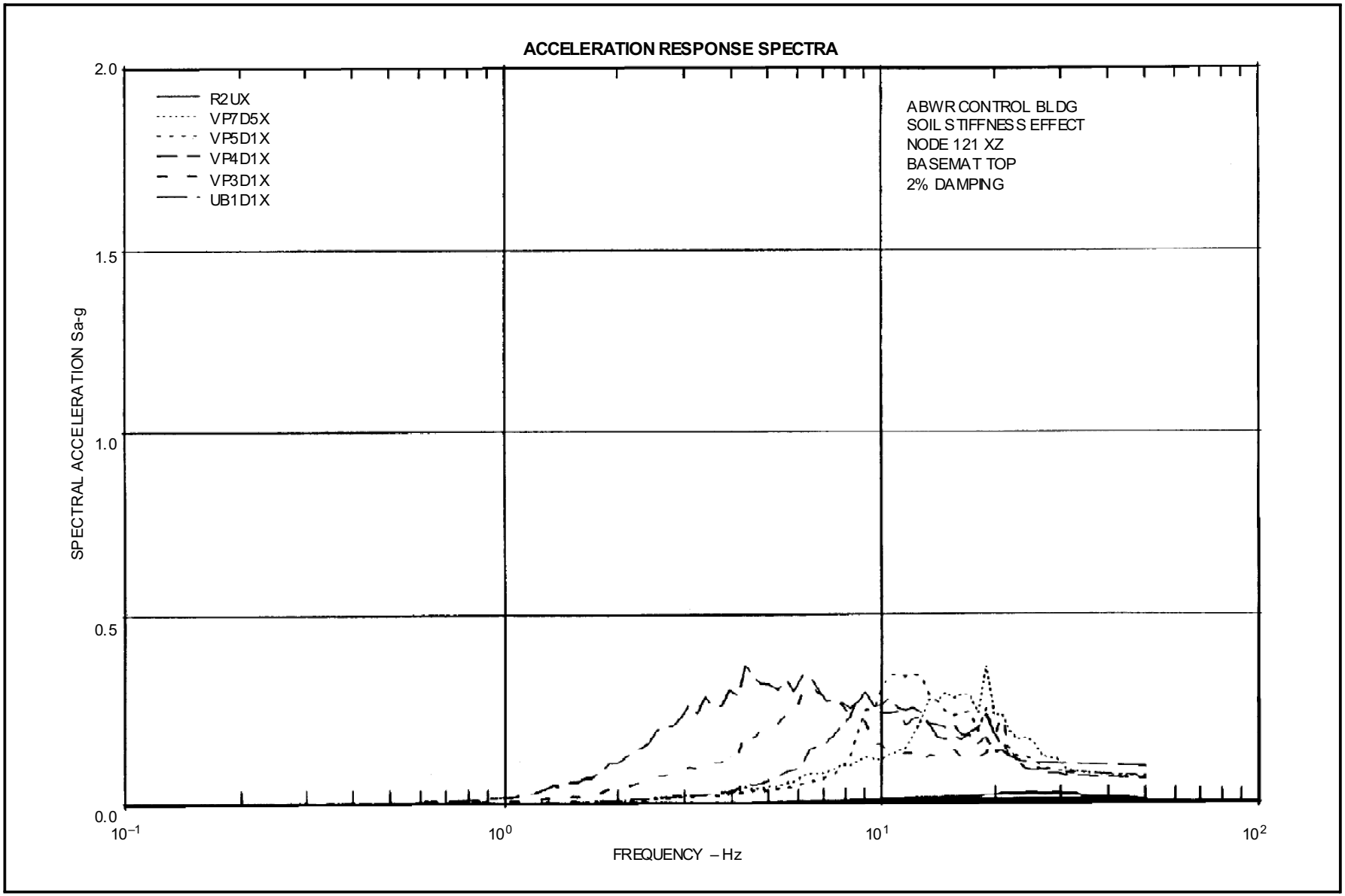

Figure 3A-52 ABWR Control Bldg. Soil Stiffness Effect, Node 121 XZ Basemat Top, 2% Damping

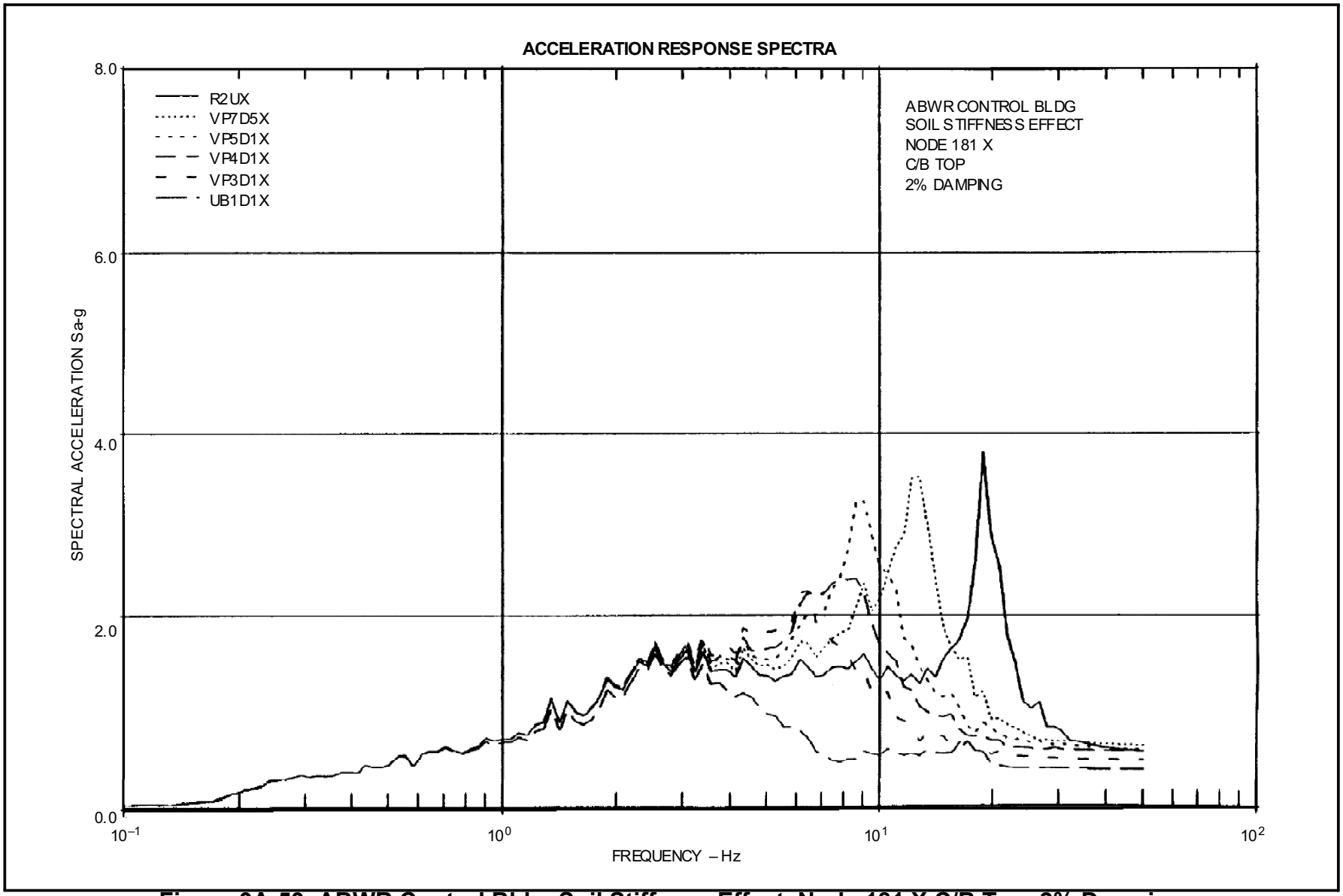

Figure 3A-53 ABWR Control Bldg. Soil Stiffness Effect, Node 181 X C/B Top, 2% Damping

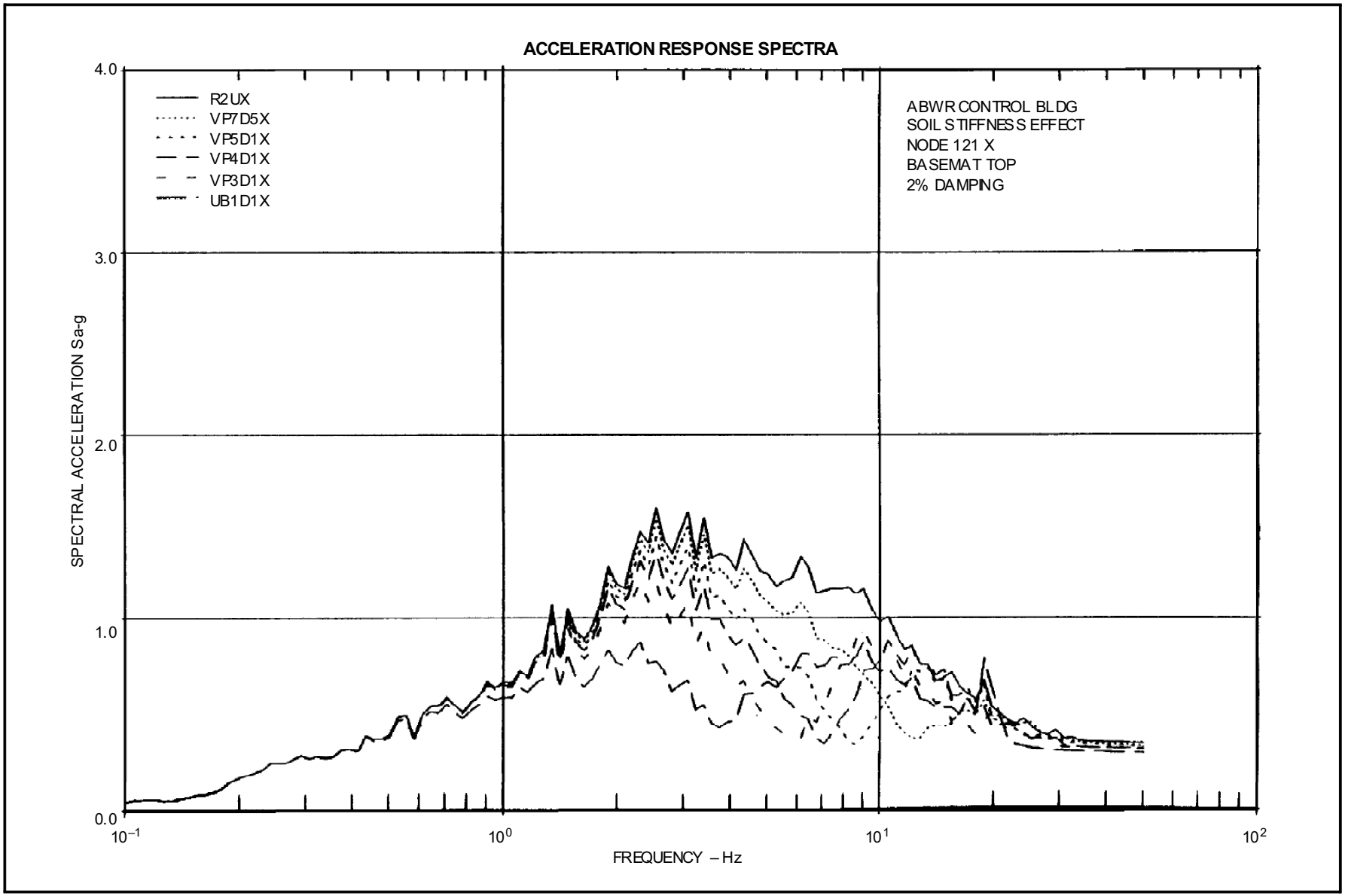

Figure 3A-54 ABWR Control Bldg. Soil Stiffness Effect, Node 121 X Basemat Top, 2% Damping

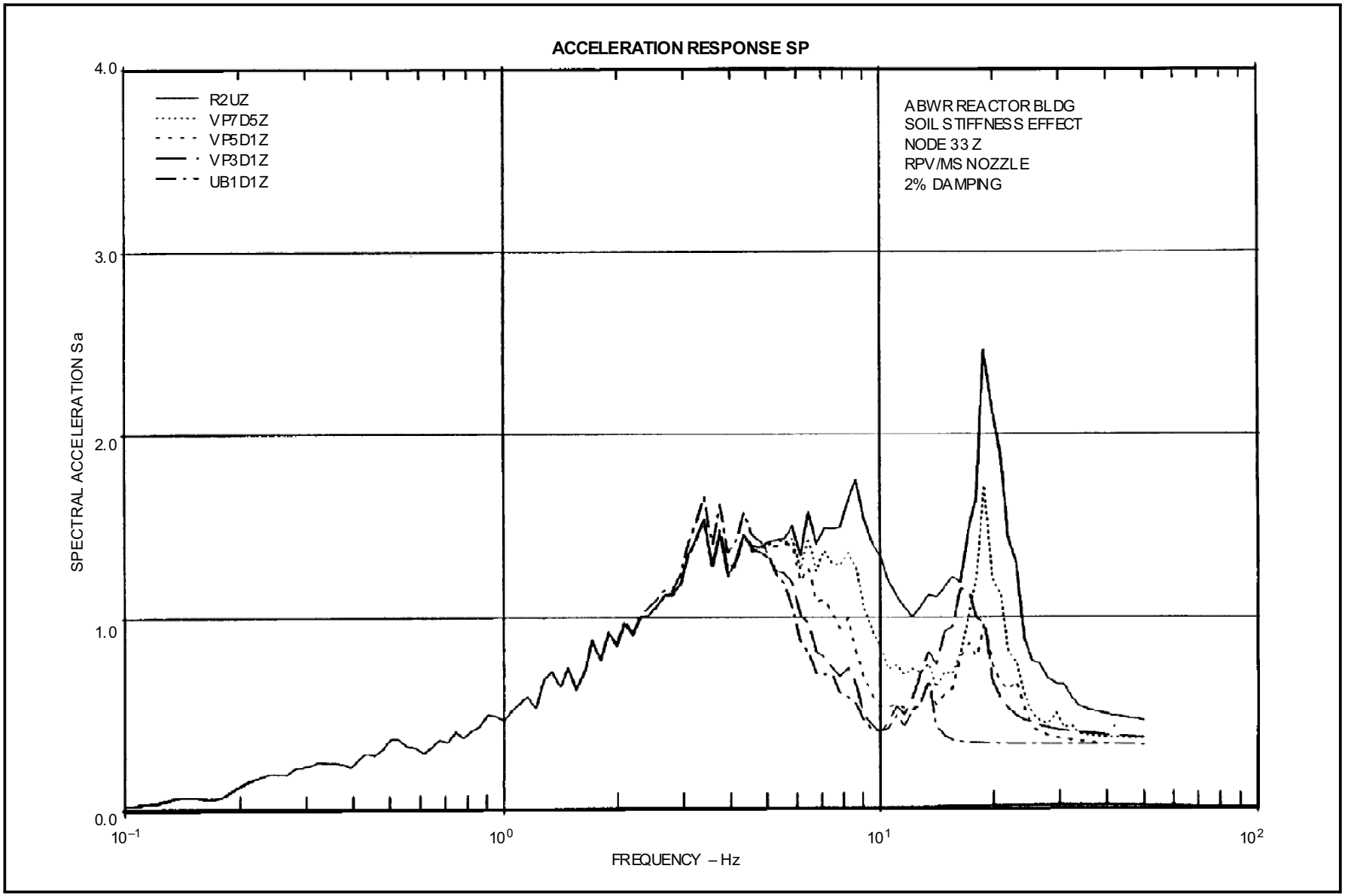

Figure 3A-55 ABWR Reactor Bldg. Soil Stiffness Effect, Node 33 Z RPV/MS Nozzle, 2% Damping

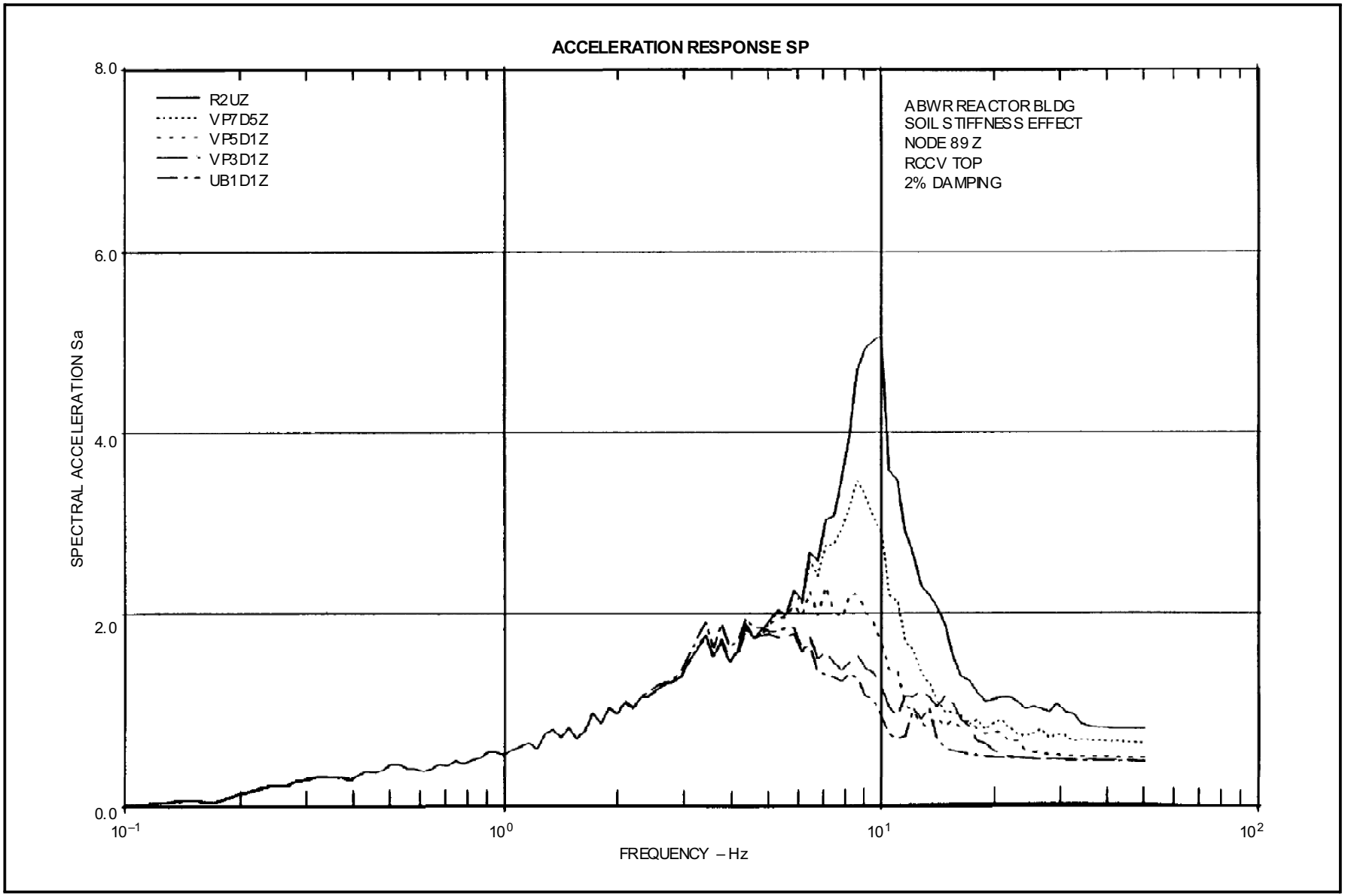

Figure 3A-56 ABWR Reactor Bldg. Soil Stiffness Effect, Node 89 Z RCCV Top, 2% Damping

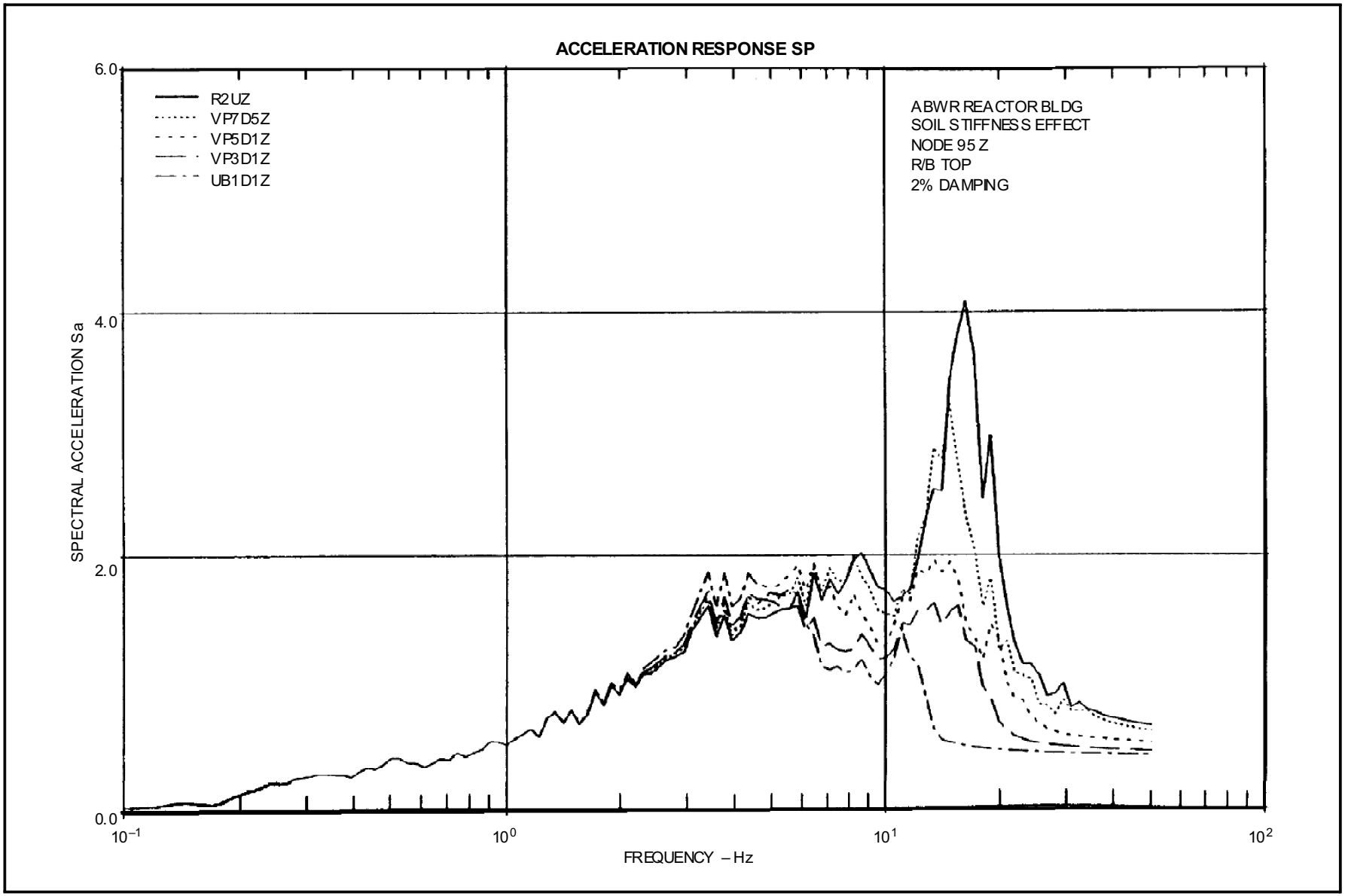

Figure 3A-57 ABWR Reactor Bldg. Soil Stiffness Effect, Node 95 Z R/B Top, 2% Damping

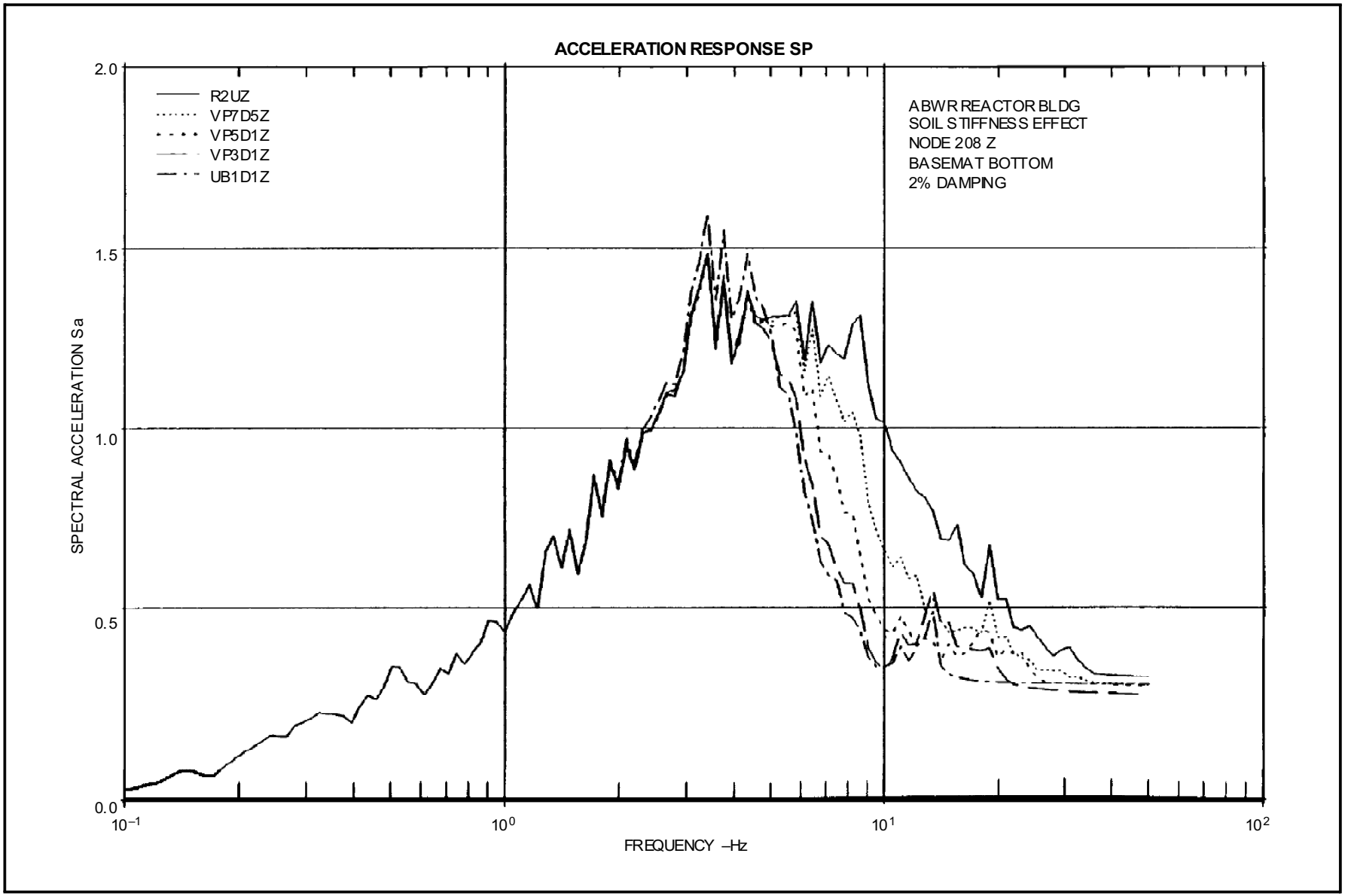

Figure 3A-58 ABWR Reactor Bldg. Soil Stiffness Effect, Node 208 Z Basemat Bottom, 2% Damping

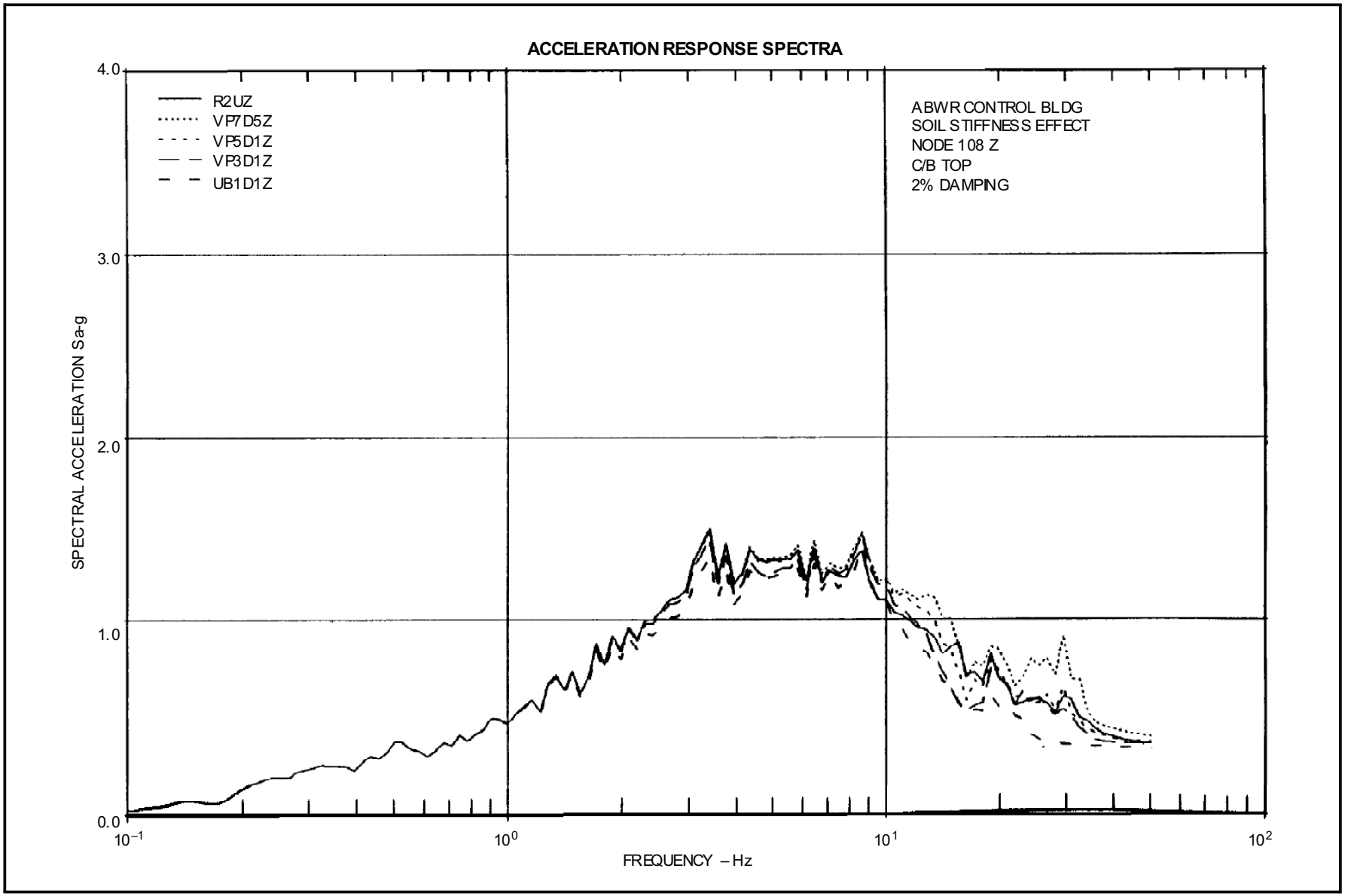

Figure 3A-59 ABWR Control Bldg. Soil Stiffness Effect, Node 108 Z C/B Top, 2% Damping

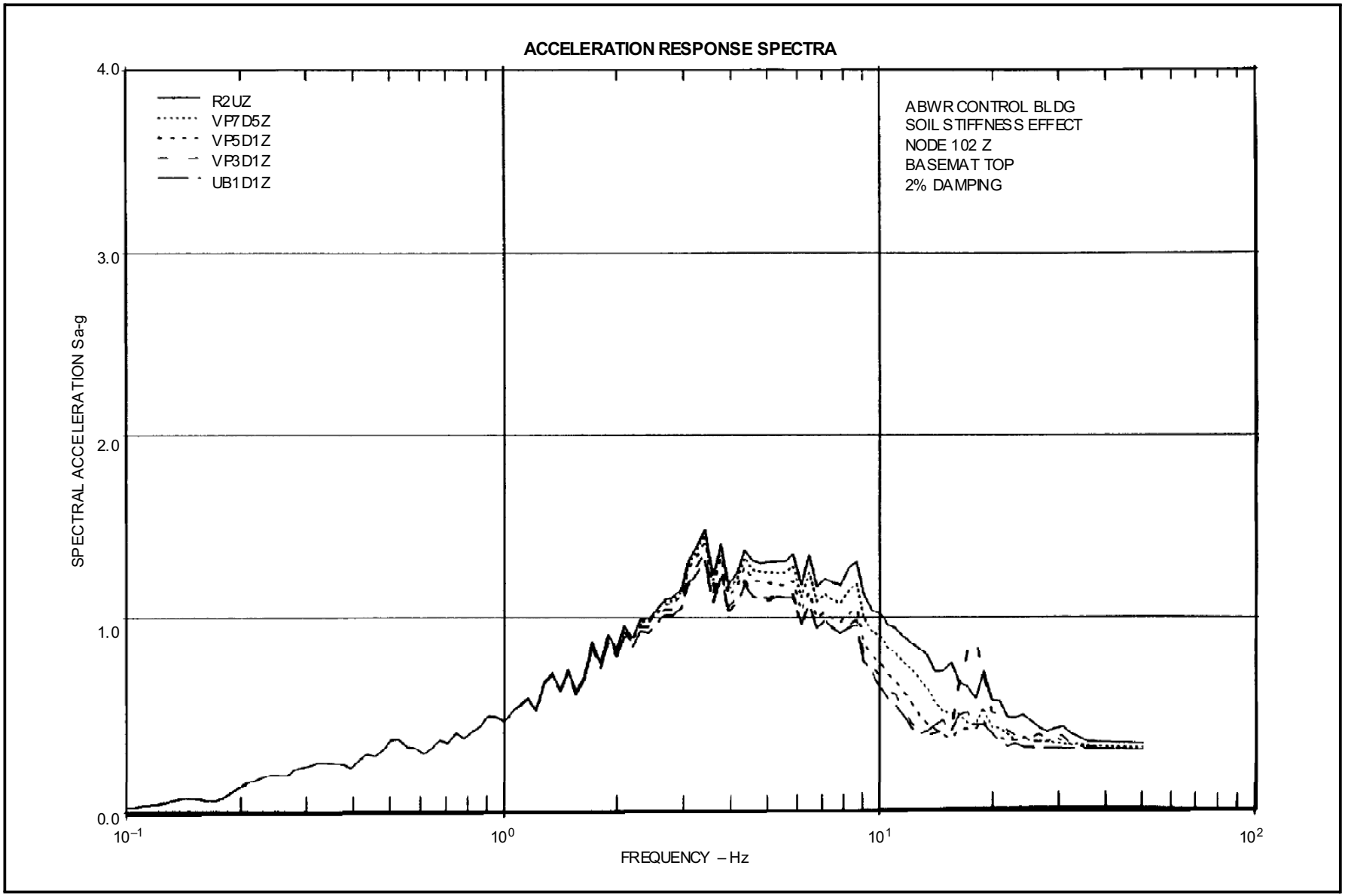

Figure 3A-60 ABWR Control Bldg. Soil Stiffness Effect, Node 102 Z Basemat Top, 2% Damping

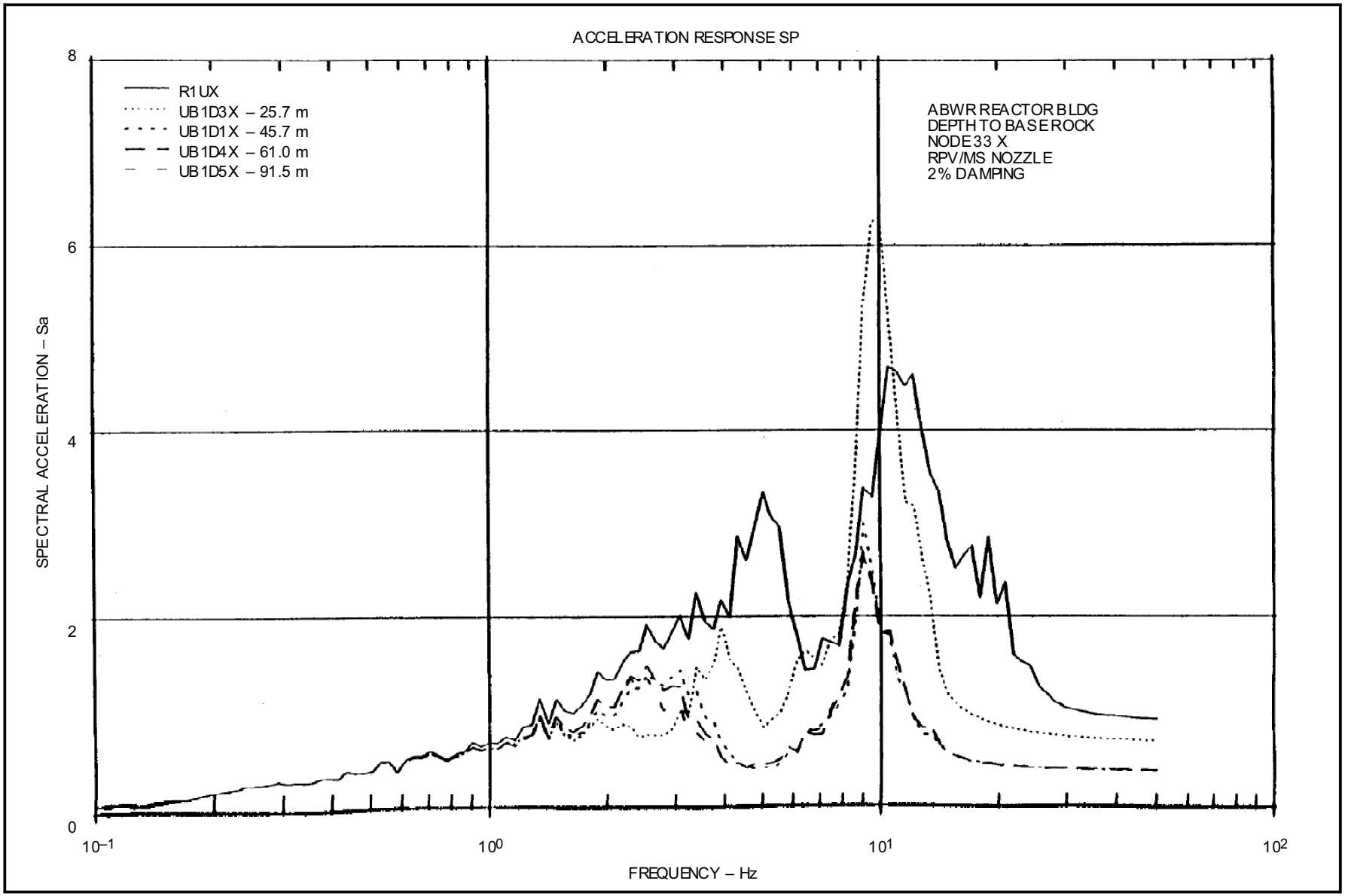

Figure 3A-61 ABWR Reactor Bldg. Depth to Base Rock, Node 33 RPV/MS Nozzle, 2% Damping, UB

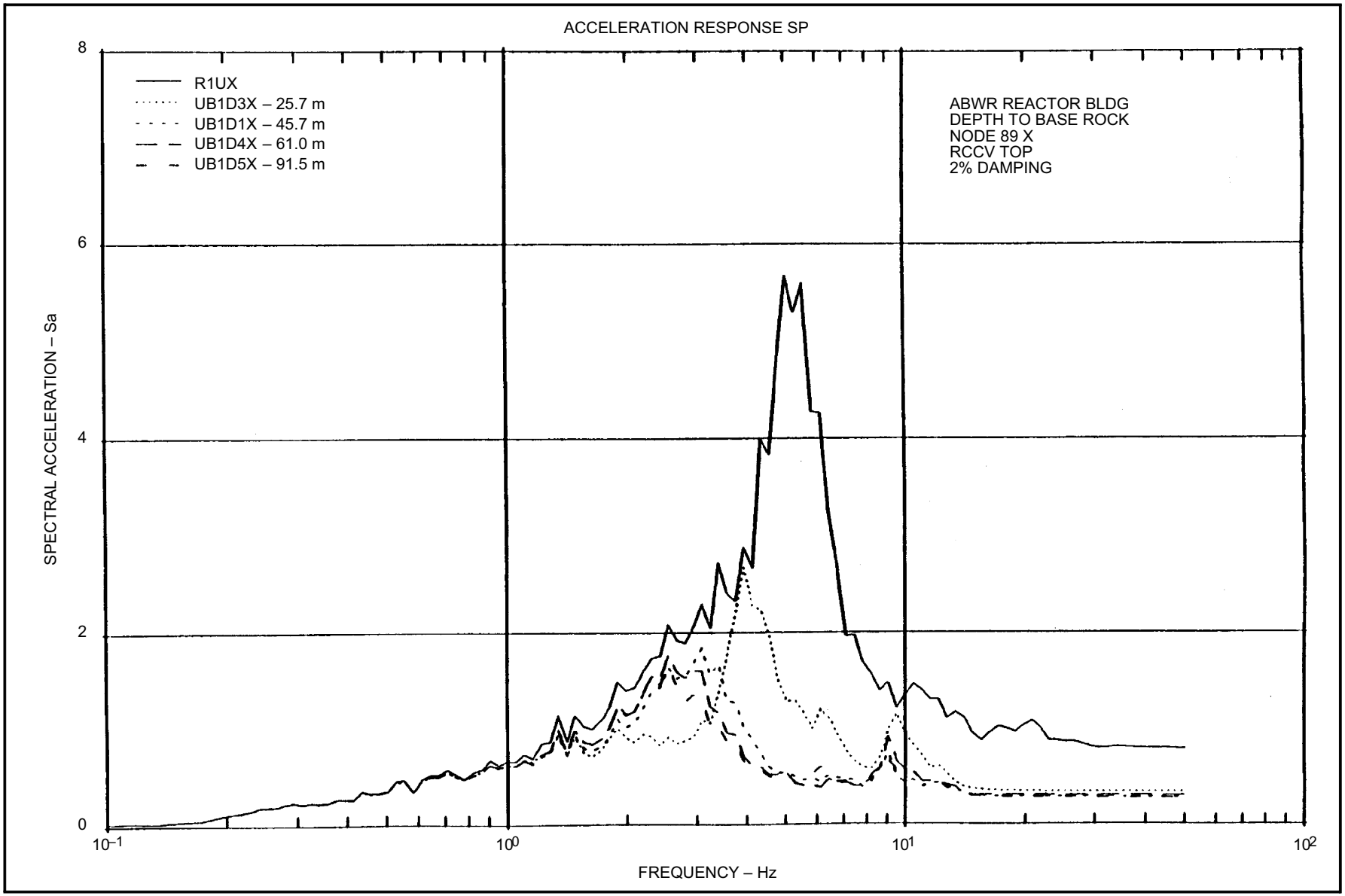

Figure 3A-62 ABWR Reactor Bldg. Depth to Base Rock, Node 89 X RCCV Top, 2% Damping, UB

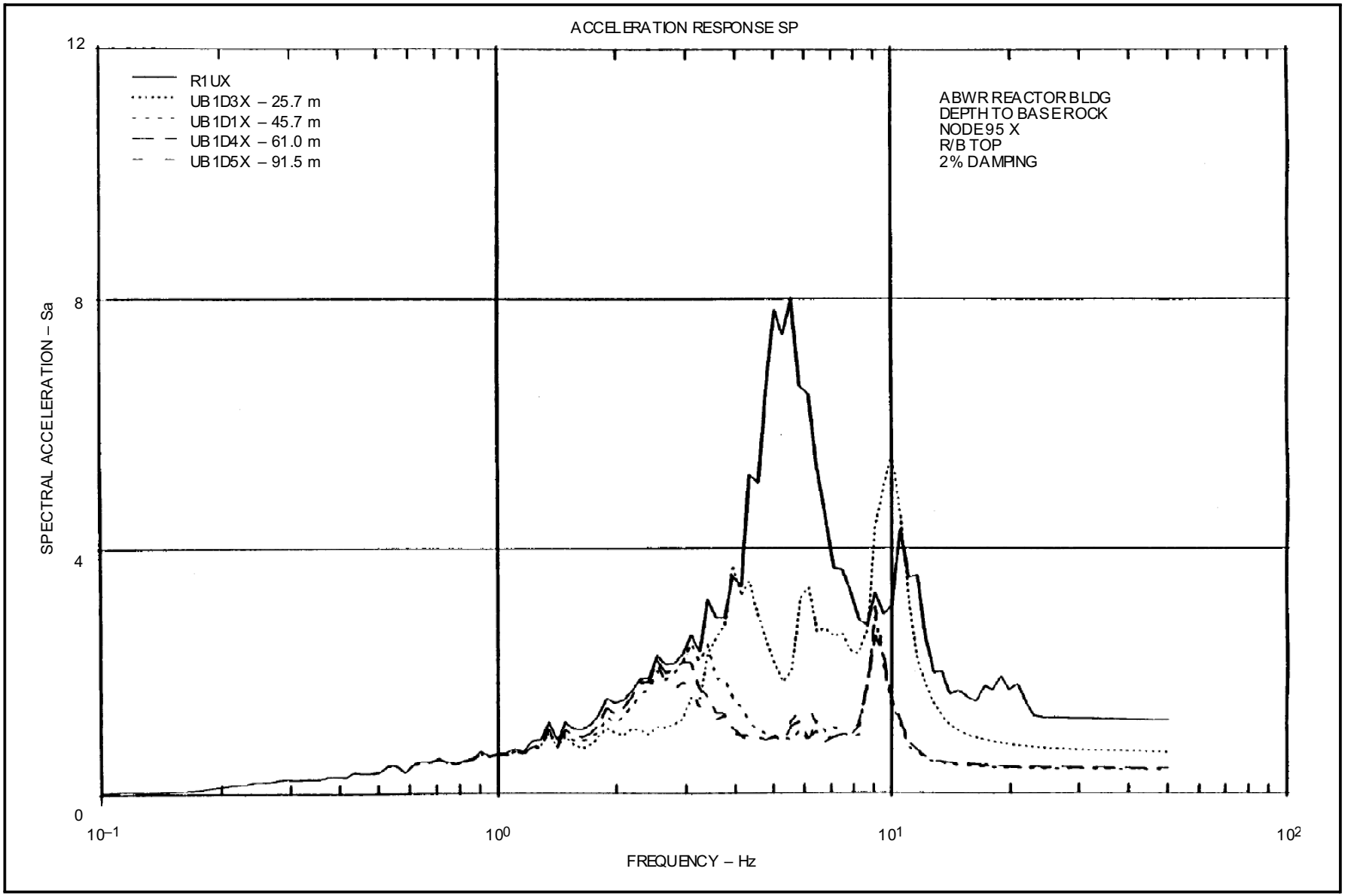

Figure 3A-63 ABWR Reactor Bldg. Depth to Base Rock, Node 95 X R/B Top, 2% Damping, UB

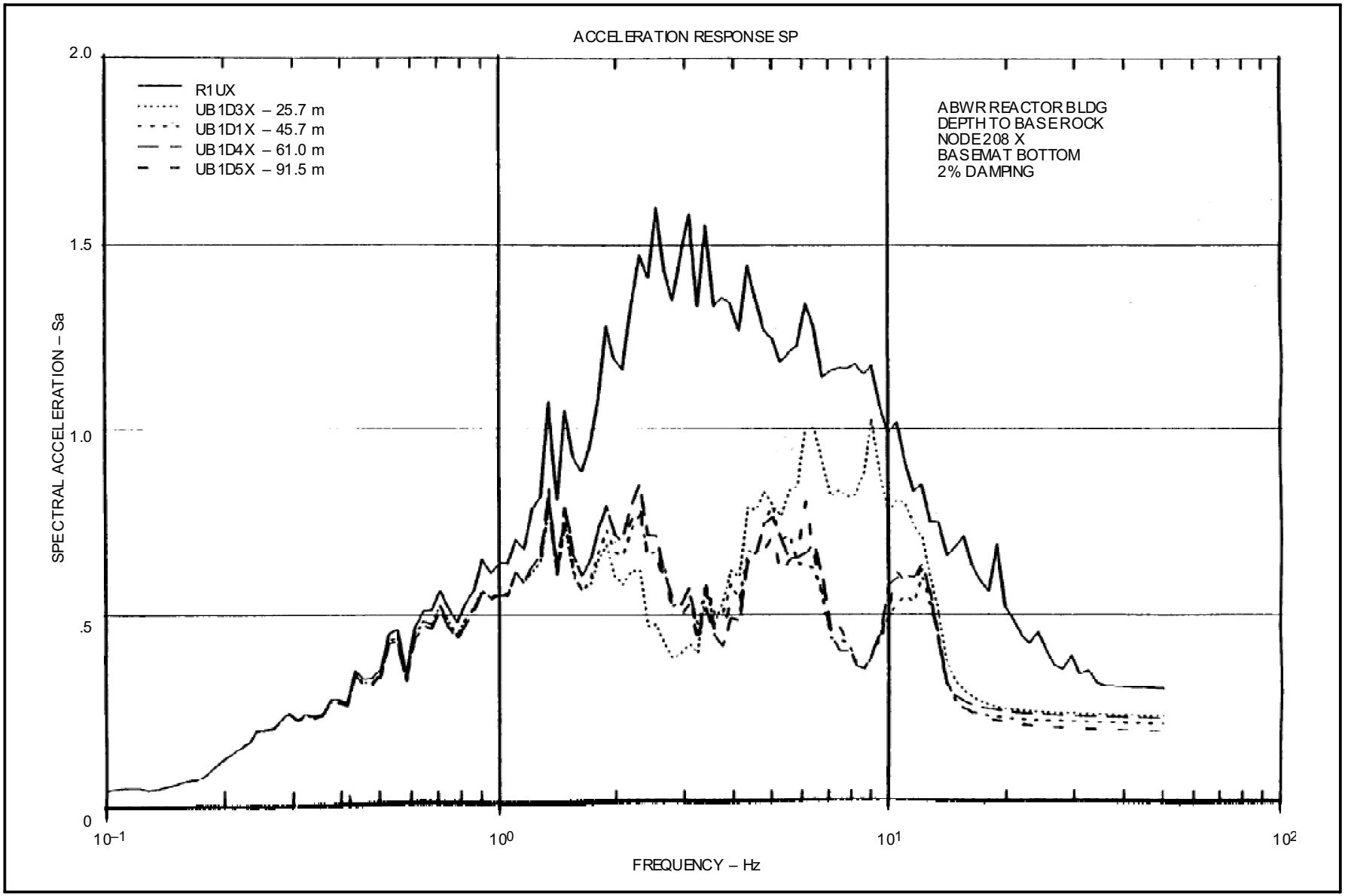

Figure 3A-64 ABWR Reactor Bldg. Depth to Base Rock, Node 208 X Basemat Bottom, 2% Damping, UB

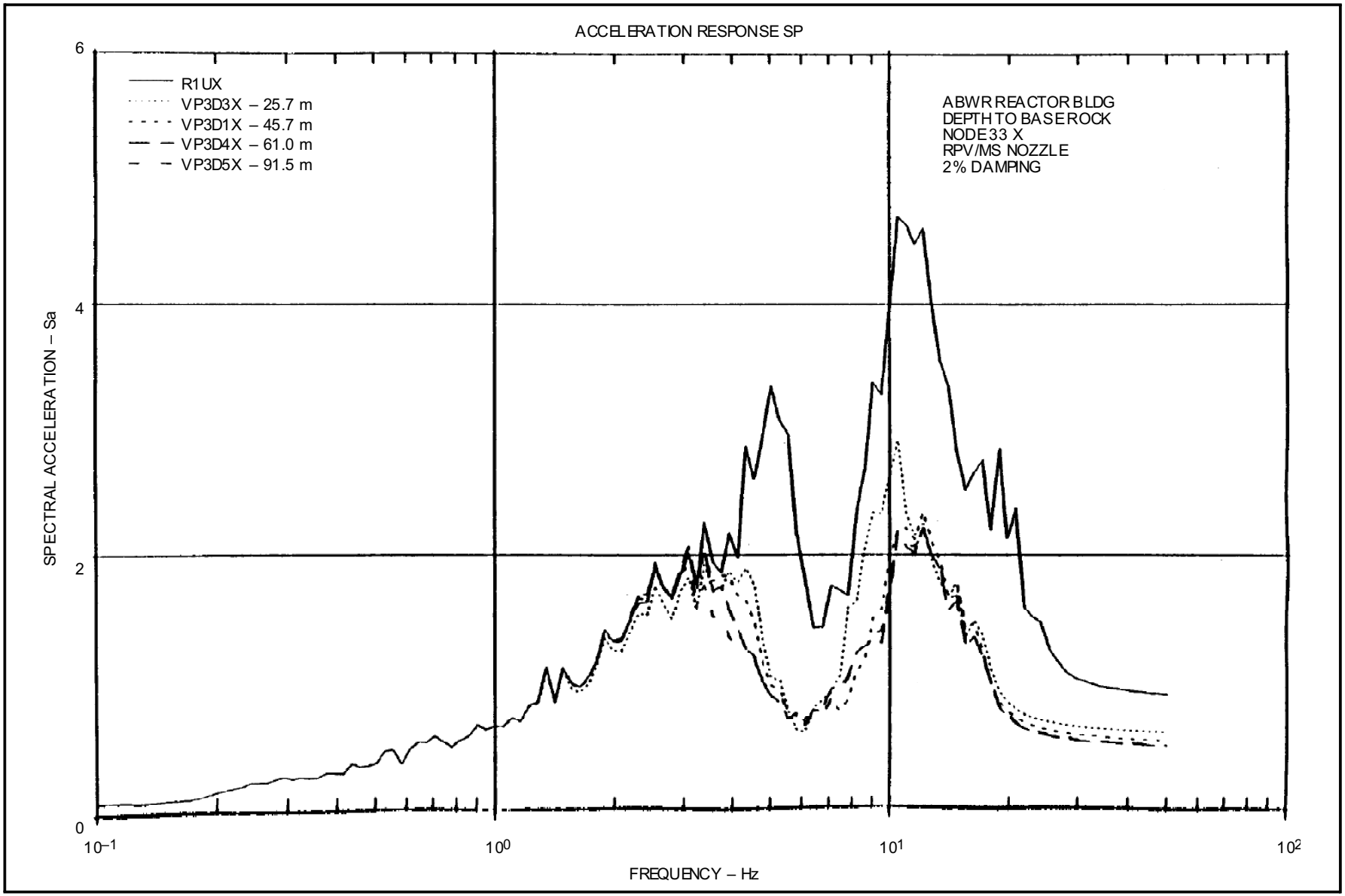

Figure 3A-65 ABWR Reactor Bldg. Depth to Base Rock, Node 33 X RPV/MS Nozzle, 2% Damping, VP3

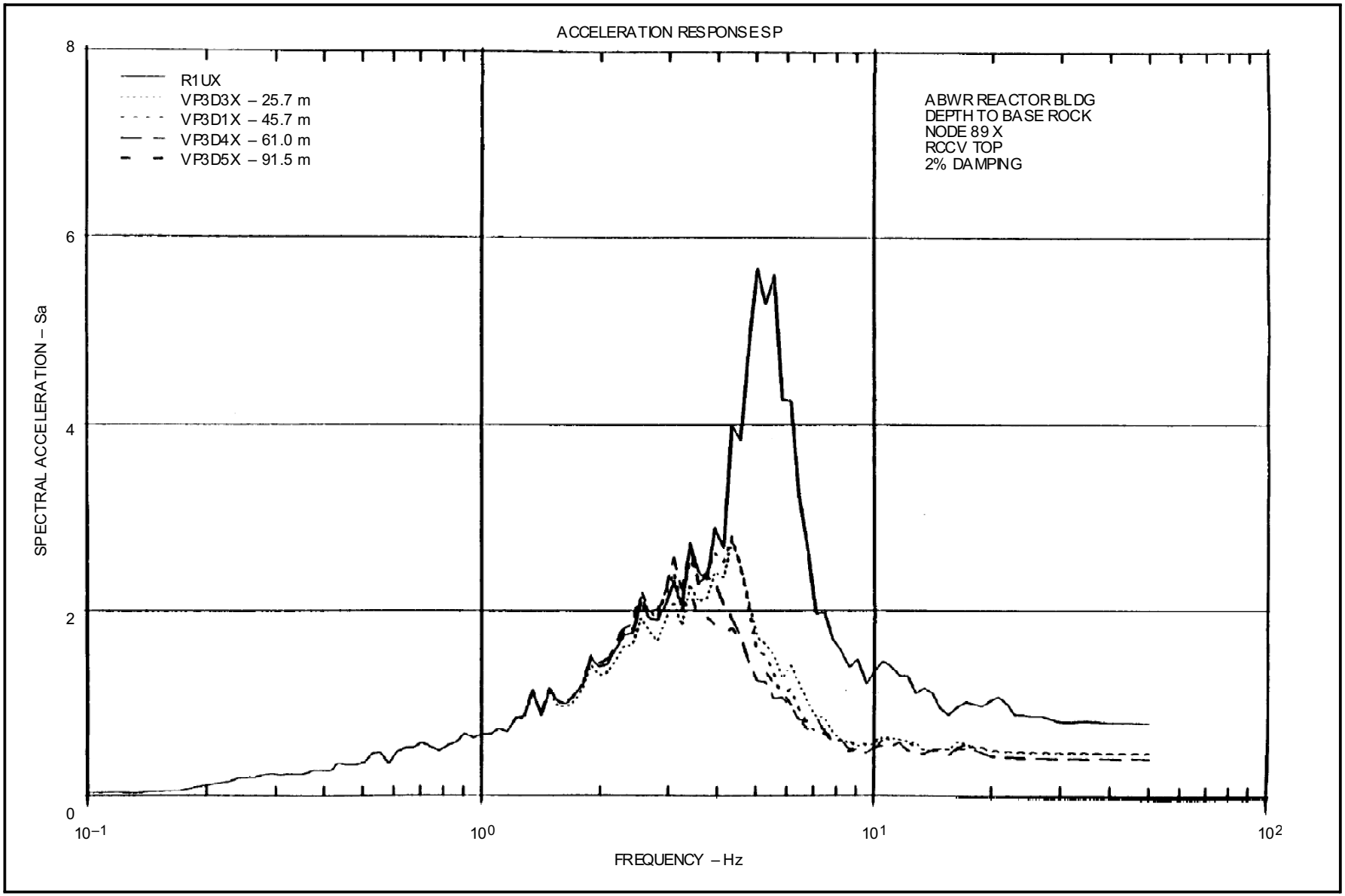

Figure 3A-66 ABWR Reactor Bldg. Depth to Base Rock, Node 89 X RCCV Top, 2% Damping, VP3

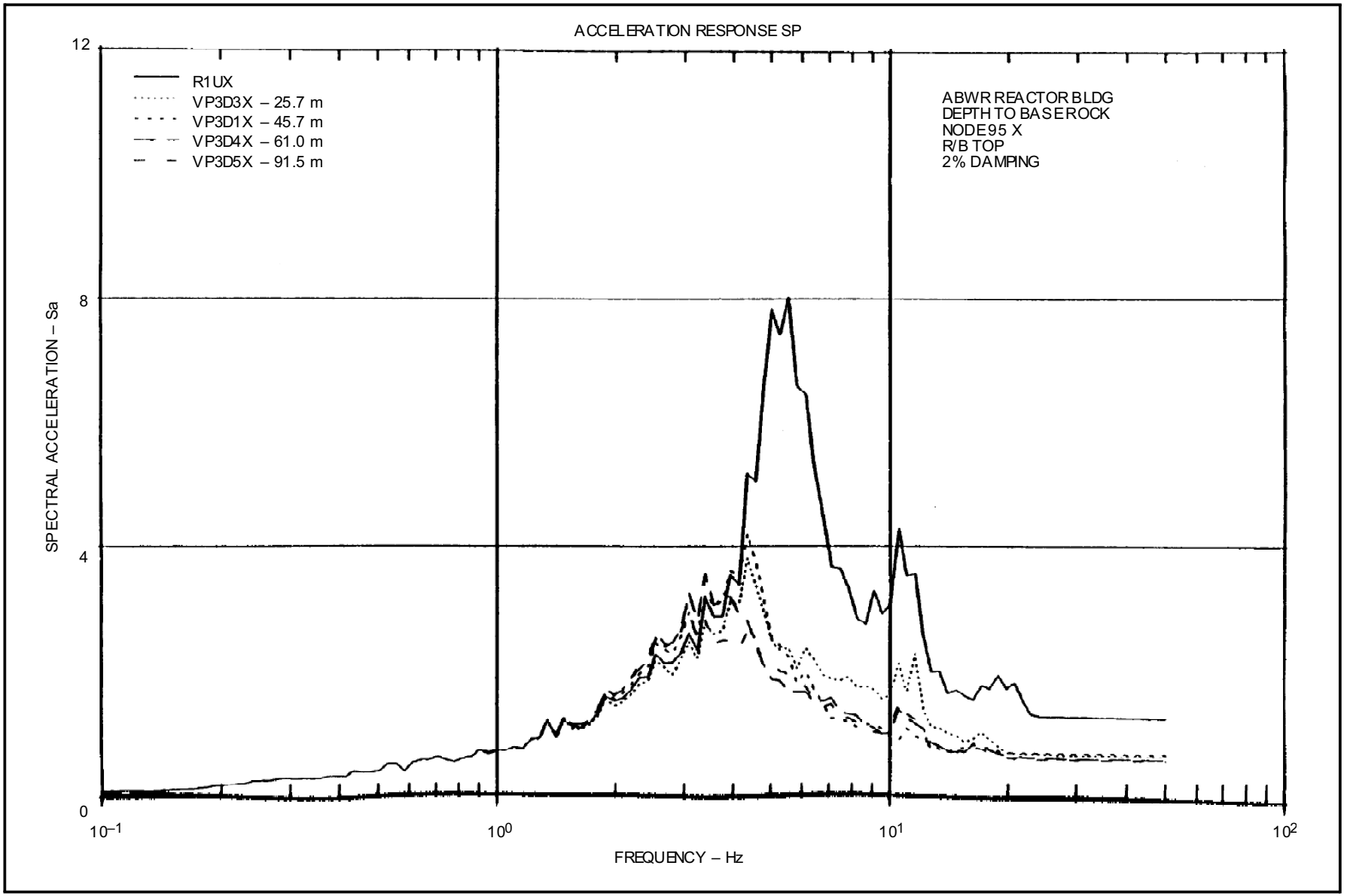

Figure 3A-67 ABWR Reactor Bldg. Depth to Base Rock, Node 95 X R/B Top, 2% Damping, VP3

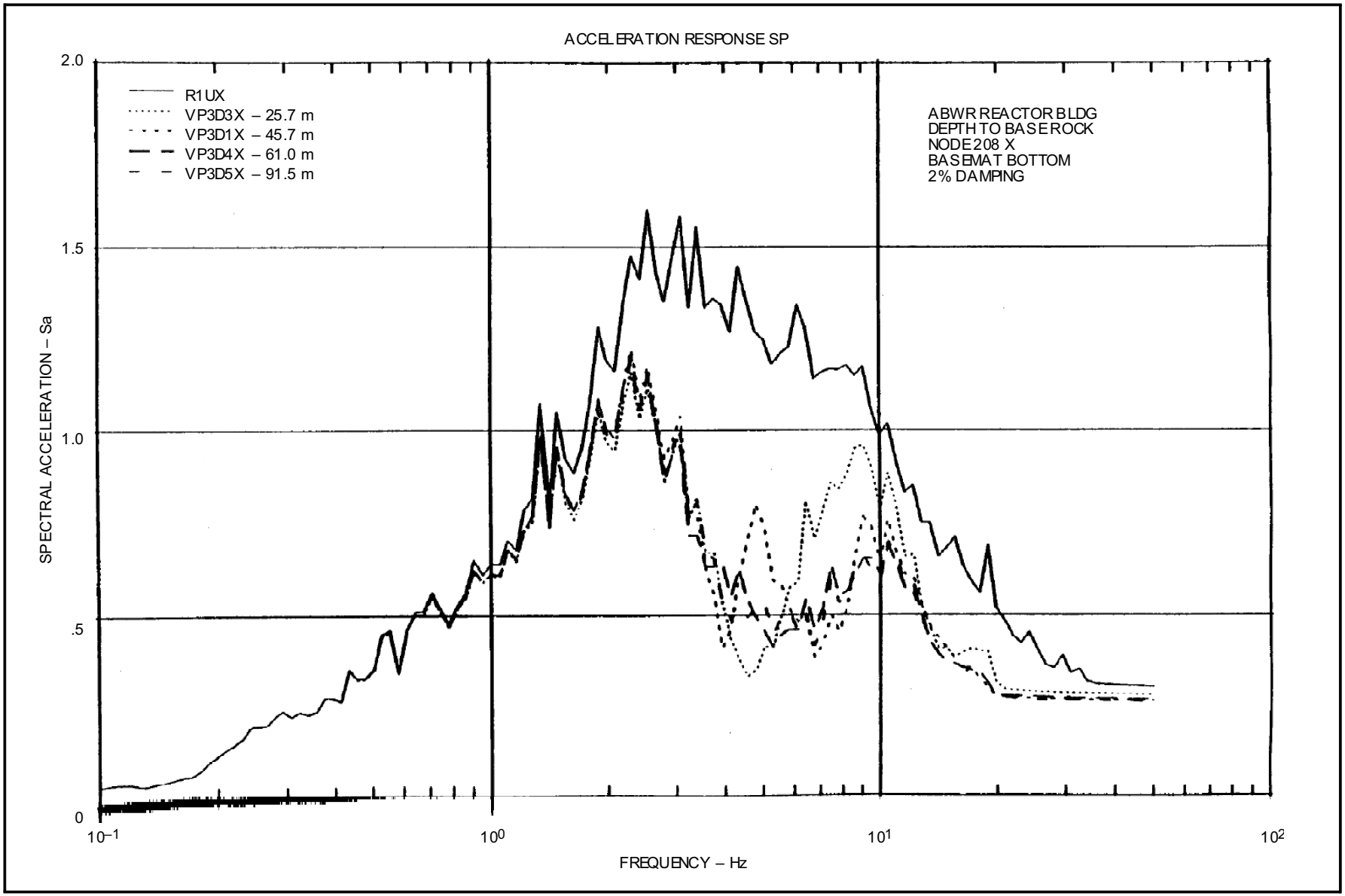

Figure 3A-68 ABWR Reactor Bldg. Depth to Base Rock, Node 208 X Basemat Bottom, 2% Damping, VP3

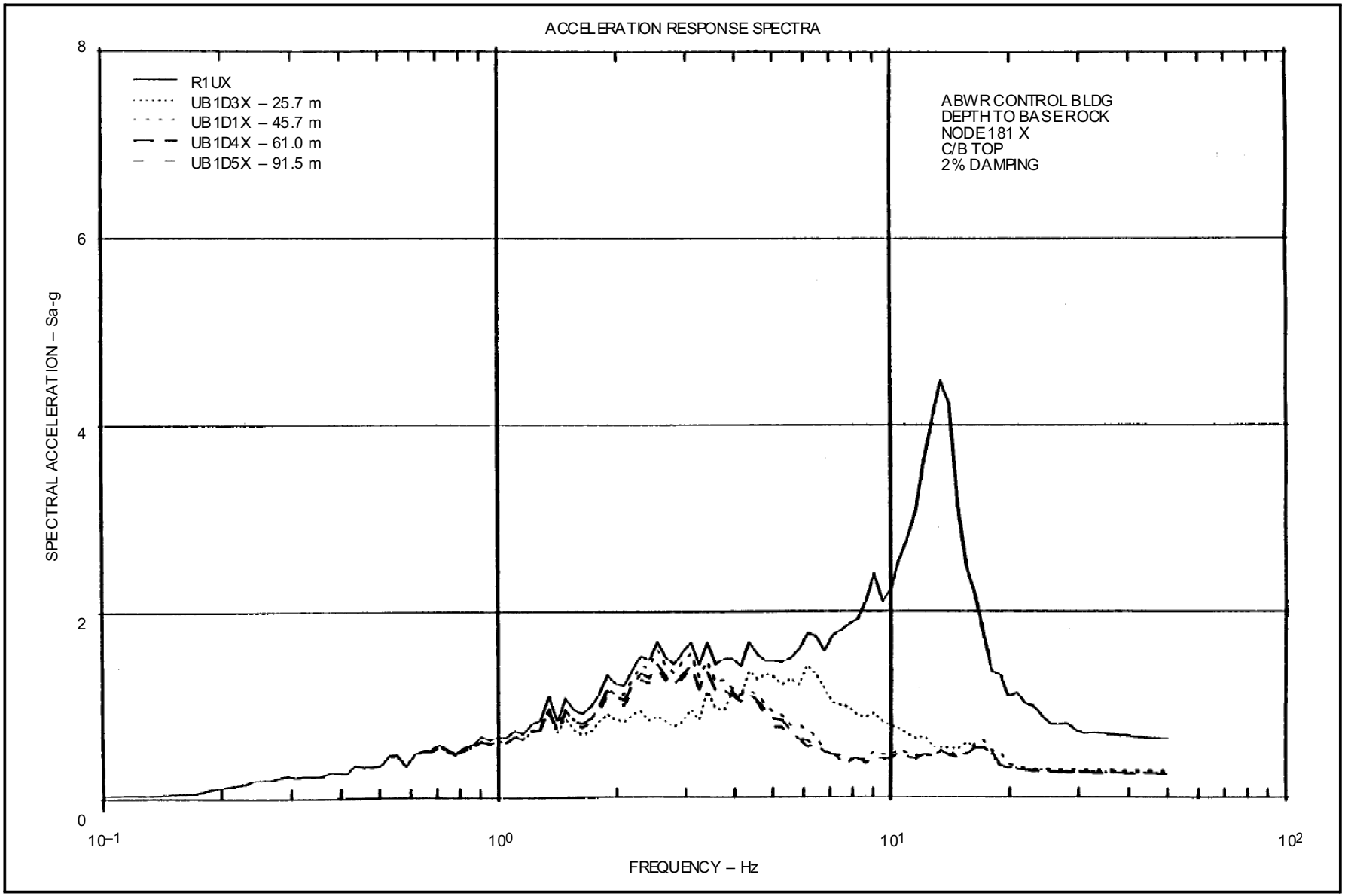

Figure 3A-69 ABWR Control Bldg. Depth to Base Rock, Node 181 X C/B Top, 2% Damping, UB

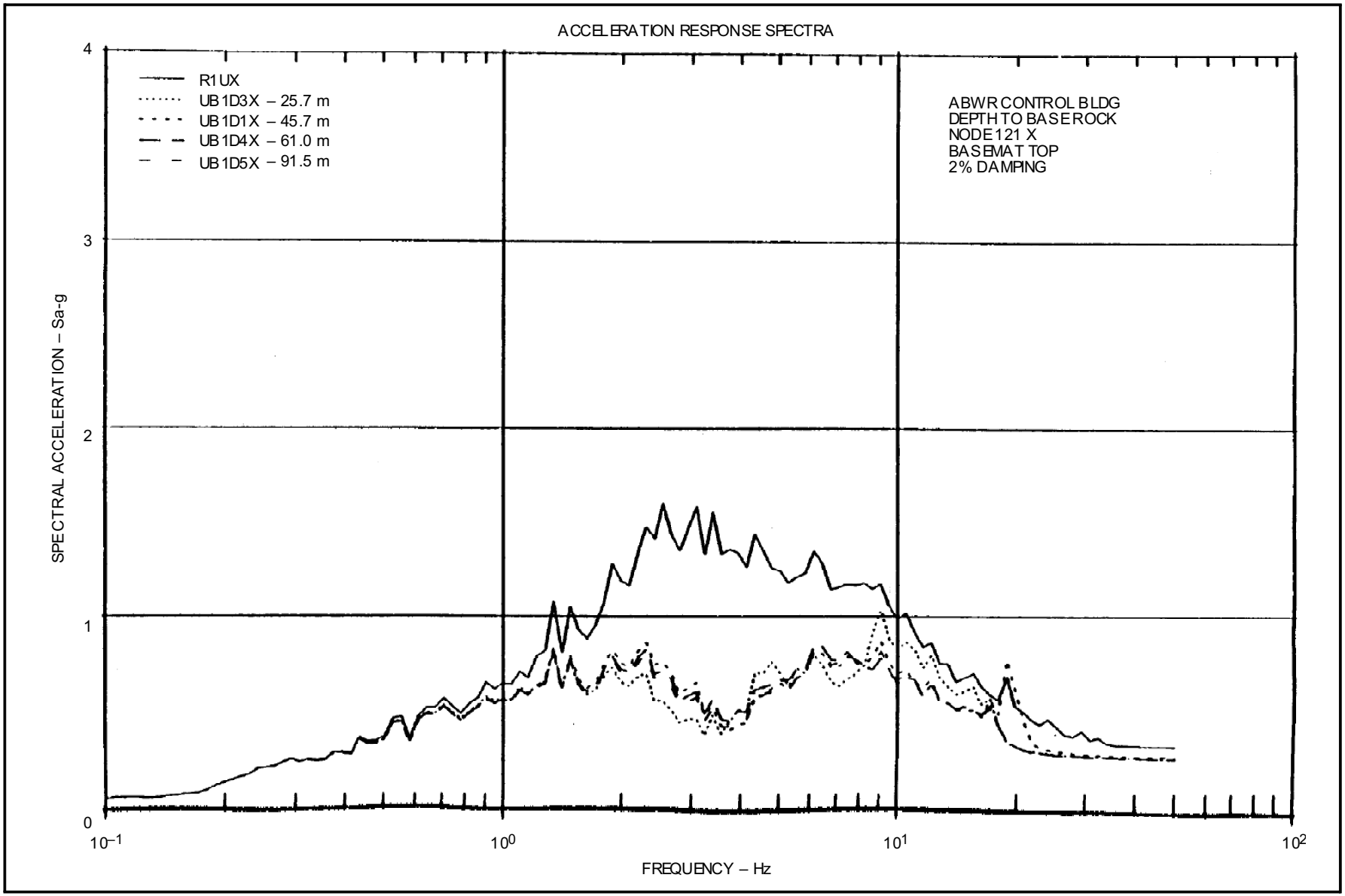

Figure 3A-70 ABWR Control Bldg. Depth to Base Rock, Node 121 X Basemat Top, 2% Damping, UB

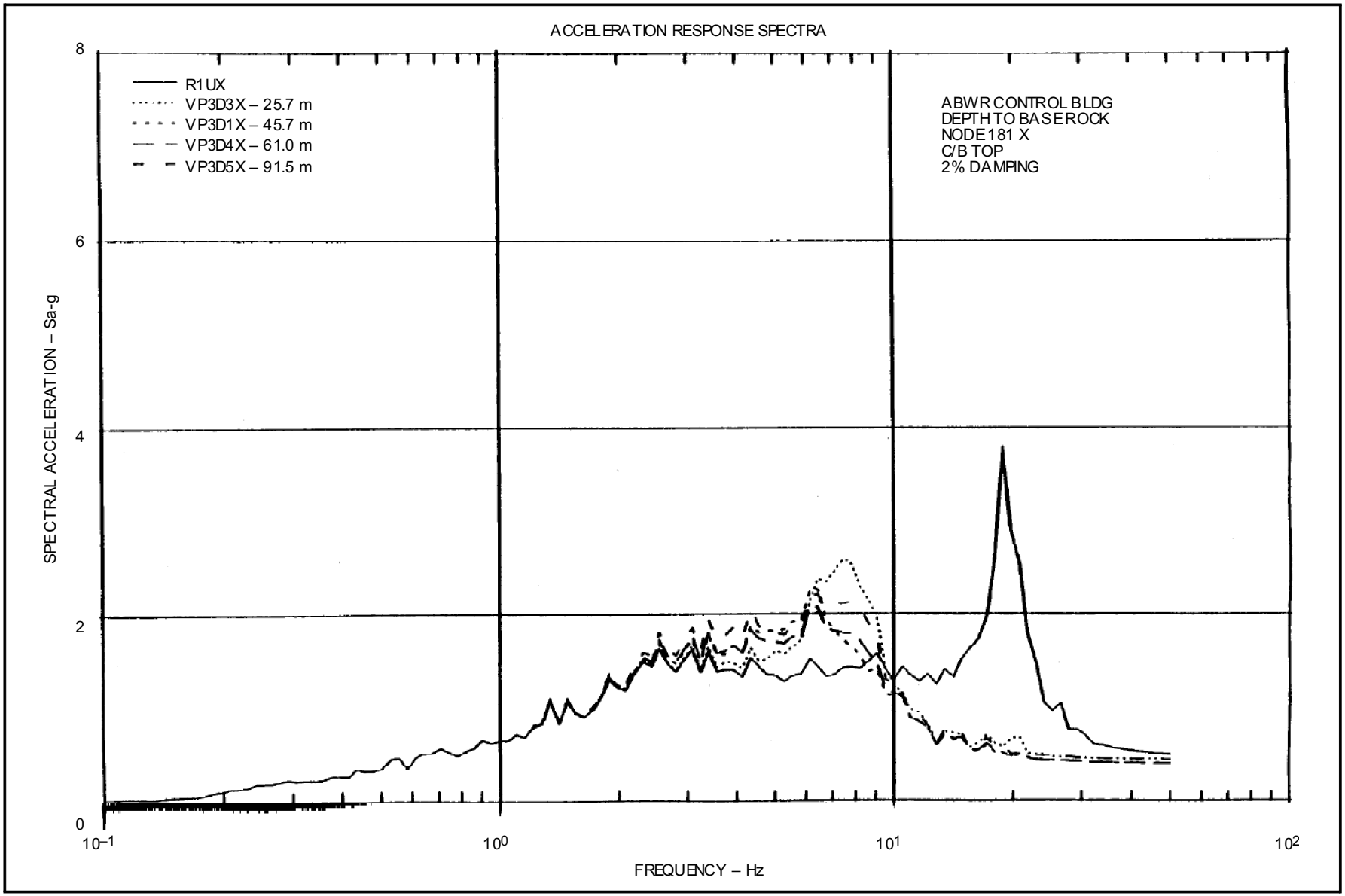

Figure 3A-71 ABWR Control Bldg. Depth to Base Rock, Node 181 X C/B Top, 2% Damping, VP3

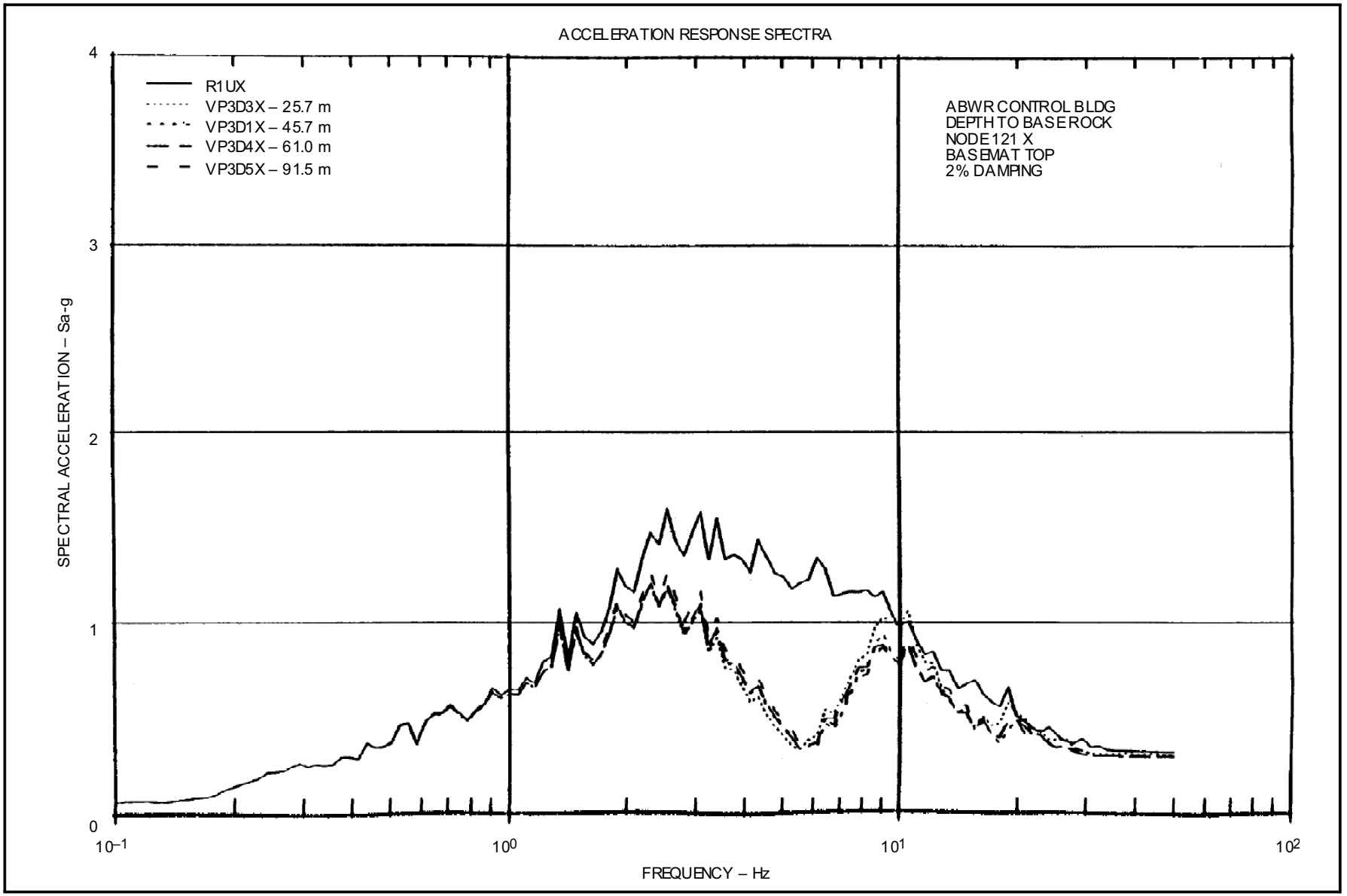

Figure 3A-72 ABWR Control Bldg. Depth to Base Rock, Node 121 X Basemat Top, 2% Damping, VP3

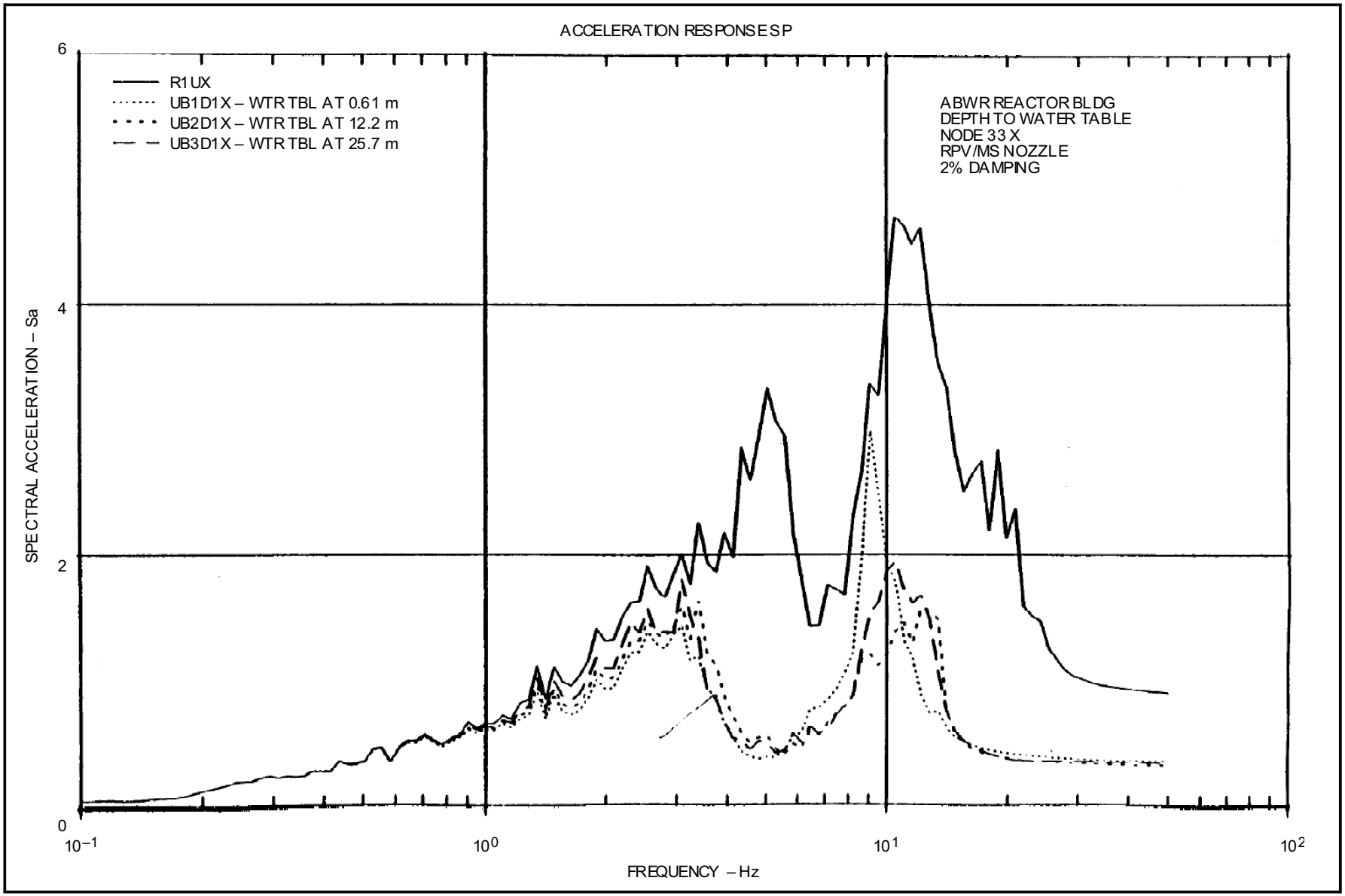

Figure 3A-73 ABWR Reactor Bldg. Depth to Water Table, Node 33 X RPV/MS Nozzle, 2% Damping

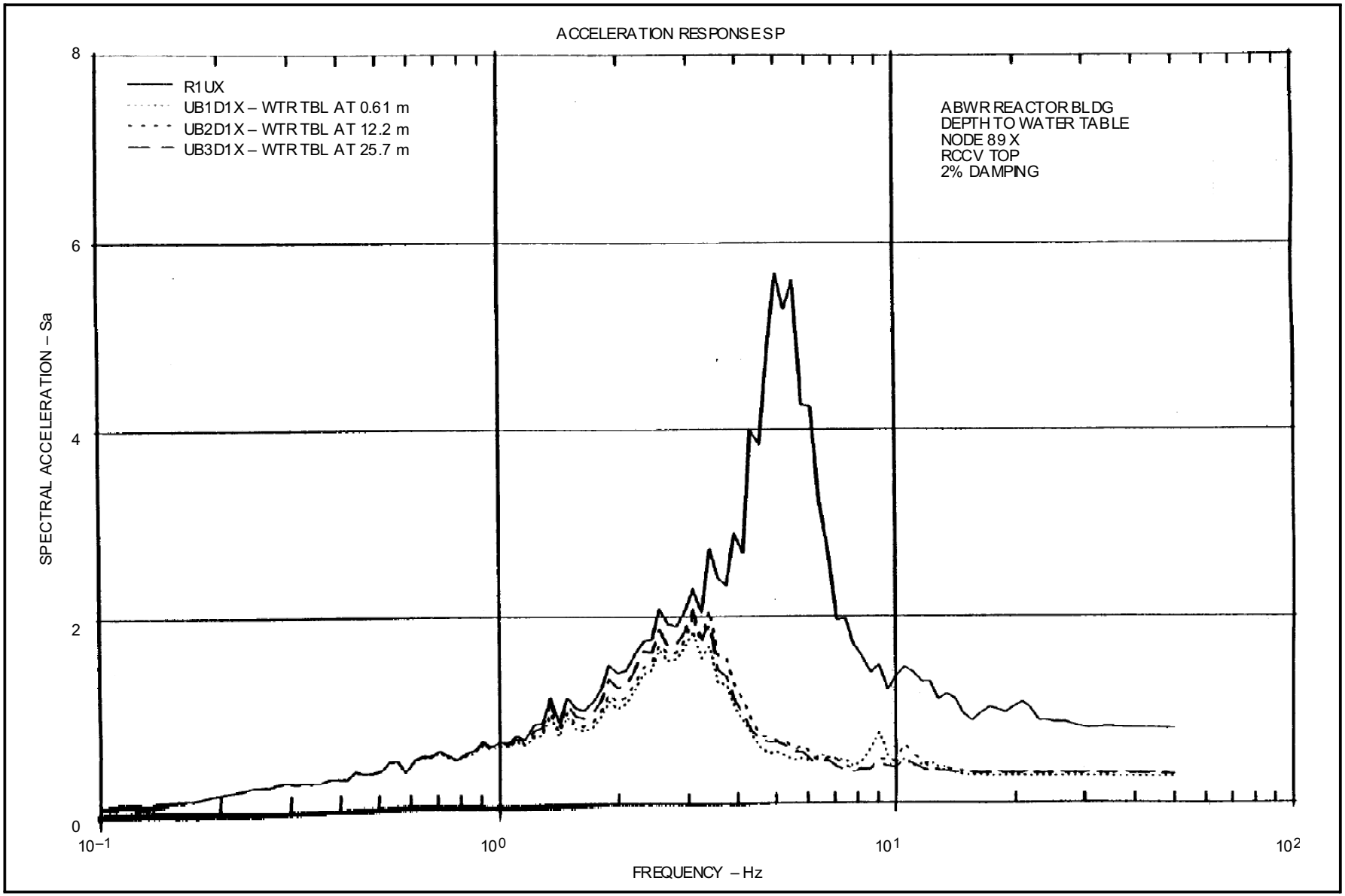

Figure 3A-74 ABWR Reactor Bldg. Depth to Water Table, Node 89 X RCCV Top, 2% Damping

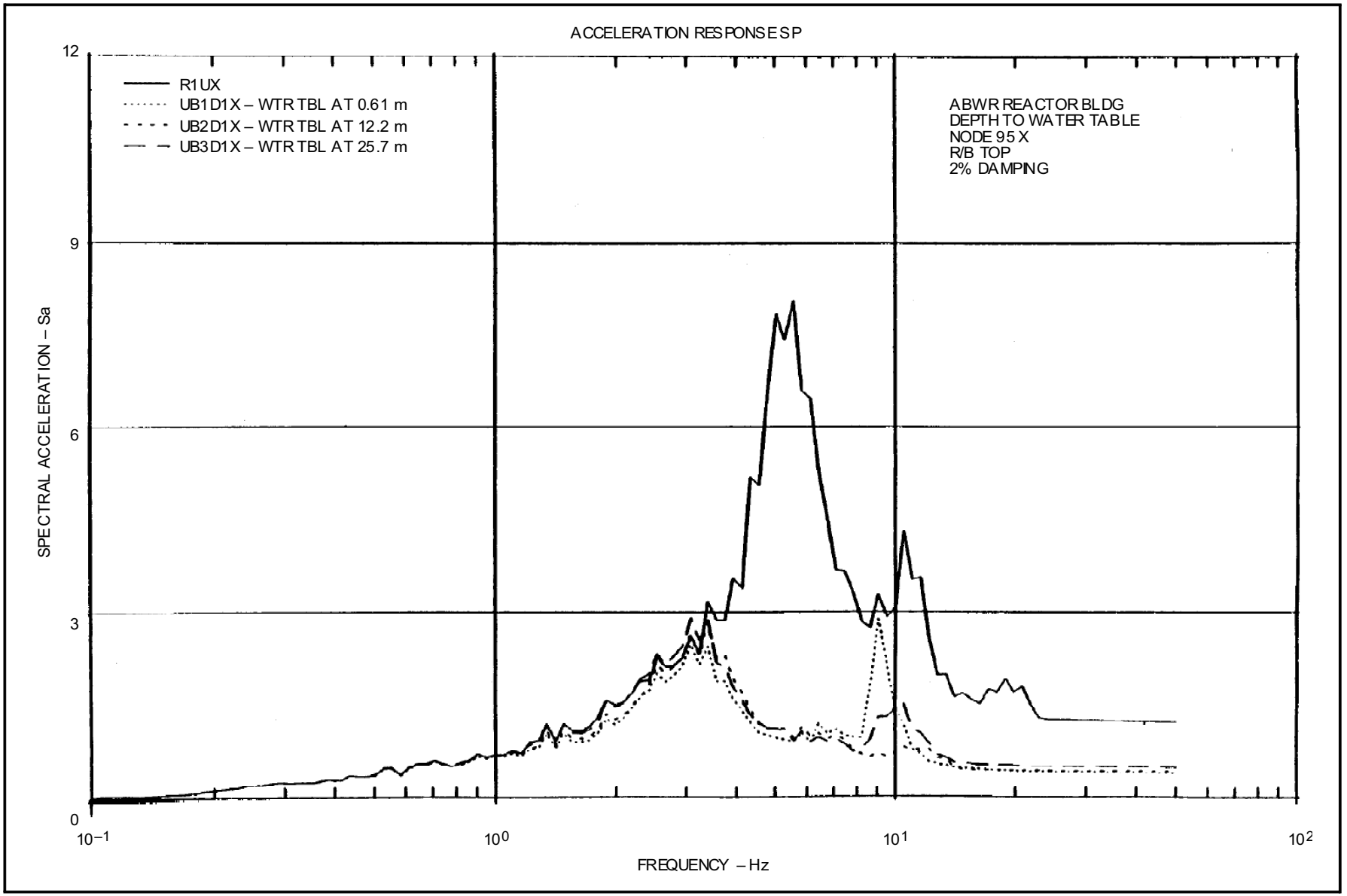

Figure 3A-75 ABWR Reactor Bldg. Depth to Water Table, Node 95 X R/B Top, 2% Damping

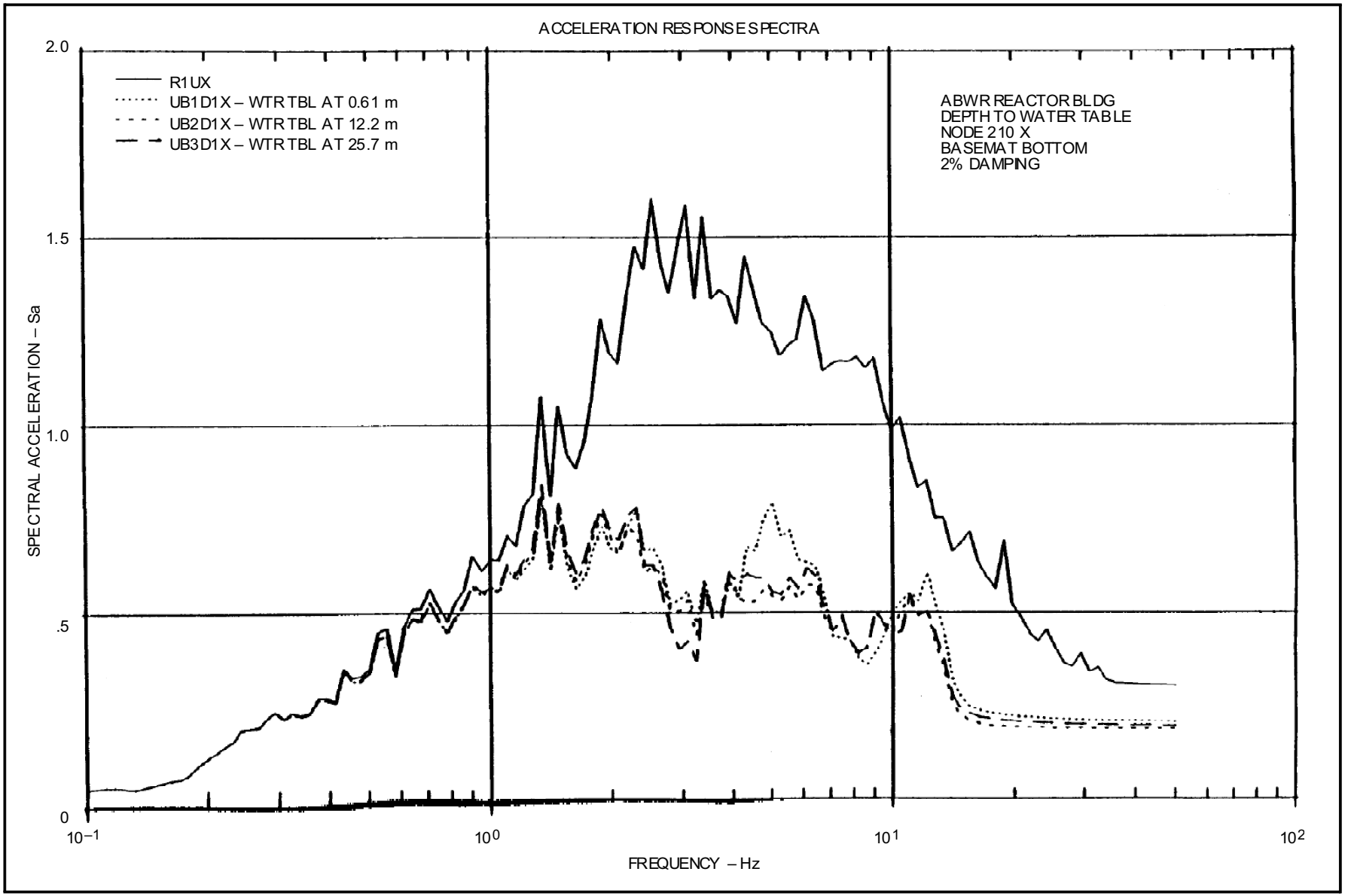

Figure 3A-76 ABWR Reactor Bldg. Depth to Water Table, Node 210 X Basemat Bottom, 2% Damping

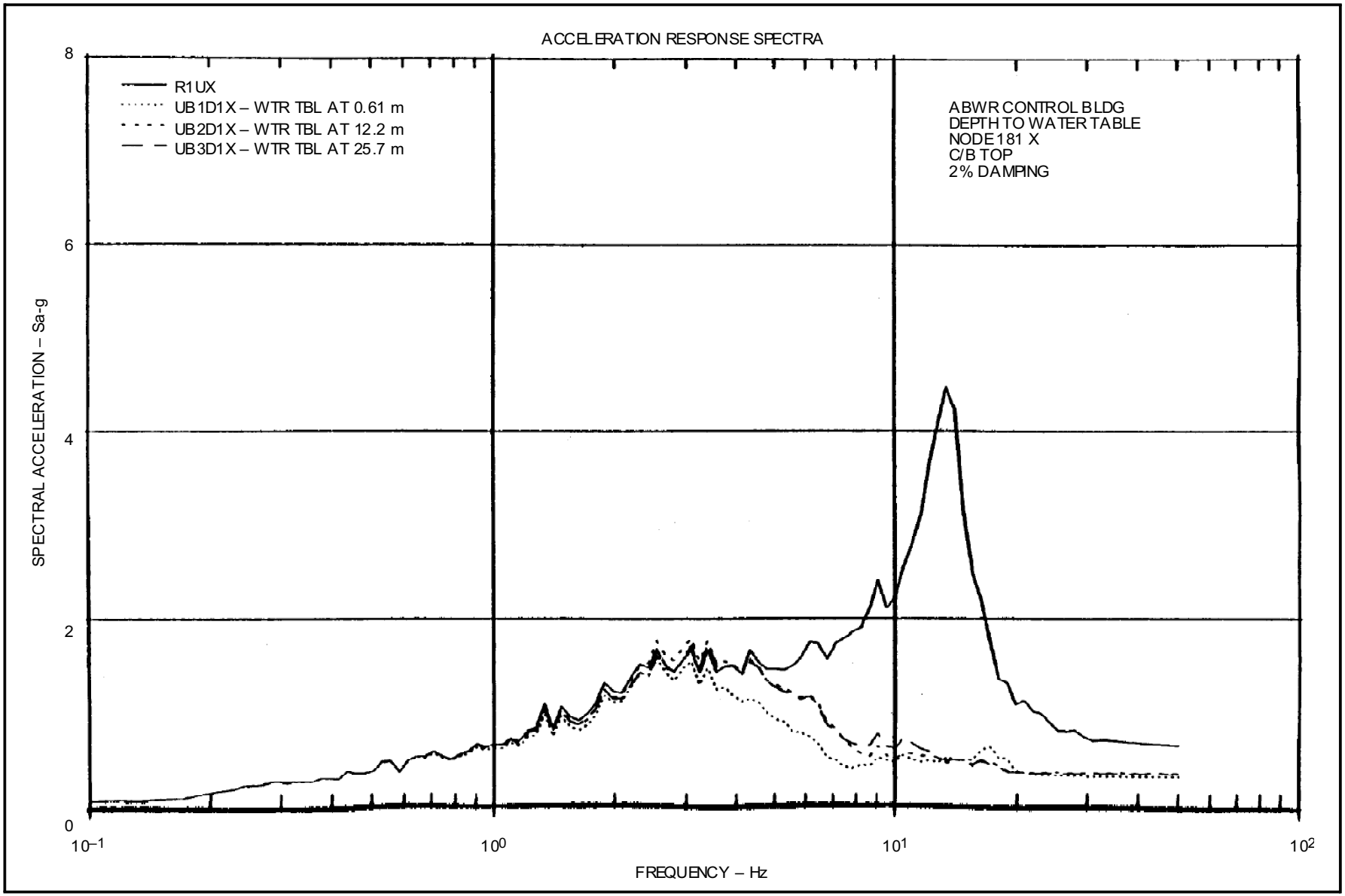

Figure 3A-77 ABWR Control Bldg. Depth to Water Table, Node 181 X C/B Top, 2% Damping

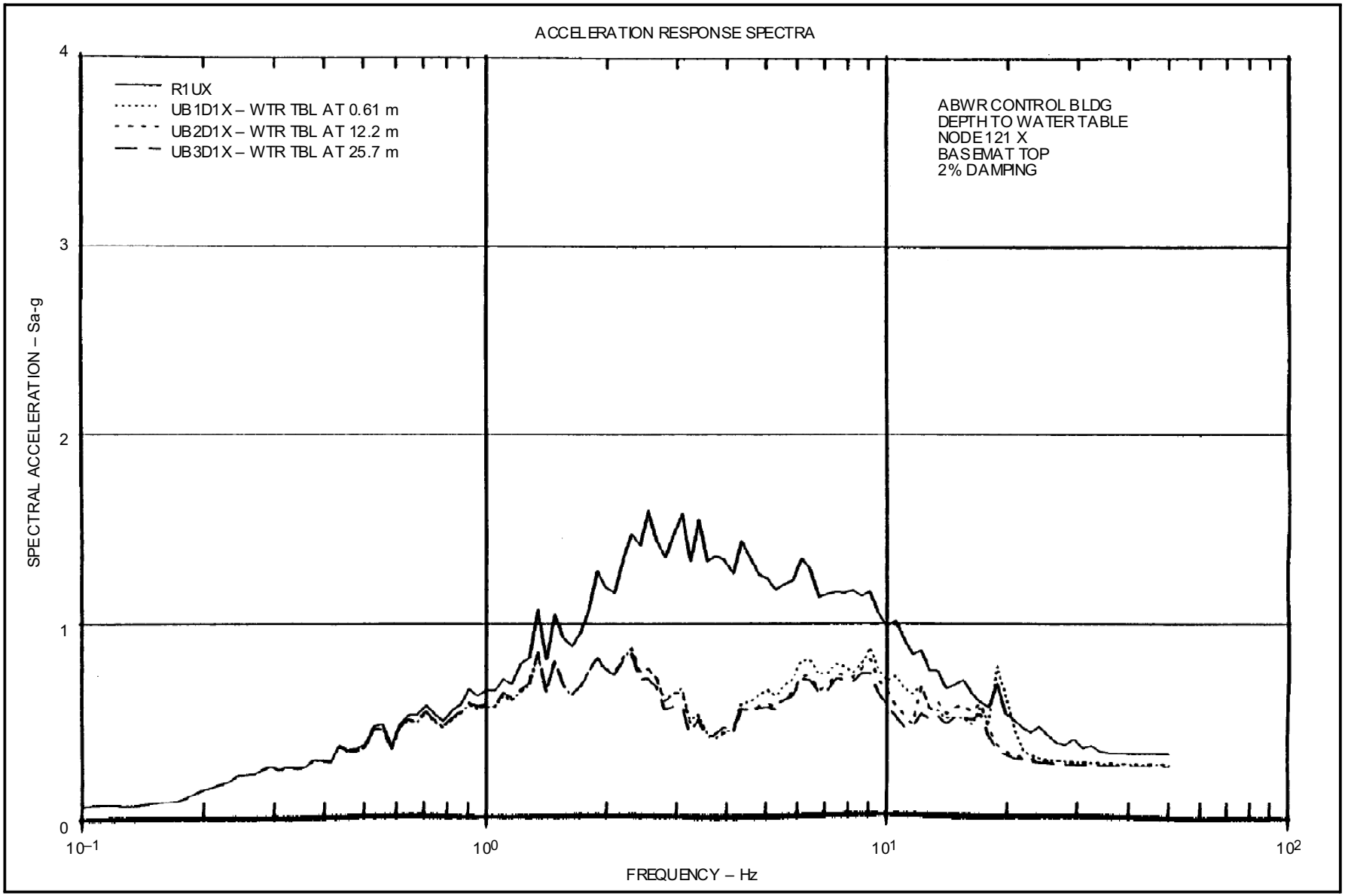

Figure 3A-78 ABWR Control Bldg. Depth to Water Table, Node 121 X Basemat Top, 2% Damping

Figure 3A-79 Not Used

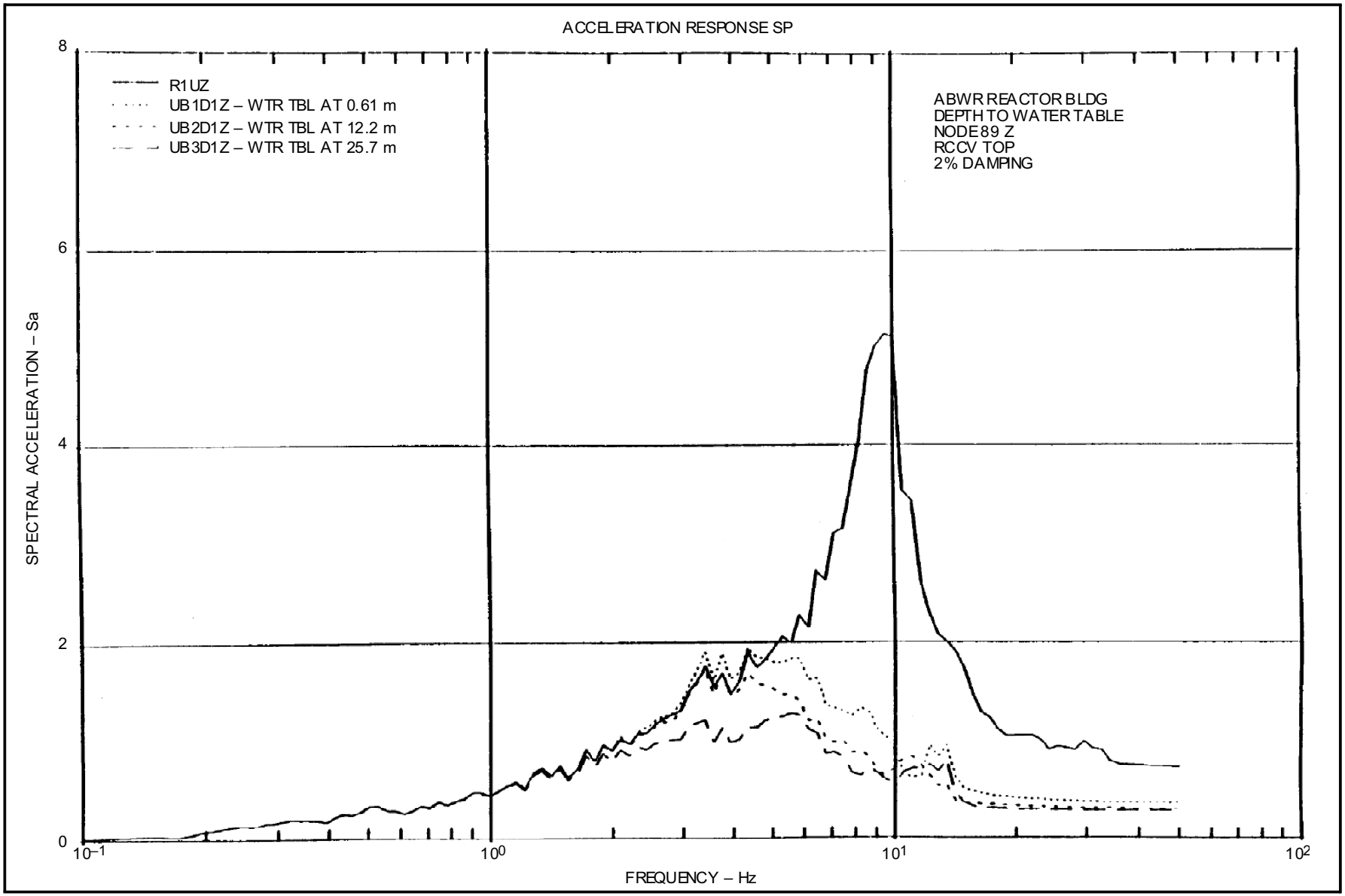

Figure 3A-80 ABWR Reactor Bldg. Depth to Water Table, Node 89 Z RCCV Top, 2% Damping

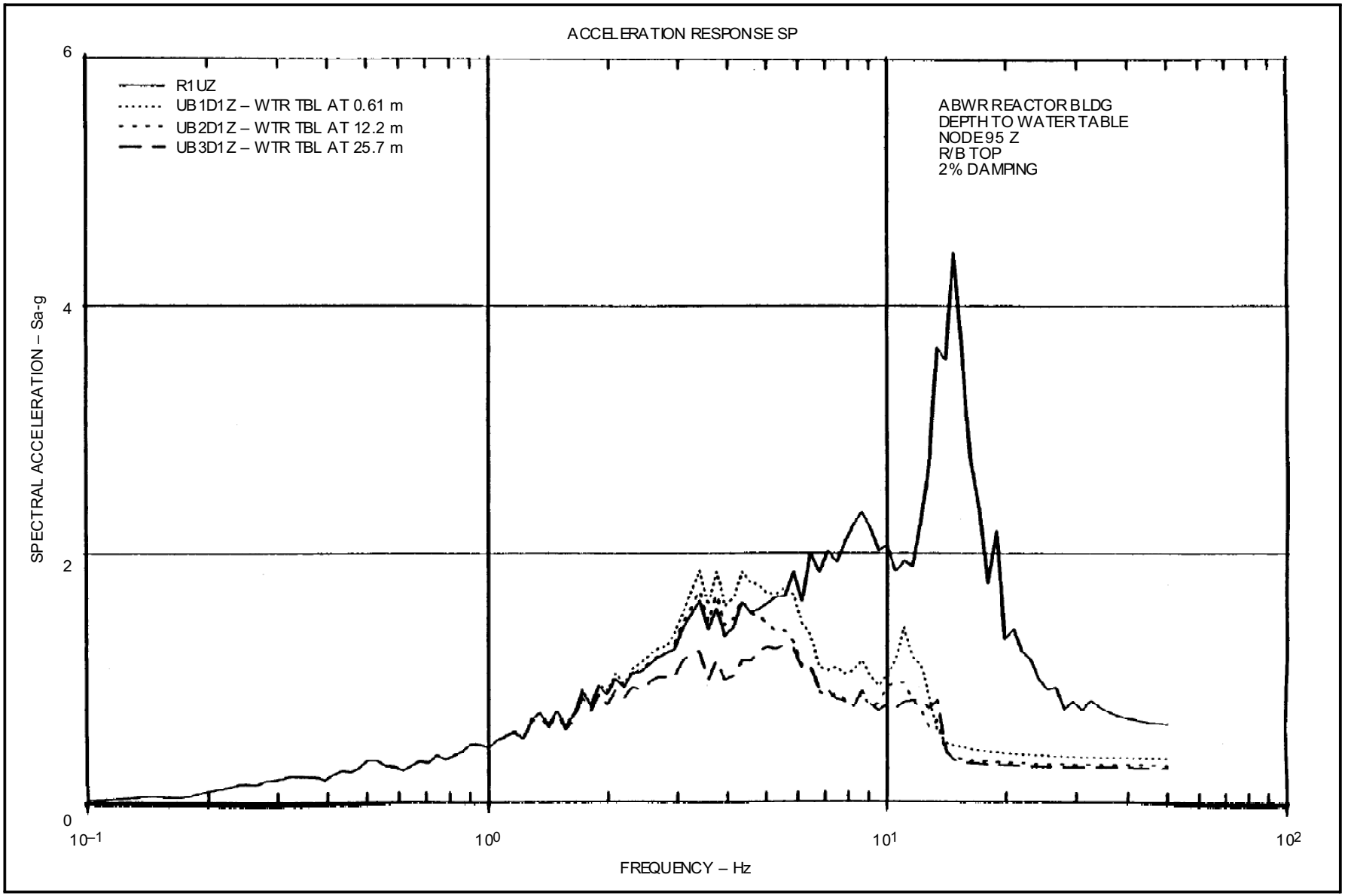

Figure 3A-81 ABWR Reactor Bldg. Depth to Water Table, Node 95 Z R/B Top, 2% Damping

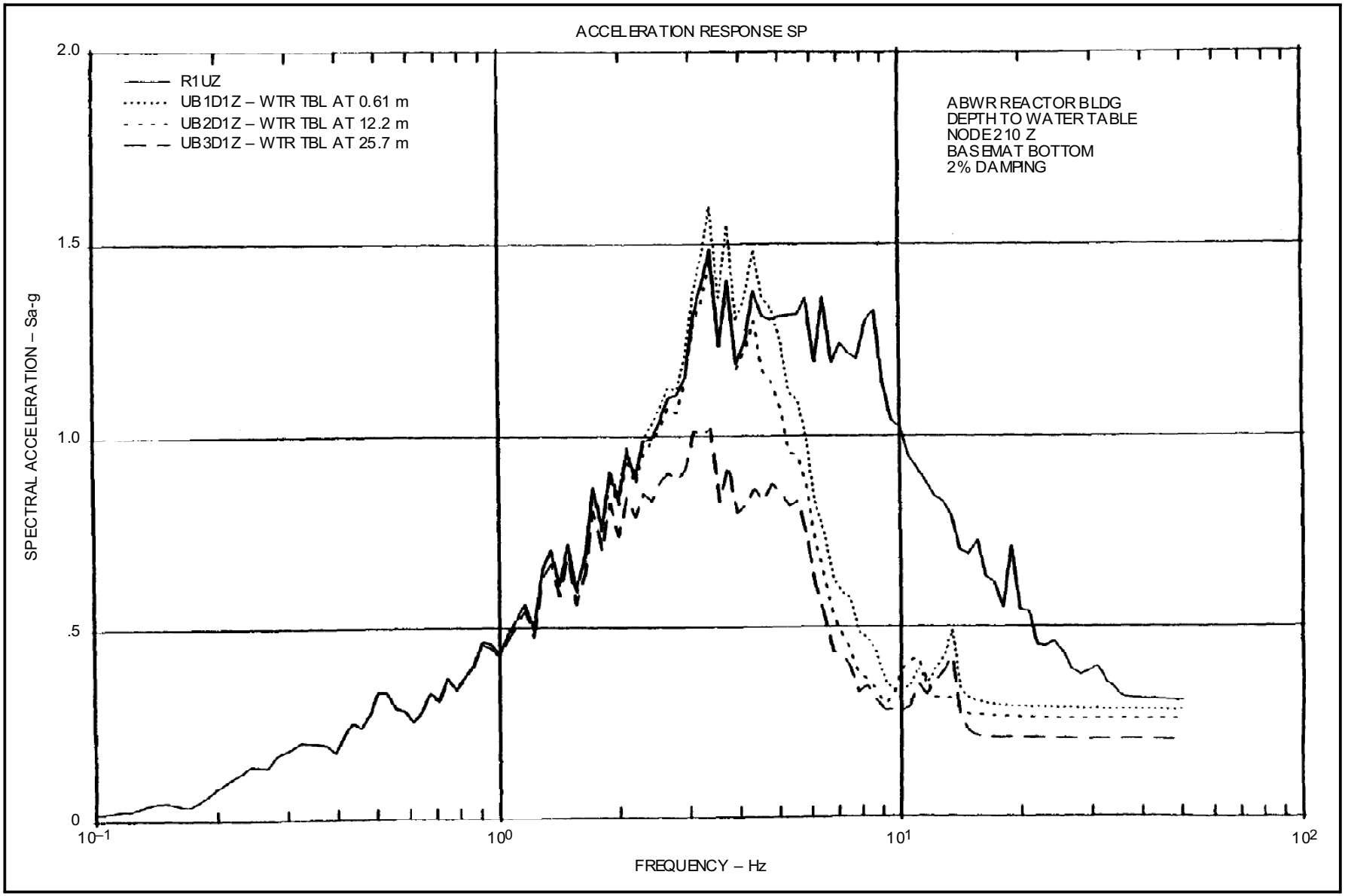

Figure 3A-82 ABWR Reactor Bldg. Depth to Water Table, Node 210 Z Basemat Bottom, 2% Damping

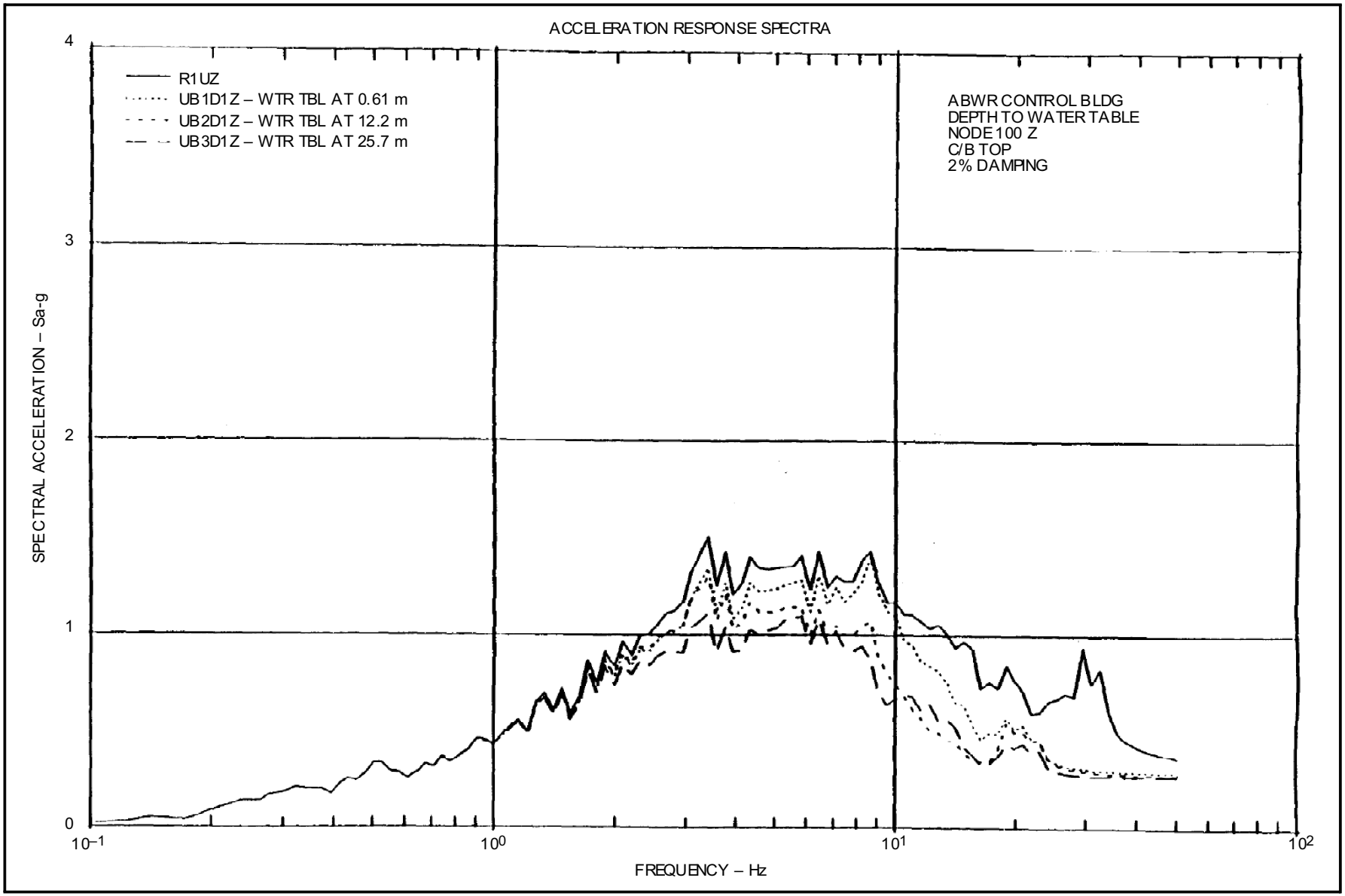

Figure 3A-83 ABWR Control Bldg. Depth to Water Table, Node 108 Z C/B Top, 2% Damping

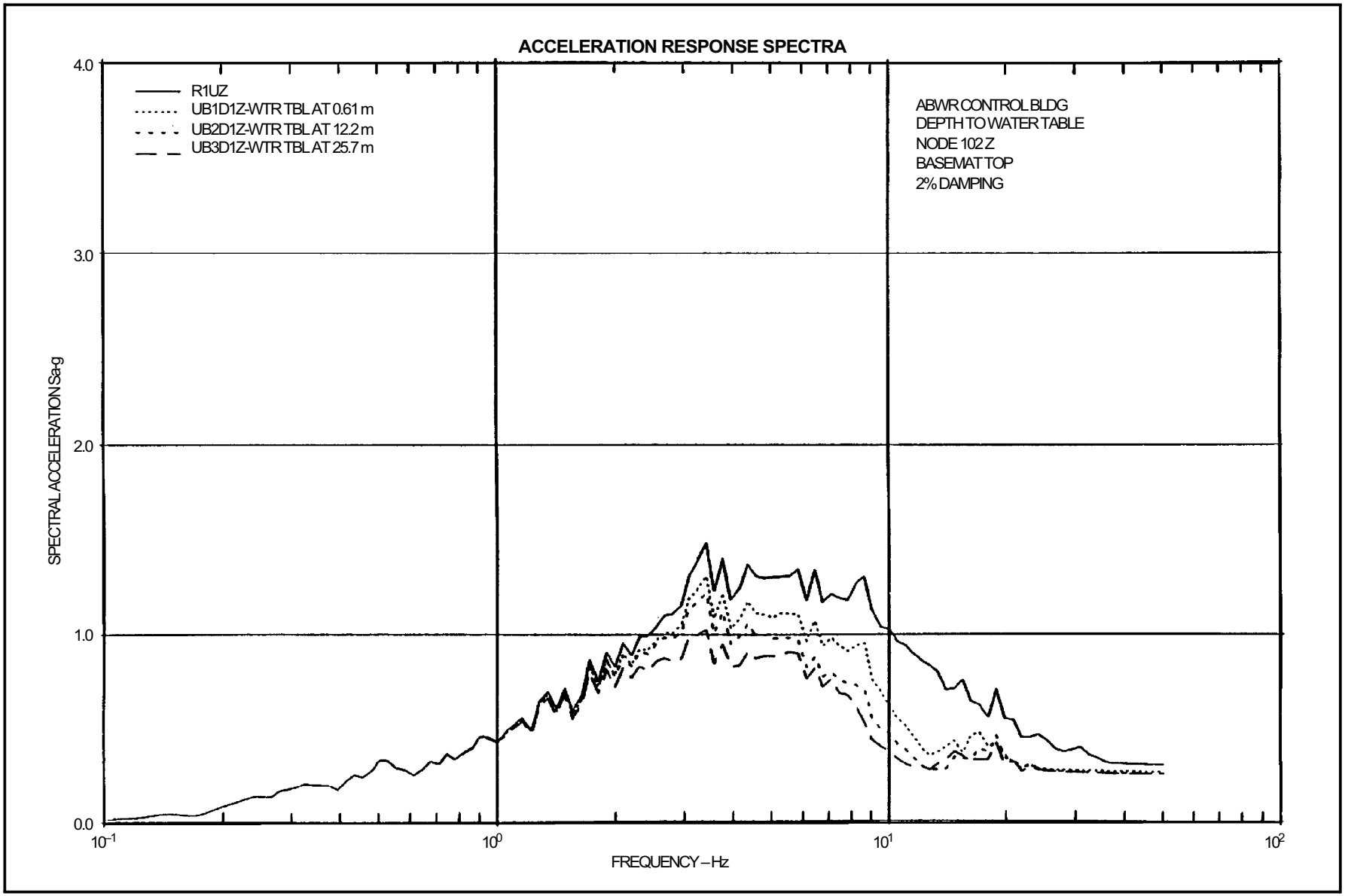

Figure 3A-84 ABWR Control Bldg. Depth to Water Table, Node 102 Z Basemat Top, 2% Damping

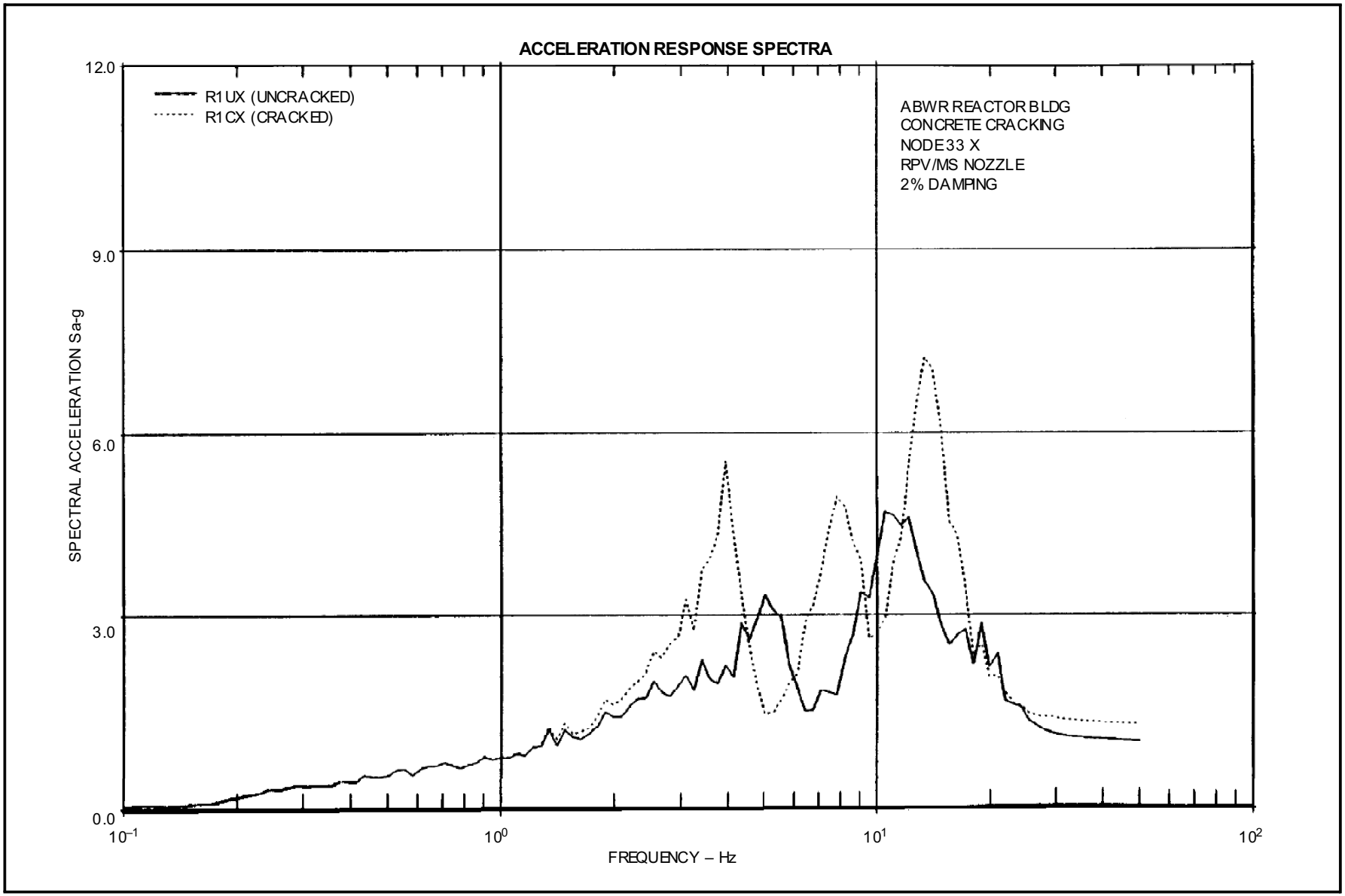

Figure 3A-85 ABWR Reactor Bldg. Concrete Cracking, Node 33 X RPV/MS Nozzle, 2% Damping

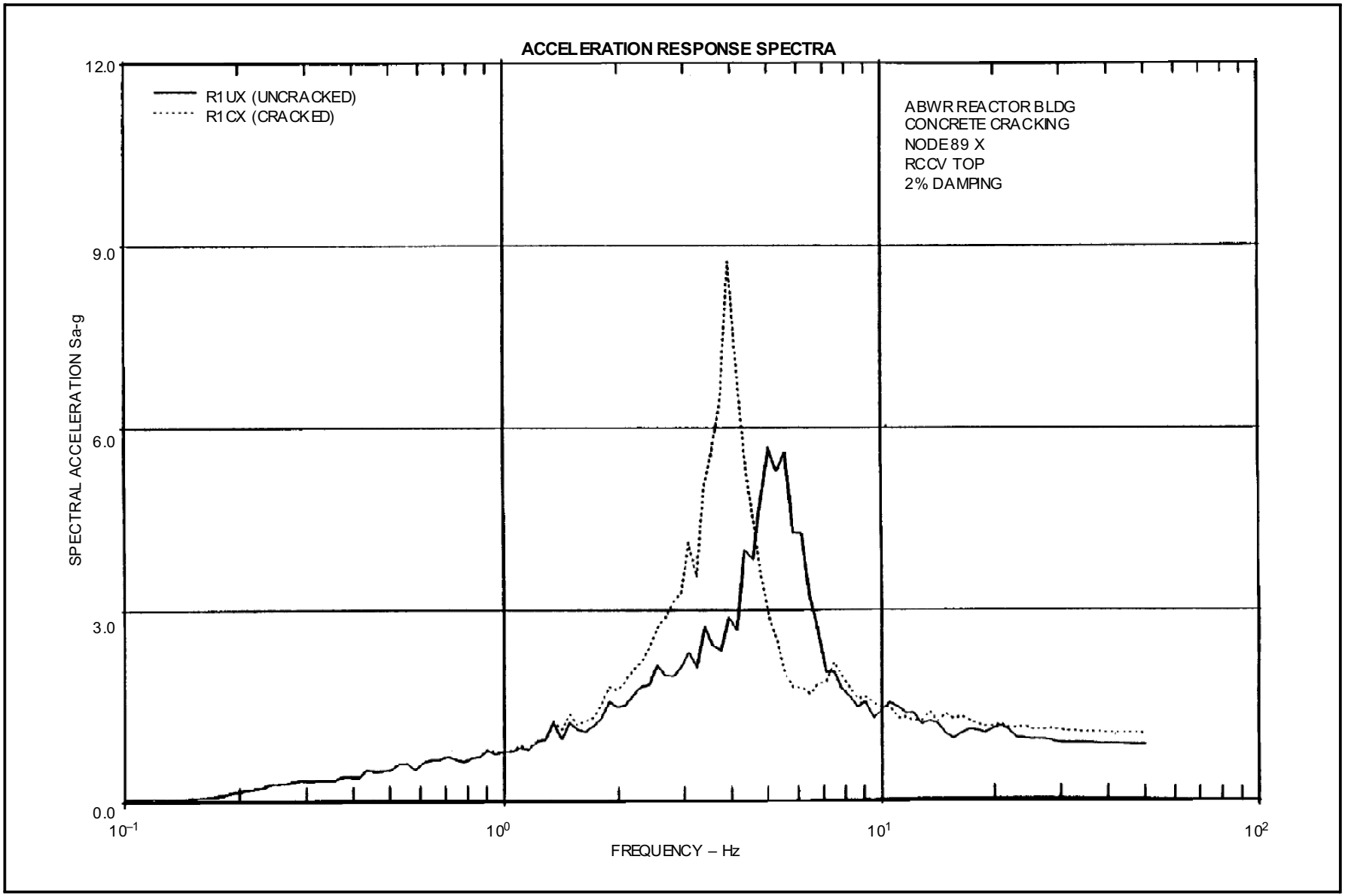

Figure 3A-86 ABWR Reactor Bldg. Concrete Cracking, Node 89 X RCCV Top, 2% Damping

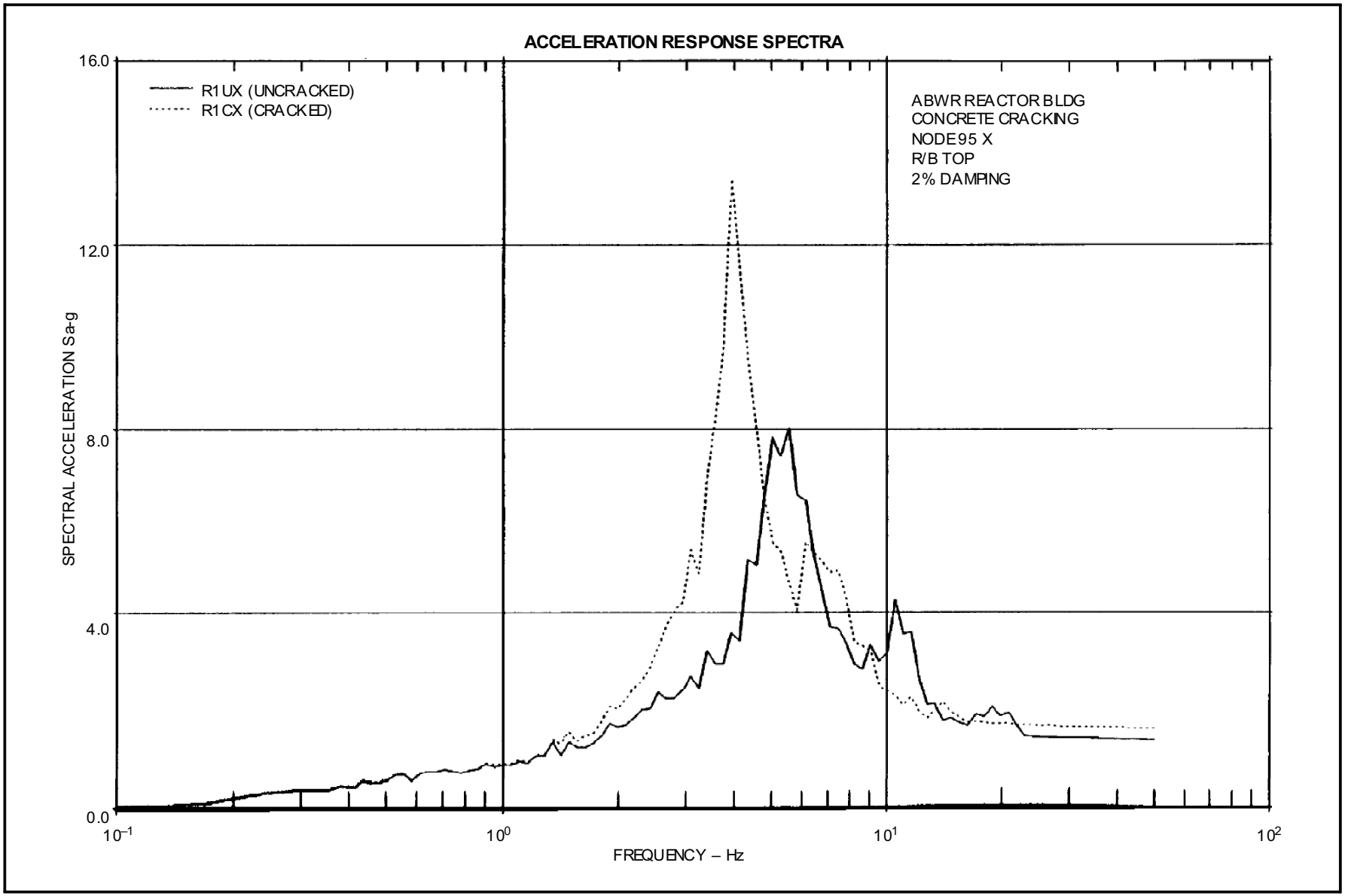

Figure 3A-87 ABWR Reactor Bldg. Concrete Cracking, Node 95 X R/B Top, 2% Damping

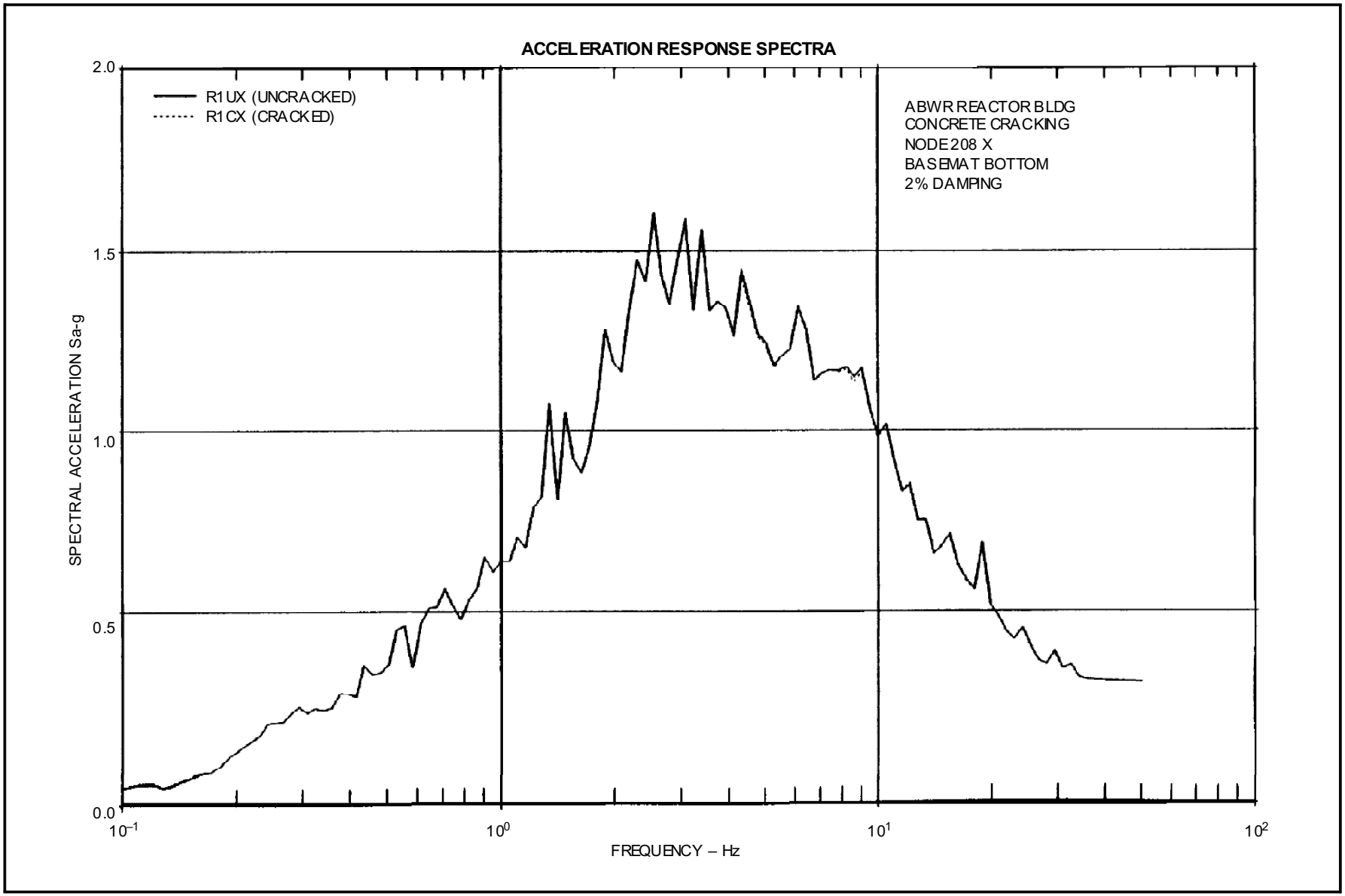

Figure 3A-88 ABWR Reactor Bldg. Concrete Cracking, Node 208 X Basemat Bottom, 2% Damping

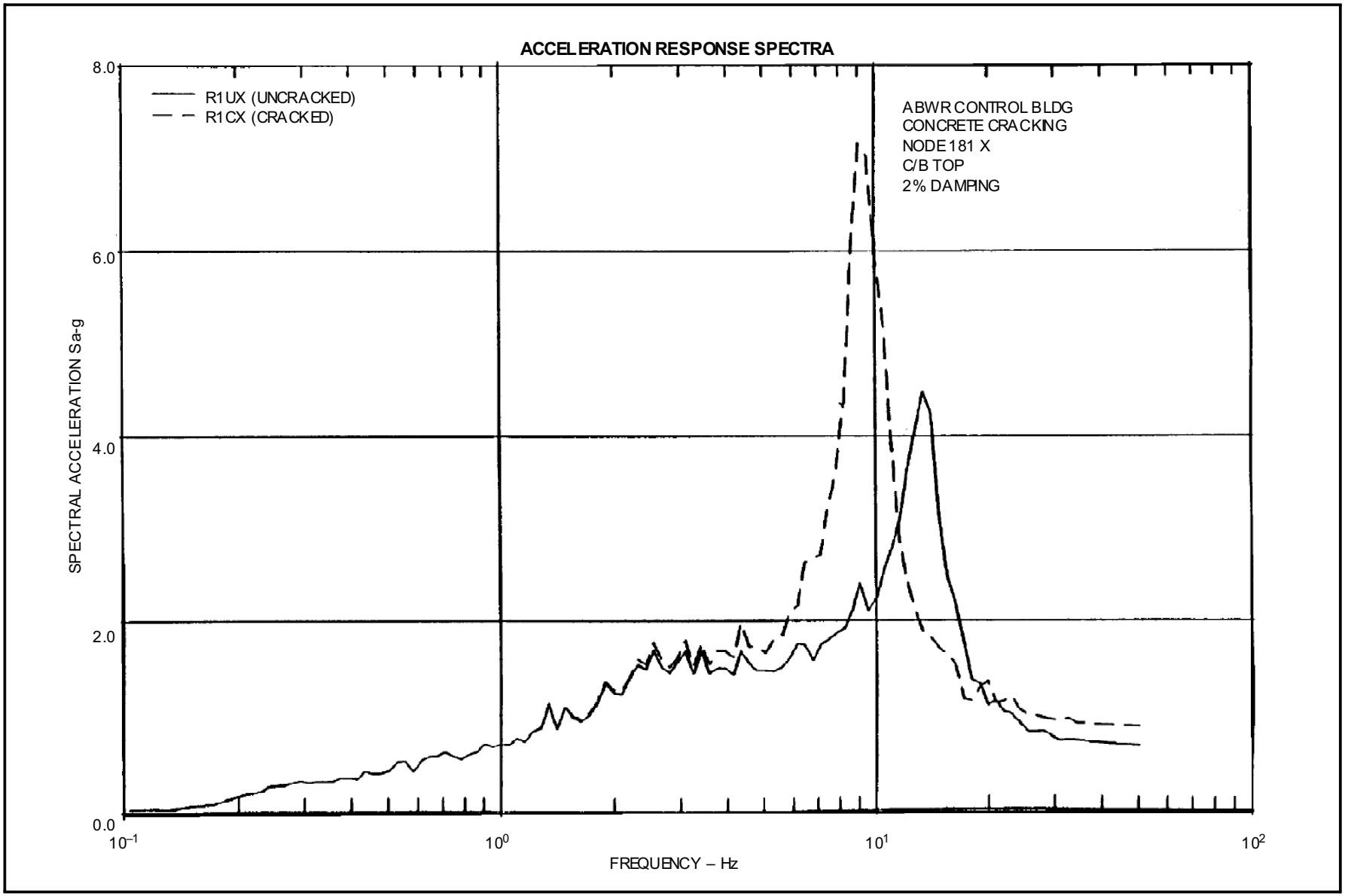

Figure 3A-89 ABWR Control Bldg. Concrete Cracking, Node 181 X C/B Top, 2% Damping

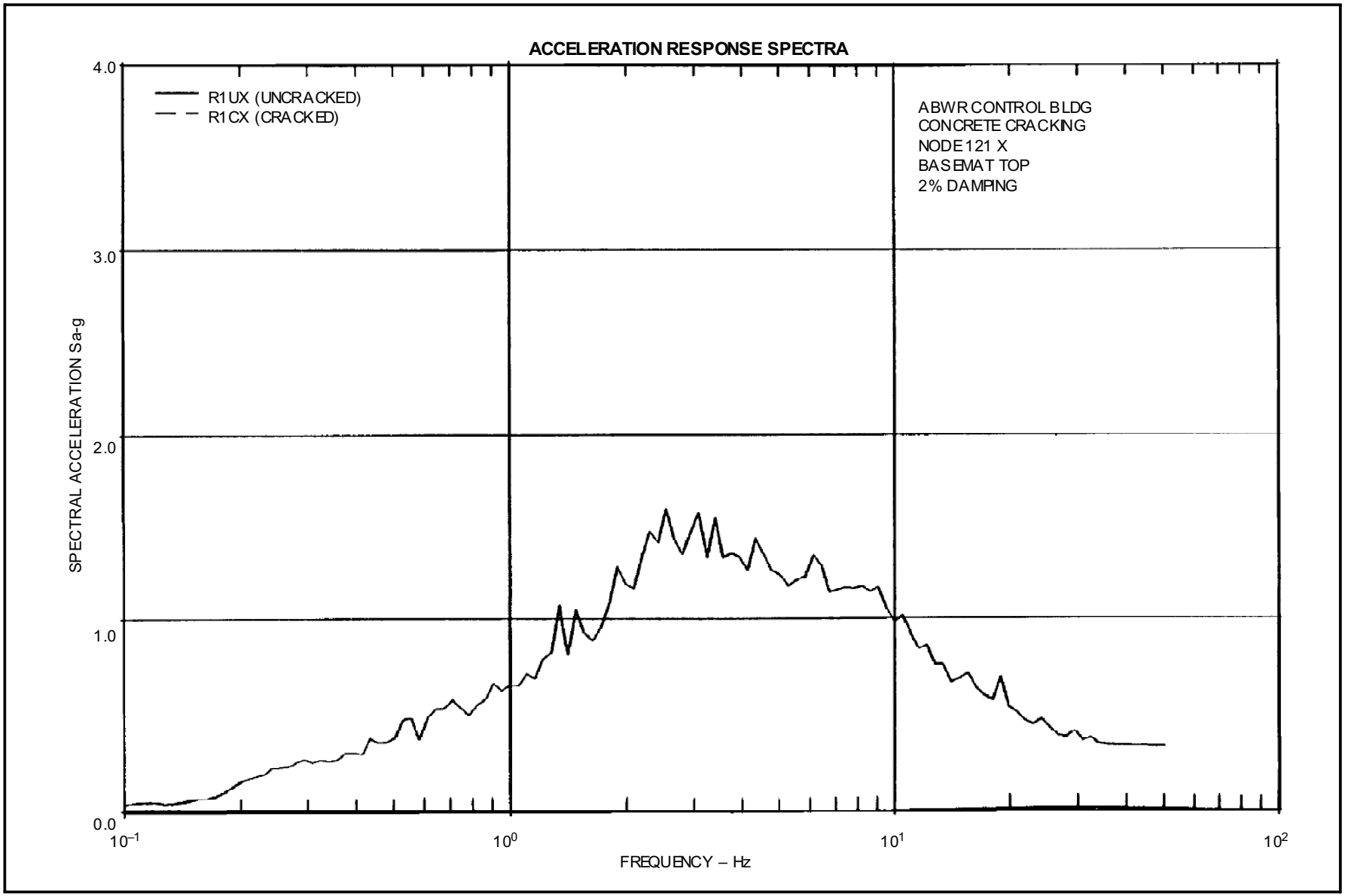

Figure 3A-90 ABWR Control Bldg. Concrete Cracking, Node 121 X Basemat Top, 2% Damping

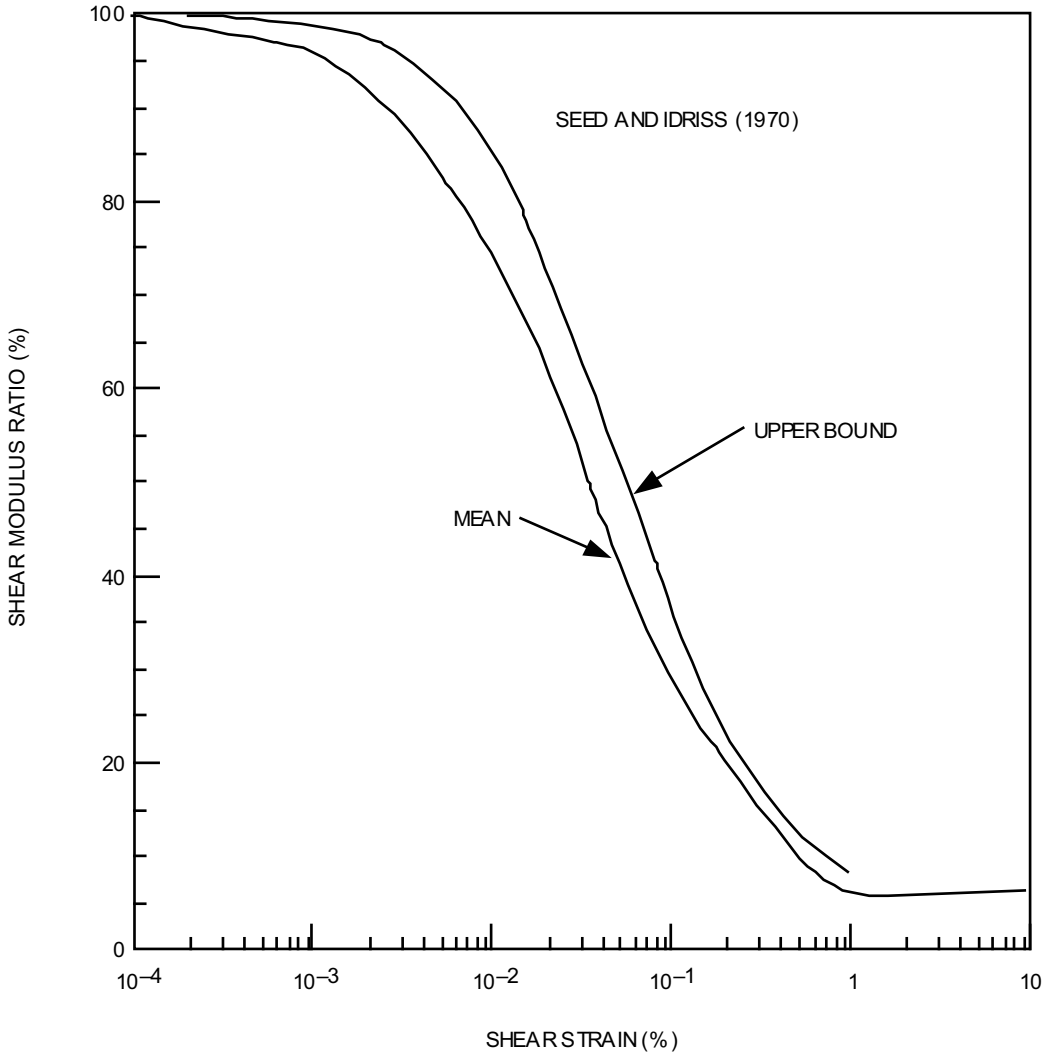

Figure 3A-91 Shear Modulus vs Shear Strain

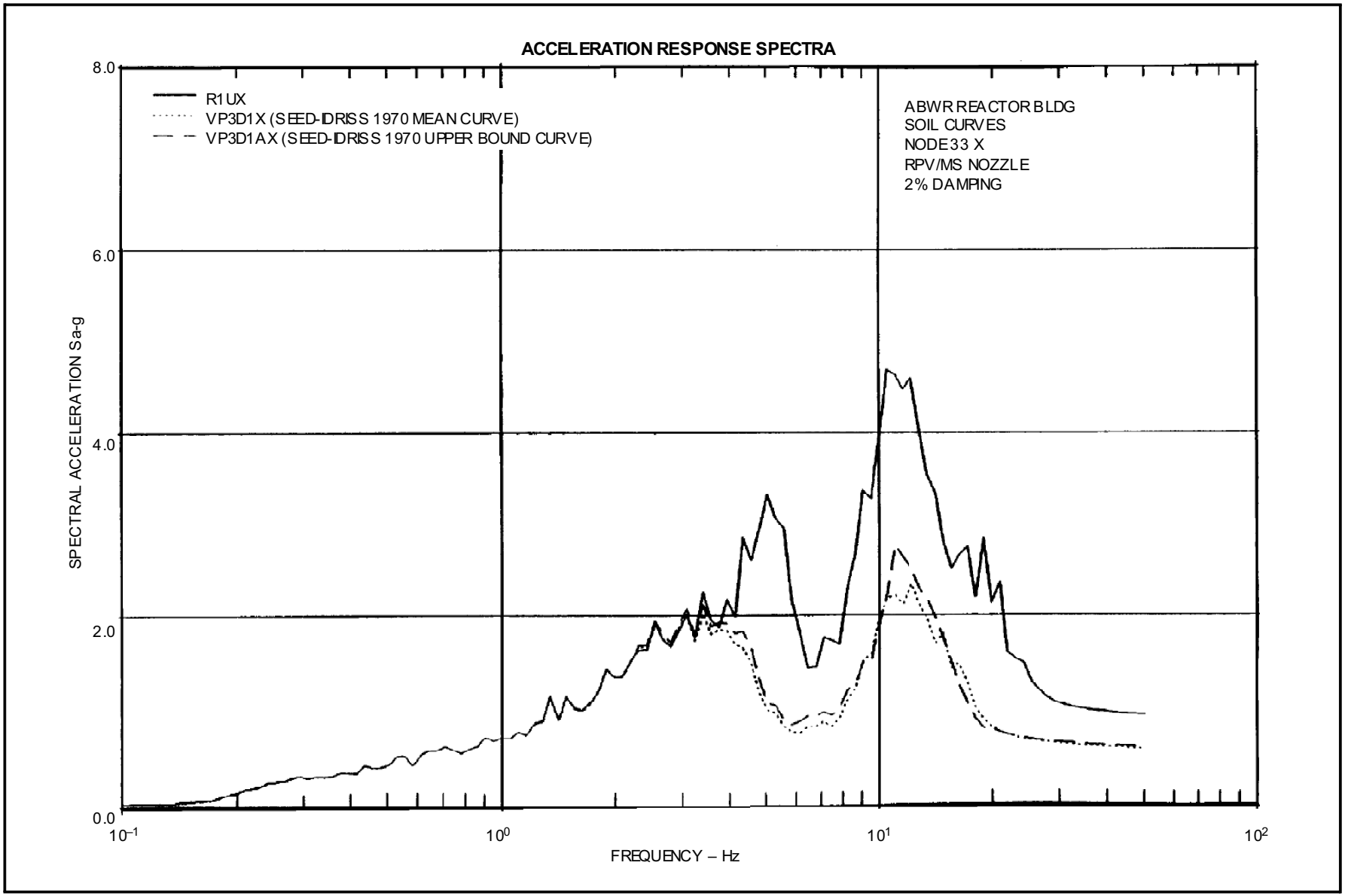

Figure 3A-92 ABWR Reactor Bldg. Soil Curves, Node 33 X RPV/MS Nozzle, 2% Damping

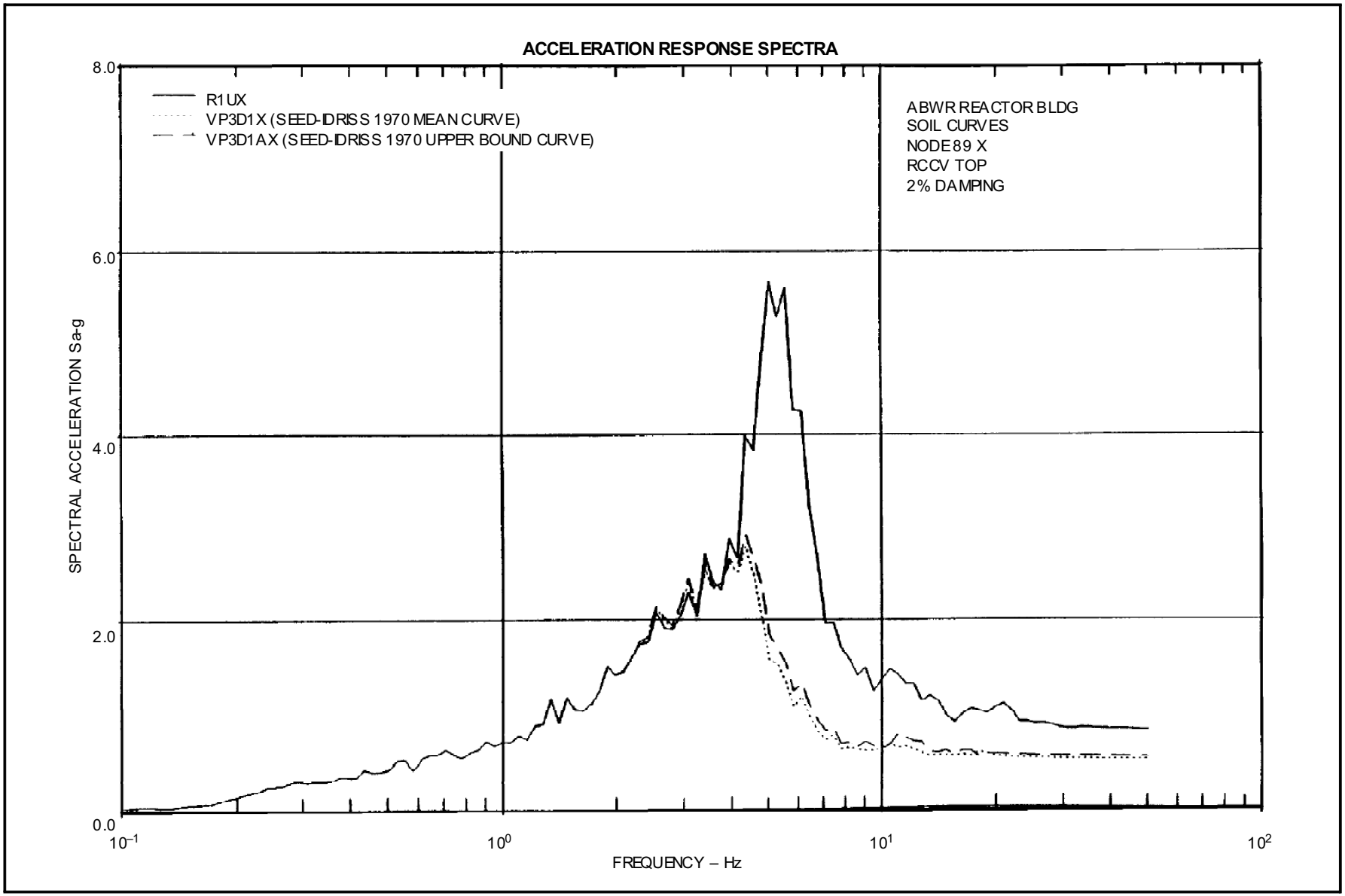

Figure 3A-93 ABWR Reactor Bldg. Soil Curves, Node 89 X RCCV Top, 2% Damping

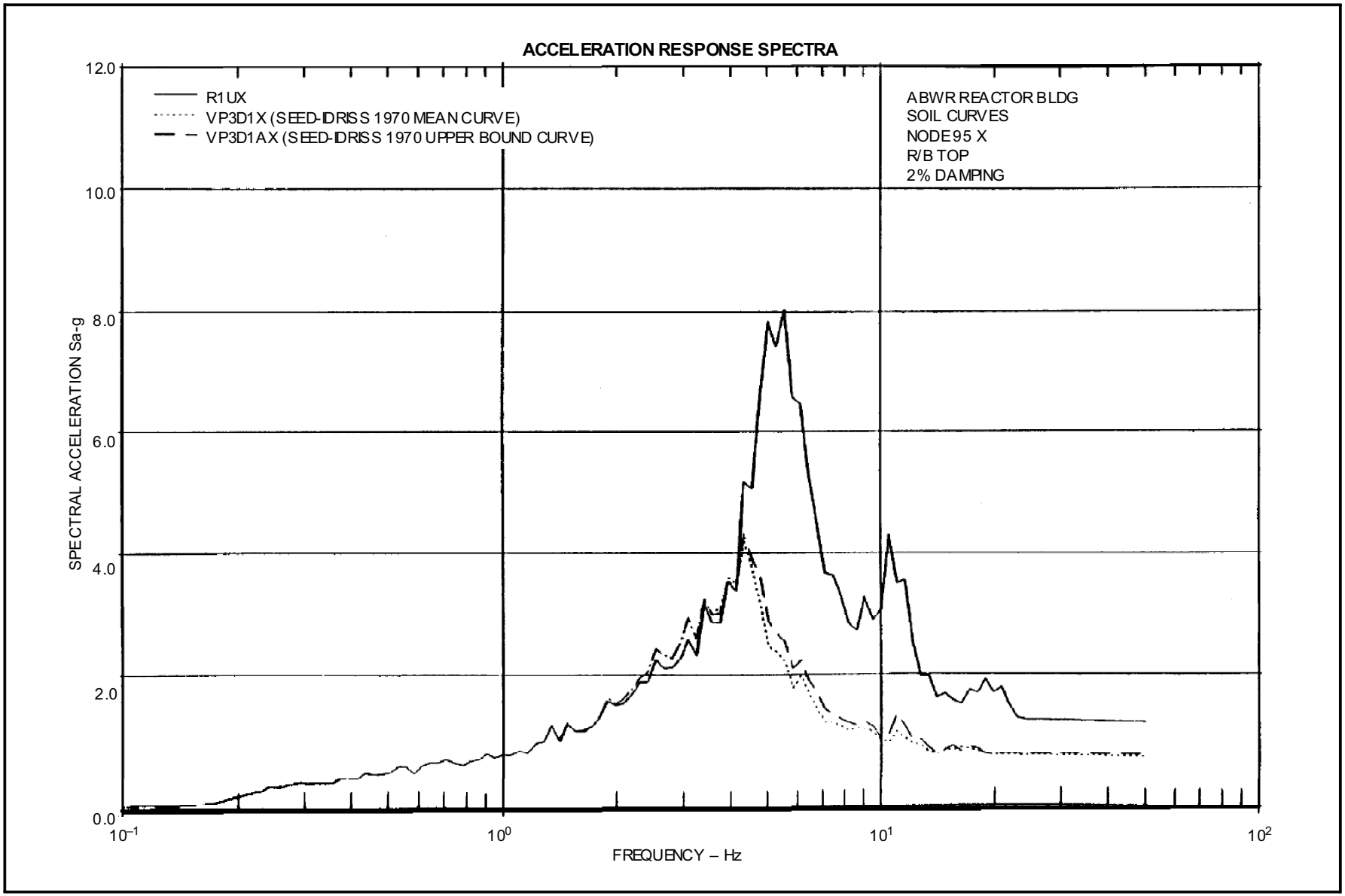

Figure 3A-94 ABWR Reactor Bldg. Soil Curves, Node 95 X R/B Top, 2% Damping

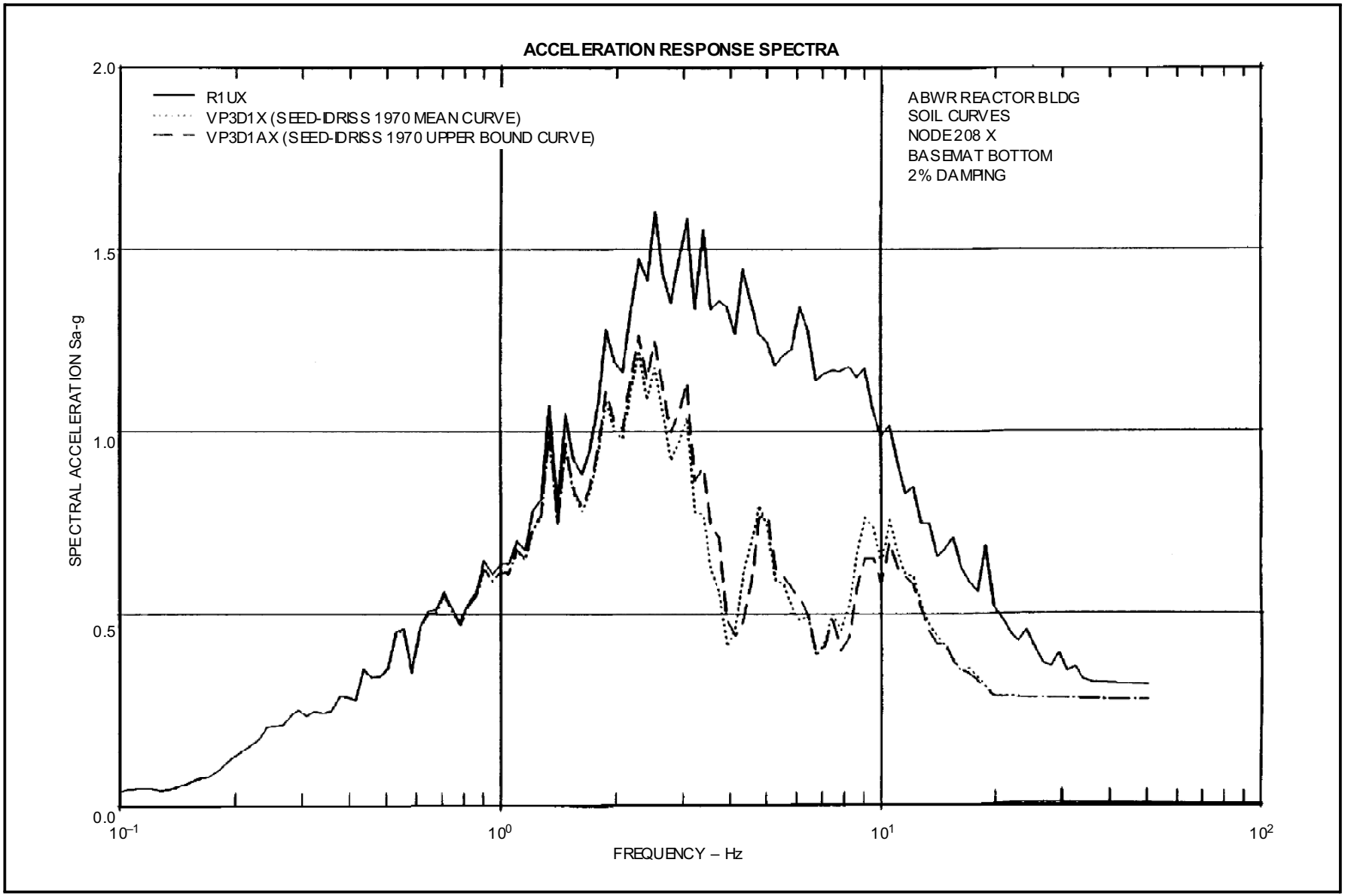

Figure 3A-95 ABWR Reactor Bldg. Soil Curves, Node 208 X Basemat Bottom, 2% Damping

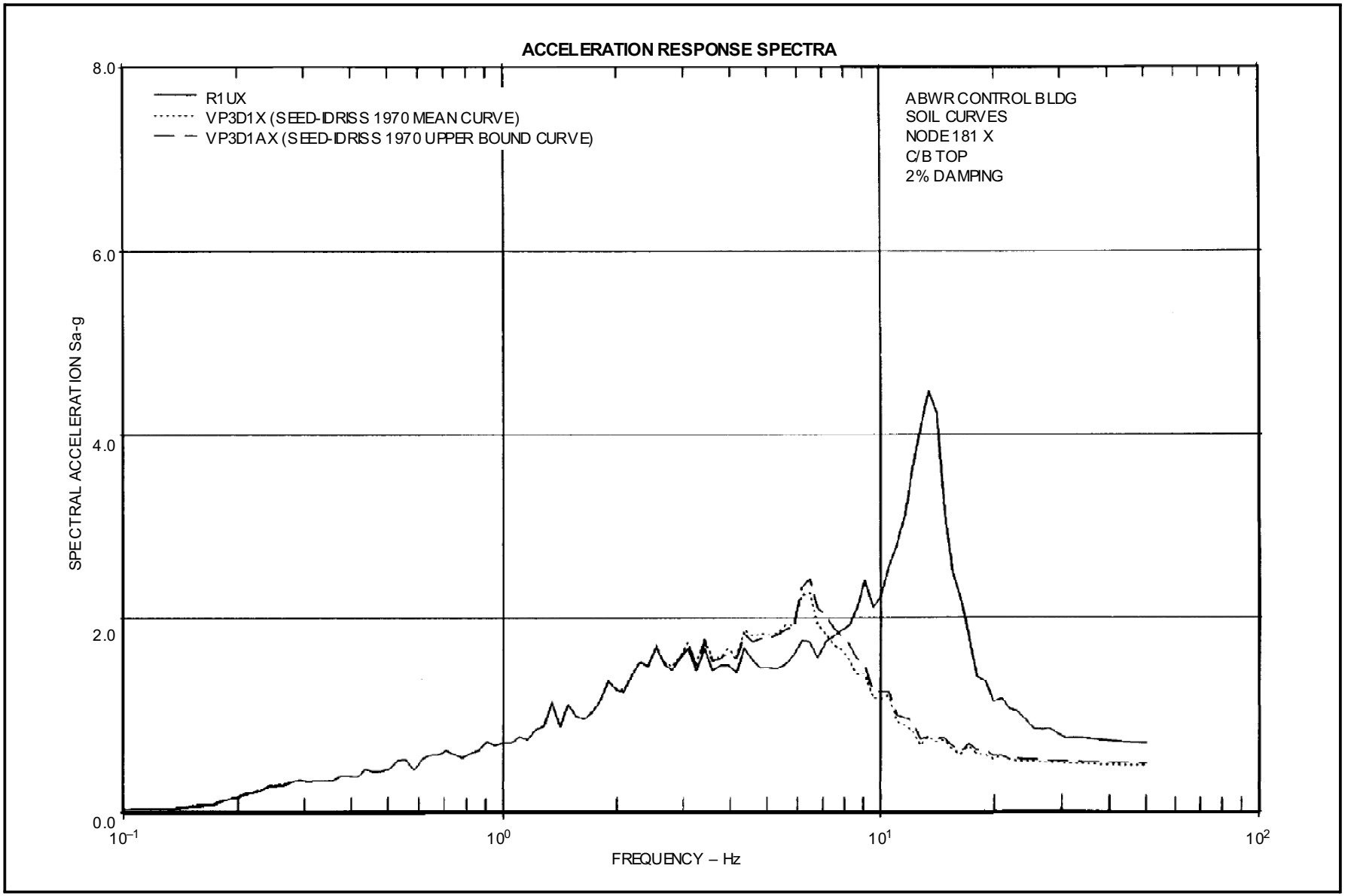

Figure 3A-96 ABWR Control Bldg. Soil Curves, Node 181 X C/B Top, 2% Damping

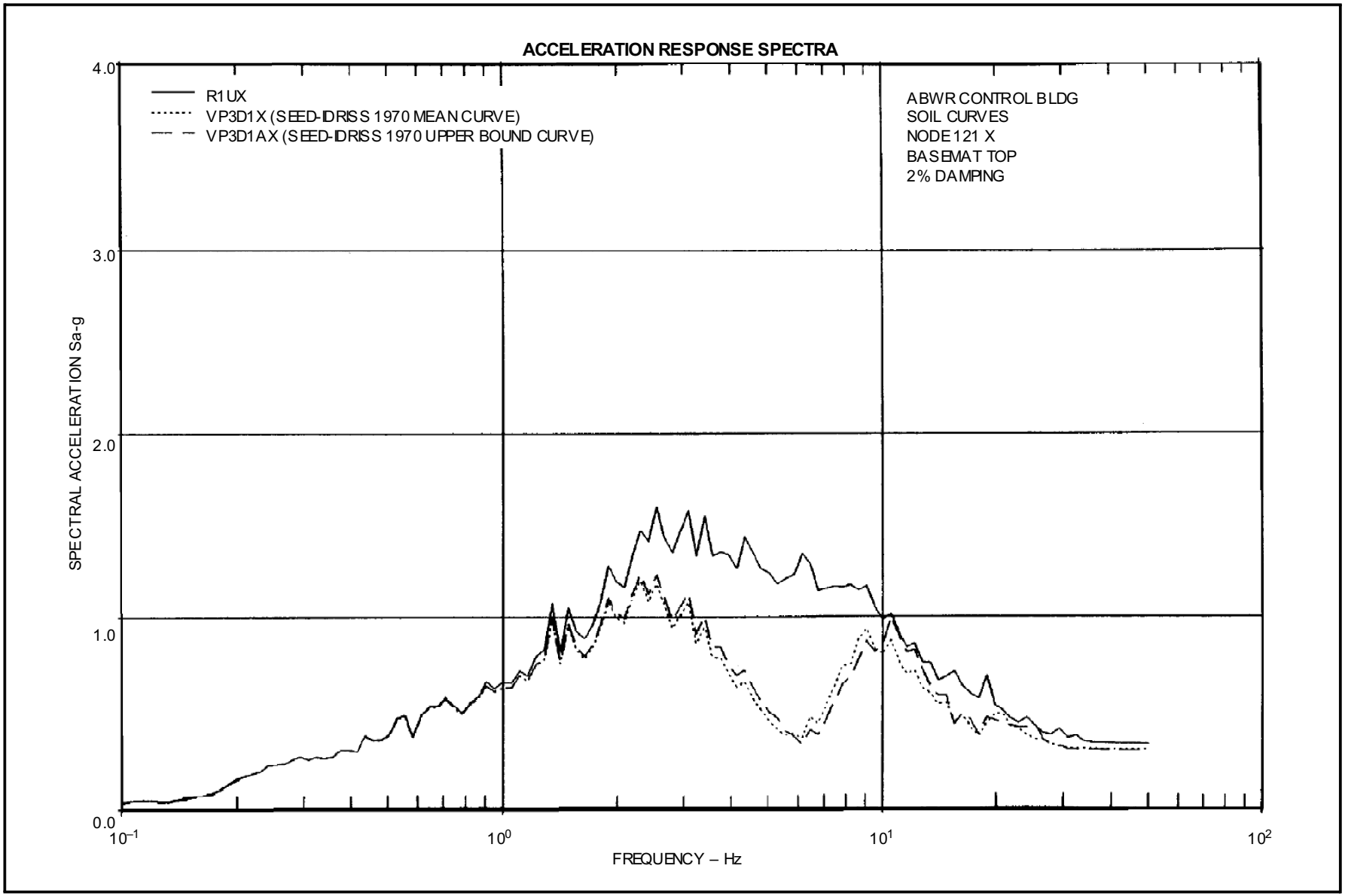

Figure 3A-97 ABWR Control Bldg. Soil Curves, Node 121 X Basemat Top, 2% Damping

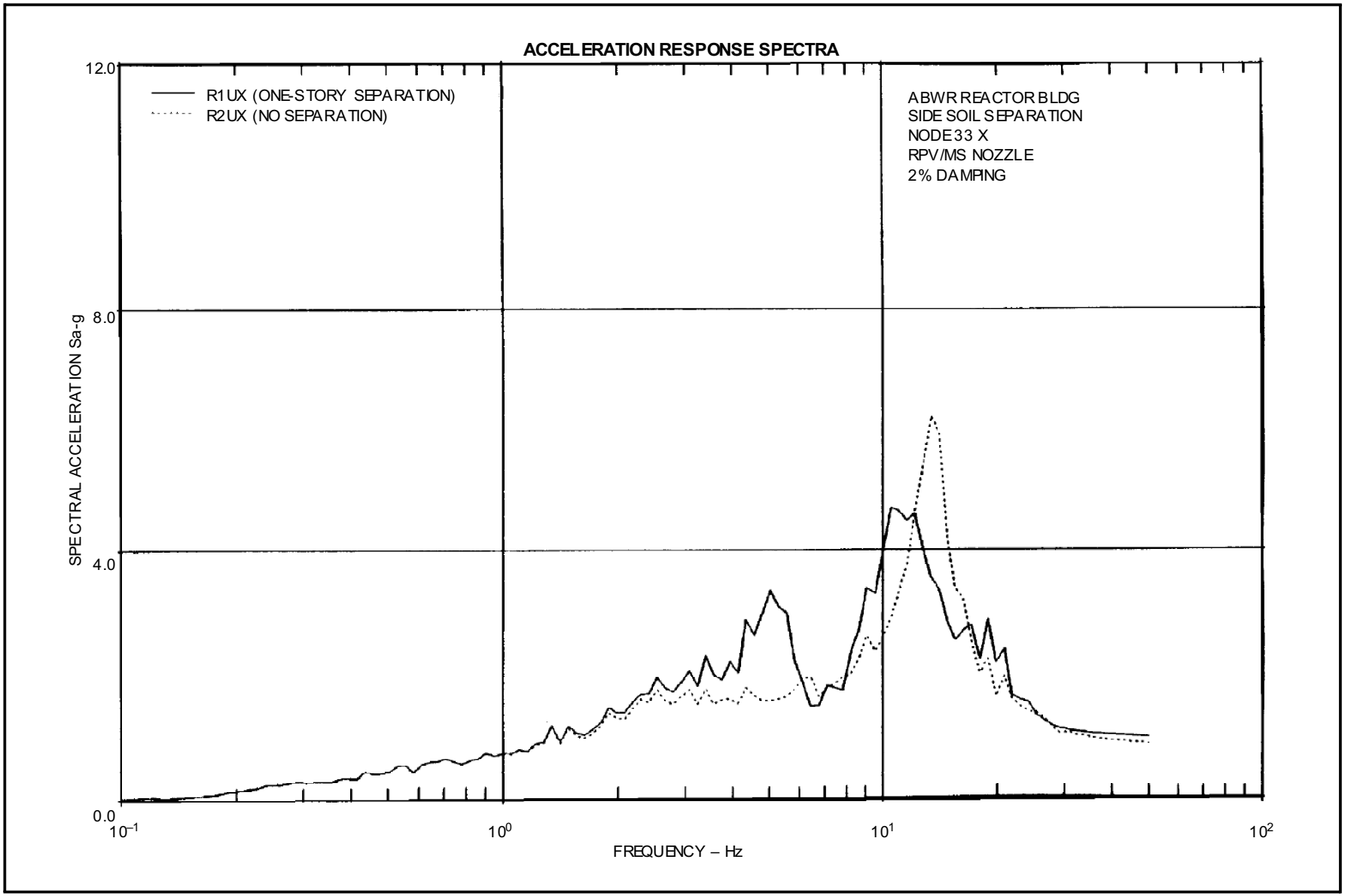

Figure 3A-98 ABWR Reactor Bldg. Side Soil Separation, Node 33 X RPV/MS Nozzle, 2% Damping

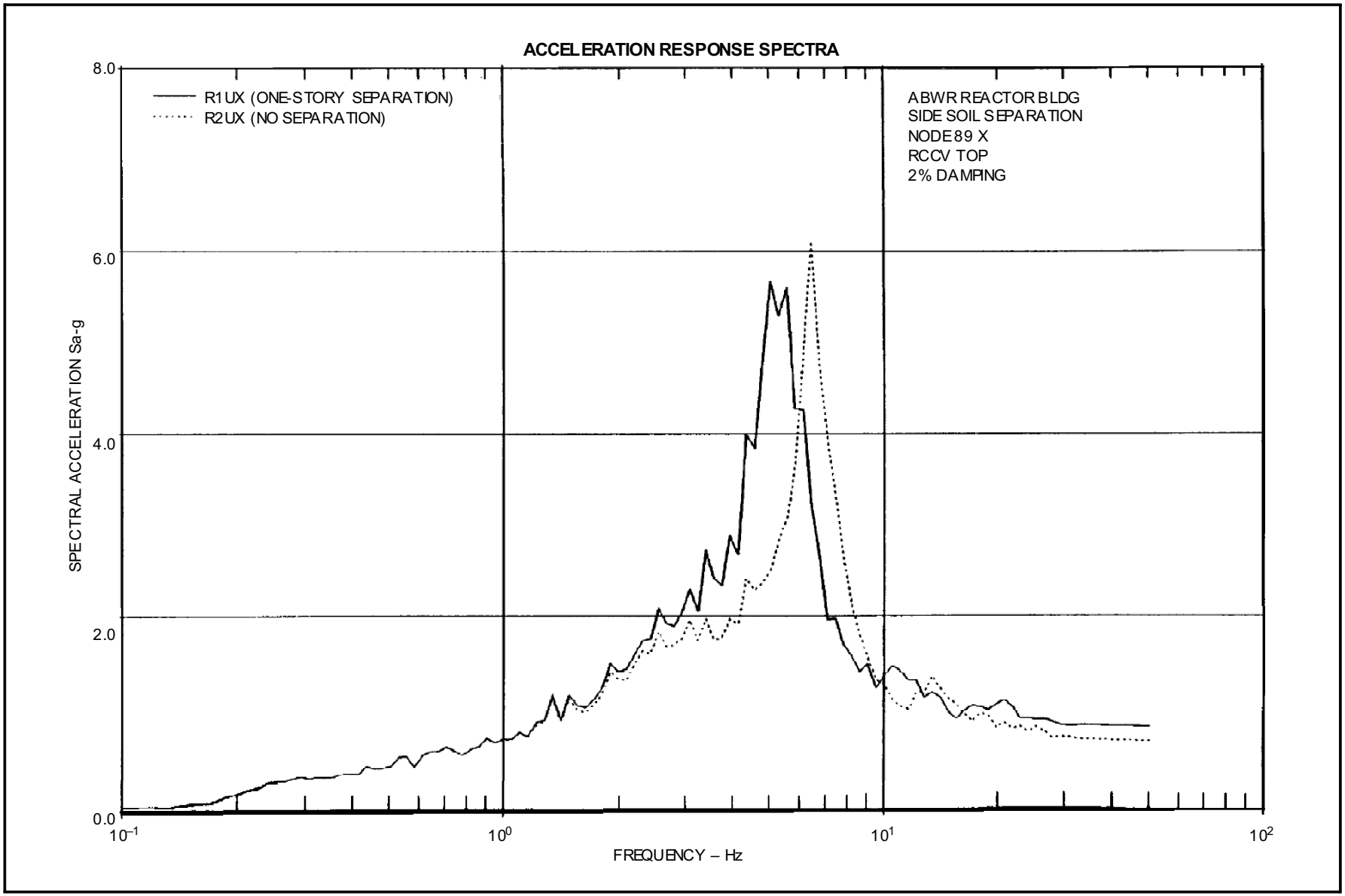

Figure 3A-99 ABWR Reactor Bldg. Side Soil Separation, Node 89 X RCCV Top, 2% Damping

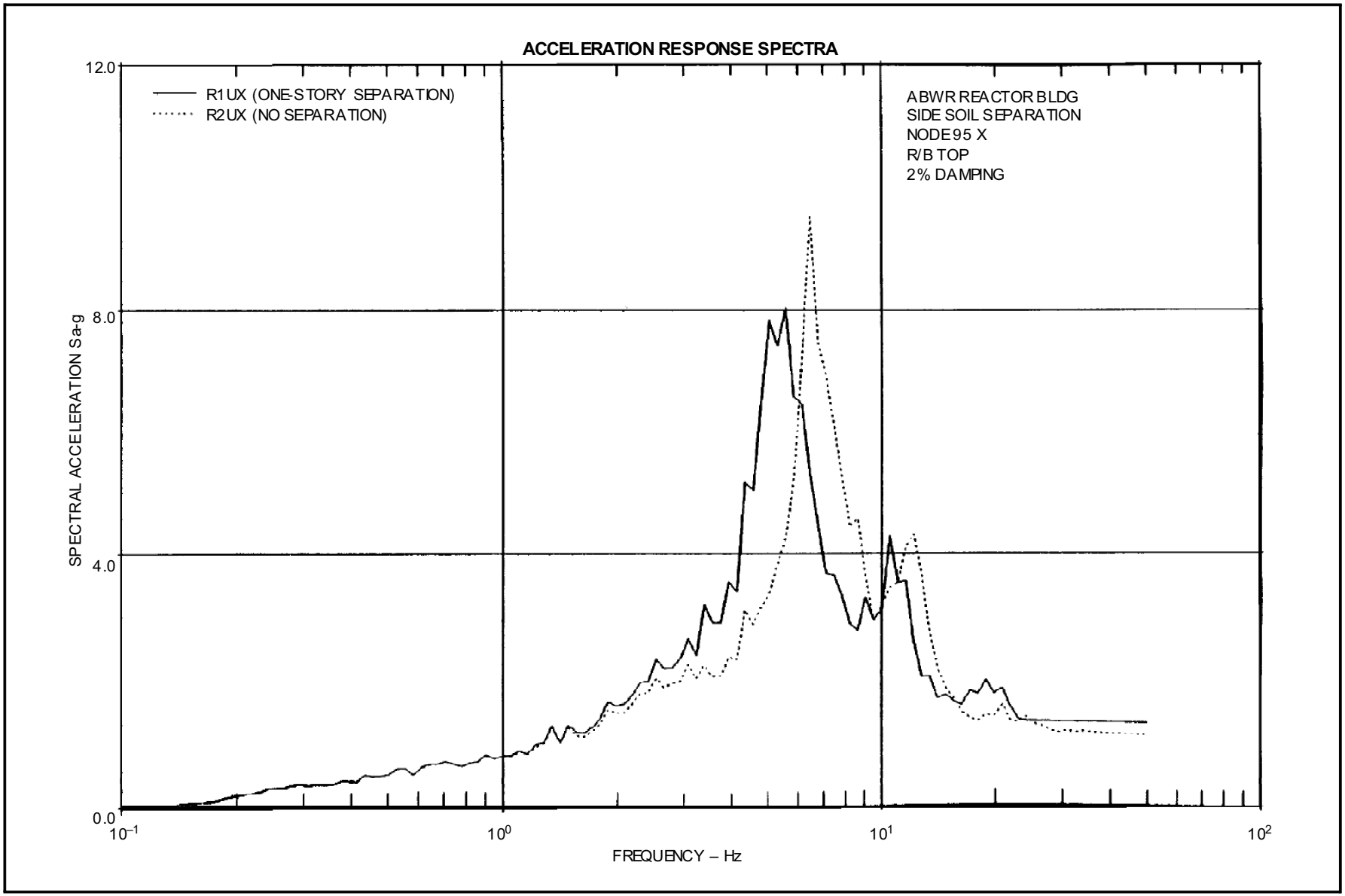

Figure 3A-100 ABWR Reactor Bldg. Side Soil Separation, Node 95 X R/B Top, 2% Damping

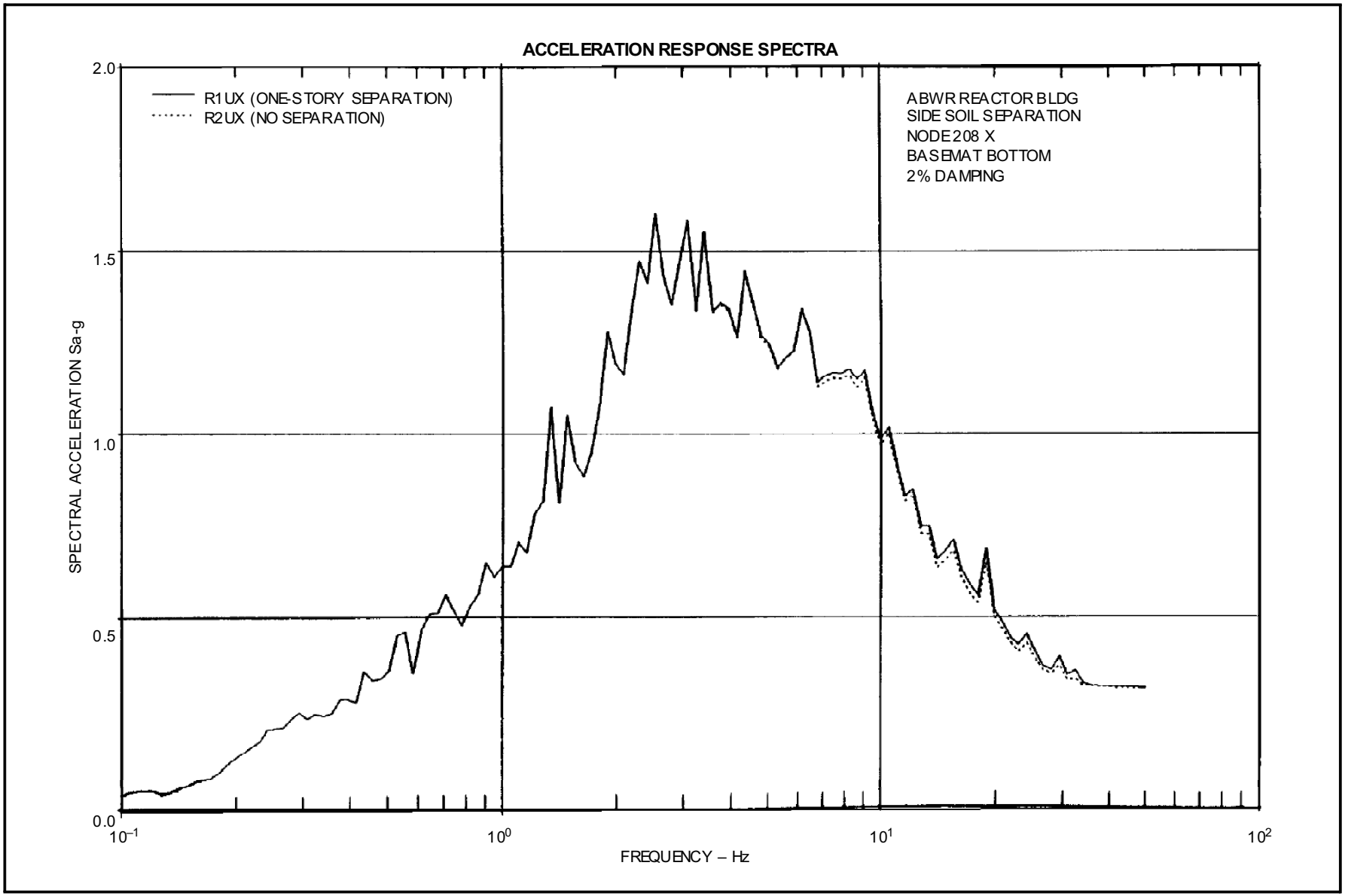

Figure 3A-101 ABWR Reactor Bldg. Side Soil Separation, Node 208 X Basemat Bottom, 2% Damping

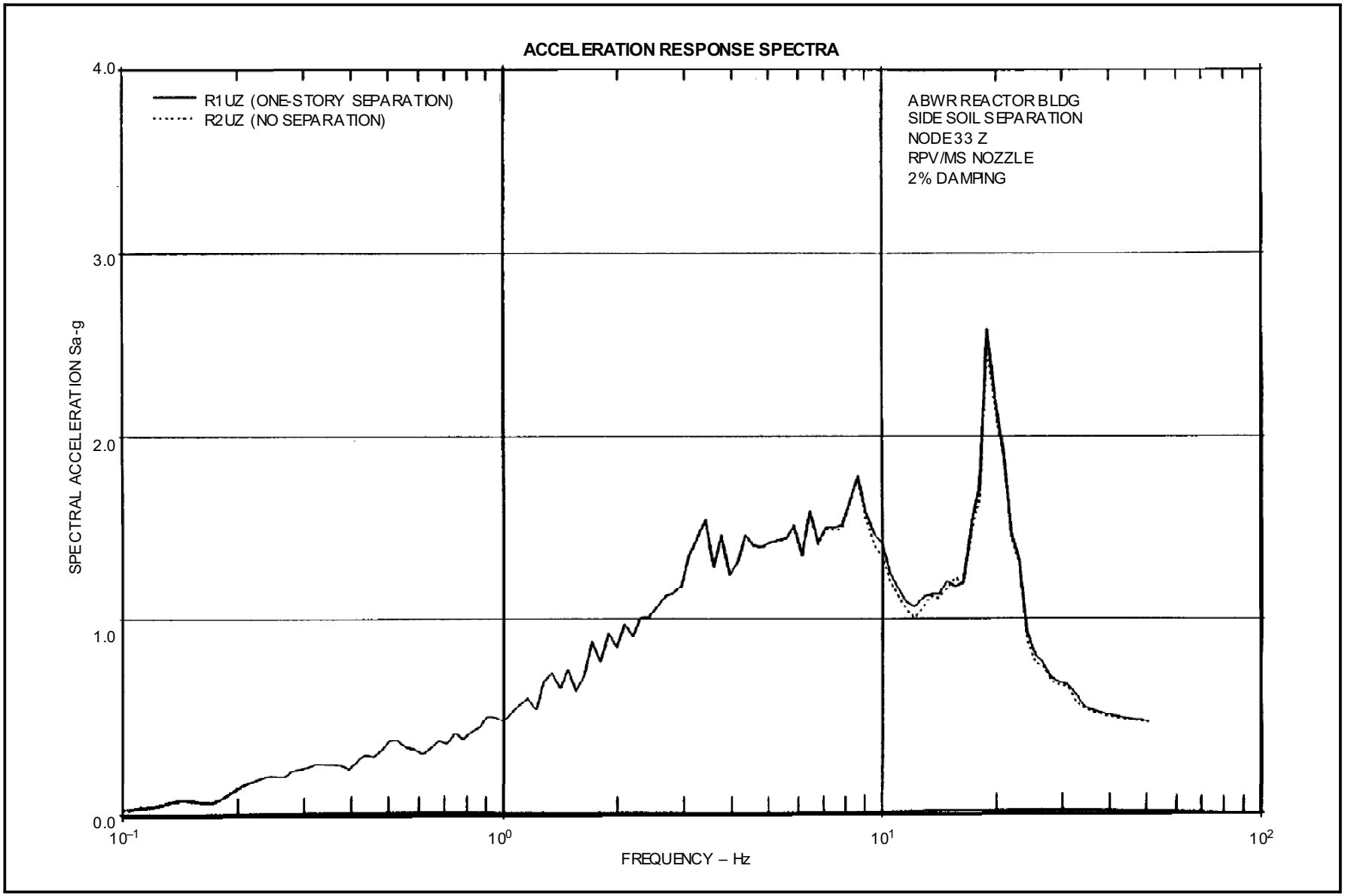

Figure 3A-102 ABWR Reactor Bldg. Side Soil Separation, Node 33 Z RPV/MS Nozzle, 2% Damping

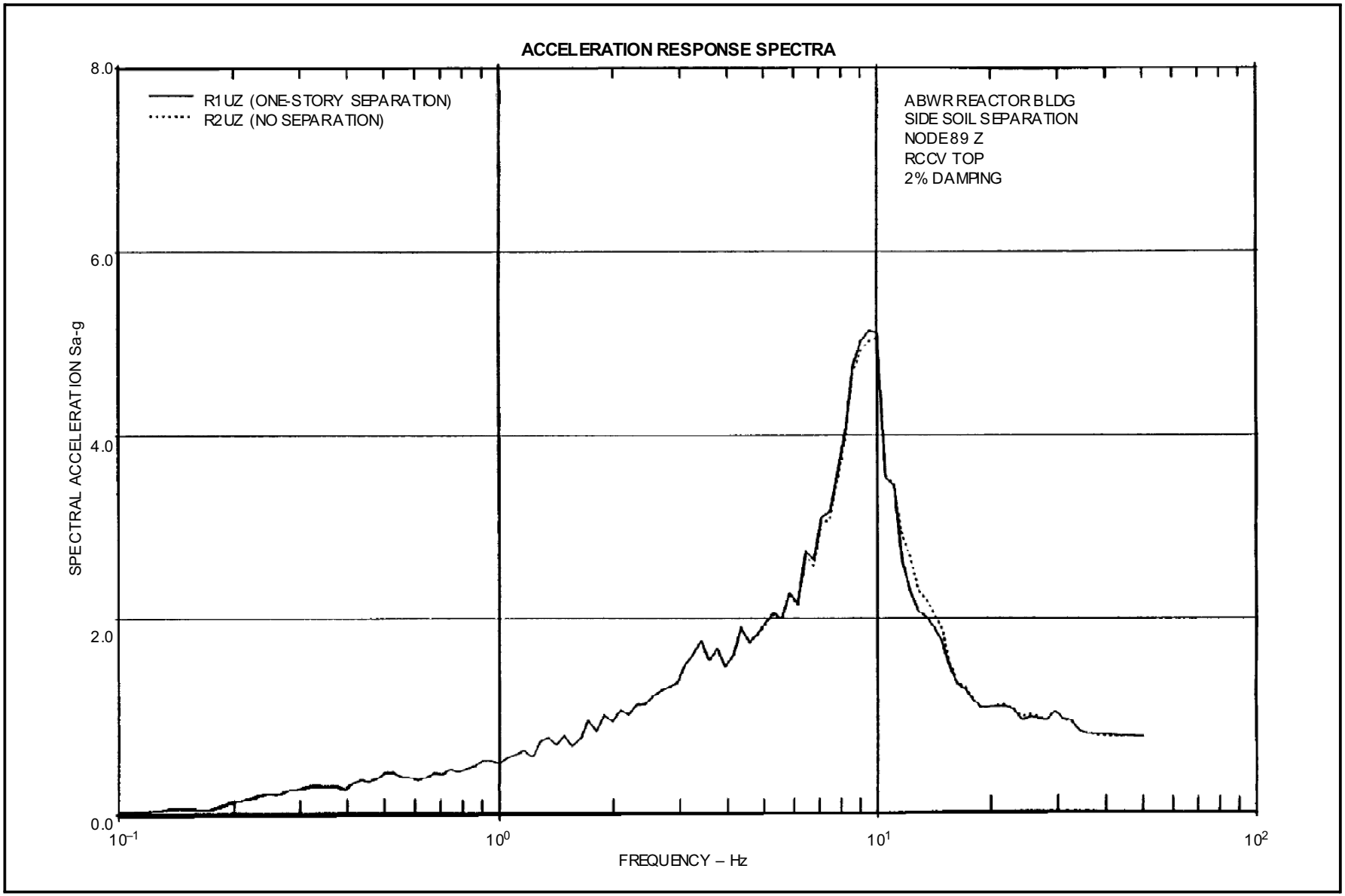

Figure 3A-103 ABWR Reactor Bldg. Side Soil Separation, Node 89 Z RCCV Top, 2% Damping

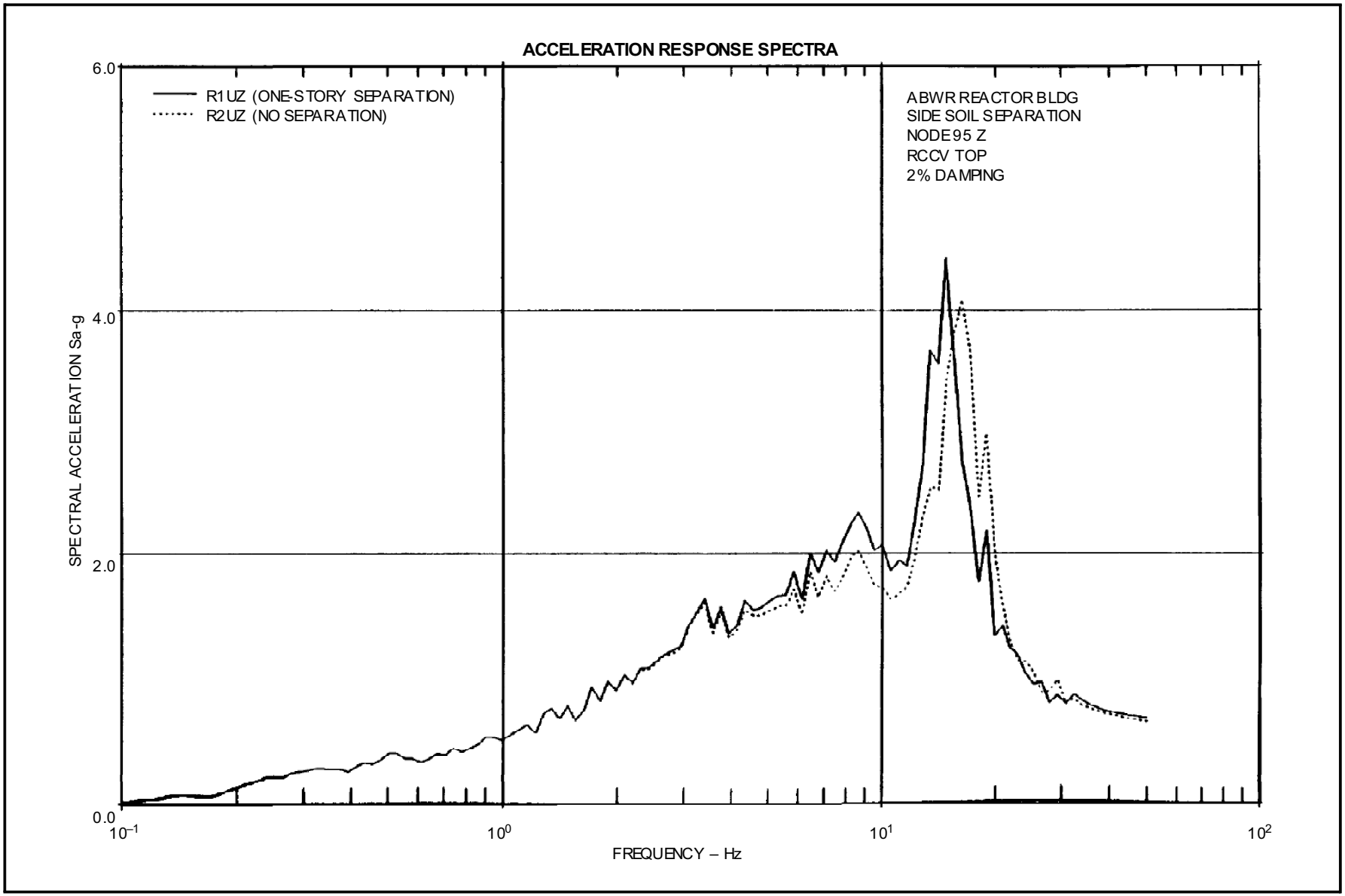

Figure 3A-104 ABWR Reactor Bldg. Side Soil Separation, Node 95 Z R/B Top, 2% Damping

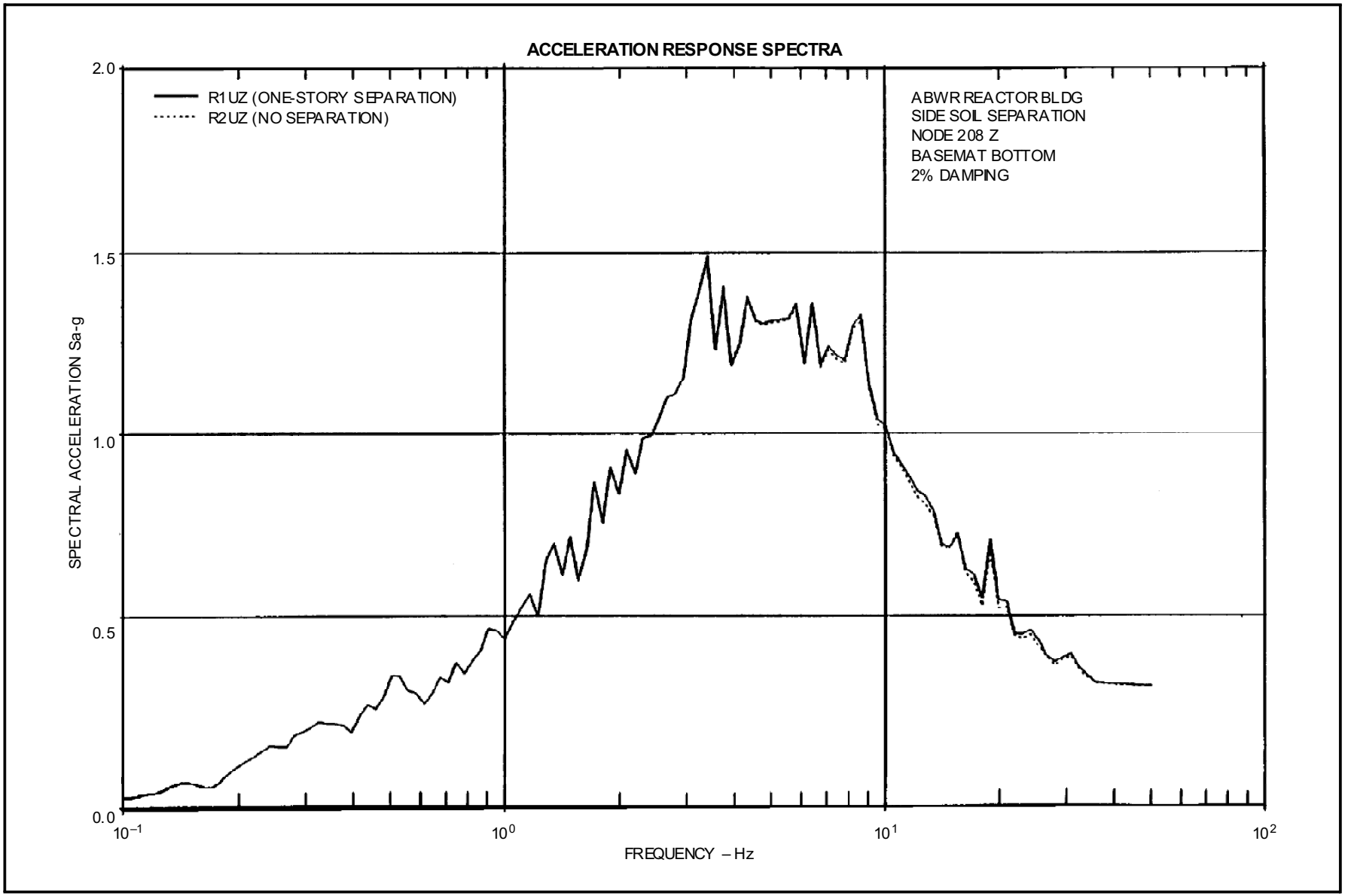

Figure 3A-105 ABWR Reactor Bldg. Side Soil Separation, Node 208 Z Basemat Bottom, 2% Damping

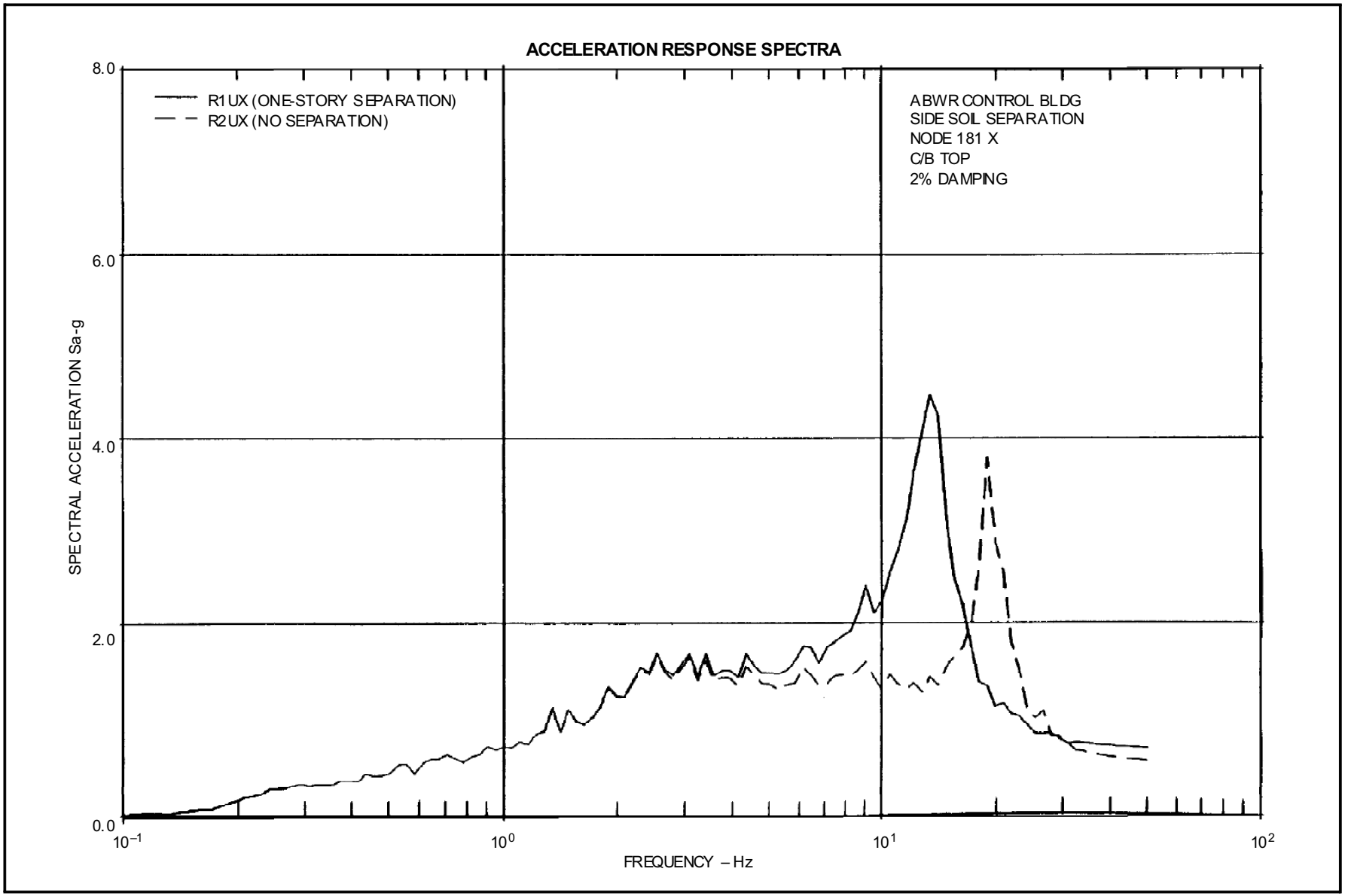

Figure 3A-106 ABWR Control Bldg. Side Soil Separation, Node 181 X C/B Top, 2% Damping

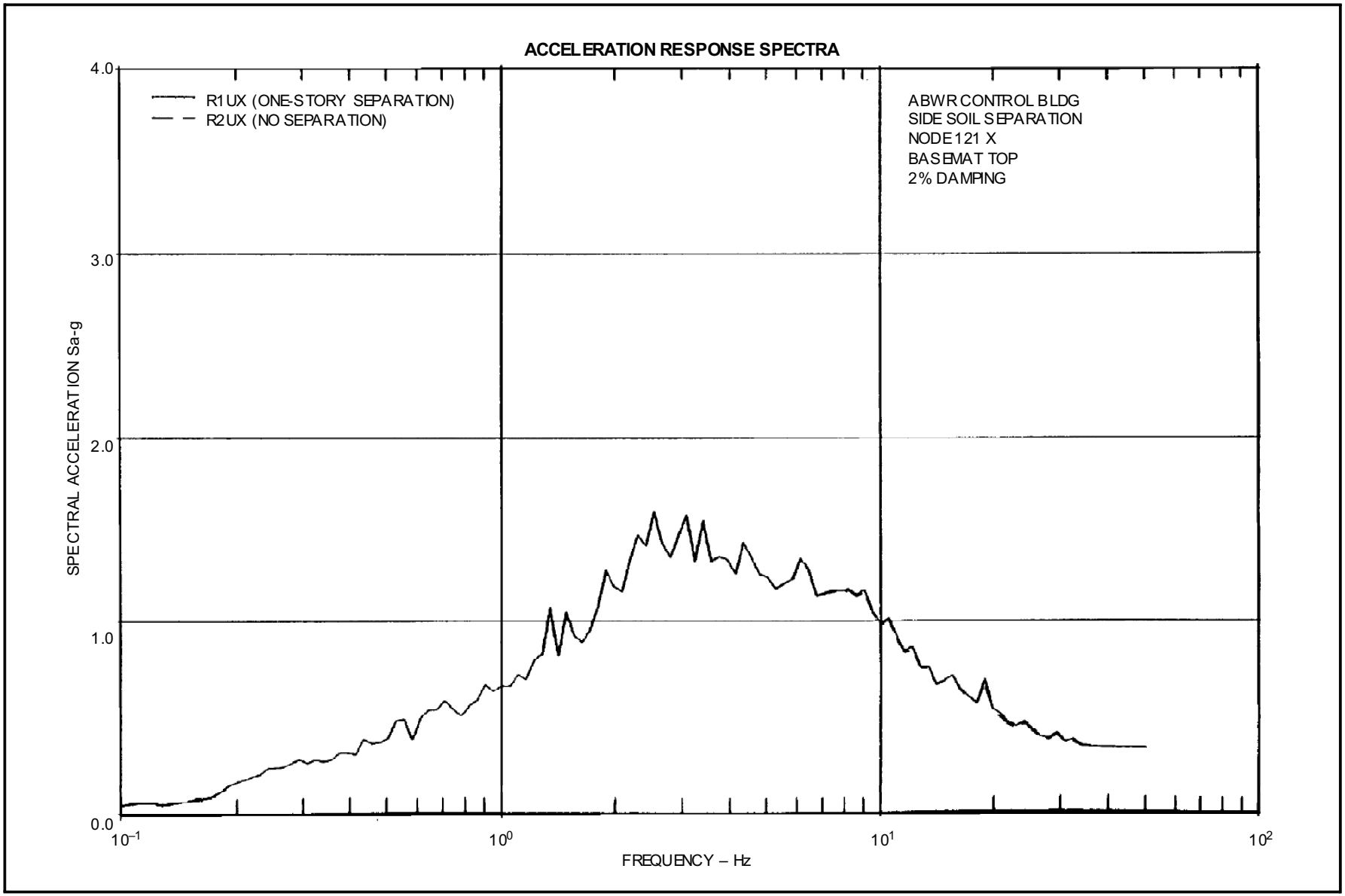

Figure 3A-107 ABWR Control Bldg. Side Soil Separation, Node 121 X Basemat Top, 2% Damping

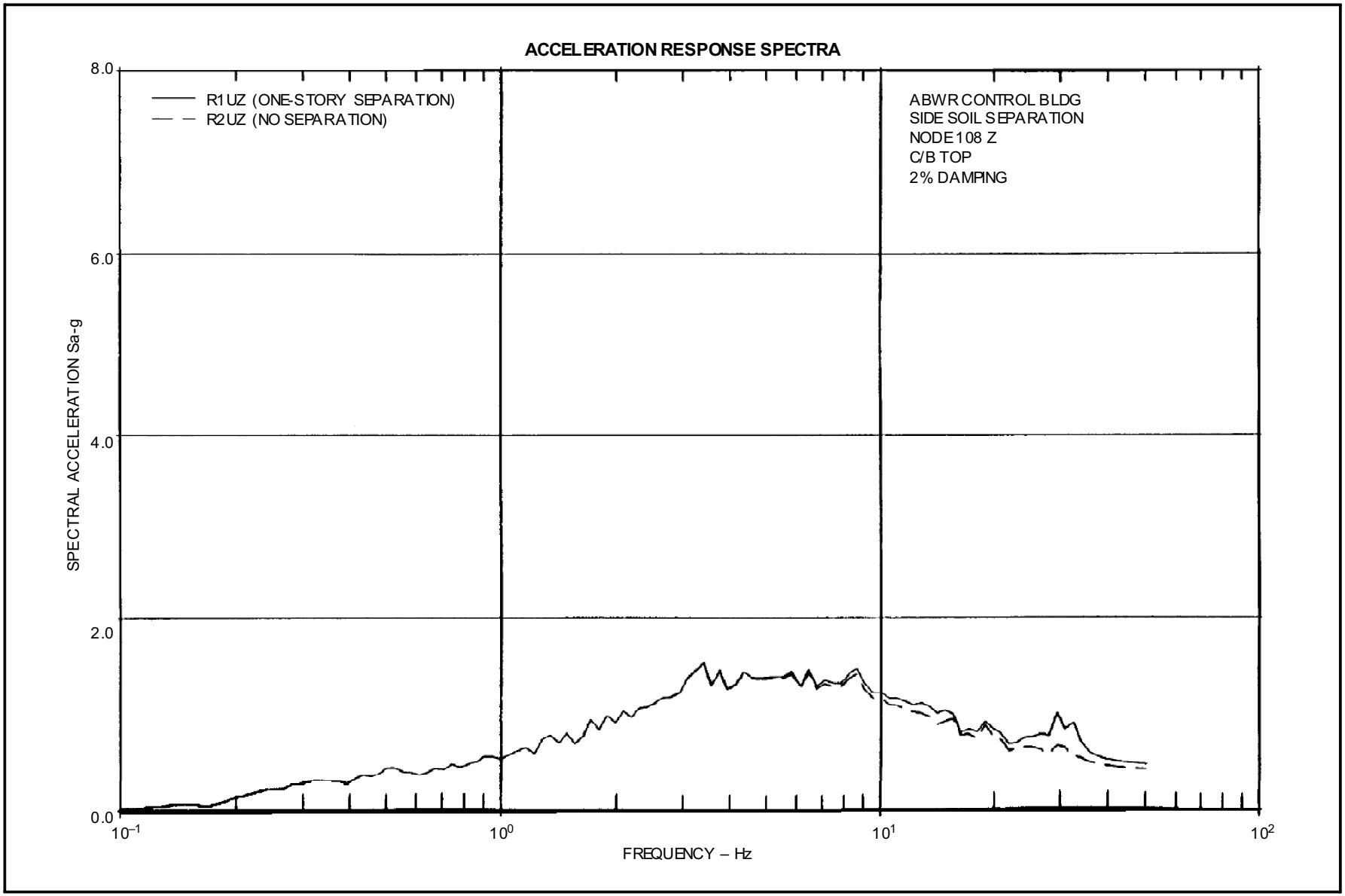

Figure 3A-108 ABWR Control Bldg. Side Soil Separation, Node 108 Z C/B Top, 2% Damping

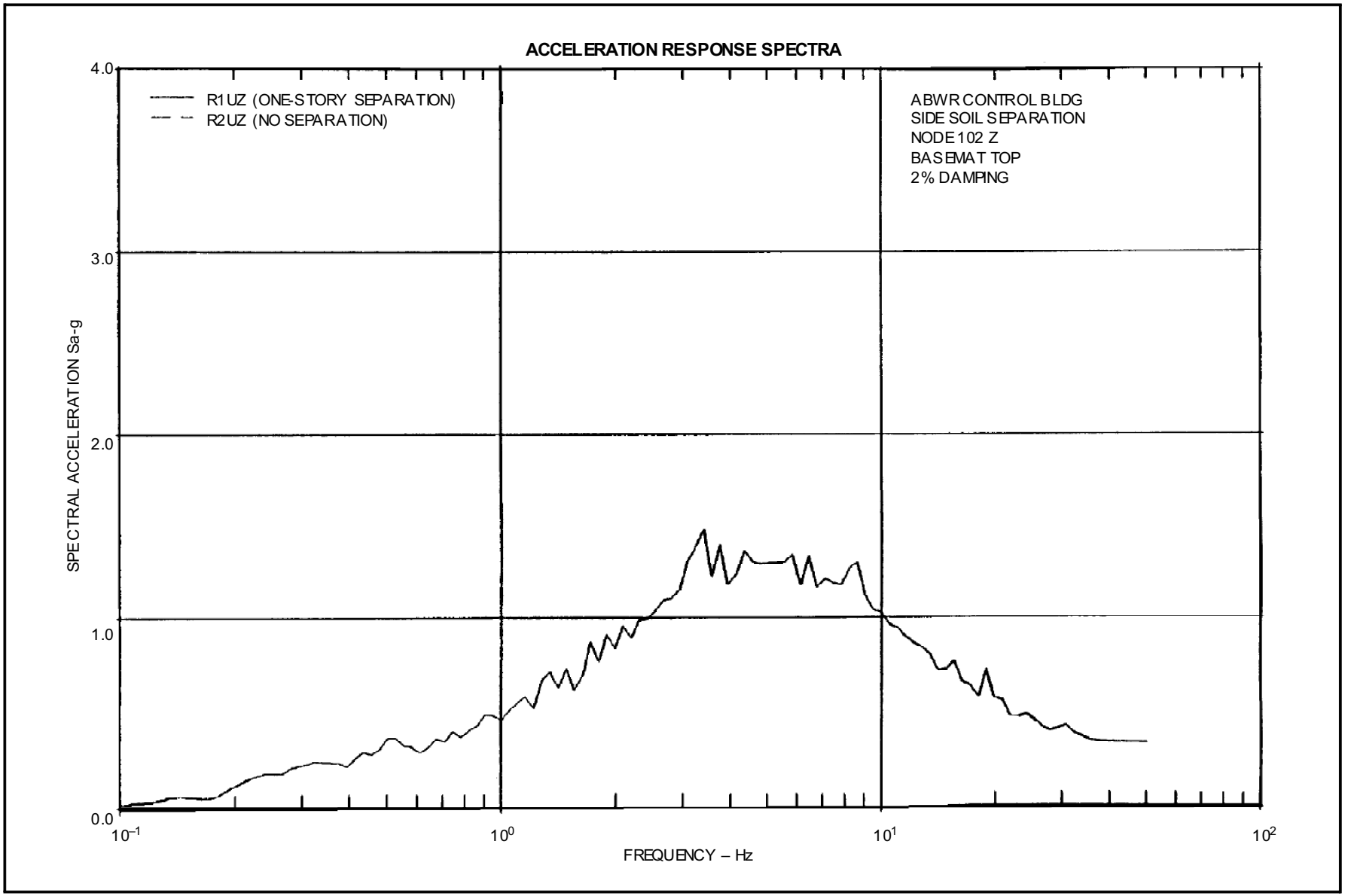

Figure 3A-109 ABWR Control Bldg. Side Soil Separation, Node 102 Z Basemat Top, 2% Damping

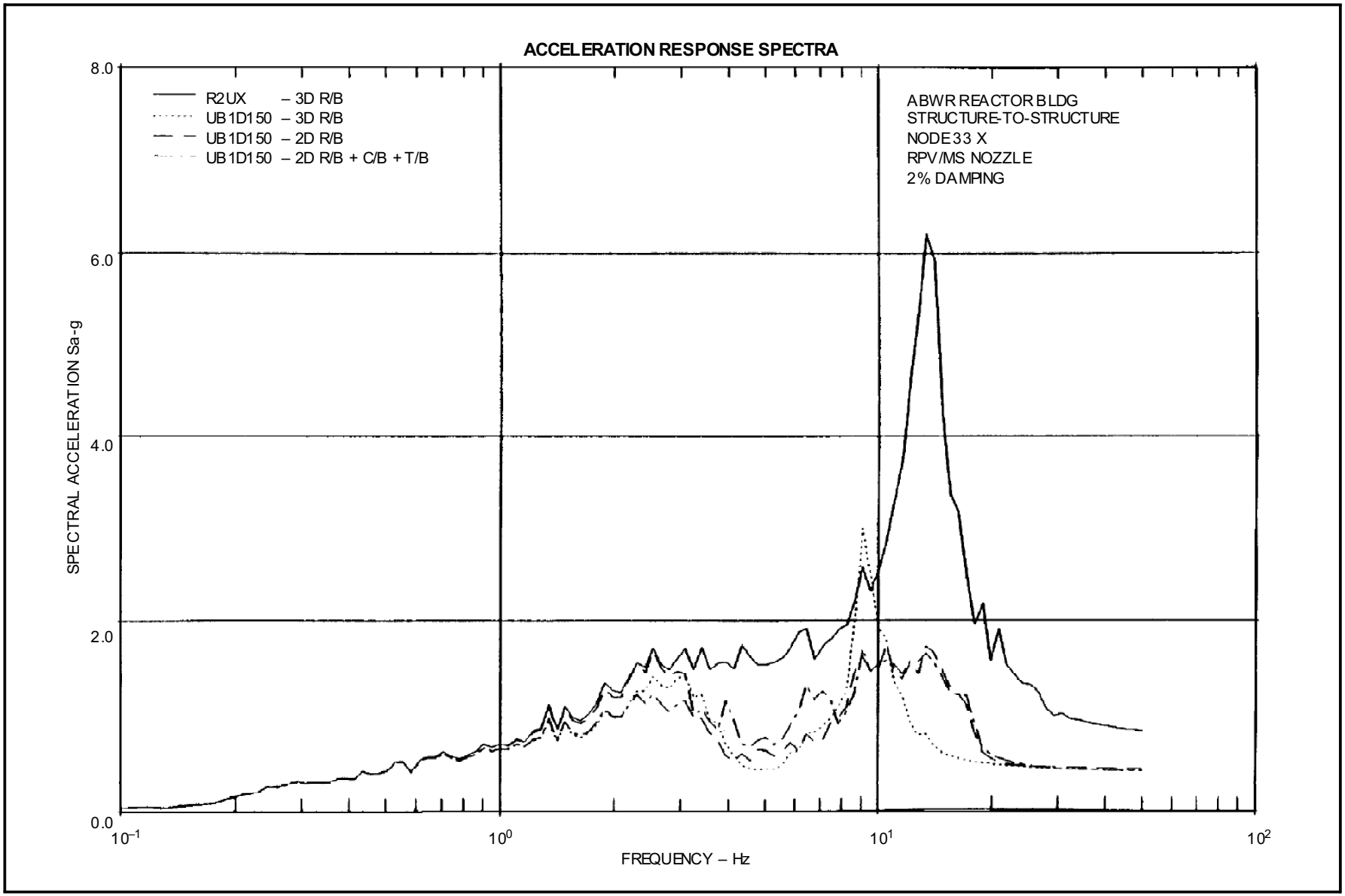

Figure 3A-110 ABWR Reactor Bldg. Structure-to-Structure, Node 33 X RPV/MS Nozzle, 2% Damping, UB1D150

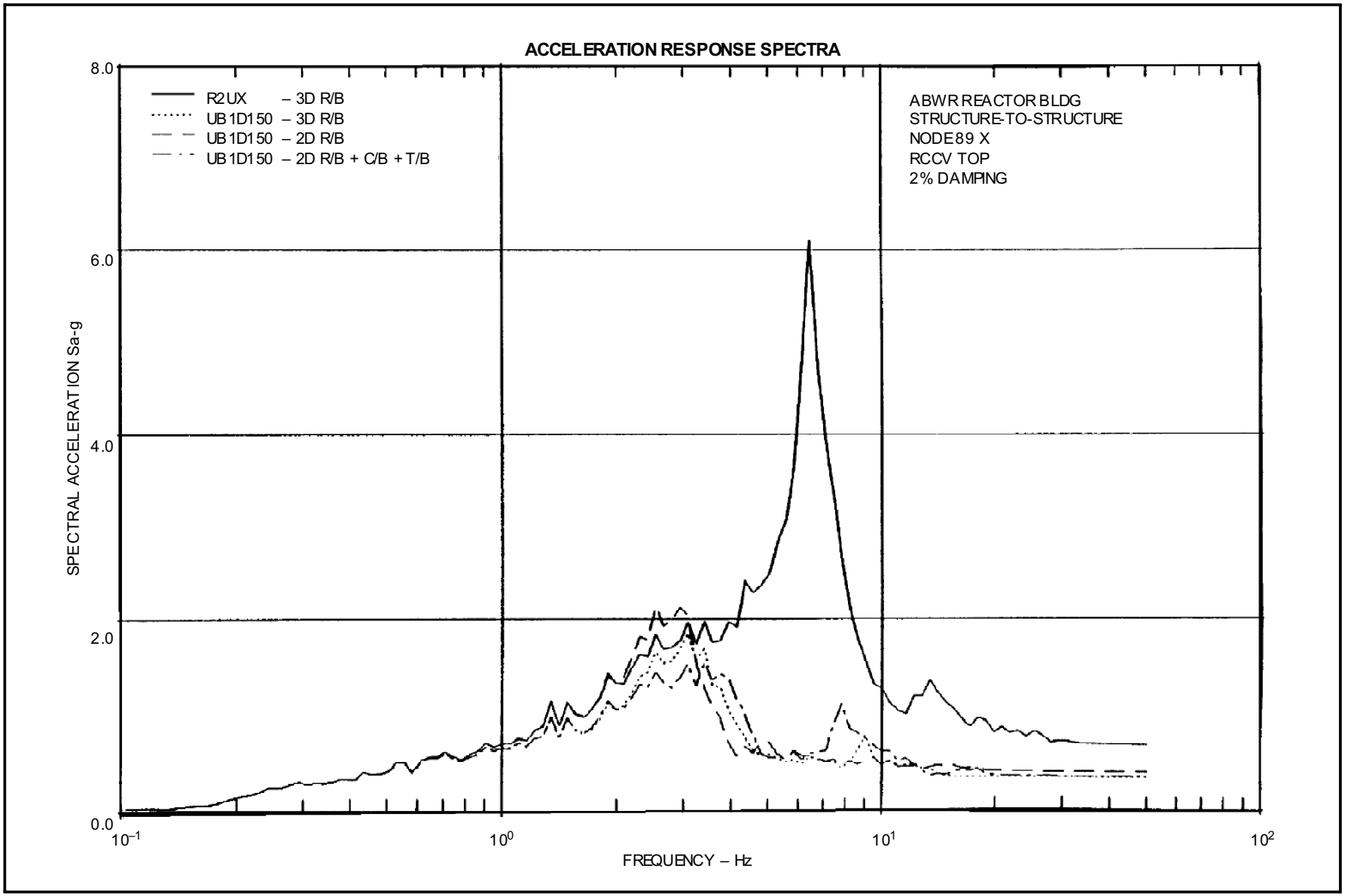

Figure 3A-111 ABWR Reactor Building Structure-to-Structure, Node 89 X, RCCV Top, 2% Damping, UB1D150

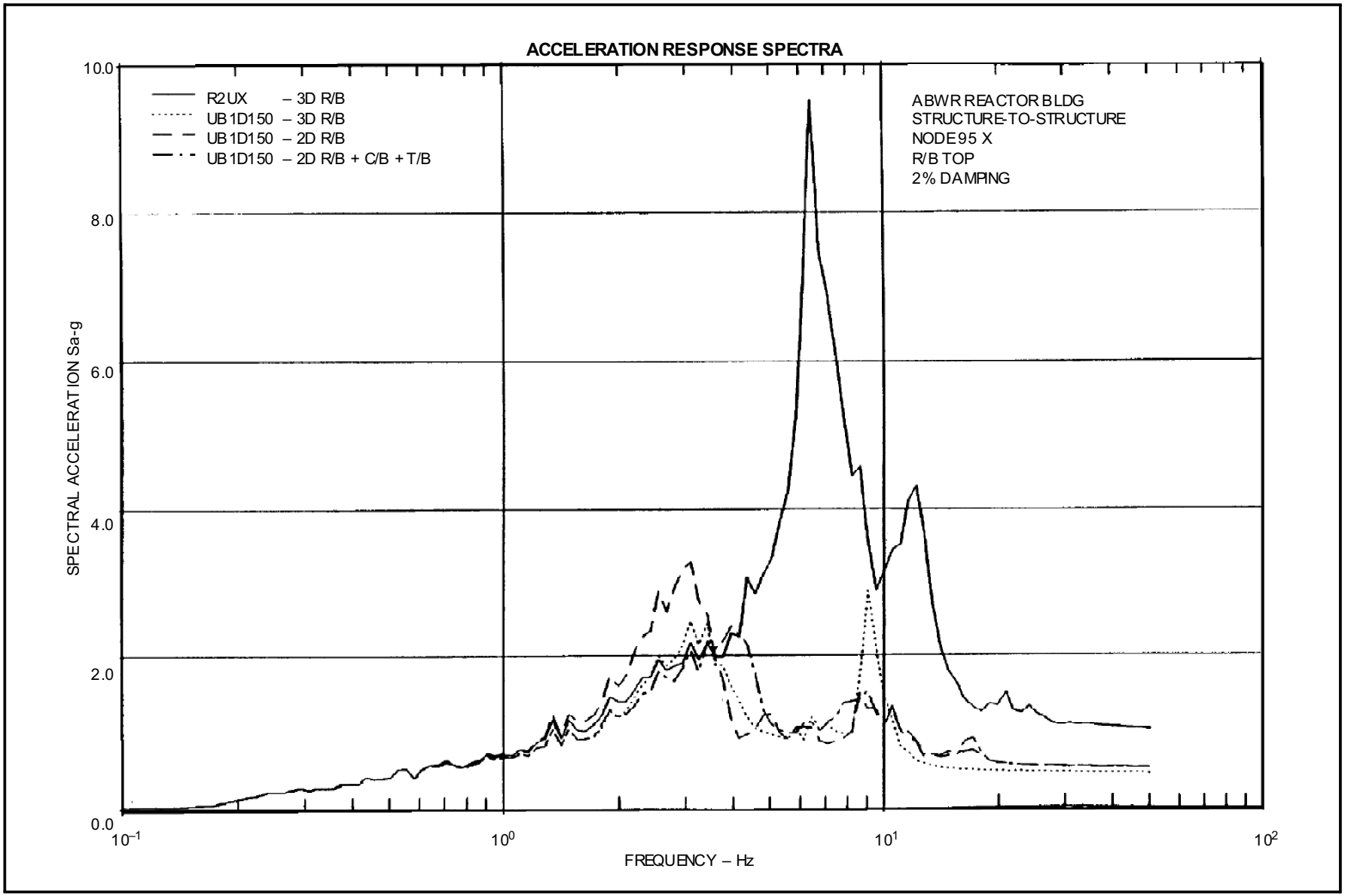

Figure 3A-112 ABWR Reactor Building Structure-to-Structure, Node 95 X, R/B Top, 2% Damping, UB1D150

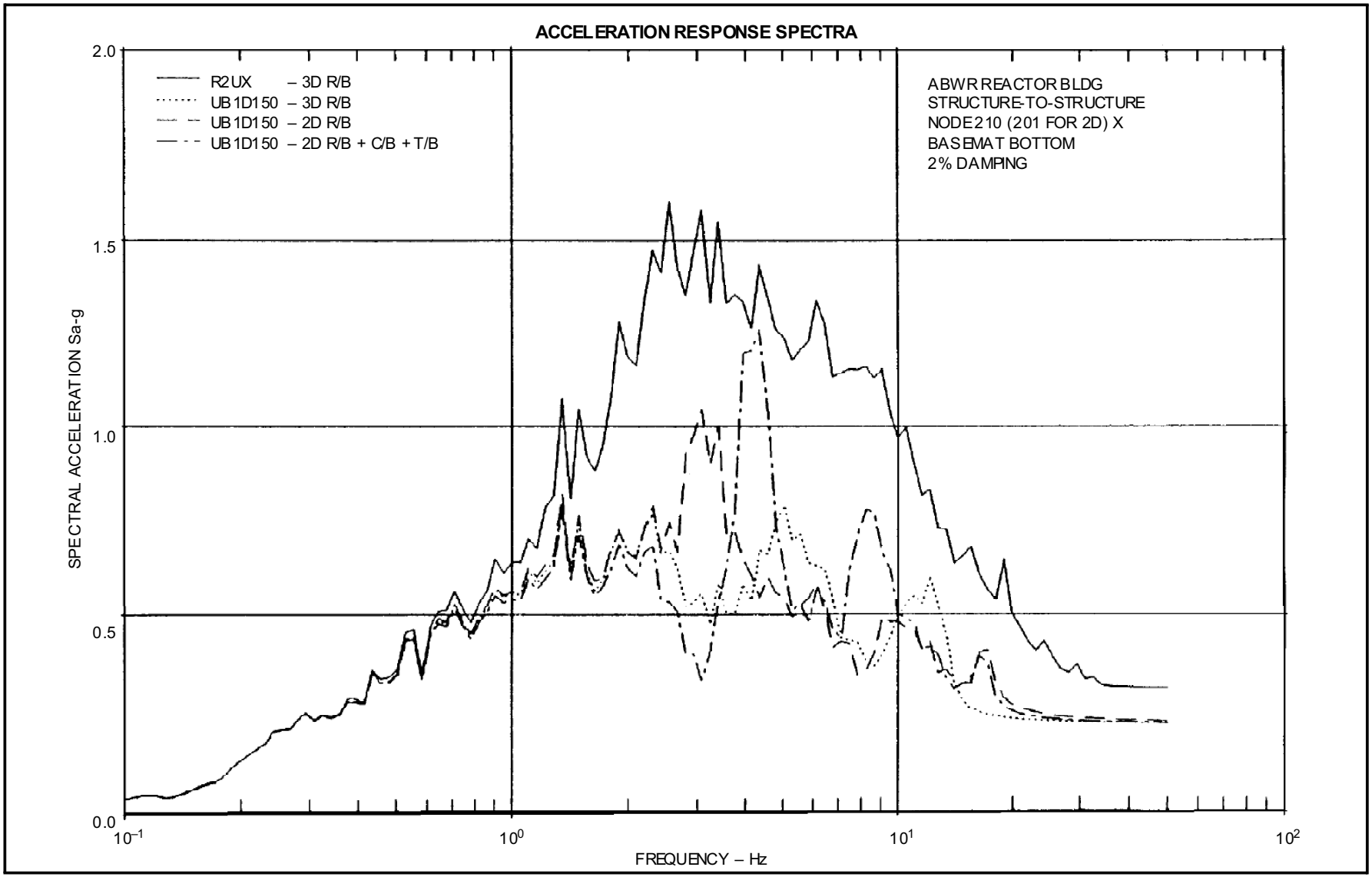

Figure 3A-113
ABWR Reactor Building Structure-to-Structure, Node 210 (201 for 2D) X, Basemat Bottom, 2% Damping, UB1D150

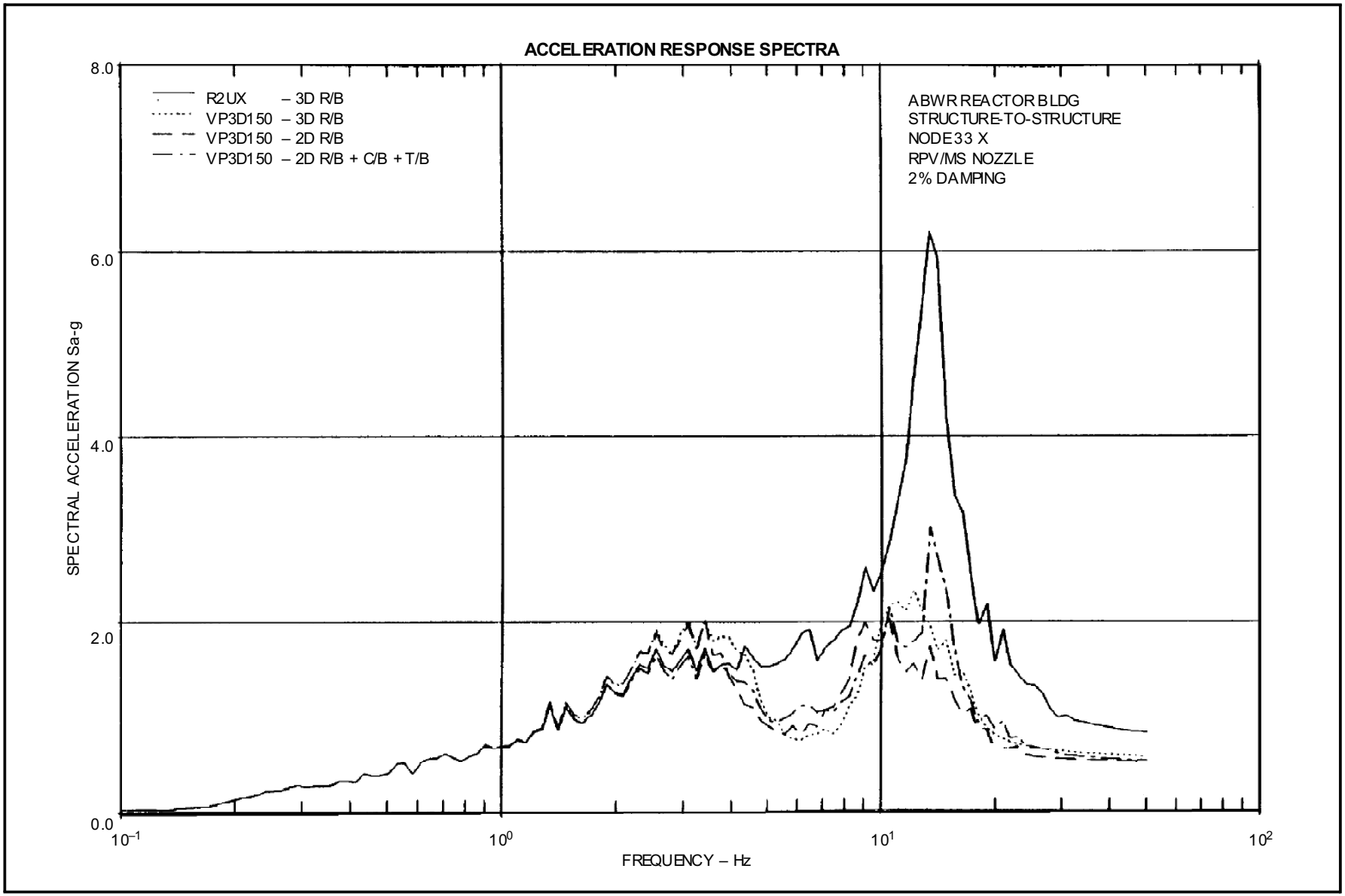

Figure 3A-114 ABWR Reactor Building Structure-to-Structure, Node 33 X, RPV/MS Nozzle, 2% Damping, VP3D150

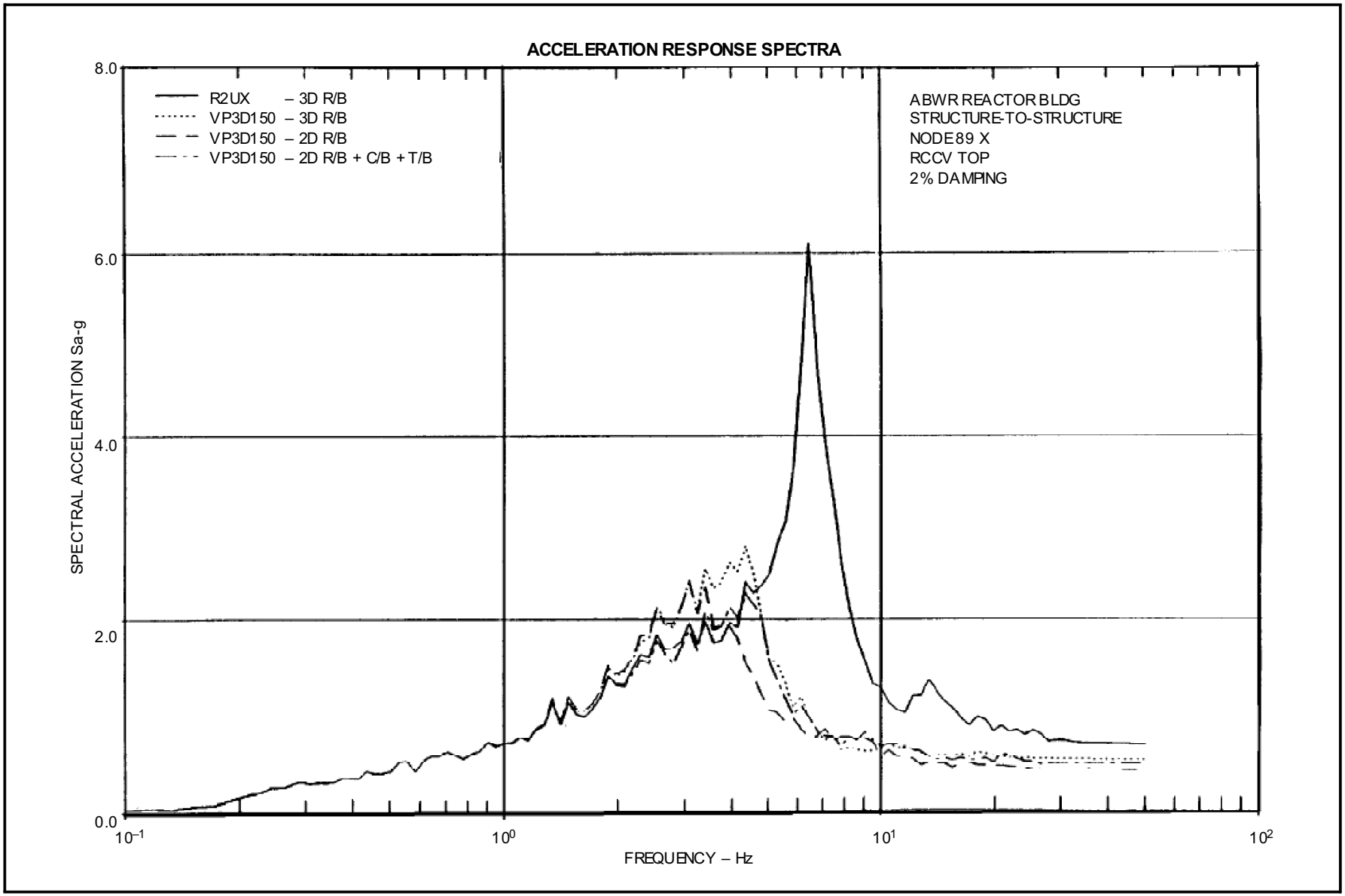

Figure 3A-115 ABWR Reactor Bldg. Structure-to-Structure, Node 89 X RCCV Top, 2% Damping, VP3D150

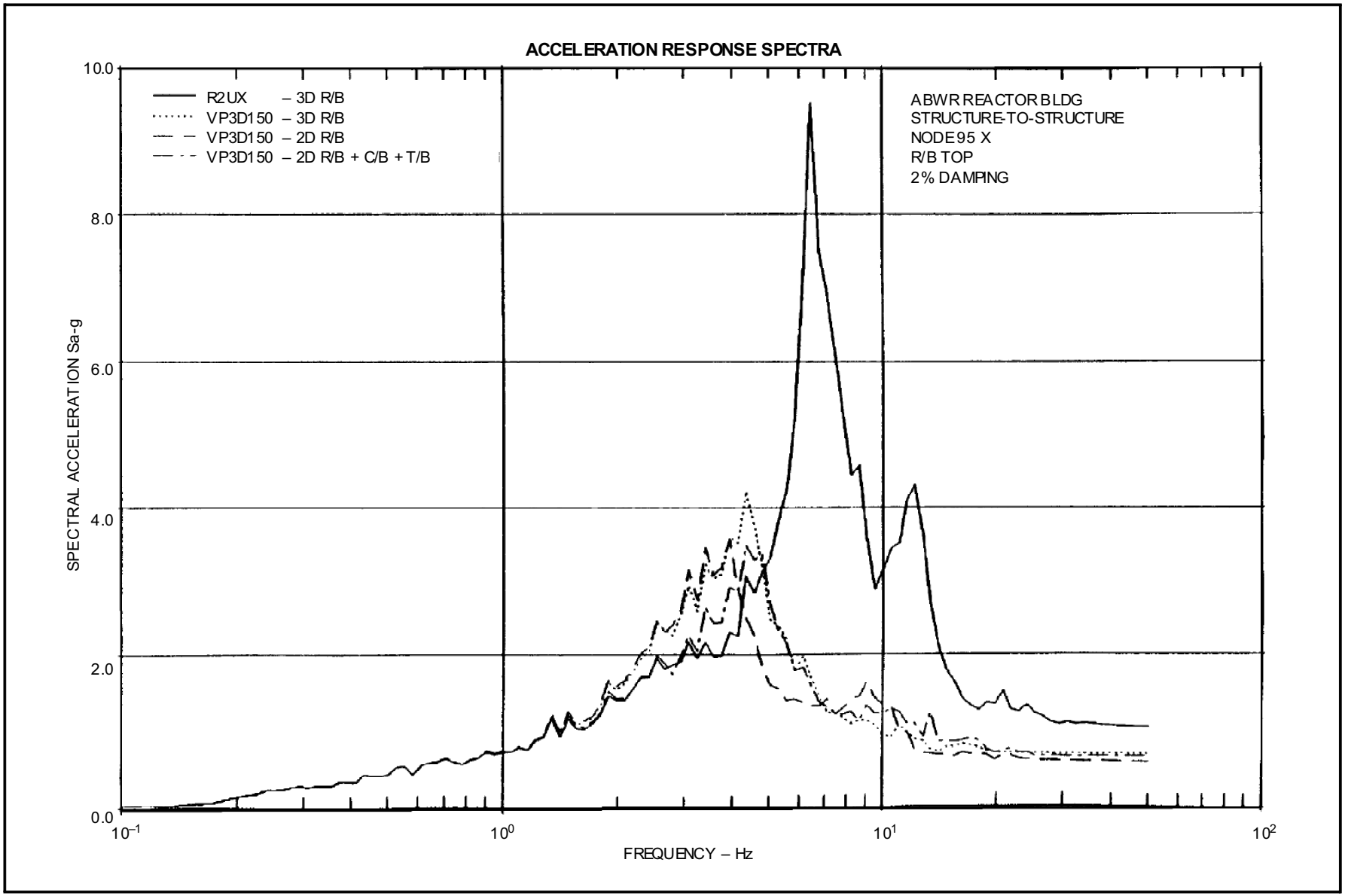

Figure 3A-116 ABWR Reactor Bldg. Structure-to-Structure, Node 95 X R/B Top, 2% Damping, VP3D150

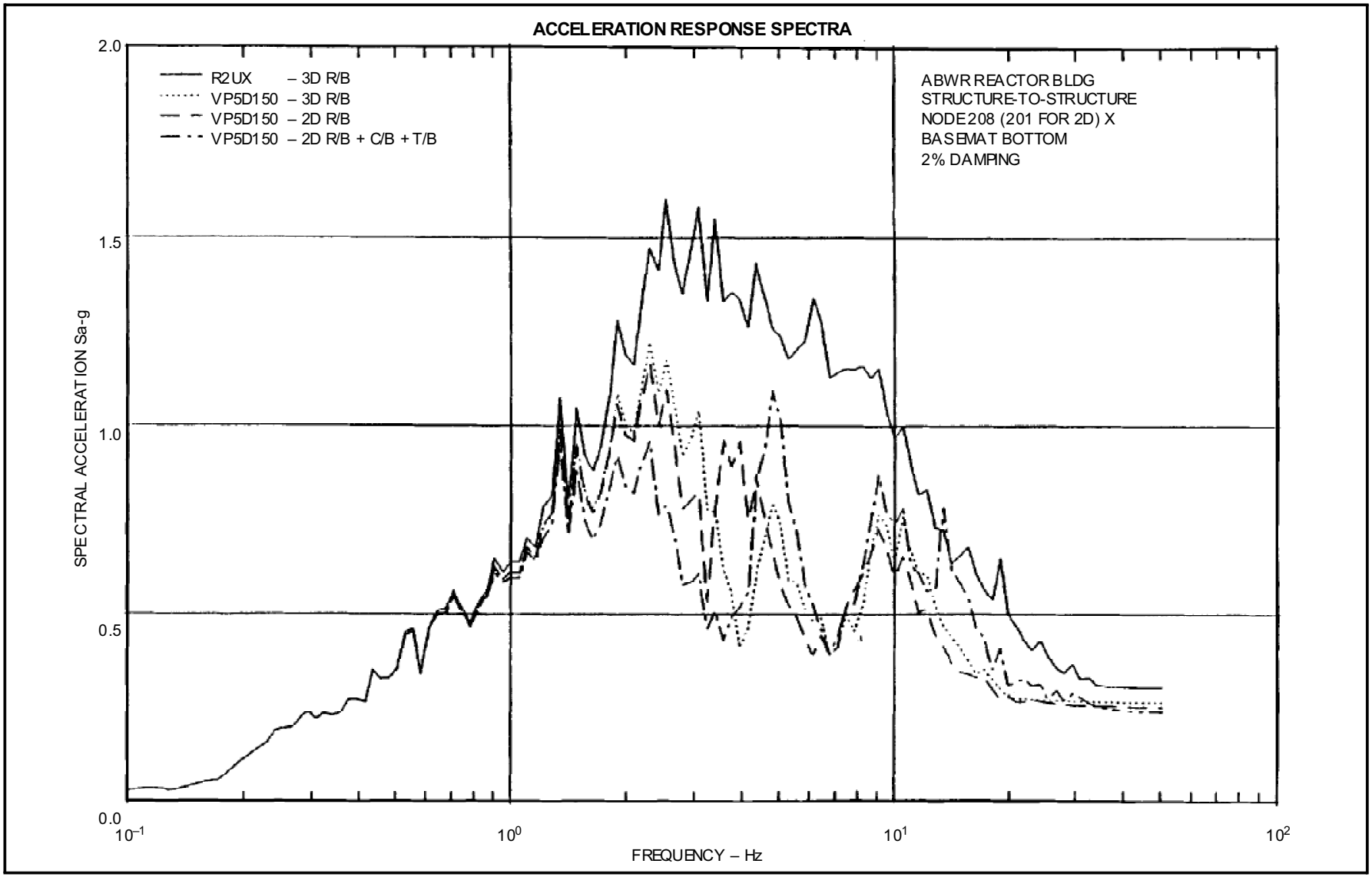

Figure 3A-117 ABWR Reactor Bldg. Structure-to-Structure, Node 208 (201 for 2 D) X Basemat Bottom, 2% Damping, VP5D150

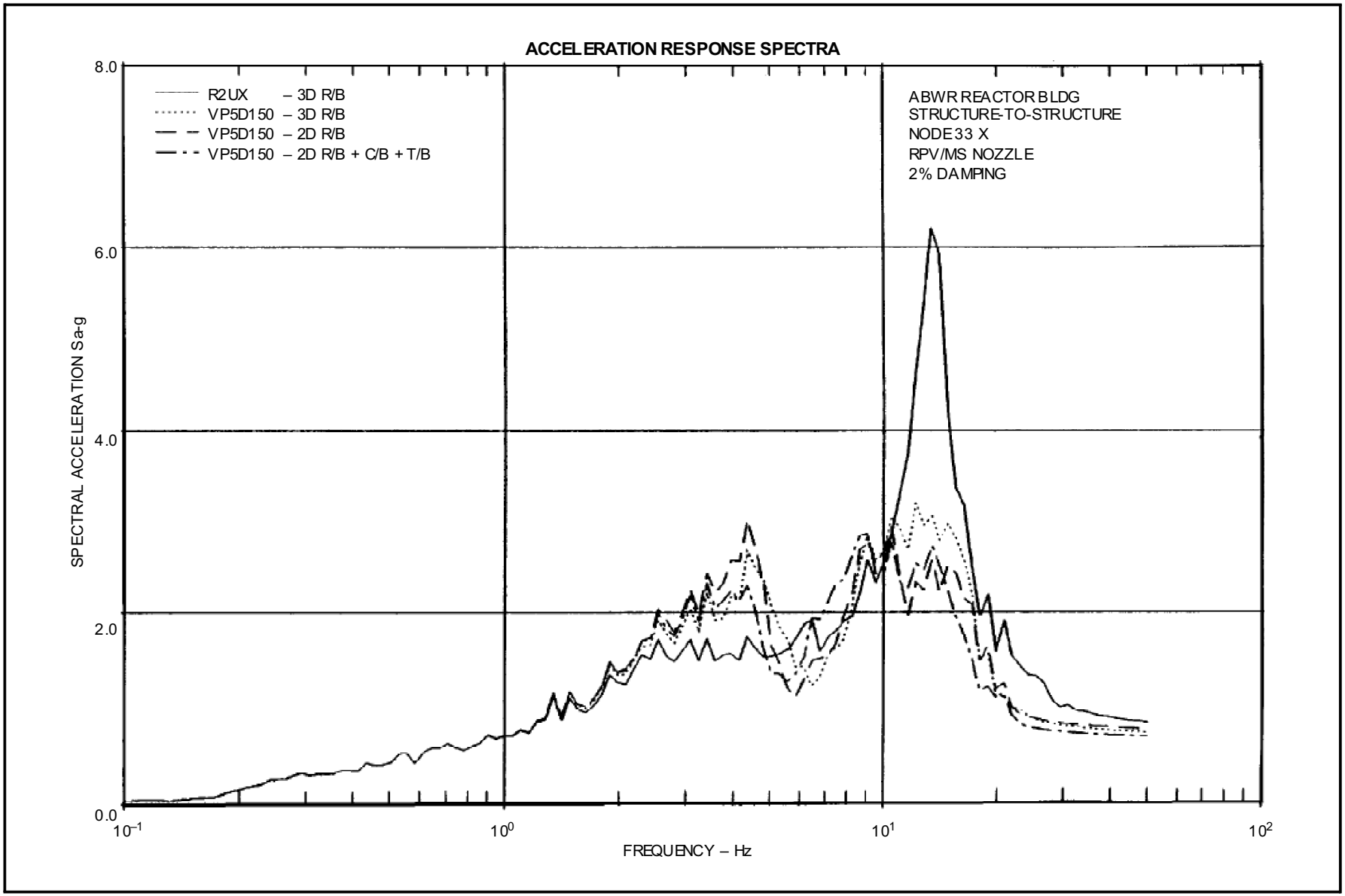

Figure 3A-118 ABWR Reactor Bldg. Structure-to-Structure, Node 33X RPV/MS Nozzle, 2% Damping, VP5D150

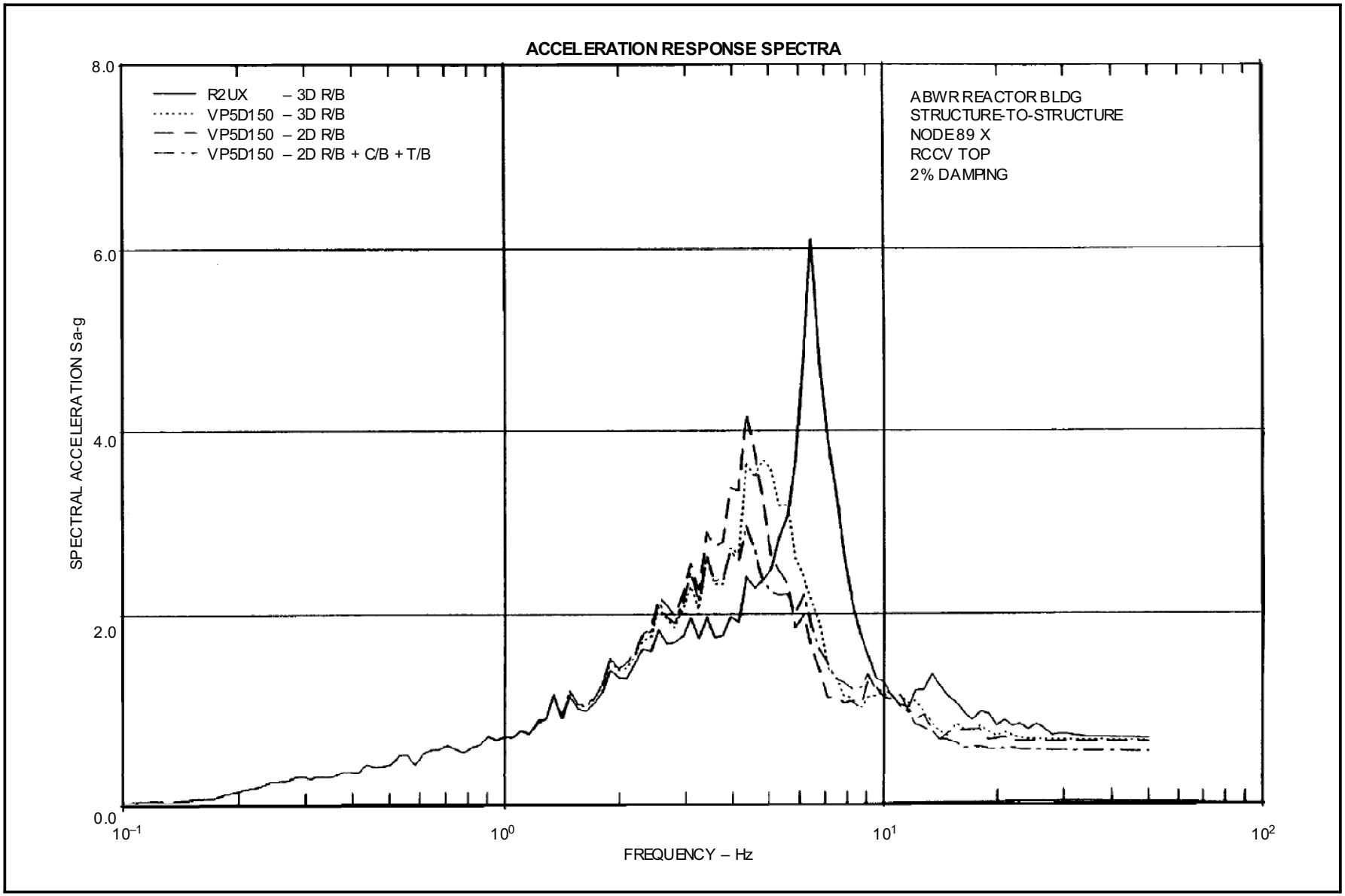

Figure 3A-119 ABWR Reactor Bldg. Structure-to-Structure, Node 89 X RCCV Top, 2% Damping, VP5D150

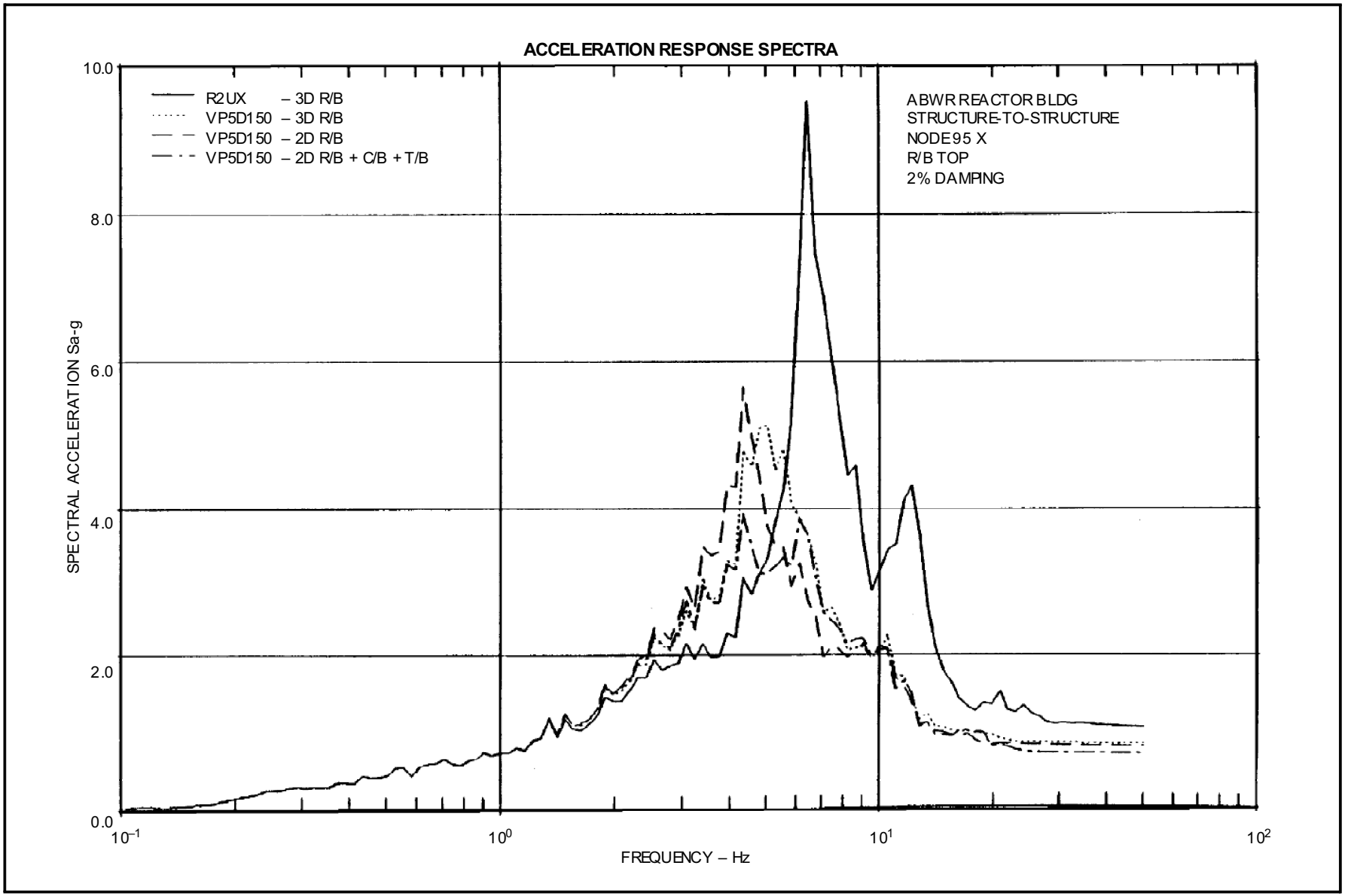

Figure 3A-120 ABWR Reactor Bldg. Structure-to-Structure, Node 95 X R/B Top, 2% Damping, VP5D150

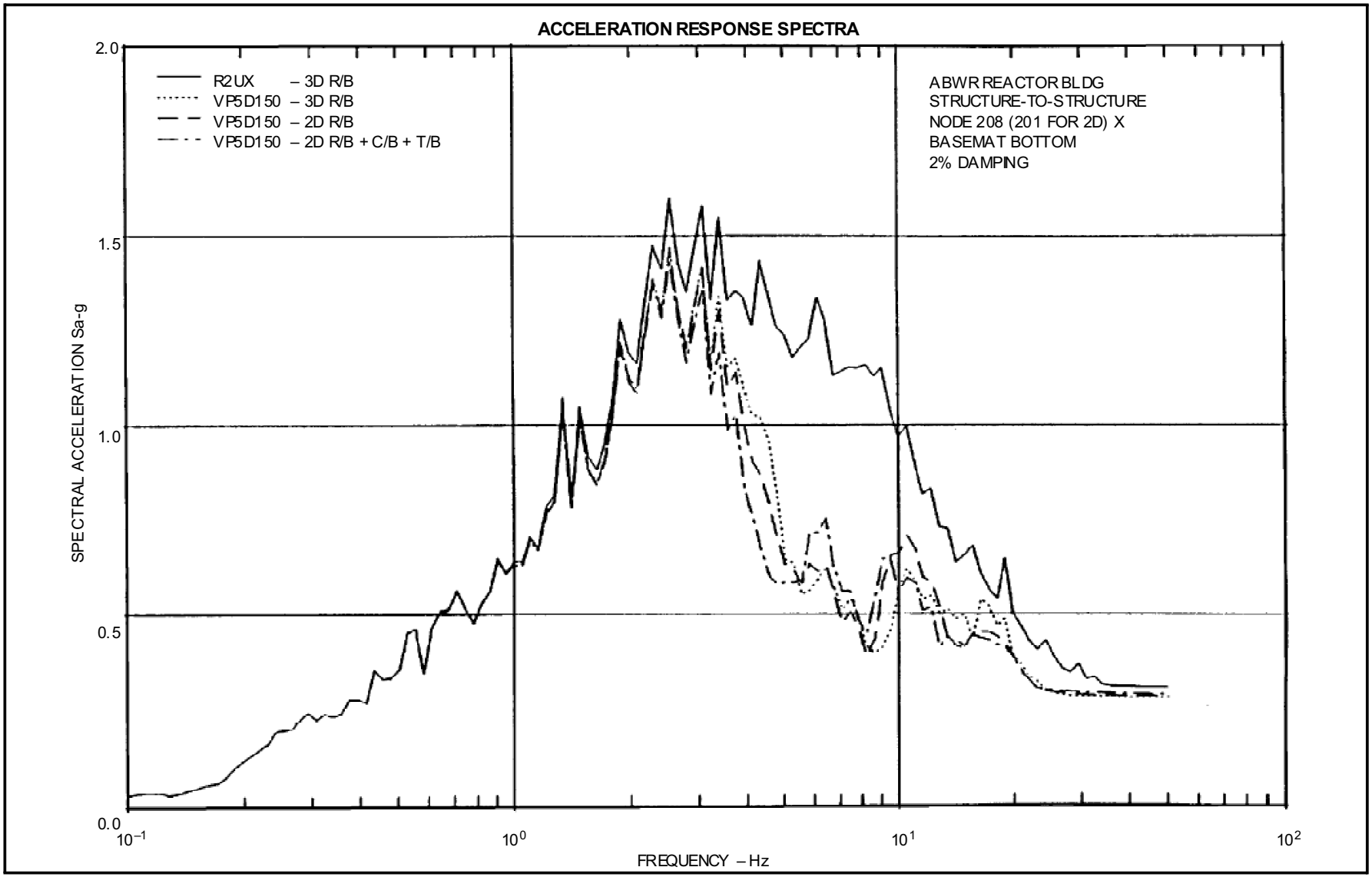

Figure 3A-121 ABWR Reactor Bldg. Structure-to-Structure, Node 208 (201 for 2 D) X, Basemat Bottom, 2% Damping, VP3D150

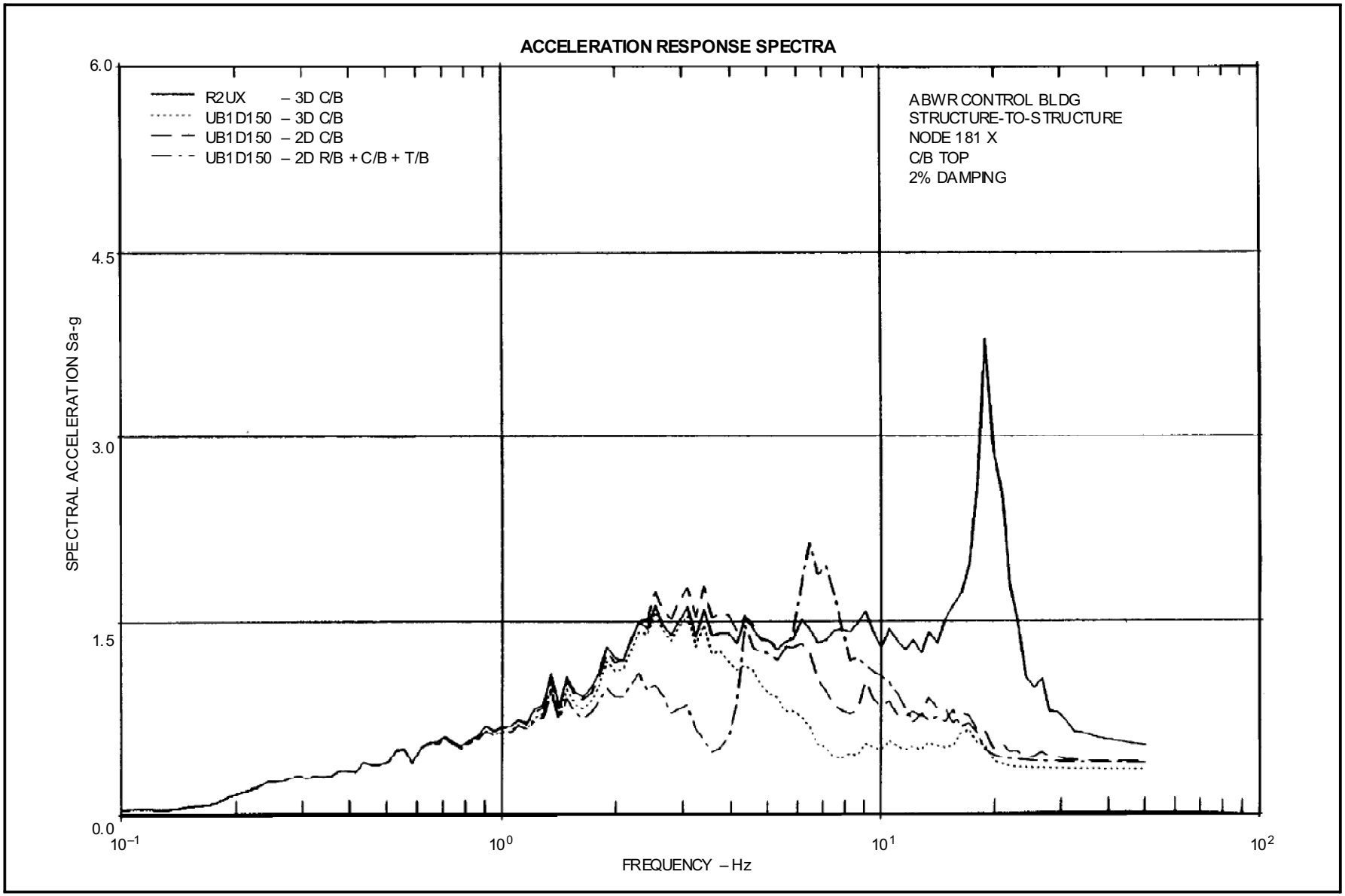

Figure 3A-122 ABWR Control Bldg. Structure-to-Structure, Node 181 X C/B Top, 2% Damping, UB1D150

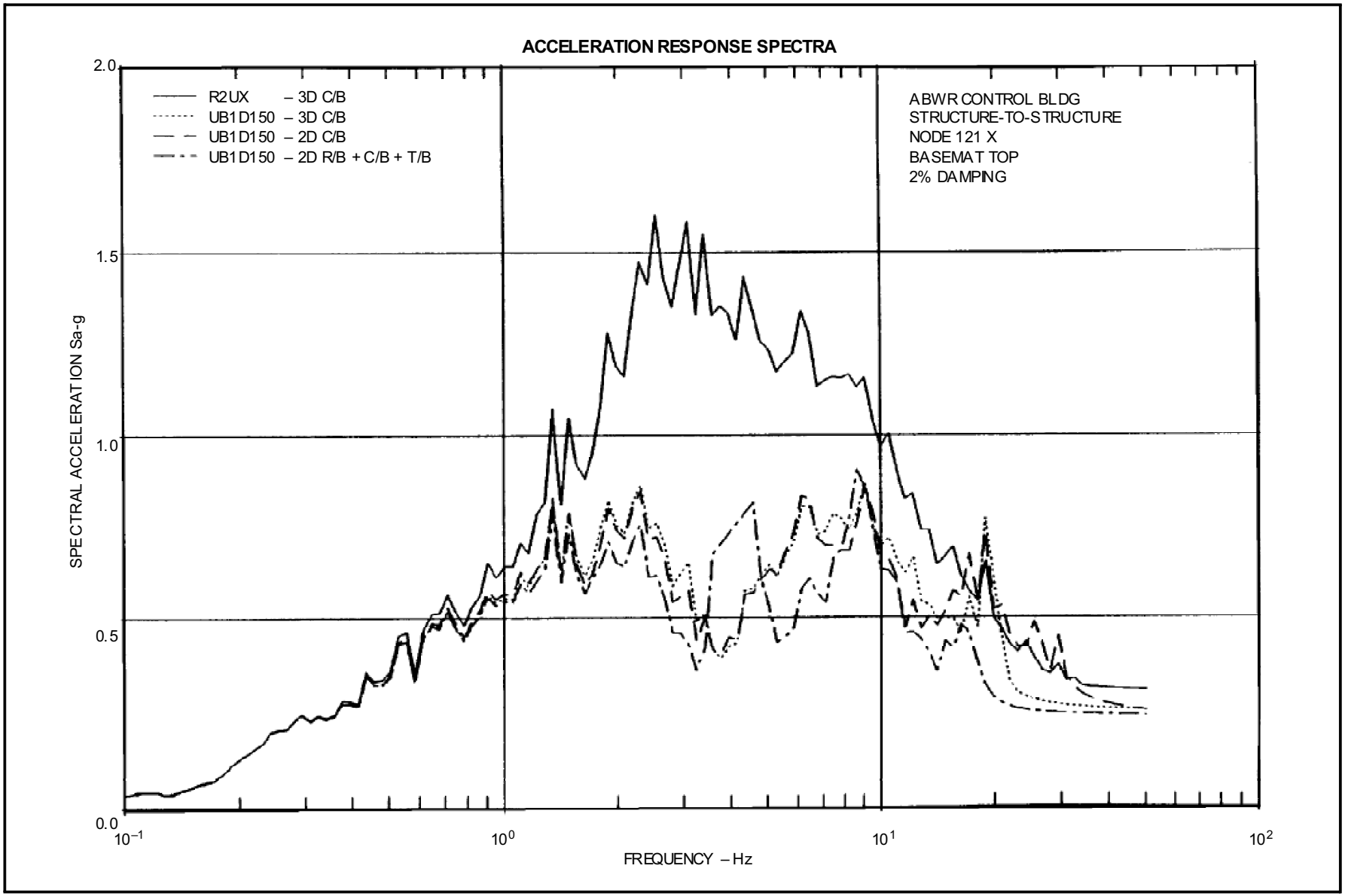

Figure 3A-123 ABWR Control Bldg. Structure-to-Structure, Node 121 X Basemat Top, 2% Damping, UB1D150

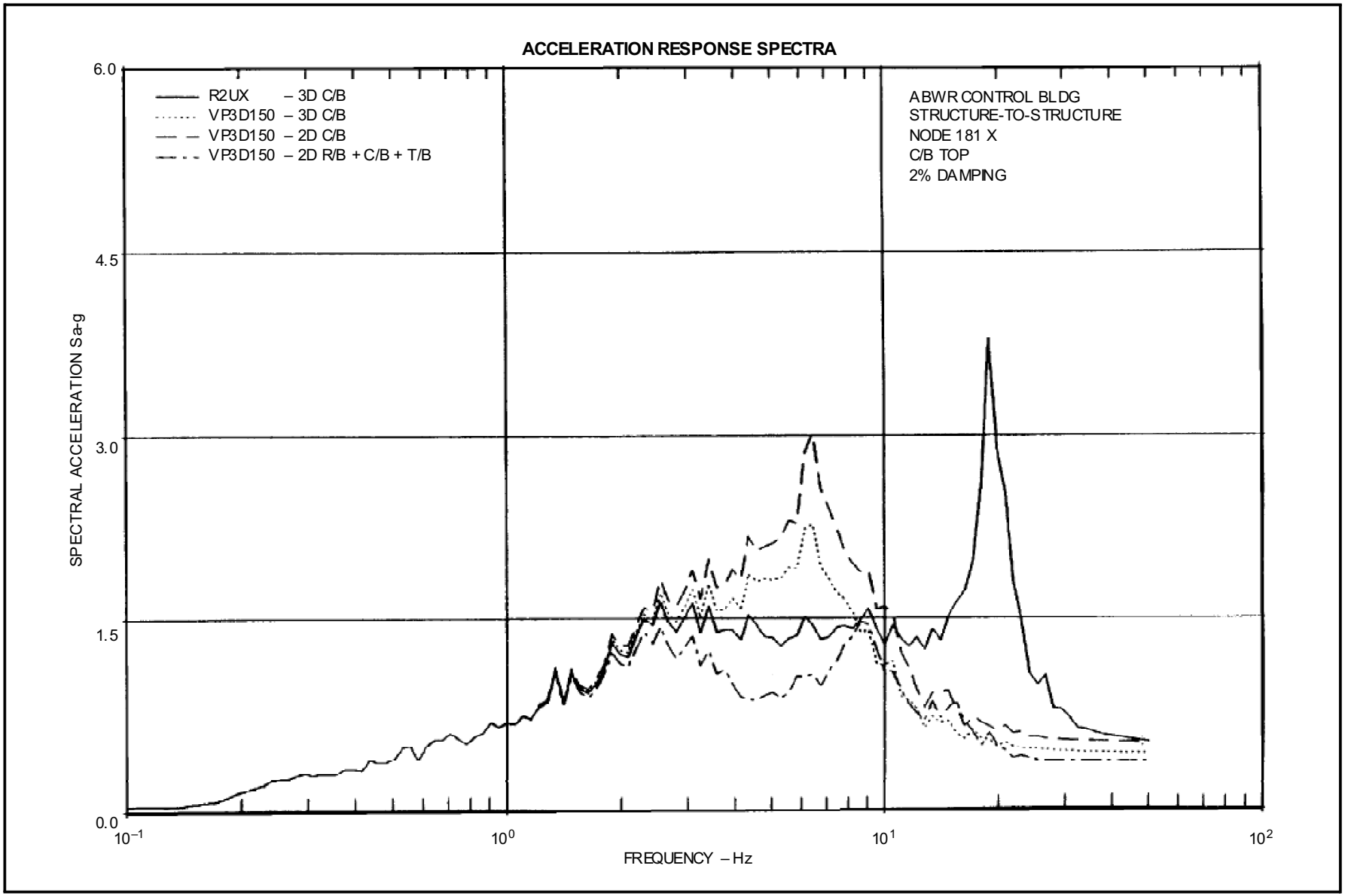

Figure 3A-124 ABWR Control Bldg. Structure-to-Structure, Node 181 X C/B Top, 2% Damping, VP3D150

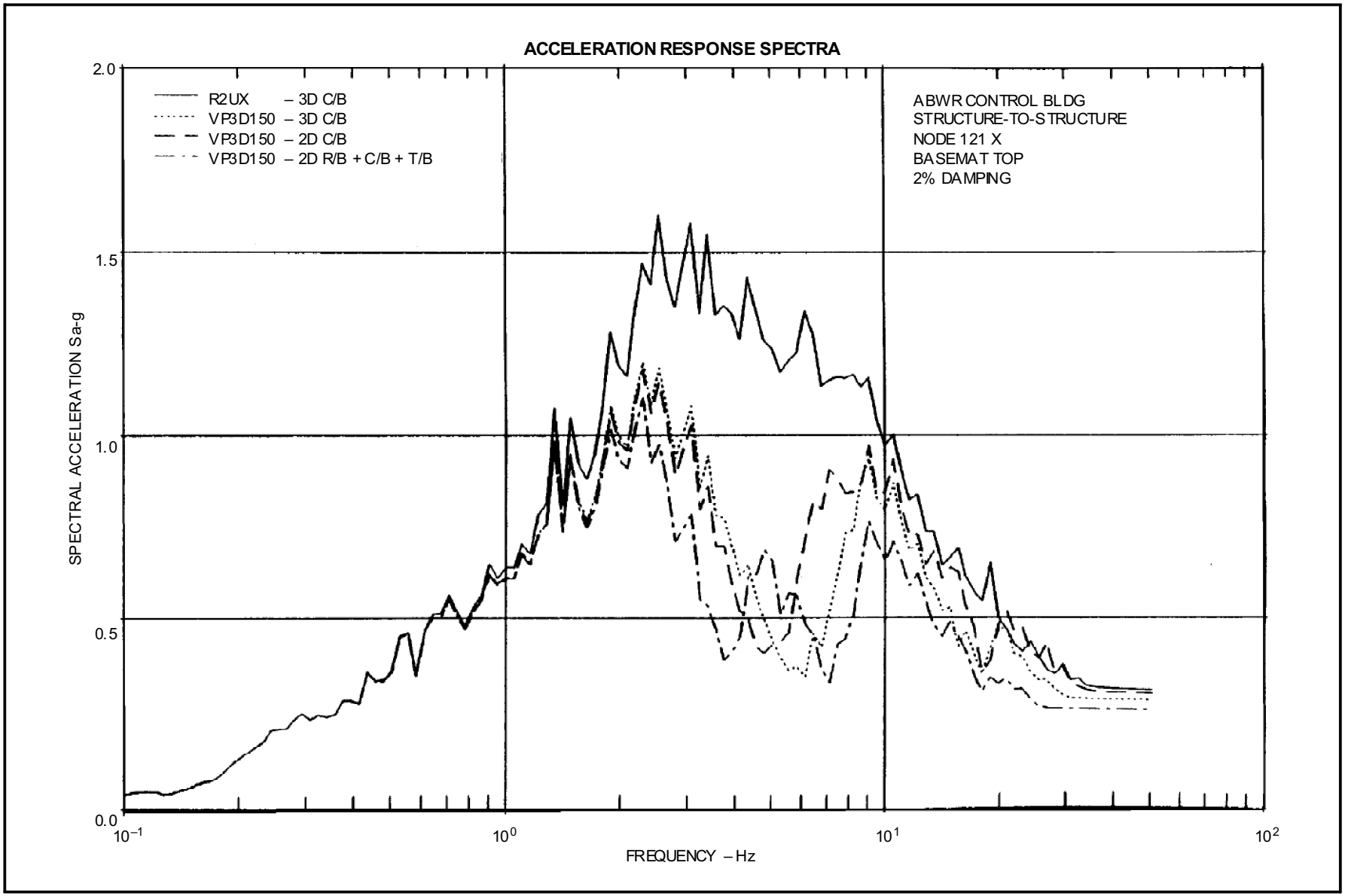

Figure 3A-125 ABWR Control Bldg. Structure-to-Structure, Node 121 X Basemat Top, 2% Damping, VP3D150

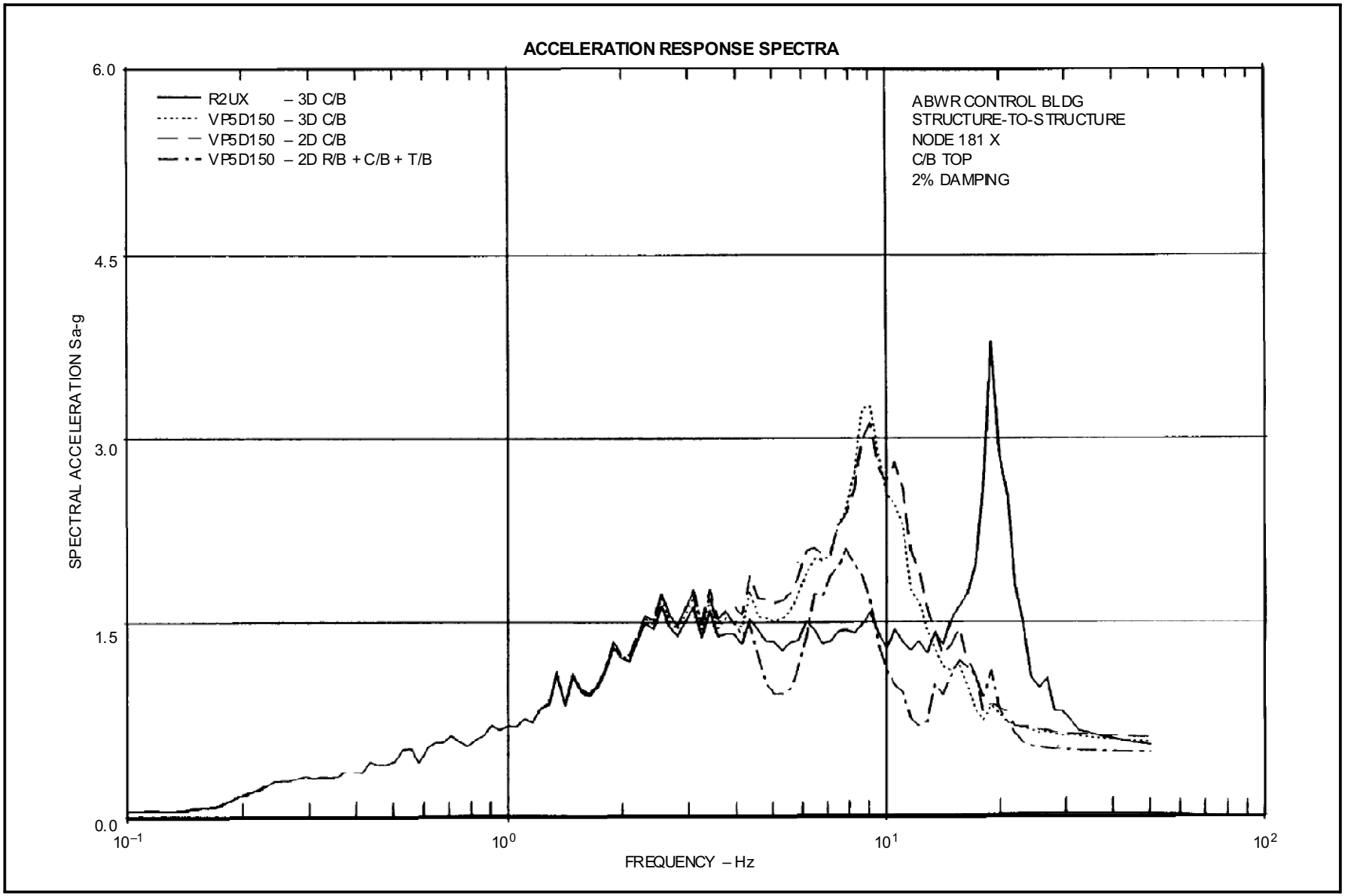

Figure 3A-126 ABWR Control Bldg. Structure-to-Structure, Node 181 X C/B Top, 2% Damping, VP5D150

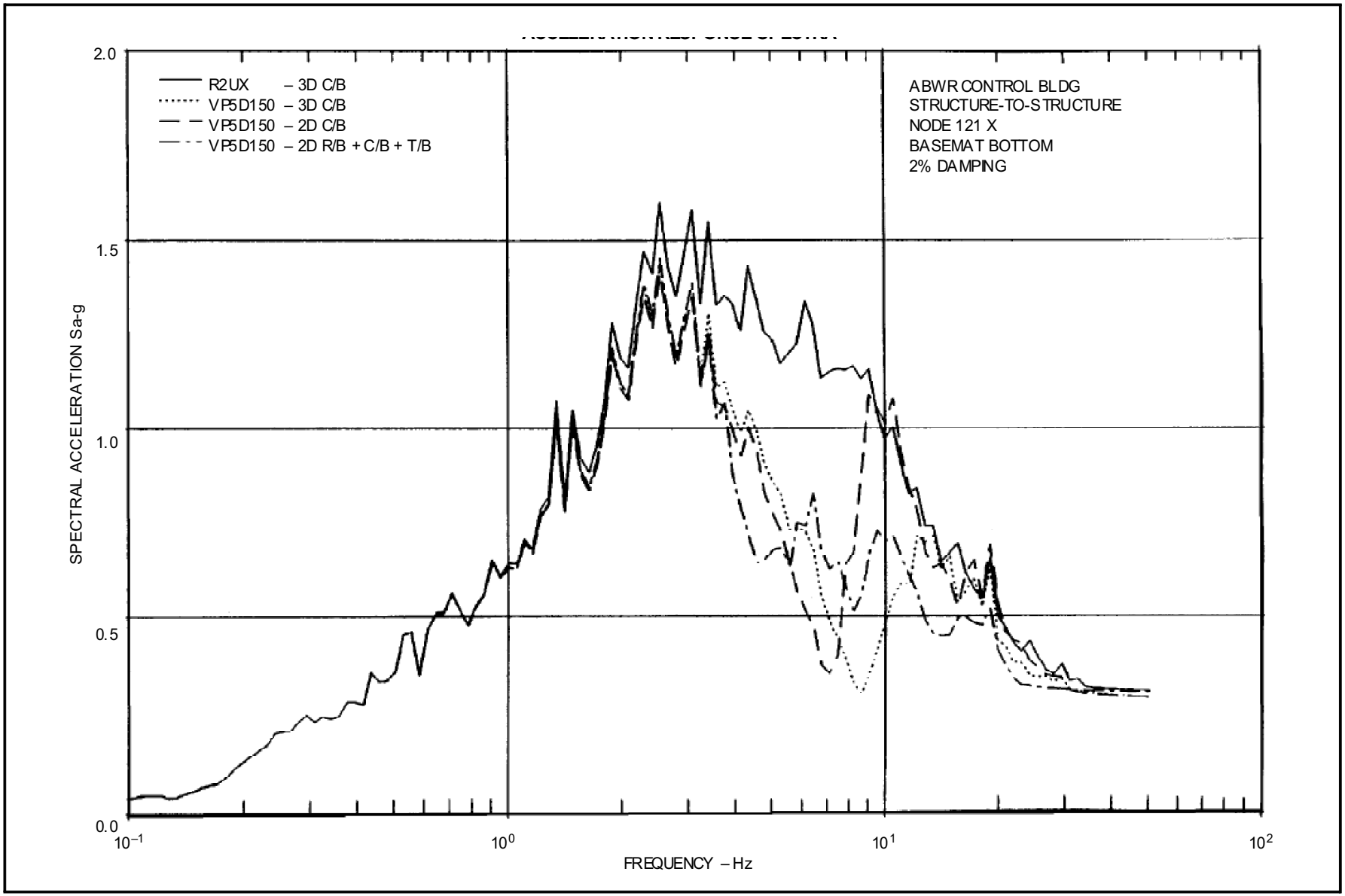

Figure 3A-127 ABWR Control Bldg. Structure-to-Structure, Node 121 X Basemat Bottom, 2% Damping, VP5D150

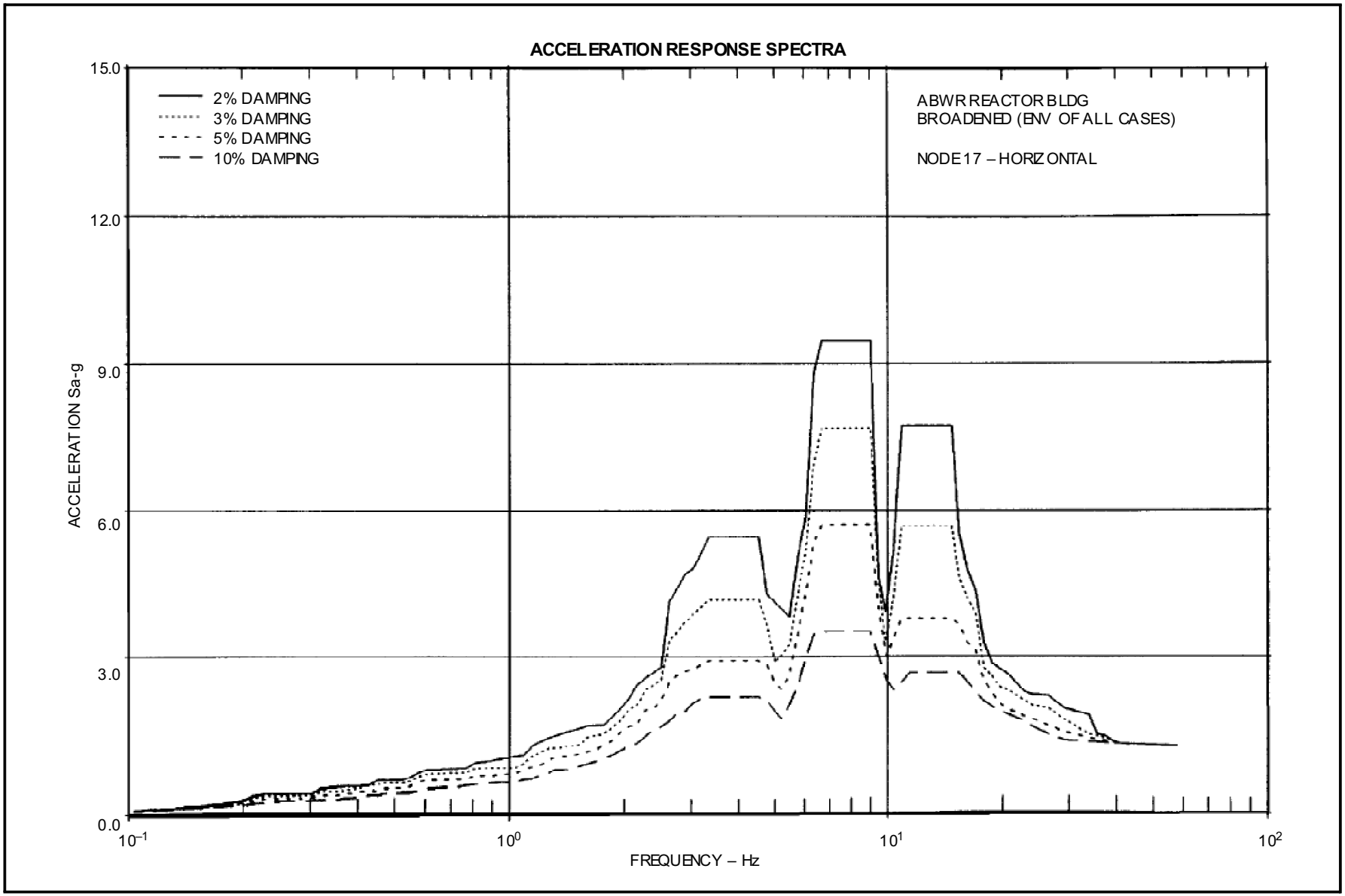

Figure 3A-128 ABWR Reactor Bldg. Broadened (Env of all Cases) Node 17–Horizontal

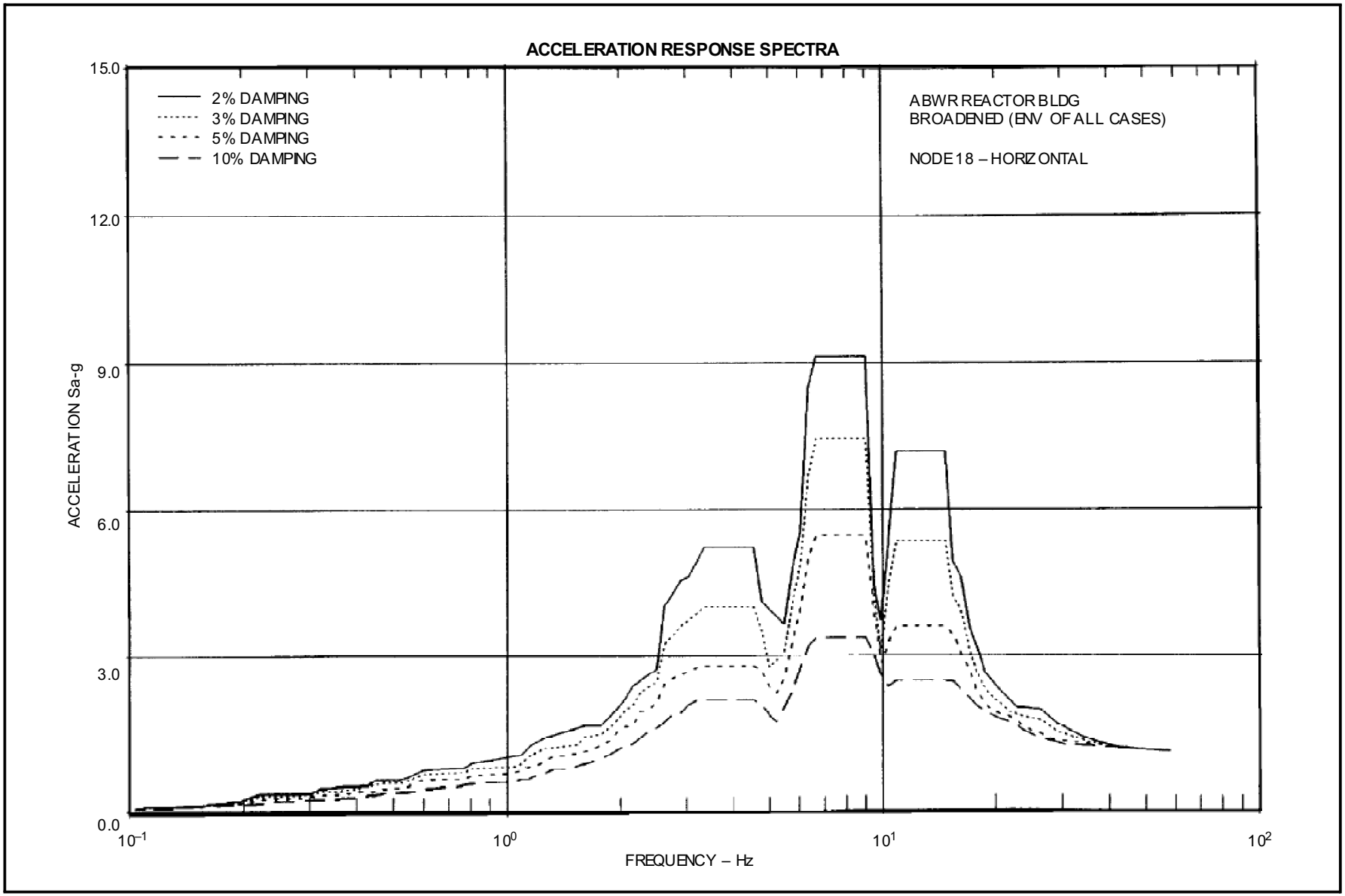

Figure 3A-129 ABWR Reactor Bldg. Broadened (Env of all Cases) Node 18–Horizontal

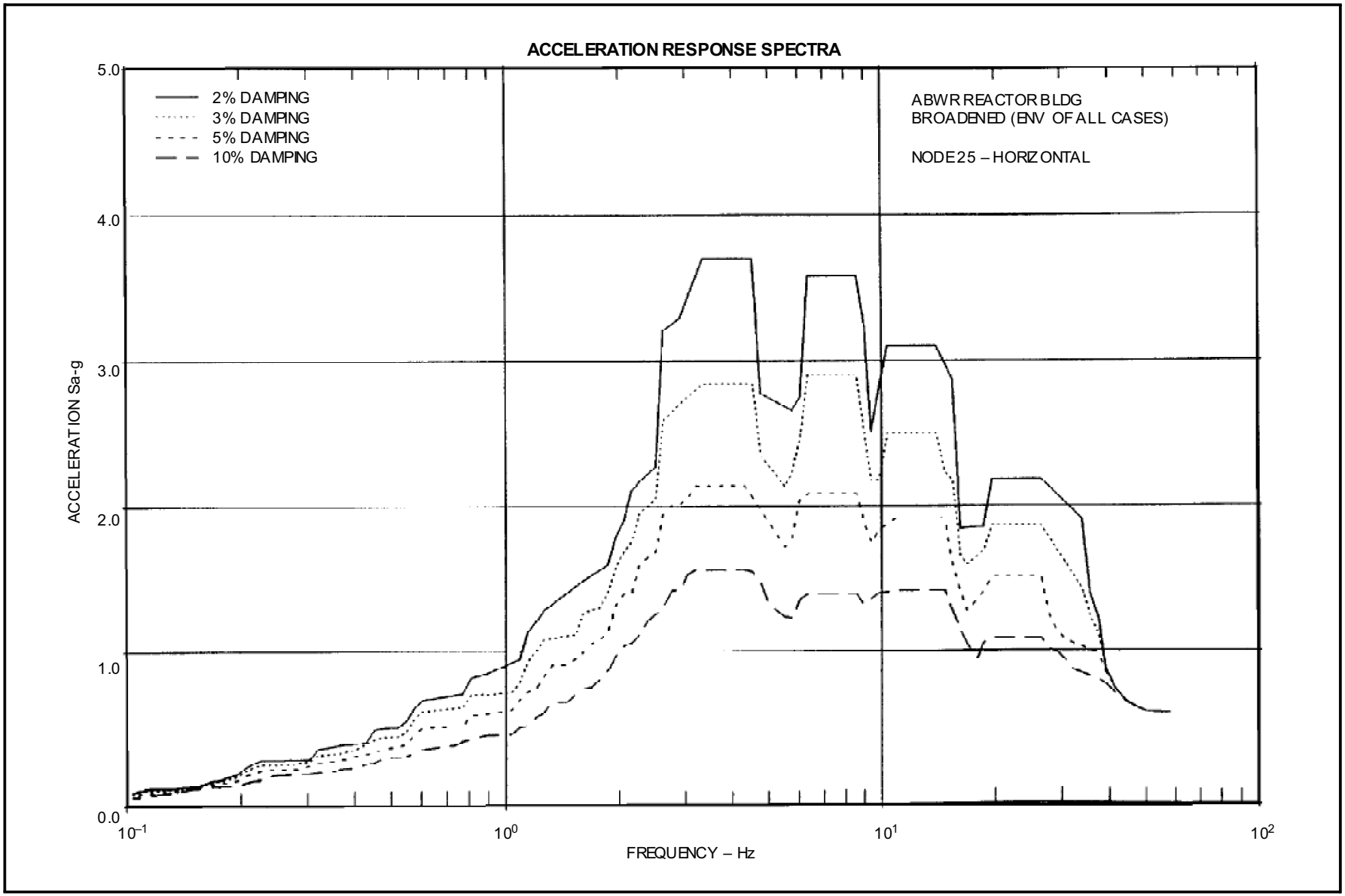

Figure 3A-130 ABWR Reactor Bldg. Broadened (Env of all Cases) Node 25–Horizontal

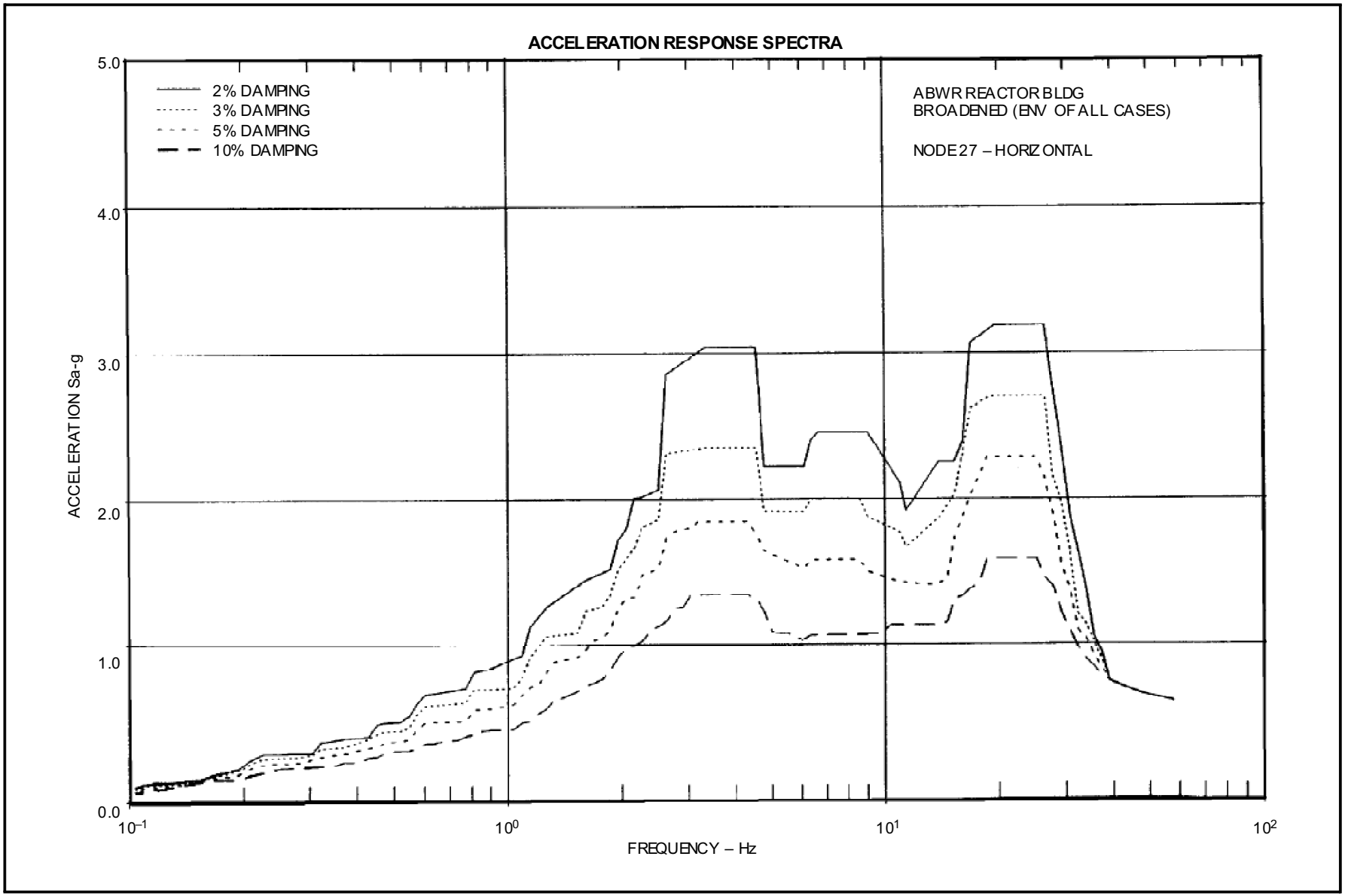

Figure 3A-131 ABWR Reactor Bldg. Broadened (Env of all Cases) Node 27–Horizontal

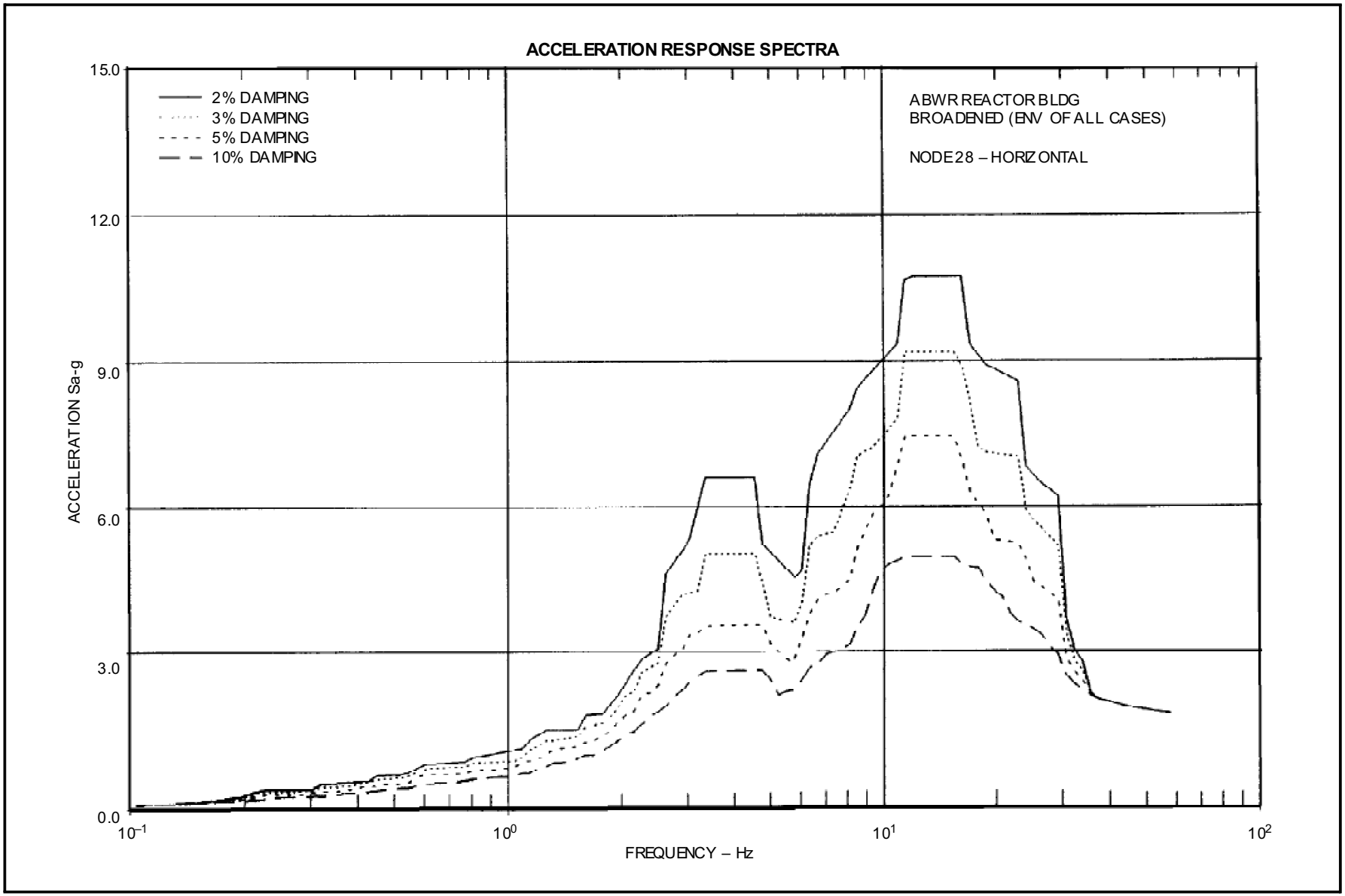

Figure 3A-132 ABWR Reactor Bldg. Broadened (Env of all Cases) Node 28–Horizontal

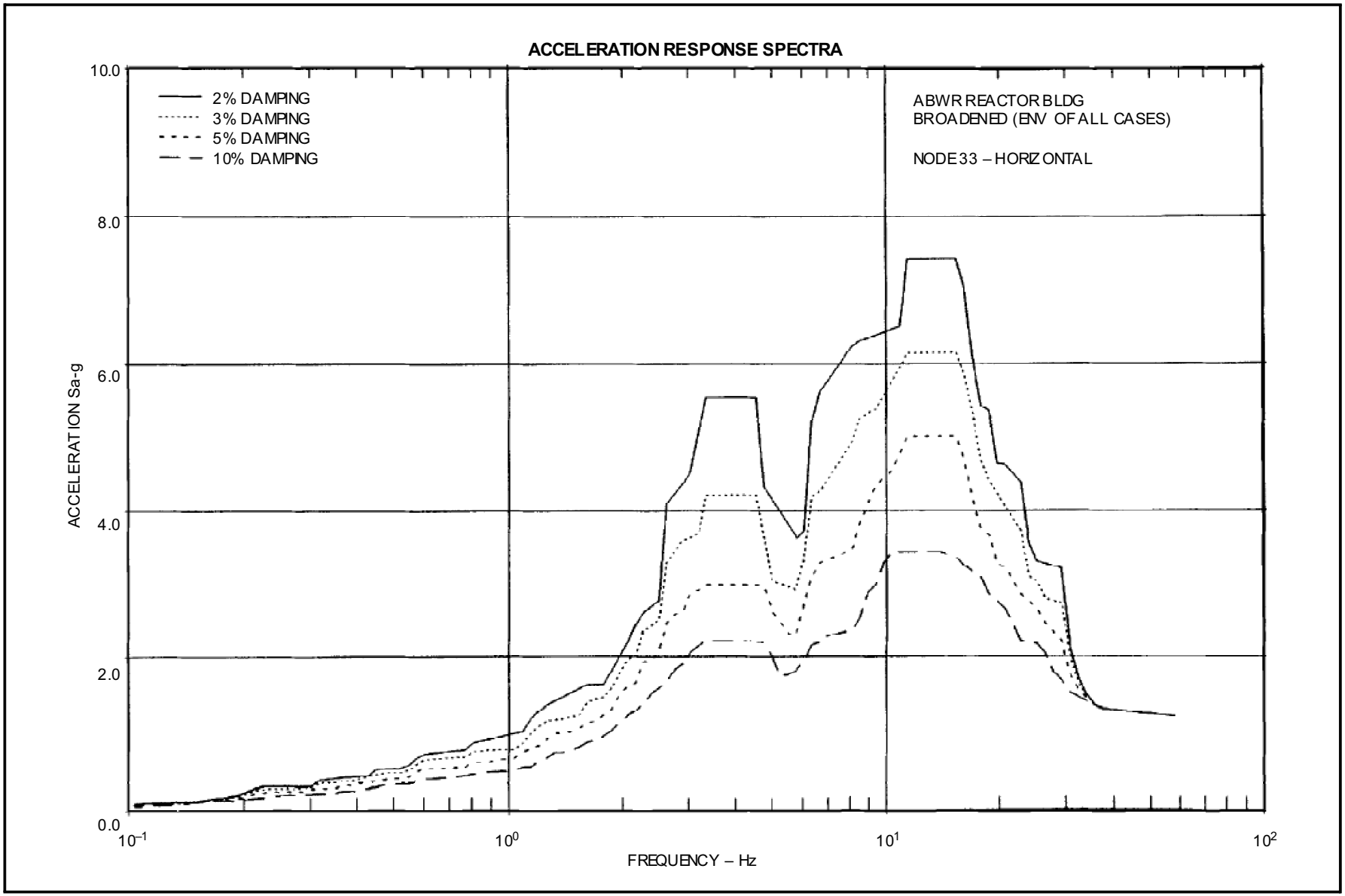

Figure 3A-133 ABWR Reactor Bldg. Broadened (Env of all Cases) Node 33–Horizontal

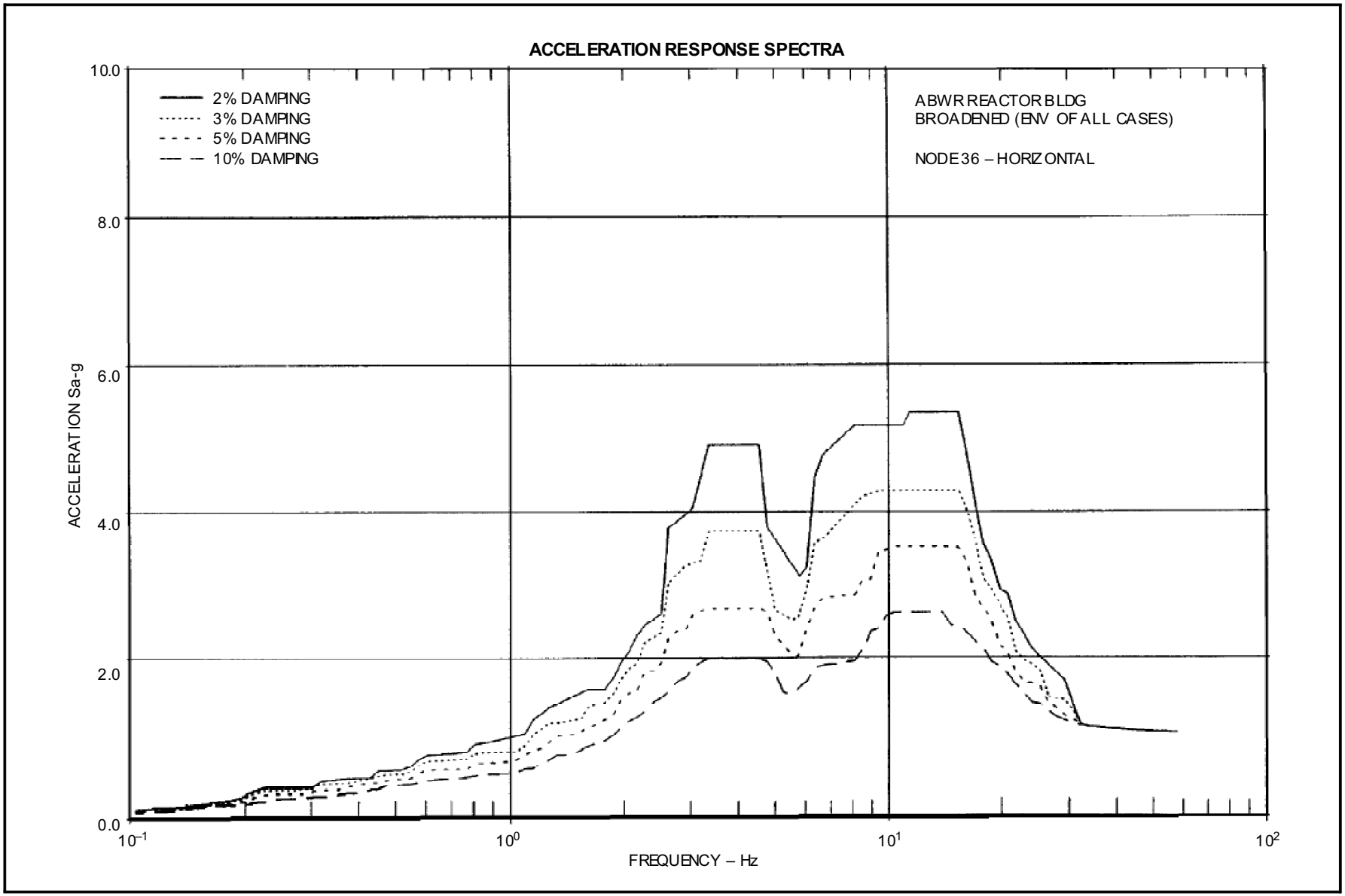

Figure 3A-134 ABWR Reactor Bldg. Broadened (Env of all Cases) Node 36–Horizontal

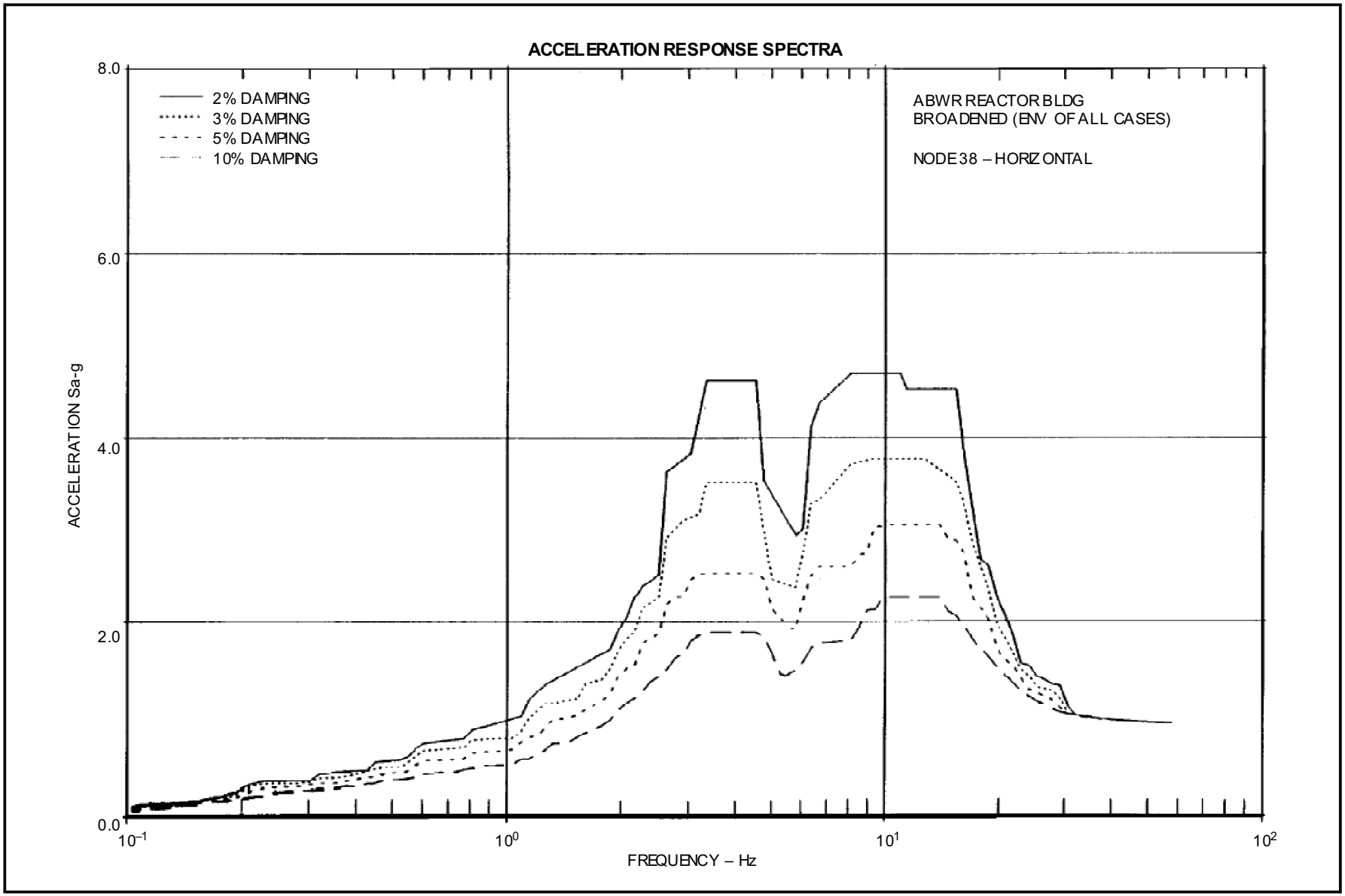

Figure 3A-135 ABWR Reactor Bldg. Broadened (Env of all Cases) Node 38–Horizontal

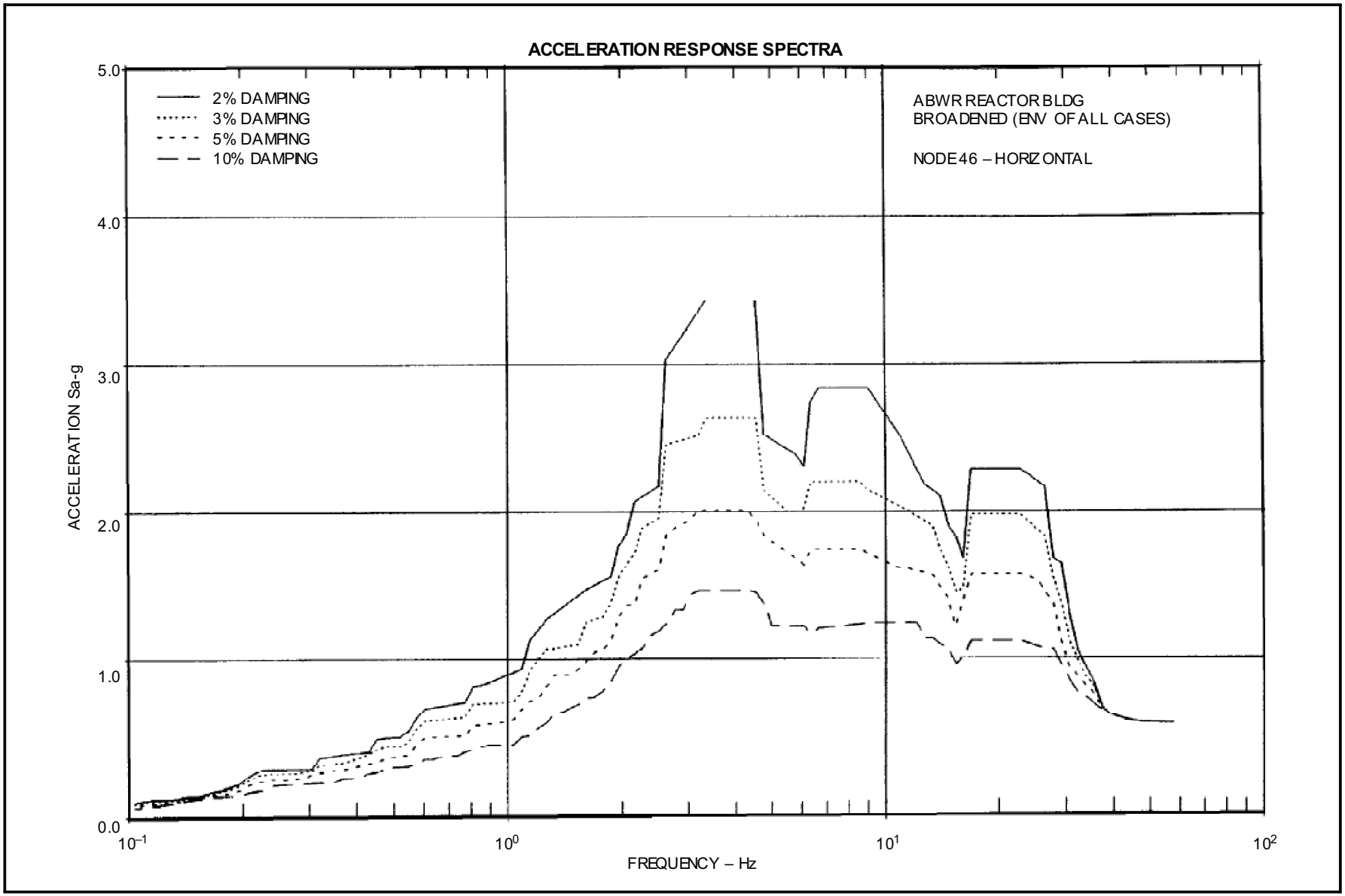

Figure 3A-136 ABWR Reactor Bldg. Broadened (Env of all Cases) Node 46–Horizontal

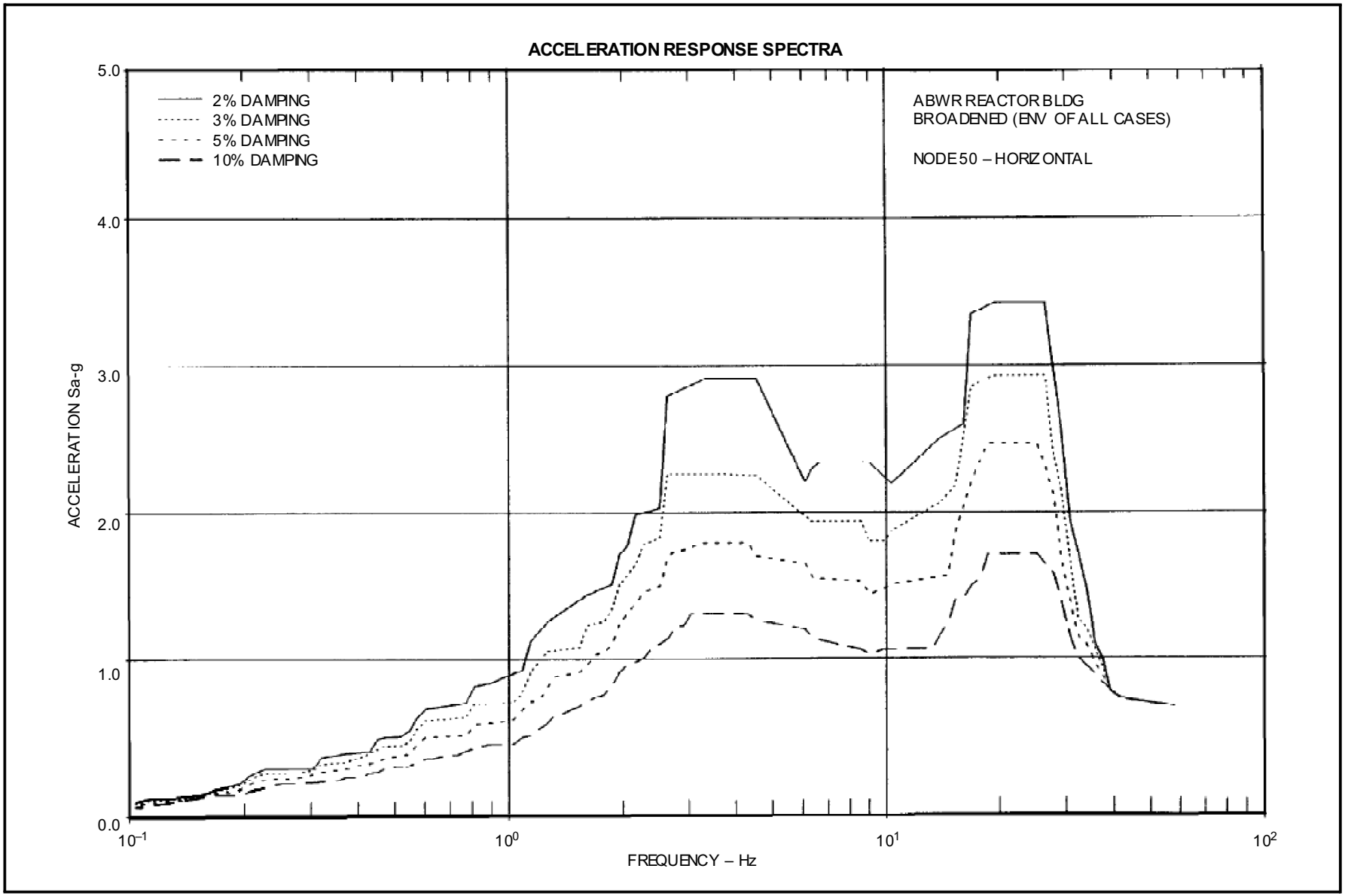

Figure 3A-137 ABWR Reactor Bldg. Broadened (Env of all Cases) Node 50–Horizontal

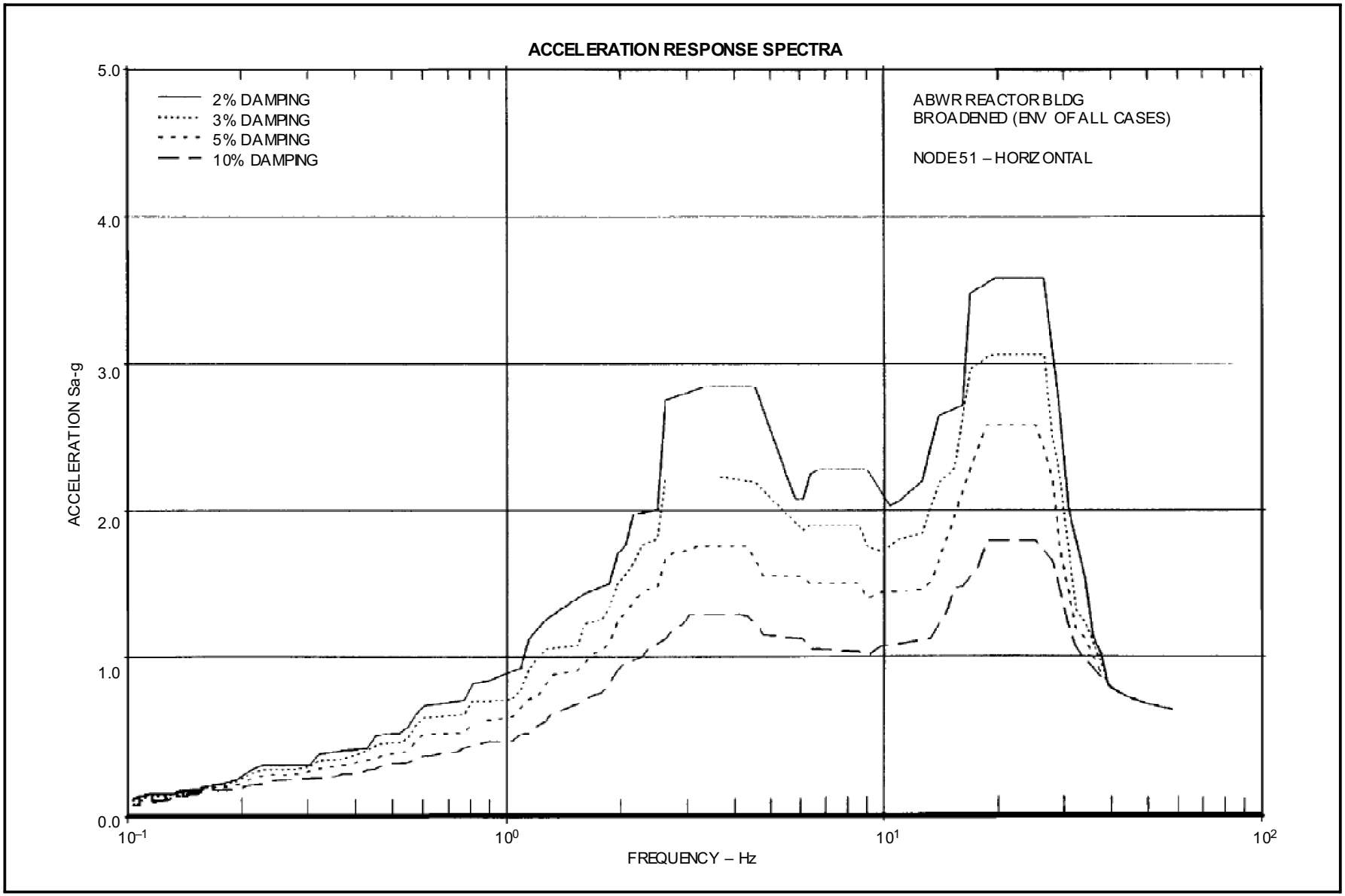

Figure 3A-138 ABWR Reactor Bldg. Broadened (Env of all Cases) Node 51–Horizontal

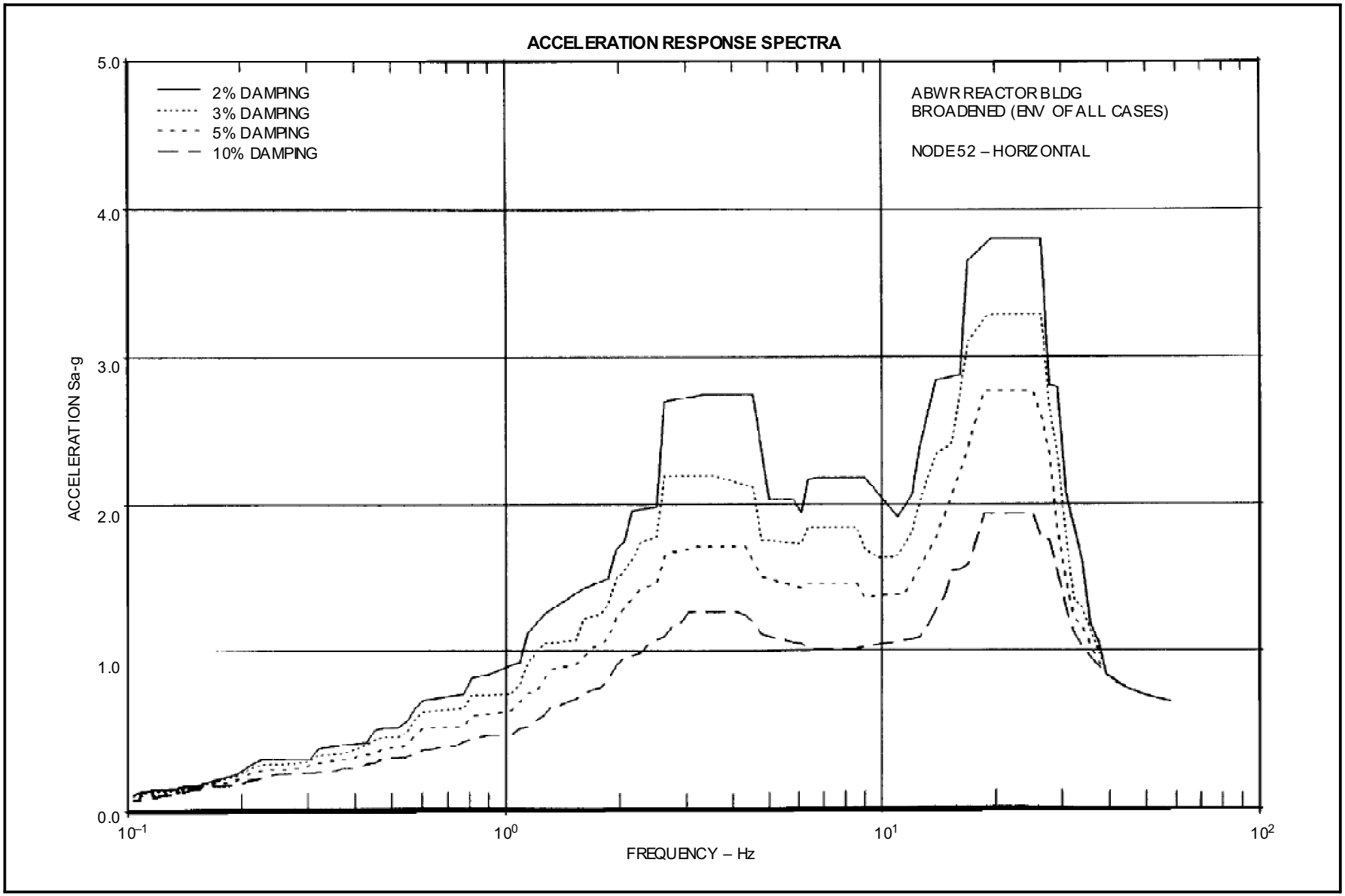

Figure 3A-139 ABWR Reactor Bldg. Broadened (Env of all Cases) Node 52–Horizontal

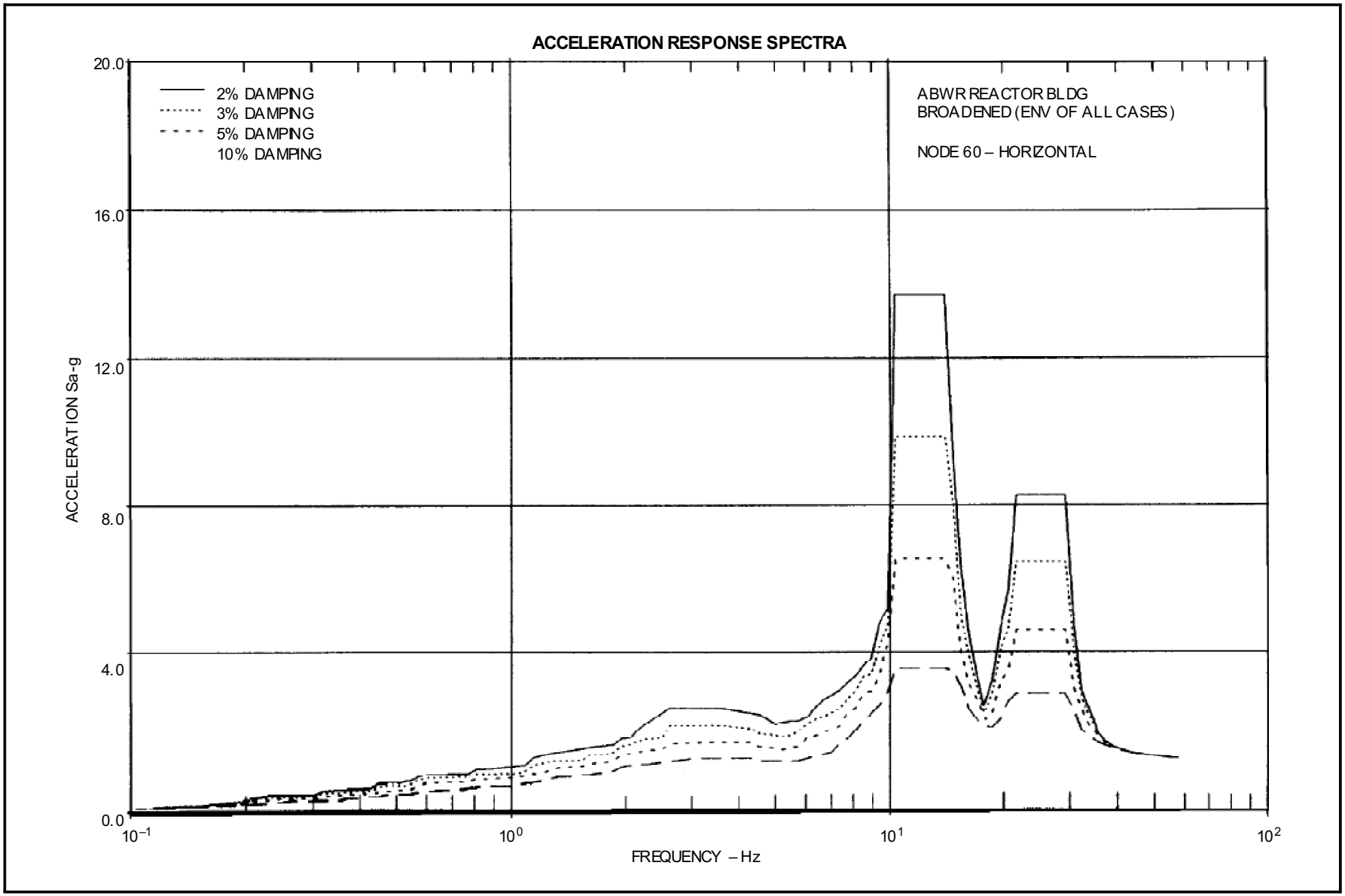

Figure 3A-140 ABWR Reactor Bldg. Broadened (Env of all Cases) Node 60–Horizontal

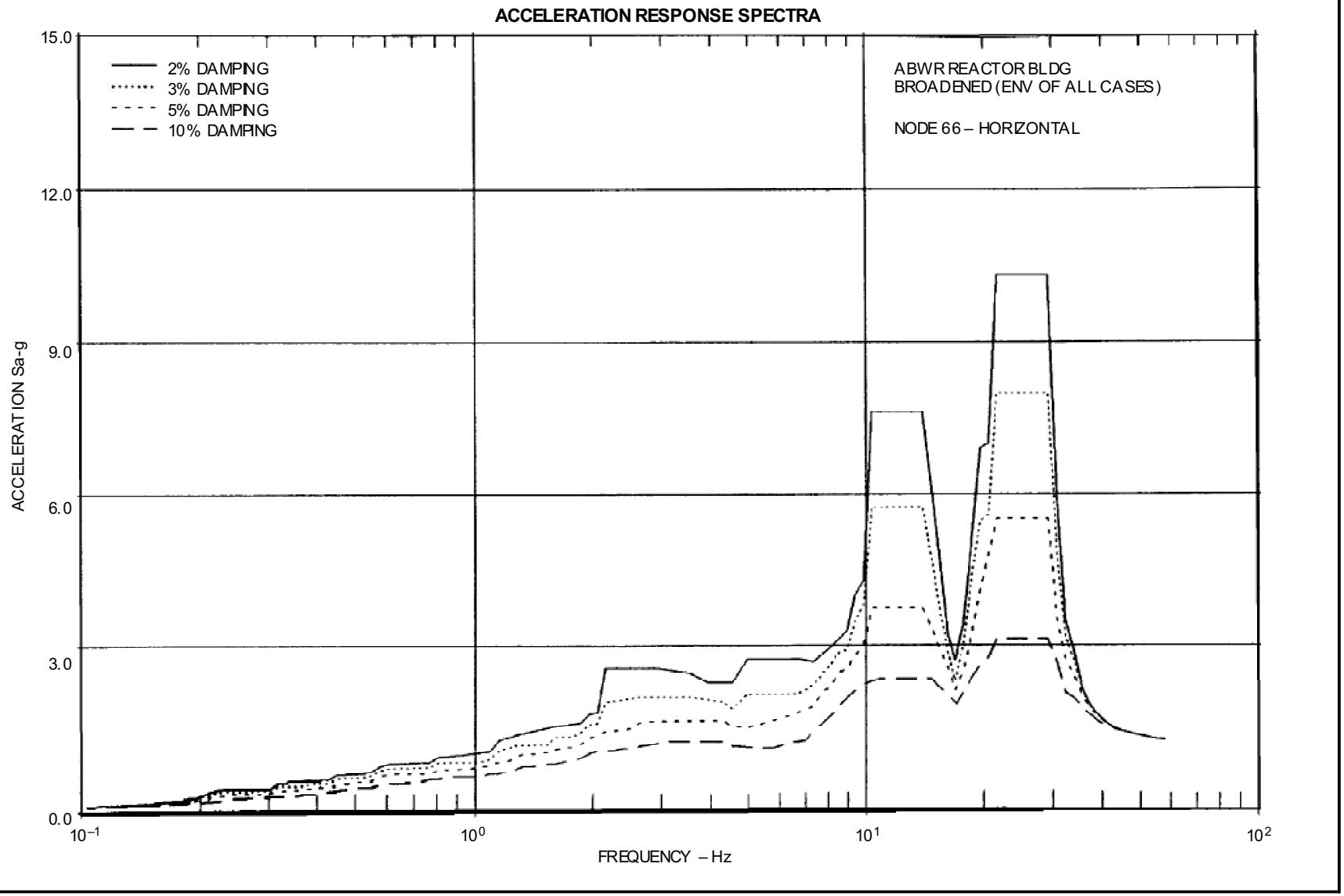

Figure 3A-141 ABWR Reactor Bldg. Broadened (Env of all Cases) Node 66–Horizontal

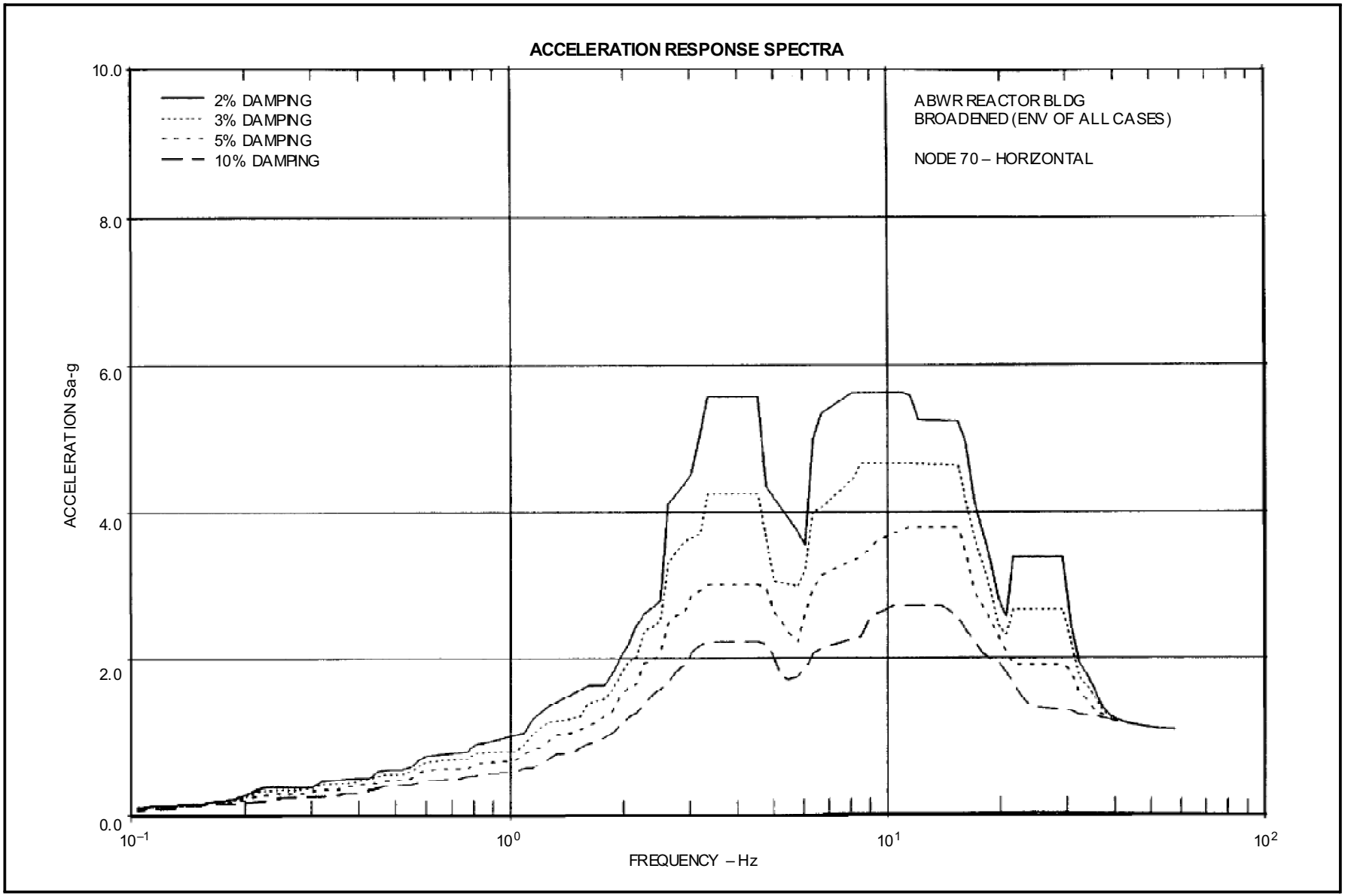

Figure 3A-142 ABWR Reactor Bldg. Broadened (Env of all Cases) Node 70–Horizontal

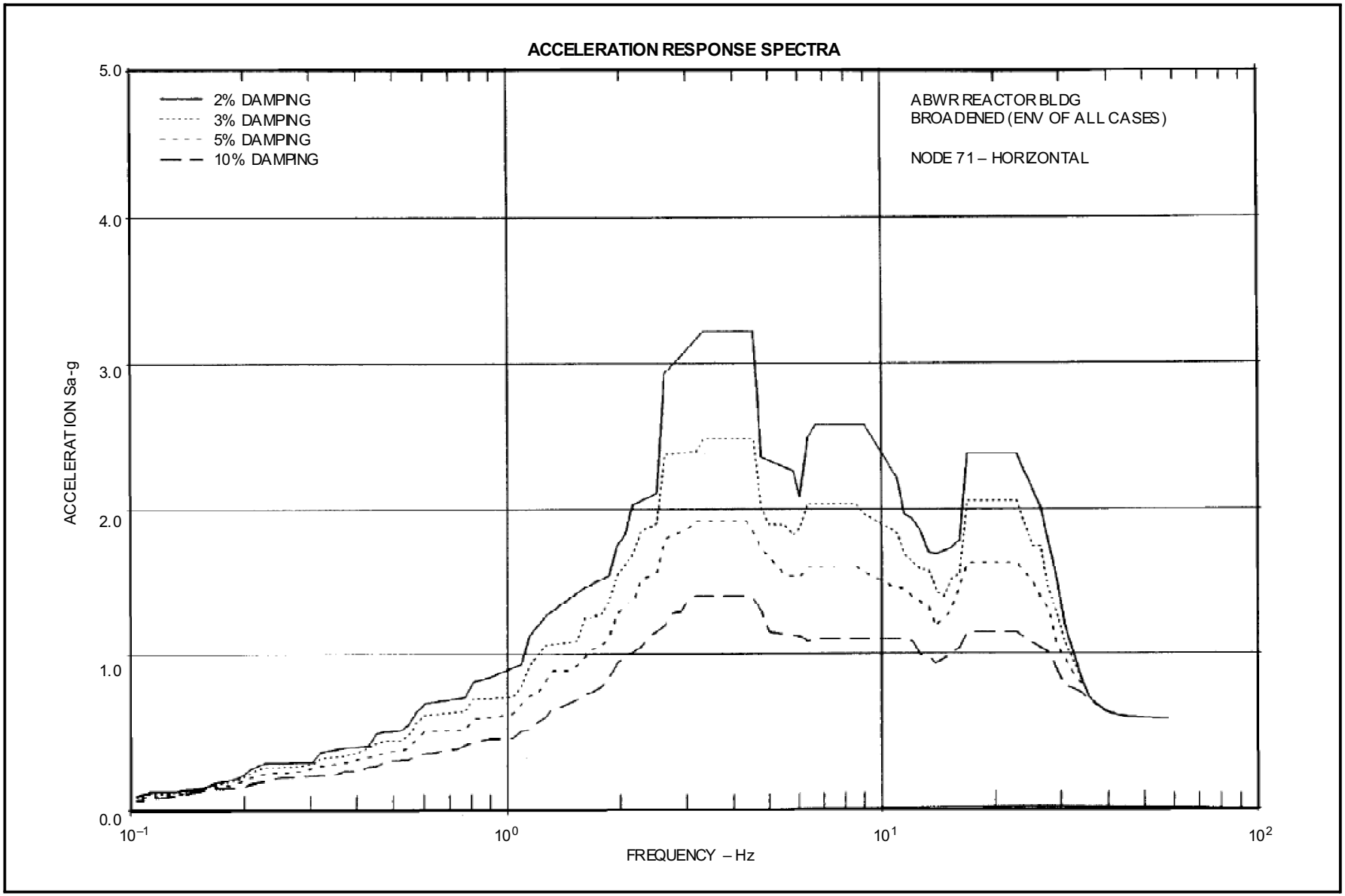

Figure 3A-143 ABWR Reactor Bldg. Broadened (Env of all Cases) Node 71–Horizontal

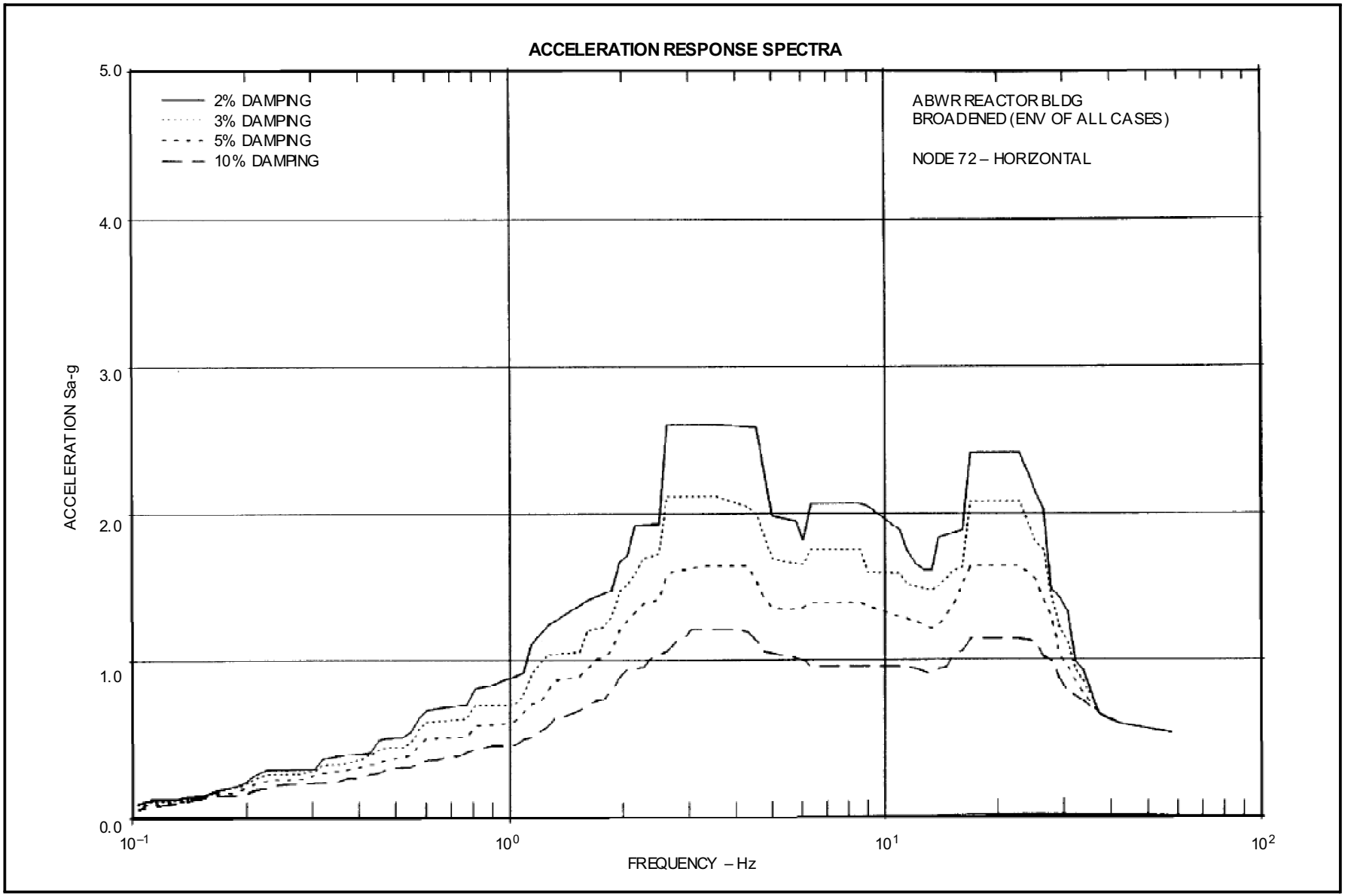

Figure 3A-144 ABWR Reactor Bldg. Broadened (Env of all Cases) Node 72–Horizontal

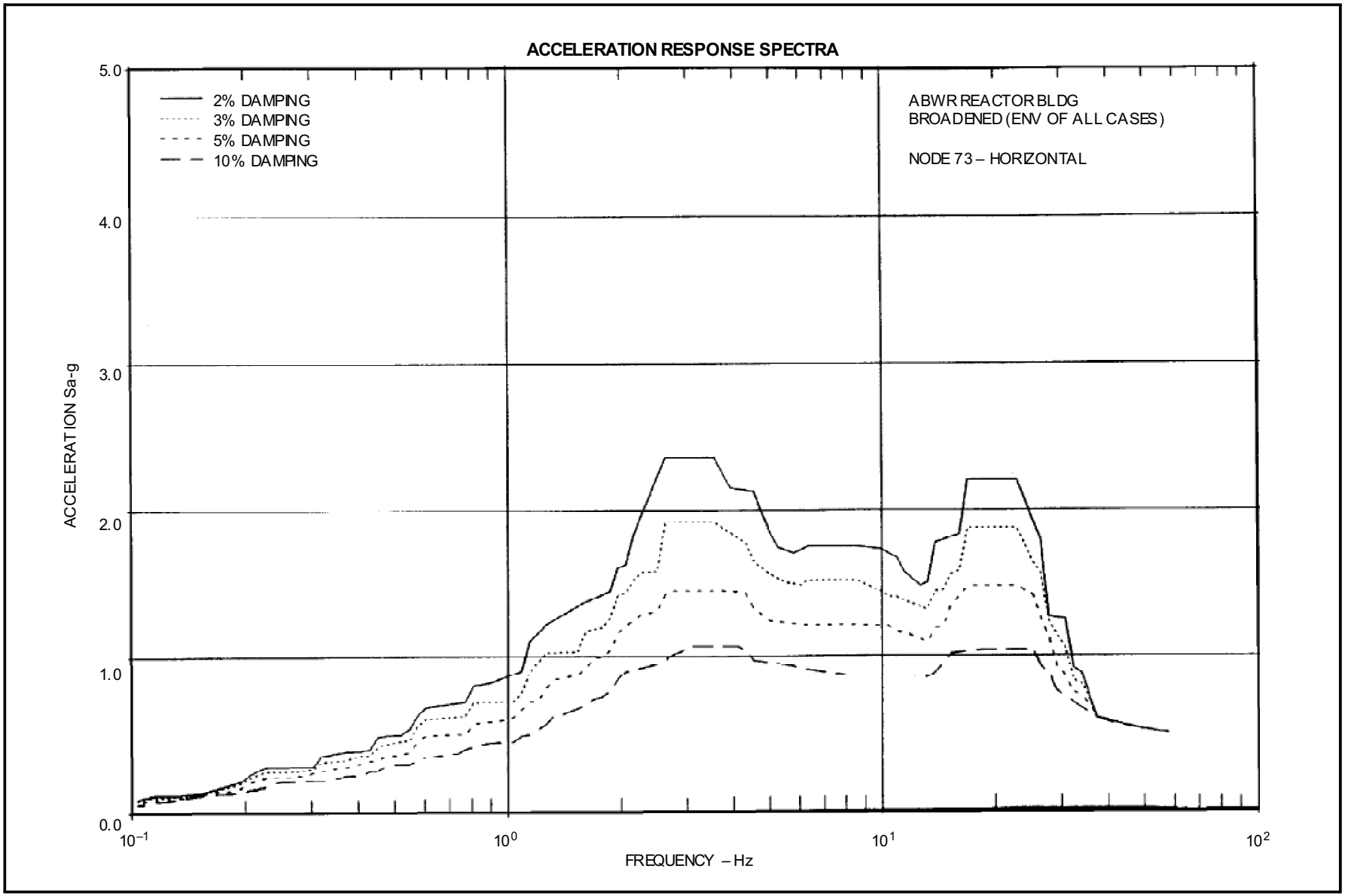

Figure 3A-145 ABWR Reactor Bldg. Broadened (Env of all Cases) Node 73–Horizontal

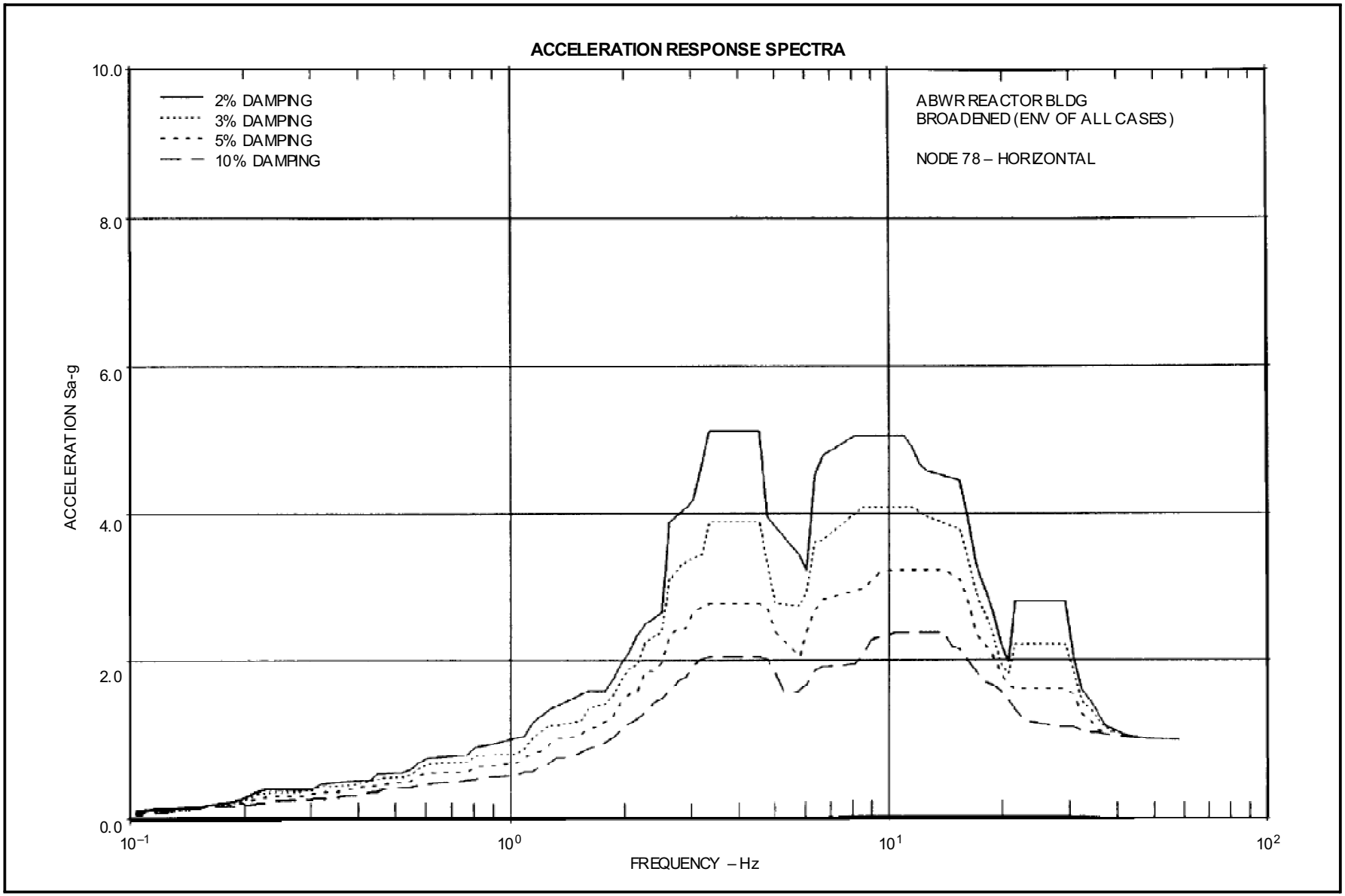

Figure 3A-146 ABWR Reactor Bldg. Broadened (Env of all Cases) Node 78–Horizontal

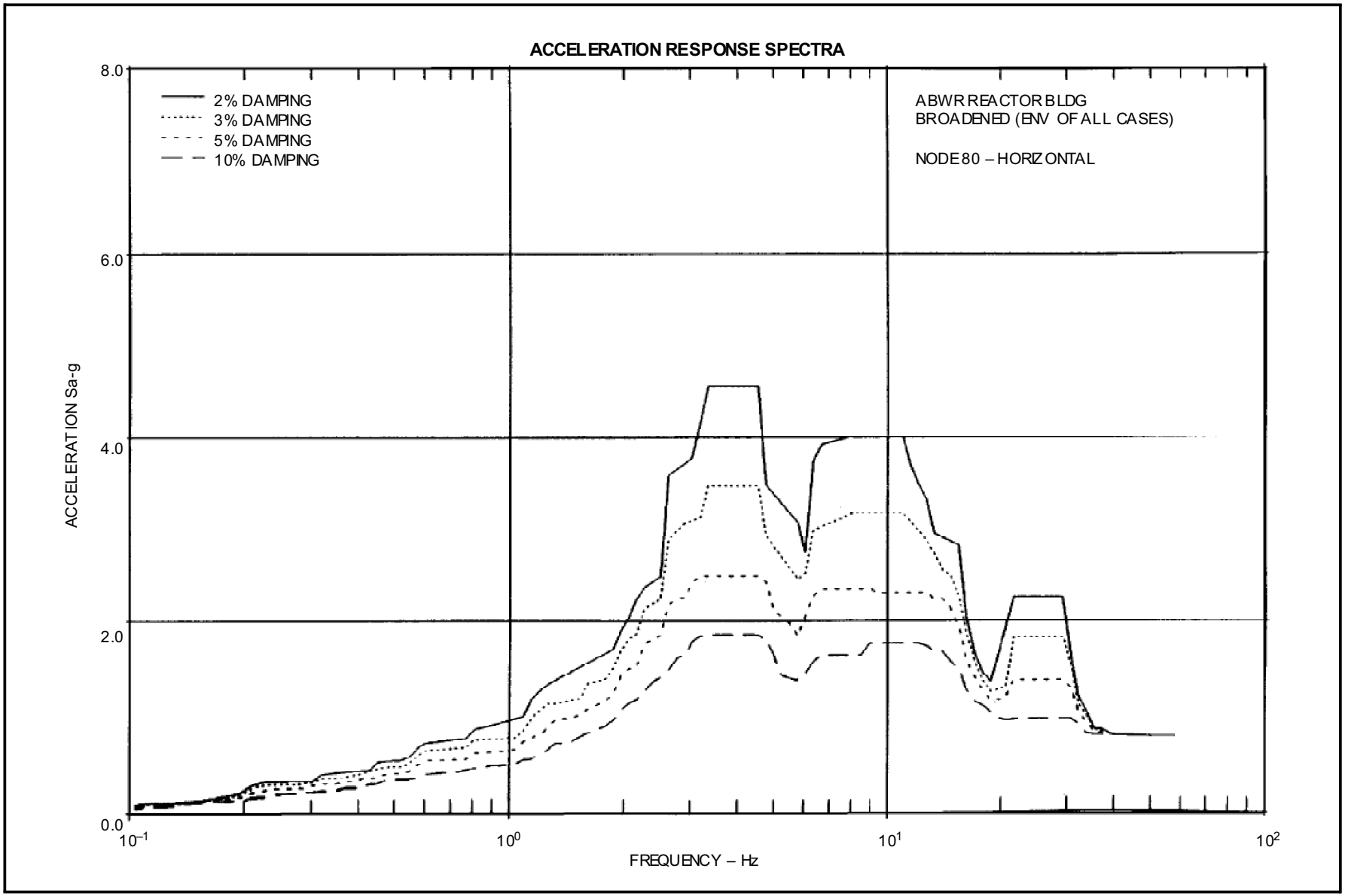

Figure 3A-147 ABWR Reactor Bldg. Broadened (Env of all Cases) Node 80–Horizontal

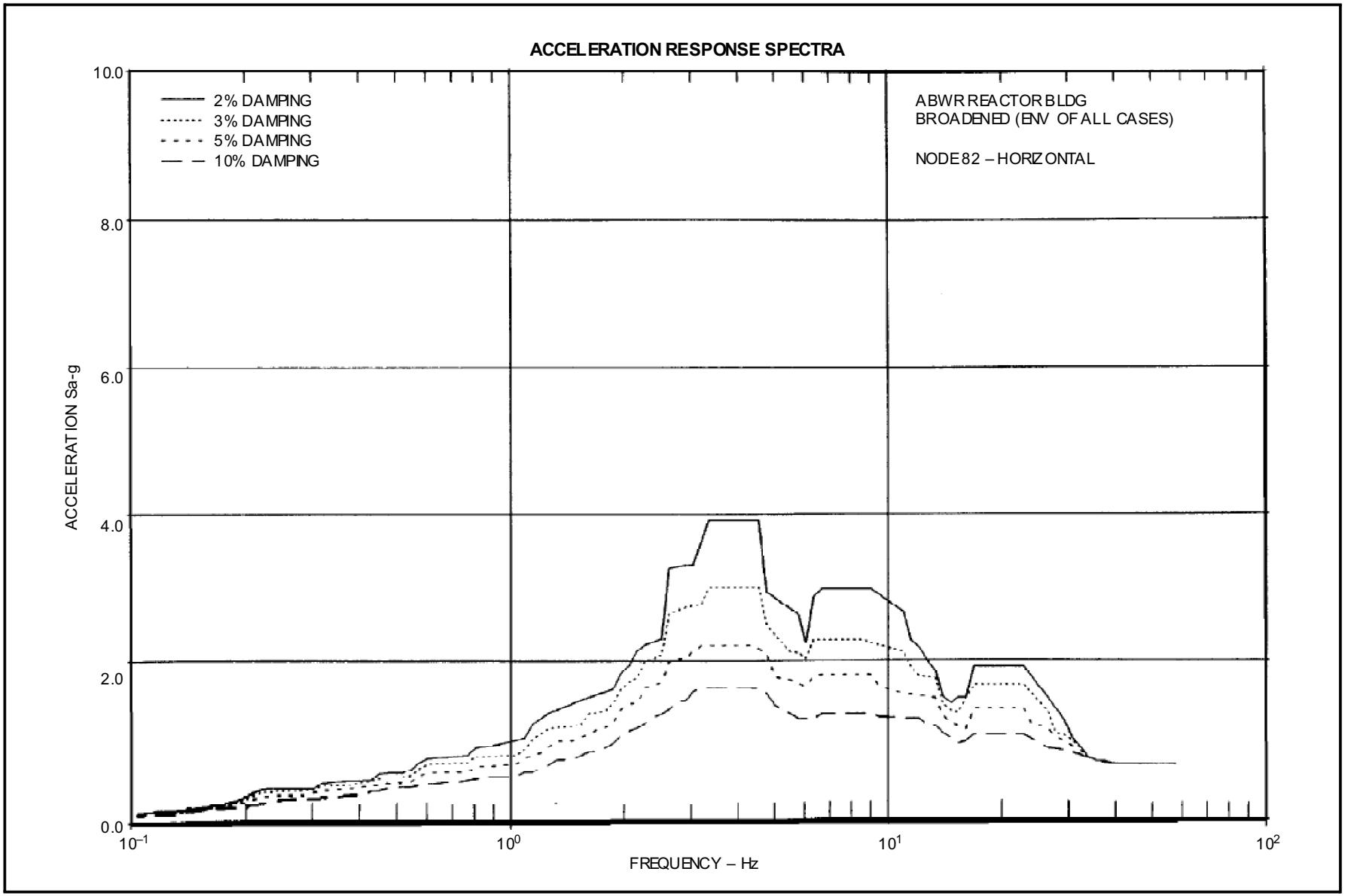

Figure 3A-148 ABWR Reactor Bldg. Broadened (Env of all Cases) Node 82–Horizontal

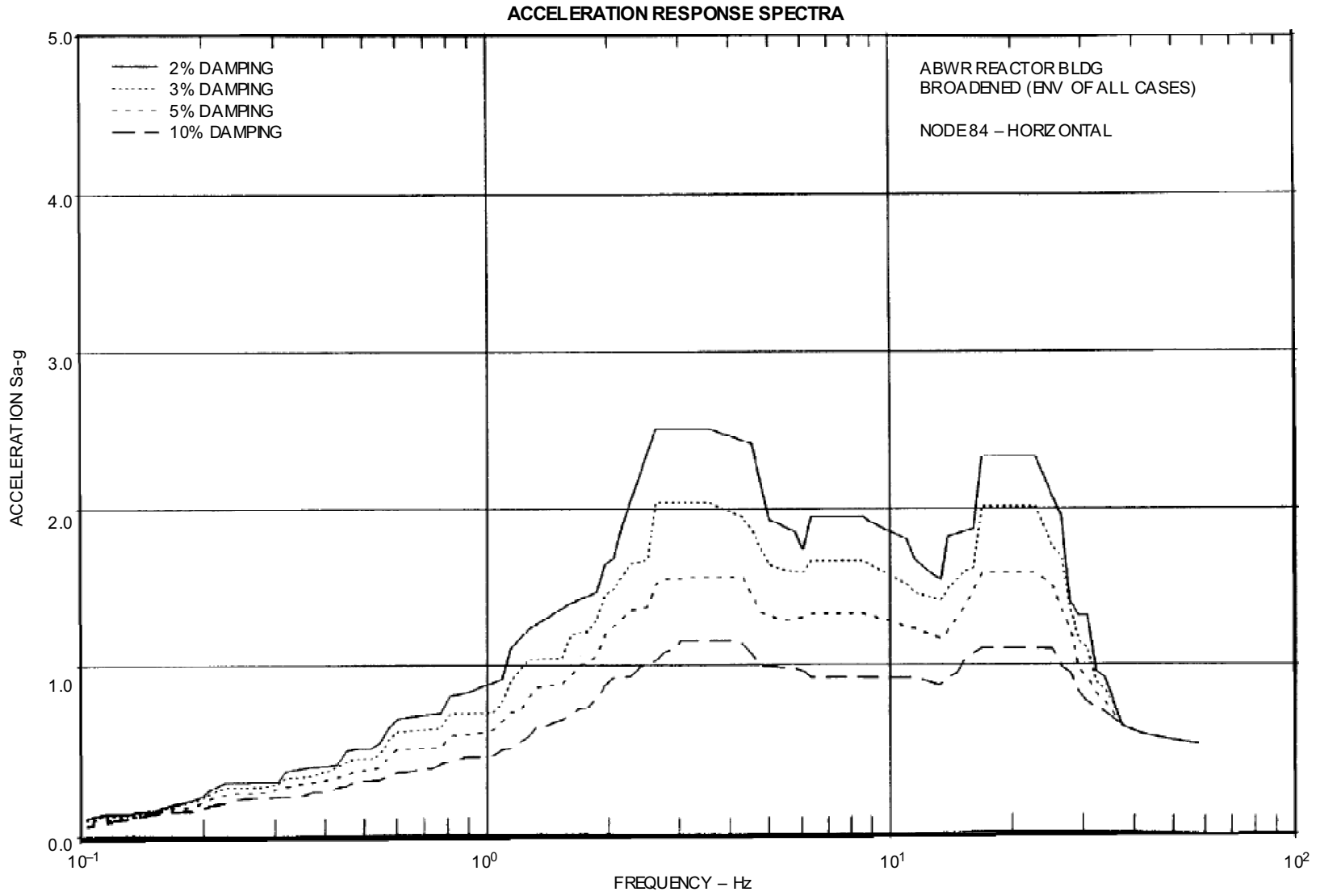

Figure 3A-149 ABWR Reactor Bldg. Broadened (Env of all Cases) Node 84–Horizontal

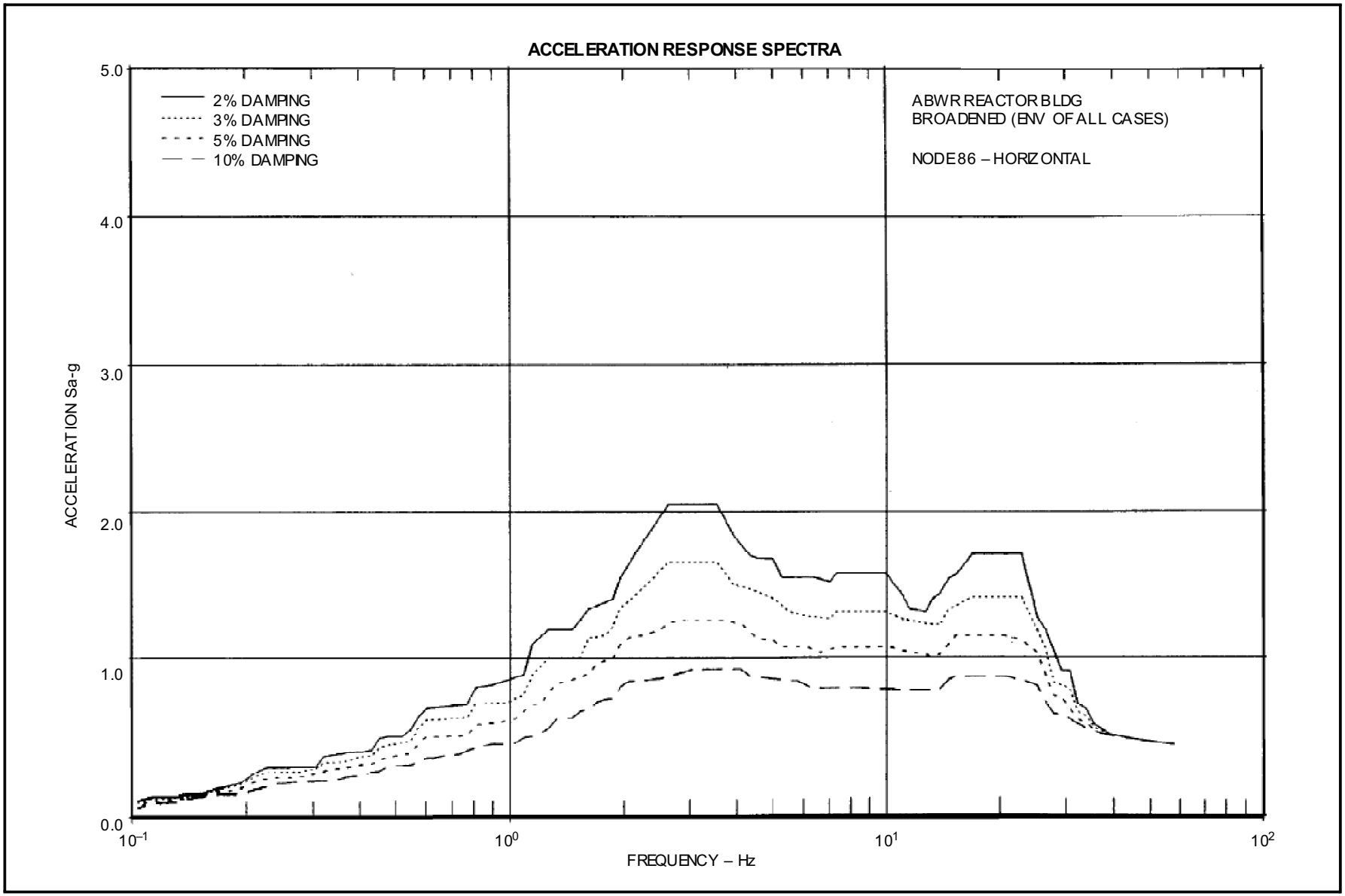

Figure 3A-150 ABWR Reactor Bldg. Broadened (Env of all Cases) Node 86–Horizontal

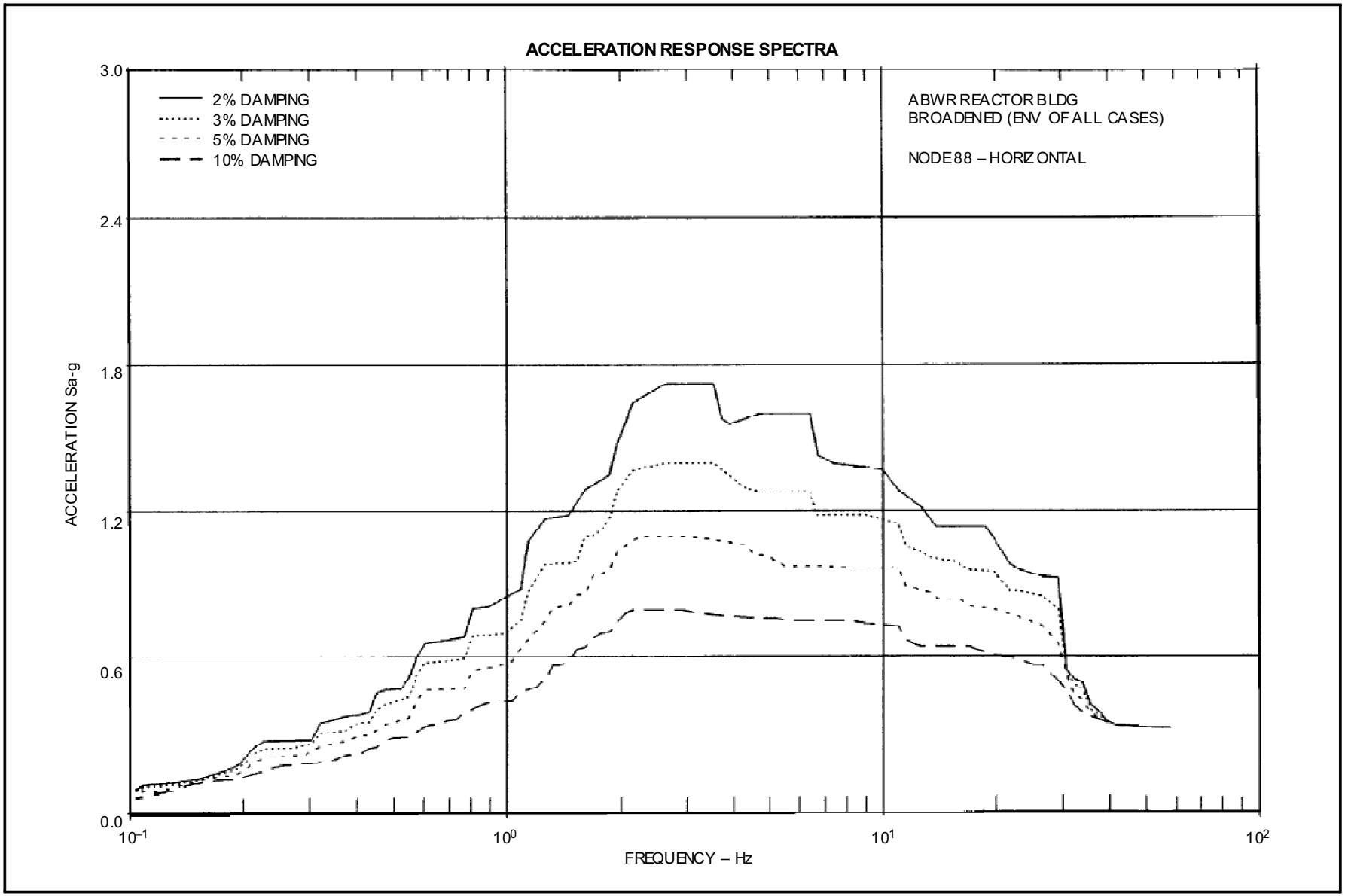

Figure 3A-151 ABWR Reactor Bldg. Broadened (Env of all Cases) Node 88–Horizontal

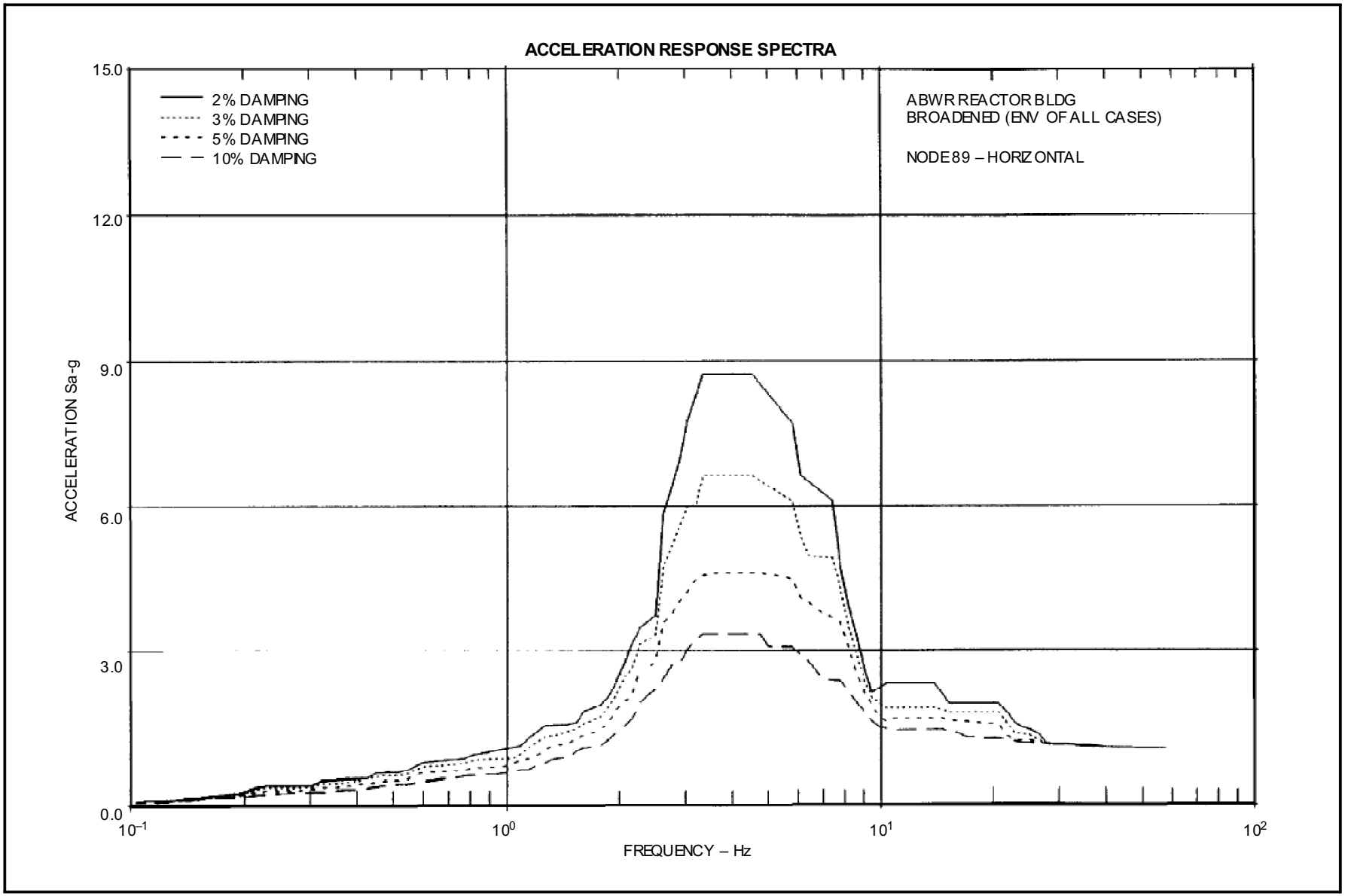

Figure 3A-152 ABWR Reactor Bldg. Broadened (Env of all Cases) Node 89–Horizontal

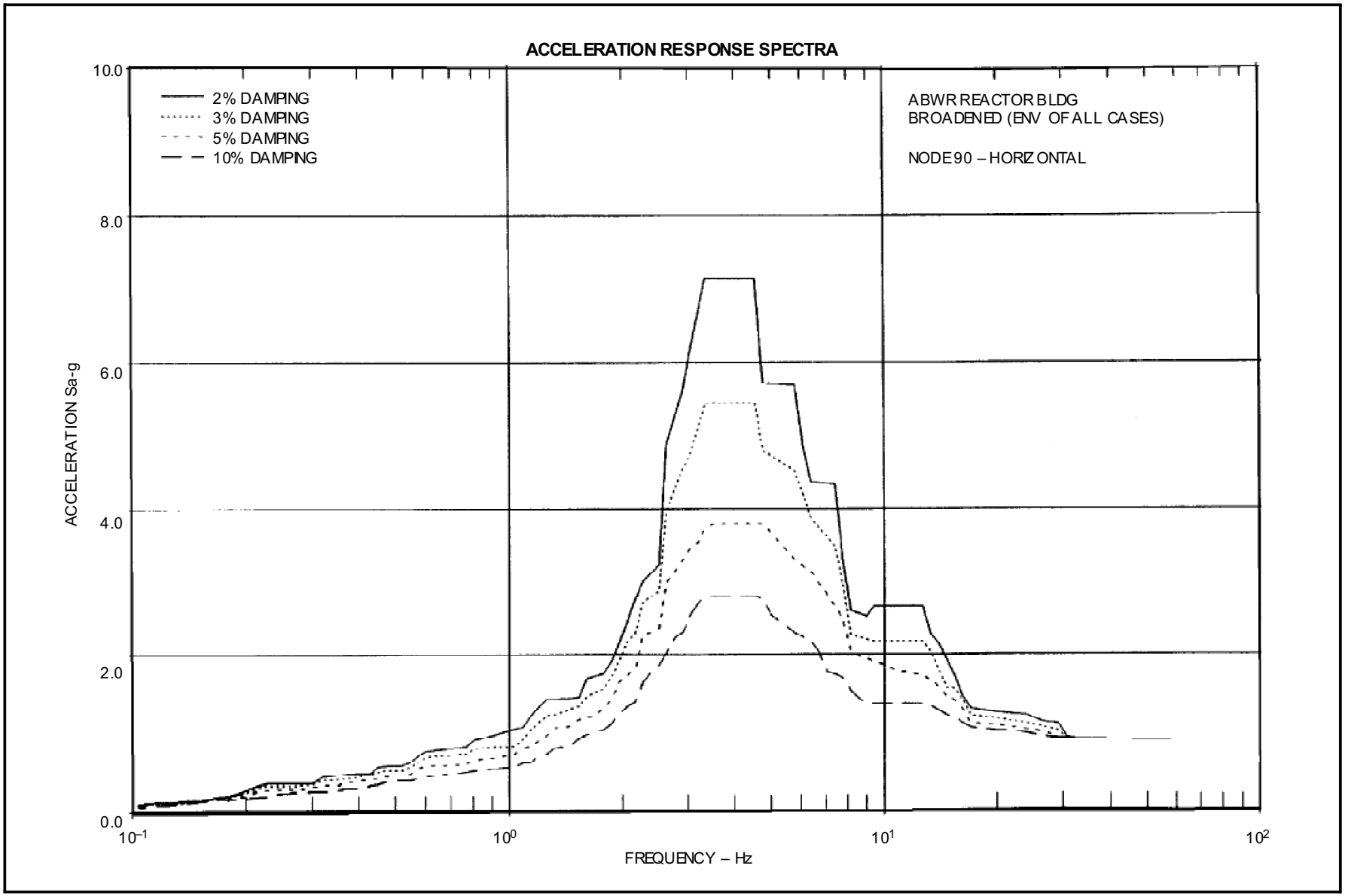

Figure 3A-153 ABWR Reactor Bldg. Broadened (Env of all Cases) Node 90–Horizontal

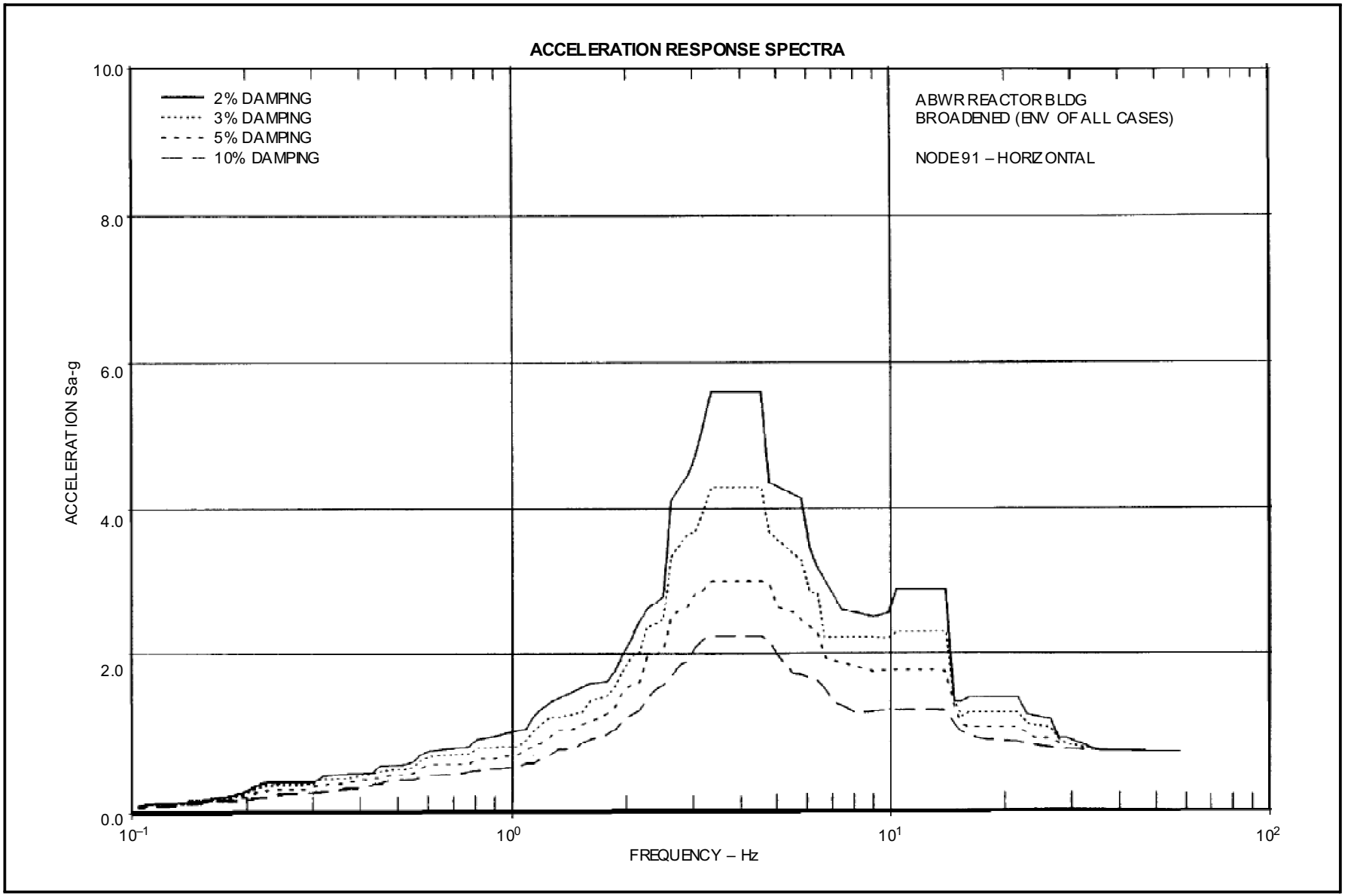

Figure 3A-154 ABWR Reactor Bldg. Broadened (Env of all Cases) Node 91–Horizontal

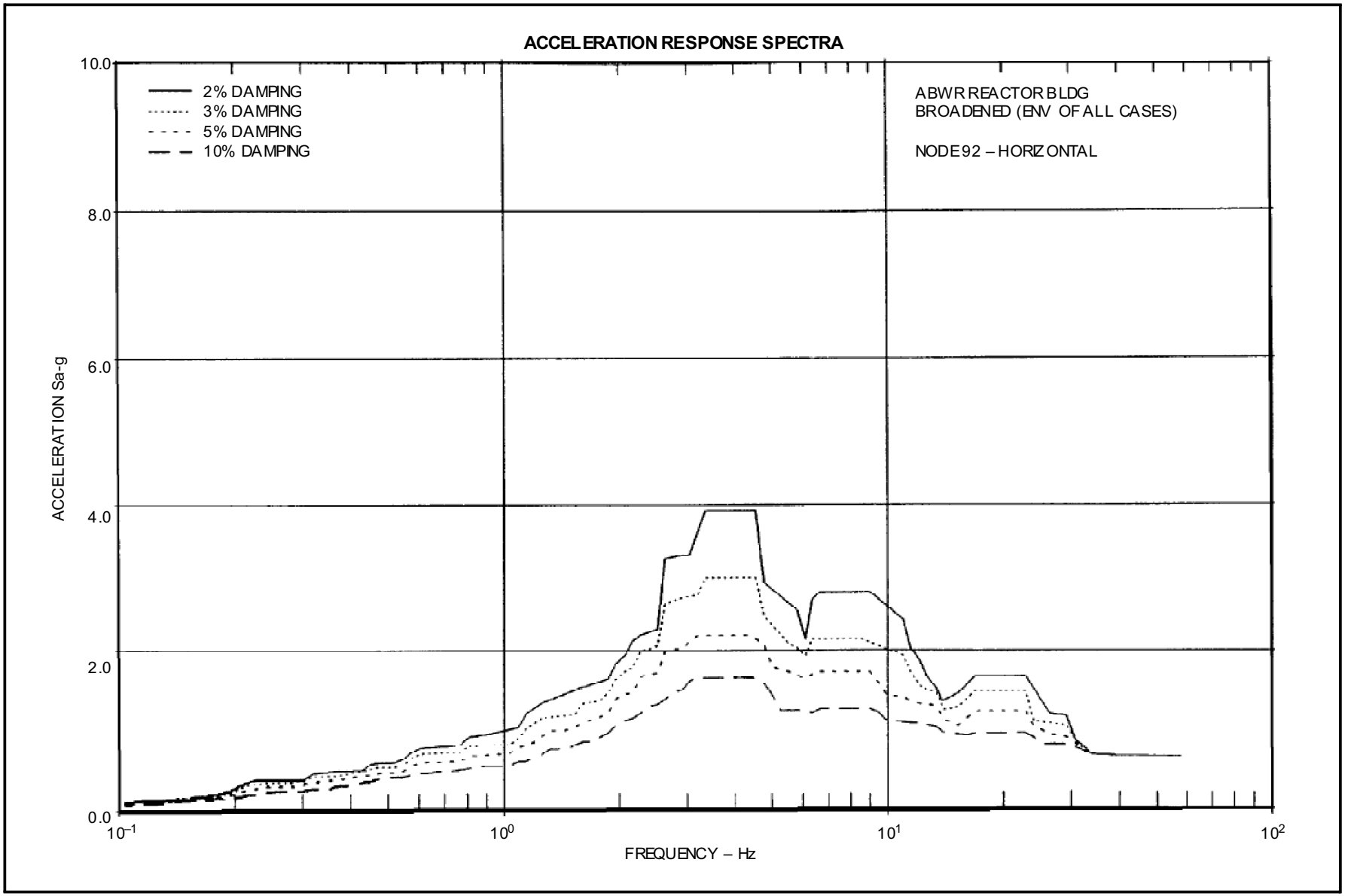

Figure 3A-155 ABWR Reactor Bldg. Broadened (Env of all Cases) Node 92–Horizontal

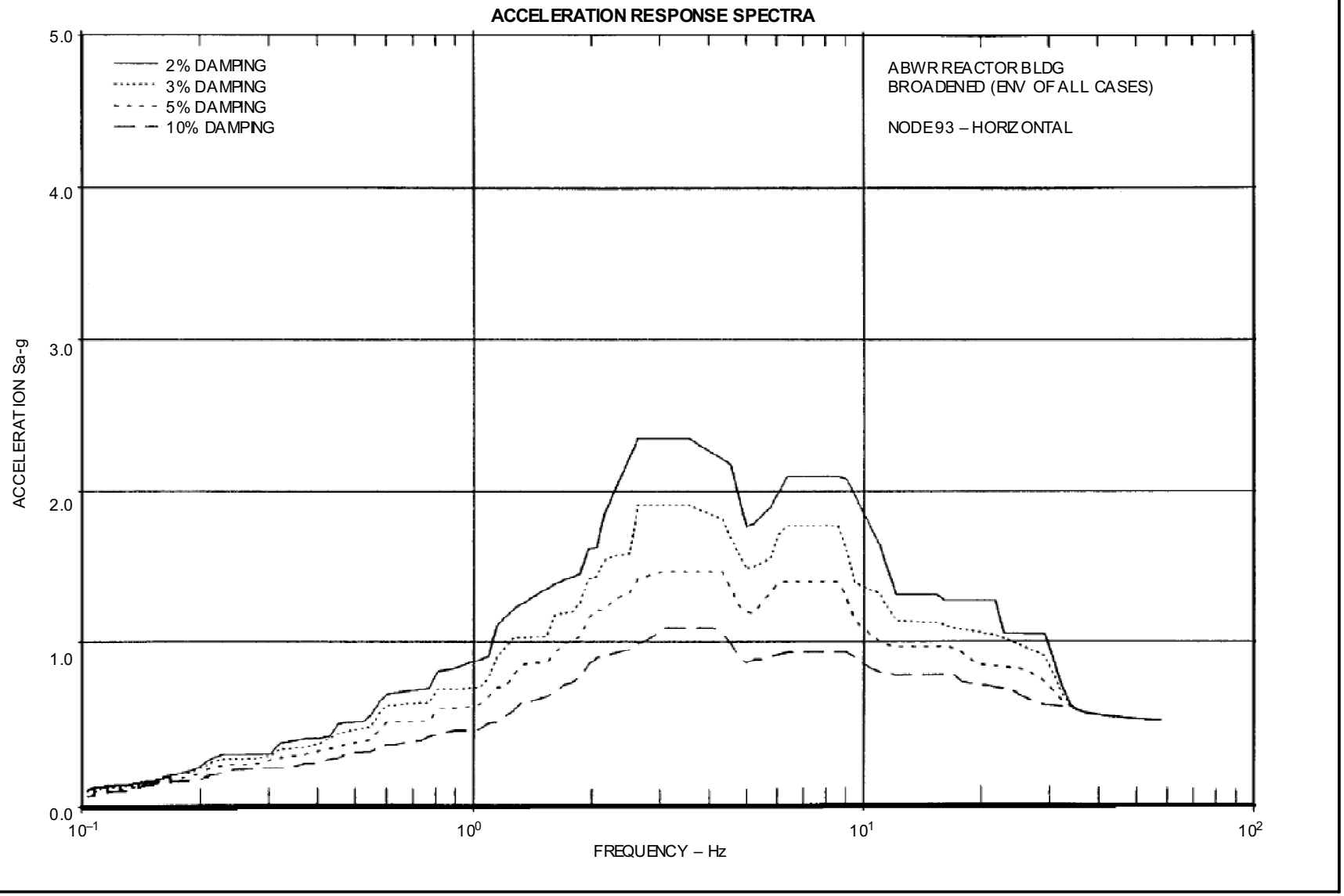

Figure 3A-156 ABWR Reactor Bldg. Broadened (Env of all Cases) Node 93–Horizontal

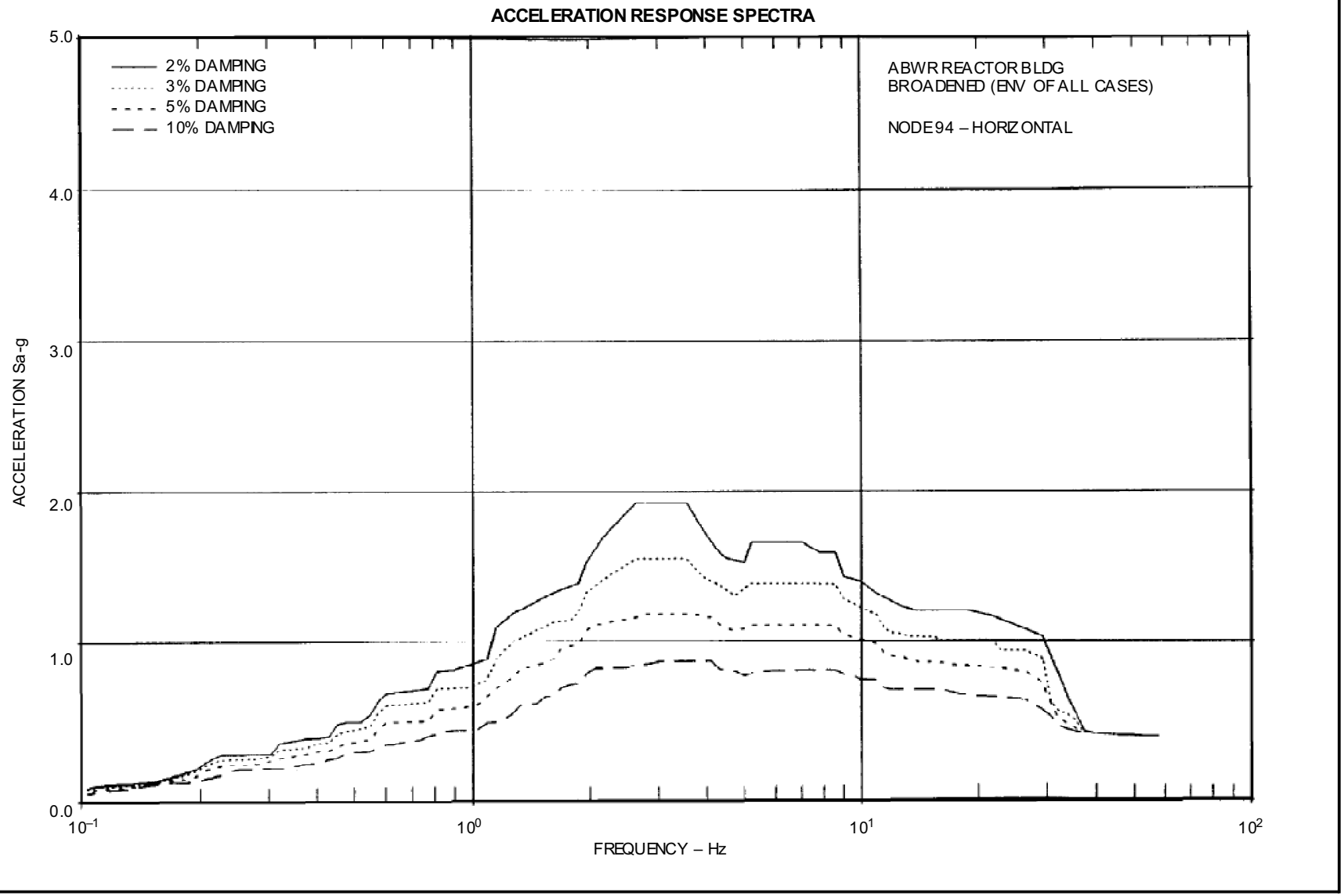

Figure 3A-157 ABWR Reactor Bldg. Broadened (Env of all Cases) Node 94–Horizontal

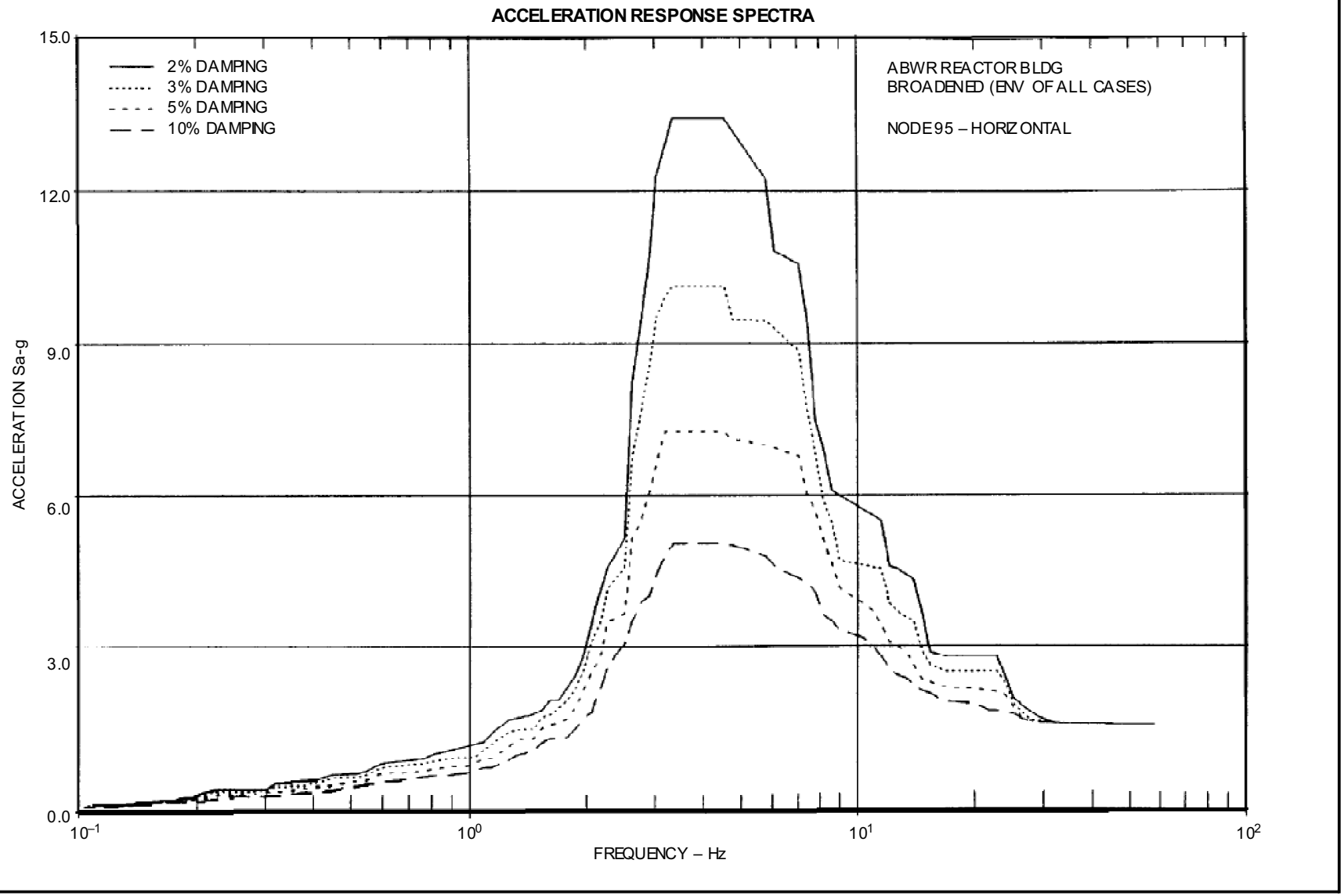

Figure 3A-158 ABWR Reactor Bldg. Broadened (Env of all Cases) Node 95–Horizontal

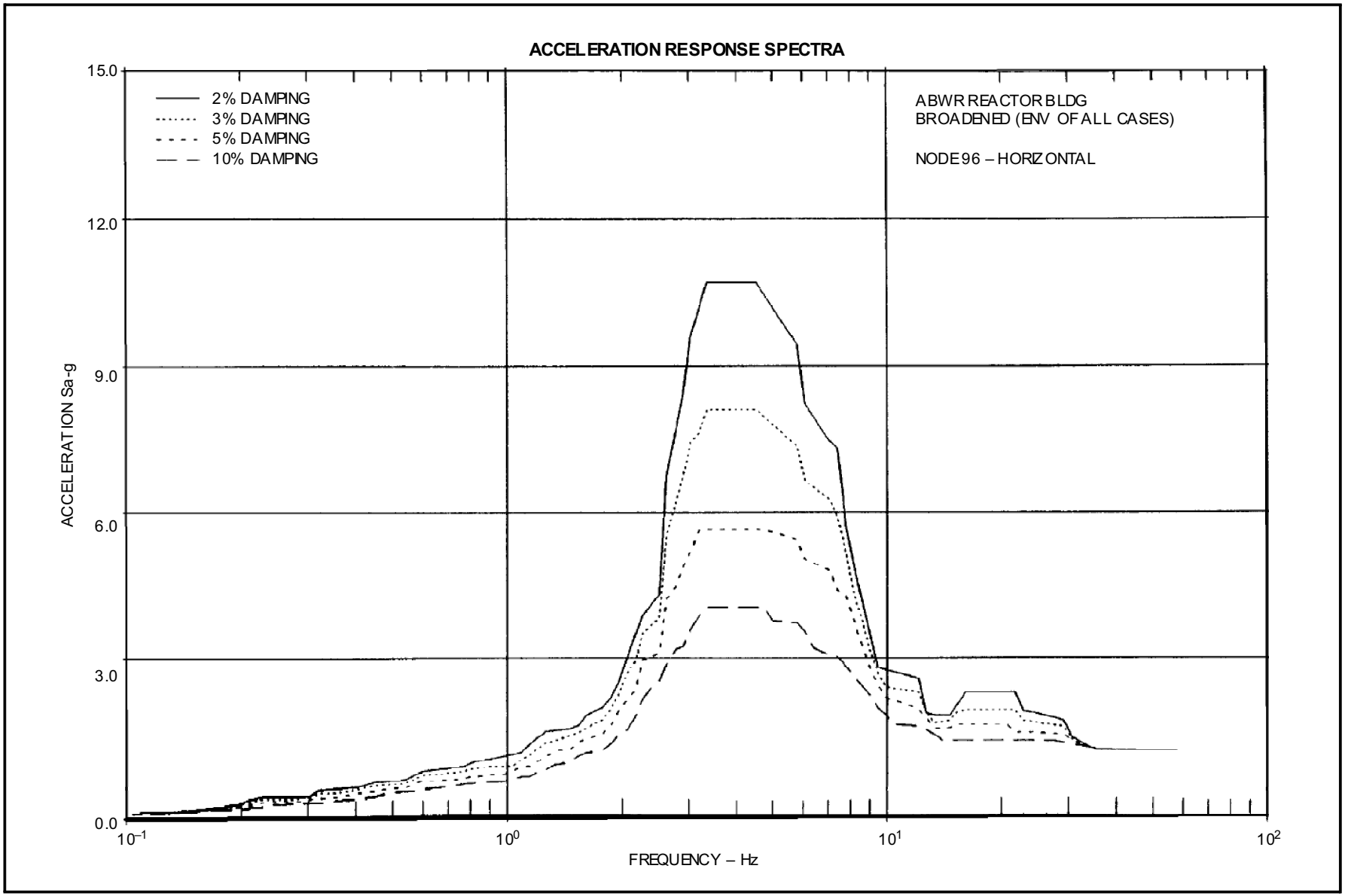

Figure 3A-159 ABWR Reactor Bldg. Broadened (Env of all Cases) Node 96–Horizontal

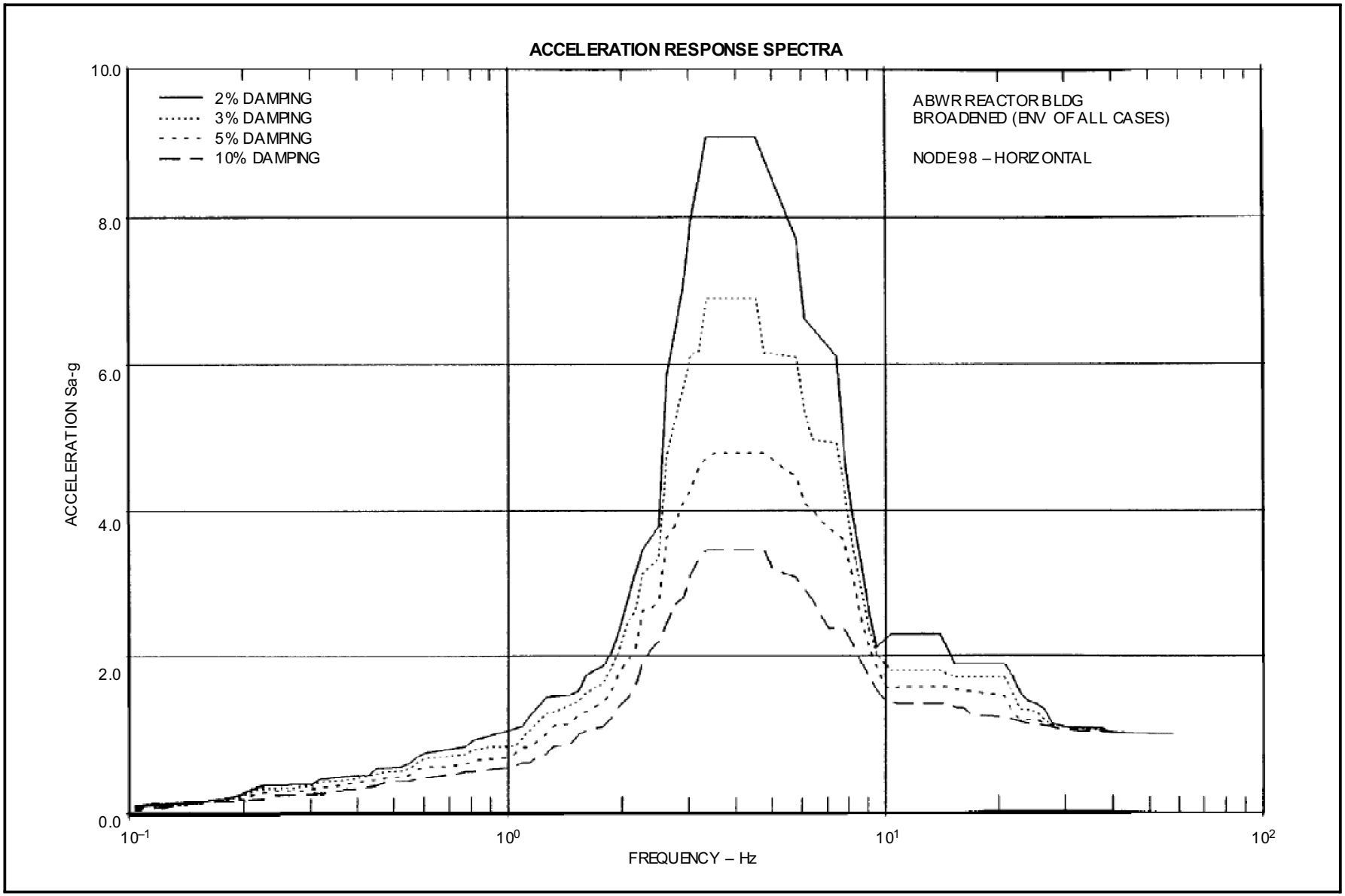

Figure 3A-160 ABWR Reactor Bldg. Broadened (Env of all Cases) Node 98–Horizontal

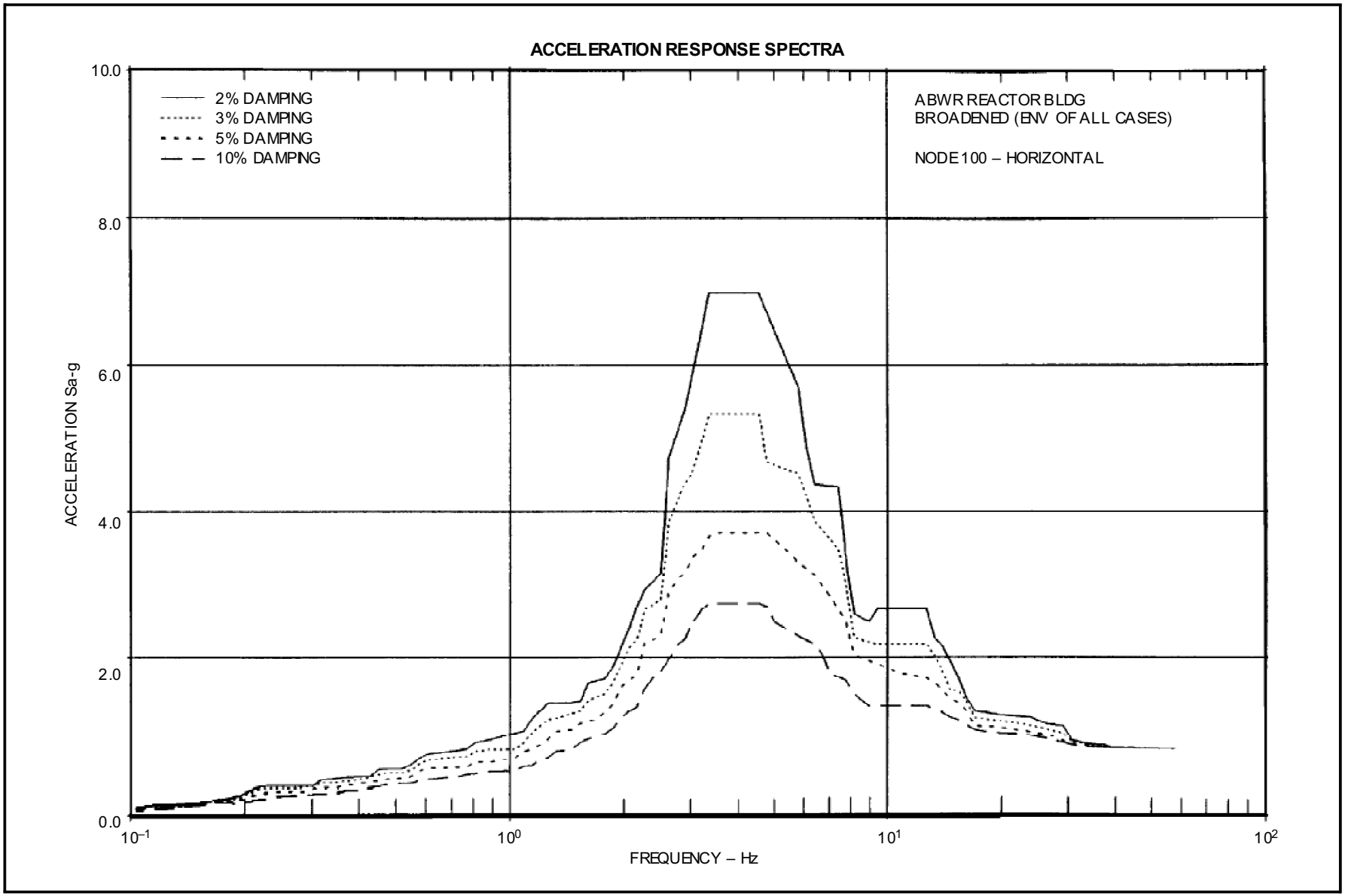

Figure 3A-161 ABWR Reactor Bldg. Broadened (Env of all Cases) Node 100–Horizontal

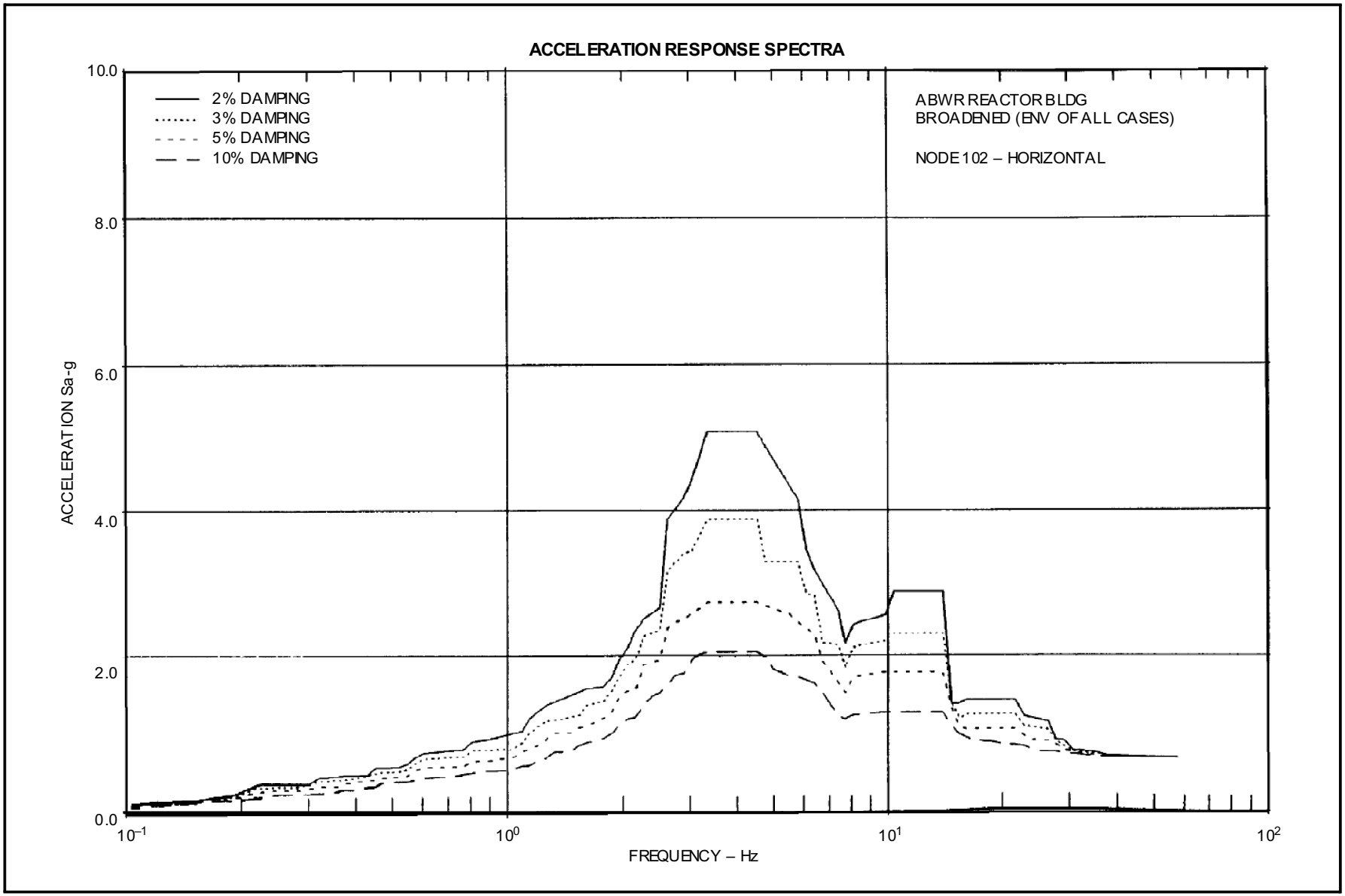

Figure 3A-162 ABWR Reactor Bldg. Broadened (Env of all Cases) Node 102–Horizontal

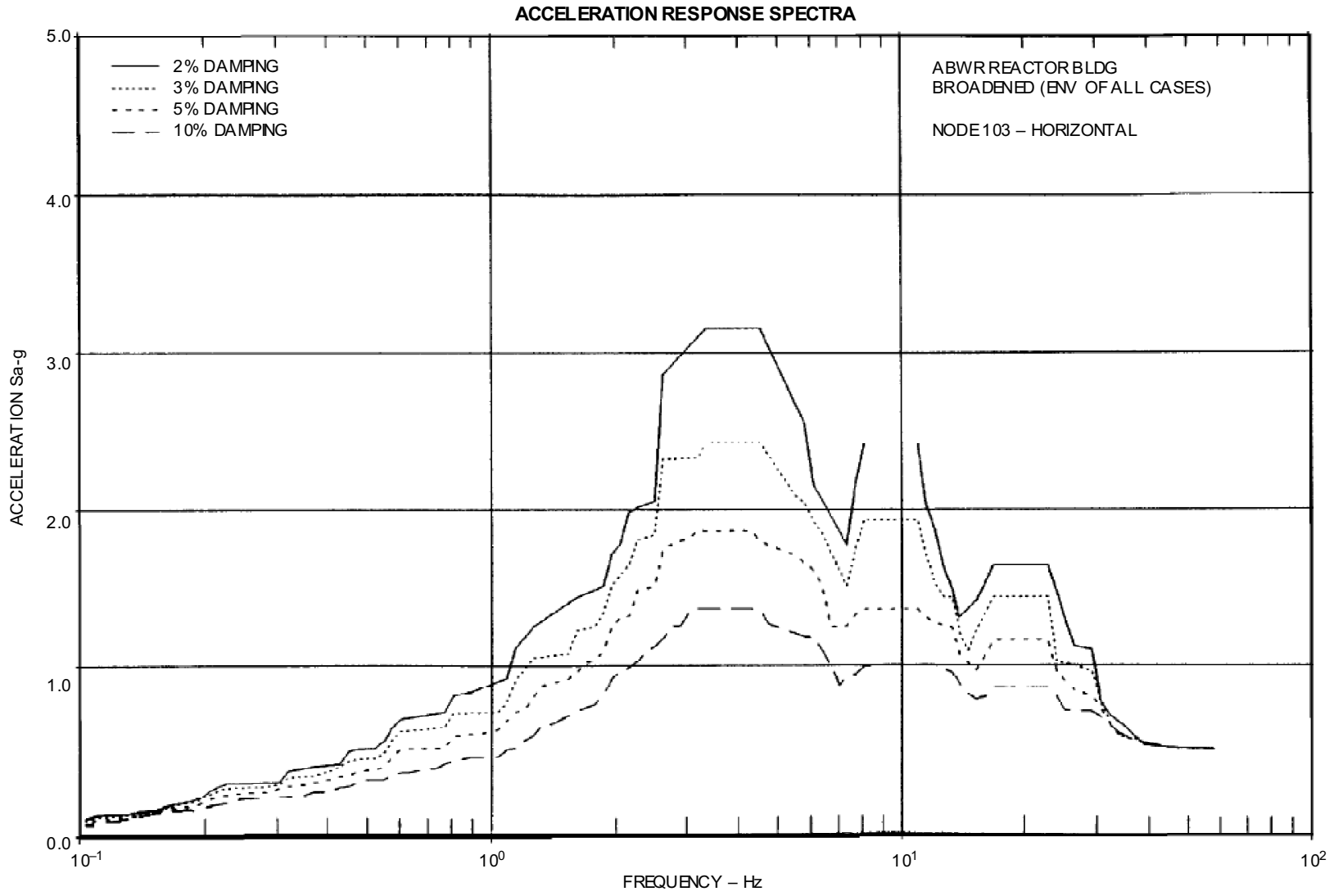

Figure 3A-163 ABWR Reactor Bldg. Broadened (Env of all Cases) Node 103–Horizontal

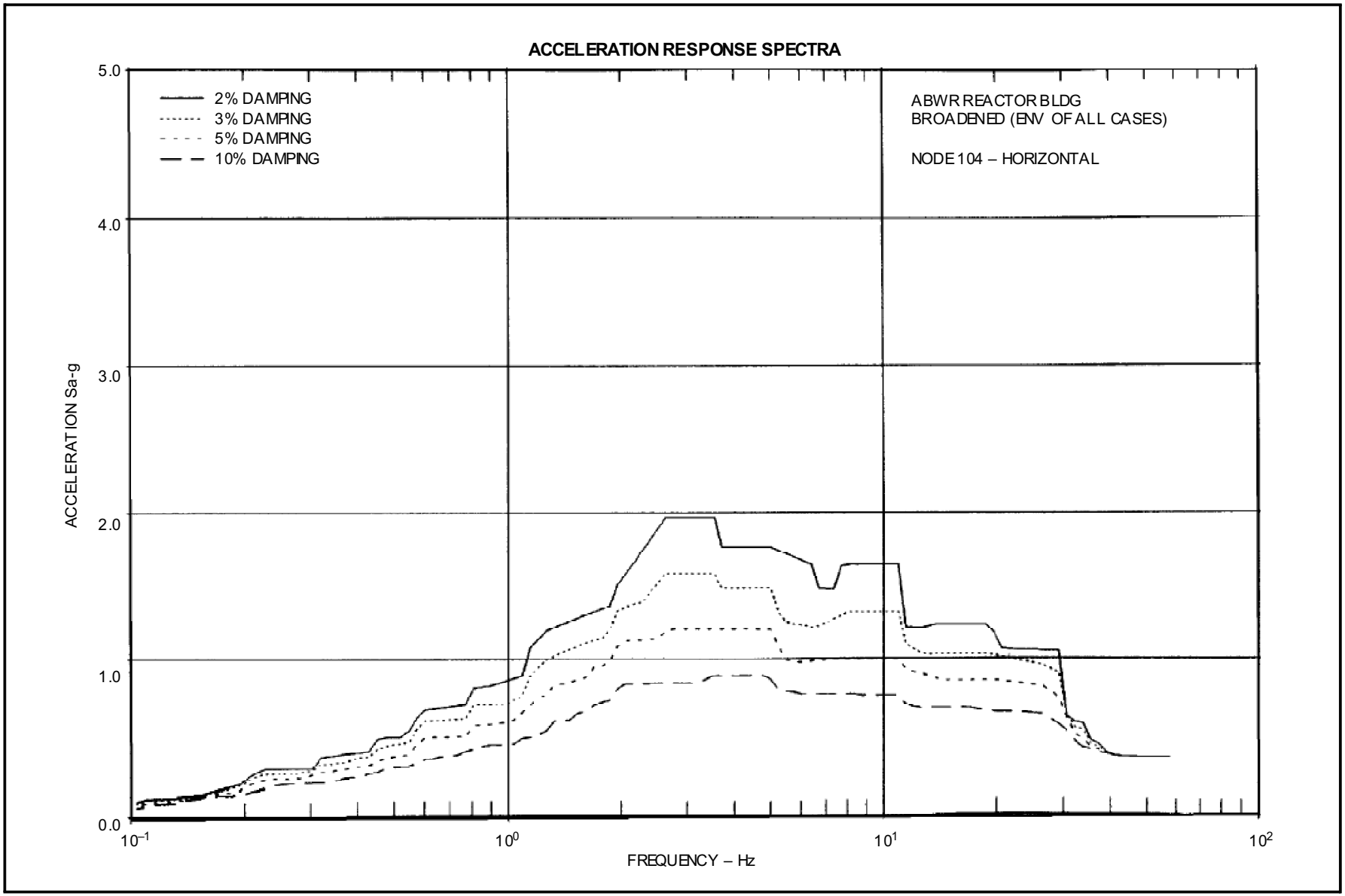

Figure 3A-164 ABWR Reactor Bldg. Broadened (Env of all Cases) Node 104–Horizontal

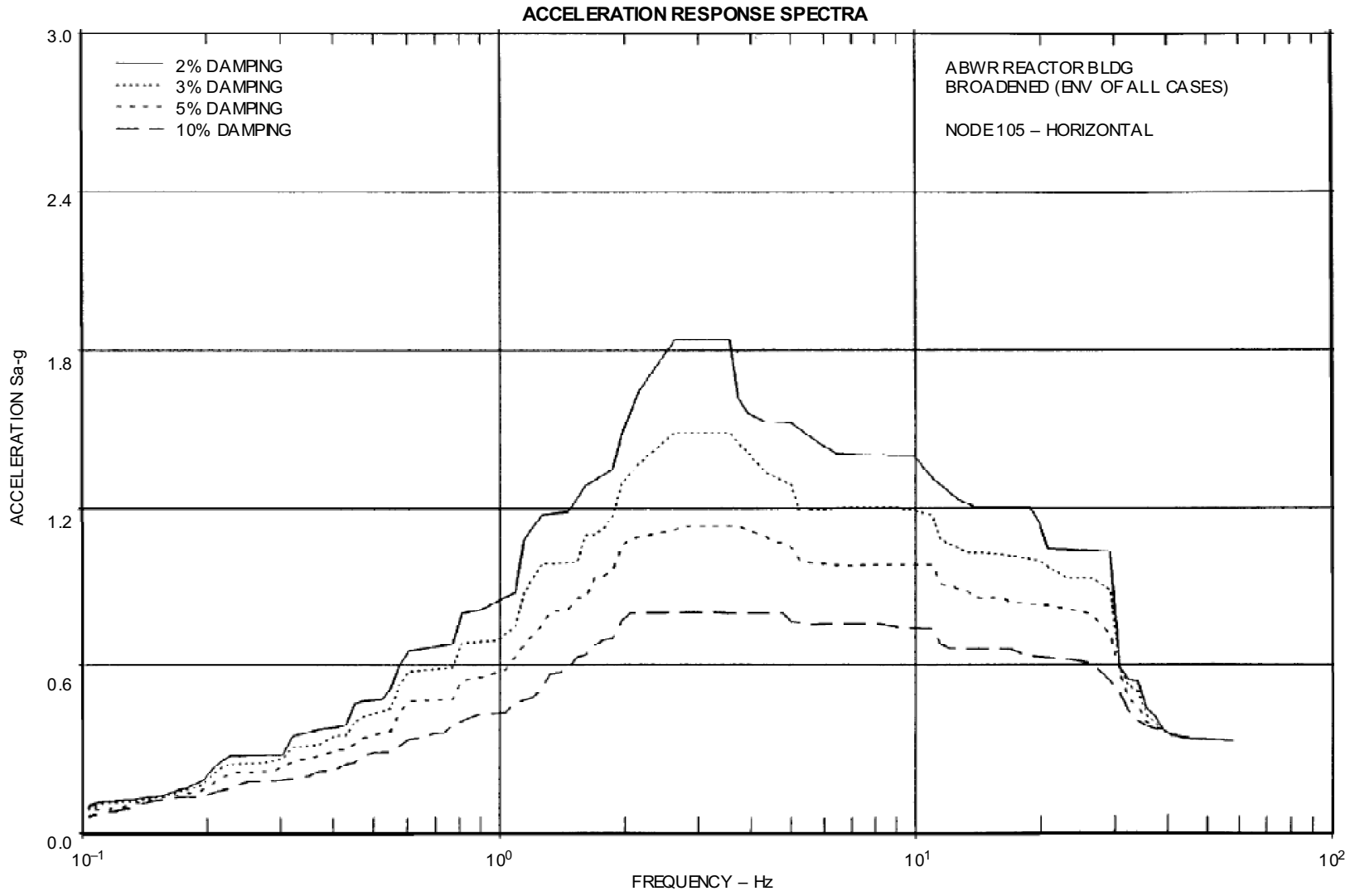

Figure 3A-165 ABWR Reactor Bldg. Broadened (Env of all Cases) Node 105–Horizontal

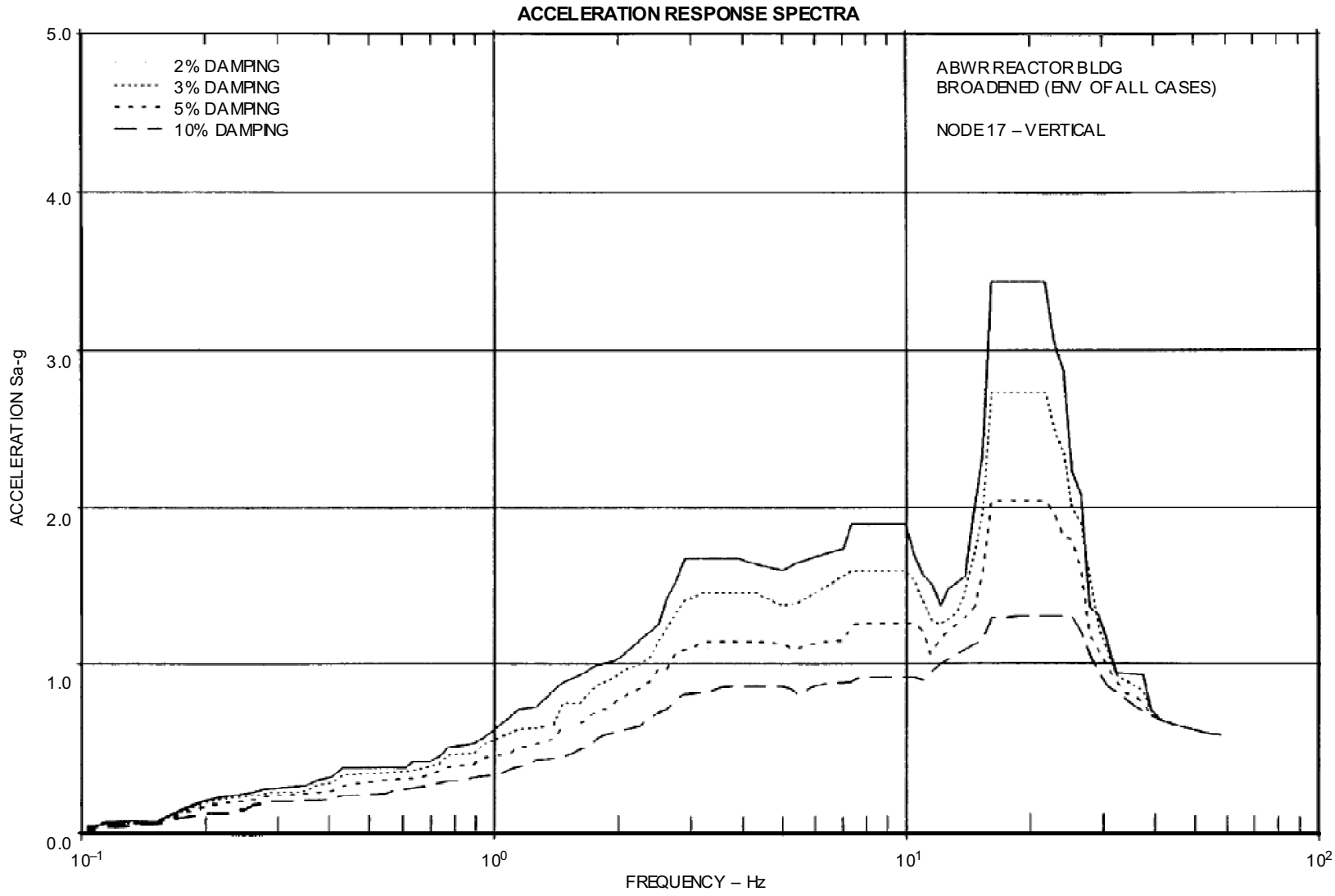

Figure 3A-166 ABWR Reactor Bldg. Broadened (Env of all Cases) Node 17–Vertical

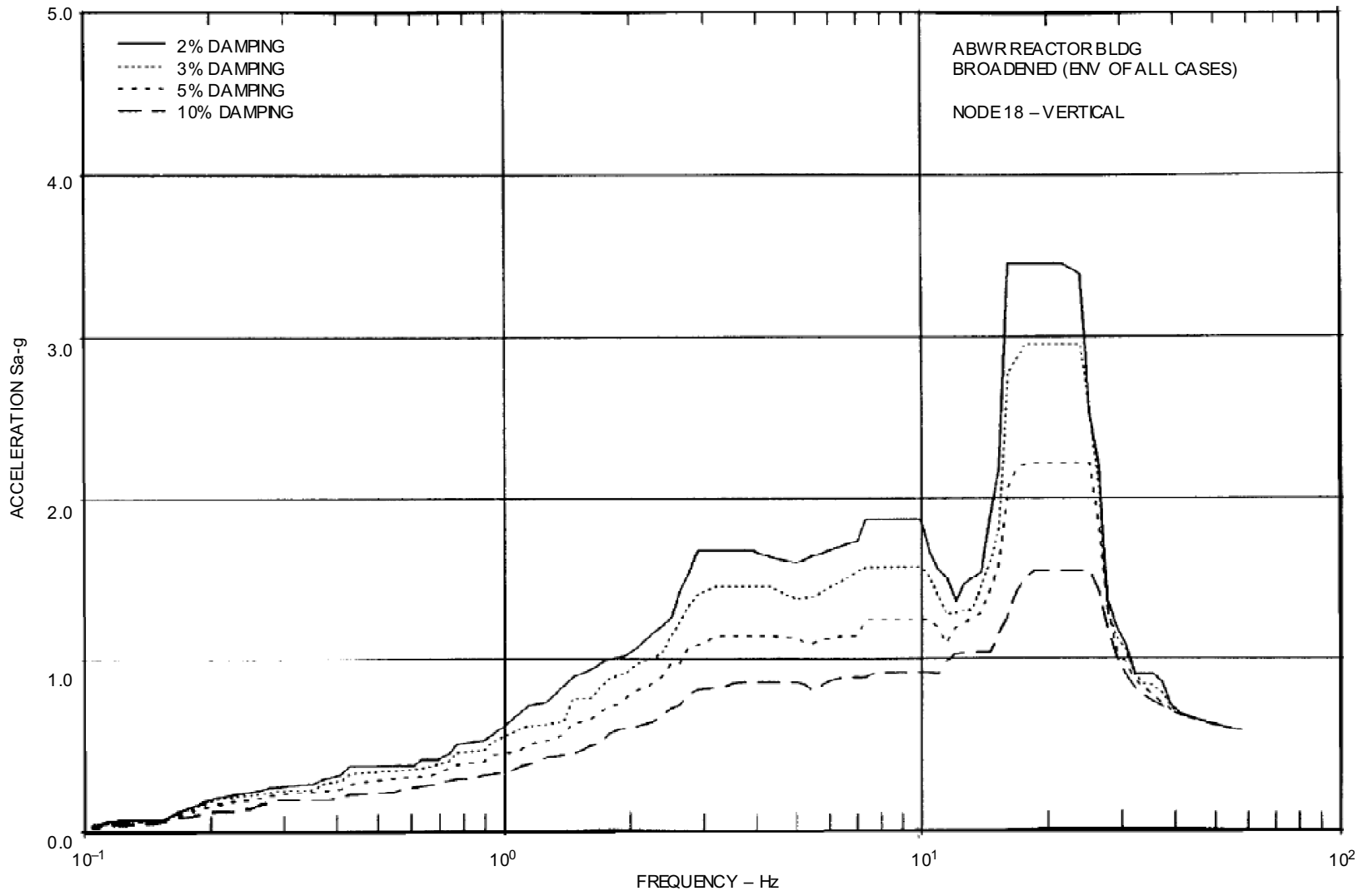

Figure 3A-167 ABWR Reactor Bldg. Broadened (Env of all Cases) Node 18–Vertical

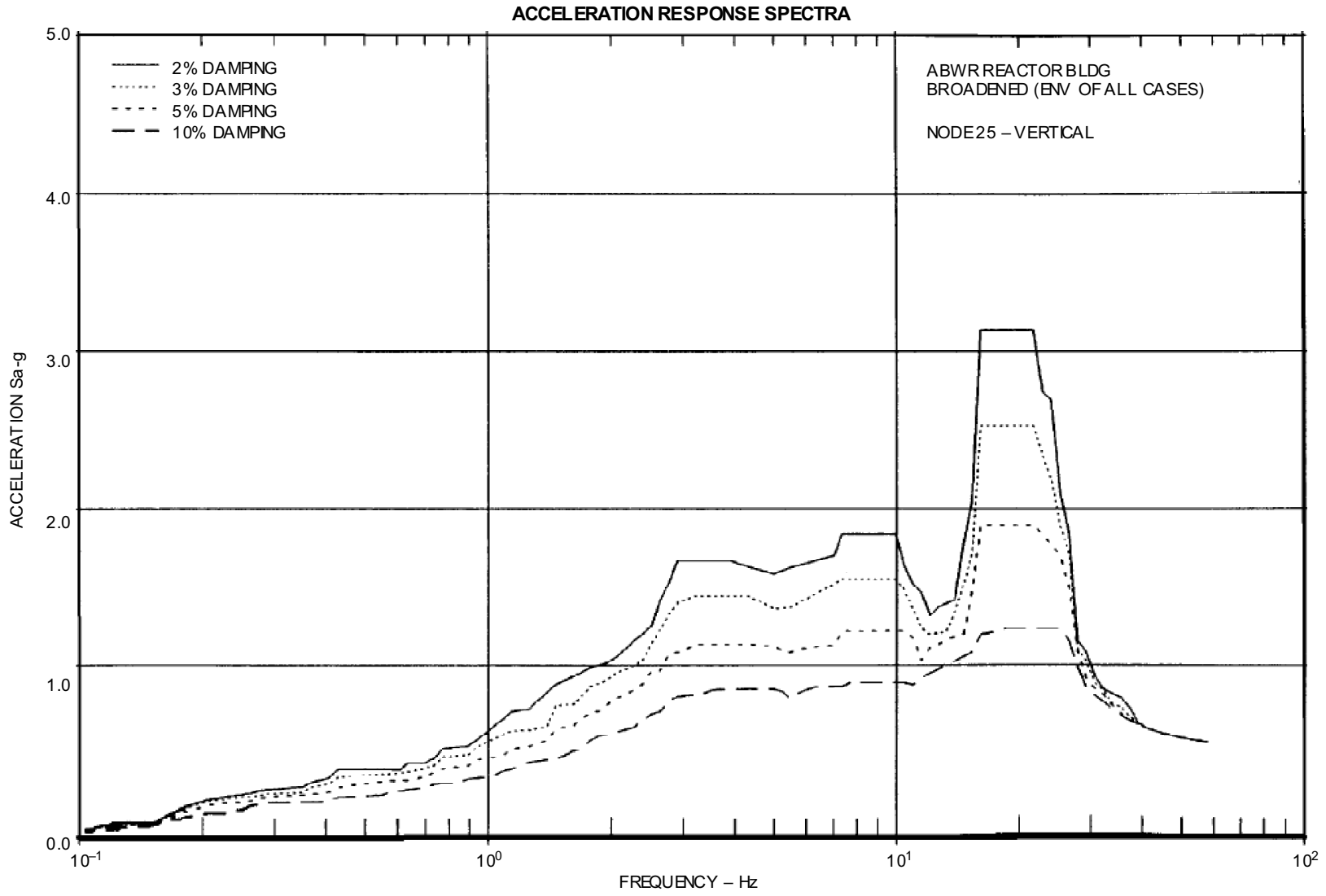

Figure 3A-168 ABWR Reactor Bldg. Broadened (Env of all Cases) Node 25–Vertical

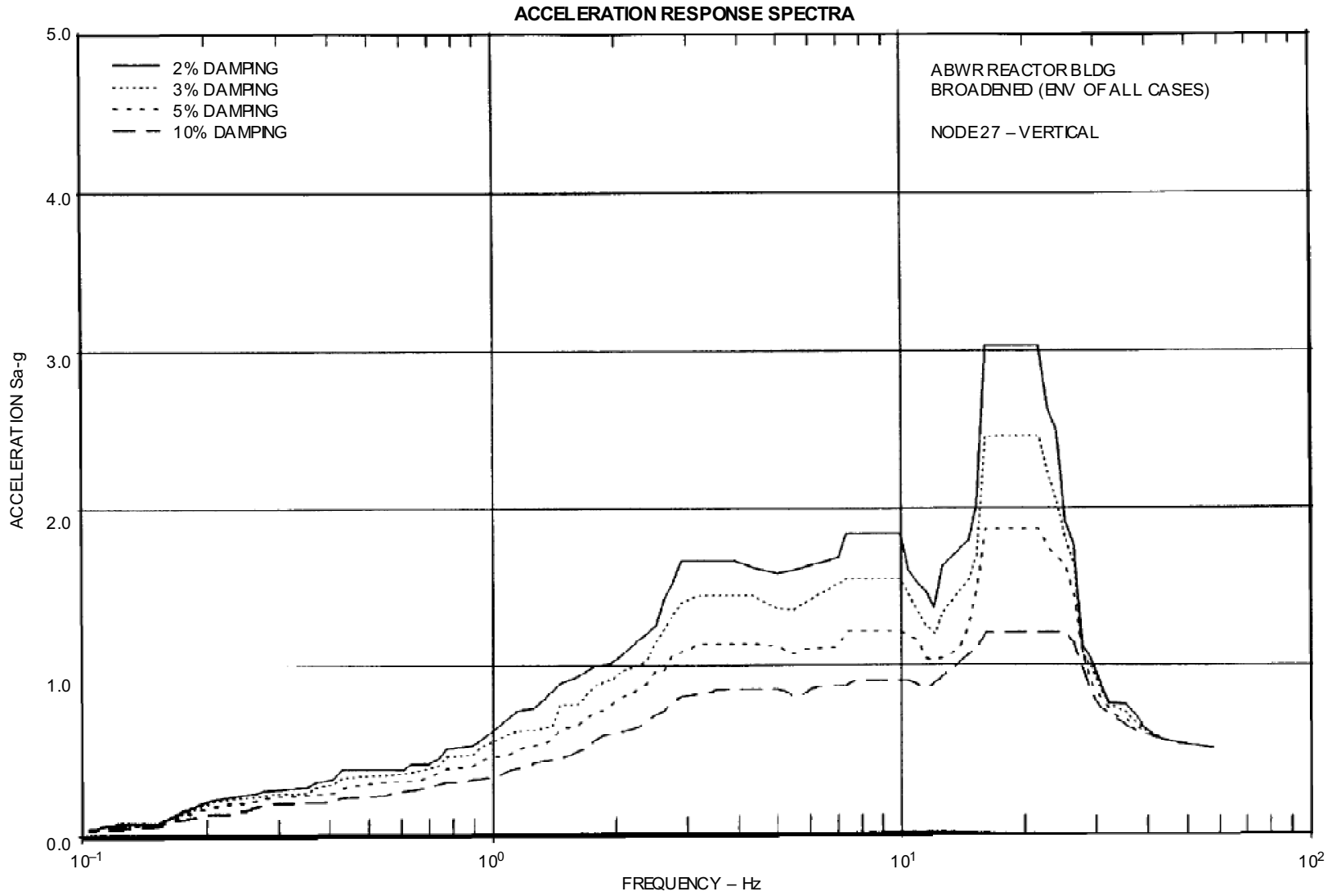

Figure 3A-169 ABWR Reactor Bldg. Broadened (Env of all Cases) Node 27–Vertical

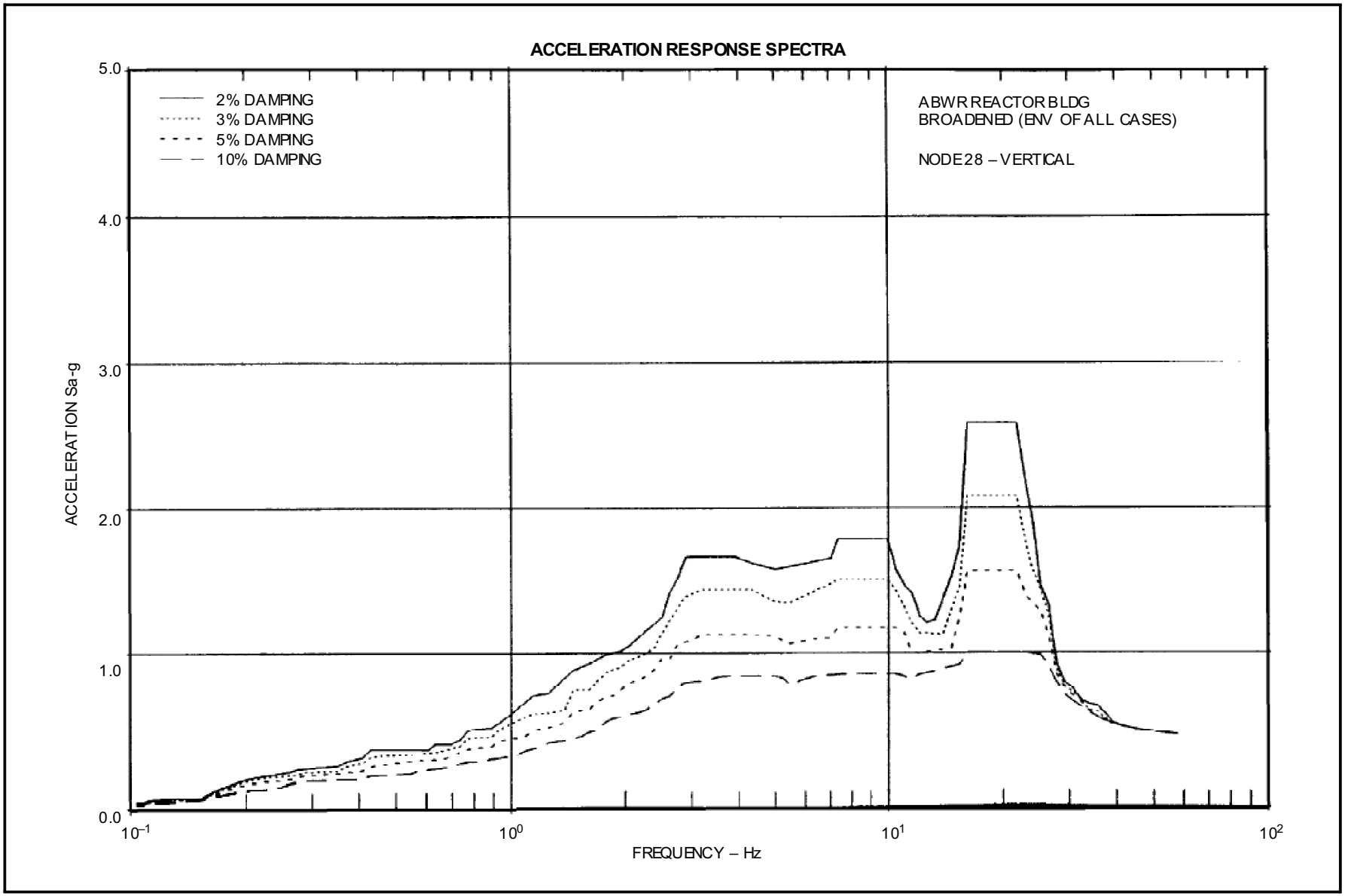

Figure 3A-170 ABWR Reactor Bldg. Broadened (Env of all Cases) Node 28–Vertical

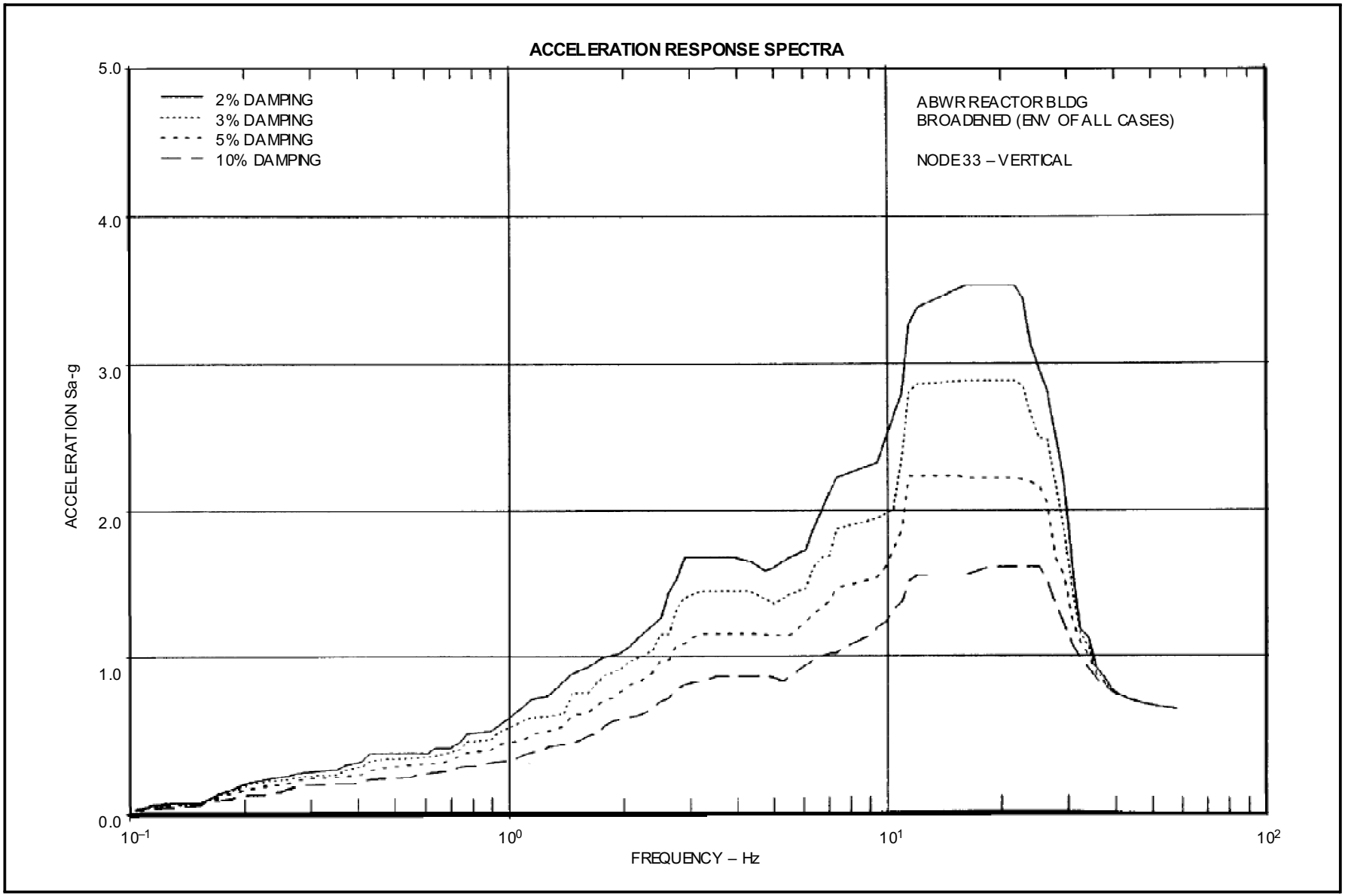

Figure 3A-171 ABWR Reactor Bldg. Broadened (Env of all Cases) Node 33–Vertical

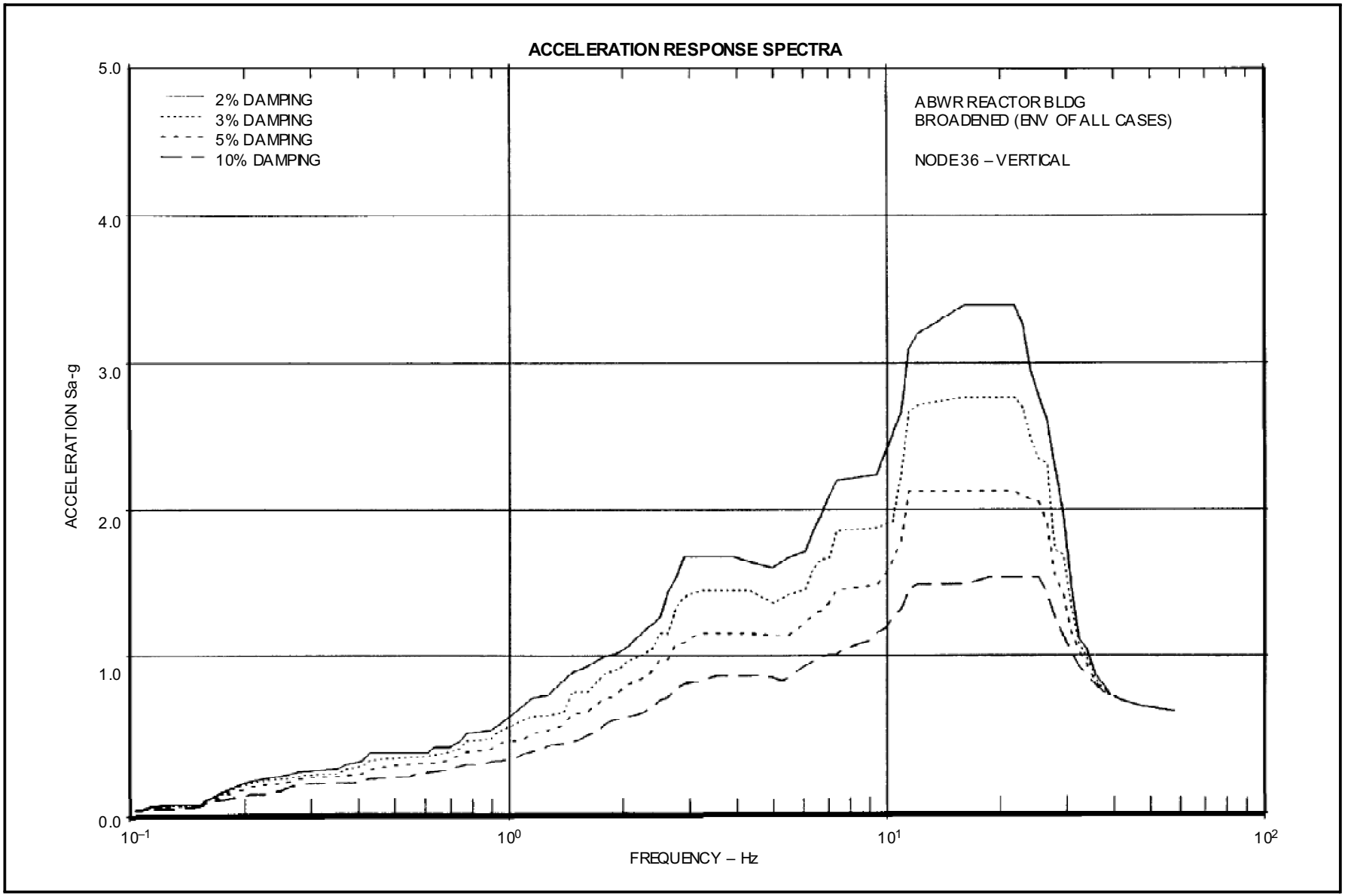

Figure 3A-172 ABWR Reactor Bldg. Broadened (Env of all Cases) Node 36–Vertical

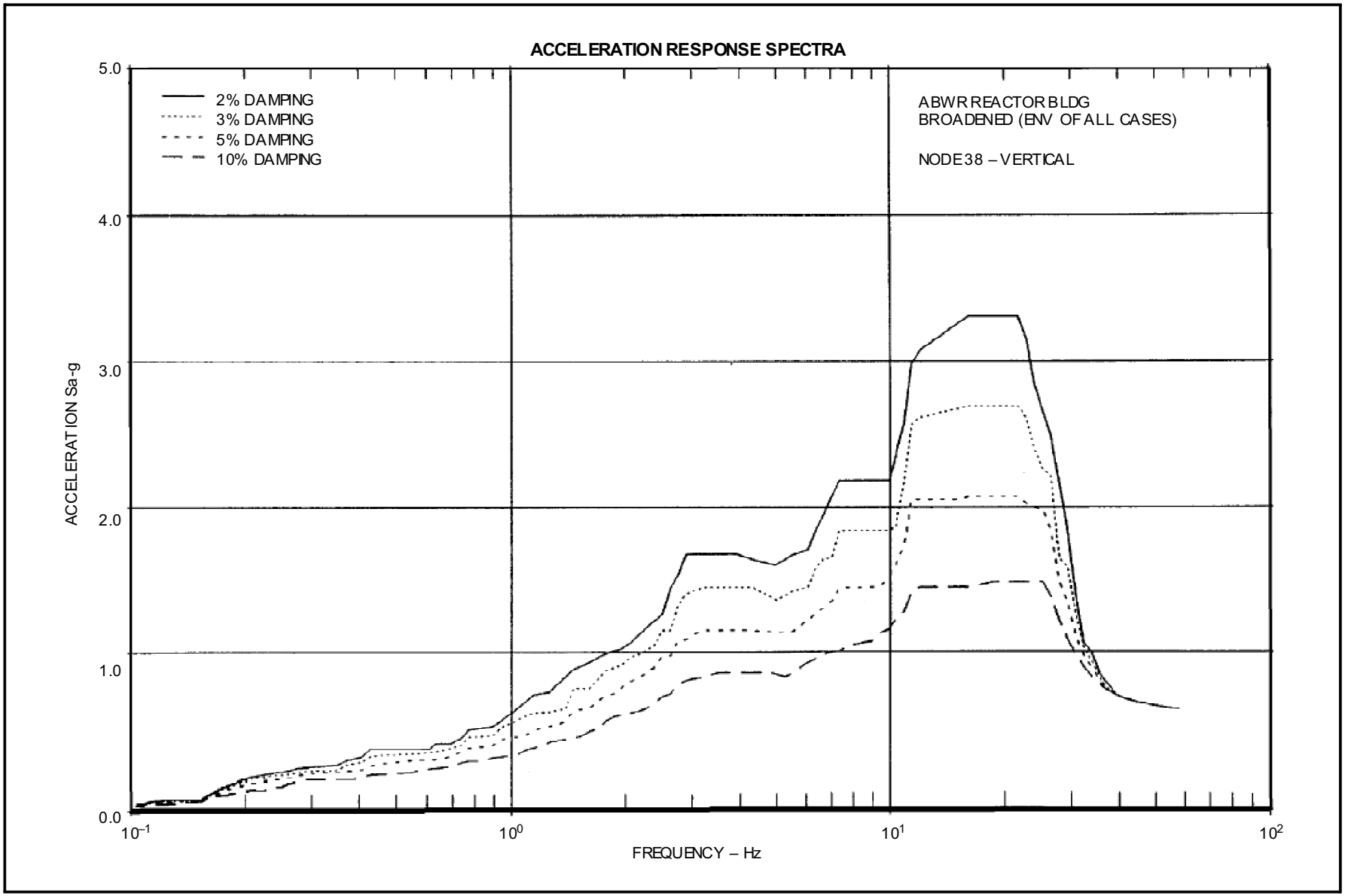

Figure 3A-173 ABWR Reactor Bldg. Broadened (Env of all Cases) Node 38–Vertical

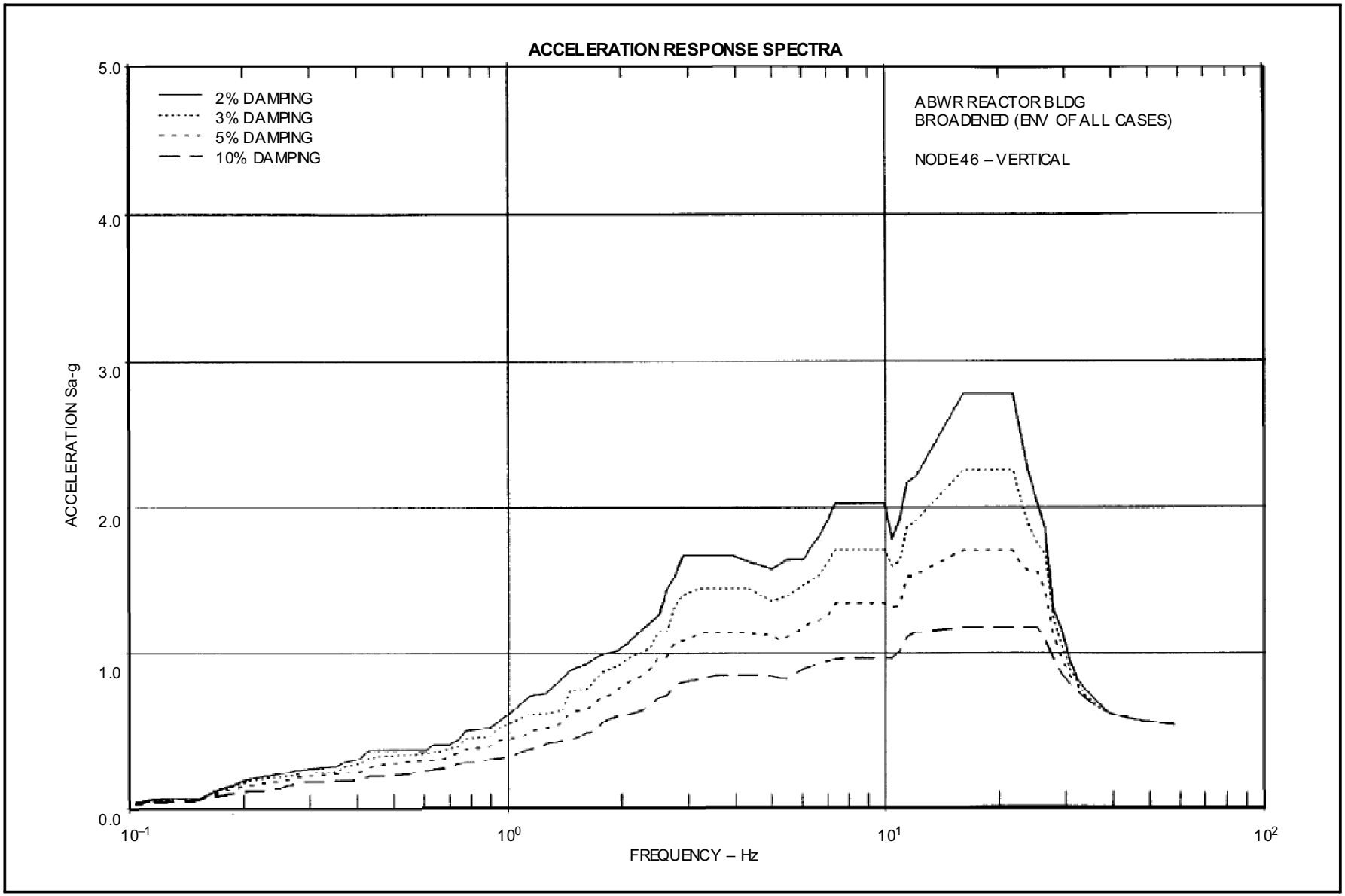

Figure 3A-174 ABWR Reactor Bldg. Broadened (Env of all Cases) Node 46–Vertical

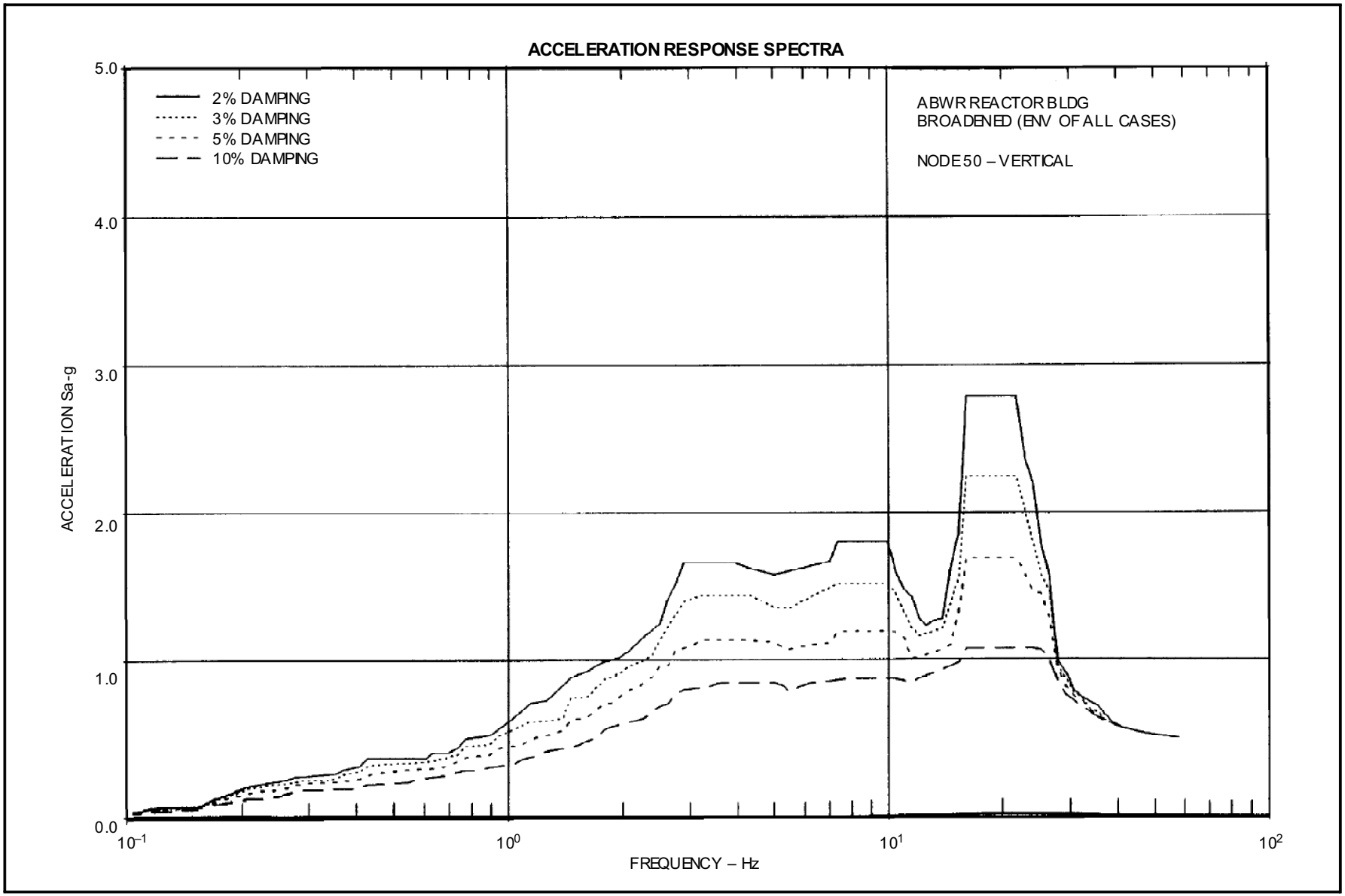

Figure 3A-175 ABWR Reactor Bldg. Broadened (Env of all Cases) Node 50–Vertical

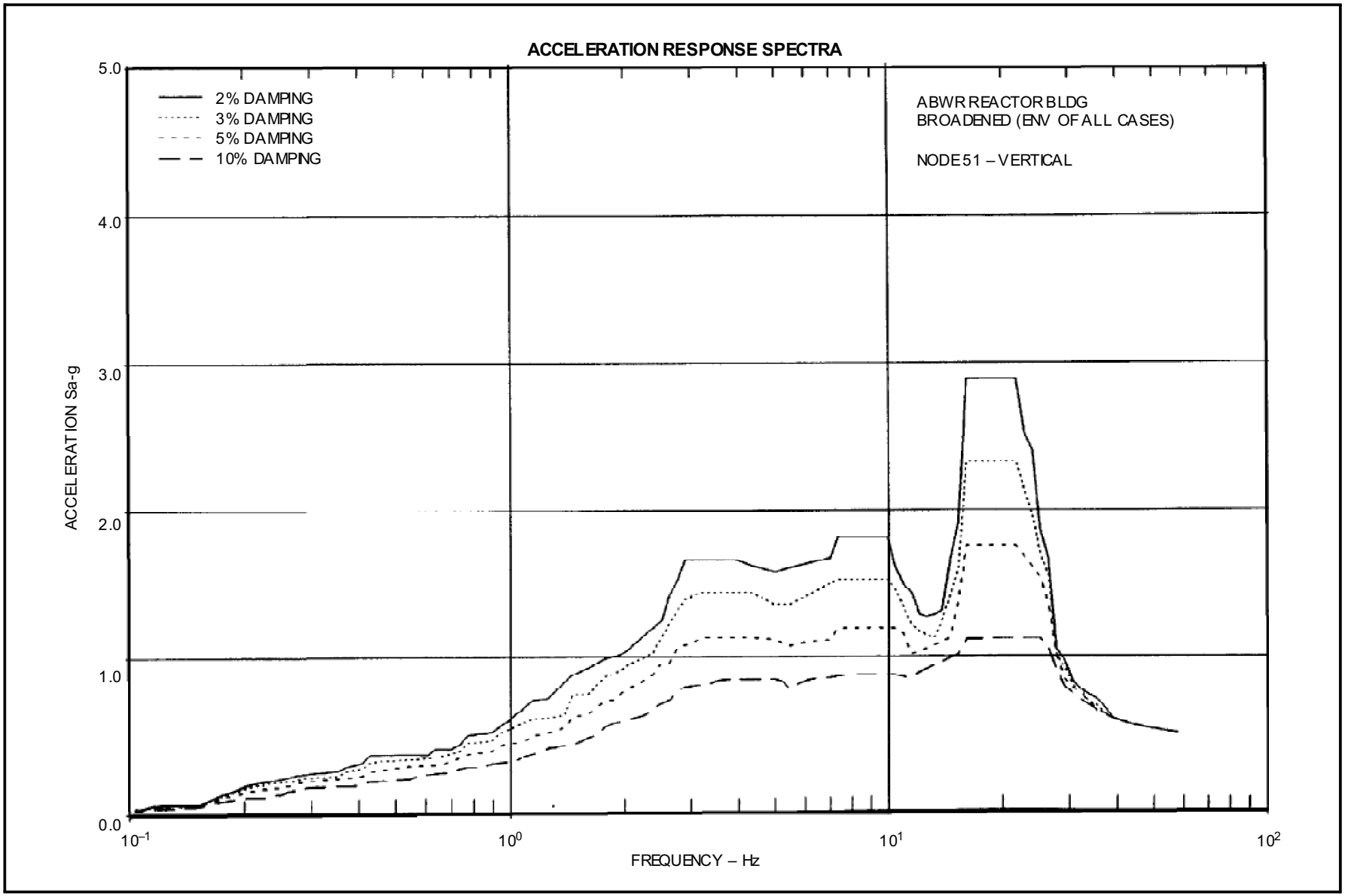

Figure 3A-176 ABWR Reactor Bldg. Broadened (Env of all Cases) Node 51–Vertical

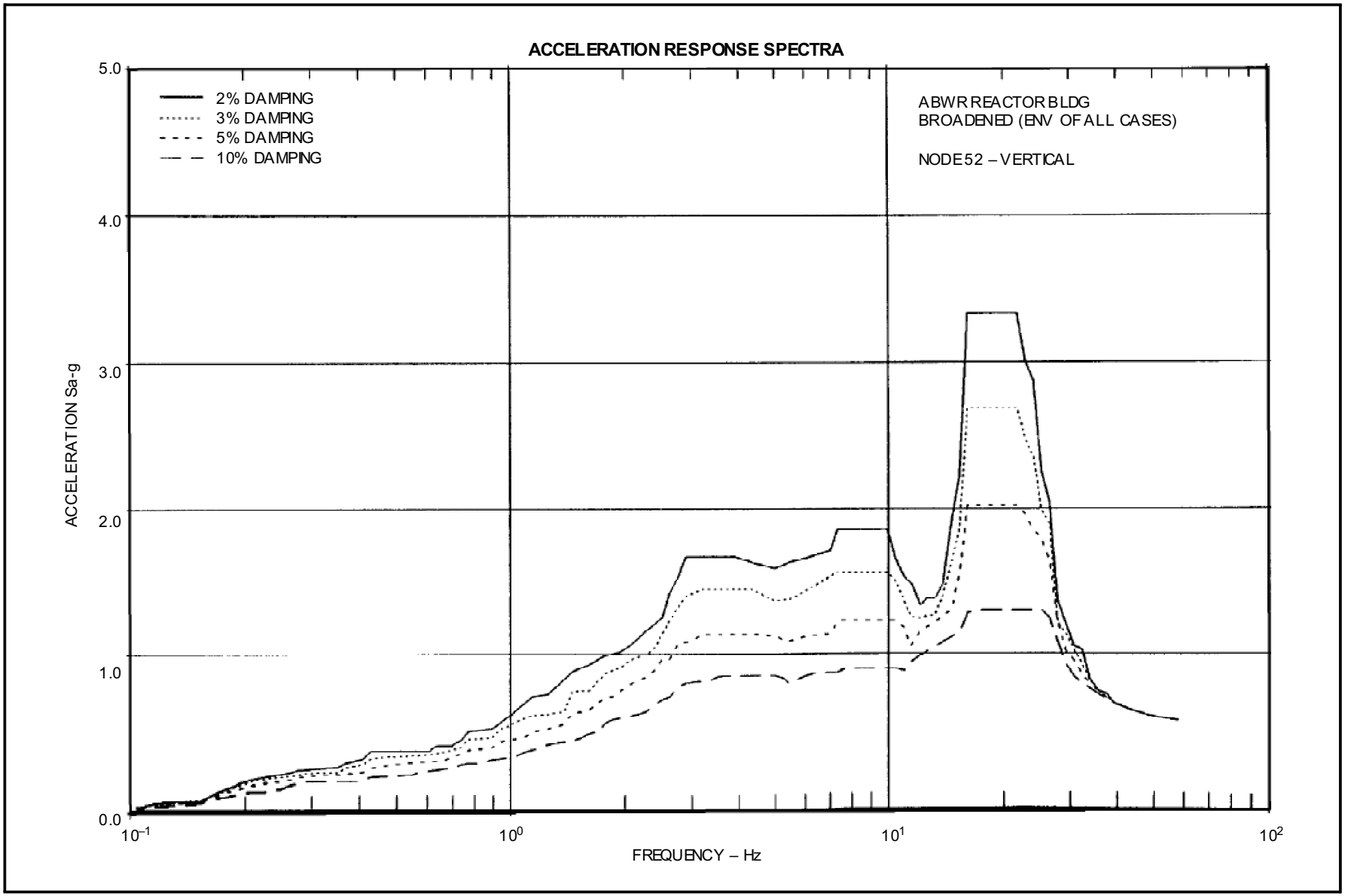

Figure 3A-177 ABWR Reactor Bldg. Broadened (Env of all Cases) Node 52–Vertical

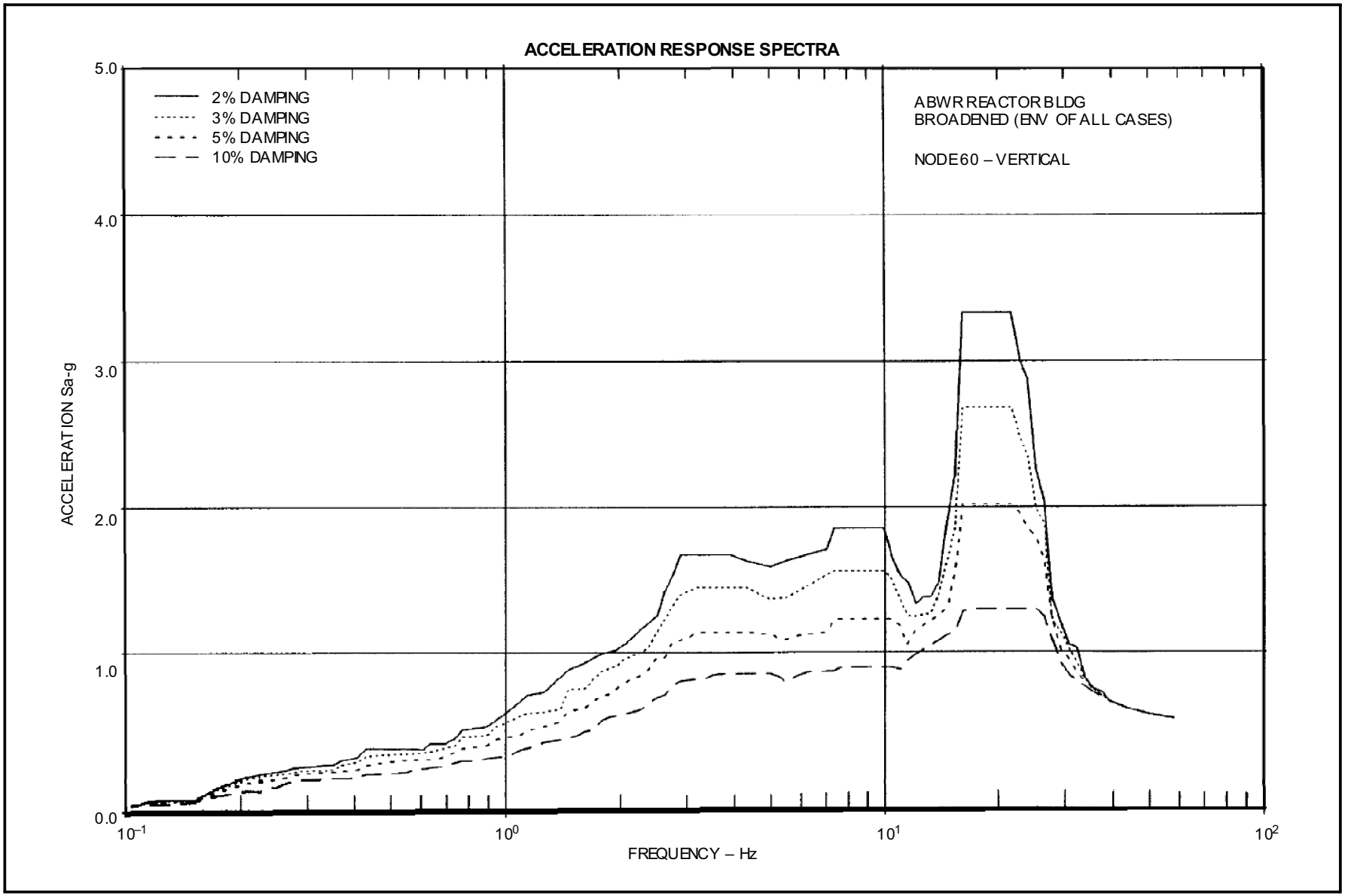

Figure 3A-178 ABWR Reactor Bldg. Broadened (Env of all Cases) Node 60–Vertical

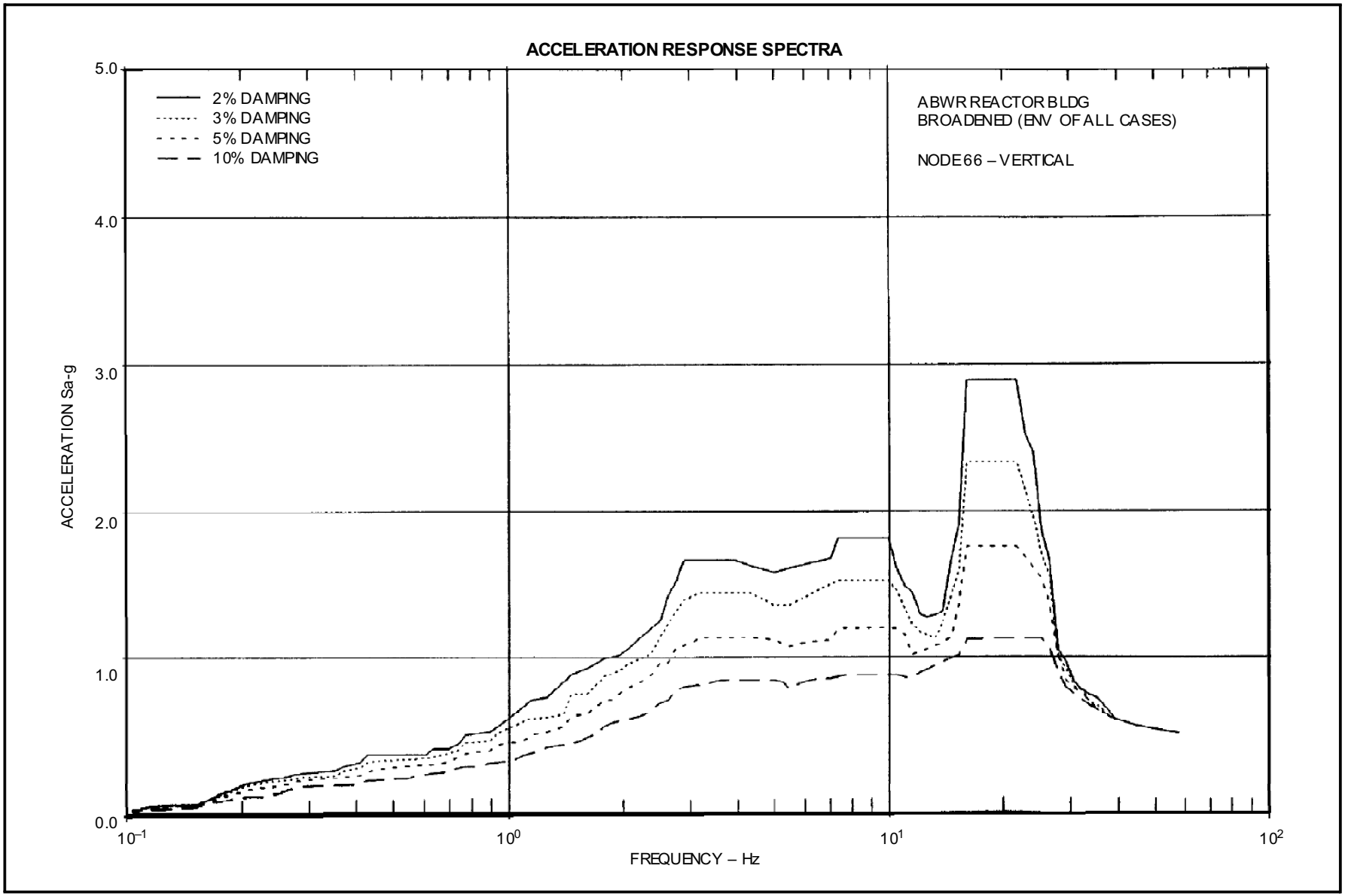

Figure 3A-179 ABWR Reactor Bldg. Broadened (Env of all Cases) Node 66–Vertical

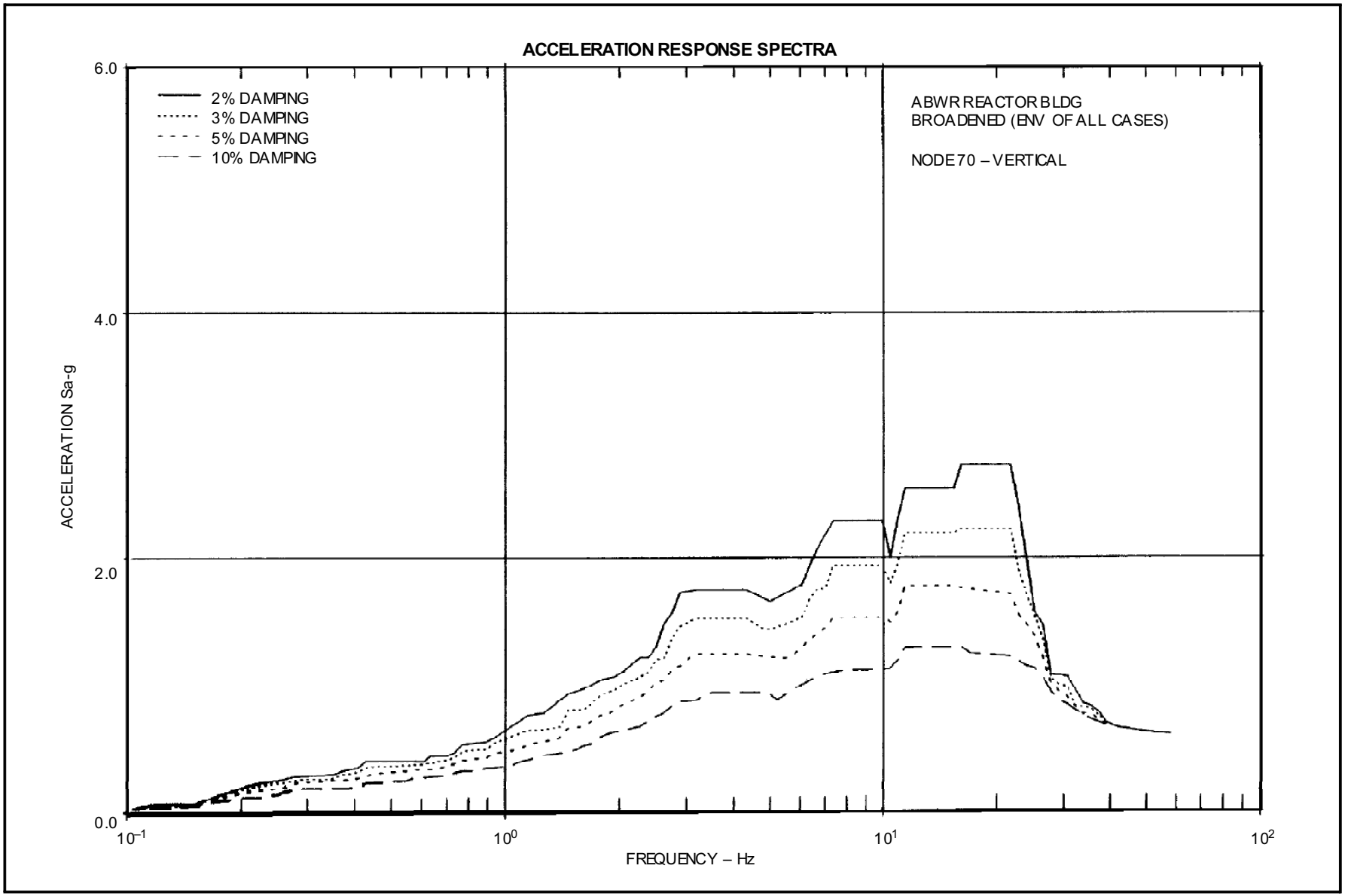

Figure 3A-180 ABWR Reactor Bldg. Broadened (Env of all Cases) Node 70–Vertical

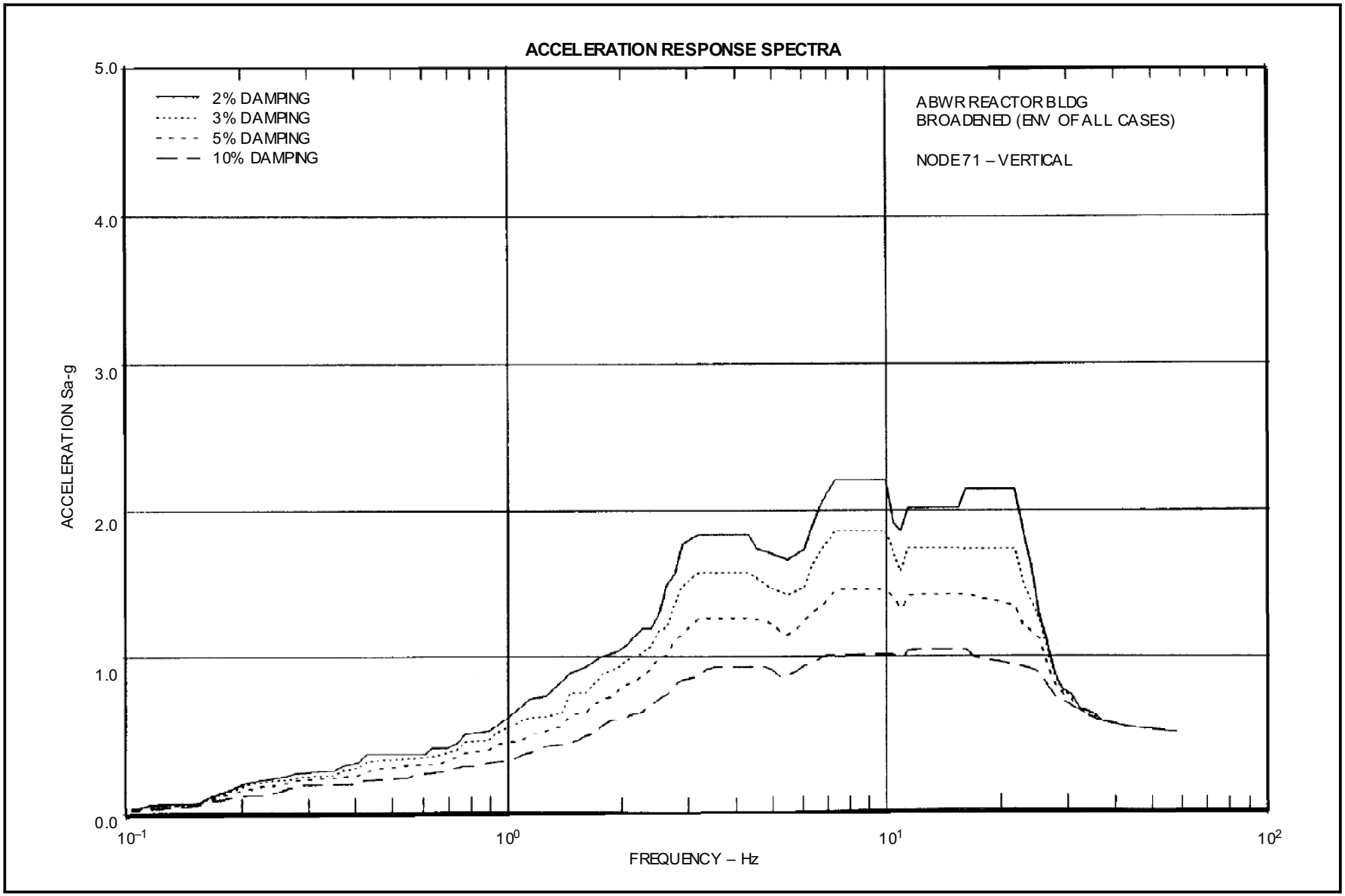

Figure 3A-181 ABWR Reactor Bldg. Broadened (Env of all Cases) Node 71–Vertical

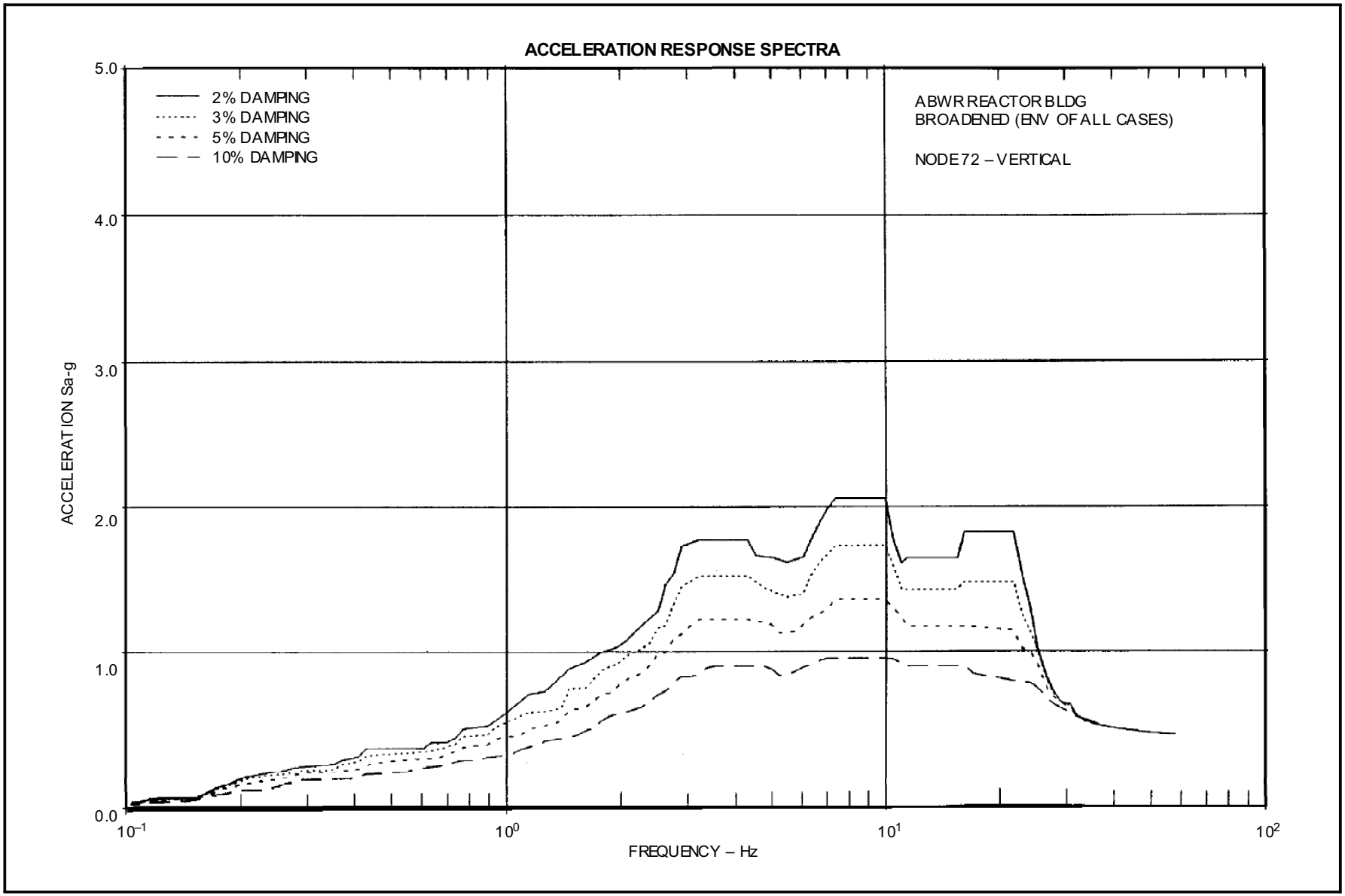

Figure 3A-182 ABWR Reactor Bldg. Broadened (Env of all Cases) Node 72–Vertical

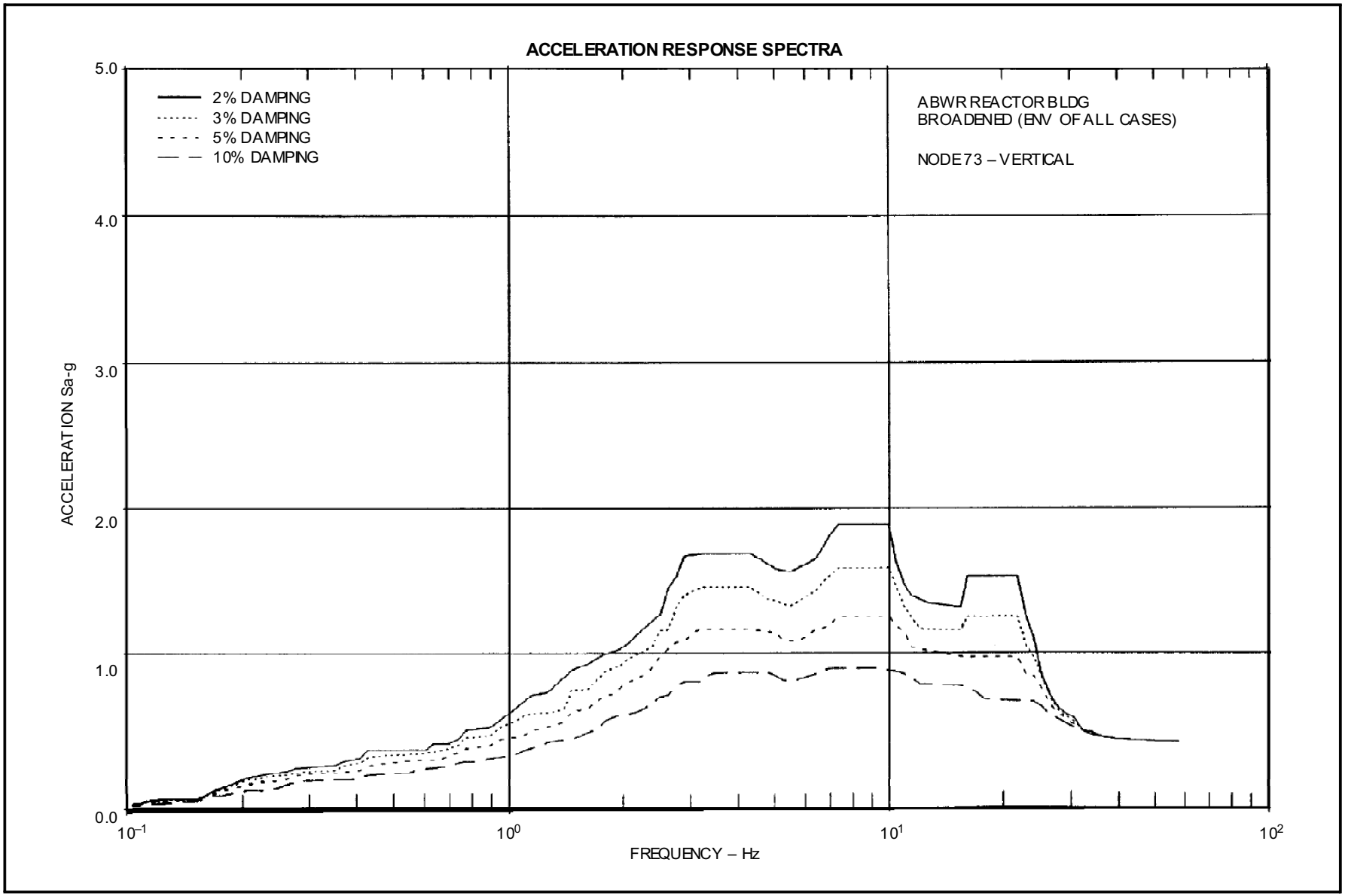

Figure 3A-183 ABWR Reactor Bldg. Broadened (Env of all Cases) Node 73–Vertical

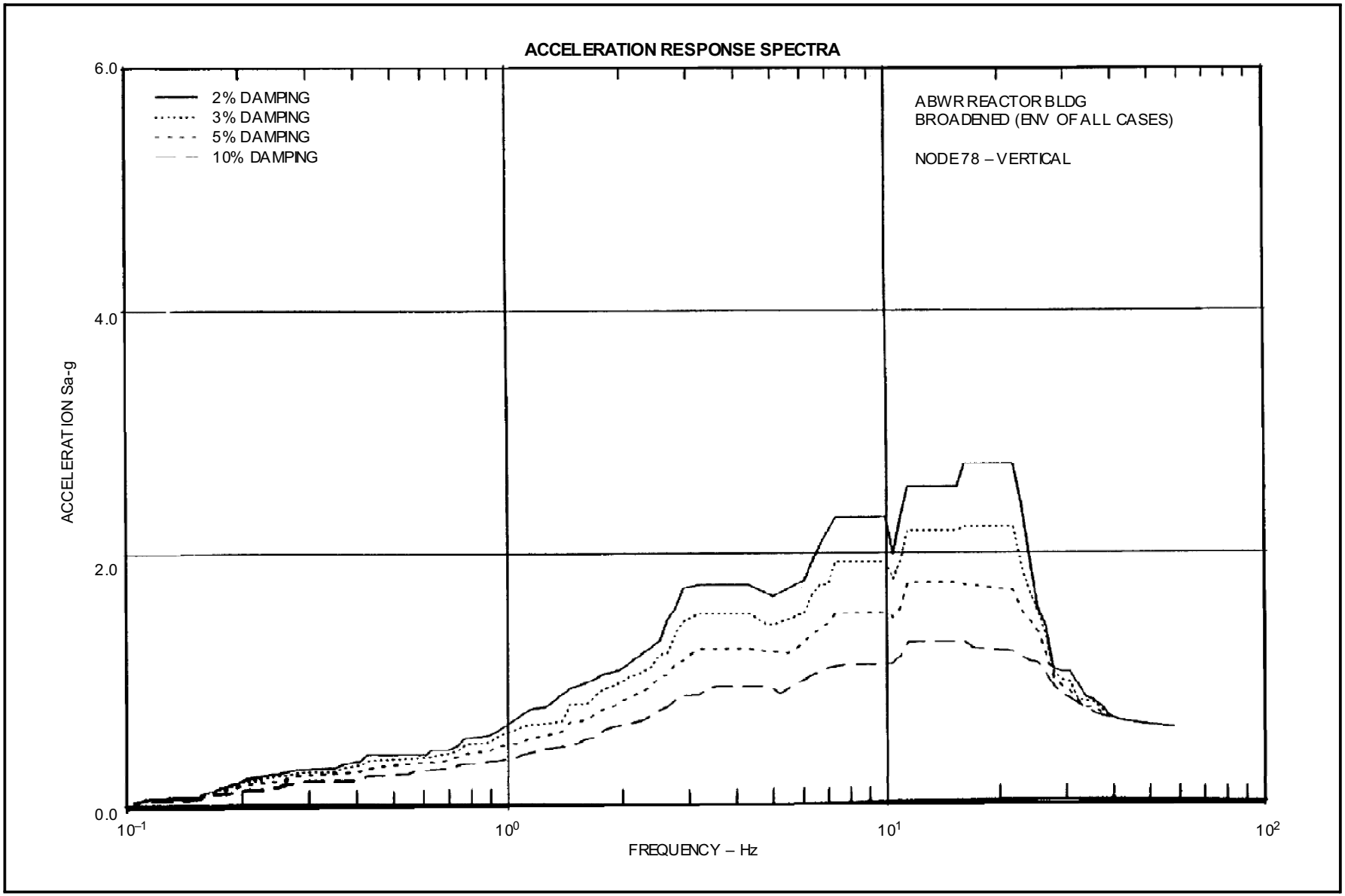

Figure 3A-184 ABWR Reactor Bldg. Broadened (Env of all Cases) Node 78–Vertical

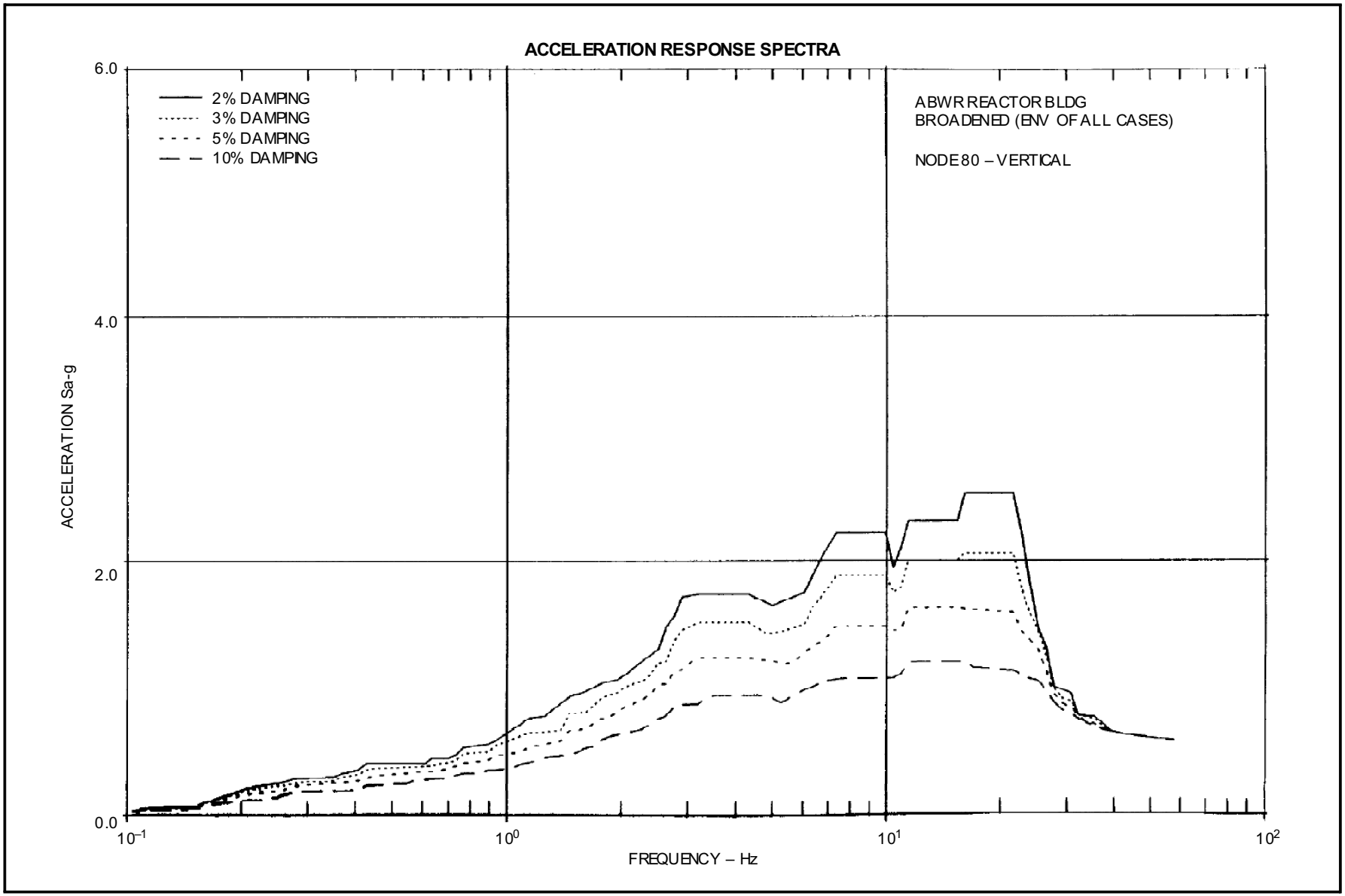

Figure 3A-185 ABWR Reactor Bldg. Broadened (Env of all Cases) Node 80–Vertical

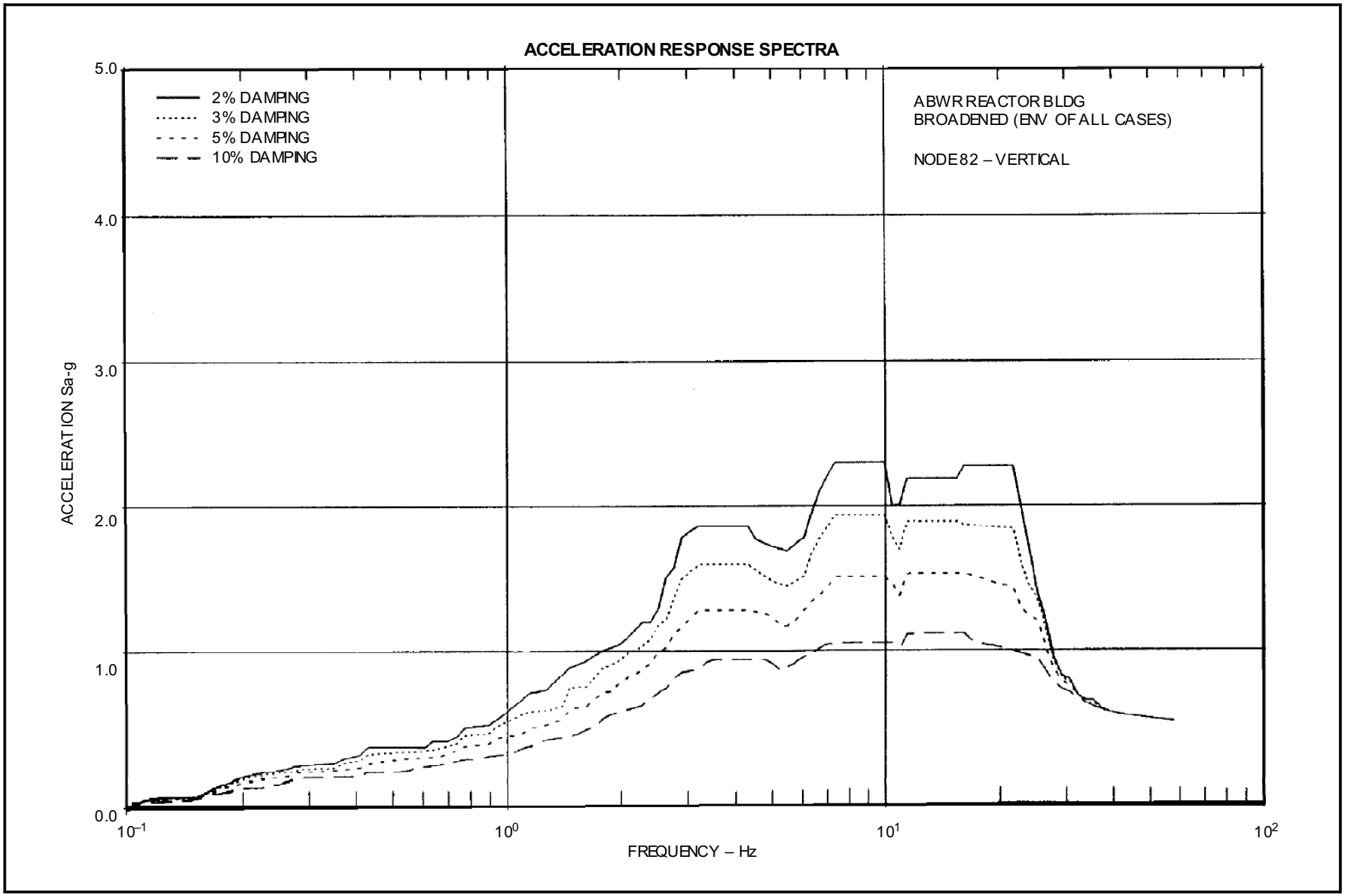

Figure 3A-186 ABWR Reactor Bldg. Broadened (Env of all Cases) Node 82–Vertical

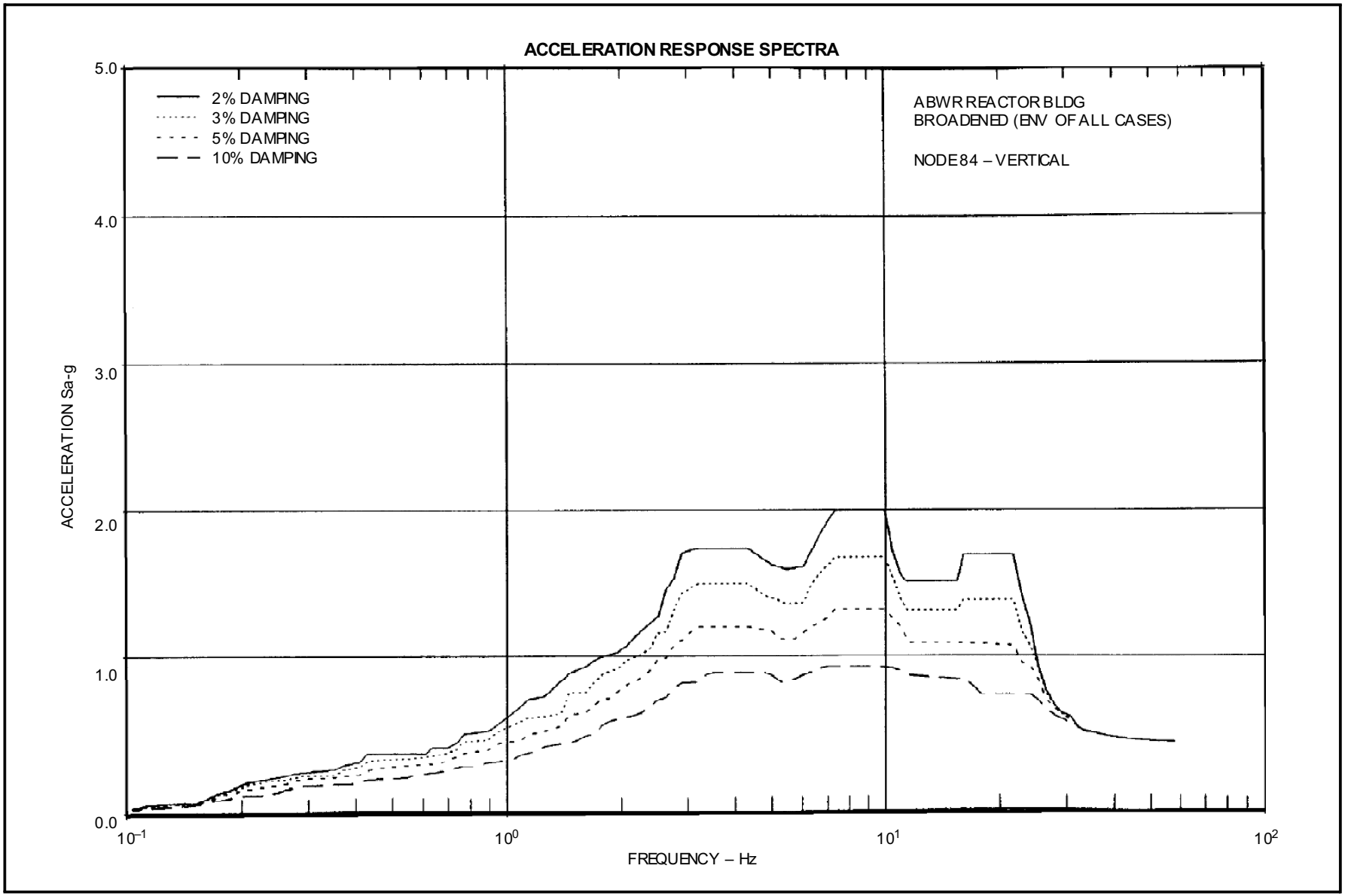

Figure 3A-187 ABWR Reactor Bldg. Broadened (Env of all Cases) Node 84–Vertical

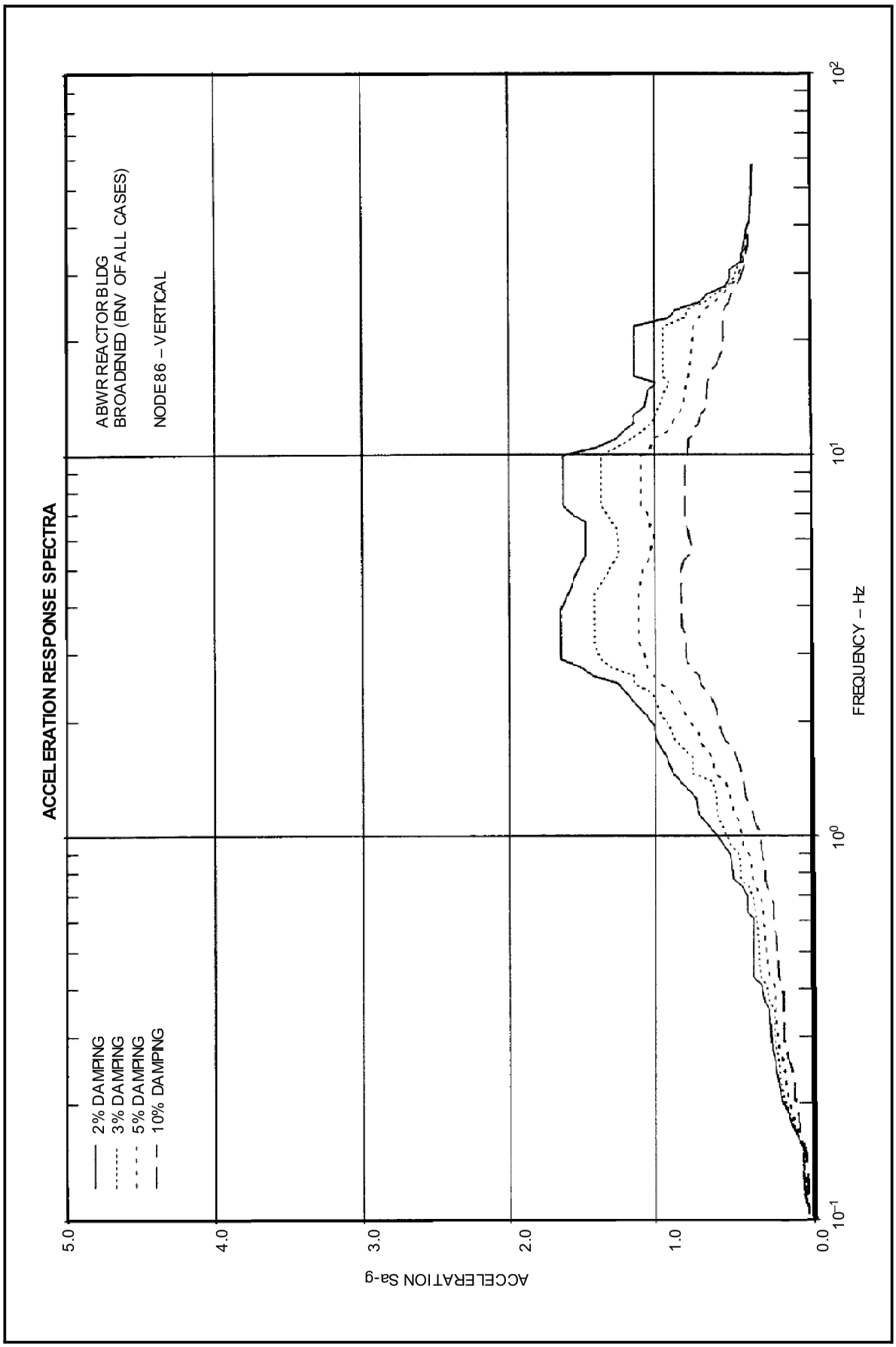

Figure 3A-188 ABWR Reactor Bldg. Broadened (Env of all Cases) Node 86–Vertical

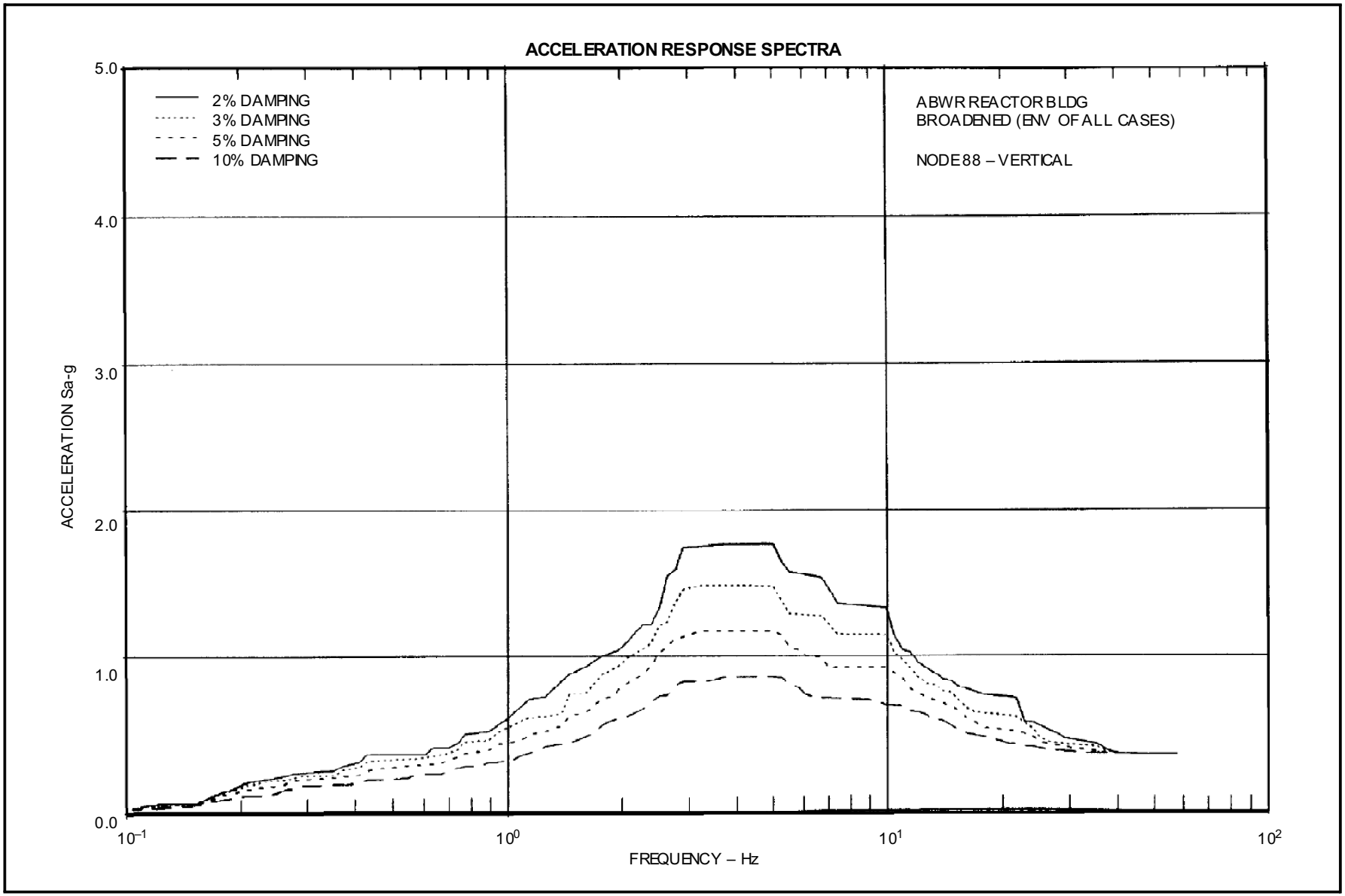

Figure 3A-189 ABWR Reactor Bldg. Broadened (Env of all Cases) Node 88–Vertical

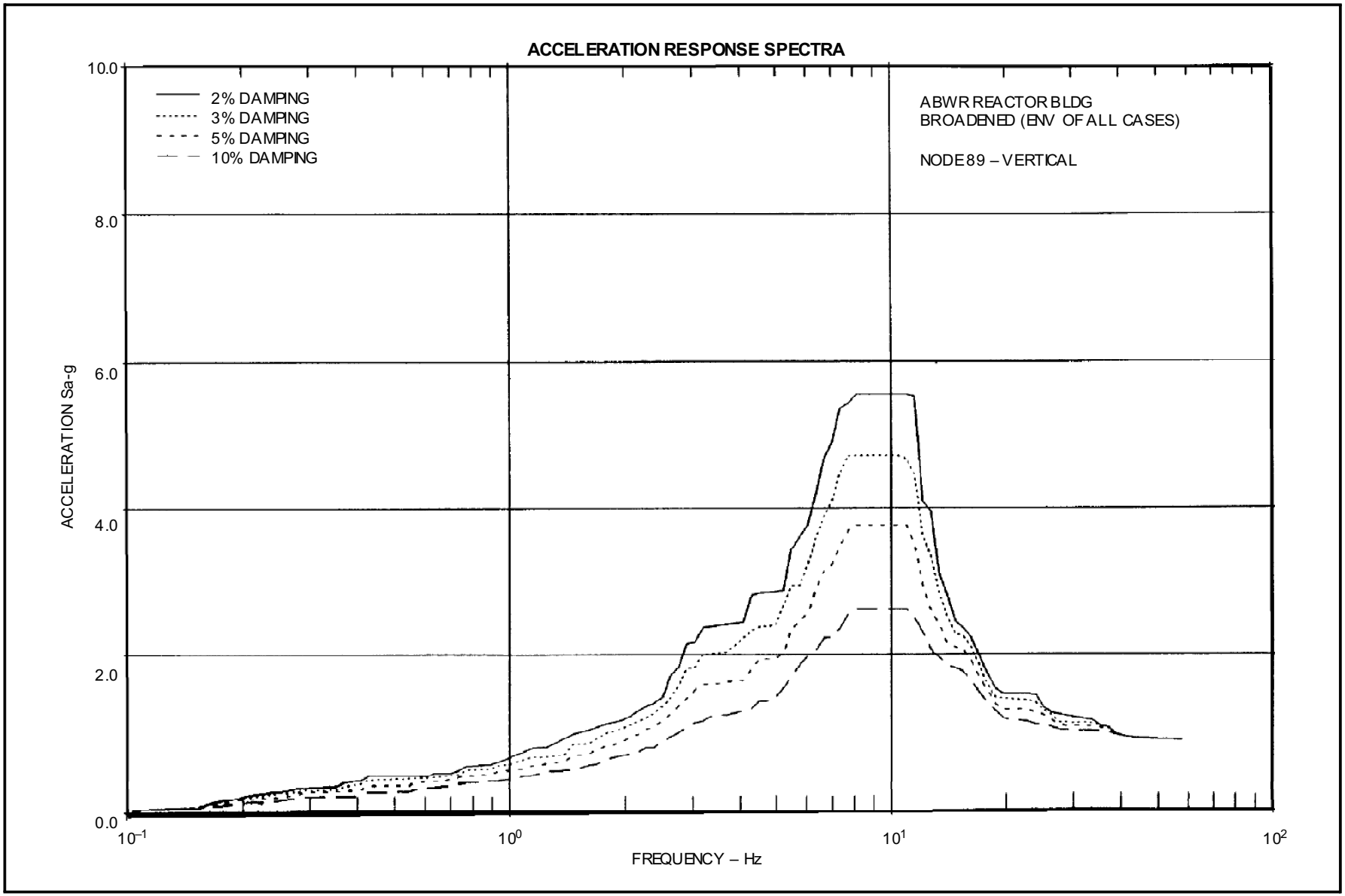

Figure 3A-190 ABWR Reactor Bldg. Broadened (Env of all Cases) Node 89–Vertical

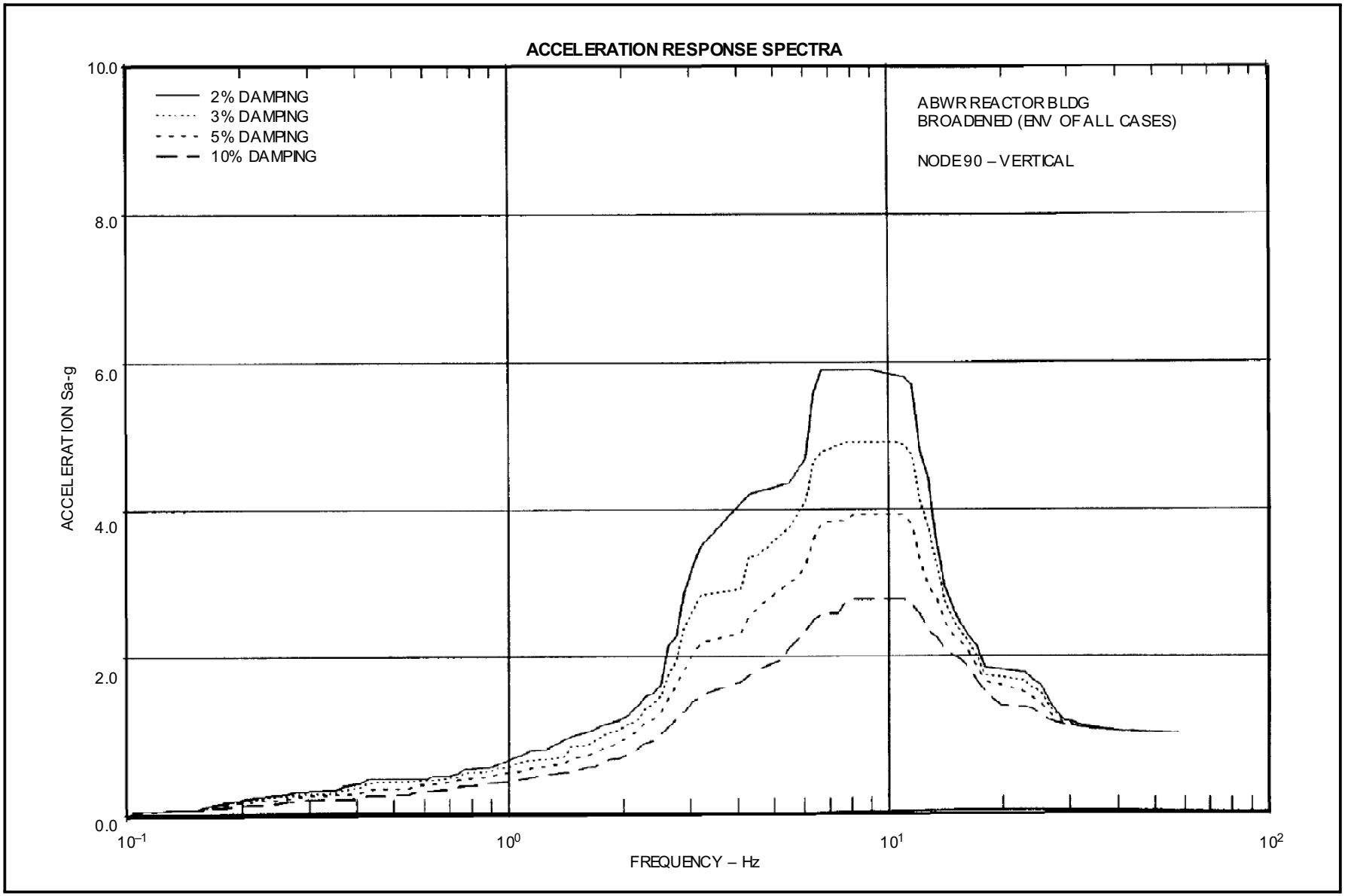

Figure 3A-191 ABWR Reactor Bldg. Broadened (Env of all Cases) Node 90–Vertical

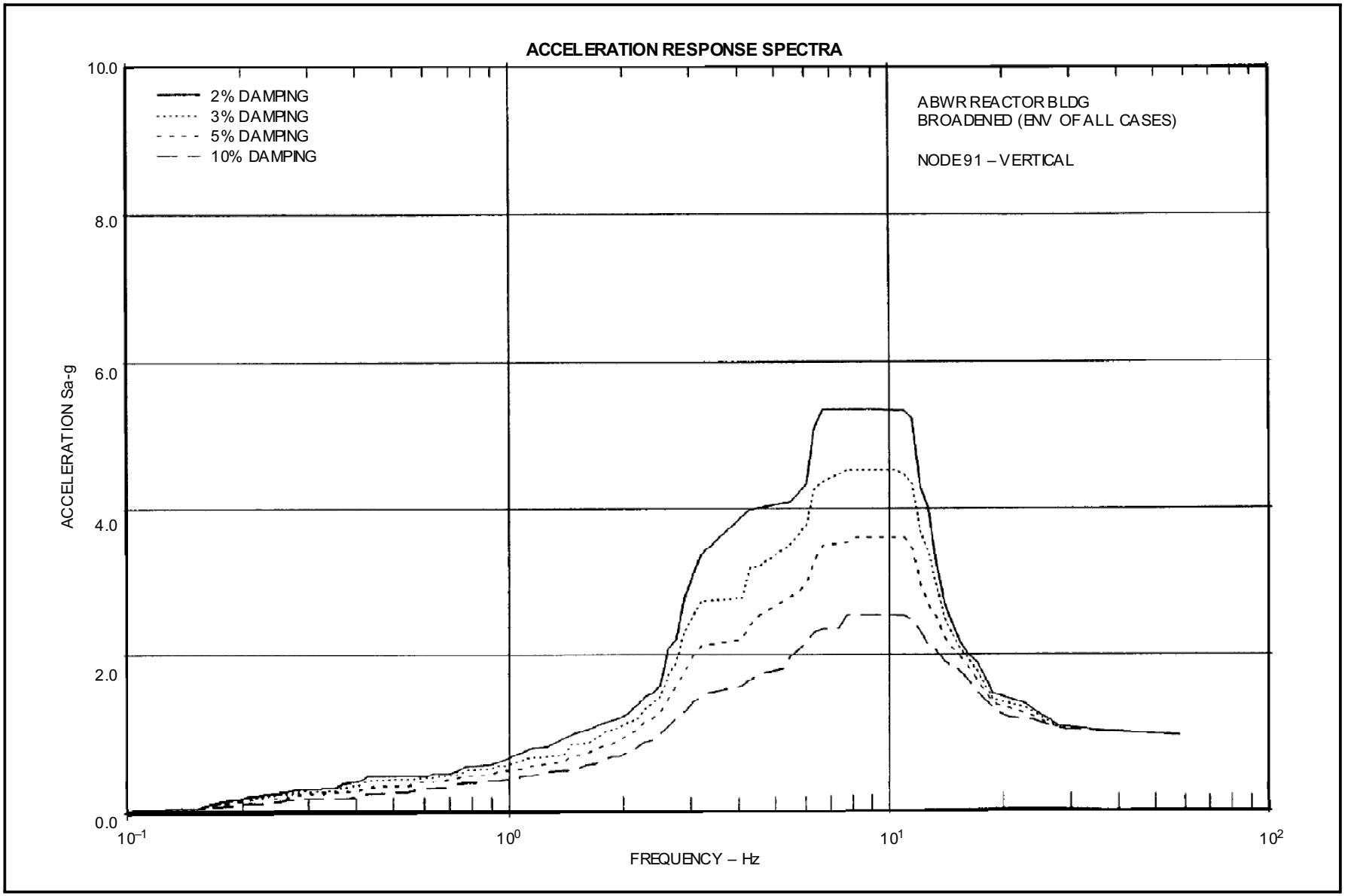

Figure 3A-192 ABWR Reactor Bldg. Broadened (Env of all Cases) Node 91–Vertical

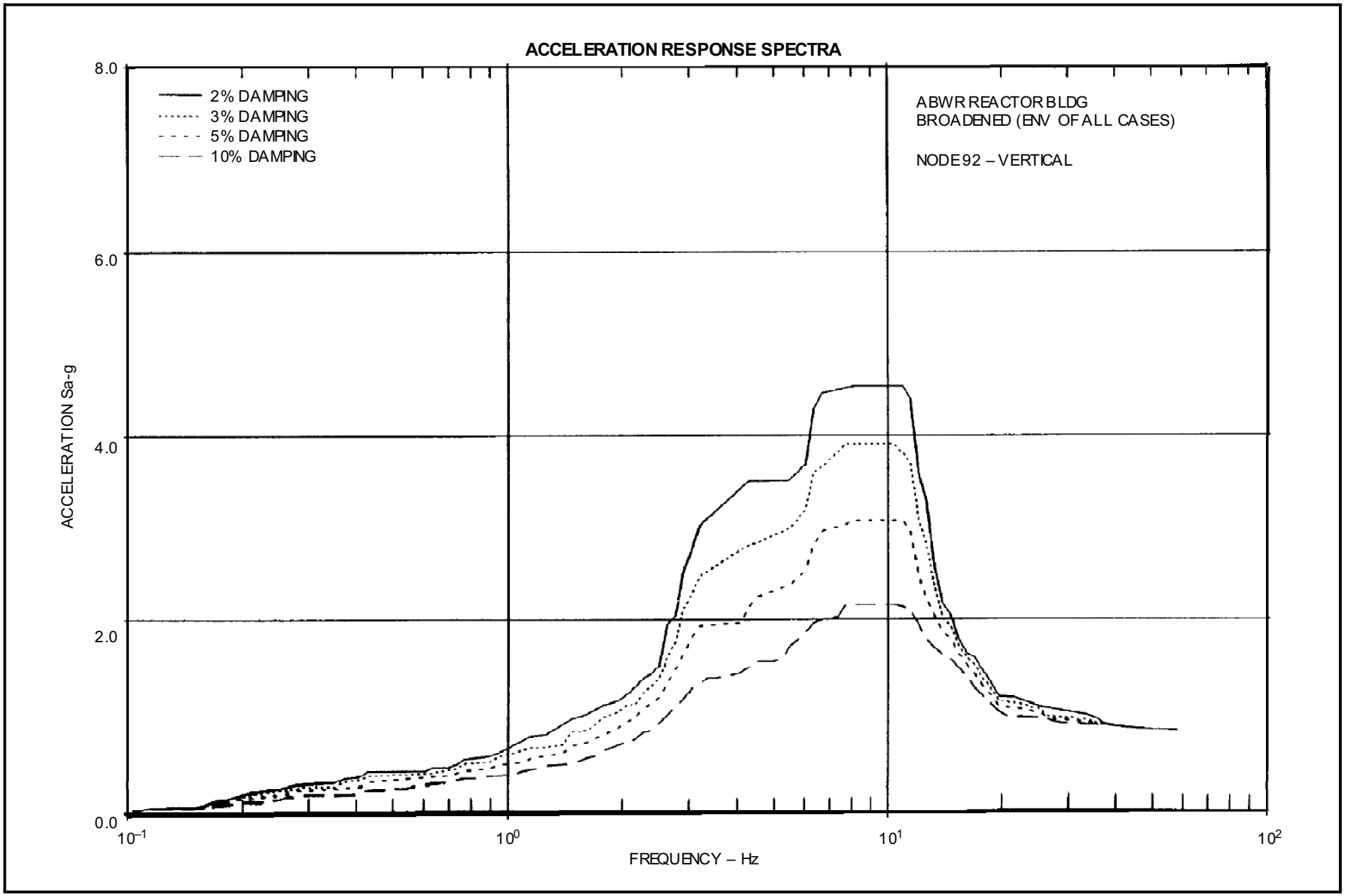

Figure 3A-193 ABWR Reactor Bldg. Broadened (Env of all Cases) Node 92–Vertical

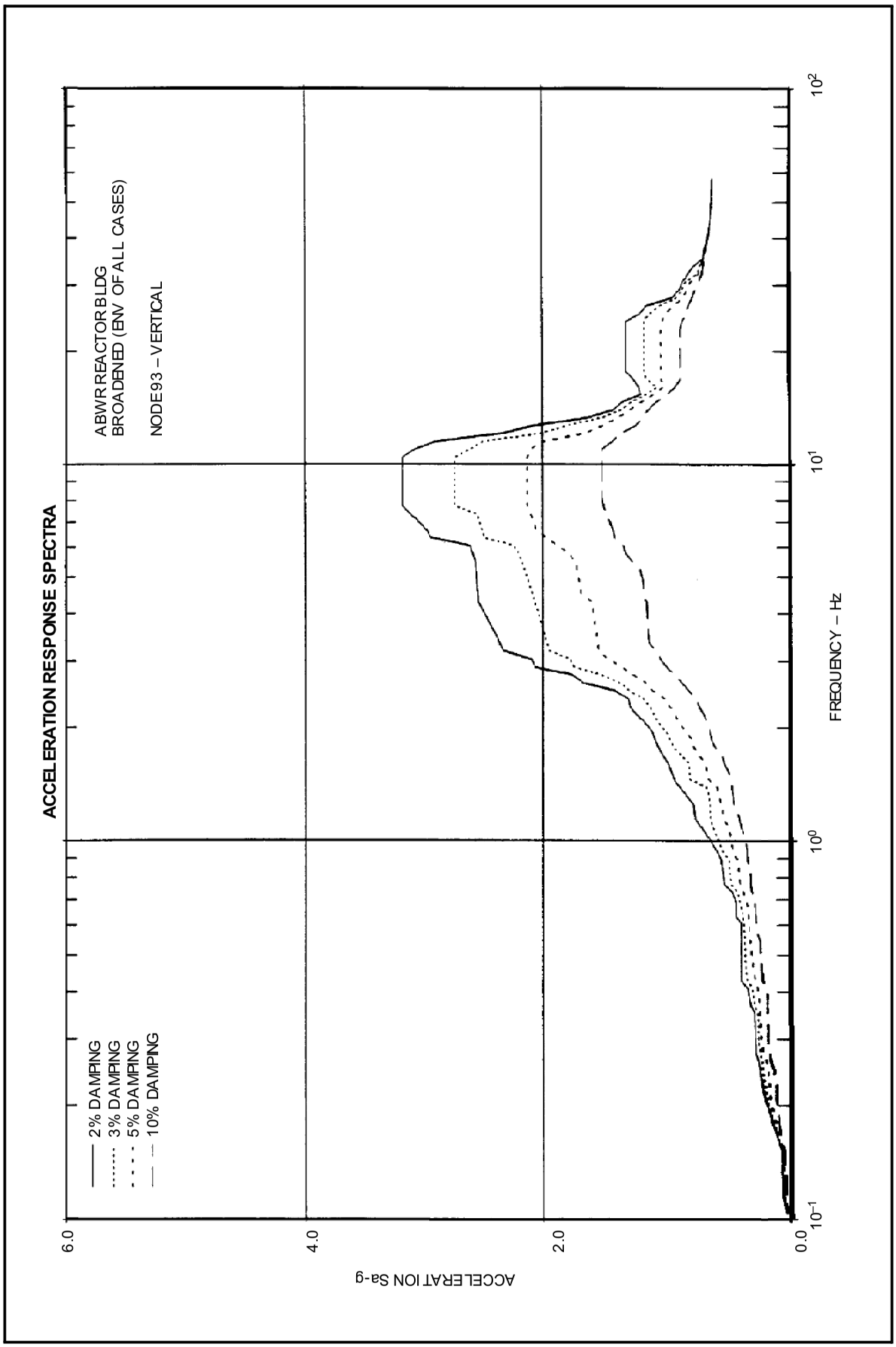

Figure 3A-194 ABWR Reactor Bldg. Broadened (Env of all Cases) Node 93–Vertical

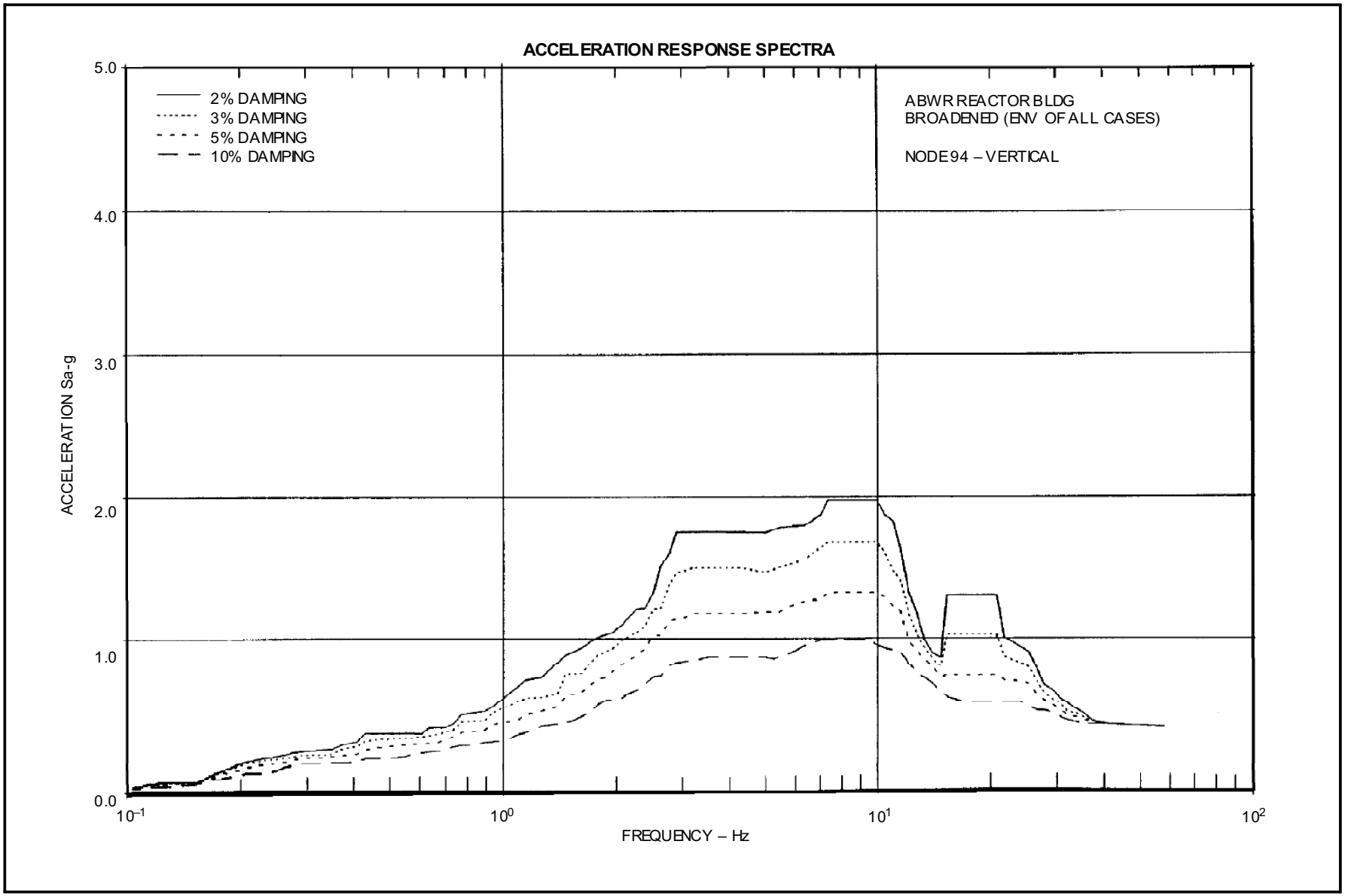

Figure 3A-195 ABWR Reactor Bldg. Broadened (Env of all Cases) Node 94–Vertical

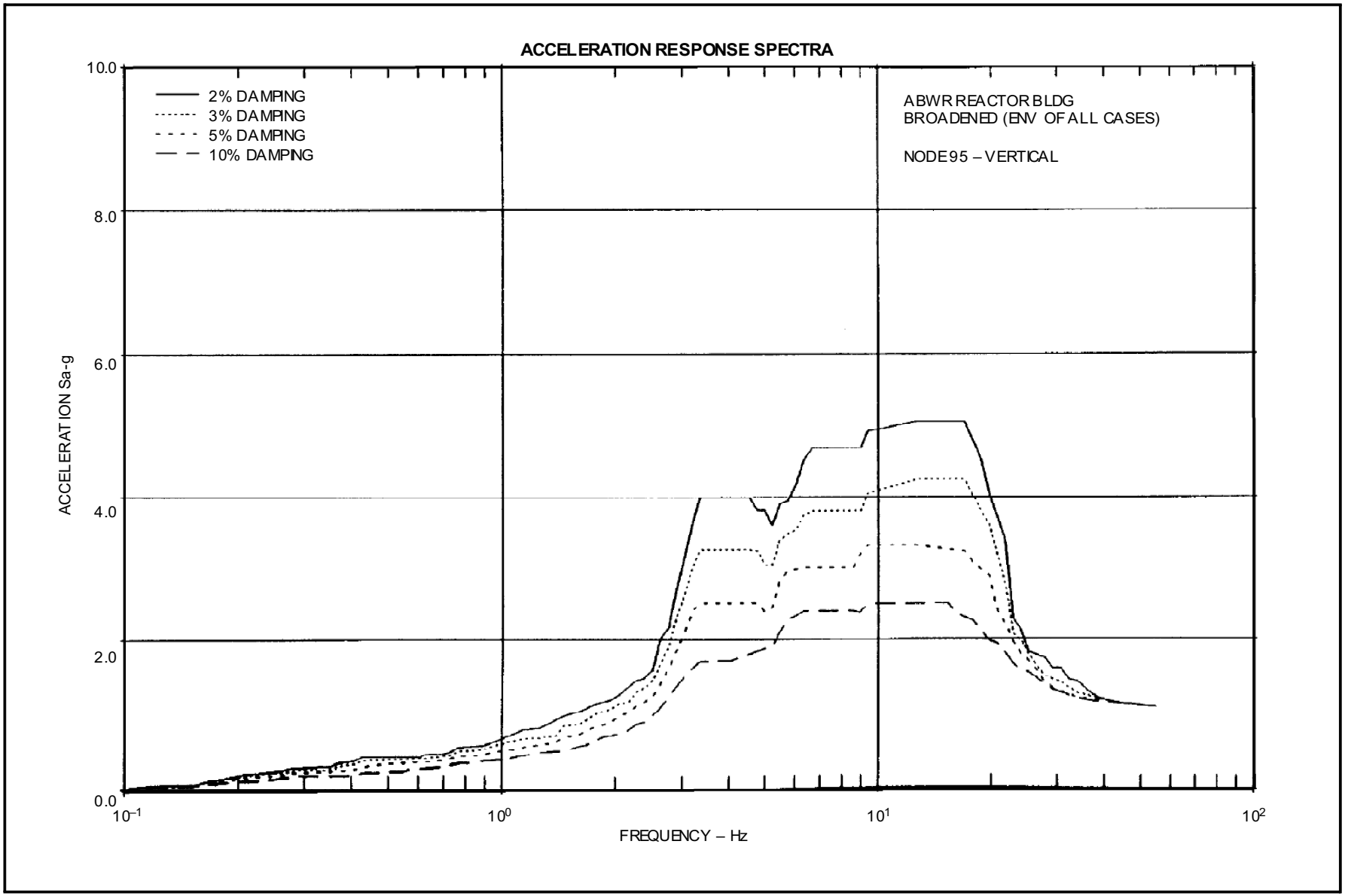

Figure 3A-196 ABWR Reactor Bldg. Broadened (Env of all Cases) Node 95–Vertical

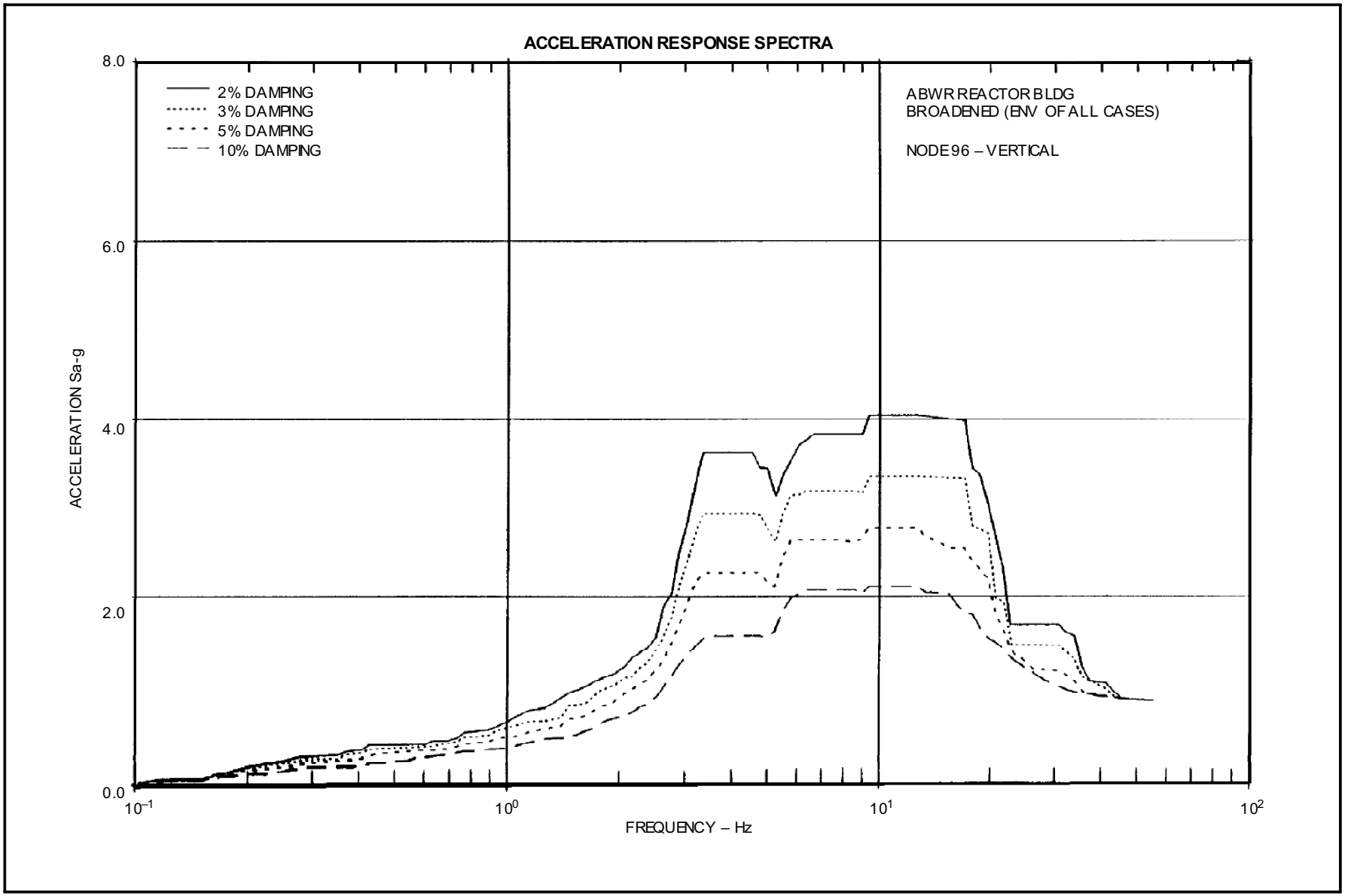

Figure 3A-197 ABWR Reactor Bldg. Broadened (Env of all Cases) Node 96–Vertical

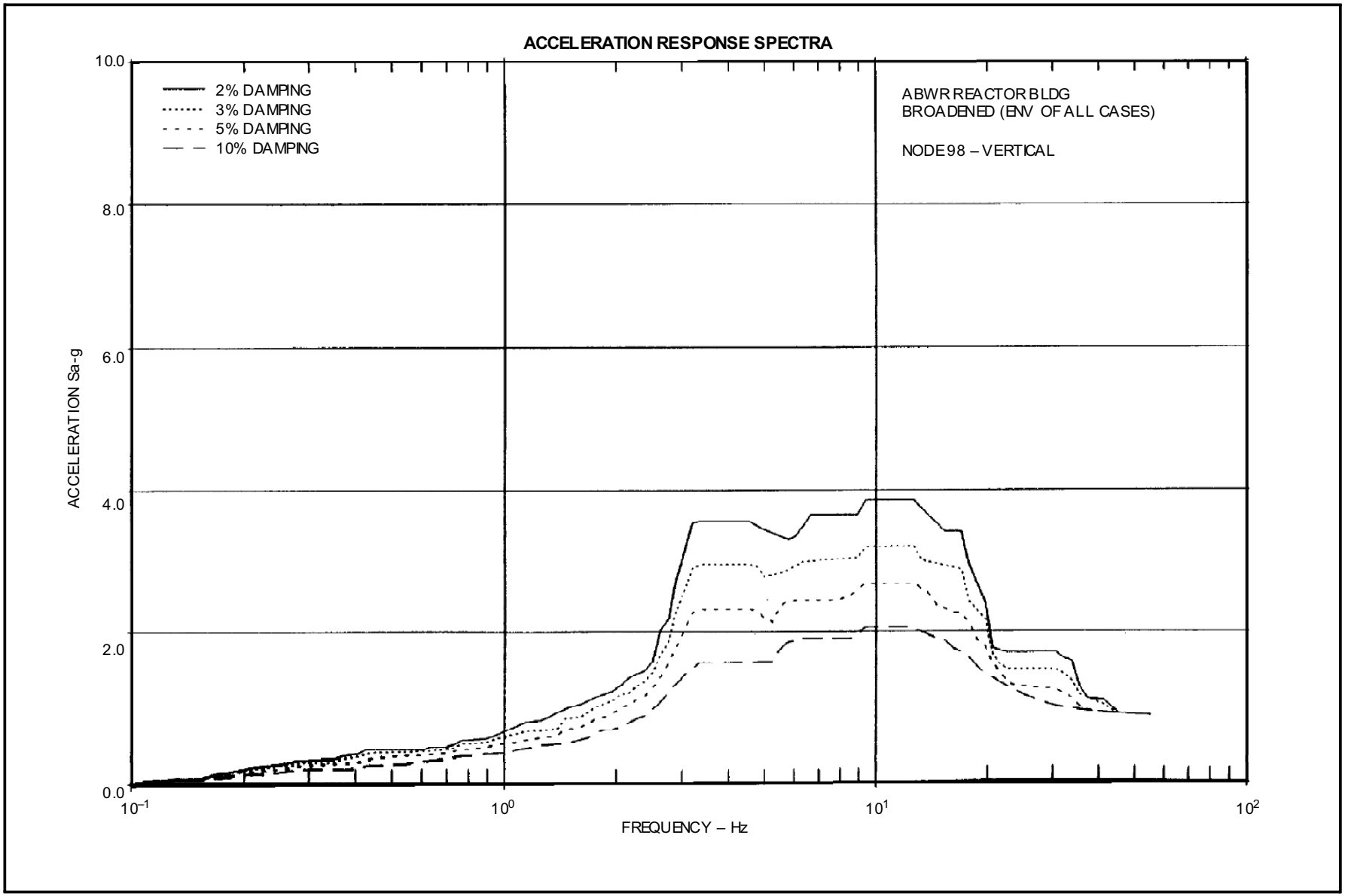

Figure 3A-198 ABWR Reactor Bldg. Broadened (Env of all Cases) Node 98–Vertical

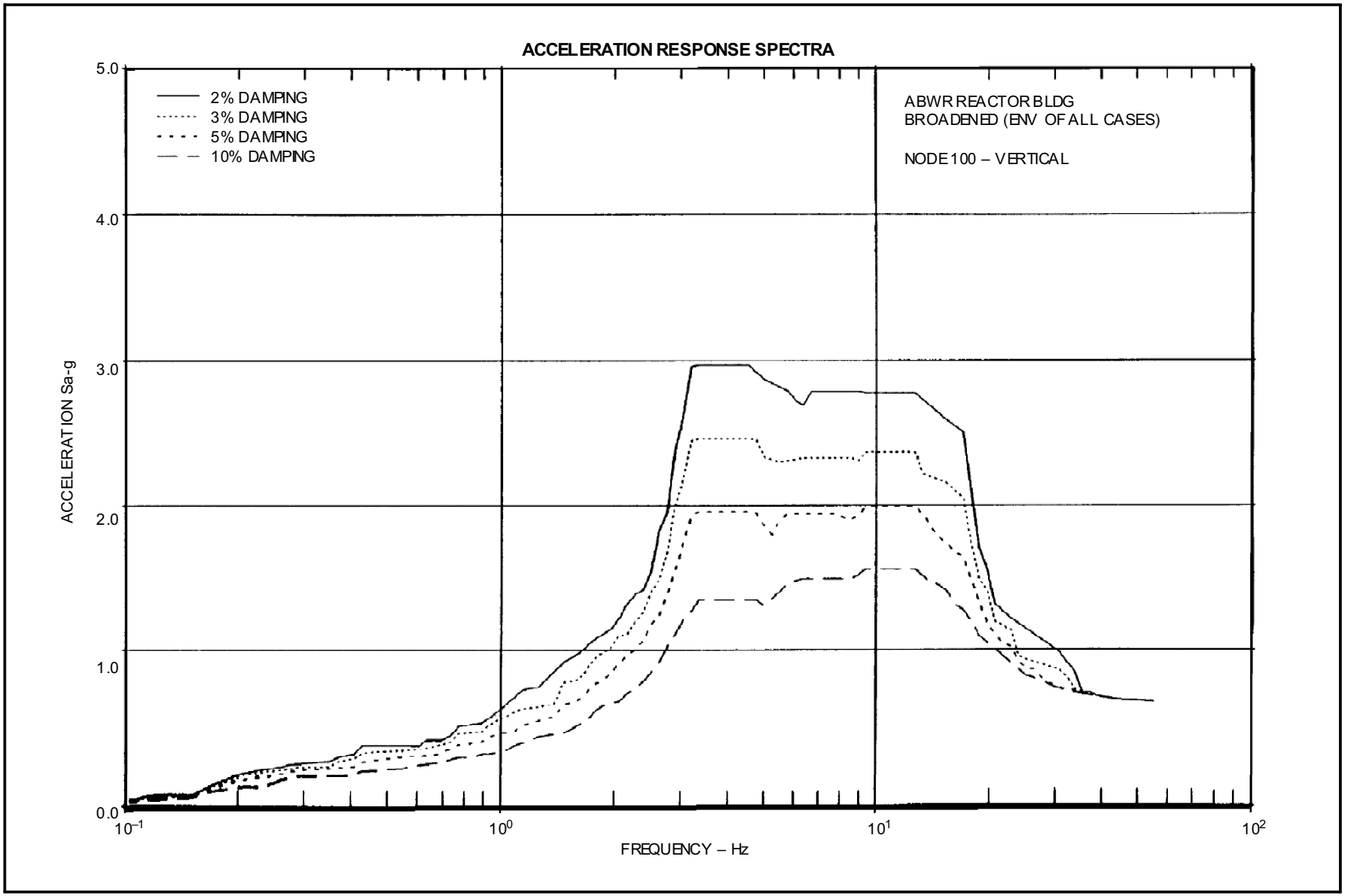

Figure 3A-199 ABWR Reactor Bldg. Broadened (Env of all Cases) Node 100–Vertical

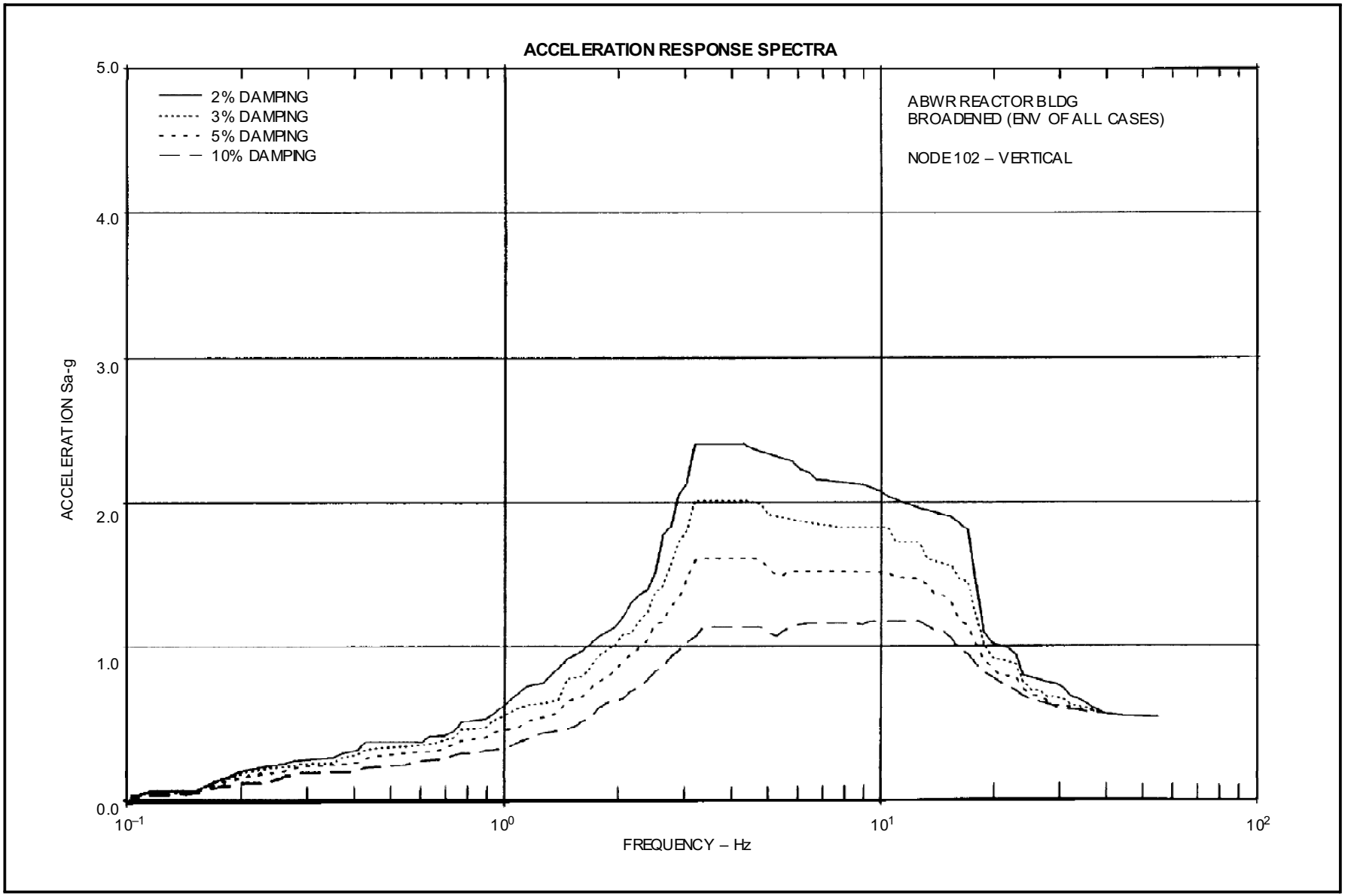

Figure 3A-200 ABWR Reactor Bldg. Broadened (Env of all Cases) Node 102–Vertical

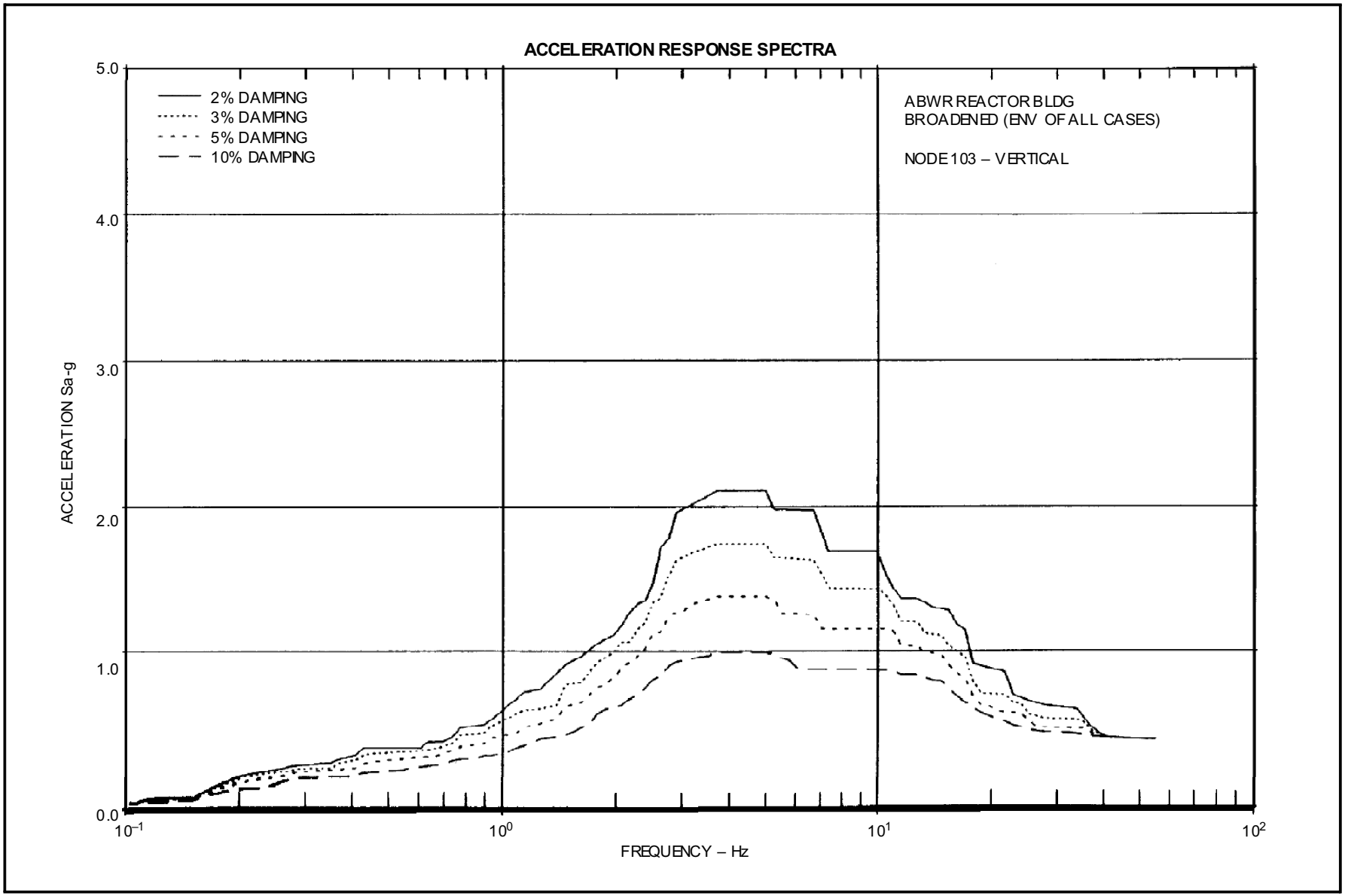

Figure 3A-201 ABWR Reactor Bldg. Broadened (Env of all Cases) Node 103–Vertical

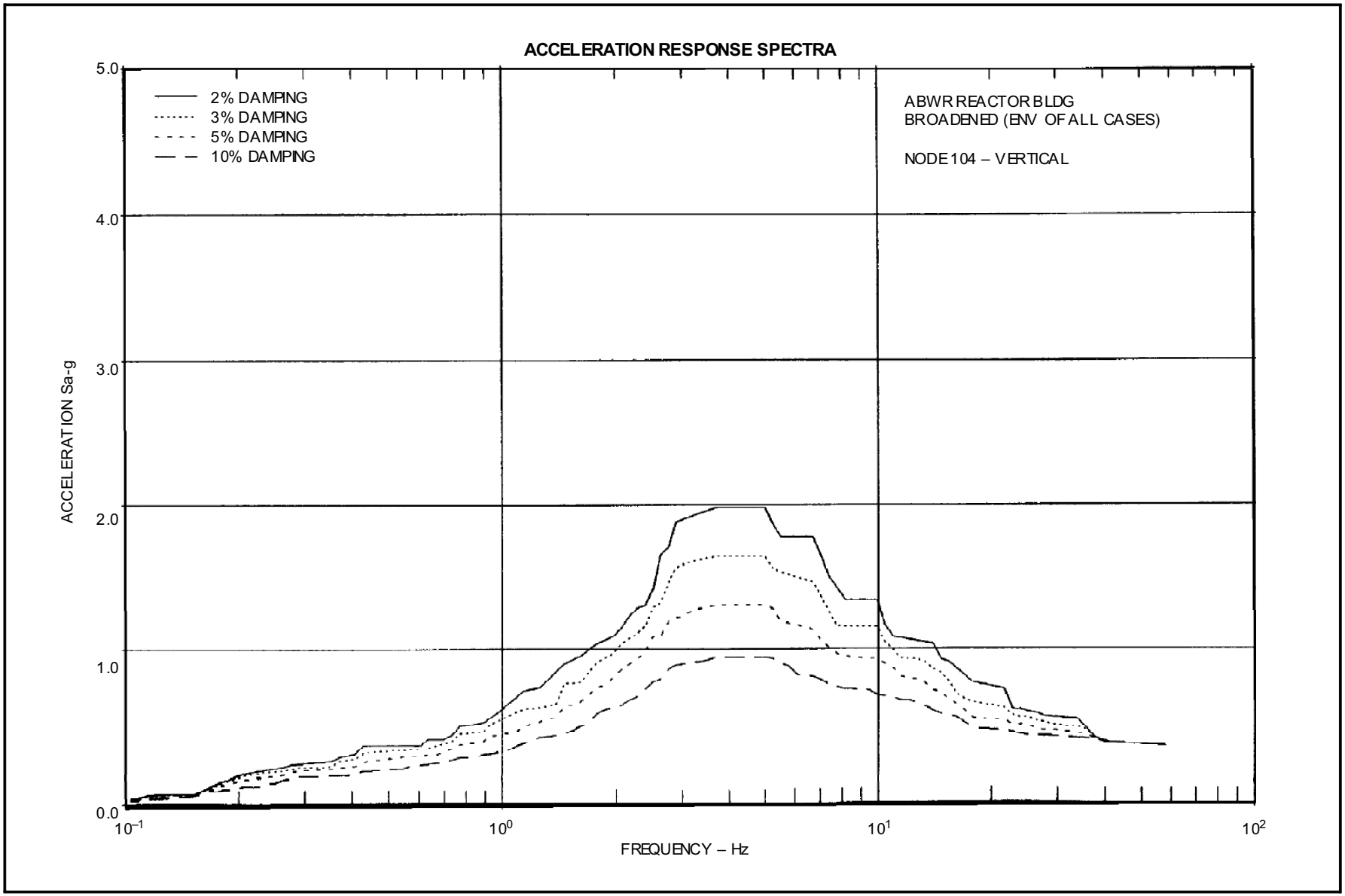

Figure 3A-202 ABWR Reactor Bldg. Broadened (Env of all Cases) Node 104–Vertical

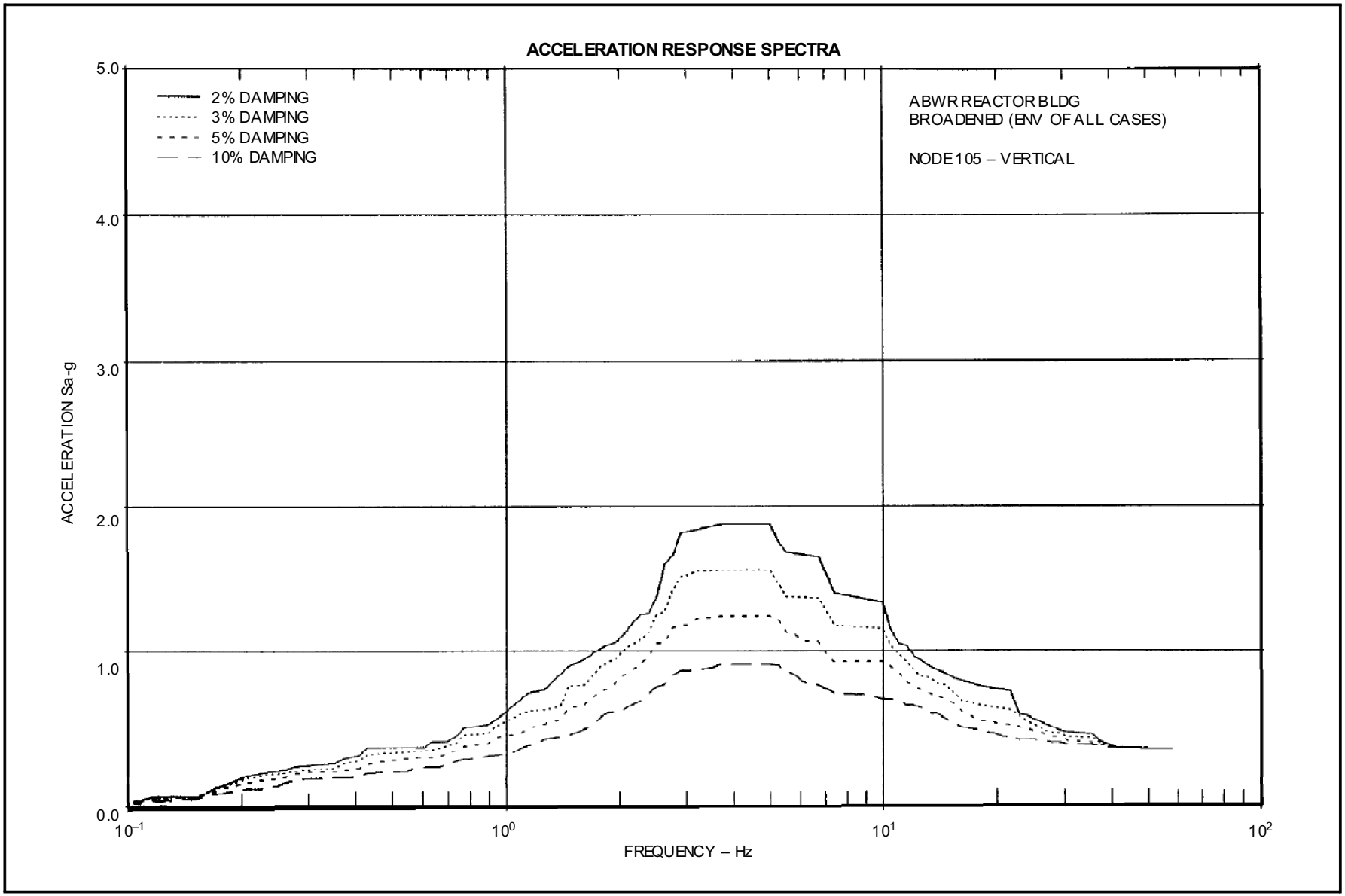

Figure 3A-203 ABWR Reactor Bldg. Broadened (Env of all Cases) Node 105–Vertical

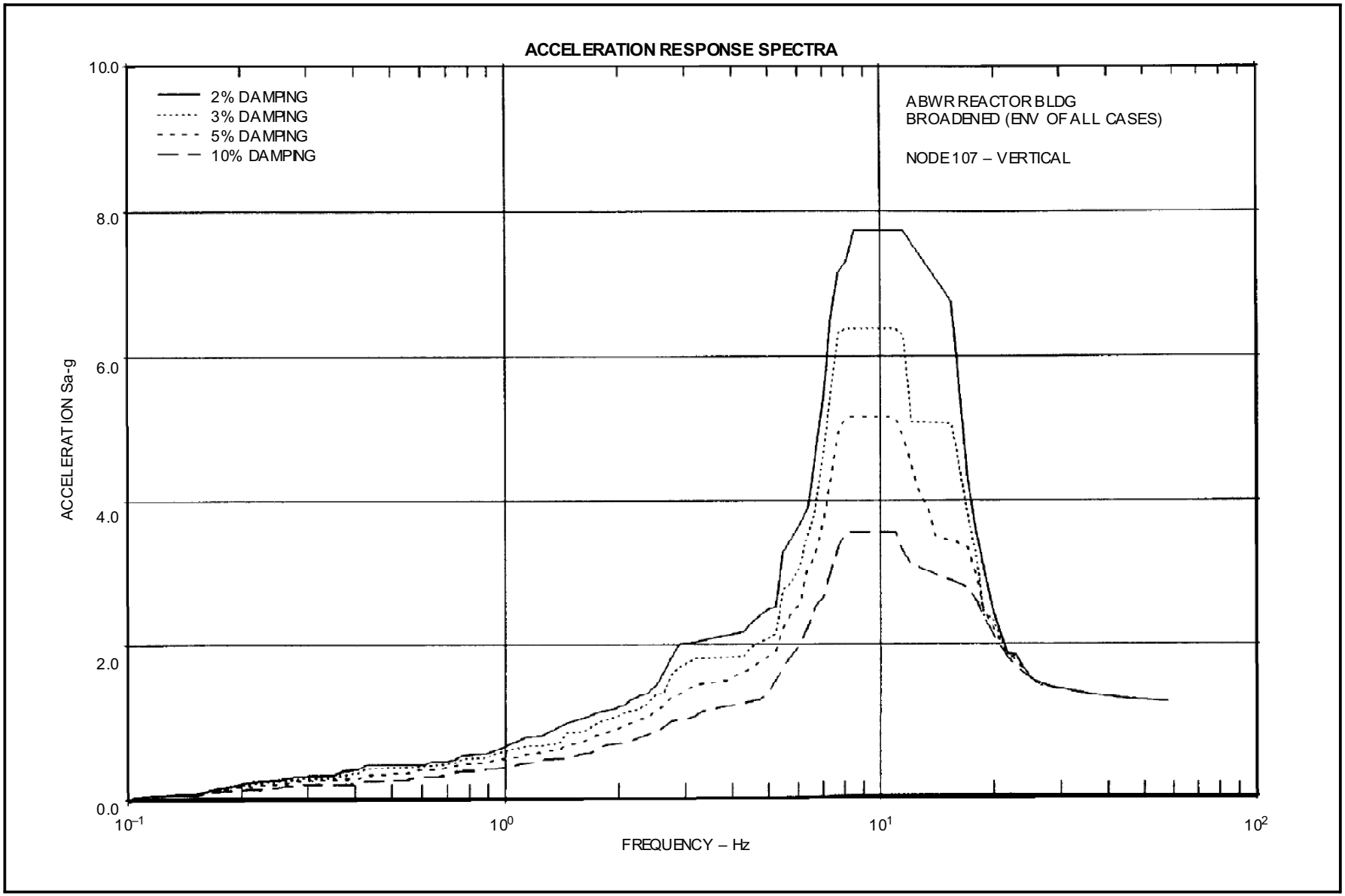

Figure 3A-204 ABWR Reactor Bldg. Broadened (Env of all Cases) Node 107–Vertical

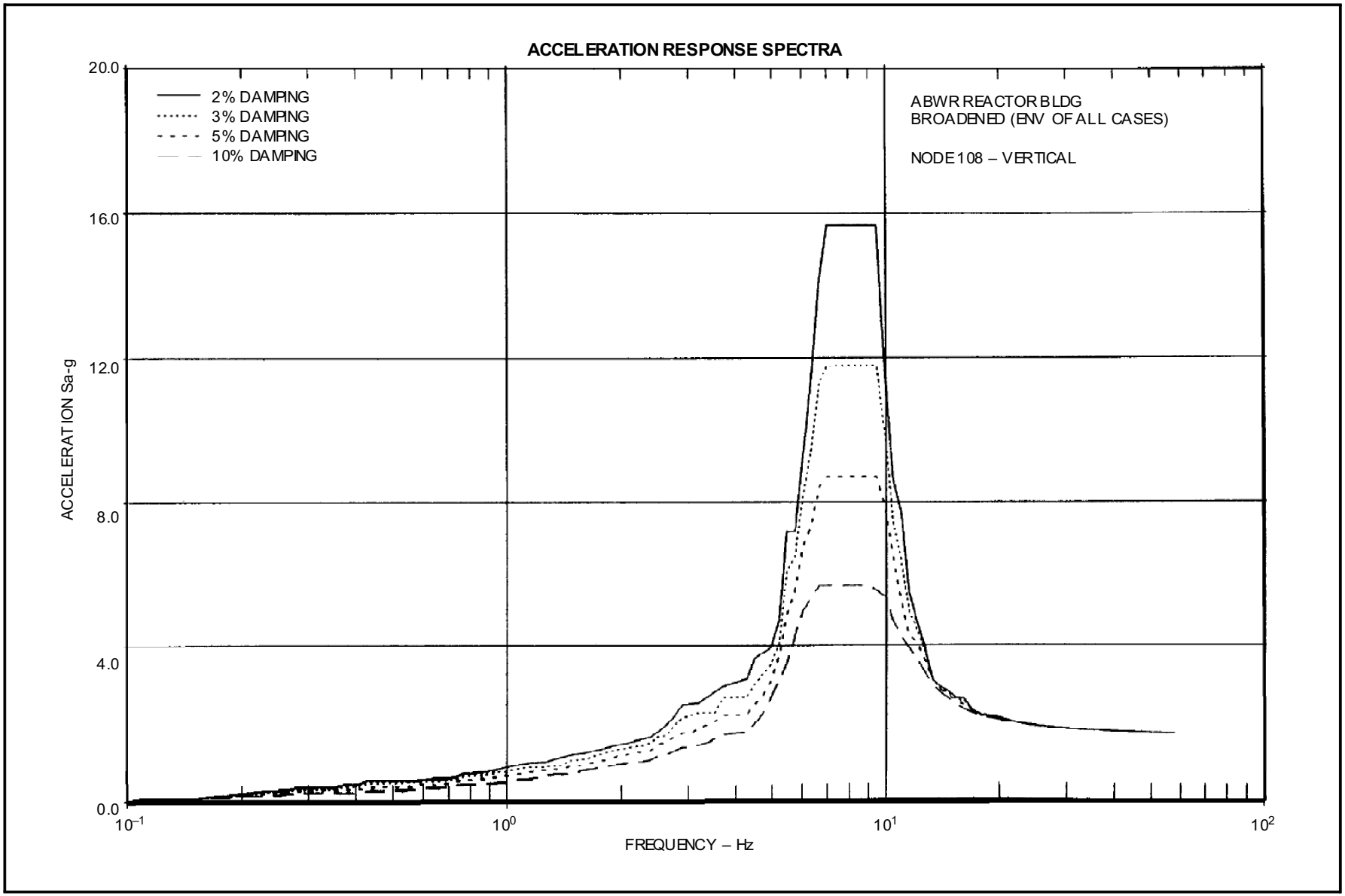

Figure 3A-205 ABWR Reactor Bldg. Broadened (Env of all Cases) Node 108–Vertical

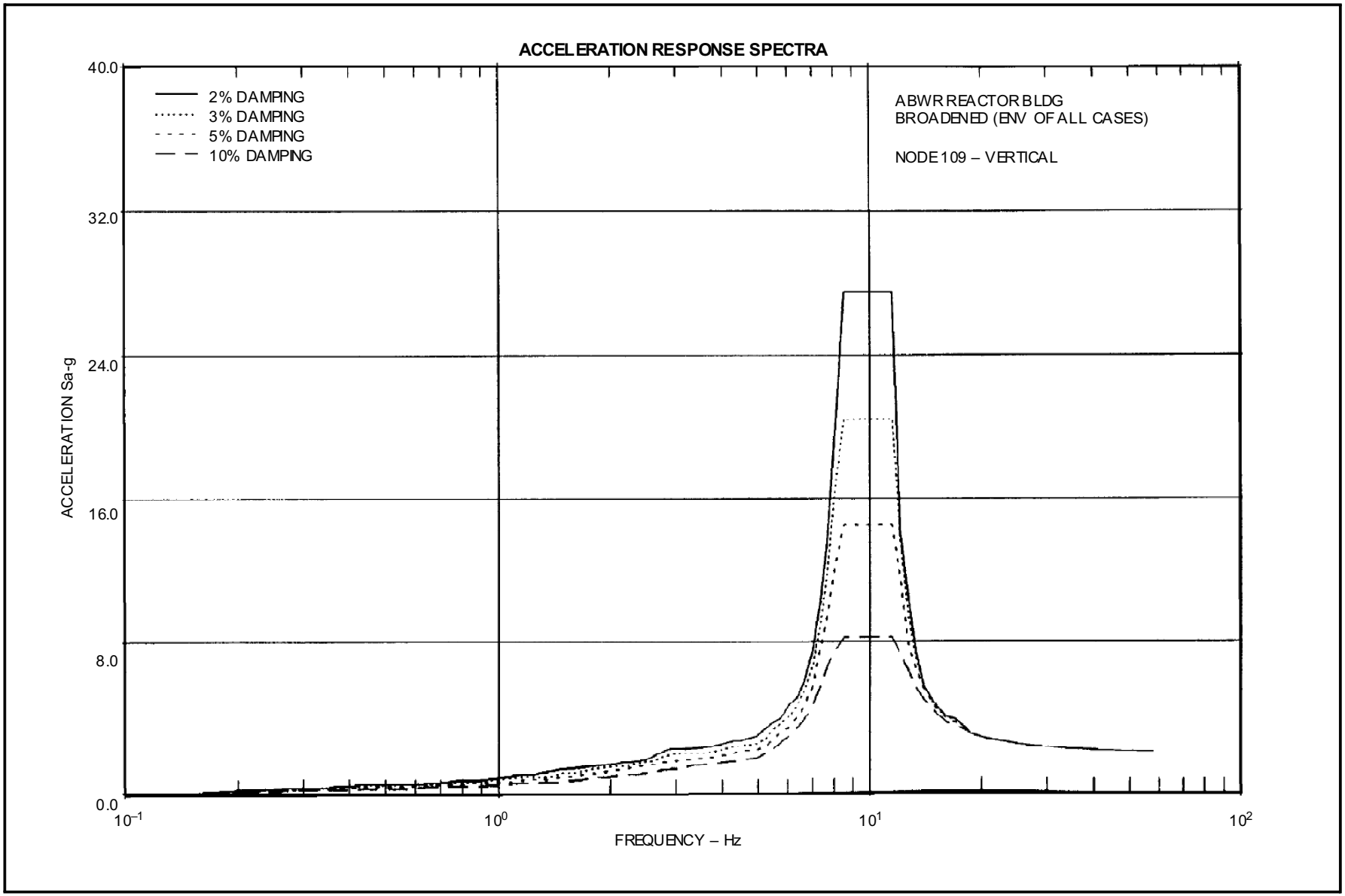

Figure 3A-206 ABWR Reactor Bldg. Broadened (Env of all Cases) Node 109–Vertical

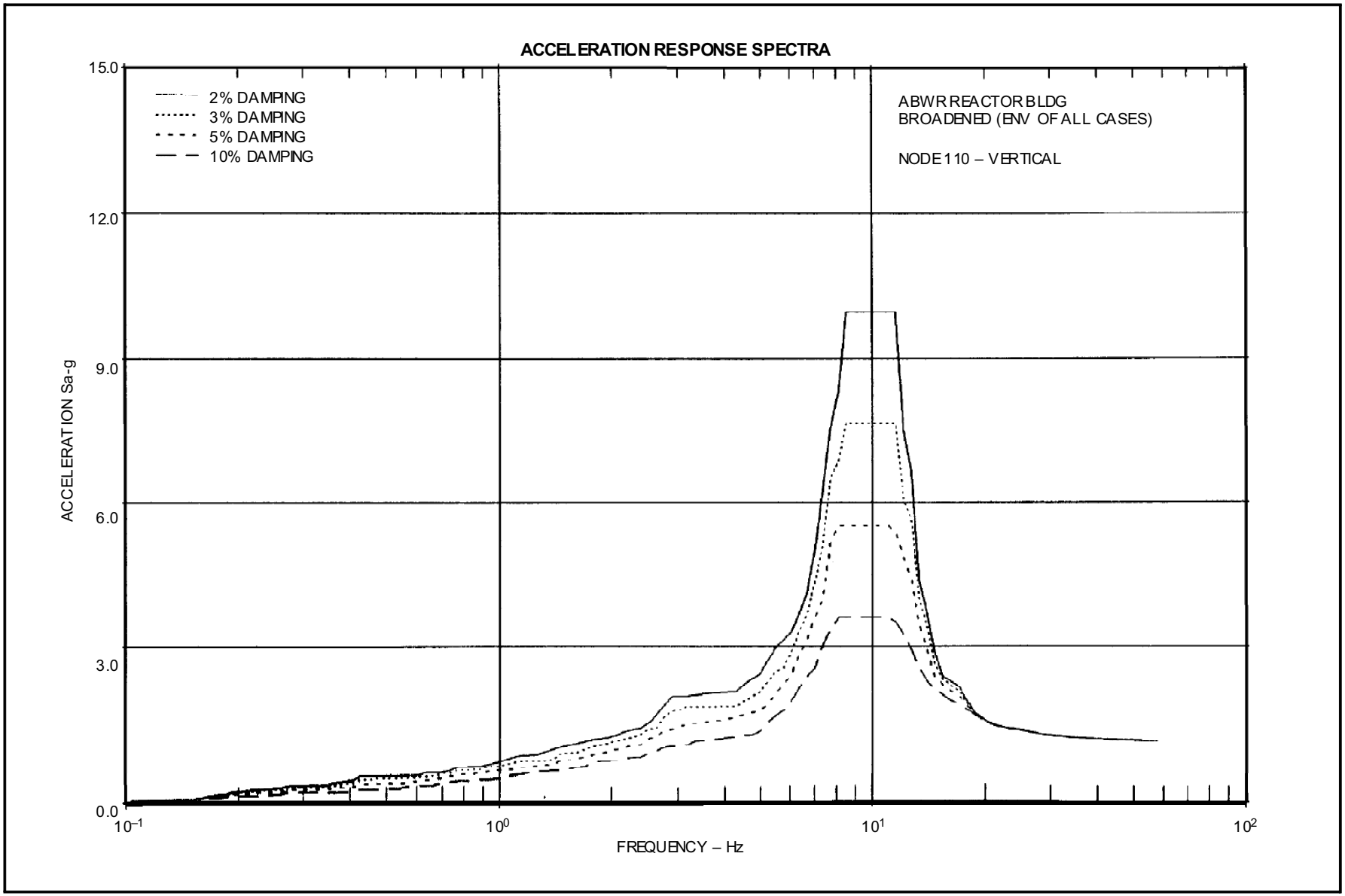

Figure 3A-207 ABWR Reactor Bldg. Broadened (Env of all Cases) Node 110–Vertical

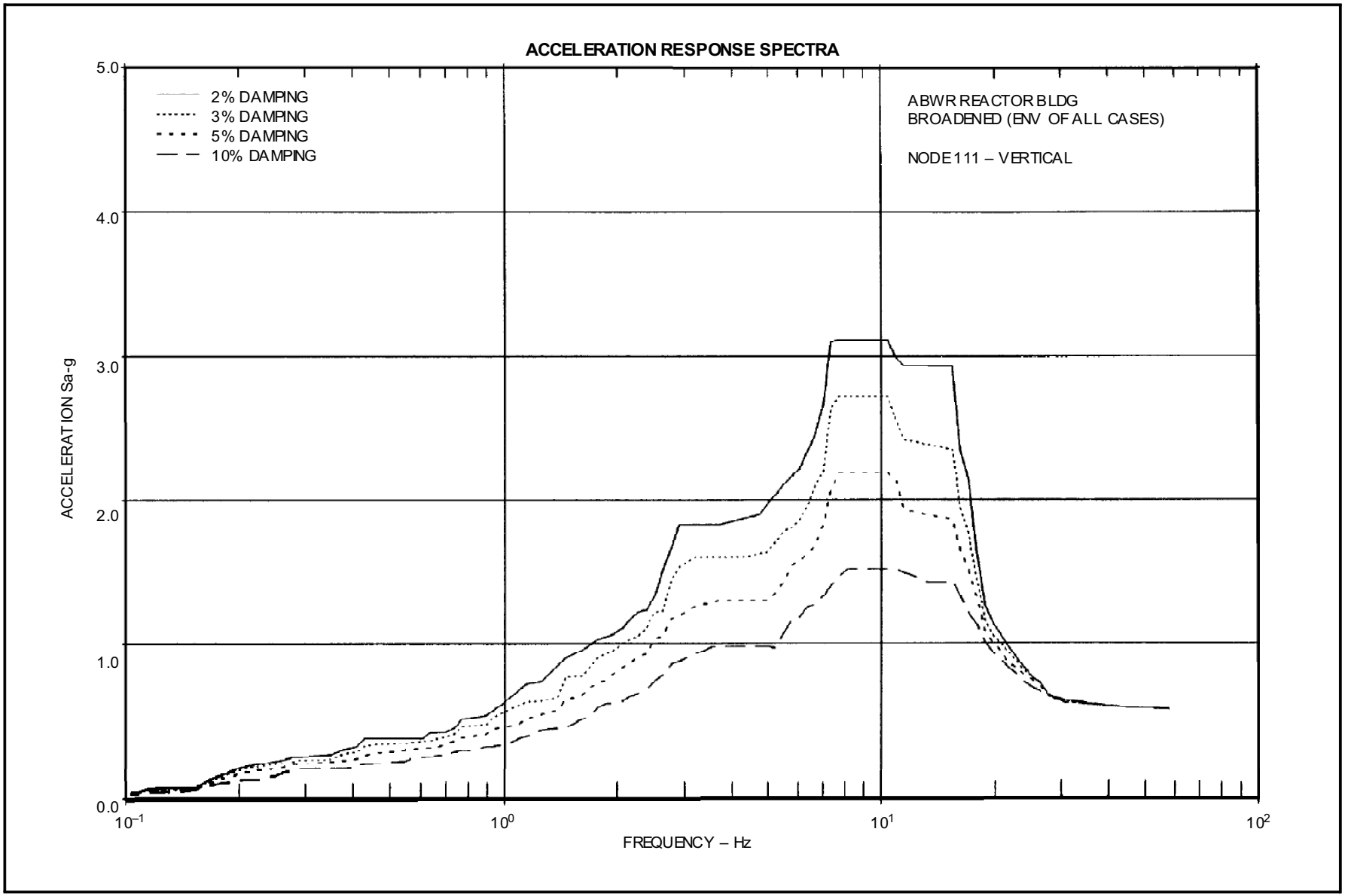

Figure 3A-208 ABWR Reactor Bldg. Broadened (Env of all Cases) Node 111–Vertical

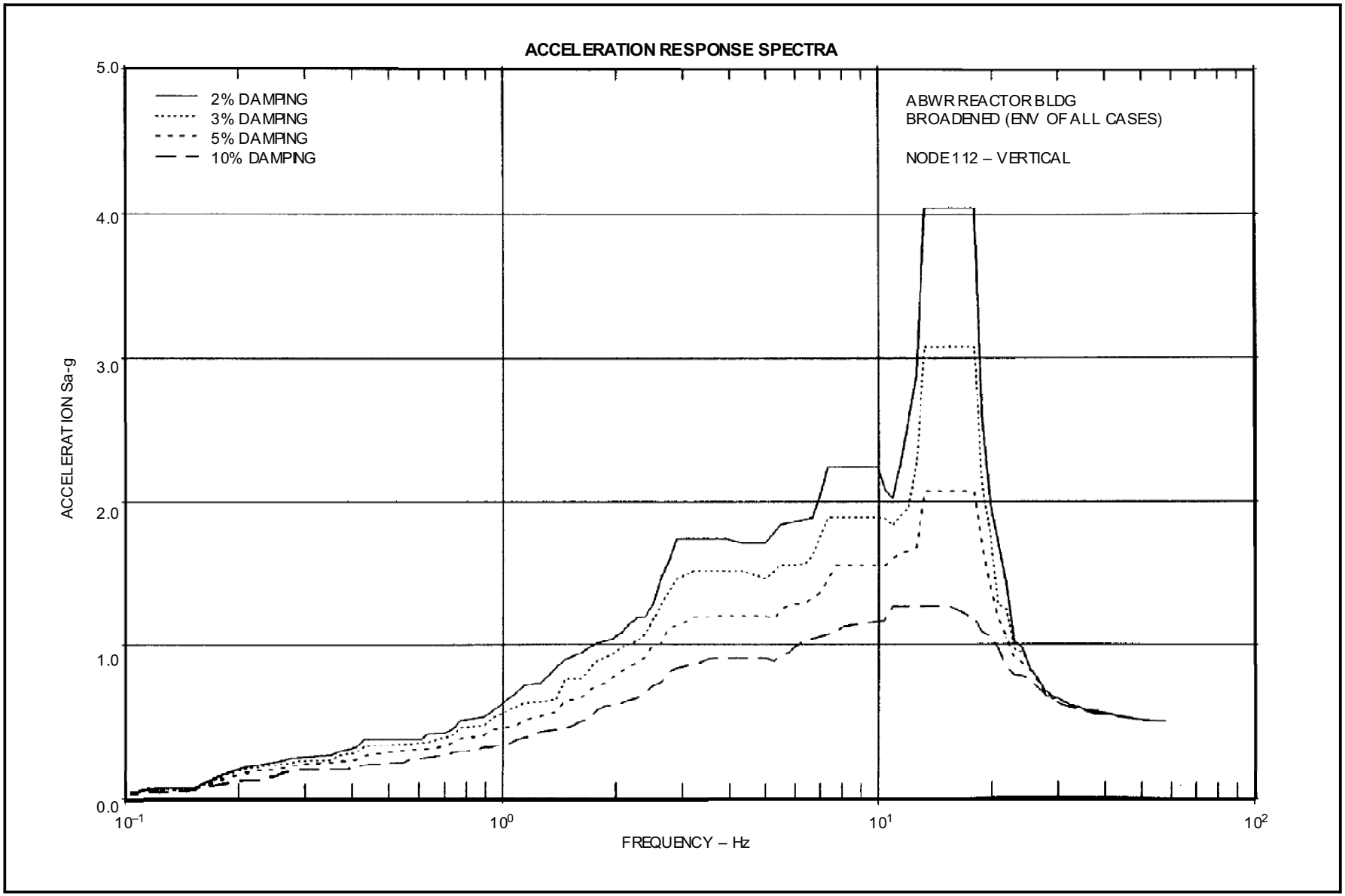

Figure 3A-209 ABWR Reactor Bldg. Broadened (Env of all Cases) Node 112–Vertical

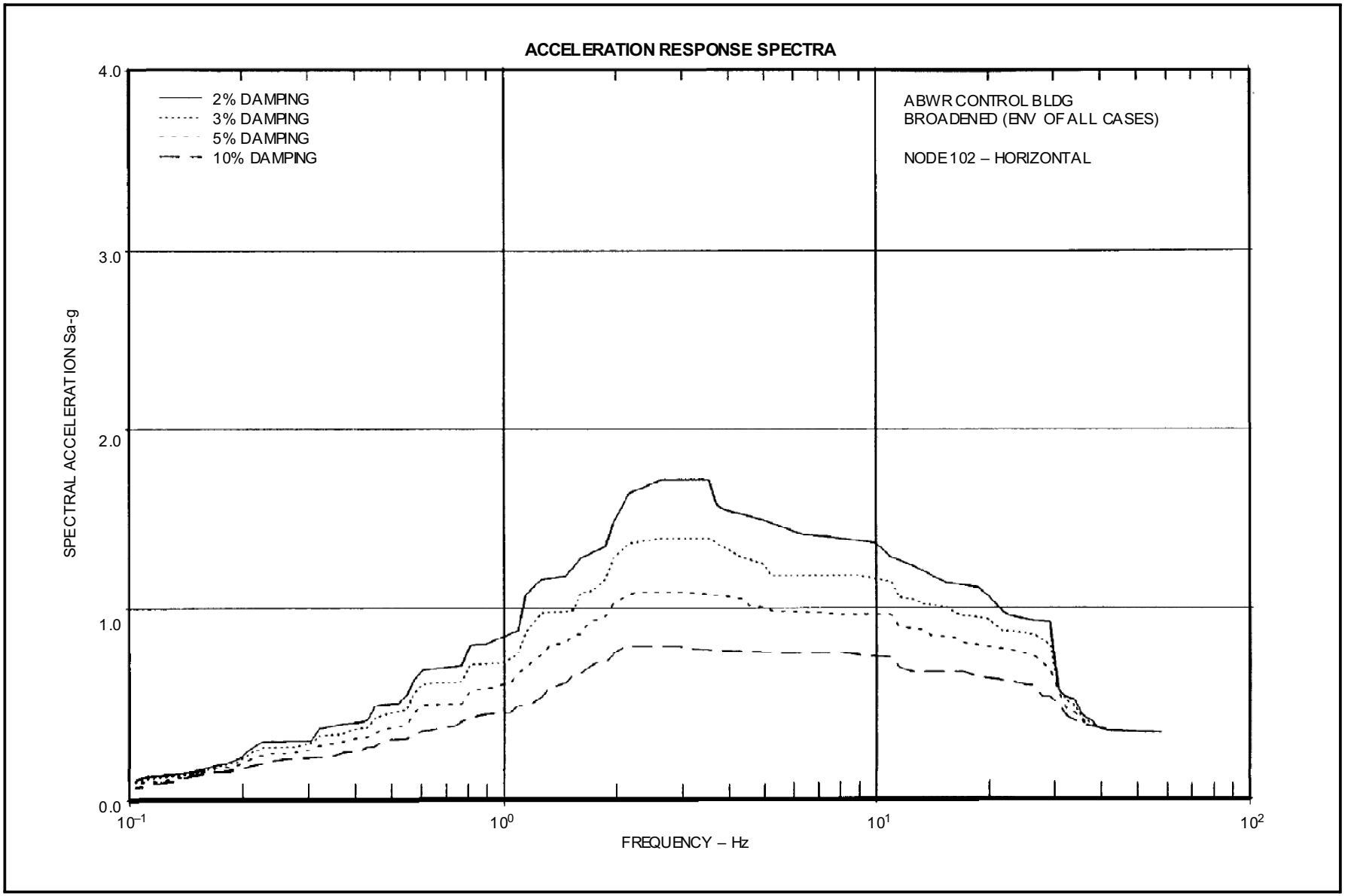

Figure 3A-210 ABWR Control Bldg. Broadened (Env of all Cases) Node 102–Horizontal

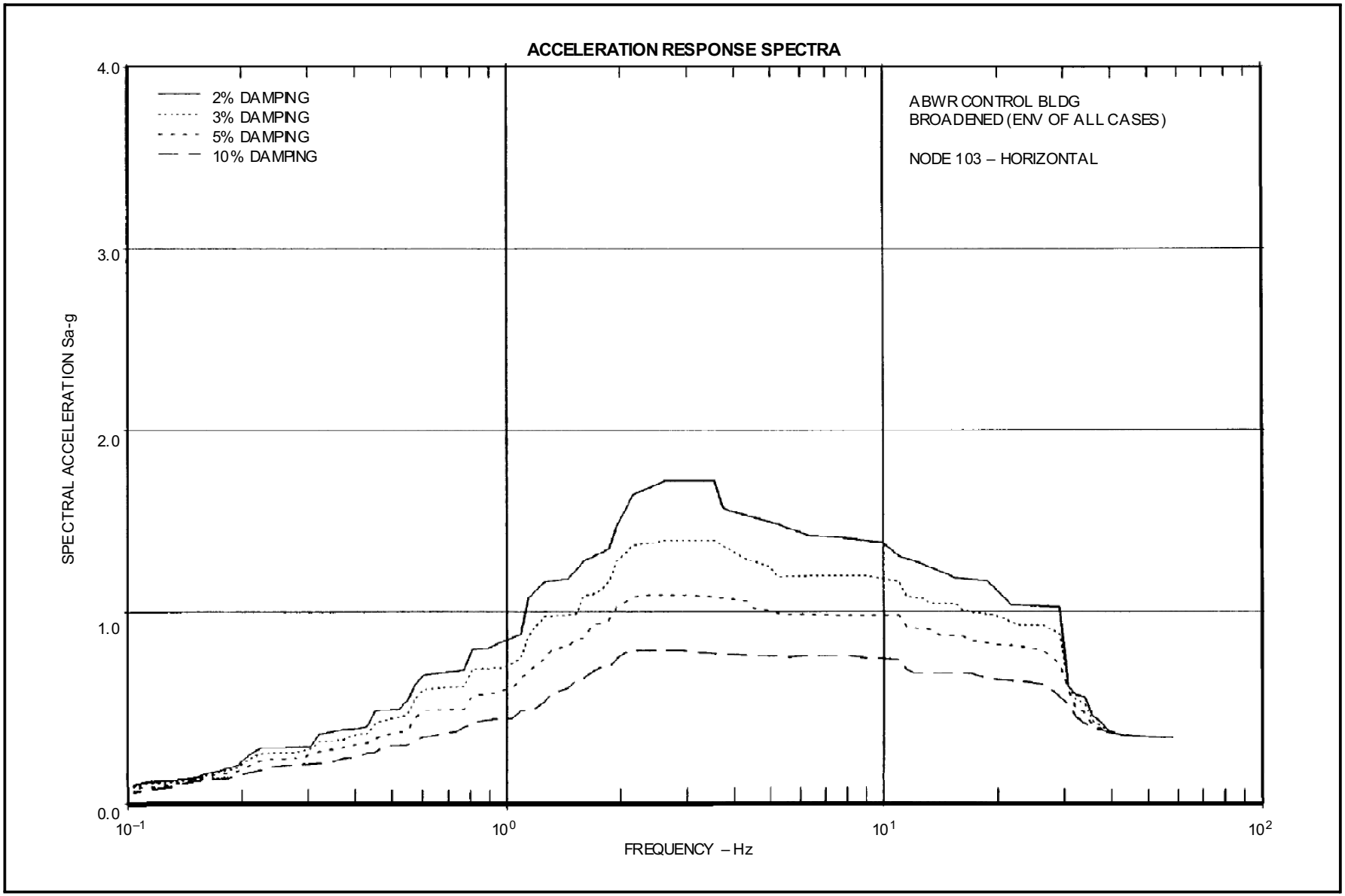

Figure 3A-211 ABWR Control Bldg. Broadened (Env of all Cases) Node 103–Horizontal

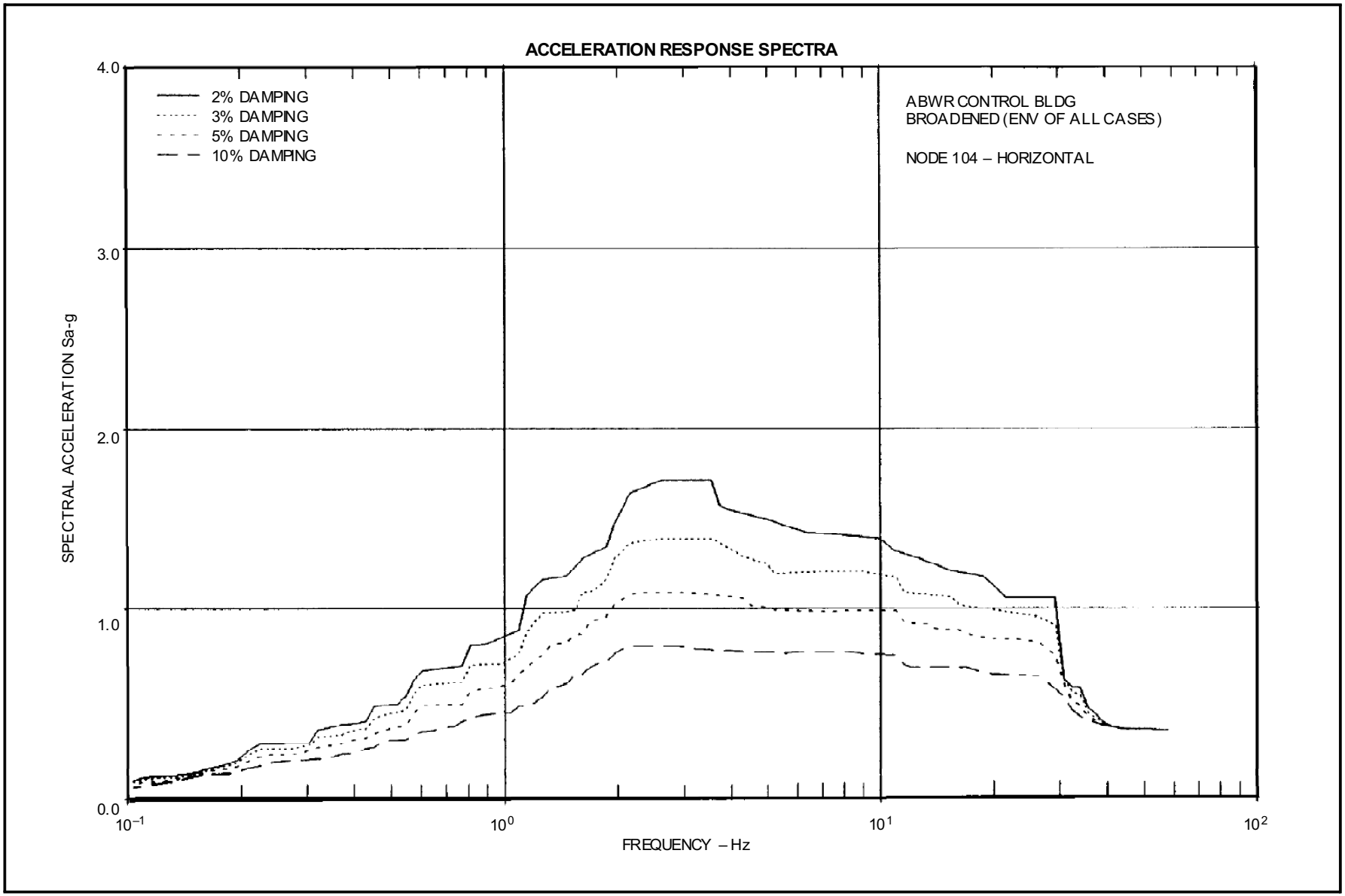

Figure 3A-212 ABWR Control Bldg. Broadened (Env of all Cases) Node 104–Horizontal

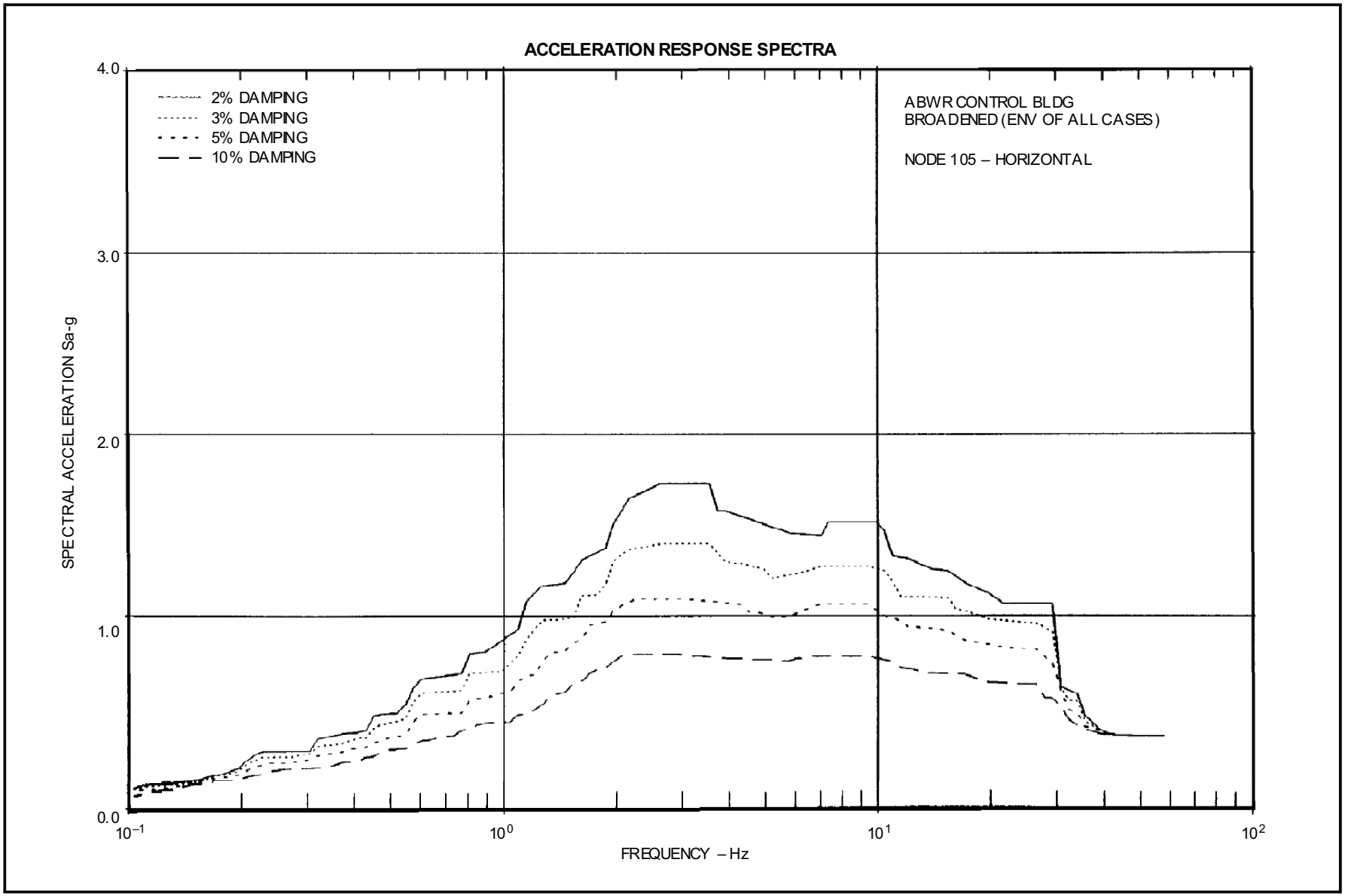

Figure 3A-213 ABWR Control Bldg. Broadened (Env of all Cases) Node 105–Horizontal

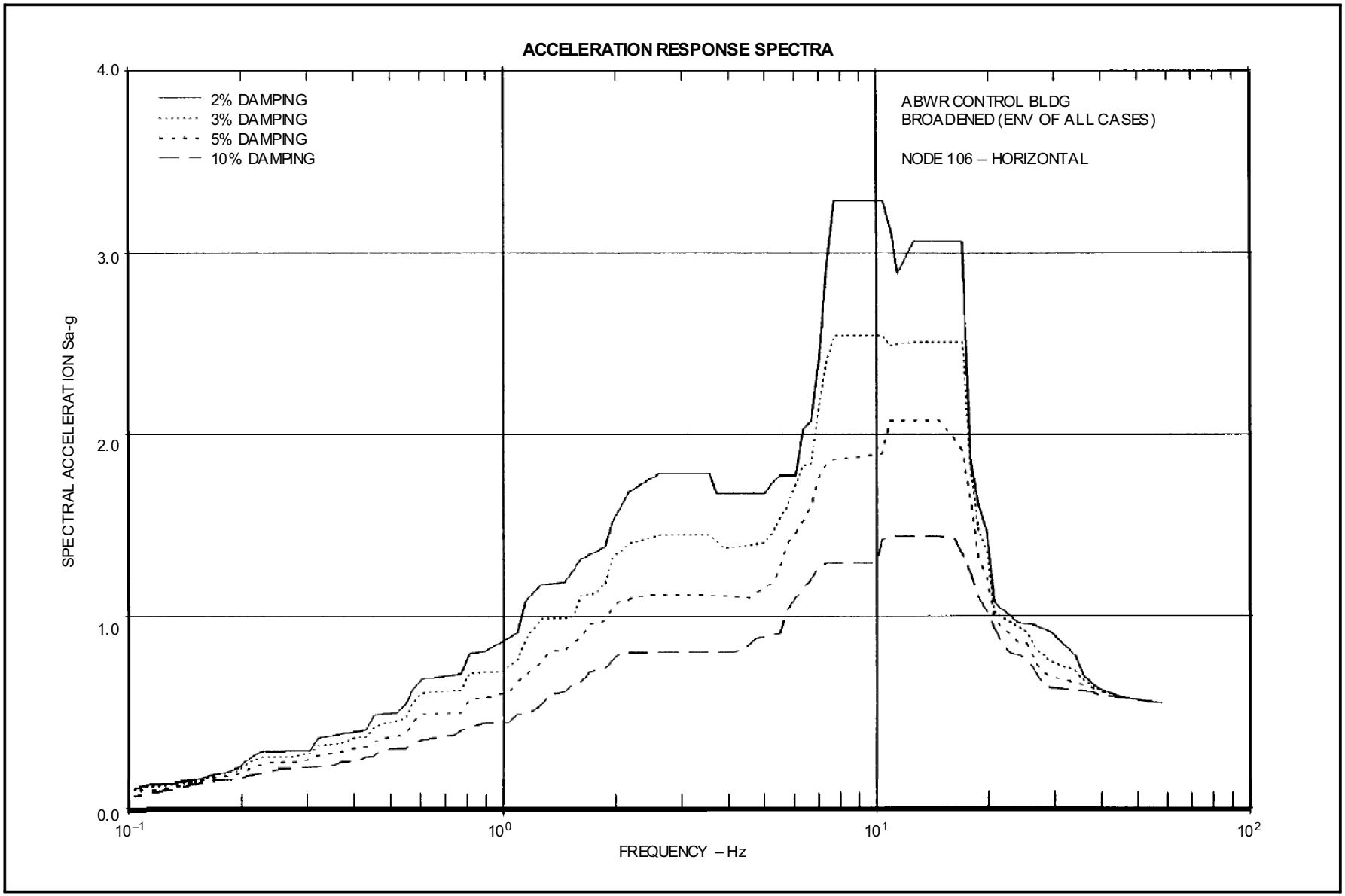

Figure 3A-214 ABWR Control Bldg. Broadened (Env of all Cases) Node 106–Horizontal

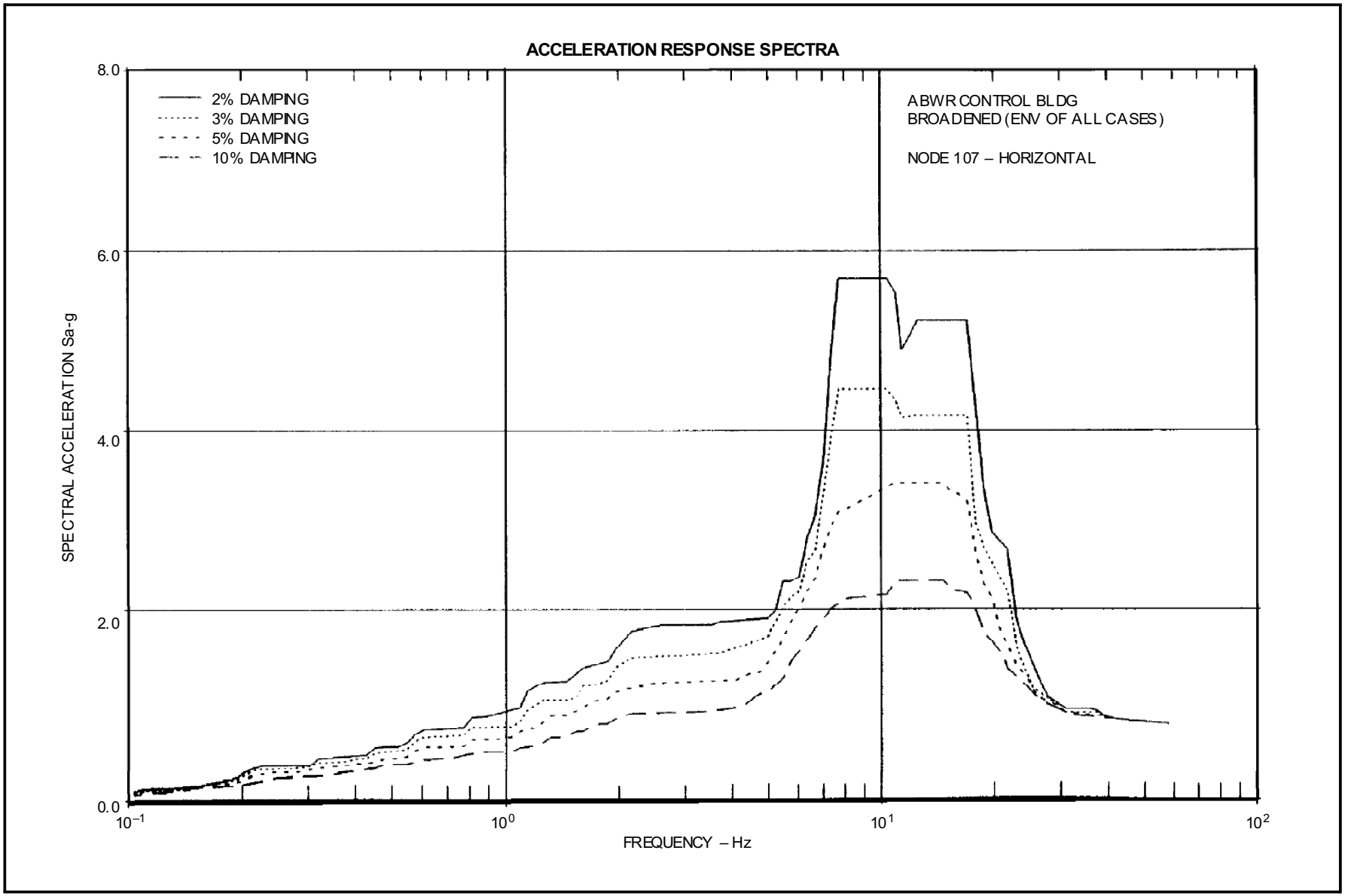

Figure 3A-215 ABWR Control Bldg. Broadened (Env of all Cases) Node 107–Horizontal

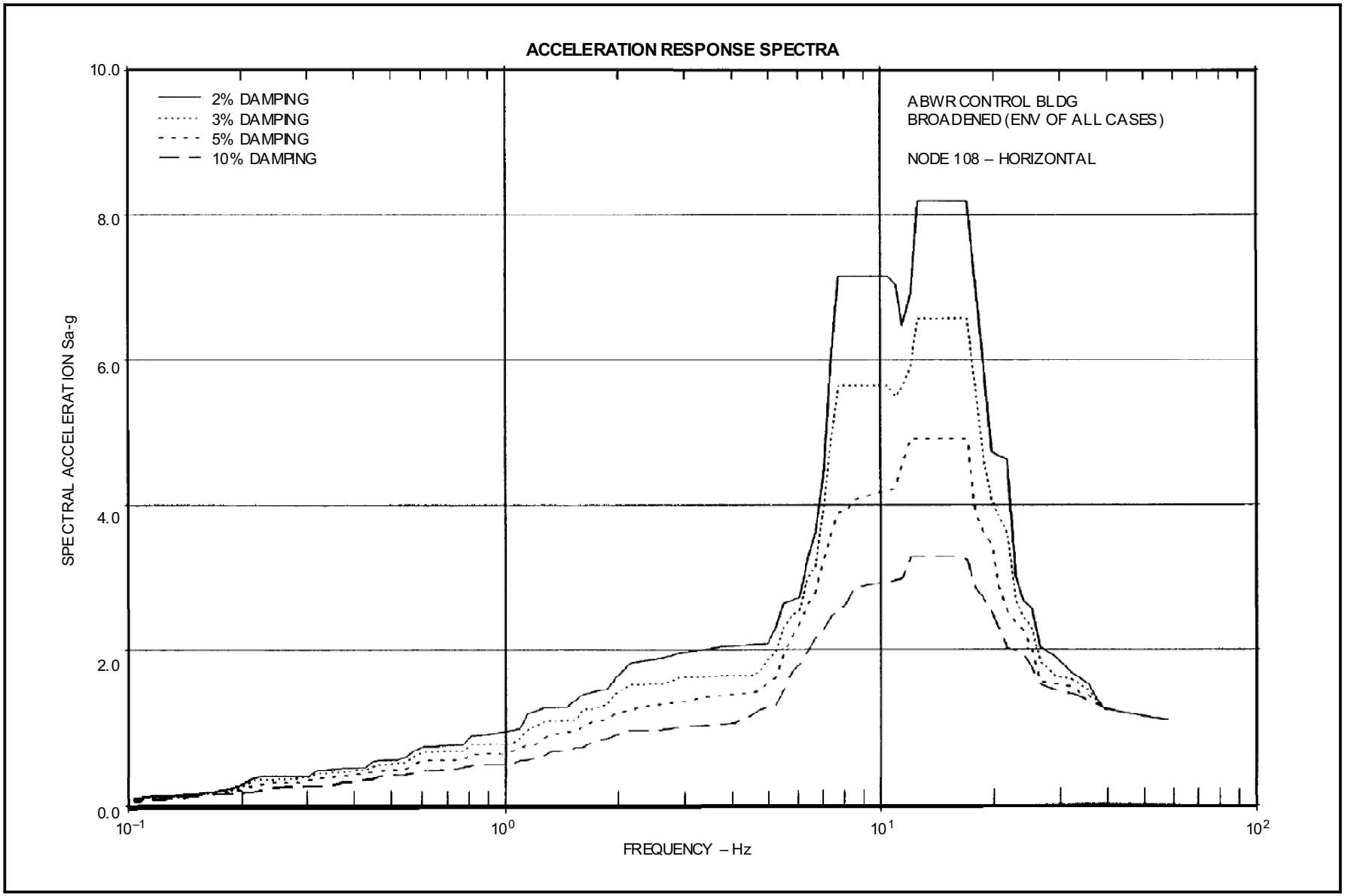

Figure 3A-216 ABWR Control Bldg. Broadened (Env of all Cases) Node 108–Horizontal

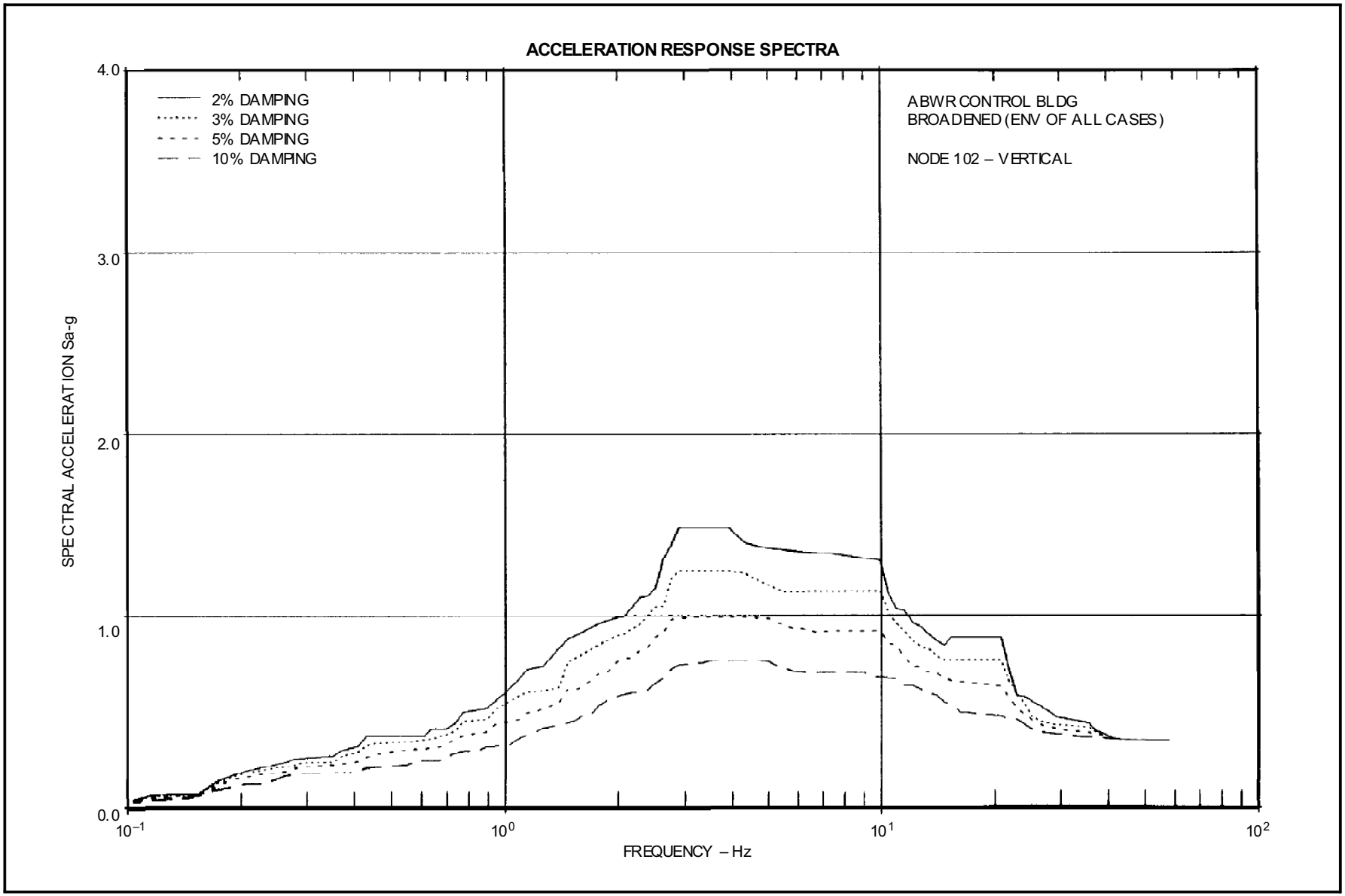

Figure 3A-217 ABWR Control Bldg. Broadened (Env of all Cases) Node 102–Vertical

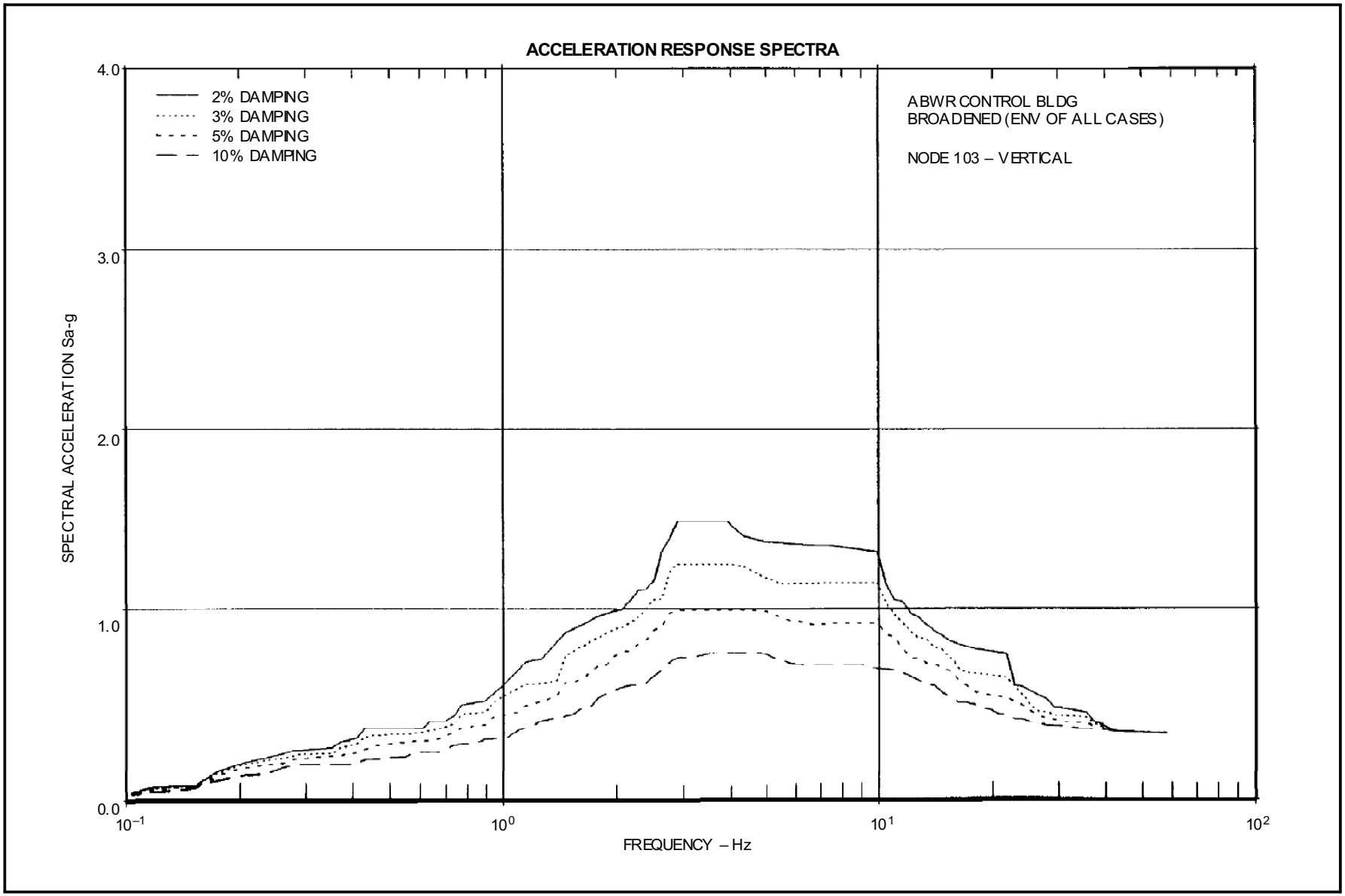

Figure 3A-218 ABWR Control Bldg. Broadened (Env of all Cases) Node 103–Vertical

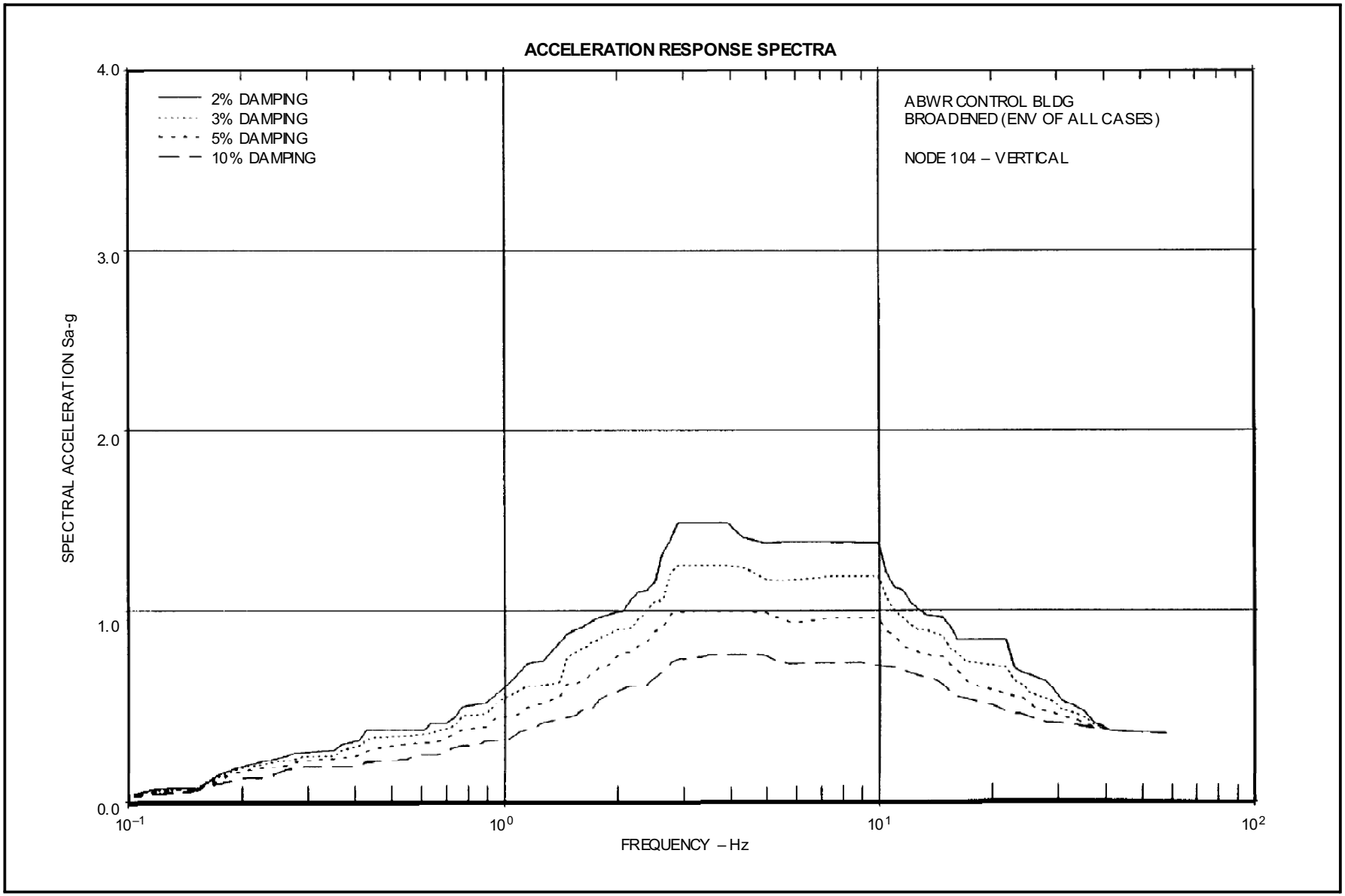

Figure 3A-219 ABWR Control Bldg. Broadened (Env of all Cases) Node 104–Vertical

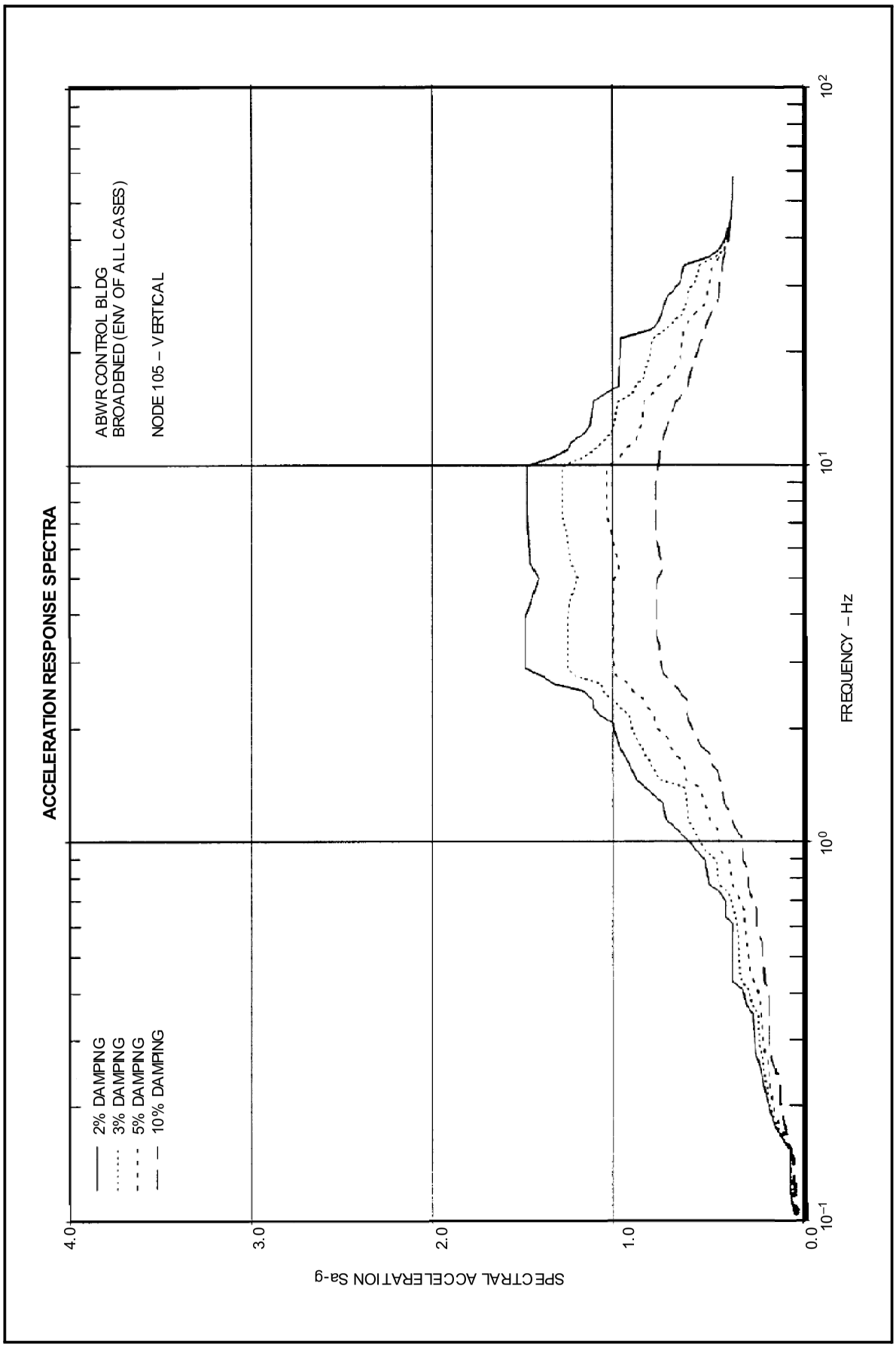

Figure 3A-220 ABWR Control Bldg. Broadened (Env of all Cases) Node 105–Vertical

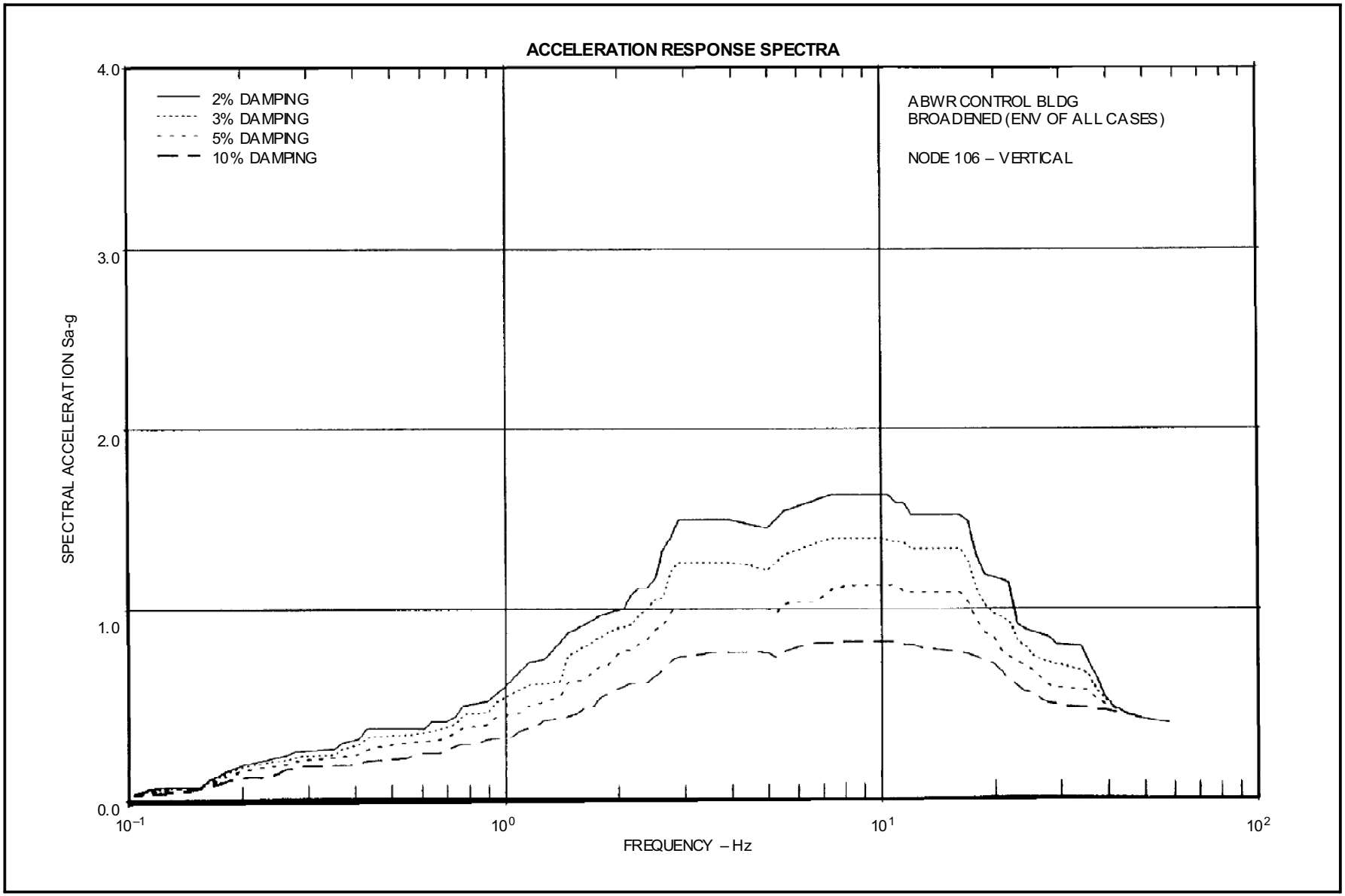

Figure 3A-221 ABWR Control Bldg. Broadened (Env of all Cases) Node 106–Vertical

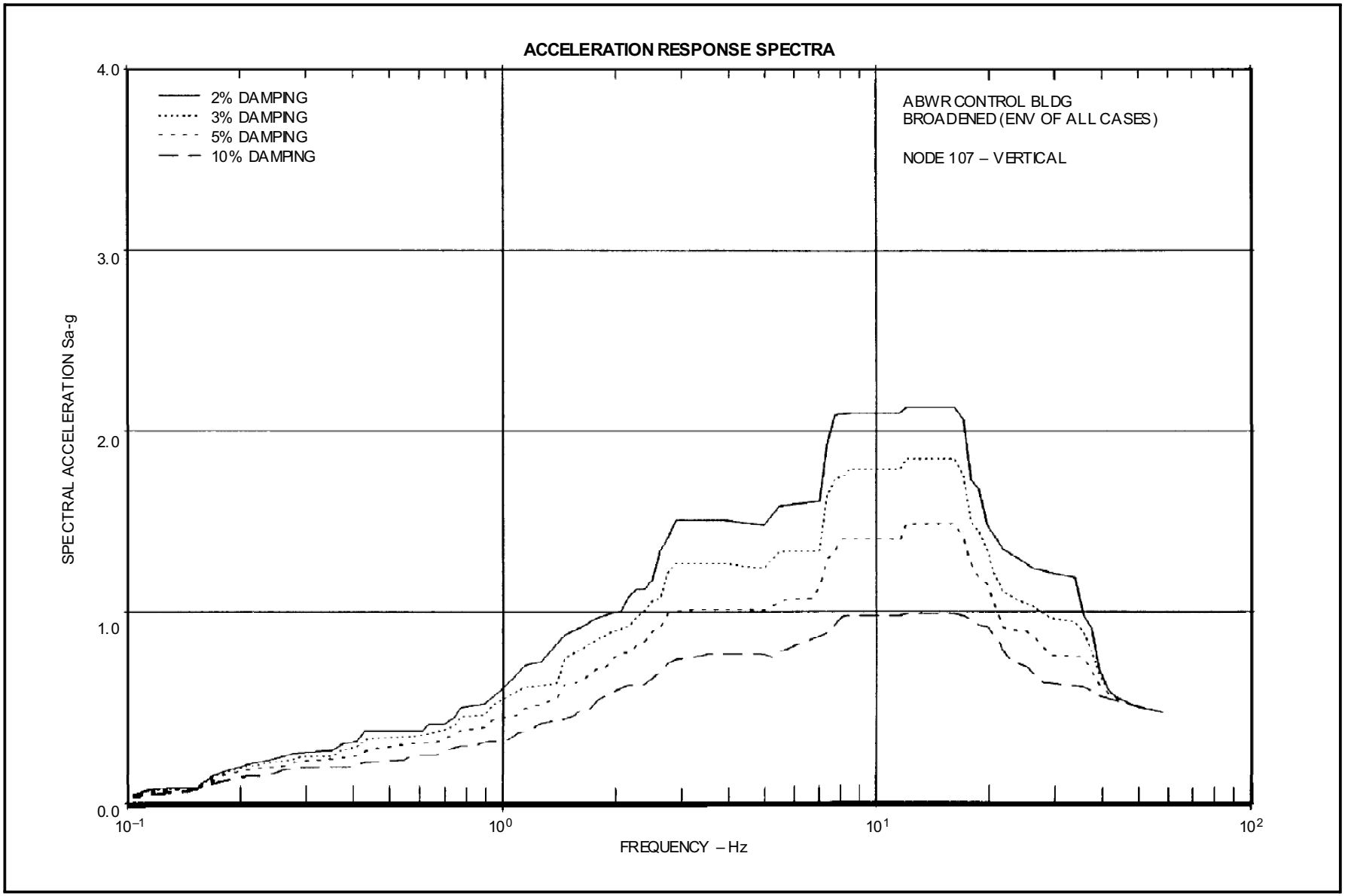

Figure 3A-222 ABWR Control Bldg. Broadened (Env of all Cases) Node 107–Vertical

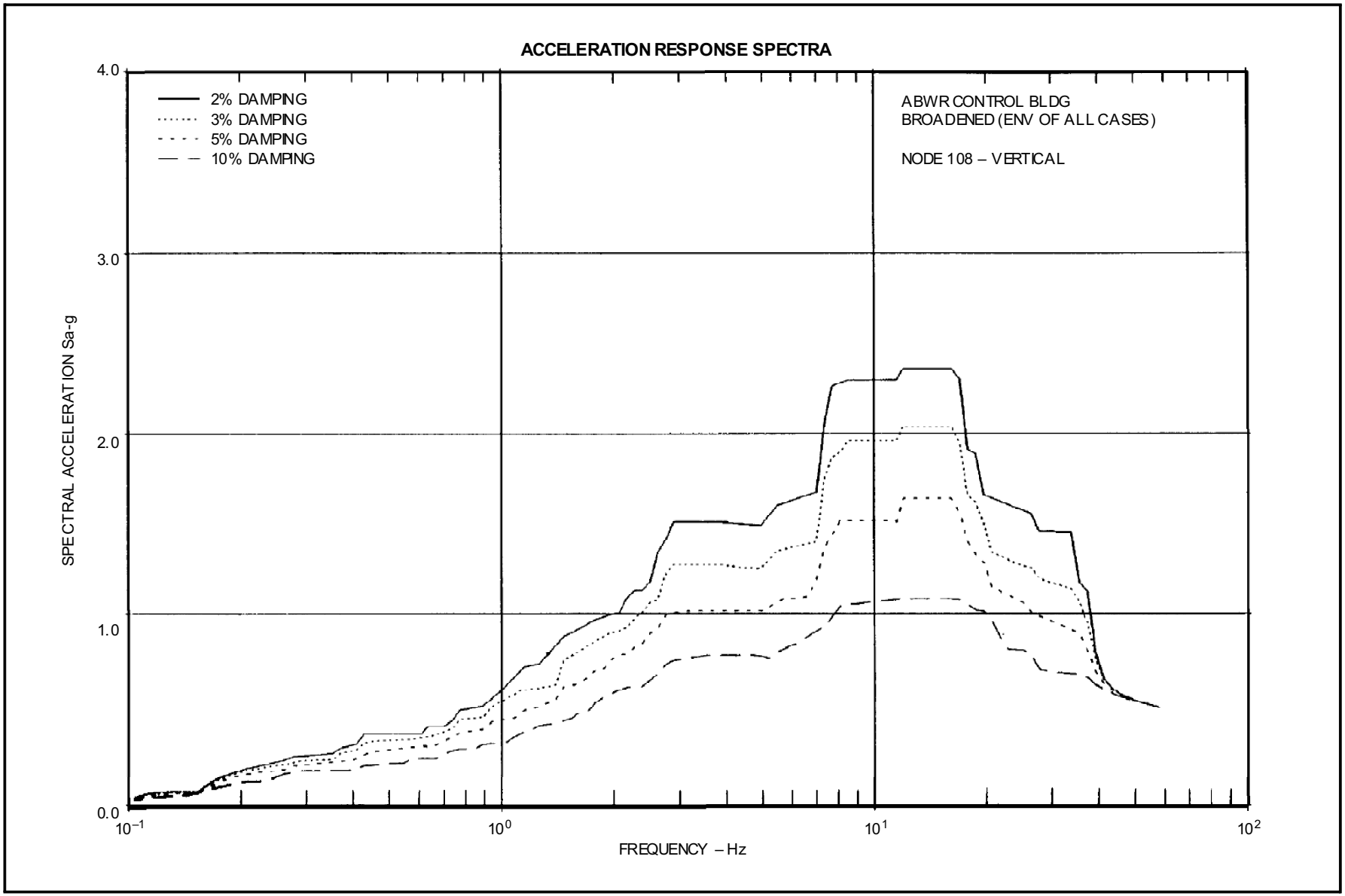

Figure 3A-223 ABWR Control Bldg. Broadened (Env of all Cases) Node 108–Vertical

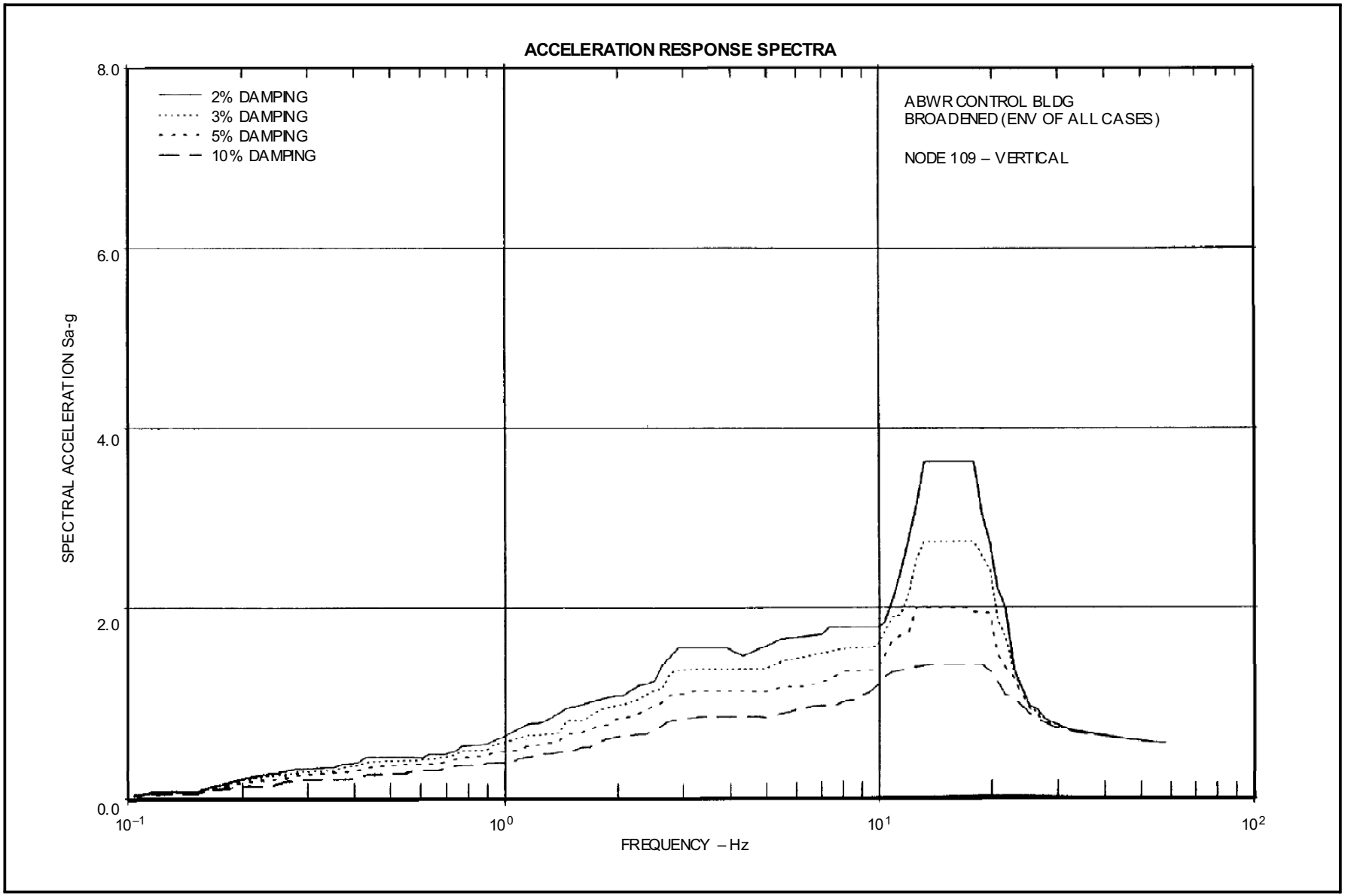

Figure 3A-224 ABWR Control Bldg. Broadened (Env of all Cases) Node 109–Vertical

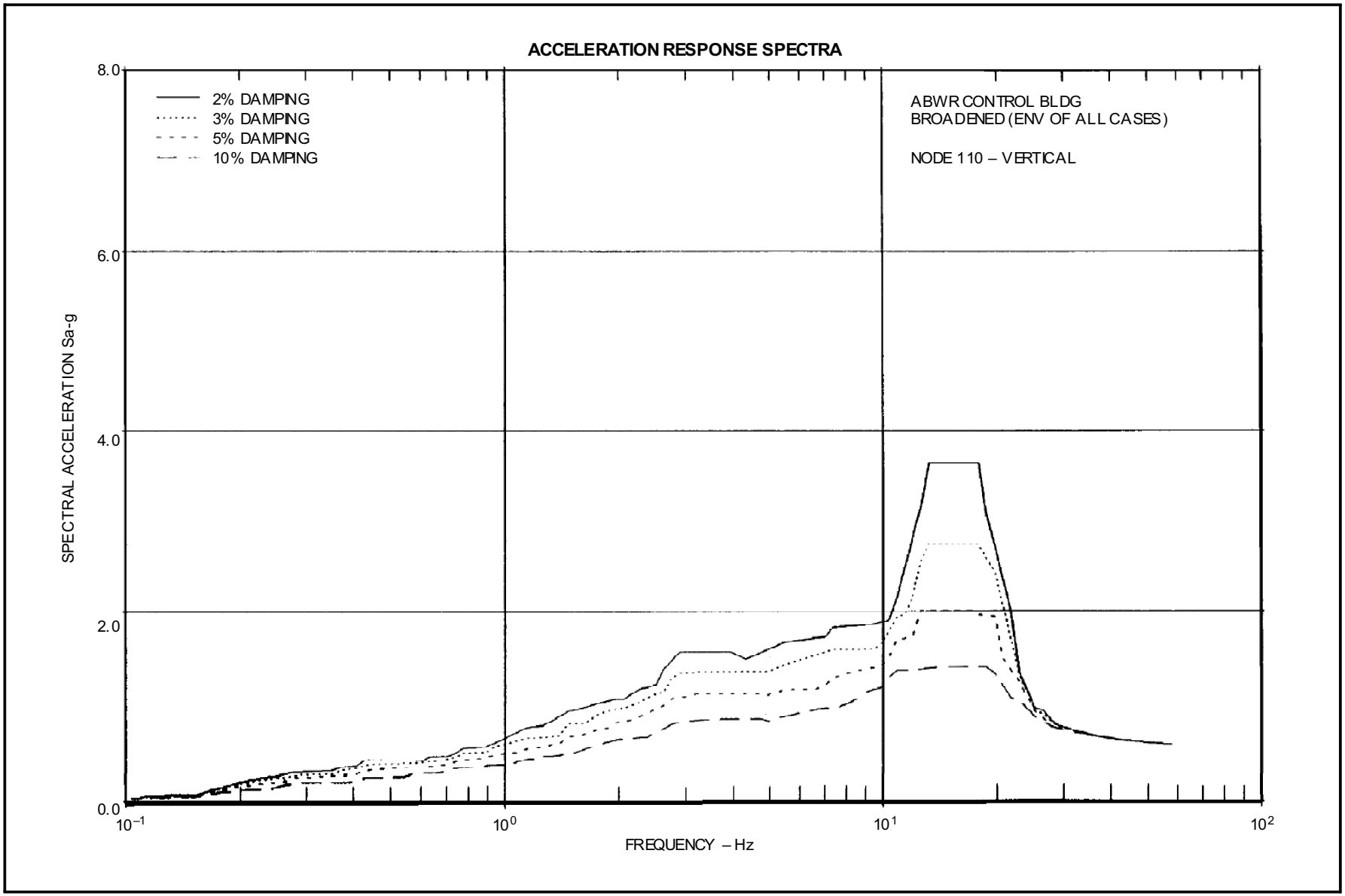

Figure 3A-225 ABWR Control Bldg. Broadened (Env of all Cases) Node 110–Vertical

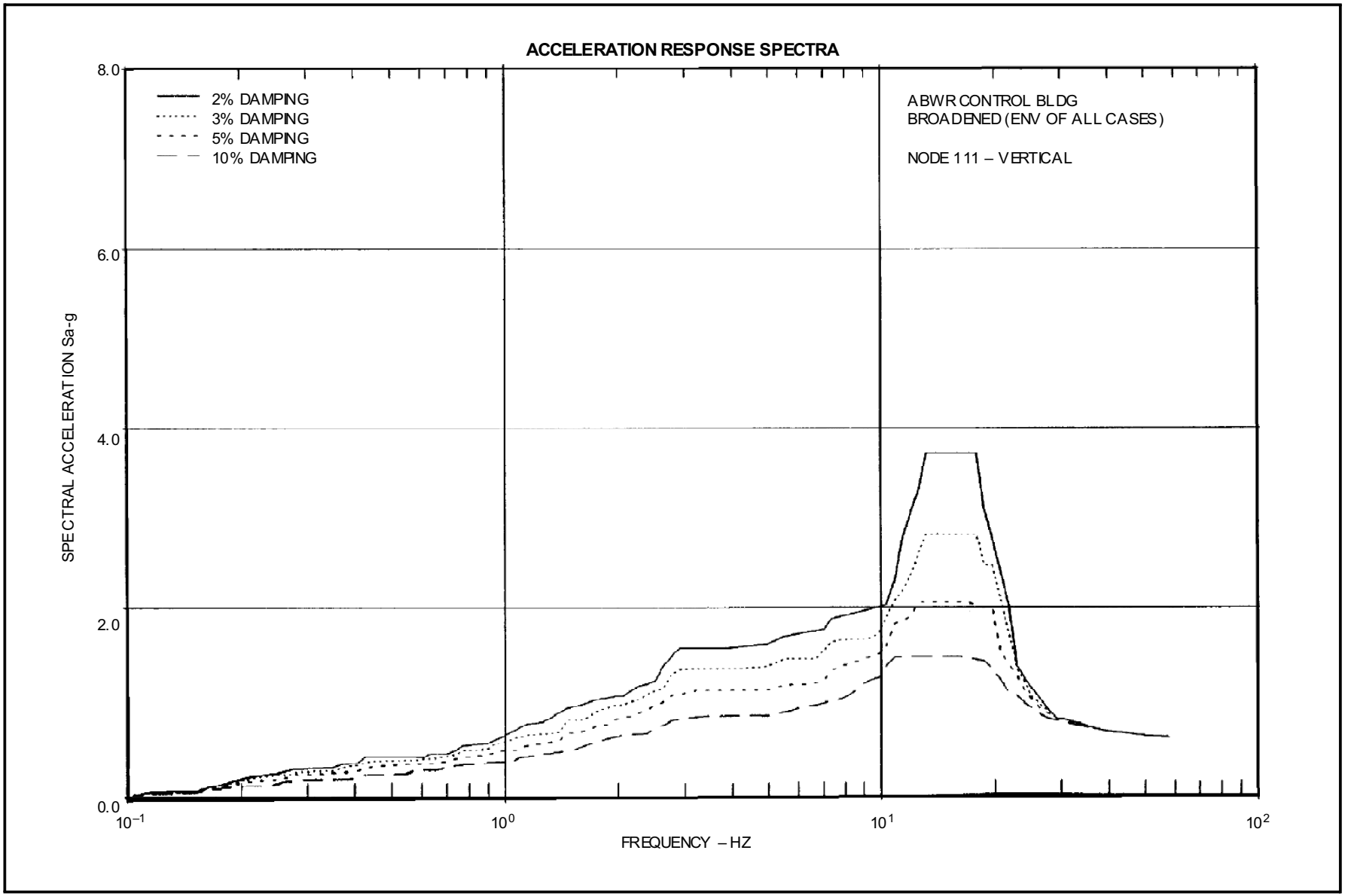

Figure 3A-226 ABWR Control Bldg. Broadened (Env of all Cases) Node 111–Vertical

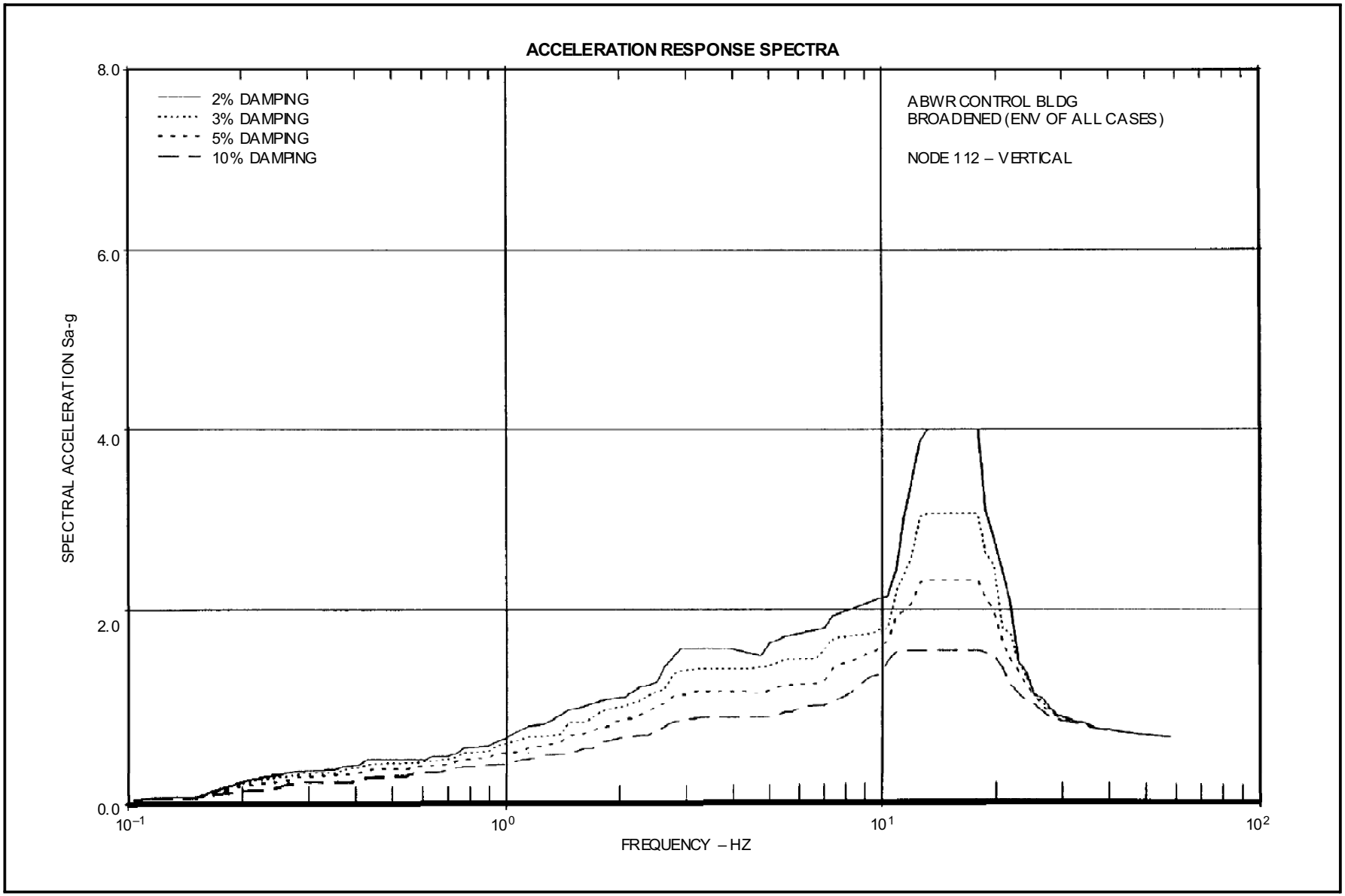

Figure 3A-227 ABWR Control Bldg. Broadened (Env of all Cases) Node 112–Vertical

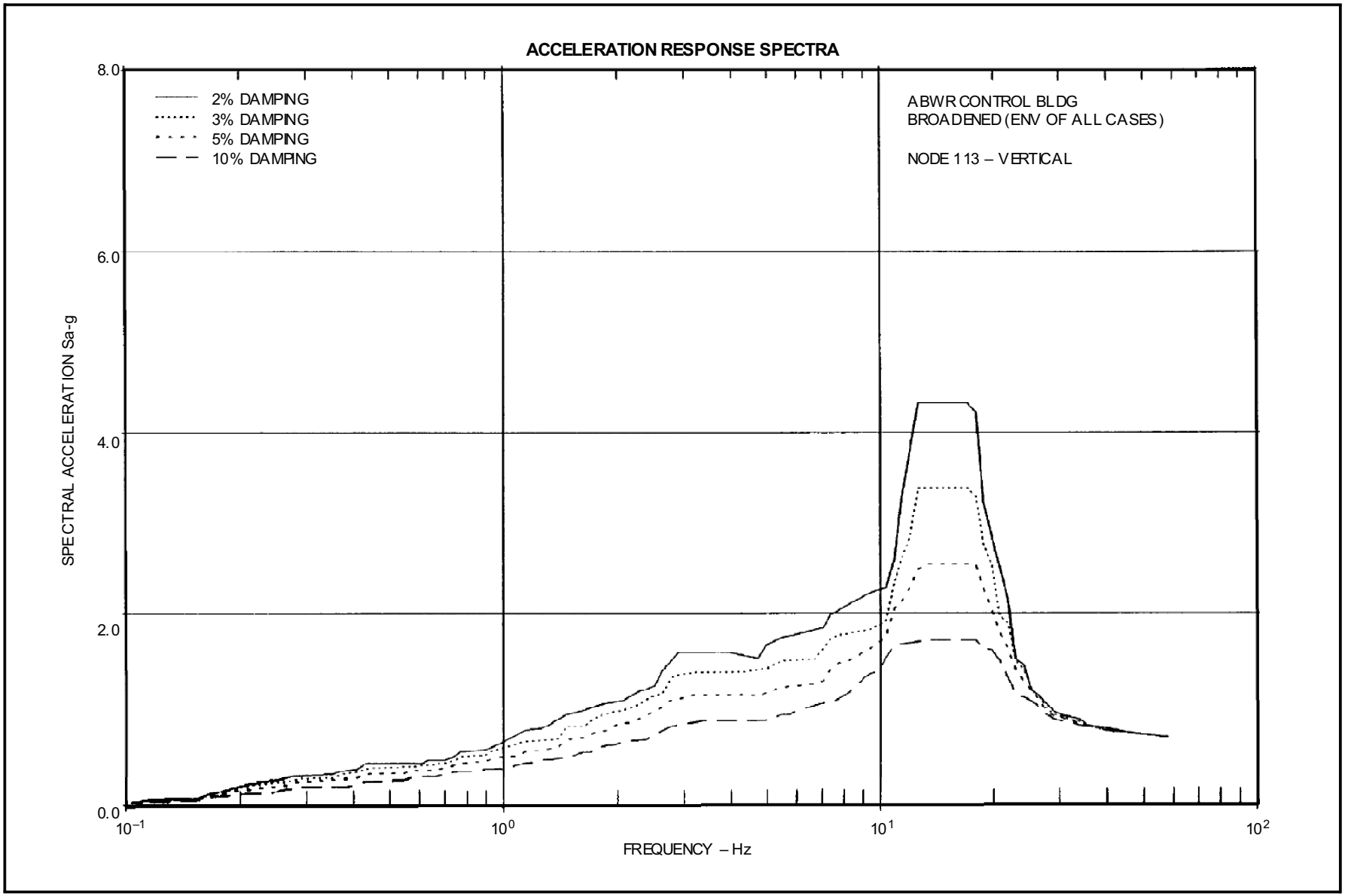

Figure 3A-228 ABWR Control Bldg. Broadened (Env of all Cases) Node 113–Vertical